REFLECTIONS III

Transmission Lines and Antennas

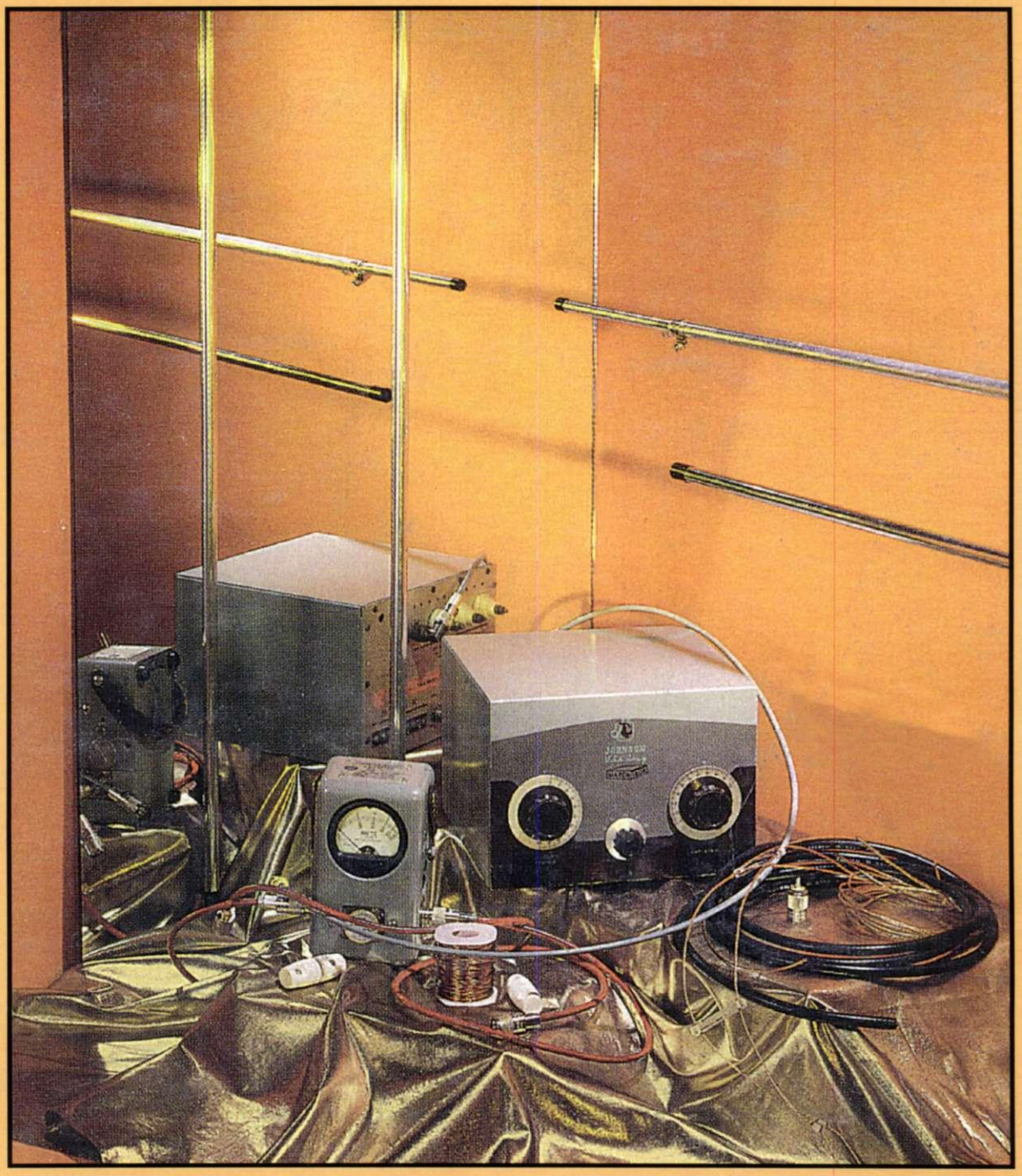

By M. Walter Maxwell, W2DU

REFLECTIONS III

Transmission Lines and Antennas

By M. Walter Maxwell, W2DU

CQ Communications, Inc.

Library of Congress Control Number 2010926394
ISBN 0-943016-43-6

Editor: Gail M. Sheehan, K2RED
Layout and Design: Elizabeth Ryan

Published by CQ Communications, Inc.
25 Newbridge Road
Hicksville, NY 11801

Printed in the United States of America.

Dedication

This book is dedicated to my father, William W. Maxwell, W8YNG (SK), who inspired and pointed me in the scientific direction. My interest in radio originated when I was three, while watching him build radios, and has continued since that year, 1922. With his support, when I was six I built my first one-tube broadcast receiver using a UV-200 detector.

My father operated his own engineering and machining business. He was a mechanical engineer, machinist, innovative welder, astronomer, telescope builder, and radio amateur. Growing up under his guidance in his machine shop fostered my creative ability. I learned from observing his methods for solving problems that required ingenuity, and his attention to precision and detail was not lost on my impressionable mind. In short, I owe my successful and enjoyable lifetime career in the scientific world to his early teachings and continued support.

He was a member of the ARRL for many years, was very active on all the phone bands, and for a long time before becoming a Silent Key in 1958 he was the net control station for the 75-meter Michigan Emergency Net, a position I held as W8KHK from 1938 until 1940.

Preface to the Third Edition

The previous two editions of this book have enjoyed great success, having sold over 13,000 copies since first published 1990. *Reflections III* now provides several additions and changes that will better serve the reader:

An addition to Chapter 19 that begins with Sec 19.10 presents further experimental data reaffirming that a conjugate match can exist when the source of power is an RF power amplifier. Several professional RF engineers reviewed the material appearing in Chapter 19, and found it to be a factual representation of RF power amplifier operation with respect to conjugate matching to its load. In their expert opinion, the facts as stated in Chapter 19 resolve any controversy that may ever have existed regarding this material. Three of these engineers are retired from the RF transmitter design group of the Collins Radio Corp. They are Jan Hornbeck, NØCS; Warren Amfahr, E.E., WØWL; and a third who wishes to remain anonymous. Others include Robert P. Haviland, E.E, W4MB, retired RF engineer from GE; John C. Fakan, Ph.D., E.E., KB8MU, consultant, formerly consultant to NASA; the late Forrest E. Gehrke, BSEE, K2BT, retired microwave engineer of the former RCA; and Al Helfrick, Ph.D. in Applied Science, K2BLA, Professor of Avionics, Embry-Riddle Aeronautical University.

A continuation of Chapter 21, Sec 21.11 describes the origin of the W2DU ferrite-bead current balun, which is a spin-off from the development of the antenna system the author developed for the TIROS weather satellites.

New additions to the previous section "Antennas In Space," retitled "Antennas in Space from an Historical and Archival Perspective," now Chapter 28, describe in detail the author's work in the design and development of the VHF antenna system that flew on the world's first weather satellite, TIROS 1, plus his work on the world's first orbiting communications repeater, the SCORE project, in which an ATLAS ICBM rocket was placed in orbit carrying the repeater that broadcast President Eisenhower's famous "Christmas Message from Space" in 1958. The author believes this book is an appropriate place to archive his work on these important early space-age projects.

Some readers have expressed confusion in a portion of Chapter 23 concerning how virtual open and short circuits are established by wave interference and how wave actions in a $\lambda/4$ transmission-line transformer transform impedances. Some have failed to appreciate how virtual open and short circuits are established by certain magnitudes and phase angles of specific resultants of voltage and current reflection coefficients appearing at the matching point in the matching device. As a result, the original Chapter 23 has been replaced with a new version that explains more clearly how the virtual open and short circuits are achieved, and includes figures that detail the wave actions occurring in $\lambda/4$-wave transformers, reflection by reflection. The section "Virtual Open and Short Circuits Established by Wave Interference" appearing in the new Chapter 25 further clarifies the confusion with more detail concerning the action of the voltages and currents, and of the E and H fields in the wave mechanics leading up to the establishment of the virtual open and short circuits.

Some amateurs, as well as professional engineers, are uncomfortable when considering conjugate conditions in networks having real vs lossless elements. In Chapter 24, Figs 24-2 through 24-8 contain eight mathematical analyses using Mathcad which will eliminate the discomfort. Fig 24-9 contains a summary of the eight analyses and is entitled, "Comparison of Lossless vs Real Elements and Forward vs Reverse Directions in Pi-Networks."

The new Chapter 25 also exposes and corrects some new myths and misconceptions that have crept into the recent literature. The reader may recall that the first seven chapters of all editions are copies of the

seven-part *QST* series "Another Look at Reflections," published during the 1970s. These earlier articles were written specifically to expose and correct the then prevalent misconceptions concerning the mechanics of transmission-line operation. From the feedback received by the ARRL, *WorldRadio*, and the author over the years following publication of the *QST* articles and the two editions of *Reflections*, it is evident that these publications have made a valuable contribution to both the Engineering and Amateur communities. Recent literature has introduced entirely new misconceptions concerning the use of transmission lines. Continual vigilance is needed for exposing and correcting misconceptions as they appear. Chapter 25 was written to correct this erroneous material and to provide proof that it is erroneous.

Appendix 11, "On the Fundamentals of Impedance Matching," in the first two editions of *Reflections* has been moved to become Chapter 26; and Appendix 13, "Investigation of the Shaped-Beam Capabilities of the Quadrifilar Helix Antenna," has been moved to become Chapter 27.

I want to acknowledge the late George Baker, W5YR, and James Reid, KH7M, with thanks for their support in the writing of Chapter 25, and the identical material appearing in *QEX* (*Ref 154*). I also want to acknowledge Robert Lay, W9DMK, James Kelley, AC6XG, and William Klocko, N3WK, for their support in my new analysis of the quarter-wavelength transmission-line transformer appearing in revised Chapter 23, and again to Robert Lay for the excellent critiquing of the addition to Chapter 19.

I want to acknowledge my son Rick's (W8KHK, ex-WB4GNR and WB2HKX) work in making the material from *Reflections I* and *II* into a format usable by CQ Communications to help create *Reflections III*. However, I especially want to thank Gail Sheehan, K2RED, Managing Editor, *CQ* magazine, for the humongous task she performed in editing the entire book and reviewing the layout of every page.

Walter Maxwell, W2DU
May 2010

About the Author

M. Walter Maxwell, W2DU, is an ARRL Technical Adviser (TA) in the specialty field of antennas and transmission lines. Walt was born in Daytona Beach, Florida in 1919, and grew up in Mount Pleasant, Michigan. At age six he built his first one-tube receiver using a UV-200 detector and with the inductor wound on a Mother's Oats cereal box. A life member of both the ARRL and QCWA, and a Fellow of the Radio Club of America, he was licensed at age 14 as W8KHK in 1933, and as of 2010 he has been licensed continuously for 77 years. He was graduated from high school and entered Central Michigan University in Mount Pleasant in 1935, earning a BS degree in mathematics and physics. He played in professional *dance bands, and* specialized in designing, building, and using auditorium and outdoor sound systems until early 1940. Then Walt joined the announcing and technical staff of WMFJ, Daytona Beach, and was assigned the call W4GWZ. In the absence of teletype at that time, Walt also copied Press Wireless News Service from WCX/WJS, 38 wpm CW, while at WMFJ.

With the FCC from September 1940 to April 1944, he was a Monitoring Officer with its Radio Intelligence Division (RID) (see Table of Contents, "Tasks While with the FCC"). His professional antenna experience during that time included participation in designing and building antenna farms at FCC monitoring stations in Hawaii and Allegan, Michigan. Then until 1946 he was in the U.S. Navy as instructor of Aviation Electronic Technicians at Corpus Christi, Texas. While in the Navy he played trumpet in the big band of Alvino Rey, W6UK. From 1946 to 1949 in his own electronic and mobile-communications business, Walt did broadcast-engineering consulting, and was chief engineer of WCEN, having engineered and built that AM station in 1948, Mt. Pleasant's first radio station (see Table of Contents, "Broadcast Engineering Consulting").

In 1949 Walt joined the RCA Laboratories (the David Sarnoff Research Center) in Princeton, New Jersey as an electrical engineer. He was hired at RCA by Clarence D. Tuska, the founder of *QST* and co-founder of the ARRL. Walt later became a charter member of its new Astro-Electronics Division in Princeton. From 1960 until retirement in 1980 he was in charge of Astro's Space Center Antenna Laboratory and Test Range. More than 30 Earth-orbiting spacecraft utilize antennas that were designed solely by Walt, which include the world's first weather satellite, TIROS 1, and the follow-on TIROS-ESSA-NOAA weather satellites, ECHO 1, the first satellite used in an attempt to achieve global TV (see Chapter 28, "Antennas in Space from a Historical and Archival Perspective"). He assisted in the design of many other spacecraft antenna systems, including the data-link antennas on NOAA's TIROS-M and TIROS-N, and on RCA's SATCOM communications satellites. He also designed the Search and Rescue (SAR) system quadrifilar helix antennas flying on TIROS-N, which are used worldwide for relaying signals from emergency locator transmitters (ELT) aboard aircraft in distress. He was one of a three-man team that designed the Moon-to-Earth TV dish antenna used on the Moon on Apollo's lunar rover—the moon buggy. (See Table of Contents, Chapter 28, "The Lunar Rover (the Moon Buggy)". He also set up its test-range facilities and performed all of its final pattern, gain, and impedance-matching measurements prior to acceptance by NASA. He engineered ground-based antenna systems at the Kennedy Space Center, Cape Canaveral, for pre-launch communication with the TIROS and RELAY spacecraft while on the launch pad. In addition he had total engineering responsibility for the receivers, transmitters, and antennas of the five ground stations set up across the U.S., used in Project SCORE, the orbiting Atlas rocket carrying the world's first communications repeater in space which broadcast President Eisenhower's "Christmas Message from Space" in December 1958 (see Table of Contents, Chapter 28 "The SCORE Chronicles").

Having been originally licensed as W8KHK, Walt has also held callsigns W4GWZ, W8VJR, W2FCY, and PJ7DU, the Extra Class license since 1967, and the callsign W2DU since 1968. (His son Rick now has

his dad's original call, W8KHK.) Every full-time position in his career resulted from association with amateur radio. He has served as antenna consultant for AMSAT, as a member of the FCC's advisory committee for WARC-79, and as trustee for K2BSA at National Headquarters, Boy Scouts of America, before they moved from North Brunswick, New Jersey to Texas. By petition to the FCC, Walt obtained the K2BSA callsign for the Headquarters' station to replace the original callsign K2BFW.

After retiring from RCA in 1980, he moved to DeLand, Florida, where he writes and edits using state-of-the-art computers, and still enjoys music, playing string bass in small jazz combos and in a professional 14-piece 1940's Glenn Miller style big band. His favorite big bands are Benny Goodman, Glenn Miller, Duke Ellington, and Count Basie. He also enjoys Florida boating in his 17-ft outboard sportster. From 1992 to 1997, he was President, Frequency Coordinator, and Data Base Manager of the Florida Repeater Council, administering to the more than 1000 Florida repeaters. A three-generation family of hams, Walt's father was W8YNG, and his three sons are Bill, W2WM (ex-WA2ETP, AG2B, 5A4TY), Rick, W8KHK (ex-WB2HKX and WB4GNR), and John, K4JRM (ex-KI4CVQ). His daughter Sue was KC4UBZ (license expired) and son-in-law Keith is WD9JCA.

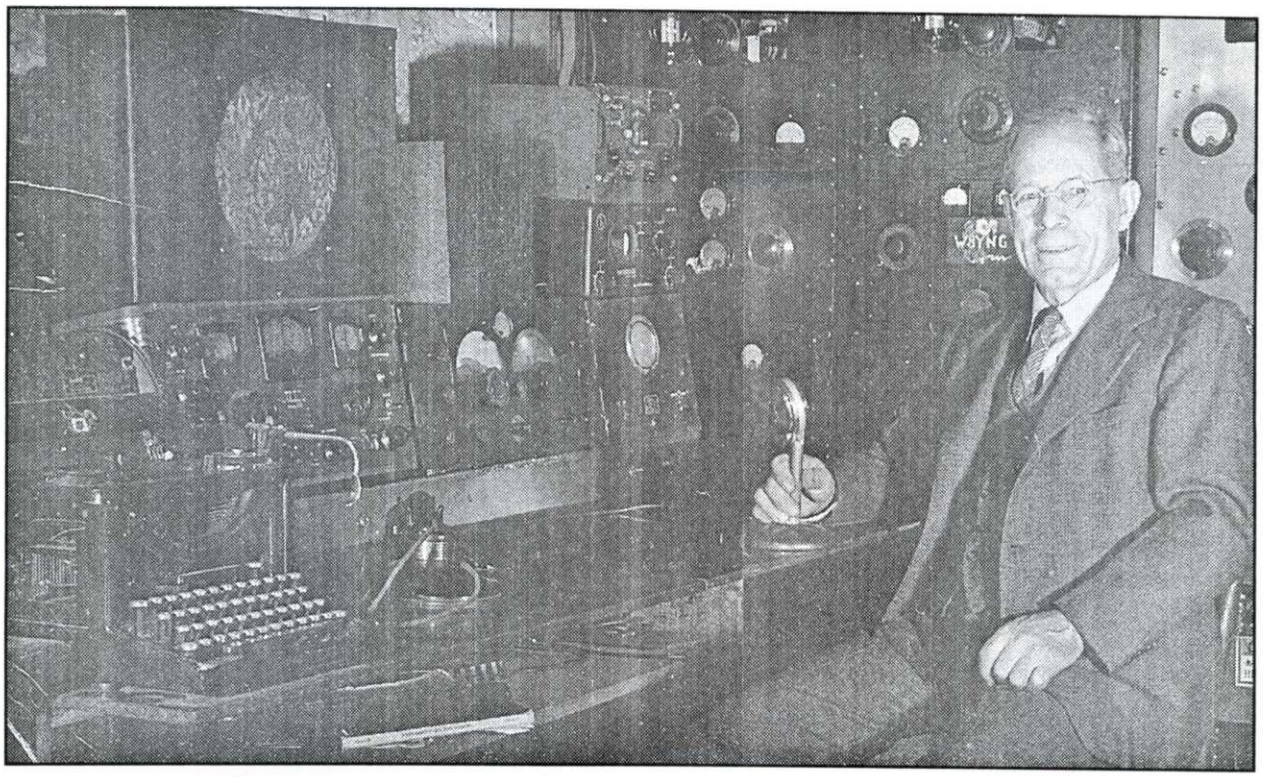

Frontispiece 1. William "Bill" Maxwell, W8YNG, in 1957. Bill was the author's father and patriarch of the three-generation Maxwell family of hams. Watching his dad build radio receivers beginning in 1922 inspired the author to enter the scientific field (see Dedication). Bill was licensed as an amateur radio operator in 1944, and was active as a ham until shortly before becoming a silent key in December 1958. Bill also taught Morse code classes for hundreds of Naval Cadets during WW II.

Frontispiece 2. The author, age 19 in 1938, first licensed in 1933 at age 14, the second generation of the Maxwell family of hams.

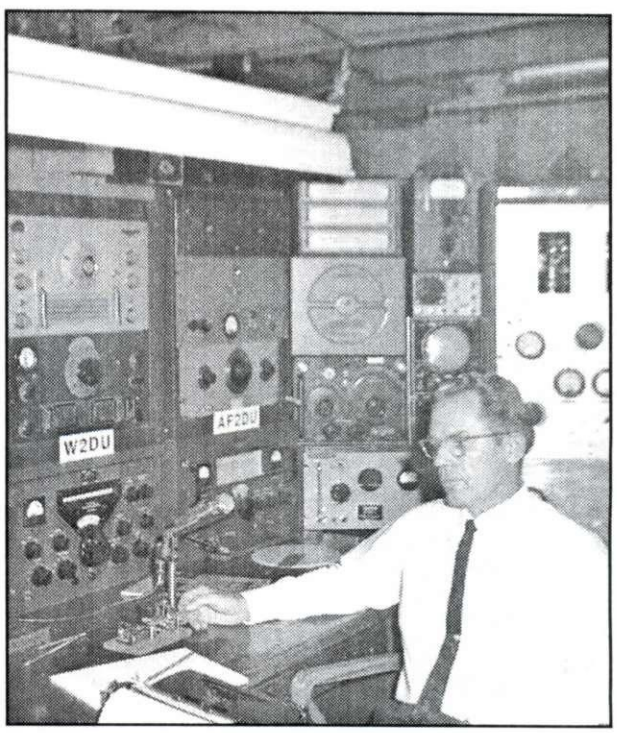

Frontispiece 3. The author in 1968.

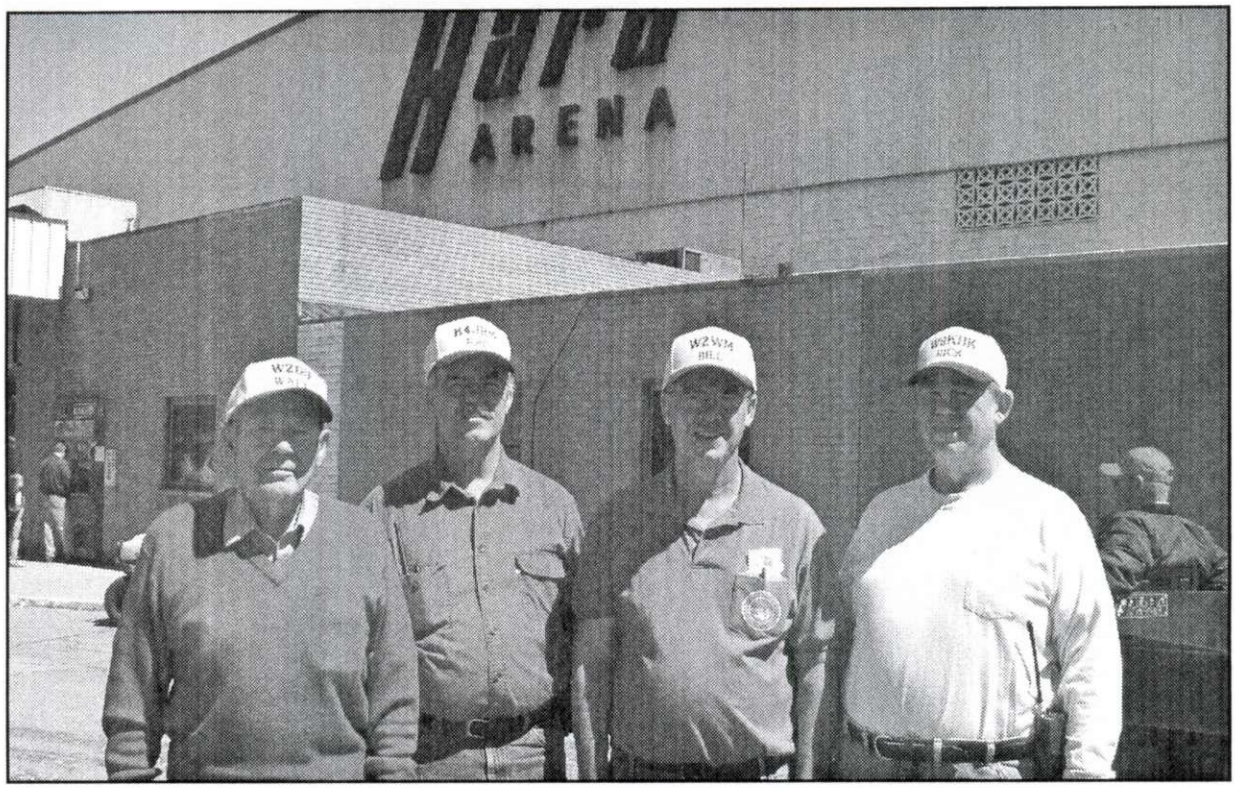

Frontispiece 4. The second and third generations of the Maxwell family of hams at the Dayton Hamvention® in 2006. From left to right: the author, third son John, K4JRM; first son Bill, W2WM; and second son Rick, W8KHK, the author's original call in 1933.

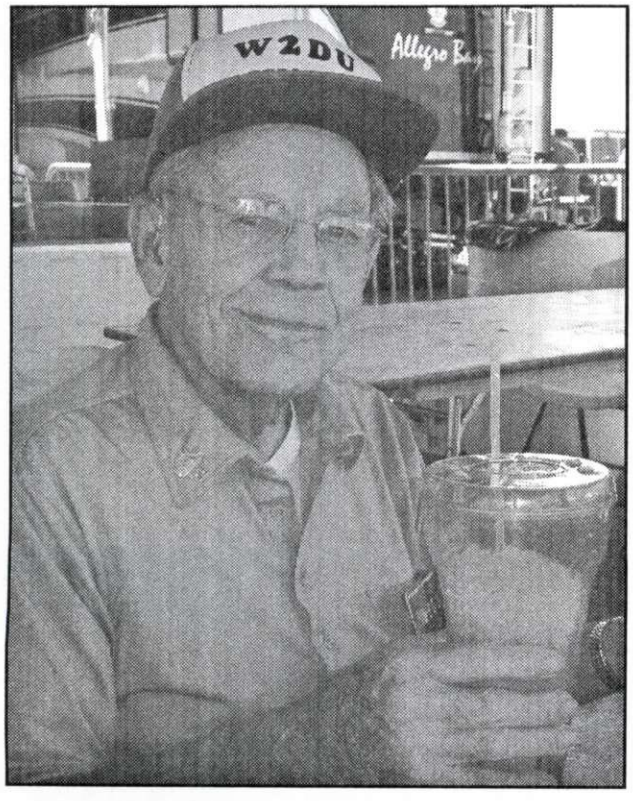

Frontispiece 5. The author, age 90, at the Orlando Hamcation℠ 2009. (Photo by Rick, W8KHK)

Frontispiece 6. The author's ham family at Orlando Hamcation℠ 2009. Back row, from left: sons Rick, W8KHK (ex-WB2HKX, WB4GNR); John, K4JRM, (ex-KI4CVQ); Bill, W2WM (ex-WA2ETP, AG2B, 5A4TY). Front row: John's twin Sue (ex-WD9AJC, KC4UBZ); the author; son-in-law Keith, WD4JCA. (Photo by Dave, K4RU)

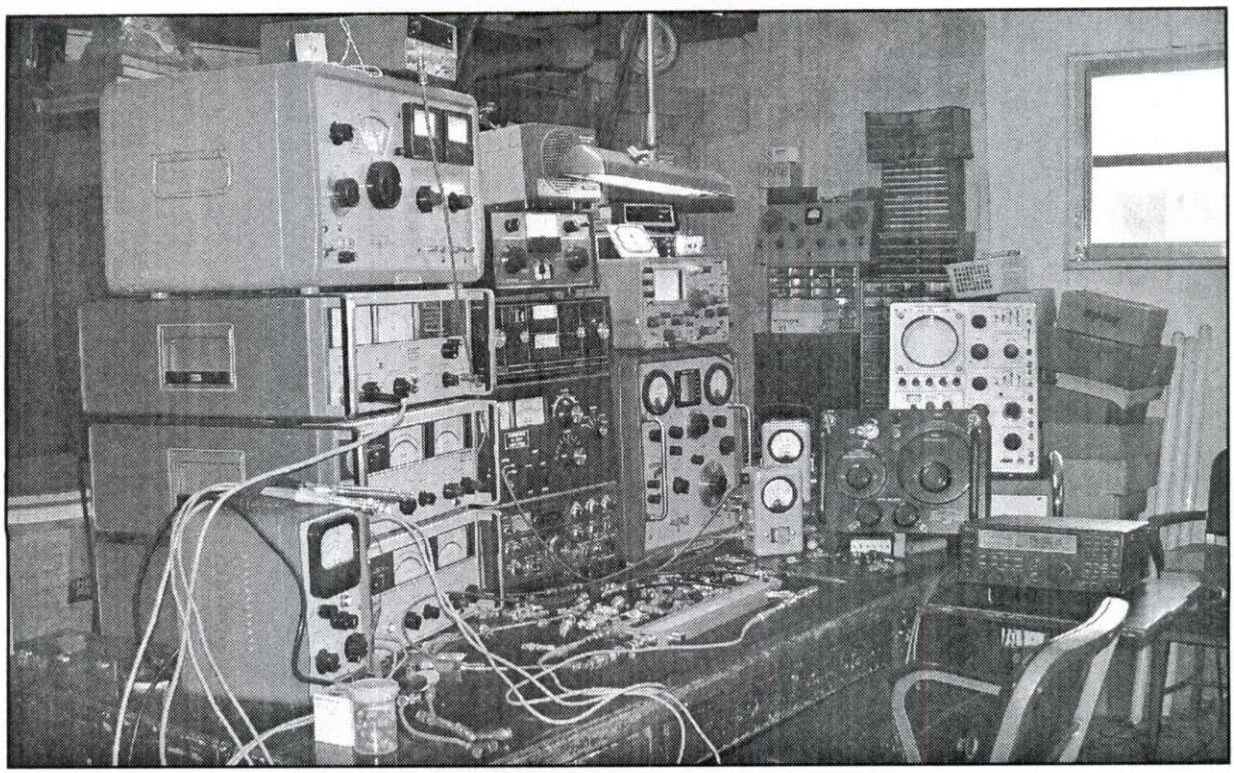

Frontispiece 7. W2DU RF Lab setup showing a General Radio GR-1606A RF impedance bridge used in measuring the impedance of various antennas, the resulting data of which are shown in both tabular and graphical form in Chapters 15 and 20. (The lab bench was formerly David Sarnoff's desk at the RCA Laboratories [the David Sarnoff Research Center], Princeton, New Jersey.)

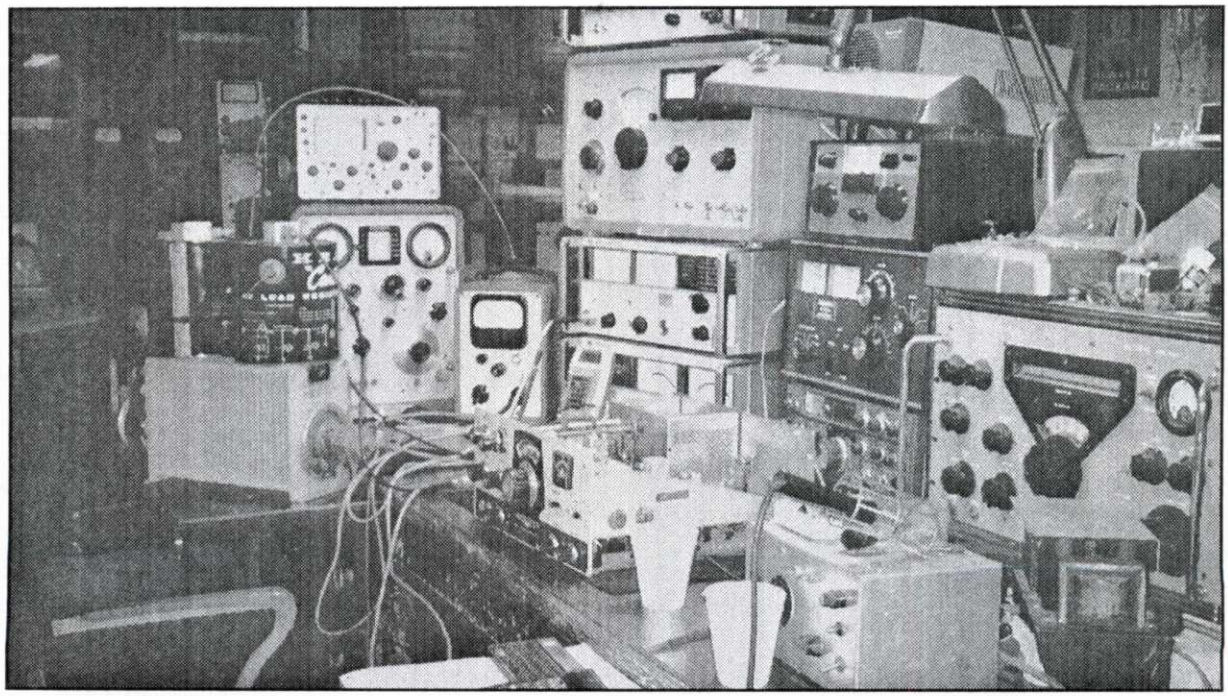

Frontispiece 8. W2DU RF Lab showing the setup when measuring output impedance of the RF power amplifiers in the Heathkit HW-100 and Kenwood TS-830S. Data resulting from these measurements appear in Chapter 19, Secs 19.8 and 19.9.

Introduction

The chapters in this book are a mixture of old and new. The older chapters comprise a collection of articles and other material I previously had published in *QST, The Radio Amateur's Handbook,* and *The ARRL Antenna Book*. Hence, the reader will find some unavoidable repetition on the subject of impedance matching among some of the chapters, because those chapters were written during different time periods, and for achieving different objectives, which did not include the continuity one obtains when the original writing is intended for a book. This third edition also includes my writings that appeared in *QST*'s "Technical Correspondence," an article from *QEX*, and the report on my research while with the RCA Space Center that led to the development of the quadrifilar helix antennas presently used on NOAA's polar orbiting weather spacecraft.

Chapters 1 through 7 are from my series of seven articles published in *QST* in the early 1970s entitled, "Another Look At Reflections." The articles were well received, and over the years both the ARRL and I had many requests for reprints. It is because of these requests that the articles are reprinted in this book, along with some of my writings from other ARRL publications. Except for Chapters 3 and 4, which have been revised extensively, Chapters 1 through 7 are essentially the same as the original articles. They are identical in substance, but I have edited them rhetorically for easier reading.

The idea for writing the original series of articles was born while listening to and participating in many discussions concerning mismatch and reflections on transmission lines. I made up a list of topics that appeared to be the most controversial among amateurs I heard or talked with. The topics themselves are not controversial, except as the amateurs misunderstood the factual realities. From the list I wrote out 27 true statements, which I presented as a true-false test in the *QST* series. Those statements are included here in Chapter 2. From the discussions I mentioned earlier, it was apparent that many amateurs would mark them false.

Those discussions also revealed that many experiments involving antennas and transmission lines were performed for which the results were predestined to futility. The reason is the experimenters were unaware that they lacked sufficient understanding of the principles involved. Then the appearance of erroneous material in amateur literature motivated my desire to do something constructive about the problem. Some of the amateur radio literature implied that little is known on the subject of mismatch on transmission lines. This is not true, unless the author was referring specifically to us amateurs, because the scientific and engineering literature is replete with voluminous data on the subject, going back to the late 19th century with the works of James Clerk Maxwell, Oliver Heaviside, and many others.

One of the problems that limits the understandability and quality of our experiments on antennas and transmission lines is the limited equipment available for amateurs to make precise and complete measurements at RF, as compared to DC and audio frequencies. However, this doesn't excuse us from needing to know some of the fundamental principles of transmission lines; it actually makes knowledge of the fundamentals all the more necessary so we can diagnose and evaluate logically the limited measurement data we do obtain. Our experimental efforts can become more productive if we are able to visualize an accurate physical picture of the voltages, currents, and fields, and how they interact on the transmission line.

My original plan was to compile and publish an extensive bibliography of accurate and readily available references on the subject in *QST*. However, in 1971, the late John Marsh, W3ZF, convinced me that a mere list of references would receive little attention. John then proceeded to fire real enthusiasm for writing an extensive paper which would not only complement and unify the references, but would also underscore the problem and stimulate interest in studying the subject of antennas and transmission lines. I followed John's

suggestion, and as the work progressed it became apparent that additional references from *professional* engineering sources would be valuable in providing access to greater depth of study for the more advanced amateur, and also to make available reliable sources for verification of the points that have been clouded by controversy among amateurs.

During the study of the numerous references in the preparation of the manuscript for the articles, an interesting and valuable aspect emerged: *The ARRL Antenna Book* was seen to unify many of the other references, plus more, because in one handy volume it contains concise, sufficient, and well-presented material on nearly every point of importance to the amateur's needs concerning antennas and transmission lines, including the fundamental principles! For the amateur who has no access to the other references, but could manage to acquire just one book, *The Antenna Book* is it! Every amateur who feeds RF into an antenna should have a copy—and read it! One would be surprised to learn how many antenna engineers have a copy in their own personal libraries.

However, with the exception of *The Antenna Book,* the details of reflections and wave action in transmission lines seems to be somewhat obscure in the amateur literature. Thus, let us now examine what this book is about in more detail.

This is not a "how to" book. Instead, its theme is "how it works." It is about the care and feeding of antennas, with special emphasis on dispelling some of the prevalent myths and misconceptions surrounding the mismatched antenna and its feed line in routine operations with tuners, feed lines, and antennas. It is tutorial in that it explains certain principles of transmission-line theory that are important to the amateur's understanding of what is occurring in routine operations with tuners, feed lines, and antennas. It explains in great detail how the antenna tuner at the input terminals of the feed line provides a conjugate match at the antenna terminals and an impedance match for the output of the transceiver, and tunes a nonresonant antenna to resonance. This aspect of impedance matching is of great importance to users of modern transceivers having broadband output circuits that require a 50-ohm load to deliver full power.

The quote below typifies our actual amateur operation with transmission lines that feed antennas, while supplying the basis for tuning a non-resonant antenna to resonance and obtaining the forward-power increase factor required to achieve the conjugate match:

"Pictures or models that illuminate a mathematical formula in terms of a readily visualized physical mechanism often serve a valuable purpose. . . . In terms of such a physically attractive picture the instantaneous potential difference at any point along a terminated transmission line is the resultant of all the contributions reaching that point simultaneously from both directions after an infinity of successive reflections at the ends. The terminated line is thus seen to play the role of an infinite line folded back and forth upon itself, with discontinuities at intervals equal to the actual length and with the potential difference in these folded parts actually superimposed and combined algebraically into a single value." *(Ronold W. P. King, Ph.D.,* Transmission Line Theory*, Dover Publications, 1965)*

Reflections III also highlights some of the reasons many amateurs seek low values of SWR for the wrong reasons. It explains why a 1:1 SWR isn't always a necessary goal, and it also describes how to determine whether it's worth the effort to reduce the SWR below a given value based on the conditions at hand. However, the book is written in language easy to understand at the amateur level. In addition, a voluminous, broad-based references section is included for those who wish to seek further study.

Chapter 3 presents a simplified treatment of the interaction of the fields, currents, and voltages on a transmission line in explaining the development of the standing wave.

A simple introduction to the Smith Chart is presented, along with a novel use of the chart to assist in understanding how the impedance changes with length on a transmission line. A new phasor-type presentation using the Smith Chart is given, which enhances the *physical* picture of standing-wave development, transmission-line input impedance, and other activity along the line, and forms a basis for an analytical proof that the explanations presented are correct.

For those who are unfamiliar with the Smith Chart, it is easy to learn. See Chapter 10 in this book, Part 1 of *Ref 25*, and Chapter 28 of *Ref 71*. You'll find the chart to be a valuable tool. It has separate sets of cir-

cles for resistance and reactance. To plot a single complex impedance R + jX, you simply find the point where the appropriate resistance, R, and reactance, X, circles intersect. Knowledge of the Smith Chart is helpful in understanding and devising impedance-matching circuitry; it is actually fun to use for this purpose. Additional references of interest are included at the end of the book. Smith Charts are available at college book stores and stores that carry engineering supplies. They may also be ordered from The ARRL.

Chapter 15 includes several computer program listings for solving impedance-matching problems. Included are programs for solving T- and pi-networks, and for obtaining the frequency response of the networks. Also included are programs for obtaining precise values of the transmission-line constants—characteristic impedance, electrical length, and attenuation—obtained from measurements made on the line. There is also a program for transferring complex impedances from one end of the line to the other for accurately determining the terminal impedance of an antenna from measurements made at the input of the feed line. The efficacy of these transmission-line programs may be seen in the figures and tables they produced from data I measured—Figs 15-1 and 20-1 through 20-3, and Tables 15-1, 15-2, and 20-1 through 20-5.

Some important aspects of baluns that are not generally appreciated are presented in Chapter 21. These are taken from my *QST* article, "Some Aspects of the Balun Problem."

I hope you will find my book interesting and useful, and enjoy reading it as much as I enjoyed preparing it.

Walter Maxwell, W2DU
May 2010

Table of Contents

Chapter 1

Too Low an SWR Can Kill You

(Adapted from QST, *April 1973; won cover award)*

Sec 1.1 Introduction

Judging by what we hear on the air, nearly everyone is looking for an SWR of 1:1. *Question* why, and the answer may be, "I'm not getting out on this frequency because my SWR is 2.5:1. There's too much power coming back and not enough getting into the antenna." Another reply could be, "If I feed a line having that much SWR, the reflected power flowing back into the amplifier will burn it up." Still yet is, "I don't want my feed line to radiate." Any of these answers shows a misunderstanding of reflection mechanics and are symptomatic of the present state of thinking on this subject. Rational and creative thinking of antenna and feed-line design practice has been absent for a long time. Such thinking has been replaced with an unscientific and thought-inhibiting attitude, as in the days before Copernicus persuaded the multitudes that the universe did not revolve around the Earth. This situation originated with the introduction of coaxial transmission lines for amateur use around the time we got back on the air after World War II. It gained momentum when SWR indicators appeared on the scene and since the loading capacitor of the pi-net tank replaced the swinging link as an output-coupling control decades ago. We are in this state of mind because much misleading information has been, and is still, being published concerning (1) behavior of antennas that are not self-resonant, (2) feed-line performance in the presence of reflections when mismatched to the antenna, and especially (3) the meaning and interpretation of the SWR data.

Articles containing explicitly erroneous information and distorted concepts have found their way into print, become gospel, and continue to be propagated. These include things such as (1) always requiring a perfect match between the feed line and the antenna, (2) evaluating antenna performance or radiating efficiency only on the basis of feed-line SWR—the lower the better, (3) pruning a dipole to exact resonance at the operating (single) frequency and feeding with an exact multiple of a half-wavelength ($\lambda/2$) coax, as no other length will do, (4) adjusting the height—perhaps just lowering the ends into an inverted-V dipole to make the resistive component of the antenna terminal impedance equal to the line impedance, or (5) subtracting percent reflected power from 100 to determine usable percentage of transmitter output power. Nomographs have even been published for this erroneous method *(Ref 102).*

As a result of these misdirected concepts, we have been conditioned to avoid any mismatch and reflection like the plague. One-to-one all the way! Sound exaggerated? Not if your receiver is tuning the same amateur bands as mine! In the current vernacular, you could say we have a severe SWR hang-up. In many instances, from the viewpoint of good engineering practice, this hang-up is inducing us to concentrate our impedance-matching efforts at the wrong end of the transmission line *(Ref 16).*

It is ironic that we should be in this situation, because the amateur is generally quite practical when it comes to following theoretical considerations. In this case we have been following the perfect-match theory down the narrow path because many of the aforementioned articles have misled us to believe that all reflected power is lost. They have not had an inkling that properly controlled, reflections can be turned to our advantage in obtaining increased flexibility concerning operating frequencies that we are presently throwing away.

That so much misinformation gained a foothold is surprising in view of the correct teachings of *The ARRL Handbook* (*Ref 1*), *The ARRL Antenna Book* (*Ref 2),* the works of Grammer (*Refs 3 through 5*), Goodman (*Ref 7),* McCoy (*Refs 8 through 13 and 41)*, Drumeller (*Ref 14*), Smith (*Ref 15*), and especially two articles that addressed a subject nearly identical to this one by Grammer (*Ref 6)* and Beers

(Ref 16). One objective of this book, therefore, is to identify some of the many erroneous concepts concerning reflection principles, with sufficient clarity to make you question your own position on the subject. Once we correctly understand mismatch and reflections, we can obtain improvement in operational antenna flexibility, similar to going VFO after being rock-bound with a single crystal. Also, when we discover how little we gain by achieving a low SWR on the average feed line, we will avoid unnecessary and time-consuming antenna modifications. Such modifications often involve hazardous climbing and precarious operations on a roof or tower, which can result in injuries or even death. *Let's kill SWR misconceptions—not ham radio operators!*

Sec 1.2 Open-Wire versus Coax Feed Lines

The theory behind the transmission of power through a feed line with minimum loss by eliminating all reflections, terminating the line with a perfect match, is equally valid, of course, for open-wire and coaxial lines. However, in the days of open-wire lines prior to our widespread use of coax, theory was tempered with practical considerations. Open-wire line was, and still is, used with high SWR to obtain tremendous antenna flexibility relative to operating over a wide range of frequencies with high efficiency. This is because all power reflected from the feed-line–to–antenna mismatch that reaches the input source is conserved, not dissipated. The power is returned to the antenna by re-reflection in the antenna tuner (transmatch) at the line input. On the other hand, although the loss from reflections and high SWR is not zero, this additional loss is negligible because of the low attenuation of open-wire lines. If the line were lossless (zero attenuation), no loss whatsoever would result because of reflections. (This is discussed further in Chapter 6, in connection with Fig 6-1.)

The error in our thinking that standing waves on coaxial line must always be completely eliminated originated quite naturally, because the permissible reflection and SWR limits are much lower than in open-wire lines. When using coax for truly single-frequency operation, it makes sense to match the load and line to the degree economically feasible. However, it makes no sense to match at the load in many amateur applications where we chiefly are interested in operating over a band of frequencies! Single-frequency operators we are not, except as our misguided concern over increasing SWR restricts our departure from the resonant frequency of the antenna.

Some authors are responsible for perpetuating the unscientific and erroneous viewpoint that the coax-fed antenna must be operated at its self-resonant frequency. They have continually overemphasized the necessity for the antenna to be matched to the line within some arbitrary, low SWR value to preserve transmission efficiency, implying that efficiency equals 100 minus percent reflected power. The viewpoint is wrong and unscientific, because it neglects the most important factor in the equation for determining efficiency—line attenuation. It is also erroneous because efficiency does not relate to reflected power by simple subtraction. Setting an SWR limit alone for this purpose is meaningless, because the amount of reflected power actually lost is not dependent on SWR alone. The attenuation factor for the specific feed line must also be included. This is because the only reflected power lost is the amount dissipated in the line because of attenuation; the remainder returns to the load. Some authors have so wrongly conditioned us concerning what happens to the reflected power, that many of us have overlooked the correct approach to the subject. It is clearly presented in both *The ARRL Handbook* and *The Antenna Book* that transmission efficiency is a two-variable function of both mismatch and line attenuation. With this knowledge and by using a graph of the function appearing in *The ARRL Handbook,* presented here as Fig 1-1, the amateur can determine how much efficiency he will lose for a given SWR with the attenuation factor of each specific feed line. He can then decide for himself what the realistic SWR limit should be.

Sec 1.3 Unimportance of Low SWR Values

In our efforts to obtain low feed-line SWR values of 1.1, 1.2, or even 1.5 to 1, we have gone far past the diminishing-returns point with respect to efficient power transfer, even for single-frequency operation. It is like installing no. 4 or no. 6 wire in a house-wiring run where no. 12 wire is sufficient.

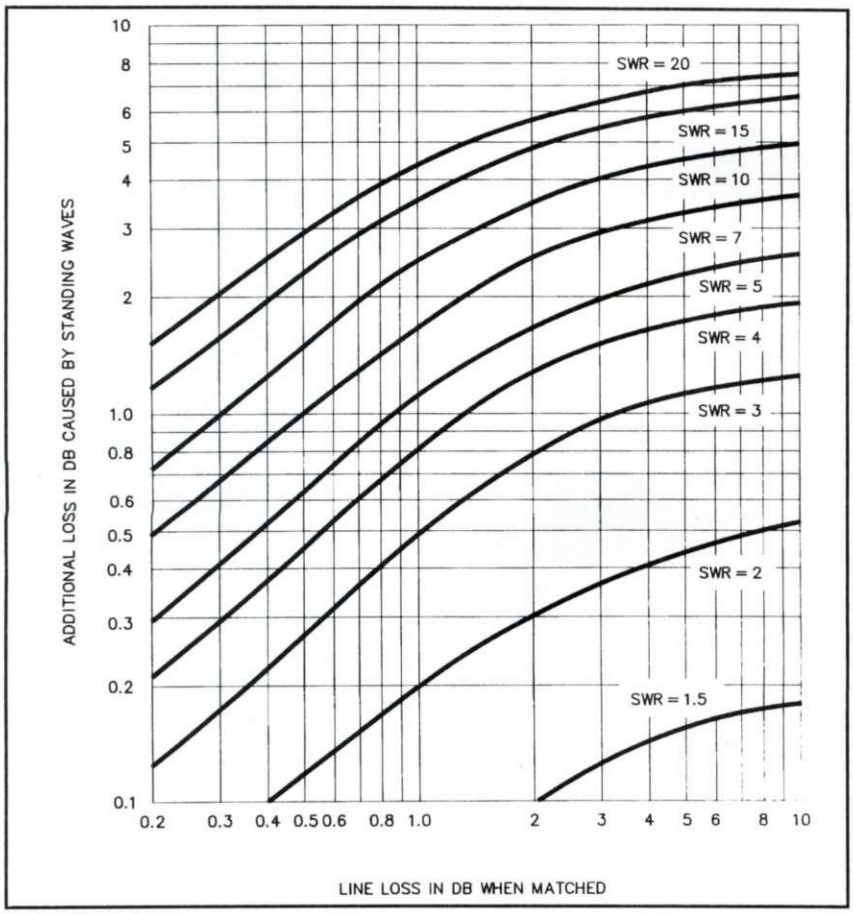

Fig 1-1. Increase in line loss because of standing waves (SWR value at the load). To determine the total loss in decibels in a line having an SWR greater than 1, first determine the loss for the particular type of line, length, and frequency, on the assumption that the line is perfectly matched. Locate this point on the horizontal axis and move up to the curve corresponding to the actual load SWR. The corresponding value on the vertical axis gives the additional loss in decibels caused by the standing wave. (Also see Fig 6-1.)

Reference to the basic transmission-line equations, which have always been readily available in engineering texts and handbooks (*Refs 1, 2, 17, 18, 19, and 33*) verify this analogy. In addition, such references make it clearly apparent that authors who simply insist on low SWR, or find 1.5:1 or 2:1 objectionably high, have failed to comprehend the true relationship between reflected and dissipated power. From the viewpoint of amateur communications, it can be shown mathematically, and easily verified in practice, that the difference in power transferred through any coaxial line with an SWR of 2:1 is imperceptible compared to having a perfectly matched 1:1 termination. This is true no matter what the length or attenuation of the line. Further, it can be shown that many typical coaxial feed lines we use on the HF bands with an SWR of 3 or 4, and often as high as 5 to 1, have an equally imperceptible difference at the receiving end. When feed-line attenuation is low, allowing such higher values of SWR permits operating over reasonably wide-frequency excursions from the self-resonant frequency of the antenna with the imperceptible power loss just described, in spite of the prevalent impression to the contrary.

The relative unimportance of low SWR when feed-line attenuation is low is demonstrated rather vividly in the following two examples of spacecraft antenna applications.

First is NOAA's TIROS-ESSA-ITOS-APT weather satellites, and the design of the entire antenna system fed by four transmitters operating simultaneously on different frequencies was the work of the author. (See the accompanying story at the end of this chapter.) The terminal impedance of each of four crossed dipoles (radiating circular polarization) at the beacon-telemetry frequency (108 MHz in early models) was $150 - j100$ ohms, for an SWR of 4.4, and reflected power of 40%. Matching was performed at the inputs of four separate feed lines by a complex stripline matching network fed by two 30-milliwatt telemetry transmitters. (We can't afford much power loss here!) The combined attenuation of the feed line and matching network was 0.2 dB, and the additional loss from the SWR on the feed line was 0.24 dB (5.4%), for a total loss of 0.44 dB

(only 9.6%). On the prevalent but erroneous assumption that all reflected power is lost (40%), only 18.1 milliwatts would reach the antenna. Efficiency determined on the same erroneous basis would only be 60%. However, 27.1 milliwatts was measured at the antenna. Of the 2.9 milliwatts lost in total attenuation, only 1.6 milliwatts was lost because of the 4.4:1 SWR. Thus, the real efficiency would have been 95.5% if the feed lines had been perfectly matched at the antenna, but reduces only to 90.4% by allowing the 4.4 SWR to remain on the feed line.

Second, in the Navy Navigational Satellite (NAVSAT), which is used for precise position indications for ships at sea, the antenna terminal impedance at 150 MHz is $10.5 - j48$ ohms, for an SWR of 9.3, reflected power 65%. Also matched at the input to the feed line, the matched-line attenuation is 0.25 dB, and the additional loss from SWR is 0.79 dB, for a total system loss of 1.04 dB. This equates to approximately one-sixth of an S unit. This is an insignificant amount of loss for this situation, even in a space environment where power is at a premium.

Why did we match at the line input rather than at the antenna? Because critical interrelated electrical, mechanical, and thermal design problems made it impractical to match at the antenna. Line-input matching (which is exactly what we do in using an antenna tuner, or transmatch) provides a simple solution by permitting the matching elements to be moved to a noncritical location. This design freedom afforded tremendous savings in engineering effort with negligible compromise in RF efficiency, in spite of SWR levels many unenlightened amateurs would consider unthinkable.

Another factor that has contributed to a misunderstanding concerning power lost because of mismatched loads is the confusion among three different conditions of line usage: (1) one in which the incident, or forward, *voltage* on the line is constant, independent of the load terminating the line; (2) one in which the forward *power* is constant, also independent of the load; and (3) one in which the forward power *varies* with changes in the load. (For the relative amplitudes of the SWR and line voltage two cases see *Ref 19, Fig1-3, p 6, and Fig 3-6, p 29*).

The first condition involves laboratory and experimental work, which generally requires holding the forward *voltage* constant with variations in the load terminating the line. A constant-voltage source is usually obtained for this purpose by using a signal generator having a pad of from 20 to 30 dB of attenuation between its source and output terminals to absorb the reflected power. Absorbing the power in the pad prevents it from reaching the source in the generator where it would otherwise alter the line coupling and cause the output voltage of the source to vary. Consequently, the generator sees a perfect match for all terminating load conditions, and *all reflected power is lost in the pad.* This is a condition that is required to obtain certain laboratory test data.

The second condition involves a power source, or generator, which maintains a constant forward *power* on the line independent of the load. The distinguishing feature of this condition is that the generator has an internal source impedance Z_S that is equal to the characteristic impedance Z_C of the transmission line into which it delivers its power. If the line is lossless, conservation of energy demands that power reflected from a mismatched load termination must cause the generator to deliver less power to the line by exactly the amount of power reflected. This is because the arrival of the reflected waves of voltage and current at the input of the line causes a change in line-input impedance from the characteristic impedance Z_C to a new value that presents a mismatch to the generator equal to the mismatch appearing at the mismatched termination of the line. However, the phasor voltage appearing at the input terminals of the line is the sum of the reflected and source phasor voltages at that point. The result is that the addition of the reflected power to the reduced source power equals the original source power; thus, the power entering the line remains the same as before the reflected power returned. Consequently, the forward power remains constant, but the power absorbed in the load is still reduced by the amount of the power reflected. However, the reflected power is not lost, because the reduction of the power absorbed in the load is simply because the source is now delivering less power to the line (*Ref 70*). The fact that reflected power is mistakenly thought to be lost under these conditions is probably the chief reason why many

have been misled to believe reflected power is also absorbed in the plate resistance of the output amplifier of our transmitters, which is not true for the reason explained above.

The third condition involves the power amplifiers in our transmitters, or transceivers, in which the forward power in the transmission line varies directly in response to the power reflected from a mismatched load, such as a mismatched or nonresonant antenna. The reason is that for whatever power we adjust the amplifier to deliver, any power reflected from the mismatched load is returned, either to the tank circuit of the amplifier or to an external line-matching network. There, by the action of re-reflection, the reflected power is added to the power delivered by the amplifier and returned to the mismatched load. In this third case, *no reflected power is dissipated in the plate circuit of the amplifier because it doesn't reach the plate circuit*, and with lossless line (and an ideal lossless tuner), *no reflected power is lost!*

As a result of these various misunderstandings, many amateurs never even wonder whether there are any benefits to be gained by not matching at the junction of the feed line and the antenna. Many even shun the use of open-wire lines (not the old-timers). They completely miss the joy of a QSY to the opposite end of the band with only a simple readjustment of the antenna tuner. The fear of reflections engendered by the exaggerated application of the theory to coax has crept into their thinking concerning any form of mismatched connection.

Adding still further to the confusion is the old-wives' tale that the reflected power is dissipated in the transmitter, causing tube and tank-coil heating and all kinds of other damage. This myth developed out of ignorance of the true mechanics of reflections and became the easy, but fallacious, explanation of what seems to be abnormal behavior in the transmitter when feeding a line with reflections. What really happens at the transmitter in the presence of reflected power is simply a change in coupling caused by a change in impedance at the input terminals of the feed line. This is explained in detail as we proceed from chapter to chapter. Then we may understand how to operate with absolutely no danger of damaging the amplifier while feeding into a line with high SWR. Although some rigs having solid-state output amplifiers have no provision for working into any load other than 50 ohms, rigs with tubes and pi-network output coupling circuits can work into impedances that far exceed the 2:1 SWR limits the manufacturers put on their warning labels.

Sec 1.4 Engineering an Antenna System

Engineering is the process of making workable compromises in design goals where theories and practical applications guiding different aspects of the design are in conflict, making it impossible to optimize all the goals. Good engineering is simply recognizing the correct choices in the compromises and relaxing the right goals, as in the spacecraft-antenna design described earlier. We amateurs spend many hours building and pruning antenna systems. Wouldn't it be worthwhile spending some of that time learning how to engineer the design in order to make correct trade-off decisions among related factors instead of letting old king SWR dictate the design?

First, we need to improve our knowledge of reflection mechanics and transmission-line propagation to understand:

(1) Why reflected power by itself is an unimportant factor in determining how efficiently power is being delivered to the antenna.

(2) The effect of line attenuation to discover why it is the *key* factor that tells us when and how much to be concerned with reflected power and when to ignore it.

(3) Why *all* power fed into the line, minus the amount lost in line attenuation, is absorbed in the load *regardless of the mismatch at the antenna terminals*.

(4) Why reflection loss (mismatch loss) is canceled by reflection gain through re-reflection obtained by the impedance matching device at the input of the line (*Ref 19, Ref 2, and Ref 136*).

(5) Why a low SWR reading by itself is no more a guarantee that power is being radiated efficiently than a high SWR reading guarantees it is being wasted.

(6) Why SWR is not the culprit in transmitter-loading problems; why the real culprit is the change in line-input impedance resulting from the reflected power, and why we have complete control over the input impedance without necessarily being concerned with the SWR.

(7) The importance of thinking in terms of *resistive and reactive components of impedance instead of SWR alone*, and why SWR by itself is ambiguous, especially from the viewpoint of the selection and adjustment of the coupling and matching circuitry of an external line-matching network.

Second, we need to become aware that with moderate lengths of low-loss coax, such as we commonly use for feed lines, loss of power because of reflected power on the HF bands can be insignificant, no matter how high the SWR. For example, if the line SWR is 3, 4, or even 5 to 1 and the line attenuation is low enough to ignore the reflected power, reducing the SWR yields no significant improvement in the radiated power because practically all the power being fed into the line is already being absorbed in the load (the antenna). This point has special significance for center-loaded mobile whip antennas, because of the extremely low attenuation of the short feed line, which is explained in detail later in this book.

Third, we should become more familiar with the universally known, predictable behavior of off-resonance antenna-terminal impedance and its correlation with SWR (*Ref 2, Fig 2-7; Ref 7).* This knowledge provides a scientific basis for evaluating SWR-indicator readings in determining whether the behavior of our system is normal or abnormal, instead of blindly accepting low SWR as good, or rejecting high SWR as bad. The following two examples emphasize the importance of this point by showing how easily one may be misled by a low SWR reading.

(1) A ground system having a hundred properly installed radials has negligible loss resistance (*Ref 20*). AM broadcast stations operating in the 540- to 1600-kHz band use either 120 or 240 radials, while the FCC requires a minimum of 90. With such a ground system the terminal impedance of a thin quarter-wave ($\lambda/4$) vertical is approximately the theoretical value of $36.5 + j22$ ohms, and becomes approximately 32 ohms resistive when the antenna is shortened to resonance. Thus, when fed with a 50-ohm line, the SWR at resonance will be close to 1.6, rising predictably on either side of resonance. However, a ground system having only 15 radials has approximately 16 ohms of ground-loss resistance with this antenna. Thus, if we remove a few radials at a time from the 100-radial system, the increasing ground (loss) resistance adds to the fixed radiation resistance, increasing the total resistance terminating the feed line. Hence, as each radial is removed, the terminating resistance comes closer and closer to 50 ohms, reducing the SWR. When enough radials have been removed for the ground-loss resistance to reach 18 ohms, the terminating resistance will be 18 + 32 = 50 ohms, for a perfect one-to-one match! While the SWR went down, though, so did the radiated power, because now the power is dividing between 32 ohms of radiation resistance and 18 ohms of ground resistance! In cases where losses are very small, it is unnecessary to improve an impedance mismatch that produces an SWR of only 1.6:1, because only a 0.24 dB increase in power will result by reducing the 1.6:1 mismatch to 1:1. However, in this antenna situation, reducing the 1.6:1 mismatch to 1:1 by removing radials will cause a 36% decrease in radiated power, a loss of 1.93 dB in the ground resistance.

Ground resistance with 100 to 120 radials is typically in the range of 1 to 2 ohms, or less. However, ground systems having from two to four radials may have a loss resistance as high as 30 to 36 ohms, so now the SWR at the resonant frequency will be around 1.3 or 1.4. However, when operating at other frequencies, instead of rising from this low value of SWR, as it should at frequencies away from resonance, the ground-loss resistance holds the off-resonant SWR to lower values than would result with a good ground. The low SWR simply indicates that the line is well matched, but it offers no clue that approximately half the power is heating the ground. Thus, the low SWR in this case is misleading; instead of verifying that the antenna system is efficient over a wide frequency band, it is actually telling us that the efficiency is very poor indeed!

(2) Some amateurs who employ a one-to-one balun believe that "one-to-one" means it provides an impedance match between the feed line and the antenna. This is an erroneous concept, because "one-to-one" only specifies the output-to-input impedance ratio of the balun. No matter what antenna impedance terminates the output of the balun, approximately the same impedance is seen at the input, depending on the quality of the balun. Nevertheless, these amateurs are convinced the baluns are matching the feed line to the antenna, because the SWR sometimes goes down dramatical-

ly when the balun is inserted. When using some baluns having ferrite cores, the SWR is less than 2:1 over the entire 75–80 meter band, where somewhat over 5:1 is normal at the ends of the band when the antenna is cut to resonate at the center of the band. Off-resonance SWR is sometimes reduced with these baluns, because the ferrite core saturates while attempting to handle the reactive current which exceeds the maximum core-current level. Thus, the full excursion of the reactive component of antenna impedance is prevented from appearing at the input of the balun. All power above the saturation level is lost in heating the balun, while the low SWR is deceiving the unsuspecting amateur. The true SWR will be unchanged by a 1-to-1 balun if it has a core capable of handling the current without saturating and if it has no significant leakage reactance. However, most transformer-type baluns having a ferrite core do have significant leakage reactance and less than perfect coupling. Hence, these baluns cannot provide a true 1-to-1 impedance transfer, and the resulting SWR will not be the same as it would if the balun did have a true impedance transfer ratio. This is because when the leakage reactance is inserted between the antenna and the feed line, this reactance can either improve or worsen the match, depending on the magnitudes and signs of both the leakage and antenna-terminal reactances. In addition, an SWR indicator may not show the true SWR without a balun if antenna current on the outside of the coax is present at the SWR indicator (*Ref 36*). These aspects of the balun problem, and how to avoid them, are discussed in detail in Chapter 21.

Therefore, it is important to know approximately what SWR to expect: If it is low, determine whether it should be low. Don't assume that a low SWR indicates success or that it guarantees a great system! Be especially suspicious if the SWR remains low or relatively constant over a moderate frequency range, unless specific broad-banding steps have been performed on the radiating system. This knowledge is elementary and routine for an antenna engineer, but too little information in this area has been available for the amateur, considering the degree of his involvement with antennas. The variation of antenna-terminal impedance versus frequency is shown in *The ARRL Antenna Book* (*Ref 2, Fig 2-7, and Ref 71, Fig 2-6*). In addition, correlation of the impedance change with SWR is covered in detail in Chapter 12 in this book to enable us to predict normal SWR, within limits with a non–resonant antenna terminating the feed line.

Fourth, we need to re-examine the use of open-wire feed lines as tuned lines (*Ref 3, Ref 10, Ref 2*), to discover that the principles used there are exactly what we have been discussing. Remember, with tuned lines we completely ignore the mismatch at the junction of the feed line and the antenna. Then we compensate for the mismatch with the tuner at the input of the line over the entire frequency range of the band. The SWR may run as high as 10, 15, or even 20 to 1, but the power reflected from the mismatch is re-reflected back to the antenna by the tuner. Adjusting the tuner to obtain maximum feed-line current simply adjusts the phase of the reflected waves to re-reflect back up the line in phase with the forward wave, again reaching the antenna. Thus, the reflection *loss* from the mismatch is canceled by the reflection *gain* of the tuner. The phenomenon of reflection *gain* is explained in detail in Chapters 4 and 7.

Many of us older amateurs know from age-old practice that a 600-ohm line made of two no. 12 wires with 6-inch spacing would work every time. We had little incentive in the earlier days to learn how they worked and why they transferred power *efficiently* with such high reflected power and SWR. Nor did we particularly care that tuning the plate tank for a dip in plate current was really canceling the reactance appearing at input of the feed line, or that the plate-current dip was just another way of viewing the phase adjustment of the reflected waves to coincide with the waves emanating from the source. Also, we didn't realize that at the current dip the reflected waves of voltage and current would add in phase with the voltage and current supplied by the source to obtain maximum feed-line and antenna current. This is probably one of the reasons for our misunderstanding of the similarity between open-wire and coaxial-line operation with mismatched loads. The principle is the same in both; only the degree of mismatch is different. In other words, for many applications, *coax can be used as a tuned line in precisely the same manner as open wire, especially with lines of low loss that are not*

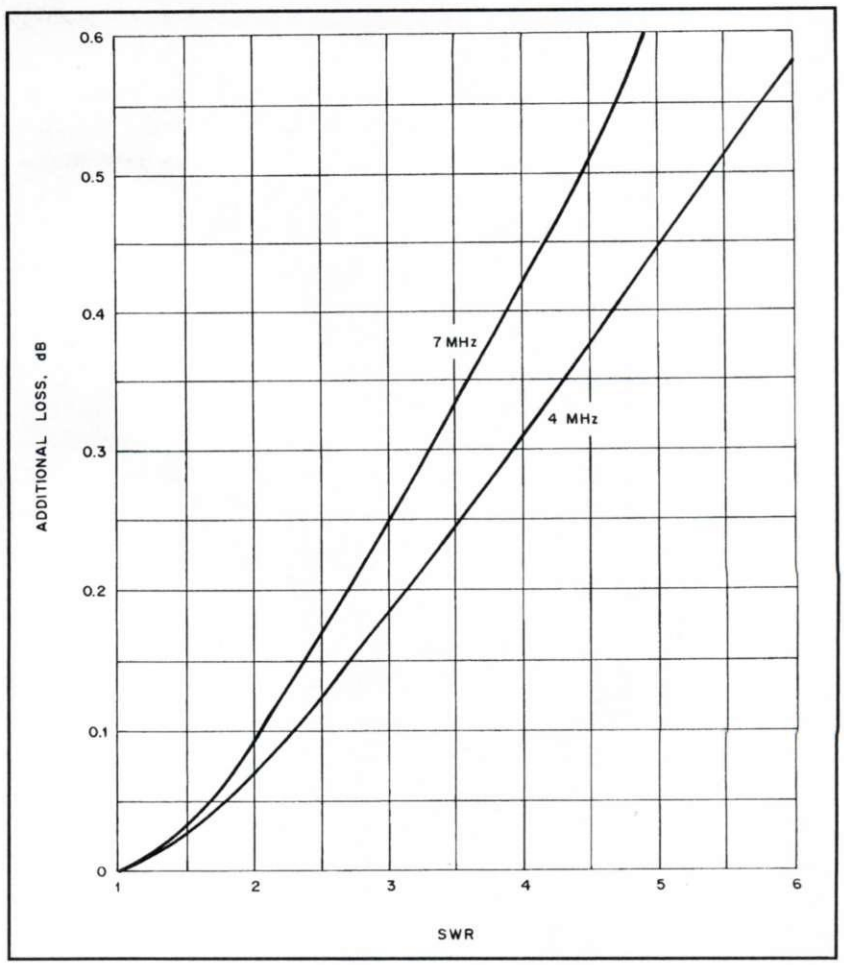

Fig 1-2. Effect of standing-wave ratio on line loss at 4 and 7 MHz. The ordinates show the additional loss in decibels over those for a perfectly matched 100-foot length of RG-8 line for the SWR values shown on the horizontal scale.

unreasonably long. The spacecraft antenna systems mentioned earlier are typical examples.

Thus, coax connected directly into the antenna may be operated successfully with substantial mismatch, in which case the SWR limits while operating away from the self-resonant frequency of the antenna are determined entirely by power lost because of line attenuation. Voltage breakdown and current heating is not a problem at our legal power limit with RG-8, RG-213, or RG-11, or with RG-58 or RG-59 at lower powers. This is because voltage at an SWR maximum is only the *square root* of the SWR times the voltage appearing on the line when the line is matched. The impedance at the input of the line will no longer be 50 ohms, but we can determine whether the output tank of the transmitter has sufficient impedance-matching range to permit feeding the line directly. This depends on the magnitude of the mismatch and the length of the line. The range is surprisingly high in some rigs, while little in others (*Ref 4*). If the matching range of the rig is insufficient, an external matching device (antenna tuner, transmatch, or ATU) can be used to obtain an impedance match and the correct coupling between the input of the feed line and the transmitter (*Refs 9 through 12 and 22*). The point I am emphasizing here is that within the limits mentioned, *all required line matching can be transferred back to the operating position* instead of forcing the match to occur at the antenna feed point, without suffering any *significant* loss in radiated power. The use of this technique, which may come as a surprise to many, does not contradict any theory. It is actually an embodiment of the fundamental principle of network theory called conjugate matching (*Ref 17, Ref 19, Ref 35, Ref 69*), which is the basis for all antenna tuner, or transmatch, operation with either open-wire or coaxial lines.

After learning of the benefits obtained with line-input matching in the two spacecraft examples described earlier, it is interesting to compare the

results using this same input matching technique in typical 80- and 40-meter situations. The 80-meter amateur band is the widest in terms of percent of center frequency, and thus suffers the greatest SWR increase with frequency excursion to the ends of the band. A dipole cut for resonance at 3.75 MHz yields a mismatch, or SWR in a 50-ohm feed line somewhat above 6:1 at 3.5 MHz and about 5:1 at 4.0 MHz. As shown in Fig 1-2, in a 100-foot length of nonfoam RG-8 an SWR of 5:1 adds only 0.46 dB loss to the matched (that is, flat) line loss of 0.32 dB at 4.0 MHz. Therefore, out almost to the ends of the band, less than 1/12 of an S unit is lost because of the SWR, an imperceptible amount at the receiving end. This further verifies the principle and proves that full-band, coax-fed dipole operation on 80 meters also is practical. Even with the high SWR at the ends of the band, the loss cannot be distinguished from what it would have been had the SWR been a perfect one-to-one! On 40 meters, with the dipole resonated at 7.15 MHz, something is amiss if the SWR exceeds 2.5 at the band ends. Also, from Fig 1-2 it may be seen that this SWR adds only 0.18 dB to the matched loss, which at 7 MHz is 0.44 dB for 100 feet of RG-8 coax.

Sec 1.5 Non-reflective Load versus Line-Input Matching

Now is a good time to contemplate the distinction between the no-reflection, perfectly matched load, requiring an inaccessible matching network at the antenna feed-line junction, and matching at the input of the feed line. From the standpoint of good engineering, as long as the SWR does not exceed the value above which one cannot afford to compromise further power in exchange for improved operating flexibility, the convenience and increased bandwidth afforded by matching at the line input is obvious.

However, line-input matching also presents a real challenge to learning more about complex impedance, because in the presence of reflections, the line-input impedance is no longer simply the characteristic impedance Zc, but now has resistive and reactive components, both of which vary with changes in line length and with frequency. Thus, we need to understand complex impedance in order to choose and adjust corrected external conjugate-matching circuitry to couple the transmitter to the line, or to adjust the transmitter directly to the line if sufficient matching range is available. Practically all problems encountered while attempting to obtain proper coupling or loading to a line with reflections can be traced simply to not understanding the correlation of line length and relative phase of the forward and reflected waves with the resulting complex impedance seen at the input terminals of the feed line.

A detailed discussion of reflection mechanics and feed-line propagation is presented in subsequent chapters. Included is a novel means for explaining impedance transformation along the line in direct relation to forward and reflected waves that simplifies the understanding of what does and what does not happen when a line length is changed, and how to select the correct length for given conditions. The relation of line attenuation to permissible SWR while using conjugate matching techniques, along with details on how to obtain proper coupling and loading of a transmitter to a line for which the input impedance has changed because of reflections, is also presented.

Chapter 2

Countdown for a Journey from Mythology to Reality

(Adapted from QST, *June 1973)*

Sec 2.1 Introduction

In Chapter 1 we saw that obtaining a low SWR is relatively unimportant for an efficient transfer of power when line attenuation is low. Four steps to assist in understanding the operation of transmission lines with reflections due to a mismatched termination were presented. In addition, the concept of matching the complex impedance appearing at the *input* of a transmission line with reflections was introduced, based on the principles of conjugate matching. One of the articles of the Conjugate Match Theorem is that a conjugate match exists whenever all of the available power from the source is being delivered to the load (*Ref 137, IEEE*). In the following paragraphs we will discuss some of the basic principles involving efficient transfer of power in a system comprising a source, and a transmission line terminated in a mismatch.

A conjugate match exists throughout the entire system, and all the available power will be delivered by the source when the output impedance of the source is made equal to the resistive component of the line-input impedance, and when all reactance components in the source and line-input impedances are canceled to zero by a matching network, which can be either the pi-network tank circuit or a separate matching network such as an antenna tuner. In this condition the entire *system* is resonant, including the output circuitry of the amplifier. All available power from the source enters the line, and reflections from any terminating mismatch or other line discontinuities are compensated by a complementary reflection, which cancels the original reflection at the matching point in the matching device. Such a reflection is obtained by introducing a non-dissipative mismatch at the match point. This non-dissipative mismatch is one which, if placed in the system by itself, would produce the same magnitude of reflection, or SWR, as is produced by the mismatched line termination. The result is a precise and total re-reflection of the arriving reflected wave. Andrew Alford makes an elegant presentation of this concept (*Ref 39, pp. 10–15; also see Ref 136*). Although this sounds very complicated, the entire set of conditions is automatically fulfilled simply by completing a correct tuning and loading procedure. It matters not whether a transmitter having sufficient matching range feeds the line directly, or whether an external matching network (antenna tuner) is used where additional range is required. If the transmitter, or source generator, is now replaced by a passive impedance equal to its source impedance (equal to its optimum load resistance), the line can be opened at any point. Then, from this open point, and looking in either direction, one will see the conjugate of the impedance seen in the opposite direction; whatever $R + jX$ value is seen in one direction, $R - jX$ is seen in the other.

Contrary to what many believe, it is not true that when a transmitter delivers power into a line with reflections, a returning reflected wave sees an internal generator resistance as a dissipative load. Nor is the reflected wave converted to heat and lost, while at the same time damaging the final amplifier. When a matched RF power amplifier is actively supplying power when the reflected wave returns, the reflected wave encounters total re-reflection at the match point appearing at the input terminals of the pi-network tank circuit, and the reflected power is entirely conserved because it never sees the source *impedance* of the amplifier as a dissipative terminating load, but not because the source impedance is non-dissipative. (Incidentally, the source impedance of the RF power amplifier *is*

non-dissipative, as will be explained in detail in Chapter 19.) The concept of a non-dissipative impedance is one of the most misunderstood concepts in electrical engineering today. This is because the source and reflected voltages and currents superpose, or add (in phase) at the match point, just as if the reflected power had been supplied by a separate generator in series with the source. The phasor sum of their voltages yields a net current flow that is always in the forward direction. The reflected power thus adds to the source power, deriving reflection gain, which compensates for the reflection loss suffered at the mismatched termination. More details on the reflection phenomenon are presented in subsequent chapters.

Sec 2.2 Line Losses

All power reflected from a mismatched line termination that reaches the source is re-reflected and returned to the load, as part of the forward or incident wave. The only reflected power lost is that from line attenuation during its return to the source and once again during its return to the load. The higher the line attenuation, the less reflected power reaches the source to add to the forward power. Thus, the lower the line attenuation, the higher the allowable SWR for a given loss because of SWR. No reflected power is lost in a lossless line, no matter how high the SWR, because it all ultimately arrives at the load. This is why open-wire line functions so efficiently as a tuned line with any reasonable mismatch value; its attenuation is almost negligible. Since the attenuation is higher in coax, the attenuation imposes lower limits on the mismatch and may require calculation of the loss penalty for a given SWR. Line attenuation and SWR both must be quite high to incur any substantial additional loss over and above the matched-line loss. The additional loss due to SWR and line attenuation may be determined graphically from *Figs 1-1* and *6-1*, or calculated using Eq 6-1.

Coax has higher RF losses than open wire at HF for two reasons:

(1) It has a lower impedance, causing higher current flow at lower voltage for the same power. This results in higher I^2R loss for the same effective conductor size. (Electric power distribution lines minimize I^2R loss by using high voltage and low current.) Skin effect also increases the loss with rising frequency because of decreased effective conductor size.

(2) The increased amount of dielectric material separating the conductors in coaxial line (air vs. solid dielectric) is also a substantial contributor to the attenuation loss factor. The attenuation increases with frequency, especially at VHF and UHF. (The attenuation due to resistance, R, in the conductors increases as the square-root of frequency, and the attenuation due to conductance, G, of the dielectric increases directly with frequency.) Hence, it is understandable why RG-8, especially the foam type with its larger center conductor (*Ref 23*), allows higher SWR (thus more bandwidth) than RG-58 for the same additional loss penalty. Also, for any cable, the shorter it is, the less loss is added for a given SWR.

A fifth step in improving your understanding of the reflected-power problem is to view the situation objectively, asking yourself, "Have I fallen prey to any of the erroneous teachings? Can I spot the wrong info when I hear it discussed? Do I understand the principles well enough to convince others of the correct version if the opportunity arises?" Several pertinent short statements follow which may be used as self-test material. They highlight and summarize many reflection-related concepts known to be generally confusing to many amateurs. In the interest of brevity they are not intended to be completely self-explanatory, but sufficient material for obtaining a complete understanding of each point appears later, or is available from references in the bibliography. Support for nearly every statement can be found in *The ARRL Antenna Book*.

Sec 2.3 True or False?

(1) Reflected power does not represent lost power except for an increase in line attenuation over and above the matched-line attenuation. In a lossless line, no power is lost because of reflection. Only when the matched-line attenuation and SWR both are high is there significant power lost from reflection. On all HF bands with low-loss coax, the reflected power loss is generally insignificant, although at VHF it becomes significant, and at UHF it is of extreme importance.

(2) Reflected power does not flow back into the transmitter and cause dissipation and other dam-

age. Damage blamed on reflections is really caused by improper output-coupling adjustment, not by SWR. Tube overheating is caused by either or both overcoupling and reactive (mistuned) loading. Tank-coil heating and arc-overs result from a rise in loaded Q caused by undercoupling. With some manipulation, proper output coupling indicated by a normal resonant plate-current dip at the correct loading level can be attained no matter how high the SWR. The transmitter doesn't "see" an SWR at all, only an impedance resulting from reflections giving rise to the SWR. Also, the impedances are matchable without concern for the SWR. This is one of the most important issues contributing to the confusion.

(3) Any effort to reduce an SWR of 2:1 on any coaxial line is completely wasted from the standpoint of any significant increase in power transfer (*see Figs 1-1 and 6-1*).

(4) A low SWR is not proof of a good-quality antenna system or an indication that it is working efficiently. On the contrary, lower than normal SWR values exhibited over a frequency range by a dipole or a vertical over ground is a clue to trouble in the form of undesired loss resistance. Such resistance can be from poor connections, poor ground system, lossy cable, etc.

(5) The radiator of an antenna system need not be of a self-resonant length for maximum resonant current flow, the feed line need not be of any particular length, and a substantial mismatch at the junction of the line and the antenna does not prevent the radiator from absorbing all of the power available at the junction (*Ref 3, Ref 24*).

(6) If a suitable matching network cancels all the reactance developed by a non-resonant-length radiator and a random-length feed line that is mismatched at the antenna feed point, the antenna system is resonant, the mismatch effect is canceled, maximum current flows in the radiator, and all the power available at the feed point is absorbed by the radiator.

(7) The majority of tower radiators used in the standard AM broadcast band (from 540 to 1600 kHz) are of heights that are not resonant lengths at the frequency of operation.

(8) The SWR on the transmission line between the antenna and a matching network at the input to the line is determined *only* by the mismatch conditions at the load and is not changed or "brought down" by the matching network. "Low SWR" obtained by using the device indicates only the mismatch remaining between the input impedance of the network and the impedance of the line from the transmitter.

(9) Adjusting the matching network, or antenna tuner, for maximum line current creates a perfect mirror termination for the reflected wave, causing it to be totally re-reflected on arrival at the input end of the line. The tuner provides the proper reactance to cancel the equal but opposite reactance between the source and reflected wave at the input. This causes the reflected wave to add *in phase* to the source wave to derive the total incident, or forward, power, which is the sum of the source and reflected power.

(10) Total re-reflection of the reflected power at the line input is the reason for its not being dissipated in the transmitter, and why it is conserved, rather than lost.

(11) With a good antenna tuner and a well-constructed open-wire feeder, a 130-foot center-fed dipole does not radiate significantly more power on 80 meters than one 80 feet long for the same power fed from the *transmitter* (*Ref 3, Ref 7, Ref 10, Ref 21*).

(12) A dipole cut to be self-resonant at 3.75 MHz and fed with either RG-8, RG-213, RG-214, or RG-11 coax does not radiate significantly more on 3.75 MHz than on 3.5 or 4.0 MHz with any feeder length up to 150 or 200 feet.

(13) With a 3.75-MHz dipole, the SWR on a 50-ohm feed line rises to around 6.5 at 3.5 MHz, and around 5.0 at 4.0 MHz, thus utilizing the coax as a tuned feeder, but with *insignificant* loss in radiated power across the entire 80-meter band.

(14) With the use of a transmatch or a simple L network at the line input, proper coupling between the transmitter and the tuned-coax feeder can be attained over the entire 80-meter band *with any random coax length*.

(15) From the standpoint of line loss because of SWR resulting from the change in quality of the impedance match between the line and antenna, changing the height of the dipole above ground or lowering the ends of a horizontal dipole to make an inverted-V dipole has an *insignificant* effect on the amount of power it absorbs from the transmitter.

(16) As a tuned line at 4.0 MHz, RG-8 can handle 700 watts CW *continuously* within ratings, at an SWR of 5:1. With the duty cycle of SSB, it is far below maximum ratings at 2 kW PEP. With a 100-foot length, the *total* attenuation with a 5:1 SWR is just 0.78 dB (0.46 dB due to the SWR), which results in an insignificant loss of power in terms of received signal strength.

(17) If the line length is critical in order to satisfy a particular matching condition, the same input impedance can be obtained with any length of line, shorter or longer, by adding a simple L network of only two components: either two capacitors, two inductors, or one of each, determined by the specific impedance change required of it. This statement is pertinent to coiled-up coax in mobiles (*Ref 19, Ref 24, Ref 30, Ref 31*).

(18) High SWR in a coaxial transmission line caused by a severe load mismatch does not produce antenna currents on the line, nor does it cause the line to radiate (*Ref 2, Ref 3; see also Chapter 20, Sec 20.3, for the answer*).

(19) High SWR in an open-wire line at HF caused by a severe load mismatch does not produce antenna currents on the line, nor cause the line to radiate if the feed currents in each wire are balanced, and if the spacing is small at the wavelength of operation (also true at VHF if sharp bends are avoided (*Ref 2; see also Chapter 20, Sec 20.3, for the answer*).

(20) Both coax and open-wire feed lines may radiate (*Ref 32*), although not at a significant level, by re-radiating energy coupled into the line from the antenna because of asymmetrical positioning with respect to the antenna. The energy coupled from the antenna results in antenna currents flowing on the *outside* of the outer coax conductor, or *in-phase* (common mode) currents flowing on the wires of the open-wire line. However, this condition has no relation to the level of the SWR on the line in either case (*Ref 2; see also Chapter 20, Sec 20.3, for the answer*).

(21) SWR indicators need not be placed at the junction of the feed line and the antenna to obtain a more accurate measurement. Within its own accuracy limits, the indicator reads the SWR wherever it is located in the line. The SWR at any other point on the line may be determined by a simple calculation involving only the SWR at the point of measurement, the line attenuation per unit length, and the distance from the measured point to the point where the SWR is desired. In any case, the primary reason for using the SWR indicator is to assist in proper loading of the transmitter.

(22) The SWR in a feed line cannot be changed, adjusted, or controlled in any practical manner by varying or adjusting the line length (*Ref 7*). *(Also see Chapter 21.)*

(23) If SWR readings change significantly when moving the SWR bridge a few feet one way or the other in the line, it indicates either "antenna" current flowing on the *outside* of the coax, or else an unreliable instrument, or both, or even a reliable bridge incorrectly adjusted to the line impedance, but it is not because the SWR is varying with line length. Some insist the bridge must be placed at a $\lambda/2$ interval from the load to obtain a correct reading. This is *incorrect*. All readings are invalid if they change significantly along the line, even though they may repeat at $\lambda/2$ intervals (*Ref 2*). *(Also see Chapter 21.)*

(24) Any reactance added to an already resonant (resistive) load of any value for the purpose of compensation to reduce the reflection on the line feeding the load will, instead, only increase or worsen the reflection. It is for this reason, although contrary to the teaching of several writers, that the lowest feedline SWR occurs at the self-resonant frequency of the radiating element it feeds, completely independent of feed-line length. Any measurements that contradict this indicate that either the measuring equipment or the technique (or both) are in error.

(25) Of the several types of dipoles such as the thin-wire, folded, fan, sleeve, trap, or coaxial, none radiates more field than another, providing each has insignificant ohmic losses and is fed the same amount of power (*Ref 3*).

(26) If coax at least the size of RG-8 is used in mobile installations (80 through 10 meters), any matching required to load the transmitter may be done at the input end of the coax without significant power loss compared to matching at the antenna terminals, and with improvement in operating bandwidth.

(27) With center-loaded mobile whips of equal size having no matching arrangement at the input terminals, the best radiating efficiency is obtained on models having the lowest measured terminal

resistance (highest resonant SWR, model for model). Models having lowest SWR are wasting power in the loading coil, because of either a low value of coil Q or excessive distributed coil capacitance, or both. *(See Chapter 6 for more details.)*

(28) The resonant frequency of an antenna cannot be determined by probing the input terminals of a feed line for resonance with a grid-dip oscillator or a noise bridge that has no capability for measuring reactance. Resonances measured at the feedline input are resonances of the combination of the antenna and the feed line, not the resonance of the antenna alone. A change in length of the feed line results in a different resonant frequency of the combination for every different length of feed line. A $\lambda/2$ feed line is not the answer, because since the resonant frequency of the antenna is unknown, the frequency at which the feed line should be $\lambda/2$ is also unknown. If the feed line is $\lambda/2$ at some frequency other than the resonant frequency of the antenna, the resonant frequency measured at the input of the feed line will be different from that of either the antenna or the feed line.

Sec 2.4 How Did You Do?

Did you mark all of the statements correctly? If you marked each one as true, then yes, *all* of the above statements are true. These examples have been centered around 80-meter operation, because bandwidth and dipole length on this band present the maximum SWR problem. Of all the amateur bands, 80 meters has the largest bandwidth: 13.3% of center frequency, as compared to 4.2% on 40 meters; 2.5% on 20 meters; 2.1% on 15 meters; and 5.9% on 10 meters. Having the longest wavelength, except for 160 meters, of course, 80 meters poses the greatest problem with respect to physical construction of radiating systems on existing real estate. Some antenna sites just won't permit an entire $\lambda/2$ on 80 meters. Thus, these examples should have a special interest if you wish to work 80 meters but are forced to use a short antenna. Since the bandwidth and antenna-length problem are really one and the same, the 80-meter examples have maximum practical value. However, practices recommended at the 80-meter level are also valid on the higher frequencies. Interestingly enough, as we go to the higher bands, the line losses increase, but the percentage bandwidth of the amateur bands decreases. This means inherently lower maximum SWR values will be obtained during frequency excursions from the design center to the ends of the band.

Chapter 3

Going Around in Circles to Get to the Point

(Adapted from QST, *August 1973)*

Sec 3.1 Basic Reflection Mechanics and Wave Propagation

In this chapter, I discuss traveling waves and their reflections on transmission lines, how they are developed, and how they both effect and affect operations on the lines. In describing the direction of wave travel, the terms "forward" and "incident" are used interchangeably.

It is well known that the size, or magnitude, of a reflection arising from a mismatched line termination is determined by the degree of the mismatch, or the amount of power in the forward, or incident, wave that is not absorbed by the load terminating the line. In this book the symbol ρ (rho) represents the *magnitude* of a reflection, called the *reflection coefficient,* which expresses the ratio of the voltage reflected by the mismatch relative to the forward voltage, the voltage incident on the load.

However, for a complete description of the reflection, in addition to its magnitude, we must also consider its *phase.* The phase of the mismatch reflection, represented by the symbol θ (theta), is the phase angle of the reflected voltage relative to that of the forward voltage at any given point on the line. In combination, the magnitude ratio ρ and phase θ comprise the *complex* reflection coefficient $\bar{\rho} = \rho\angle\theta$, which becomes important in later discussions of transmission-line wave propagation and impedance matching techniques. The complex coefficient, $\bar{\rho}$, is determined quantitatively from the line and load impedances by the expression:

$$\bar{\rho} = \frac{Z_L - Z_C}{Z_L + Z_C} \qquad \text{(Eq 3-1)}$$

where

Z_L = the complex load impedance, $R + jX$

Z_C = the characteristic impedance of the transmission line.

This expression shows that $\bar{\rho} = 0$ (no reflection) when $Z_L = Z_C$. However, for zero reflection, the load must be purely resistive ($R + j0$), because here we are considering only lossless and low-loss lines with a characteristic impedance Z_C that is real—that is, $Z_C = \text{Re}(V/I) + \text{Im}(0)$. (Re is the dissipationless, *real part,* of impedance.)

For those of you who are wondering why I use ρ instead of Γ to represent reflection coefficient, I digress here to present a note of historical significance that will answer your question. Prior to the 1950s, ρ (rho), σ (sigma), and sometimes S were used to represent standing-wave ratio. The symbol of choice to represent reflection coefficient during that era was Γ (upper case gamma). However, in 1953 the American Standards Association (now the NTIA) announced in its publication ASA Y10.9-1953 that ρ was to replace Γ as the standard symbol for reflection coefficient, with SWR to represent standing-wave ratio (for either voltage or current), and VSWR specifically for *voltage* standing-wave ratio. Most of academia responded to the change, but some individuals did not. Consequently, Γ is occasionally seen representing reflection coefficient, but rarely.

Before delving into the details of the reflection mechanics of wave reflections on transmission lines, it will be helpful to understand the mechanics if we first examine the origination of waves on transmission lines and how they travel on the line. We'll begin by introducing an AC voltage across the input terminals of the line, which sets up an electric field between the conductors of the line. Because the voltage introduced into the line is AC, the resulting electric field is constantly changing. At this point an *electromagnetic* field is developing, because a changing electric field produces a changing magnetic field. In turn, the changing magnetic field causes current flow on the conductors. The changing magnetic field also produces a changing electric field, which produces a magnetic

field, and so on indefinitely, until the voltage at the input of the line is cut off. However, with the continuing alternate production of the electric and magnetic fields a series of energy transfers is started. The magnetic energy does not appear at precisely the same point on the line as the electric energy from which it is derived, but a little beyond, and then the succeeding electric energy is formed still a little farther down the line, so that as the energy is changing from form to form it is also being propagated along the line. The result is a traveling wave of electromagnetic energy propagating along the line. It is therefore evident that if there is a changing electric field, there must also be a changing magnetic field. Thus the name *electromagnetic* field: If it exists, it must contain both electric and magnetic fields simultaneously.

To digress from the discussion of propagation on transmission lines for a moment, it is also of interest to know that the same phenomenon occurs in space as just described for the transmission line. The electromagnetic field radiated from an antenna propagates through space in precisely the same manner. Although we didn't discuss it above, it should be known that the electric and magnetic fields are always at right angles or perpendicular to each other, and in directions that are also perpendicular to the direction of the wave travel. This geometric relationship holds true for the propagation in transmission lines, as well as in space. Consequently, we can define polarization of the electromagnetic field. It is universally accepted that the polarization is determined by the orientation of the *electric* field. When the electric field is vertical, the polarization is said to be vertical, and when the electric field is horizontal, the polarization is horizontal. Therefore, you know that when your antenna elements are oriented in the horizontal position, and receiving the maximum signal with respect to orientation of the elements, the incoming wave is horizontally polarized, and the magnetic field is vertical.

We are now ready to return to the discussion of reflections and reflection coefficients. We begin by first describing the nature of reflections, and how they are produced. An open circuit (an infinite impedance), a short circuit (zero impedance), or a pure reactance terminating a transmission line is incapable of absorbing any power from a forward wave, and therefore causes total reflection of the energy in the forward waves of both voltage and current. The magnitude ρ of the reflection coefficient at such a load impedance is therefore 1.0 (unity) for both voltage and current.

The step-by-step process by which the reflections arise on lossless and low-loss transmission lines, both coaxial and open-wire, is as follows, beginning with the manner in which waves of voltage and current on transmission lines are formed initially. If a sinusoidal alternating voltage is applied across the input terminals of a transmission line, a forward-traveling voltage wave is launched into the line traveling toward the load. Simultaneously, a forward-traveling current wave is launched into the line, accompanying the voltage wave in its travel toward the load. Together, the voltage and current waves develop a forward-traveling electromagnetic field comprising an electric field and a magnetic field. One-half of the energy in the electromagnetic field is stored in the electric field because of forward voltage, and the other half is stored in the magnetic field because of forward current. The input impedance that the electromagnetic field encounters as it leaves the generator in its forward travel down the transmission line is the *surge* impedance of the line, also known as the *characteristic* impedance, Z_C. In ideal lossless lines the voltage and current travel in perfect phase with each other because the characteristic impedance Z_C is real, since $Z_C = \mathrm{Re}(V/I) + \mathrm{Im}(0)$, as stated earlier. However, in real lines of low loss, such as those generally used in amateur and commercial RF practice, there is a small negative reactance (capacitive, $-X_C$) in the characteristic impedance, but it is so small that it can usually be neglected. Therefore, the voltage and current in real lines are essentially in phase during travel along the line. On the other hand, the capacitive reactance appearing in lossy lines cannot be neglected, and must be taken into consideration when lossy lines are used in engineering applications.

Now we'll proceed to the generation of reflections. When the electromagnetic field reaches the end of the line, if the load terminating the line is an open circuit, the magnetic field collapses because the current goes to zero due to the infinite impedance of the open circuit. The changing magnetic field at the open circuit produces a new electric field equal in energy to the magnetic field, which

induces a new voltage into the load circuit that is equal to, and in phase with, the voltage in the forward wave. (Keep in mind that a voltage is induced, or generated, by mutual motion between a magnetic field and a conductor, a phenomenon generally known as *motor-generator action*. Thus, it can be said that the reflected voltage was developed and delivered by a generator, a *reflection generator*. Although in this case the *field* is changing while the conductor is stationary, as in a transformer, it is motor-generator action nonetheless.) The new electric field induced by the changing magnetic field adds *in phase* to the existing electric field, and the new induced voltage (delivered by the reflection generator) adds *in phase* to the voltage in the forward wave, resulting in an increase of voltage at the open circuit to twice the voltage of the forward wave. At this instant, a standing wave is developing, because now there is a current minimum and a voltage maximum at the open-circuit termination, where an instant before, current and voltage were constant all along the line.

The new voltage at the open-circuit termination, along with its new electric field, starts a voltage wave traveling in the rearward direction, as if it had been launched by a *separate generator* at the open-circuit point. (It has. Remember the induced voltage *generated* by the changing magnetic field?) Since no energy was absorbed by the open-circuit load, the new rearward-traveling voltage wave has the same magnitude as the original forward wave, which is why $\rho = 1$, indicating total reflection. As the new electric field starts its rearward travel, it produces a new magnetic field, which in turn produces a new current, launched into the line as the reflected current wave with the same magnitude as the forward current wave, but with opposite polarity and direction. The new electric and magnetic fields combine to form the reflected electromagnetic field and, as in the forward electromagnetic-field wave, the energy in the reflected electromagnetic-field wave also divides equally between its electric and magnetic fields. (*Ref 17, Ref 19, Ref 35, Ref 43, Ref 70*)

To continue, the total voltage (or current) at the load at any instant is the sum of the voltages (or currents) of the forward and reflected waves. The in-phase reflected voltage wave is verified because the sum of the two voltages at the load is equal to two times that of the forward voltage. In addition, since the two current waves of opposite polarity add to zero at the open-circuit load, the generation of the reversed-polarity, out-of-phase reflected-current wave is also verified. The phase angles, θ, of the reflection coefficients at the open-circuit load are therefore 0° for voltage and 180° for current.

When the load impedance is a short circuit, the reflection-generation process is the same as the open-circuit process described above, except that the electric- and magnetic-field actions and the polarities of the reflected-wave components are reversed. This is expected when we recall that while current goes to zero in an open circuit, voltage must be zero in a short circuit. For the voltage to be zero, the forward and reflected voltages must cancel one another at the load, thus verifying the reversed polarity of the reflected voltage with the short-circuit termination. The corresponding currents are of the same polarity, and add at the short-circuit load to equal twice the forward value, as the voltages did when the load was an open circuit. The phase angles θ of the reflection coefficients at the short-circuit load are therefore 180° for voltage and 0° for current. When the load impedance is a pure capacitance, it is equivalent to an additional length of open-circuited line, while a purely inductive load is equivalent to an additional length of short-circuited line.

We have observed that on reflection at a mismatched load termination, either the voltage *or* the current changes polarity, *but not both.* Repeating for emphasis and clarity, when the load is an open circuit the current changes polarity, but not the voltage; when the load is a short circuit the voltage changes polarity, but not the current. Hence, it is evident that while the forward voltage and current travel in phase, the reflected voltage and current are 180° out of phase, and maintain that phase relationship during their entire rearward travel on the line.

When the load impedance contains resistance that is not equal to the characteristic impedance Z_C, the reflection is generated in the same manner as with infinite- or zero-impedance loads described earlier, except that the reflection is less than total, the magnitude depending on the amount of power absorbed in the resistance. The reflected wave is again generated by the changing electric and magnetic fields in the mismatched resistance due to the

change in voltage and current when the forward wave encounters a change in impedance relative to the characteristic impedance Z_C of the transmission line. Hence, the reflection coefficient ρ is dependent on the difference between the forward-wave voltage on the line and the resulting voltage appearing across the load. If the load contains no reactance, and its resistance is greater than Z_C, the reflection angles θ are the same as for the open-circuit termination; if the load resistance is less than Z_C, the θ angles are the same as for the short-circuit termination.

No reflection arises when the load is a pure resistance equal to Z_C, because all of the forward-traveling energy is absorbed in the load, and because there is no variation in voltage or current when the energy passes from the line to the load. Thus, there is no change in the electric and magnetic fields, no new voltage or current generated, and hence no reflected wave.

Returning now to the wave action on the line, after being launched rearward the reflected wave travels back up the line as a new electromagnetic traveling wave, separate and distinct from the forward-traveling incident wave. As the reflected wave travels rearward, it encounters only the same real line impedance Z_C encountered by the forward wave in its forward travel to the load. Hence, the magnitudes of both the reflected voltage and current waves remain constant as they plow rearward, retaining the same values as when leaving the reflection generator. (This is exactly true only on lossless lines. However, there is a *gradual* reduction in magnitudes with line length in real lines due to line attenuation, as discussed later.) The magnitudes of the reflected waves are completely unaffected by the standing wave that is developing as the reflected and forward waves slide past one another traveling in opposite directions. The forward voltage and current waves are similarly unaffected, continuing in their forward travel with constant magnitude until reaching the load. Also, as in the forward wave, both the reflected voltage and reflected current pass through zero simultaneously (twice per cycle) and reach their maximum values one-quarter cycle later, because the line impedance Z_C is real.

Thus, you now ask, are not the reflected voltage and current then also in phase with each other, like the forward voltage and current? *No!* As explained earlier, only the voltage *or* the current changes polarity during reflection, *but not both,* so they cannot be in phase. In fact, the maximum of the reflected voltage is positive when the maximum of the reflected current is negative, and vice versa, which means, as stated earlier, the reflected voltage and current are *always* 180° out of phase with each other. However, does the phase really matter here? *Indeed it does: There is no other relationship more important to wave propagation on a transmission line! The 180° out-of-phase relationship between the reflected voltage and current is directly responsible for the development of the standing wave, and for the change in the input impedance of the transmission line from Zc to a complex value when the load terminating the line is mismatched.*

To continue, although the forward and reflected waves travel separately in opposite directions, they are inescapably related to each other through their common line and load characteristics. Their respective voltages and currents add vectorially at every point along the line, forming the standing waves as the two waves slide past each other. In other words, the phasor sum of the forward and reflected voltages (or currents) at every point along the line produces the amplitude of their respective standing wave at each corresponding point on the line. In addition, the amplitude and angle of the resultant phasor voltage divided by the corresponding resultant phasor current determines the complex line impedance at each corresponding point on the line. Hence, the polarity relationships between the voltages and currents in the forward and reflected waves determine both the characteristics of the standing wave and the line impedance appearing at every point along the line, including the impedance appearing at the input terminals. We will explore the development of the standing wave in more detail later in this chapter, and again from a different viewpoint in Chapter 9.

Sec 3.2 Wave-Travel Analysis

Some people have difficulty in understanding the polarity relationships between voltage and current waves on transmission lines, so now let's examine polarity and the establishment of a polarity reference for convenience. Let us consider a single wave traveling on a two-conductor line. By follow-

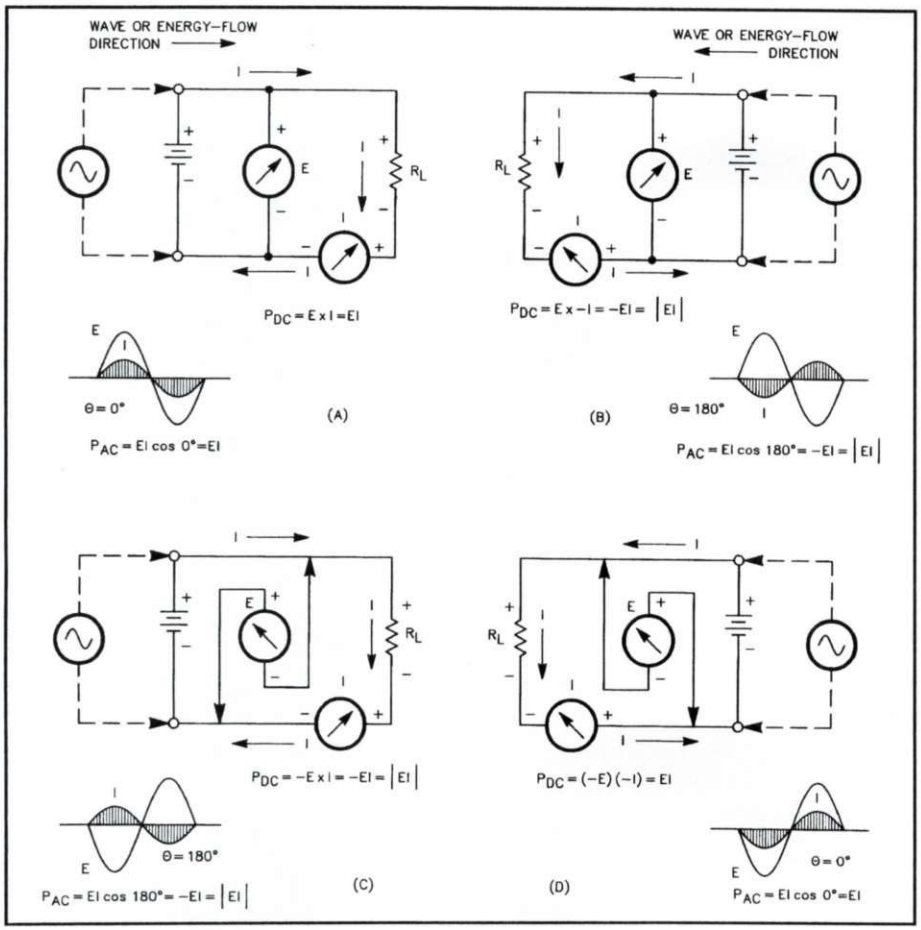

Fig 3-1. Illustrating relationships between current and various combinations of voltage reference and energy-flow direction.

ing conventional current flow we can select the appropriate conductor as the voltage-polarity reference for a given direction of wave travel which causes the voltage and current maxima to occur with the same polarity. This polarity relationship may be reversed simply, either by selecting the opposite conductor for the voltage reference or by reversing the direction of wave travel. Obtaining the opposite polarity or phase relationship by reversing the conductors is a simple enough concept, but obtaining it by reversing the wave-travel direction has been a point of confusion for many people.

To reduce the confusion, a set of simple current-flow diagrams showing both AC and DC treatment is presented in Fig 3-1. Use of DC with zero-center meters as indicators makes the explanation of polarity easy. Conventional needle movement is to the left for negative polarity and to the right for positive. Once polarity is clear, the battery may be replaced with an AC generator, and phase will also become clear using the waveforms as indicators. The circuits in A and B of Fig 3-1 are the same as in C and D, respectively, except that the voltmeter terminals have been reversed. Observe that the wave or energy-flow direction and voltage-polarity reference selected in A cause line voltage and current flow to be in the same polarity. Now notice that reversing either the wave direction (as in B) or the voltage reference (as in C) both result in *opposite* voltage and current polarities, as stated previously. Observe also that reversing both direction and voltmeter reference polarity (as in D) again results in line voltage and current flow with the same relative polarity, although reversed from A. It may be helpful at this point to perceive that changing the wave or energy-flow direction is equivalent to reversing the terminal connections of the current meter, because the source changes sides. This is the key to understanding the polarity-reversal problem, because for a given voltage-polarity reference, the current-flow direction must reverse when the wave-flow direction reverses.

Based on these conditions, assume a generator is now placed at each end of a single two-conductor

transmission line. Then, a reference that is selected to make the voltage and current in phase on the line for one generator will result in 180° out-of-phase voltage and current for the other generator. This is the situation that exists with the mismatched RF transmission line—a source generator at one end of the line and the reflection generator at the other end. By selecting the conventional reference that makes forward voltage and current in phase with each other, it verifies that reflected voltage and current are 180° out of phase with each other (*Ref 35*).

It is of interest at this point to be concerned with the nature of the power in the forward and reflected waves. Some writers contend erroneously that the voltage-current phase relationship in the reflected wave is 90°. If this were true, then the reflected wave would contain only reactive volt-amperes and no real power. The evidence presented above disproves this contention, since we have seen that the voltage-current phase relationship in the reflected wave is 180°, not 90°. Moreover, we will certainly agree that if real power is conveyed in A of Fig 3-1, it is also real power in B, or C, even with reversed current-meter or voltmeter terminals. We will agree that *real* power P equals EI cosine θ, in which cosine is the power factor. It matters not whether the phase angle is 0° or 180°, because cos 0° = 1, and cos 180° = –1. This simply denotes the polarity difference discussed above.

When conductor spacing in a transmission line is restricted to the near field—i.e., a spacing that is a very small fraction of a wavelength—the fundamental principles governing transmission-line propagation are the same as those which govern all general AC circuit relationships, including electric power transmission. From these principles we know that real power flows for all values of θ in all four quadrants, except when θ is 90° or 270°, where cosine θ is zero, yielding zero power factor. However, whenever phase θ is other than 0°, 90°, 180°, or 270°, both real power and reactive volt-amperes are present. Nevertheless, at 0° or 180°, only real power exists because the absolute value of the power factor is 1.0 in either case. This clearly proves that reflected power and forward power in a transmission line are both *real* power, and that no fictitious power, or reactive volt-amperes, exists in either one. This is indeed true because, as I have shown earlier, the voltage and current in the forward wave are always in phase, and the voltage and current in the reflected wave are always 180°, out of phase.

The misunderstanding concerning *real*-versus-*reactive* power in the reflected wave arises in part from confusion between traveling and standing waves, because of insufficient familiarity with both types. To broaden the familiarity, I have concentrated first on the *traveling* waves. From the physical viewpoint, as stated earlier, standing waves are derived from the resultant interaction between the forward and reflected traveling waves. Thus, sufficient knowledge of traveling waves is essential before one can correctly understand the formation of standing waves and other correlated phenomena occurring on the transmission line. These other phenomena will become apparent as we proceed.

Now that you have a reasonably enlightened background concerning the ingredients of standing waves, we'll begin exploring the details of their development. Then it will be appropriate to return to the real-versus-reactive power misunderstanding for a few brief comments to clear away any remaining confusion.

Sec 3.3 Vector Graph Explanation and Standing-Wave Development

The newly launched reflected voltage and current waves, in their rearward travel toward the generator, add vectorially to their respective forward waves at every point on the line, with the result that their continuously changing relative phase differences along the line cause alternate cancellation and reinforcement of the voltage and current distribution on the line. This addition produces a continuous variation in the resultant voltage E and current I on the line that results in the formation of the standing wave and a change in the input terminal impedance, Z_{IN}, from the initial value of the line characteristic impedance, Z_C.

A physical picture of this complex relationship enhances the understanding of the phenomenon. Accordingly, the W2DU Vector Graph of Fig 3-2 graphically illustrates the progressive phase relationships between the forward and reflected voltages and currents as they travel in their respective directions along the line. Circular insets at every 22.5 (λ/16) along the line show accurately scaled phasor diagrams for visual comparison of the

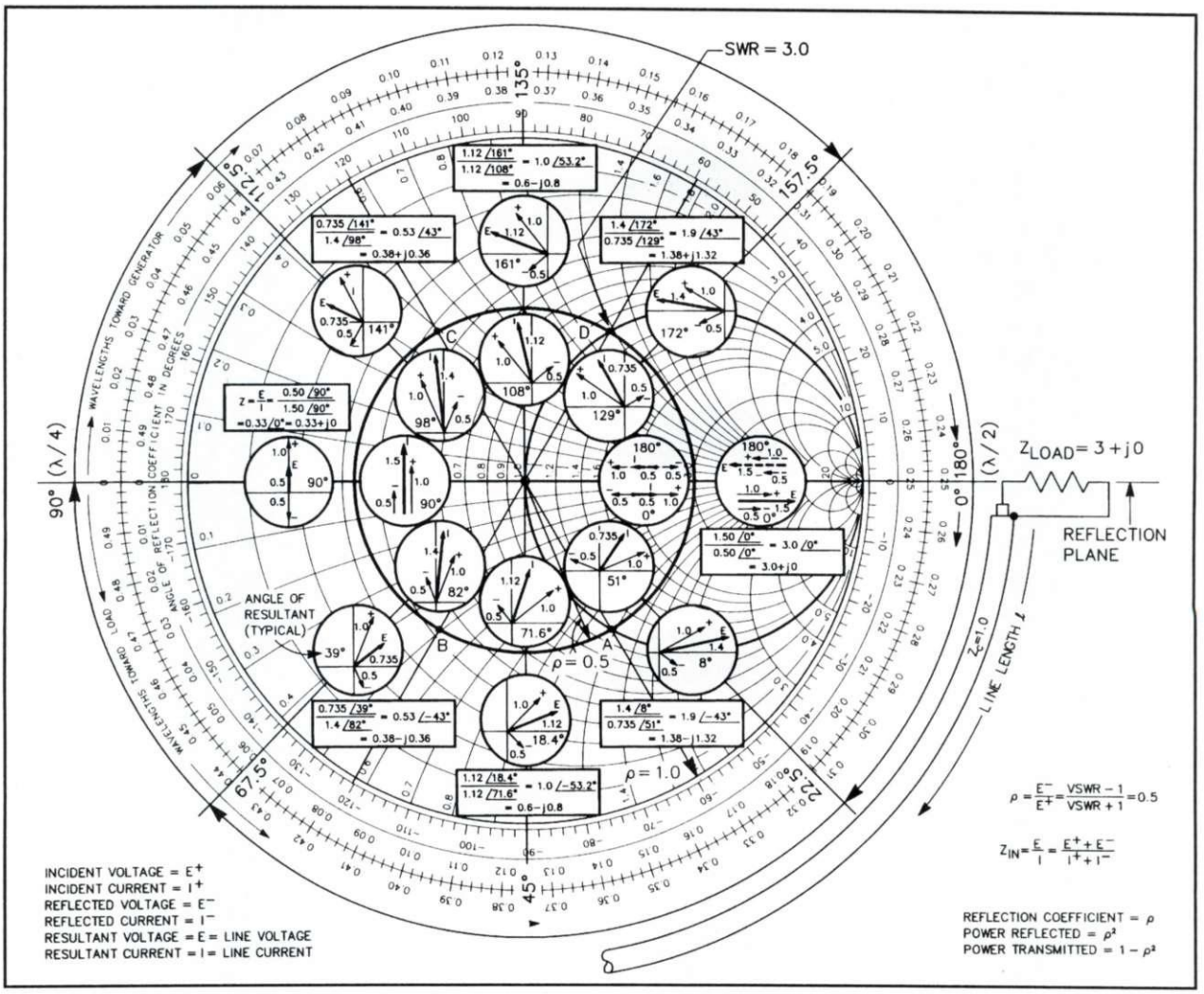

Fig 3-2. The W2DU Reflection Mechanics Vector Graph. (For an enlarged version see the back of the book.)

amplitude and angles of the forward and reflected waves relative to their position along the line. The reference for the angular distance along the line begins at the load termination point (the reflection plane where length $\ell° = 0°$, drawn at the right), with angular movement progressing clockwise toward the generator. These phasor diagrams superimposed circularly around the Smith Chart present certain symmetrical voltage-current phase-angle relationships with respect to line length, or distance from the load, which are not obvious in previously published displays (*Ref 2, p 72*; *Ref 17, p 146*; *Ref 18, p 110*). In addition to providing a new way to show the formation of the standing wave, Fig 3-2 provides a new visual basis to explain many other aspects of transmission-line operation, such as the development of capacitive and inductive components of complex impedance, the understanding of λ/4 impedance inverting action, the impedance-repeating phase-inverting action of the λ/2 line, and the reciprocal relationship between impedance and admittance.

For this illustration we are letting the line impedance Zc = 1.0, which is the basis for handling normalized impedances on the Smith Chart, and we have terminated the line with a pure resistance of 3 ohms, three times the line impedance Zc. Hence, a circle representing an SWR of 3.0 is shown. The line length $\ell°$ is measured from 0° at the reflection plane, and is represented by clockwise rotation around the chart.

Phasors representing voltage are displayed in the insets outside the 3:1 SWR circle. Phasors marked "+" represent incident, or forward, voltage (ampli-

tude = 1.0), phasors marked "–" represent reflected voltage (amplitude = 0.5), and phasors marked "E" represent the resultants of the forward and reflected phasors, both as to length and angle at the corresponding points on the line. (The resultant voltage, E, is also the *line voltage* appearing at the corresponding points. The corresponding current phasors appear in the insets directly opposite and inside the SWR circle. The resultant phasors marked "I" represent *line current*. The number in degrees shown with each phasor set indicates the angle of the resultant in that set. The phasor lengths are proportional to the amplitudes of their respective voltages and currents at each point along the line. By setting the lengths of the forward phasors equal to 1.0, the length of the reflected phasors inherently indicates the amplitude of the reflection coefficient, ρ. Hence, the lengths of the reflected voltage and current phasors in this example are 0.5 because ρ = 0.5 for an SWR of 3.0 from the relationship:

$$\rho = \frac{SWR - 1}{SWR + 1} \qquad \text{(Eq 3-2)}$$

While the phasor lengths are proportional to each other, the lengths are not scaled to the chart dimensions. However, the various phasor diagrams on the graph contain the necessary amplitude and phase information to define both the standing wave and the impedance at each corresponding point on the transmission line.

The SWR = 3.0 (or ρ = 0.5) circle is based on the chart scales and may be observed to have a radius of one-half the chart radius. The perimeter of the chart has a radius of 1.0, representing total reflection—that is, an infinite SWR. The radius of the ρ circle is thus directly proportional to the reflection coefficient, ρ. Thus, an SWR or ρ circle may be constructed for any value of reflection by making the radius equal to either SWR or ρ.

To make valid phase comparisons between various points on the line, wave motion has been frozen at an arbitrary point in time so that all phasors are shown in their true position relative to each other. It makes no difference when the motion is stopped, but the symmetry of the presentation is enhanced by stopping the motion when the forward phasors at the reflection plane (where $\ell^\circ = 0^\circ$) are pointing in the zero direction in the standard polar coordinate system (to the right).

Observe that at any point on the line, the phasors representing forward voltage and current are always pointing in the same direction, indicating that they are in phase. In contrast, observe that the phasors representing reflected voltage and current are always pointing in opposite directions, indicating that they are always 180° out of phase, as explained previously. Also observe that at the reflection plane, where $\ell^\circ = 0^\circ$, all components are in phase except the reflected current, which is 180° out of phase from all of the others. This is as it should be when the terminal impedance lies between Zc and an open circuit. These phasor relationships graphically illustrate the concluding comments of Sec 3.2.

With clockwise travel from the reflection plane toward the generator, observe that each forward and each reflected phasor rotates the same number of degrees as those in the angular change in position along the line. However, note the following statement carefully, because it is a crucial element in understanding the mechanics of wave travel on mismatched transmission lines: *The forward-wave phasors (+) rotate counterclockwise (phase leading), while the reflected-wave phasors (–) rotate clockwise (phase lagging).* For example, at 45° from the reflection plane, the forward-voltage phasor is at +45°, while the reflected-voltage phasor is at –45°, for a total phase difference of 90°. *Thus, for every degree of motion along the line, the relative phase angle between the forward and reflected voltage changes two degrees.* (The relative phase angle between the forward and reflected voltage is θ, which determines the *angle* of the reflection coefficient. Also observe on the graph that the degree scale labeled "Angle of Reflection Coefficient" increases at twice the rate of that of the line-length scale, ℓ°.) This phenomenon becomes clear when you consider that in the distance from the reflection plane to our observation point at 45° along the line from the termination, the reflected wave has traveled twice as far as the forward wave. From the observation point, the forward wave travels only to the reflection plane, while the portion of the forward wave that is reflected travels an equal additional distance in returning to the observation point.

Now let's see what happens in traveling 90°, or λ/4 from the load toward the generator. Beginning at the load, where $\ell^\circ = 0^\circ$, we see that the forward

and reflected phasor voltages (1.0 and 0.5, respectively) are exactly in phase with each other and adding, yielding the reinforcement mentioned earlier, indicated by the resultant E phasor length of 1.5. However, at the point 90° toward the generator, the forward and reflected voltage phasors have each rotated 90° in opposite directions, so they are now 180° out of phase and canceling, or subtracting, with the resultant E phasor length of 0.5.

Continuing on to $\ell° = 180°$, or $\lambda/2$ from the load, we see that both voltage phasors have now rotated 180°, having continued rotating in opposite directions. Hence the forward and reflected phasors have rotated 360° relative to each other, and are again exactly *in phase with each other*, and reinforcing to 1.5 volts, *but note that all phasors are 180° out of phase with those at the starting point at* $\ell° = 0°$. Consequently, the *dashed* phasor lines appearing at $\ell° = 0°$ (really $\ell° = 180°$) indicate the phasor angles that occur 180° from the load relative to those at the load, clearly illustrating the impedance-repeating, phase-inverting properties of half-wavelength ($\lambda/2$) transmission lines.

However, at all points between $\ell° = 0°$ and $\ell° = 90°$, the resultant voltage phasor, E, is seen to diminish gradually from the maximum of 1.5 at $\ell° = 0°$, to the minimum of 0.5 at $\ell° = 90°$, and then increase back to the 1.5 maximum at $\ell° = 180°$. In Fig 3-3, the values of these resultant phasor amplitudes at each 22.5° point along the line have been plotted on the more familiar rectangular coordinate graph. The smooth curves connecting the plotted amplitude values generate the familiar standing-wave patterns of voltage and current. The curves verify the relationship:

$$\text{SWR} = \frac{1 + \rho}{1 - \rho} = 3.0 \qquad \text{(Eq 3-3)}$$

which is the algebraic expression for the addition and subtraction of the forward and reflected voltage phasors explained above. With $\rho = 0.5$, the E and I curves of Fig 3-3 show how adding ρ to the forward voltage of 1.0 at $\ell° = 0°$, and then subtracting it at $\ell° = 90°$ generates the 3:1 SWR curves of voltage and current. Also bear in mind that the amplitudes at any given point of the SWR curves of voltage and current indicate the *line voltage* and *line current*, respectively, at the corresponding points on the transmission line.

Line lengths greater than $\lambda/2$ (180°) are accommodated simply by continuing on around the Vector Graph circle again (Fig 3-2), repeating the same values encountered 180° earlier, and thus establishing the periodicity of the standing wave. Only lossless line is being considered here; correction factors for attenuation, which change the SWR circle into an inward spiral, are presented later. The basis for the phase- or polarity-reversing characteristic of the half-wave, or 180°, line may be observed on the Vector Graph: Note again that the specific phase of the voltage phasors at the $\ell° = 180°$ point on the line is 180° from their phase orientation at the reflection plane, at $\ell° = 0°$.

The significance of the constant 180° phase difference between the reflected voltage and current emerges if we now compare the phase and amplitude of the current phasors with that of the voltage phasors just discussed. We see that at the reflection plane $\ell° = 0°$, where the forward and reflected voltage waves are in phase and adding to create a voltage maximum, the corresponding currents are out of phase and opposing to create a current minimum. Also, at $\ell° = 90°$, where the voltage waves are out of phase and opposing, resulting in a minimum, and the currents are *in phase*, resulting in a maximum. This is the reason, illustrated graphically, why *the maxima and minima of the voltage standing wave are always separated by 90° from the corresponding maxima and minima of the current standing wave*. This phenomenon is caused specifically by the constant 180° phase difference between the reflected voltage and current, as stated earlier and as shown here on the phasor display.

You can make a visual comparison of the voltage and current phasor resultants in Fig 3-2 (both angular positions and amplitudes) with the corresponding positions along the plot of Fig 3-3. This comparison should enhance your understanding of the important concept of a 180° voltage-current phase difference in the development of the standing wave. The concept is of further importance because, as we proceed, you'll see that this phase difference is the basis for the impedance-transforming properties of the transmission line, including the $\lambda/4$ and $\lambda/2$ sections (which are only two specific conditions of the general case).

As we discuss the concept of impedance in Chapter 4 and later solve matching problems, try to

Fig 3-3. Illustrating how the voltage and current standing waves relate to the magnitude of the reflection coefficient.

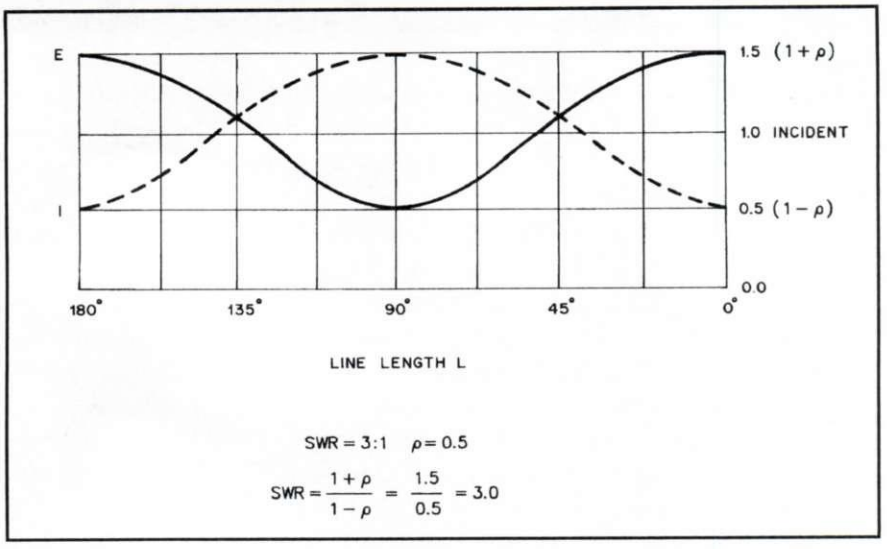

conjure up a mental image of the action occurring on the line. At times, this will be more helpful in understanding the difficult concepts than through logical reasoning alone. It is especially important to have a clear image of the formation of the reflected wave. Remember that the reflected wave must be considered as a *separate traveling wave.* It is identical to the forward wave except for the *direction* of travel and, usually, the magnitude. This point is important, because it helps us keep in mind that the reflected voltage and current waves travel the line 180° (not 90°) out of phase with each other, and thus transfer real voltage and current, and real power during their travel. It is essential to the process of reinforcement and cancellation of voltage and current along the line in the formation of the standing wave that *real power* be conveyed in the reflected wave, as if it had been developed by a separate source of power at the load end of the line. It will also become clear in the chapter to follow why the impedance along a line changes in the presence of reflections because ***real power*** *is flowing in* ***both*** *directions on the line* (*Ref 2*, *Ref 35*, *Ref 42*).

I stress this point because, as mentioned previously, some writers have presented the erroneous viewpoint that the reflected wave conveys no real power, with the argument that the reflected voltage and current are 90° out of phase with each other and are therefore wattless. The reflected wave would indeed convey zero power if its voltage and current really were 90° out of phase, but the argument is incorrect, because, as explained previously and shown in the Vector Graph, they actually travel 180° out of phase. At least three writers, Woods (*Refs 67* and *97*), DeLaMatyr (*Ref 98*), and Drumeller (*Ref 68*) would have us believe otherwise. It is easy to reach the wrong conclusion, however, because of the lack of a clear image of the reflection process and the somewhat complicated wave mechanics on the line. Woods and Drumeller apparently have confused the *reflected wave* with the *standing wave*, while all three writers have apparently confused *reflected* voltage E^- and *reflected* current I^- with *line* voltage E and *line* current I. Drumeller says, ". . . application of logic has demonstrated that reflected power is a vicious fiction." Unfortunately, Drumeller's logic is flawed, because, as explained in detail earlier, we know that reflected power is indeed *real, not fictional.* The true nature of the reflected wave as a separate electromagnetic traveling wave must be appreciated. It is also interesting to note that Woods states, ". . . re-reflection of power at the input end (of the line) is impossible to accept since the necessary conditions of impedance mismatch are not present." However, his Fig 2 shows a circuit which, when properly tuned to resonance as in all pi-network coupling circuitry, forms a conjugate impedance-matching network that *totally re-reflects all reflected power reaching it.* (There will be much more discussion in later chapters concerning the action of conjugate matching in relation to re-reflection of reflected power that reaches the pi-network.) This is also true in his Fig 1, since he implies that his final amplifier is loaded and tuned properly. Now the very essence of this impedance-

matching network is its totally reflecting mismatch for reflected waves traveling toward the generator, while presenting a perfect match for forward waves traveling toward the load. Misunderstanding of this important basic concept is widespread among us amateur radio operators. This concept is basic to the operation of the pi-network for matching the output load impedance Z_L of the RF amplifier to its source impedance Z_S. The mechanism behind its operation involves wave interference and reflections, which are described in detail in Chapter 4, again using the Vector Graph as a visual aid, and again, from a different viewpoint, in Chapter 19, and from still another viewpoint in Chapter 23.

Mistaking the 180° difference in phase between the reflected voltage and current for the *90° difference of position on the line* that exists between the voltage and current maxima (or minima) of the standing wave (described a few paragraphs earlier and shown in Fig 3-3) is understandable. Also, the similarity between *line* voltage and *line* current behavior with the voltage-current relationship in conventional AC circuitry also makes it easy to understand why line voltage E and current I are being confused with reflected voltage E^- and current I^-. This is because, in addition to the in-phase line voltage and current components, which convey only the net power flow, line voltage and current do contain reactive components which are out of phase with each other when reflections exist on the line. Obviously, these reactive components convey no real power. Unfortunately, some people who are well versed in AC circuitry using lumped constants, but who are less familiar with the principles of transmission lines, sometimes make the error of assuming that the two circuit types are identical in electrical performance. Hence, we should be wary of making unwarranted comparisons that can bring about disastrous consequences of the type we are attempting to straighten out here.

Another erroneous argument set forth is that reflected power cannot be real power because it cannot perform work. I'll prove this argument false by showing how power in the reflected wave *does do work.* Now a simple RF voltmeter connected across the line indicates the line voltage at that point, and an RF ammeter in the line at the same point indicates the line current at that point. As stated earlier, line voltage and current are the *resultants* of the combined forward and reflected waves (E and I on the Vector Graph), the product of which, when multiplied by the cosine of the phase angle between them, yields only the net power that is absorbed by the load. Nevertheless, there are several devices in common everyday use that selectively extract either the reflected or the forward wave from the line, independent of the standing wave. These devices permit separate measurement of the power associated with the waves traveling in either direction. One such device is the directional coupler. Another is the circulator. The circulator is a three-port directional device using port one as the input port. The wave reflected from a mismatched load that terminates port two is completely diverted away from the input feed line, and emerges only from port three. The reflected wave cannot get back onto the feed line to interact with the forward wave to develop a standing wave, or to change the line-input impedance at the source feeding port one. However, current flow through a matched resistor terminating port three develops I^2R heat equal to the amount of power reflected from the mismatched load that terminates port two.

A four-port hybrid coupler can be connected to perform in the same manner as the circulator. Directional RF devices most familiar to amateurs are the simple reflectometer SWR indicator and the directional wattmeter (*Ref 18, p 188,* and *Refs 38, 40, and 42*). The meter in either instrument is actuated by RF power absorbed from one of the traveling waves on the line—either the forward wave or the reflected wave, as selected. If the reflected wave were wattless reactive power, no power would be available to actuate the meter movement in SWR indicators, or to produce heat from the current flow in the resistor on port three of the circulator. Furthermore, for power to become wattless on being reflected would violate the most general and fundamental of all physical laws, namely the law of conservation of energy (*Ref 35, p 25*). Based on this law, if all the energy flowing in the line toward the load cannot be absorbed in or dissipated by the load, then that portion of the energy that is not absorbed must appear somewhere else. It cannot just disappear or cease to exist as if by magic. The reflected power recovered as heat in the resistance terminating the circulator is a typical

proof of this fact, which is also proof that *reflected power is real power.*

Here is another way to express net power flow through a transmission line, one that enables us to break down power into its separate forward and reflected components. The final expression is obtained from the transmission-line power equations found in many engineering textbooks on transmission lines. The equations that follow are quoted from Johnson (*Ref 18*).

$$\text{Power} = P = E \times I \qquad \text{(Eq 3-4)}$$

$$P = \frac{E^2}{Z} \qquad \text{(Eq 3-5)}$$

On RF lines,

$$P = E_{MAX} \times I_{MIN} \qquad \text{(Eq 3-6)}$$

and

$$P = \frac{E_{MAX} \times I_{MIN}}{Z_C} \qquad \text{(Eq 3-7)}$$

Now E_{MAX}, produced by $E^+ + E^-$,occurs as shown in Fig 3-2, where the forward and reflected voltages are in phase at $\ell^\circ = 0^\circ$ and 180°, and E_{MIN}, produced by $E^+ - E^-$, where they are 180° out of phase, $\lambda/4$ away at $\ell^\circ = 90^\circ$. Later we shall see that both the resultant voltage E and resultant current I are non-reactive at these points on the line, while being reactive everywhere else along the line between these points. However, because E_{MAX} and E_{MIN} are also non-reactive at these points on the line, respectively, the product of these voltages divided by the line impedance, Z_C, *yields the net power flow, exactly,* as expressed in (Eq 3-7)**.** But recalling that E^+ and E^- are always non-reactive, we can replace the term E_{MAX} with $E^+ + E^-$, and the term E_{MIN} with $E^+ - E^-$ and thus:

$$P = \frac{E_{MAX} \times E_{MIN}}{Z_C} = \frac{(|E^+| + |E^-|) \times (|E^+| - |E^-|)}{Z_C} \qquad \text{(Eq 3-8)}$$

Multiplying out the numerator terms gives the separate desired forward and reflected components of power.

$$P = \frac{|E^+|^2}{Z_C} - \frac{|E^-|^2}{Z_C} = \text{net power flow} \qquad \text{(Eq 3-9)}$$

The first term on the right of the equal sign in Eq 3-9 expresses the power associated with the forward wave and the second term expresses the reflected power. This simple separation of power into two components, each associated with one of the traveling waves, can be performed on a lossless or low-loss line, where the characteristic impedance Z_C is real. However, if the line has appreciable loss, the interaction of the two waves gives rise to a third component of power, which we need not consider, because lines normally used by amateurs are generally in the low-loss category (*Ref 18, p 150*; *Ref 37, p 129).*

This separability of the forward and reflected powers forms the physical basis for the operation of reflectometers and directional wattmeters. These devices sense either the forward or reflected component by taking advantage of the 180° out-of-phase relationship of the reflected voltage and current, while the forward voltage and current are in phase with each other.

Bruene's published explanation of directional wattmeter operation is a classic paper (*Ref 38*). In these instruments, a sample of the voltage across the line is added to a sample of voltage derived from the current in the line. When the voltage and current samples are adjusted to the correct amplitude relationship determined by line impedance Z_C, the difference between the two samples derived from the reflected wave cancel, while the sum of the samples represents only the voltage of the *forward* wave. However, by reversing the polarity of either the voltage sample or the current sample, the difference between the two samples now derived from the forward wave cancel, while the sum of the samples represents only the voltage of the *reflected* wave. The scale of a meter connected to indicate these voltage sums can now be calibrated in *power*, because the voltage squared is proportional to power. The reversal of the polarity of the voltage or current samples is accomplished in SWR indicators simply by changing the position of the Forward-Reflected switch.

It is also important to note that *the meter-needle movement in simple SWR indicators is directly proportional to the voltage reflection coefficient.* In other words, *the SWR indicator measures the reflection coefficient, not SWR,* but the meter scale is graduated to convert reflection coefficient to

SWR. The scale conversion is derived from the mathematical expression, presented earlier:

$$SWR = \frac{1 + \rho}{1 - \rho} \qquad \text{(Eq 3-2)}$$

This scale calibration can be verified by first adjusting for a full-scale reading in the forward-power position, and then switching to the reflected-power position with a 3:1 SWR on the line. Because a 3:1 SWR results in the reflection coefficient $\rho = 0.5$, it indicates that the voltage of the reflected wave is half that of the forward voltage. Under these conditions, as in our previous example, the needle of the SWR meter will point to *exactly half scale*, but the reading at the half-scale point on the SWR meter is "3." Check your own SWR indicator. I'm betting the "3" is at half scale on *your* meter!

The marvelous feature of the directional wattmeter is that, when properly calibrated, it indicates the *true power* in the transmission line regardless of the impedance of the load terminating the line; the load can be either an impedance match or a mismatch, and it can be either reactive or non-reactive. The meter achieves this because the forward power is equal to the sum of the line-input power and the reflected power. Hence, in the forward-power position, the meter indicates the *total* power that is incident on the load. In the reflected-power position the meter indicates the amount of the forward power that was *not absorbed* by the load, but that adds to the line-input power from the transmitter at the line input, or at whatever point in the line the match is performed (*Ref 18, p 191*). Hence, the difference between the forward- and reflected-power readings is the *net power flow* in the line at whatever point the wattmeter is inserted. In a lossless line, the net power flow indicates the line-input power, which is the absorbed power exactly; the two are identical anywhere on the line. In a line with attenuation, the meter indicates the line-input power if it is placed at the line input, or it reads the absorbed power if it is placed immediately ahead of the load. The difference between these readings is related to the line attenuation. Of course, for practical reasons there may be small, or even large errors in the actual results versus those obtained by SWR measurements—for one example, diode non-linearity at various power levels (*Ref 40*).

A further explanation of why the concepts discussed above are realized in practice and the beginning of a discussion on the wave mechanics of impedance matching appear in Chapter 4.

Chapter 4

A View into the Conjugate Mirror

(Adapted from QST, *October 1973, edited June 1999)*

Sec 4.1 Introduction

In Chapter 3 I discussed basic concepts concerning the generation of wave reflections on transmission lines, wave propagation along the line, and the development of standing waves. I then explained mathematically how RF power traveling on a transmission line is separated into its forward and reflected components. I concluded with mathematical expressions representing forward and reflected power as evidence, which proves that if the line is mismatched at its termination, RF energy, or power, does indeed travel in both directions on the transmission line. It then followed logically to explain how the power separation is physically realized by directional devices, such as SWR indicators and directional wattmeters. While learning about wattmeter operation, and how to interpret the indications, we observed that when the line is terminated in a mismatched load impedance and conjugately matched at the line input, the reflected power is re-reflected by the matching device. Due to the addition of the reflected power and the source power at the matching point, the incident or forward power in the line between the matching point at the line input and the load is greater than the power supplied by the source generator. In this chapter I explore this transmission-line phenomenon in detail, because it is of great importance to the amateur in relation to the operational flexibility of the antenna system. Appreciation of the fundamentals involved in this seemingly anomalous situation will free you from the prevalent opinion that we are restricted to operating with little or no mismatch at the junction of the transmission line and the antenna terminals.

The explanation of directional wattmeter operation in Chapter 3 should clarify why the forward power appearing on the line between a transmatch and a mismatched load (the antenna) is greater than that delivered by the transmitter. This is a normal condition that enables a mismatched load to absorb all the power delivered by the transmitter, while at the same time reflecting a portion of the total power it receives. To do this, the load must receive enough more forward power than what is delivered by the transmitter so it can absorb the power delivered and still reflect the portion demanded by the mismatch. The basis for understanding this rather subtle concept lies in the wave mechanics behind the principles of impedance matching introduced in Chapter 1 and defined in Chapter 2. As far as I know, the *wave* aspect of this subject has been presented in the literature only by Slater, Alford, (*Refs 35, 39*, and this author in Chapter 23*)*. Perhaps this restricted exposure may account for some of the confusion in this area among engineers and amateurs alike. For example, the many "cook book" recipes and graphic directions for stub-matching a mismatched line tell "how" to do it, but offer little insight concerning the wave mechanics through which the match is accomplished. (but this author does in Chapter 23). However, this insight goes to the heart of the transmitter-to-line coupling problem. It clarifies how the reflected wave becomes re-reflected at the matching point. If the matching did not produce this effect, the reflected wave would travel along the line back to the generator, reducing the amount of power made available by the generator due to the mismatch now appearing to the generator at the input of the line (*Ref 19, p 37*).

Sec 4.2 The Normalizing of Impedances

I will shortly be discussing the reflection mechanics involved in impedance matching, using the technique of employing a matching stub on a mismatched transmission line. In this discussion we use *normalized* impedances, represented graphically on the Smith Chart W2DU Vector Graph, Fig 3-2. Therefore, I'll now digress briefly to explain normalization. We are rather accustomed to think-

ing of 50 ohms as a standard *system* impedance because of the preponderance of RF components and coaxial lines using that impedance. However, many calculations are greatly simplified by using *normalized* impedances, in which all impedance values have been divided by the system impedance. The characteristic impedance Zc of the transmission line being used generally determines the system impedance. Normalizing an impedance by dividing it by Zc amounts to a change of scale such that the unit of impedance is 1 chart ohm, rather than Zc ohms. The W2DU Vector Graph uses the normalized system to take advantage of the simplification in the calculations. To obtain normalized values occurring in a system based on any specific impedance, simply divide all impedances by the system impedance. For example, in a 50-ohm system, 150 ohms becomes 3.0 chart ohms. To convert back to the 50-ohm system, simply reverse the process and multiply the normalized values by 50. For example, the normalized impedance $z = 0.6 - j0.8$, found at $\ell° = 45°$ becomes $Z = 30 - j40$ when de-normalized. When working with the Smith Chart the normalized values of resistance and reactance appearing on the chart are often called "*chart ohms.*" Also note that normalized values of impedance components are customarily shown in lower case, and non-normalized values are capitalized.

Sec 4.3 Reflection Mechanics of Stub Matching

We will now examine the mechanics of wave interference and reflection, which are the basis for all impedance-matching operations. An approach that will provide a clear understanding of the wave action that occurs in the matching process uses complex reflection coefficients to represent the magnitude and phase of the waves at various points on the line. The complex reflection coefficient, represented by $\overline{\rho} = \rho\angle\theta$, with magnitude ρ and angle θ, were introduced in Chapter 3, and are discussed in greater detail in Chapter 9. As stated along with the definition of the conjugate match in Chapter 2, the matching is accomplished by inserting a non-dissipative mismatch at the matching point, which produces a complementary reflection that compensates and cancels the waves reflected from the mismatched load. It was also stated that matching can be achieved by a correct adjustment of either the final tank tuning circuit (*Ref 4, Part III*), or of a line-matching network (antenna tuner or transmatch) if one is used. Because stub matching uses the same principles as used with a matching network, and is easier to visualize, we will use the stub technique to demonstrate the wave mechanics that perform the matching function.

In stub matching, the stub provides what may seem like an anomaly—a non-dissipative discontinuity, or mismatch. While we usually think of the stub as providing a *match* (which it does), rather than a mismatch, we will discover that the impedance match achieved by the stub results from constructive and destructive wave interference introduced by the stub. The destructive interference causes mutual cancellation of two complementary reflected waves generated by two complementary mismatches. One of the two waves is the original undesired wave reflected from the terminating load mismatch, the wave that needs to be eliminated to achieve the match. The second wave is a new reflected wave generated by the stub mismatch, introduced to cancel the undesired wave. This new reflected wave generated by the stub is equal to the undesired load-reflected wave in both magnitude and phase *but with opposite phase sign*. The ***de**structive* wave interference between these two complementary waves at the stub point causes a complete cancellation of energy flow in the direction toward the *generator*. This cancellation results from the *difference* between these two equal but oppositely phased reflected waves. Conversely, the ***con**structive* wave interference produces an energy *maximum* in the direction toward the *load*, resulting from the *sum* of the two reflected waves and the source wave. The cancellation of energy flow rearward from the stub, toward the generator, results in no reflected power on the line between the stub and the generator. This means that the impedance now appearing at the input of the line is simply the characteristic impedance Zc of the line. Thus, the SWR on the line from the input to the stub is 1:1, although the original SWR between the stub and the load remains at 3:1.

The effect of the energy-canceling wave interference creates either a virtual one-way open circuit or a one-way short circuit at the stub point (the matching point) to waves traveling rearward

toward the generator.[1] How the wave interference creates the virtual one-way open or short circuit will be explained shortly. This one-way circuit blocks both the load-reflected waves and the stub-reflected waves at the stub point from any further rearward travel, and causes these waves to be totally re-reflected toward the load, in phase with the forward waves. Hence, the power in the re-reflected waves adds directly to the forward waves, causing the forward power to be greater than that delivered by the transmitter, as stated earlier.

This wave-interference mechanism, which accomplishes the virtual one-way open or short circuit that is vital to the impedance-matching phenomenon, will become clearer as we investigate the complex reflection coefficients of the load and stub mismatches with the aid of an example using the Vector Graph in Fig 3-2. In this example we are using *normalized* values of impedance Z, resistance R, and reactance X. Here we observe a terminating load of $3 + j0$ chart ohms, which yields a reflection-coefficient magnitude $\rho = 0.5$, resulting in a 3:1 standing-wave ratio along the whole line. The SWR of 3 is shown by the dark concentric circle, which is the locus of impedances anywhere on the line when the terminating load is $3 + j0$. This circle intersects the unity resistance circle marked 1.0 at the two points A and D, as shown. At these corresponding points on the transmission line, the resistive component[2] of the line impedance equals 1.0 times the characteristic impedance Zc of the line. Hence, points A and D are appropriate positions for attaching a *series* matching stub to cancel the line reactance appearing at that point.[3] Points A and D on the graph are also intersected by reactance circles marked 1.15. At point A the reactance is negative, –1.15 times Zc, and at point D the reactance is positive, +1.15 times Zc. Thus, the line reactance is $-j1.15$ ohms at stub point A, and $+j1.15$ ohms at stub point B. It is therefore evident that the line impedances appearing at points A and D are $1 - j1.15$ and $1 + j1.15$ chart ohms, respectively. It should be understood that when we relate these values to real transmission lines, whose characteristic impedance Zo value is, for example, the commonly used 50 ohms, the line impedances above would be denormalized by multiplying by 50. Thus, the real values of these line impedances would be $50 - j57.5$ and $50 + j57.5$ ohms, respectively.

The conditions for obtaining reflected-wave cancellation by wave interference are the well-known stub-matching requirements, as follows:

(1) A series stub is placed where the resistance component of the line impedance equals Zc, such as at points A or D on the unity-resistance circle, and

(2) The stub is tailored to produce a reactance equal in magnitude and opposite in sign to the line reactance appearing at the stub point, which is the reactance that results from the phase relationship between the forward and reflected waves superposed at the stub point. Thus the stub and line reactances cancel to zero at the stub point, which is also the matching point. (See *Ref 2, p 116* and *Ref 19, p 97.*)

This sounds almost like the conjugate-match definition itself, doesn't it? The correct point for inserting a reactance-canceling stub in series with the line nearest the load is at point A on the SWR circle.[4] Alternatively, the stub may also be placed at point D, or at any $\lambda/2$ interval along the line from point A or D. This is possible because the line impedances are repeated at every $\lambda/2$ distance around the diagram, and along the line. However, it should be understood that a stub placed at point A must have a positive (inductive) normalized reactance, $+j1.15$ ohms, to cancel the equal, but negative reactance component of the line impedance at that point. Conversely, a stub placed at point D, must have a negative (capacitive) normalized reactance, $-j1.15$ ohms to cancel the positive reactance component of the line impedance appearing there.

Using the complex voltage and current coefficients of reflection, magnitude ρ and angle θ, we'll now examine how reflections add at a stub matching point to produce the matching effect. We'll see why a directional wattmeter gives a true reading of forward power between the matching point and the load—power that is greater than that delivered by the transmitter when the line is terminated with a mismatched load. A little later we'll also see how these principles apply to practical feed-line matching networks, including the ubiquitous antenna tuner performing the matching at the input of the line.

To clarify the following operations used in explaining the matching function using reflection coefficients, it should first be understood that any impedance $Z = R + jX$ may also defined in terms of its equivalent complex reflection coefficient $\overline{\rho} =$

$\rho\angle\theta$. At point A, which is 30° from the load at $\ell° = 30°$ in Fig 3-2), while the normalized line impedance E/I is $1 - j1.15$ ohms, the unmatched voltage reflection coefficient is seen to be $\overline{\rho}_E = 0.5\ \angle{-60°}$. This means that the magnitude of the reflected voltage wave is one-half the value of the forward wave, and the phase of the reflected voltage wave lags the forward wave by 60° at point A. (The superposition of the forward wave and the lagging reflected wave at point A result in the formation of the normalized line reactance, $-j1.15$ chart ohms at point A.) A match can be effected by connecting an inductive reactance, such as a stub (or a lumped inductance) of $+j1.15$ chart ohms in series with the line at point A. The reactance-cancellation effect of the positive-reactance stub on the equally negative reactance of the line impedance is generally understood, but several points are not always clear regarding the effect on the component wave. What characteristics of the stub cause it to counteract the reflections from the load? Also, why does the stub cause the forward power to increase between the matching point and load?

In answer to these questions, let's first determine the reflection coefficient produced by the stub if it were inserted at point A in a perfectly matched line—i.e., with the line terminated with a normalized 1-ohm resistance instead of the 3-ohm resistance appearing in Fig 3-2. In this condition we may analyze the reflection generated by the stub in the absence of any other reflection on the line. If we observe from a position just on the load side of stub point A with the stub attached, and look into the line toward the matched termination, we will see a pure resistance R equal to the characteristic impedance of the line, Z_C.

We know from transmission-line theory that if we replace the matched line portion extending from the stub to the load with the terminating resistance $R = Z_C$ alone, in series with the stub across the otherwise open-ended line, we may look into the line toward the stub from the generator and see the same conditions of reflection as were present before the line section was removed and replaced with the resistor. Thus, the series circuit comprising either the stub and the matching resistor, or the stub and line section terminated with the matching resistor alone, develops a $1 + j1.15$-ohm impedance on the line at the stub point. Consequently, a reflection is generated by the stub at the stub point that is of precisely the same magnitude as that generated by the 3-ohm mismatched load in Fig 3-2, and precisely this same reflection is produced no matter where the stub is inserted in a matched line. The Vector Graph shows this impedance of $1 + j1.15$ ohms to appear at point D, for which the complex voltage reflection coefficient is $\overline{\rho}_E = 0.5\ \angle{+60°}$. Note that this is the same magnitude and phase *but of opposite phase sign* of the reflection coefficient appearing at point A resulting from the load mismatch of $3 + j0$.

Thus, the stub mismatch produces the same magnitude of reflection (and thus the same SWR) as was produced by the load mismatch, but the stub-reflected voltage wave *leads* the forward wave by 60°, while the load-mismatch wave *lags* by 60°. If the series stub is now inserted at matching point A (corresponding to $\ell° = 30°$ on the Vector Graph Fig 3-2) with the $3 + j0$ load terminating the line, both the stub-mismatch and the load-mismatch reflections will appear simultaneously at the same point. As a result of their opposite-sign phase relationship, the *leading* stub-reflected wave and the *lagging* load-reflected wave cancel each other at the match point due to destructive wave interference.

The voltage reflection coefficients of the load ($\angle{-60°}$) and stub ($\angle{+60°}$) thus add vectorially to a resultant of zero degrees, $\overline{\rho}_E = 0.5\ \angle 0°$, which tells us that the resultant of the two voltage reflections is exactly in phase with the forward voltage wave at match point A, as shown in Fig 4-1(A). The amplitude resulting from this trigonometric addition is considered later, but knowledge of these angular relationships should clarify the understanding of the mechanics of line-reactance cancellation by the stub.

Now that we know what is happening with the voltage waves, we also need to investigate the current waves to learn about the complex impedance Z = E/I appearing at the matching point. As defined earlier, reflected current is always 180° out of phase with reflected voltage. Hence, the complex reflection coefficient for current at point A on the line is found on the Vector Graph 180° away at point C, diametrically opposite the corresponding voltage-coefficient point. Thus, we find the current reflection coefficient for the load mismatch at point C with $\overline{\rho}_I = 0.5\ \angle{+120°}$. Similarly, the complex reflection coefficient for current of the stub mis-

match is found diametrically opposite point D, at point B, and is $\rho_I = 0.5 \angle -120°$. Note that similar to the case with voltage, the current coefficients of the load and stub are also of equal magnitude and phase, but of opposite phase sign. However, while the voltage angles added vectorially to the resultant 0°, the current angles add to the resultant 180°. Hence, the resultant of the two reflected *current* waves is 180° out of phase with the forward current, as shown in Fig 4-1(B). Therefore, we now have forward and reflected voltages in phase (at 0°), and forward and reflected currents 180° out of phase; hence, the wave arriving at the match point from the generator sees a perfect match. Why a perfect match to waves arriving from the generator? Because these specific magnitudes and angles of the reflected waves of both voltage and current send a significant message which we will now

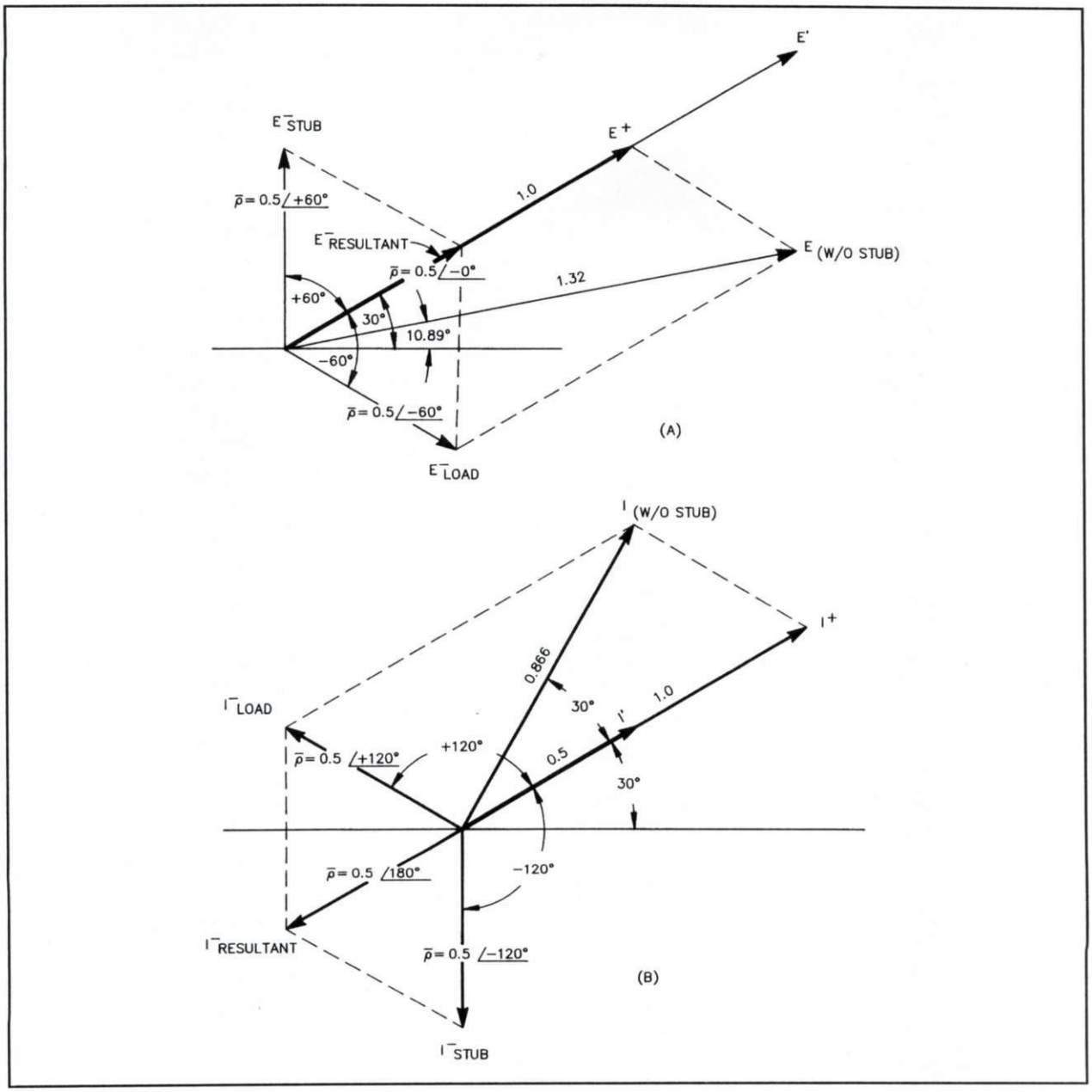

Fig 4-1. At A, various voltage-vector relationships, and at B, various current-vector relationships at $\ell° = 30°$.

reveal. With reflected voltage and current phasors of equal magnitude, and the voltage phasor at 0° and the current phasor at 180°, a virtual open circuit to rearward traveling waves is established at the stub point, which I will now explain.

In the opening paragraphs of Chapter 3, I described the wave mechanics involved in a line terminated by an open circuit. There we learned that angle theta (θ) of the voltage reflection coefficient at an open circuit is 0° and that of the current is 180°. With an open-circuit termination, the voltage wave that is incident on the termination is totally reflected with no change in phase, while the current wave is totally reflected with a change in phase of 180°, a complete *reversal* of current polarity.

The significance of the reflection conditions appearing at the open circuit described above is that the phase relationships of the resultant reflected waves at the stub matching point, which we established earlier ($\theta_E = 0°$ and $\theta_I = 180°$), are identical to those which prevail in a line terminated in a real open circuit so far as the reflected waves are concerned (but not the forward waves). Therefore, the effect of the two oppositely-phased reflected waves arriving simultaneously to superpose at the match point is to establish a virtual open circuit at the match point to the waves generated by the load and stub mismatches. Consequently, the waves from the two mismatches become totally re-reflected at the match point and undergo *open-circuit* phase changes, as described above. Hence, on re-reflection at the match point, the angle of the resultant re-reflected voltage wave, already at 0°, does not change phase. However, the resultant *current wave changes phase* by 180° on re-reflection. In addition, because it was 180° out of phase with the forward current wave just prior to re-reflection, its 180° reversal on re-reflections places it also in phase with the forward current wave. Now that both voltage and current re-reflected waves are in phase with their corresponding forward waves, direct addition of the voltages and currents of the forward and reflected waves occurs at the stub-matching reflection point. Thus the conclusion: (1) *On re-reflection the power contained in the reflected waves adds directly to the forward power,* increasing it between the matching point and the load in the manner stated earlier; (2) *a 1:1 impedance match to source waves from the generator appears at stub matching point.*

Now let us consider that the above conclusion assumes a virtual open-circuit was established at the match point for the reflected waves traveling toward the generator. The assumption was based on the identical relationship between the reflection coefficients, which we established at the match point by wave interference and those known to exist at a real open-circuit termination. We can verify this assumption by an alternative method. The method is based on the discussion in Chapter 3 concerning the electric- and magnetic-field relationships that occur at an open-circuit termination.

Let us first observe the net value of all currents flowing at the match point at the instant the two superposed reflected currents form their resultant angle $\theta = 180°$. At this instant we will see an initial sudden drop in resultant line current, I, because of wave cancellation as the reflected-wave resultant becomes aligned exactly 180° out of phase with the forward current. This drop is shown graphically in Fig 4-1(B), where the original resultant current, I (as with no matching stub present), suddenly drops to the new instantaneous resultant value I' from the effect of the stub discontinuity.

Now recall the open-circuit field theory presented in the early part of Chapter 3. We know that when the current drops, the magnetic field also drops. The changing magnetic field produces an electric field equal to the energy reduction in the magnetic field. The new electric field then adds in phase to the existing electric field, producing a voltage increase at the match point. This voltage increase now starts a wave traveling in the opposite direction, which is now in the same direction as the forward wave, and thus adds to it. The increased electric field (now an enlarged *forward* electric field), as it moves toward the load, produces a new magnetic field. The new field is equal in magnitude but of opposite polarity to that of the original field. The new magnetic field now causes current to build up again to the same magnitude as the original reflected current, but of opposite polarity and direction. Thus, the new current wave is now also traveling in the same direction, and with the same polarity as the forward current wave. The new current wave adds to the forward wave, enlarging it just as the re-reflected voltage wave added to and enlarged the forward voltage wave.

By following these field-current-voltage reactions through their natural sequence of events, you can see that we have obtained the same conclusions as those previously obtained on the basis of reflection coefficients. This justifies the assumption that the resultant reflection coefficients at the stub-matching point have defined a virtual open circuit to the reflected waves, thus preventing any further travel of the reflected waves toward the source. The existence of the reflectance (ratio of reflected power to forward power) at the matching point is therefore verified, with the result that both the reflected voltage and current have indeed been re-reflected, and the power associated with them has thus been effectively added to the power contained in the source wave. Therefore, when the line is terminated in a mismatch causing reflected power to exist on the line, the *sum* of the source and re-reflected powers (traveling only toward the load) must be greater than the power delivered by the generator alone, when conjugate impedance matching is performed at the input of the line. Also, since we have shown how the stub acts to counteract reflections from the load, our original questions concerning the stub characteristics have been answered.

Sec 4.4 Effect of Line Attenuation on Reflected Power

Now we'll consider the effects of line attenuation, alpha (α) with respect to the increase in the loss of power delivered to a load when the load is mismatched to the transmission line impedance, Z_C, but conjugately matched at the input of the line with a matching device such as an antenna tuner. When determining the effects due to attenuation on transmission lines, it is customary to first determine the pertinent parameters while considering the line to be lossless (zero attenuation), and then re-calculate to include the attenuation. The next step then is to determine the total forward power in the lossless line resulting from the addition of the power re-reflected at the match point to that from the source, the transmitter. Let's consider a mismatch that yields a reflection coefficient $\rho = 0.5$, resulting in a 3:1 SWR, and that the transmitter delivers 100 watts into the line. Because of the addition of the re-reflected power to the power delivered by the transmitter, after a few cycles of round trip travel to establish the steady-state condition, the forward power in the line with the 3:1 mismatch is 133.33 watts, and the reflected power is 33.33 watts. The 133.33 watts of forward power results from multiplying the 100 watts from the transmitter by the "forward-power-increase factor" $1/(1 - \rho^2)$. With the reflection coefficient $\rho = 0.5$, ρ^2 is the *power* reflection coefficient, 0.25, and $(1 - \rho^2)$ is the power *transmission* coefficient, 0.75. Thus, $1/(1 - 0.25) = 1/0.75 = 1.3333$, and 1.3333 times 100 watts equals 133.33 watts, which is incident power at the load. On the lossless line used for the reference, 100 watts will be absorbed in the load, and 33.33 watts will be reflected, because reflected power $\rho^2 = 0.25$, or 25% of the forward power. This leaves 75% absorbed by the load, and because 75% of 133.33 watts is exactly 100 watts absorbed in the load.

Now we'll apply the data obtained with lossless line to a realistic line with attenuation. As an example, the matched-line attenuation in 175 feet of RG-213 at 4 MHz is 0.5 dB, and our problem is to find the additional loss sustained with this line attenuation when the load mismatch is 3:1. If the load were perfectly matched to the line, for a 1.0 SWR, the 100 watts delivered by the transmitter would be attenuated to 89.13 watts by the 0.5-dB line loss during travel to the load. However, with a 3:1 mismatched load the *additional one-way* line attenuation *because of the SWR* is 0.288 dB.[5] We can now determine the power absorbed by the mismatched load by adding the 0.288 dB additional attenuation to the 0.5 dB matched attenuation, for a total of 0.788 dB. Then we reduce the 133.33 watts of forward power obtained above with *lossless* line by the 0.788 dB. The result is 83.41 watts absorbed in the 3:1 mismatched load. To continue, the forward power at the conjugate-match point at the line input is 124.78 watts (0.288 dB below 133.33 watts), and 111.21 watts (0.5 dB below 124.78 watts) reach the load. Of the 111.21 watts reaching the load, 27.80 watts (25%) are reflected, leaving 83.41 watts to be absorbed in the load. Of the 27.80 watts reflected, 24.78 watts arrive back at the input to join the 100 watts of source power to develop the 124.78 watts of forward power. The difference between the 89.13 watts absorbed in the *matched* load, and the 83.41 watts absorbed in the 3:1 *mismatched* load is only 5.72 watts. This small

amount of power loss is insignificant, because when considering that an S unit normally refers to a change of 6 dB, the loss in this case amounts to less than 1/12 of an S unit. A circuit model illustrating the effects of the line attenuation in this example appears in Appendix 6, Fig 6-2(B), and Example 5. Procedures for calculating these values appear Appendices 7, and 8. These values are typical of data obtained during actual routine measurements in a professional laboratory. They provide additional evidence that reflected power is real, not fictitious. If it were fictitious power, no more than 66.85 watts (75% of 89.13 watts) would be available for delivery to the 3:1 mismatched load. However, the 83.41 watts actually absorbed in the mismatched load is 93.58% of the amount absorbed in the matched load, the additional loss of 6.42% being completely accounted for in the line attenuation encountered by the reflected power.

Sec 4.5 Matching Networks and Reflection Mechanics

Now we'll delve further into the wave-interference principles demonstrated with the stub technique in Sec 4.3. These principles also apply to both the resonant $\lambda/4$ series matching-transformer operation and the typical amateur "antenna tuner," line-matching network, or transmatch. In order to visualize the inherent generality of these principles, we need to develop some additional concepts concerning stub matching and embark on a somewhat different line of reasoning. As you can surmise from the example presented earlier, the fundamental principle behind the elimination of reflections is this: Have the original reflected wave canceled at the point where the elimination of the reflection is desired, by destructive wave interference from another wave of equal magnitude and phase but of opposite phase sign (*Ref 35, p 58, and Ref 39*). A transmission line of the appropriate length, which has one end effectively open circuited and the other end short circuited, possesses the reflection-producing characteristics required to develop canceling waves of the correct phase in relation to the wave to be canceled.

Using other line arrangements can also develop canceling waves, but for the purpose of demonstrating the principles, I will use the arrangement just stated. Fig 4-2 shows how a stub of this arrangement performs the matching function in practice. Fig 4-2A is the conventional representation of a typical series-stub circuit (using the values of our previous SWR = 3 example), in which section F is called the *feed line*, section S is the *stub*, and section T is an impedance-transforming section which I will call the *transformer*. We'll now examine these in greater detail. To clarify the approach, Fig 4-2(A) is redrawn in Fig 4-2(B), with the stub and transformer shown as one continuous straight-line section. This straight-line section will presently come to life as the heart of the wave-interference-producing mechanism found in all stub-matching operations. This is because its physical length will be adjusted specifically so that waves reflected at each end will return to the feed point with equal magnitude and phase, but with opposite phase sign.

We observed earlier that a voltage wave is reflected with zero phase change at an open circuit, or with any resistive termination *greater* than the Z_C of the line. Also it is reflected with 180° of phase change from a short circuit, or from any resistive termination *less* than Z_C. With a current wave, the opposite is true. Thus, from the viewpoint of phase angle in reflection behavior, with the $3 + j0$-chart ohm load terminating the transformer, the load end of the straight-line section is considered as being open circuited and the opposite end short circuited. As can be seen, which end is open and which end is short circuited depends on the character of the load—i.e., whether the resistance in the load is greater or less than Z_C. In our example in Fig 4-2(B), the load end behaves as an open circuit as far as wave reflection is concerned because R is greater than Z_C, while the opposite end (the stub) is short circuited. The action occurring in this line section in the process of developing the interfering wave-canceling relationship is as follows. Either a voltage or current wave is assumed to enter the line section at the feed-line entry point. The energy in the wave divides, one portion of the wave traveling toward one end of the section and the other wave portion traveling toward the opposite end. After each wave portion encounters one reflection, the returning waves will each have the same absolute value of phase but opposite sign, or polarity, on return to the point of entry. This is true for both voltage and current.

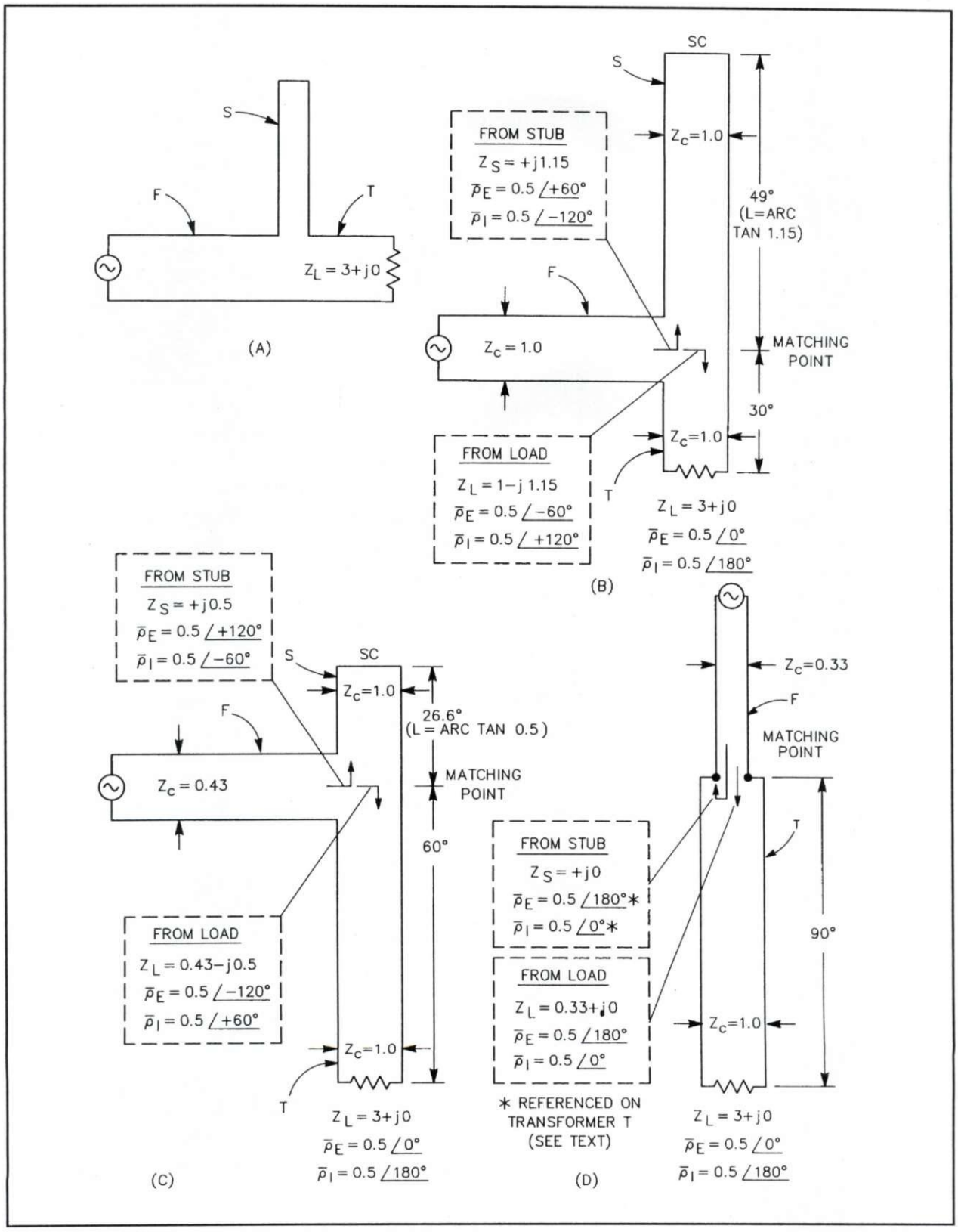

Fig 4-2. At A, the concept of stub matching with a series-connected stub. At B, the same matching arrangement redrawn. At C, a similar matching arrangement, but with different stub and transformer line lengths. At D, a λ/4 line-transformer section evolves as the stub length goes to zero. Sc = short circuit.

The opposite phase or polarity between the two reflected waves arriving from opposite directions results because reflection at one end is accompanied by a 180° phase reversal, while reflection from the other end is not. As stated above, the phase reversal of one wave but not the other is caused by the opposite conditions of reflection at the two ends of the line, one end open-circuited and the other end short-circuited. Note in the dashed-line boxes in Fig 4-2(B) that in each case the phase of the reflected wave (of both voltage and current) is of opposite polarity on opposite sides of the feed line as they return from the stub and load directions. The wave-entry point, where the feed line is attached, is the matching point. This point divides the line section into its two complementary portions: the *stub* portion, S, and the *impedance-transformer* portion, T. Electrically, each portion is the complement of the other, because the waves reflected from the end of each portion returning to the match point are complementary in their phase relationship and equal in magnitude. Herein lies the basis for the term *complementary mismatches* as used earlier, because each portion presents a complementary mismatch to the feed line.

Later I show that this complementary mismatch concept is of great importance to matching in general, because the complementary relationship holds no matter where the feed-line entry point is positioned on the stub-transformer line section. The importance prevails because the canceling wave and the reflected wave to be canceled will be of the same magnitude and phase, but opposite phase sign, at whatever point on the matching line section the feed line is attached. This is true with two provisions: (1) the characteristic impedance Z_C of the feed line section F must be the same as the resistive component of the transformed line impedance appearing on the transformer line at the feed point, and (2) the length of the stub portion S must be adjusted to produce a reactance equal and opposite in polarity to the line reactance appearing at the feed point in the transformer section. That length may be found from the expression:

$$S_L = \text{arc tan } \frac{jX}{Z_C} \qquad \text{(Eq 4-1)}$$

where

S_L = stub length in electrical degrees

jX = line reactance (obtained from the Vector Graph Fig 3-2)

Z_C = characteristic impedance of the stub section; Z_C = 1.0 here, because we are using normalized impedances as discussed in Sec 4.2.

Transformer section T transforms the load impedance to varying values of both resistance and reactance along its length. Hence, for a proper match, the magnitude of the feed-line section F impedance, Z_C, depends on the location of the feed point, and vice versa. This is because the feed-line impedance, Z_C, must equal the resistance component of the line impedance appearing on the transformer line at whatever point the feed line is attached to the transformer. This concept is not generally appreciated, and it is certainly not readily apparent from the usual stub-length and position-indicating graphs appearing in many publications.

Observe that, as we move from diagram "B" to "C" the feed line has moved toward the short-circuited end of the stub. We also observe the resistive component of the line impedance on the transformer section and the Z_O of the feed line decreasing from 1.0 to 0.43 ohms. However, observe also that when the total length of the transformer section T becomes 90° in length, or $\lambda/4$ in diagram "D" the stub length has gone to zero, and transformer T has evolved into the conventional $\lambda/4$ matching transformer. Note that in the case of the $\lambda/4$ transformer, the input and load resistances are reciprocally related. From this relationship it can be shown that when the input and output impedances of practical $\lambda/4$ transformers are normalized to the characteristic impedance Z_O of the transformer, the input and output impedances will always be reciprocally related. This illustration indeed demonstrates the remarkable, but simple phenomenon of wave interference in achieving the matching of impedances by introducing complementary reflections to eliminate the reflections resulting from a mismatch.

Sec 4.6 Stub Matching versus Network Matching

We are now getting closer to understanding how stub-matching principles extend to line-matching-network operation. If we look further into the reflection characteristics of what have generally been considered to be different techniques of

matching, a fascinating revelation of the similarity among all of these various techniques emerges. Stub, hairpin, λ/4 series section transformer, transmatch, L network, pi-network, and so on, are all in this category. Also, there is a logical reason for this similarity: These techniques all have one essential ingredient in common—reflections! Reflection and matching are applied in transformers that rely on reflections from the end terminals, where a change in impedance level exists. As I discussed in Chapter 3, any abrupt change in impedance level appears as a discontinuity to the smooth flow of the electromagnetic wave, and results in producing a reflection. The transformer accomplishes the task of matching its input and output impedances by controlling the phase and magnitude of the waves produced by reflection at its boundaries, or end terminals. As a result, all the reflections produced at either end are canceled by those arriving from the other end (*Ref 35, p 58*). This is what was meant in the reference to "controlled reflections" early in Chapter 1. A corollary to the seeming anomaly of a stub producing a mismatch, instead of a match, is that we match to eliminate reflections, but we can't match without using controlled reflections when different impedance levels are involved.

From Eq 3-1, we know that the ratio between the load impedance Z_L and the impedance Z_C of the line transformer determines the magnitude of a reflection from a mismatched load. To enhance the understanding of the role played by reflections in the process of impedance matching, it is interesting to make two additional observations on the Vector Graph, Fig 3-2. First, either the magnitude of the reflection, , or the SWR, determines the position on transformer section T where the resistance component (the real part^2) of the transformed line impedance Z = E/I equals the feed-line characteristic impedance Z_C on the *unity resistance circle (the R = 1 circle)*. This position, we recall, is the matching point, and fixes the length of transformer section T. In making this observation, remember that the diameter of the SWR circle is proportional to the SWR. Thus, by tracing along the R = 1 circle we can see that as the diameter of the SWR circle changes, the point where the R = 1 circle and the SWR circle intersect moves accordingly. A radial line drawn through this intersection point, and extending to the line-length scale ℓ°, indicates the angular distance (T) from the load to the matching point for a given SWR. We recognize this observation as simply the conventional method of using the Smith Chart for determining the stub position when the transformer and feed-line impedances Z_C are equal. However, in addition, using a radial indicating line in a similar fashion while tracing along the SWR = 3.0 circle as it intersects the various other resistance circles, we see that for a given SWR the resistance component^2 of the line impedance Z = E/I changes with position along the transformer. These two observations together reveal a flexibility available in the approach to a matching procedure that provides a step toward visualizing the fundamental similarity of the different matching techniques. This flexibility includes the following three conditions, which are explained in more detail later.

(1) There is no restriction on the characteristic impedance Z_C of the transformer section T that requires it to be of the same value as the section F feed-line impedance; it can range from low (coax) to high (open-wire line), whichever is to be used.

(2) The *length* of the transformer section having a given Z_C can be found which will yield the desired resistance component^2 of the transformer-line impedance that matches the feed-line section F impedance Z_C, which differs from the transformer Z_C. However, the transformer section can have a length that is not limited to the distance from the terminating load to the first point at which the resistance component^2 of the impedance is seen to equal the feed-line Z_C. The transformer can extend from the load to either of the two points where the resistance component^2 is seen to equal the feed-line Z_C on the SWR circle, or any electrical length extending beyond these points by an integral multiple of λ/2. Later I show how the use of matching networks assists in obtaining the required electrical length. This removes *all restrictions* from any specified physical transformer length—that is, from the load (the antenna) all the way to the operating position.

(3) Any device that will provide a reactance of the correct value can perform the action of the stub portion. This can be either by a lumped-constant component, or by a separate line section of any reasonable value of Z_C of the proper length to obtain the required value of reactance. The *electrical*

length of the stub is always directly related to its reactance. Now we again return to wave or reflection mechanics. We will see in those terms how matching, obtained by the various techniques recited previously, is described by three parameters: transformer impedance, transformer length, and stub reactive elements.

In our earlier example using the stub technique, the magnitude ρ of the reflections appearing at each end of the *transformer* section was the same, 0.5, or an SWR of 3:1, for the load at one end and the stub at the other. In other words, the magnitudes of each complementary mismatch were identical. For the present, we will retain the characteristic impedance $Z_C = 1.0$ for the entire stub-transformer line section. However, based on conditions 1 and 2 above, we may change the feed-line impedance as conditions dictate. Consider now the effect of increasing the length of the transformer section and shortening the stub section in accordance with Eq 4-1. For example, while referring to Fig 4-2(C) and the Vector Graph, Fig 3-2, let us move the feed-line entry point farther away from the load, from $\ell° = 30°$ to $\ell° = 60°$. This increases the transformer length to 60° and reduces the stub length to 26.6°. Now on the Vector Graph observe the radial line extending from the $\ell° = 60°$ point (where $\theta = -120°$) through point B, where the SWR = 3.0 circle and the R = 0.43 circle intersect. Observe that the corresponding movement along the SWR circle results in a change in the resistance component at the feed point, from R = 1.0 to a new resistance, R = 0.43.

Now recall from the earlier statement that the complementary mismatch relation holds constant wherever the feed line is attached. A feed line having a characteristic impedance $Z_C = 0.43$ will be perfectly matched when attached at the $\ell° = 60°$ point. The complex voltage reflection coefficient of the load-mismatch is now read as $\overline{\rho}_E = 0.5 \angle -120°$ at point B. The magnitude is the same as before, but the phase angle is *larger* because we are farther from the load. Also, applying the complementary-mismatch principle, we see that the complex voltage reflection coefficient of the stub mismatch becomes $\overline{\rho}_E = 0.5 \angle +120°$, as read at point C. So we ask the question, how does this new combination produce a canceling wave having the same magnitude as before. Recall that previously, when the line-characteristic impedance of sections F, S, and T were all $Z_C = 1.0$ as in Fig 4-2B, the canceling reflection was generated by the stub alone. This happened because no line-junction mismatch existed between the feed-line section F and the transformer T. However, now that the impedance of the feed line differs from the impedance of the transformer, we have an additional discontinuity at the feed point, which also generates a reflection. Also, the *shorter* (series) stub portion now generates a reflection which is smaller than when all the line sections had a $Z_C = 1.0$. The magnitude of the stub-reflection is reduced by the amount of the reflection presently being generated by the feed-line-to-transformer mismatch. Thus, by the complementary mismatch principle, the resulting canceling wave still retains the correct magnitude and phase to cancel the load-mismatch reflected wave at this new feed point on the transformer. This canceling wave is evidently generated by the *combined discontinuities* of both the differing line impedances at the feed-line junction, and of the stub with the corrected length. We have thus matched a feed line of $Z_C = 0.43$ to a load of $Z_L = 3 + j0$ through a transformer of $Z_C = 1.0$.

Using this same type of reasoning, to obtain a match for feed lines of higher impedance, we may conversely shorten the transformer section and change the stub section, according to the tangent relation in Eq 4-1. To accomplish this we position the feed-line entry point where the real part of the line impedance Z = E/I in the transformer T has been transformed to the value of the feed-line impedance Z_C that we wish to use. We then adjust the stub length to cancel the line reactance. As explained above, the resistance circle that is intersected by the SWR circle for a given transformer length indicates the real part of the of the feed-point impedance. This is also the Z_C value of the feed line that will be perfectly matched when connected at that feed point on the transformer. The data presented in Table 4-1, taken from points along the SWR = 3.0 circle on the Vector Graph, show a few selected transformer-length examples, and pinpoint some of the pertinent information for clarity. Notice especially that the real part of the feed-point impedance decreases as the transformer length increases. It is interesting to discover that when the feed point goes beyond the $\ell° = 45°$ position, the θ angles of the voltage- and current-reflec-

Transformer Length	Stub Length	Resistance Component	Stub Reactance	Angle of Reflection Coefficient			
				Voltage		Current	
				Load Mismatch	Stub & Line Mismatch	Load Mismatch	Stub & Line Mismatch
$\ell°$	$S_L°$	R	jX	$\theta°$	$\theta°$	$\theta°$	$\theta°$
0	0	3.0	0.0	0	0	180	180
10	48.2	2.42	+1.12	–20	+20	+160	–160
22.5	52.9	1.38	+1.32	–45	+45	+135	–135
30	49.0	1.00	+1.15	–60	+60	+120	–120
45	38.7	0.60	+0.80	–90	+90	+90	–90
52	33.0	0.50	+0.65	–104	+104	+76	–76
60	26.6	0.43	+0.50	–120	+120	+60	–60
67.5	19.8	0.38	+0.36	–135	+135	+45	–45
90	0	0.333	0.0	180	180	0	0

Table 4-1. Matching characteristics with various transformer- and stub-section lengths.

tion coefficients pass through 90° from opposite directions. The result of this is that their respective resultants shift 180°. Thus, the resultant angles of reflection coefficient interchange. The resultant angle of the voltage reflection coefficient now becomes 180° and the resultant current angle θ becomes 0°. This means that the effective reflecting termination at the match point shifts from an open circuit to a short circuit when the feed line is attached more than 45° away from the EMAX position (at $\ell° = 0°$ on the transformer).

Consider now the effect of increasing the length of the transformer section until the reactance component of the line impedance disappears by itself without requiring a stub to cancel it. The Vector Graph shows this condition to occur at $\ell° = 90°$. At this point the reflected voltage wave from the load mismatch is exactly 180° out of phase with the forward wave, and therefore no reactance component is developed. The resistance component[5] of the line impedance at this point is 0.33 × Zc, as shown on the chart. Hence, we may now connect a feed-line section F having impedance Zc = 0.33 chart ohms at this point and obtain a perfect match, as shown in Fig 4-2(D). No reflections appear on the 0.33-chart-ohm feed line. Why? Again, because of the canceling reflections in the transformer section! Note the present length of the transformer section—90°, or λ/4. The transformer section alone is now using the *entire length* of the line section, and the stub section has disappeared.

Note that simply by moving the feed point along the transformer to the point where the line reactance vanishes, the resistance component[5] becomes Zc/SWR = 1/3, and we slip smoothly from the stub form into the series λ/4 transformer form of matching. You can see what's happening by observing the numbers in Table 4-1. Remember, the characteristic impedance of the transformer is still Zc = 1.0, which has become the geometric mean between the input and output impedances that it is matching, $\sqrt{0.33 \times 3.0}$. From inside the transformer, the impedance level looking toward the input terminals is stepped down 3:1 from 1.0, giving us short-circuit reflection behavior, just as the output impedance is stepped up 1:3 from 1.0, for open-circuit reflection behavior at the output terminals. It is therefore evident that a λ/4 transformer section of line having a Zc equal to the geometric mean of its two end-terminal impedances has equal mismatches at both ends, and thus produces reflections of equal magnitude at both ends. These reflections from each end cancel each other at the junction of the feed line and the transformer input terminals, as waves reflected at the output load mismatch return to the input junction exactly 180° out of phase with the wave reflected at the input mismatch. This is because the wave reflected from the load mismatch has traveled 90° from the input point to the load mismatch, and an additional 90° in returning to the input (see Chapter 23).

To clarify further what is happening here, recall that previously when the feed-line section F and transformer T were of equal impedance Zc = 1.0 (Fig 4-2[B]), the canceling reflected wave was generated entirely by the stub mismatch. In the present

case, where the stub length is zero and the transformer length is λ/4, the canceling reflected wave is generated entirely by the 3:1 mismatch at the junction of the feed line and the transformer. The voltage reflection coefficient angle of the wave reflected from this feed-line-junction mismatch is $\theta = 0°$ referenced to the feed-line Zc, because the Zc of the transformer is greater than the Zc of the feed line. However, after the waves reflected from both the load- and input-junction mismatches have joined at the input of the transformer to cancel one another, the input-junction reflection no longer travels toward the generator, but is re-reflected back into the transformer toward the load in the same manner as with the previous stub-reflected wave. Therefore, referenced from within the transformer, the reflection coefficient angle of the feed-line-junction reflection is $\theta = 180°$, as indicated in Table 4-1. The matching point with this configuration is at the input terminals of the λ/4 transformer section. Hence, it is evident that the above discussion has explained the reflection mechanics involved in the general impedance-matching action of all series λ/4 transformer matching sections.

Chapter 12 explains why the λ/4 series transformer is an impedance *inverter for any complex terminating load.* It is not restricted to purely resistive loads.

Notes

1. The virtual one-way circuit will be either an open circuit or a short circuit, depending on the value of the resistive component R in the terminating load in relation to the characteristic impedance Zc of the transmission line. If the load resistance R is greater than Zo the one-way circuit will be a virtual open circuit; conversely, if R is less than Zo it will be a virtual short circuit.

2. When the term *resistance* is applied to a component of line impedance in a transmission line, or at terminal connections within a network, the term means the "real part, Re" of the impedance, which is non-dissipative, in accordance with the IEEE Definition (2) of resistance. Conversely, when the term *resistance* is applied to the value of resistance in a physical resistor, such as the resistive portion of a complex load impedance, the resistance is dissipative, in accordance with the IEEE Definition (1) of resistance. The IEEE definitions of resistance are stated in Appendix 9.

3. For this example we are using *series* stubs to permit *impedance* treatment for the reader who is unfamiliar with admittance treatment. Both series and parallel stubs are used in commercial short-wave transmitting systems, where balanced open-wire transmission lines prevail. However, series stubs are not practical for use with coaxial transmission lines. Thus, parallel or shunt stubs are used more prevalently in general practice, but for some, using the shunt form would also require an explanation of *admittance* treatment, which is beyond the scope of this example.

4. To avoid confusion concerning what is meant by "*series* stub," we mean a stub with its two terminals placed in series with the line, not a line-"section" inserted between two portions of the line.

5. The procedure for determining the additional one-way attenuation due to SWR for all values of mismatch and line attenuation appears in Appendix 8.

Chapter 5

Low SWR for the Wrong Reasons

Sec 5.1 Introduction

I made the statement in Chapter 1 that misconceptions concerning SWR and reflections are prevalent among amateurs, both in print and on the air. Therefore, I reiterate, this book was written with one primary goal in mind—to identify some of the misconceptions and to clarify some of the confusion resulting from the misconceptions.

One outstanding area of confusion concerns the nature of reflected power and how it is accounted for in the circuit. In short, is it *real* or *fictitious, reactive power,* and if it is real, where does it go? The nature of reflected power is discussed in Chapter 3, where it is shown why reflected power is real power not reactive. However, the understanding of this subject is so vital that an entire chapter, "The Reality of Reflected Power," Chapter 8, was written to present additional proof for those who still believe that reflected power is fictitious. Also in Chapter 4, when discussing the role of reflections in conjugate matching, I delved into the question of where the reflected power goes. I used the stub form of matching to illustrate the wave action that accomplishes the matching function, and that also derives the total forward power from the combined source and reflected power. Recall that learning of this wave action stripped away the mystery of how a mismatched load can absorb all of the power delivered by the source. We learned this as we saw how the reflected power adds to the source power at the conjugate match point so that the reflected power can be subtracted from the total, enlarged forward power at the mismatch point to leave a net power in the load equal to the source power, less only that lost due to attenuation in the line.

Now that we have established this relationship between the source, and reflected and forward power in terms of the wave mechanics of the conjugate match, we have the necessary background for identifying some of the improper usage of SWR. We can also clarify in greater detail the reasons for the misunderstanding that still prevails concerning what happens to the power reflected from an antenna that is mismatched to its feed line. Further clarification of the misconceptions will enhance the appreciation of the mismatched feed line as simply a tuned, resonant impedance-transforming device, particularly as we see somewhat later how the transmatch type of feed-line matching network and the pi-network tank circuit of the transmitter perform the matching function in the same manner as the stub. Additional perspective in relating the discussion to practical feed-line operation will be gained as some of the thoughts presented in Chapters 1 and 2 are now expanded.

If it appeared that the importance of SWR was overly minimized or downgraded in the treatment accorded it in Chapter 1, I did not intend so. The intent there was to focus attention on the importance of understanding the subject of reflection and SWR correctly and in such depth that we may retain complete control over them in our antenna system design engineering. Thus, instead of letting SWR become *king* to take control and deprive us of a breadth and flexibility of operation, we may use SWR in the system design choices in ways that many are unaware exist.

How many of us have acquiesced to *"King SWR"* in pruning an 80-meter dipole, taking great pains to obtain the best possible match to a $\lambda/2$ feed line at a specific frequency, and feared operating more than a few kilohertz from that frequency without worrying about the king's ominous threats of damage to our equipment? However, how many are aware that King SWR can be outwitted and his consequences averted without pruning either the dipole or the feed line? Also, how are aware that the matching operation can be performed at the transmitter end of the line at any frequency within the entire 75–80-meter band without suffering any significant loss in power in spite of the SWR remaining on the feed line? Although it contradicts the word published in many articles during the past

four decades, this revelation is true. This revelation indicates the flexibility, or freedom, that really is available in our choice of antenna systems designed for all the HF bands, simply by having a better understanding of SWR and reflection.

Sec 5.2 Valid Reasons for Low SWR

There are good and valid reasons for being concerned with SWR and reflection from both the amateur and commercial viewpoints—with this there can be no argument. As we well know, these reasons are concerned basically with voltage breakdown and power-handling capability, efficiency and losses, and with line-input impedance as it relates to transmitter output coupling. However, in amateur practice, power-handling capability and voltage breakdown don't become serious problems unless we try to shove the legal limit of power through RG-58 or RG-59 at a high SWR. Losses and efficiency concern us, but to a much smaller degree than is generally realized, and for a different reason than many are aware, as we'll see very shortly.

The chief reason why the amateur should be concerned with, but not alarmed by, SWR is in its relation to line-input impedance and transmitter coupling. This is discussed in great detail in Chapters 6, 7, and 13. There we see how to tame impedance and coupling for any reasonable value of SWR, and in those discussions the relative *unimportance* of having a ***self-resonant*** antenna also becomes evident. However, it is of great importance that we first clarify some of the prevalent misunderstandings of SWR and reflected power, because they are causing many amateurs to strive for a low SWR for the wrong reasons, often needlessly. Probably the most serious and widespread misconception concerning SWR prevailing throughout the amateur fraternity is the erroneous notion that there is a direct one-for-one relationship between reduction in reflected power and a resulting increase in radiated power. In other words, many believe that for every decreased watt of reflected power there is an additional watt of increased output. *Not so*, but the number of amateurs who have been misled to believe this invalid and unscientific premise is unbelievable.

Another related concept, popular but also erroneous, is that when terminated in a mismatch, the coaxial feed line becomes part of the radiator, causing radiation from the feed line because of the standing wave. (See Chapter 2, statement 18, and Chapter 20, Sec 20.4.) This is untrue because the line voltages and currents, and the standing wave resulting from the mismatch, are entirely contained in and between the outer and inner conductors, inside the coax. No standing wave develops on the outside of the coax because of impedance mismatch. However, feed-line radiation may result from standing waves on the outside of the coax because of current flowing on the outside, if a balanced dipole is fed without using a balun. This feed-line radiation may or may not be of any consequence, but the topic is covered well by McCoy (*Ref 45*). (Also see Chapter 20, Sec 20.3 and 20.4, and Chapter 21.) There is also no radiation from tuned open-wire feeders, because the current is flowing in opposite directions in each wire; hence the fields developed by the current in each wire are canceled.

Misunderstanding of how the benefits accrue from a low SWR, and of just how little benefit is obtained, is driving many of us to attain SWR values far lower than where the benefits continue to be significant in relation to the efforts expended to attain them. It is for this reason that we often set an unrealistically low limit on allowable SWR that needlessly restricts the operating bandwidth—the range of usable frequencies on either side of the resonant frequency of the antenna—to a far more limited range than is necessary. In rectifying a misunderstanding such as this, it often helps to first learn how the misunderstanding originated.

Sec 5.3 "Impedance" Bridges[1]

One aspect of the misunderstanding has been created to some extent by often erroneous interpretations of matching principles found in various instructions for instruments such as noise bridges (*Ref 100*) and the antenna-scope for determining the terminal "impedance" of an antenna. Contrary to what is stated in some of the instruction manuals, these devices cannot measure impedance—they can measure resistance only, and then only in the absence of reactance.[1] Look up and compare the definitions of impedance and resistance; the term impedance is often misused when the correct term should be resistance (*Ref 46*). Consequently, in using these devices we have been coerced into finding only the resistance component of the anten-

na terminal impedance, and only at the resonant frequency of the antenna, because this is the only frequency where the impedance has zero reactance, or R + *j*0. In following this approach, erroneous emphasis has been given to requiring the antenna radiator itself to be resonant, thus nurturing the misconception that it needs to be self-resonant to radiate all the power being supplied to it *(Refs 100 and 101)*. Thus, many have been misled to believe that the antenna just won't perform properly at any frequency except the self-resonant frequency. (See Chapter 2, statements 5, 6, and 7; also *Refs 20, 21, and 24.)* In addition, emphasis on the further necessity for obtaining an antenna-terminal resistance component equal to the line impedance Zc has in many cases caused us to go to extreme measures, such as adjusting the antenna height above ground in small increments to achieve that precise resistance reading in quest of the perfect 1.0 match (*Ref 101;* also see Chapter 2, statement 15). Adjusting antenna heights in large increments to obtain control of radiation in the vertical plane is realistic. However, controlling radiation resistance by adjusting the height is neither necessary nor practical, because the efficiency thought to be gained through this action is illusory. The truth of this will become evident somewhat later as we see why there is no justification for expending any matching effort at the load, or antenna, to improve a mismatch of 2:1 or less, simply to remove the standing wave with the expectation of improving efficiency (see Fig 6-1). Furthermore, because of the reactance that appears as we depart from the resonant frequency of the antenna, the sacred but overrated perfect match found at some carefully adjusted height can be obtained at only one frequency without retrimming the radiator length, thus continuing the vicious cycle. However, the widespread practice of this philosophy in antenna-system operation has conditioned us to think only in terms of using a $\lambda/2$ transmission line with no reflections, and to obtain its perfect 50-ohm non-reactive input impedance by operating only at the resonant frequency. Thus, we have, in effect, been deterred from learning of the real effect of reactance in antenna impedance, and how the transmission line

transforms any antenna impedance in a straightforward and predictable manner for use at the line input. In becoming so conditioned, many of us have forgotten that we can obtain the desired 50-ohm non-reactive input impedance from the line-transformed antenna impedance with a simple line-input matching network in the shack much more easily than it can be obtained at the antenna. In fact, with most tube transmitters the impedance seen by the transmitter at the input of the feed line for SWR values in excess of 2:1 can be matched for optimum loading by adjustment of the transmitter tank circuit itself. If a transmitter does not contain sufficient matching range, a separate line-matching network (antenna tuner) between the transmitter and line input offers a more judicious matching arrangement than playing games out at the antenna. Chapter 6 explains why there are many situations where this same matching approach should be considered when the load mismatch yields SWR values of even 5:1 or higher, as one departs from the self-resonant frequency of the antenna.

One further misconception exists that has also resulted in needless and unwarranted reliance on the $\lambda/2$ feed line to repeat the resonant antenna resistance at the transmitter. This one concerns the effect of line-input reactance on tank-circuit resonance when the line with reflections is fed directly by the pi network. Consider a tank circuit that is first loaded and tuned to resonance with a resistive load, and then when the load is changed to one containing reactance. If the tank components have sufficient retuning range to compensate for the reflected reactance to return the circuit to resonance at the same load level, all is well, because the tubes still see the same resistive load as before. The misconception about this point has been generated by some writers who apparently don't understand resonant circuits, for they proclaim that the retuning "introduces" reactance that detunes the circuit, causing improper loading and increasing plate current and dissipation. Wrong! Chapters 7 and 13 contain much more detail on this point.

Sec 5.4 Low SWR for the Wrong Reasons

We have discussed "low SWR for the wrong reason," as practiced (often unwittingly) in using the perfectly matched antenna operated only at the self-resonant frequency of the radiating element. However, another wrong reason for desiring a low SWR is interpreting feed-line SWR as the sole indicator of the quality of an antenna's radiating performance across a band of frequencies, with low SWR across the band getting the raves and high SWR getting the boos. This is a definite misuse of SWR information, because there are cases in which the low and high SWR values occur in just the opposite relation, with respect to indicating antenna efficiency over a given bandwidth. Reasons for this are given shortly. As a result of this misuse of SWR values, *good* antennas are too frequently rejected as "bad" because the feed-line SWR swings relatively high, and *poor* antennas are accepted as "good" when the SWR remains relatively low.

In most cases the use of feed-line SWR alone to indicate antenna efficiency is invalid, because SWR indicates only *the degree of mismatch*, not efficiency. However, we presently will see how a relative change in SWR, to a value either lower or higher than a previous value known to be correct in a given antenna system, can indicate that a possible undesirable change has occurred somewhere in the system. That change may affect its radiating efficiency. For example, the popular vertical antenna having from two to four ground radials (an insufficient number for efficient operation), or perhaps having only a buried water pipe or a driven rod for a ground terminal, is one case where a lower-than-normal SWR obtained over a frequency range indicates a poor quality of radiating efficiency, rather than a good one. Conversely, though, improving the ground system by adding a sufficient number of radials can increase the radiating efficiency to nearly 100%, and this improvement is accompanied by a *significant* ***increase*** *in SWR readings* over the same frequency range to higher values, which are the normal or expected values. With an adequate ground system, the SWR is predictable over the frequency range, because a load impedance of any specific $R + jX$ value yields an exact value of SWR on a given feed line, and because we can determine approximately what the antenna impedance should be at whatever frequency we may wish to use (*Ref 2, Fig 2-7; Refs 47, 48, 49, and 58; Ref 71, p 2-6).* However, when the ground system is inadequate there is an unknown ground-loss resistance added to the known antenna impedance, which changes the SWR to some lower and unpredictable value.

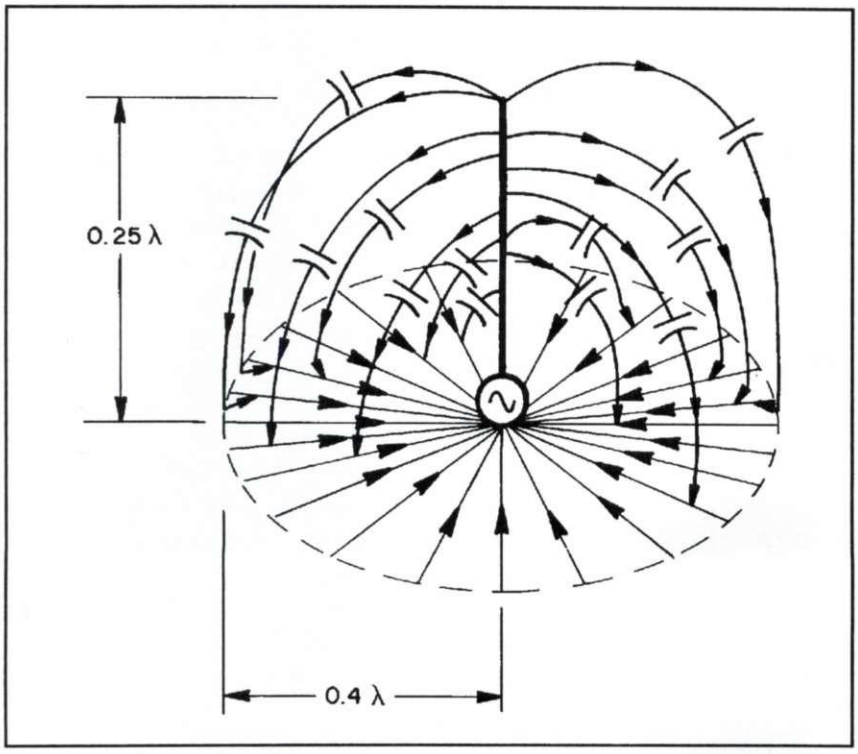

Fig 5-1. The hemisphere of displacement current that flows as a result of the capacitance of a λ/4 vertical radiator to the earth or a radial system. At frequencies above 3 MHz, RF currents flow primarily in the top few inches of soil, as explained in the text. Ground rods are of little value at these frequencies, and spikes or large nails are sufficient to secure the outside end of each radial wire. With a sufficient number of radials, annular wires interconnecting the radials offer no improvement in antenna efficiency, as the current path is radial in nature.

Yet, without being aware of these facts, we often tend to be happier in the discovery of an unsubstantiated low SWR than we are in determining whether we have SWR values that *should* be obtained with the existing configuration. This is a very important concept that requires a clear understanding if we are to avoid misinterpretation of SWR data in our effort to optimize radiated power.

It will help in understanding this concept if we have a clear physical picture of how the ground-loss resistance develops. Still another misconception exists here, this one concerning the current and field behavior in the vertical-over-ground antenna system. Most of us know that conventional grounding techniques used for lightning protection, such as rods or pipes driven deeply into the ground, provide an excellent low-resistance current path for the lightning current (DC). Many are unaware, however, that these techniques are totally inadequate for conducting the entirely different pattern of current flow with the vertical antenna system.

Sec 5.5 Vertical Radiator over Earth

Let us digress a moment for a brief look into the field and current behavior of the vertical antenna system to see what type of ground system is needed to meet the requirements of a proper current-flow pattern. Consider a base-fed vertical antenna as shown in Fig 5-1. One terminal of a generator is connected to the base of the vertical radiator and the other generator terminal is connected to ground, just below the base of the radiator. During the half cycle in which the conduction current in the antenna flows upward, all the current returns to ground through displacement currents, which follow the lines of force in the RF electric field through the radiator-to-ground capacitance, as shown in Fig 5-1.

The electric field surrounding the antenna, which excites the displacement currents, fills the entire volume of space surrounding the antenna in the shape of an oblate or somewhat squashed hemisphere. This hemisphere intersects the ground to form an imaginary circle having a radius of slightly over 0.4 λ for radiators of λ/4 in electrical height. This radius defines the distance from the antenna at which the returning displacement currents become insignificant and don't justify radials of greater length. The radius decreases as the height of the radiator decreases, because the size of the hemisphere surrounding the antenna decreases. Also, radials in or on the ground have no resonance-versus-length characteristic; when outward-

flowing current reaches the end of the radial, it continues flowing in the ground instead of going to zero and becoming reflected to flow in the opposite direction, as it does in elevated radials. The displacement currents enter the ground *everywhere over the entire surface within the circle* and then flow back radially to reach the grounded generator terminal. Therefore, to repeat for emphasis, ground radials are *not resonant*. Although some of the current penetrates somewhat more deeply, most of the current flow at frequencies above 3 MHz is restricted by skin effect to the upper few inches of the ground. Now a ground system comprising only a simple water pipe or a driven rod or two is simply a terminal—the ground-feed terminal of the antenna system. Thus, all the returning currents using this arrangement must flow entirely through the poorly conducting ground from all directions everywhere within the circle to reach the terminal. This ground system is often measured to have an "acceptably low" resistance *at DC* (which may be satisfactory for lightning protection), but it injects a loss resistance in series with the antenna *at RF*. The RF ground resistance often exceeds the radiation resistance of the antenna itself! Adding a few wire radials to the system provides good conductivity toward the ground terminal for the currents that reach those radials. However, only a tiny amount of the total current entering the Earth's surface inside the circle is intercepted by these few radials. Thus, all the remaining currents still flow only through the lossy earth, and the result is that we still have a high loss resistance.

If a sufficient number of equally spaced radials (90 to 100) extending out to 0.4 λ are present to intercept all the current, all the returning displacement currents find highly conductive paths everywhere within the circle, which lead the currents through negligible loss resistance directly back to the ground terminal of the generator. This can be visualized by examining Fig 5-1. Currents that enter the ground between the closely spaced radials quickly diffract to a radial wire, and thus travel only a short distance through lossy earth before reaching a good conductive path. Thus, with a sufficient number of radials, we have a nearly perfect ground system, which adds only a negligible amount of resistance to the true antenna impedance measurable between the base of the radiator and the ground terminals (*Refs 20, 50, 51. and 57*). From this we can see why the lightning-type ground system, although in prevalent use, is unsatisfactory for an efficient antenna system (*Ref 57, p 82*). I am not suggesting that λ/4 antennas with less than ideal ground systems should not be used, nor that fair results cannot be obtained without their use. However, the difference between no radials, or only 3 or 4 compared to 100, can amount to over 3 dB. This is far in excess of the loss resulting from an SWR of 4:1 or 5:1 on the average coaxial feed line used by amateurs. The point made here is that the value of ground resistance is unknown and unpredictable in systems using less than an adequate number of radials. This makes the resulting SWR readings unpredictable and therefore useless for the purpose of evaluating the quality of the system, unless some means is available for determining what the change in SWR would be if the loss resistance could be switched in or out.

In practical amateur installations, the ground resistance is sufficiently low if only 40 to 50 radials are used with a λ/4 radiator. The small improvement in radiated power for the addition of still another 40 to 50 radials with the λ/4 radiator probably does not justify the extra cost and effort. However, if a *short* vertical antenna (from λ/8 or less, to λ/4) is contemplated, remember that the radiation resistance decreases as the radiator is shortened. The ground resistance then becomes a larger part of the total resistance, decreasing the efficiency. Thus, the ground resistance should be kept as low as possible for the full capability of the short antenna to be realized (*Refs 51, 56, and 57*). There is practically no difference between the radiation capabilities of the λ/4 antenna and a radiator even shorter than λ/8, except for the effect of ground resistance and the loss in the resistance of the inductance coil used to cancel the capacitive reactance in the terminal impedance of the shortened antenna. The professional literature is replete with references confirming this point (*Refs 20, 52, and 53).*

Sec 5.6 Resistive Losses and SWR

In this section I discuss how *any* additional resistive losses that are separable from the true antenna impedance affect the true load SWR. By separable I mean losses such as ground-loss resistance, corroded connectors and other poor connections, cold-

solder joints, and so on. These all contribute loss resistances that we can control or reduce. In contrast is the resistive component of the antenna terminal impedance, which comprises both the radiation resistance and the inherent conductor-loss resistance in the radiating element. In most cases the conductor-loss resistance in practical radiating elements is negligible, unless excessively small wire is used. There are several useful relationships between load impedance $Z_L = R + jX$, line impedance Z_C, and SWR. For example, it is well known that when the load impedance is a pure resistance R, equal to the line impedance Z_C, the reflection coefficient ρ is zero, and the standing-wave ratio is thus one to one. However, the reflection is no longer zero and the SWR becomes equal to the ratio R/Z_C when the resistance is larger than Z_C, or Z_C/R when the resistance is smaller than Z_C. It is also well known that ρ and SWR increase with the addition of any reactance component in the load impedance that increases the total reactance, whatever the resistive component may be. This relationship may be verified by observing Eq 3-1. Also, as noted previously, any combination of $R + jX$ yields an exact value of SWR when terminating a line of given impedance Z_C. We also know that the reactance X appearing in the impedance at the terminals of an antenna contributes more to the rise in SWR at frequencies away from antenna resonance than the change in the antenna resistance. This is because the reactance changes more rapidly than the resistance during the change in frequency, and because no power is absorbed in the reactance.

However, there is an interesting relationship between the resistance and reactance components of a load impedance that is not generally well known. This relationship sheds light on how these two impedance components affect mismatch reflection and SWR, and it also explains why the unknown ground resistance and other losses mentioned above reduce the usefulness of SWR readings. When reactance is present in the load impedance, the minimum possible SWR occurs when the resistance R is greater than Z_C. The value of the resistance that yields the lowest SWR in combination with a given value of reactance in the load, which I call the minimum-SWR resistance, is dependent solely on the reactance present in the load. This value may be obtained from the relationship:

$$r = \sqrt{x^2 + 1} \qquad \text{(Eq 5-1)}$$

where

r and x are normalized to the system Z_C

r = minimum-SWR resistance

x = reactance present in the load

(For more information concerning Eq 5-1 and its proof, see Chapter 11, Sec 13.3 and Appendix 1) It can be seen from Eq 5-1 that when x becomes zero, r = 1, for an SWR of 1:1. However, it is interesting to know that the resulting SWR *always equals exactly* the arithmetic sum of the minimum-SWR resistance value r, and the reactance value x. This interesting relationship is shown in the following expression:

$$SWR_M = r + x \qquad \text{(Eq 5-2)}$$

where

SWR_M = SWR obtained with the minimum-SWR resistance

r = the normalized minimum-SWR resistance

x = the normalized reactance

The relationship shown in Eq 5-2 can help us to understand how unwanted loss resistance, separable from the true antenna-load impedance, affects SWR. In the case of the vertical radiator over earth, the unpredictable ground losses change the SWR from a predictable value, based on known available antenna impedance data (*Ref 48, p 176*) to some unpredictable and usually lower value. A general application of the relationship is presented in the following statements. When the resistance component of the true load impedance is lower than the minimum-SWR resistance, as determined for any reactance component also present in the true load, adding of resistance separate from the true load impedance will cause the SWR to decrease from the value obtained with the true load resistance. This is true until the total resistance is equal to the minimum-SWR resistance. The further addition of resistance will cause the SWR to rise again. These statements apply especially to the vertical antenna of $\lambda/4$ heights or less in proving why ground resistance which reduces the efficiency also reduces the SWR. This is because the true antenna resistance component, R, is generally less than the imped-

ance, Zc, of normally used feed lines, while the minimum-SWR resistance, R, is always equal to or greater than Zc.

The effect of reactance in the antenna impedance raises an additional factor of importance in understanding the relationship between SWR values and antenna performance. As stated earlier, the rate at which the SWR rises as the operating frequency departs from the resonant frequency of the antenna depends on the resulting change in the impedance at the antenna terminals, which in turn is dependent on the Q of the antenna. One factor that has a primary influence on antenna Q is the amount of capacitance between the opposite halves of the dipole. (Although it is more commonly called a monopole, a vertical antenna over ground can also be considered as a dipole, because the lower half is simply the image of the upper half, with the opposite polarity.) This dipole capacitance is determined by the ratio of the radiator length, L, to its diameter, D, the well-known L/D ratio.

The L/D ratio found in the usual simple thin-wire dipole is very high, resulting in a low dipole capacitance and high Q. When the frequency is changed with such an antenna, rapid changes in impedance, reflection, and SWR result. This is why a thin-wire dipole is considered a narrow-band device. However, specific broad-banding steps may be taken to increase the dipole capacitance and thus reduce the Q, thereby reducing the rate of change of SWR. One such step, for example, is decreasing the L/D ratio by using a multiwire cage configuration for each dipole half, or by fanning out multiple wires from the feed point. Curves of SWR versus frequency are valid here in comparing bandwidths obtained while you experiment with different radiator configurations. However, any separable loss resistance must now be either minimized or held constant to prevent it from introducing unknown variables. Otherwise, the unknown variables can cause differing errors in the SWR readings obtained with different configurations, and thus render the results of the experiment invalid. However, unless actual broad-banding steps have been taken to reduce the Q, the rate of change in SWR as frequency changes will not differ dramatically among various types of dipoles having roughly equivalent values of Q. These types include the inverted-V dipole. If a dramatic difference is noted with no *valid* broad-banding steps having been taken, troubleshooting is called for to determine the cause. More than likely some unwanted loss resistance will be flushed out, if this is the case. I have seen SWR curves published with descriptions of quite simple antennas, where it would have been impossible for the SWR to remain as low as indicated over the frequency range shown; the Q of the antenna configuration shown simply would have been too high. Two possible explanations for this sort of contradiction are that (1) perhaps the readings were obtained from an inaccurate SWR indicator—many read on the very low side (*Refs 40, 54*); or (2) as suggested above, an unrecognized trouble existed somewhere in the antenna system which was lowering the Q by means of a separable loss resistance. Yet these articles were published because the antennas they described were purported to have "improved SWR characteristics." How many times have you heard someone praise his newly hung skywire simply by telling how low the SWR indicator reads across an entire band? It should now be clear, and it cannot be emphasized too strongly, that an unrecognized and unwanted loss resistance in an antenna system can cause a low SWR reading when *it should not be so low*. Therefore, in Chapter 6 we will explore the relationship between antenna impedance and SWR in detail so that we may determine what is a proper SWR for given conditions.

Sec 5.7 Reflected Power and SWR

Let us now return to the subject of why we worship low SWR for the wrong reason. As stated earlier, the misunderstanding of this aspect of reflected power is based primarily on the prevalent, but erroneous, notion that any reduction in SWR or reflected power effected on a line feeding a mismatched antenna results in a direct one-for-one increase in radiated power. The erroneous reasoning behind this notion is in the assumption that if power is being reflected by a mismatched load, it cannot be absorbed in the load or radiated, and that the reflected power returns to be lost to dissipation in the transmitter. This assumption is false on both points, for the truth is, except for the power dissipated in the line itself because of line attenuation, *all* of the power delivered to the line by the transmitter is absorbed in the mismatched load. This is

true because the power reflected from the mismatch is conserved and returned to the load by re-reflection from the line-input matching circuitry, the antenna tuner, in accordance with the principles discussed in Chapter 4.

In light of the above statement, let us consider a lossless line for a moment. Adhering to the Law of Conservation of Energy, here it is axiomatic that if all power delivered to the line is already being absorbed in the load (because none can be absorbed in a lossless line), a reduction of the reflected power cannot have any effect whatsoever on the amount of power taken by the load. Also, obviously, there is no power left over to be dissipated in the transmitter.

Following this same reasoning in a real line having attenuation, *all losses in power* must be attributed to the basic I^2R and E^2/R losses arising from attenuation due to line resistance. These losses are unavoidable, even when the load is perfectly matched. The only *additional losses in power* that can be attributed to SWR or reflection occur because the same resistive attenuation is encountered by the reflected power as it travels back along the line from the load to the input. The amount of power lost in this manner is very small at frequencies in the HF range when good-quality, low-loss line is used. This is because during its return to the input, the reflected power suffers only the same amount of line-attenuation loss as the forward power suffers in its forward travel toward the load. In addition, as stated previously, all the reflected power that arrives back at the input now becomes part of the forward power due to total re-reflection at the input.

Another way of explaining the relationship between SWR and lost power is to recall from Chapters 3 and 4 that because the forward power is the sum of the source and reflected powers, the forward power is greater than the source power whenever the SWR is greater than 1.0. Thus, for a given source power, the resistive losses are somewhat higher in the portion of line where the forward power is higher than the source power, simply because the average line current I and voltage E are higher in that portion of the line.

Therefore, from this discussion concerning improper usage of SWR data, we learn that from the viewpoint of efficiency, our concern for SWR involves only the loss from line attenuation. Hence, we can tolerate a higher SWR when the attenuation is low, but when attenuation is high the SWR limit must be lower for the same amount of additional power lost from SWR. The exact relationship between SWR and line losses for different values of line attenuation is shown graphically in Figs 1-1 and 6-1. From these graphs we can easily see that the amount of power actually lost is in sharp contrast to the amount mistakenly assumed to be lost in the improper concept of SWR, where it is thought that a reduction in SWR or reflected power results in a direct equivalent decrease in the amount of power lost in the system.

There is a certain twist of irony behind these various misunderstandings of reflections that have prompted the wrong interpretation or usage of SWR. The irony is that the correct reasons why SWR should be considered are frequently overlooked in the wrong usage, while the basis so generally accepted in support of the wrong usage does not even exist in the coupling methods used by amateurs to transfer power from the transmitter to the antenna. A part of this obtuse logic seems to have originated from the confusion among both amateurs and engineers in the meaning of "a matched generator." To some it means being matched in only one direction, and to others it means being matched in both directions. A "matched" signal generator is generally considered to be Z_0 matched, or matched to the line impedance in both directions. However, in transmitter operation, the match is in one direction only—forward—because of the total re-reflection of the load-reflected wave by the matching circuitry at the input to the transmission line. This subject is treated in great detail in Chapters 6, 7, 16, 17, and 19.

Note

1. Author's note: The original *QST* text from which this chapter is adapted was written before noise bridges were constructed with the capability of measuring reactance.

Chapter 6

Low SWR for the Right Reasons

(Adapted from QST, *December 1974)*

Sec 6.1 Introduction

Chapter 5 concludes with the statement that in transmitter operation, where conjugately matched coupling is normally used to deliver power to a load through a transmission line, the match is in one direction only—forward. The transmitter (or generator) output is matched to the line, but looking back into the generator, the line is totally mismatched during the time the generator is actively supplying power to the line through the conjugate coupling of the pi-network tank. If the correct procedure is followed, the conjugate relationship may be demonstrated by making impedance measurements in either direction from any point on the line. These measurements will show an impedance $R + jX$ looking in one direction, and the equal but opposite-sign impedance $R - jX$ in the opposite direction. The net reactance of zero obtained from these two impedances proves that the system is resonant! However, these measurements cannot be performed while the generator is active; it must be *turned off* and replaced with a passive impedance equal to its optimum load impedance. When this is done the impedance terminating the generator end of the line will be seen as a dissipative load when measuring the impedance in the direction of the generator.

One of the prevalent misconceptions is that when reflected power returns to the generator, it sees the plate resistance of the amplifier tube as a dissipative terminating resistance. The fact that dissipation occurs in the impedance that replaces the generator impedance during the measurements described above is partly responsible for the erroneous inference that power reflected toward the generator is dissipated in a similar manner in the internal impedance of the generator. However, when the generator is supplying power to the line, its internal impedance is never seen as a terminating load for power reflected from a mismatched load terminating the line. This is true because of the wave interference between the source wave, the load-reflected wave, and the canceling wave supplied by the coupling network that eliminates the reactance and achieves the total re-reflection of the load-reflected wave. Hence, the line is totally mismatched looking rearward in the direction of the generator. This entire phenomenon is described in detail in Chapter 4.

On the other hand, in laboratory work the signal generator is usually matched in *both* directions. Here the generator has a Zc source impedance at the output terminals, usually 50 ohms, and it is also isolated from the line with a resistive pad or attenuator. The pad usually has an insertion loss of around 20 dB (sometimes more) with the same impedance as the generator output and line Zc. Thus, the generator sees a match looking into the pad. This is because the pad absorbs and dissipates both forward and reflected power like a lossy line, so that only about 1/100 of the source power reaches the load, and any power reflected from a mismatched load is also dissipated to 1/100 of its original value during its return to the generator. As a result, whether the load is a totally reflecting short- or open-circuit termination, the reflected power reaching the source is about 40 dB below, or only 1/10,000 of the power delivered by the generator. Consequently, the power delivered by the source of the generator remains constant, unaffected by the returning reflected power. Thus, the pad appears to the generator as either an infinitely long line, or a line having a perfect R = Zc termination. As a result, reflected power returning from a mismatched termination on the line, the device under test, does not reach the generator with sufficient power to significantly affect its output power, or to modify the impedance which the generator source sees as its load. Consequently, the forward voltage entering the transmission line at the output of the pad is held constant, independent of the load im-

pedance presented by the device under test (*Ref 19, p 48*). Thus, it is understandable that confusion between these two forms of matching can be responsible for misleading us to thinking that reflected power in the transmitter case is dissipated and lost on return to the source.

Sec 6.2 Reflected Power versus "Lost" Power

The erroneous conception that reflected power is lost is widespread, having been nurtured on the air for a long time, and supported in print in so many published articles it would be impossible to count them. Two such articles, one by Houghton (*Ref 102*) and the other an SWR-indicator review by Scherer (*Ref 103*), are especially pertinent, because they contain explicit statements supporting the erroneous concept, whereas statements in many other articles only support the error implicitly. Let us now make a further analysis of the reflection mechanics involved in generator matching. In this analysis, two important ingredients that have been overlooked for a long time will be revealed. In so doing, we will see why statements concerning lost power published in the two articles mentioned above are incorrect. We will also see why it was so easy for these ingredients to be overlooked early in the amateur use of coaxial transmission line, with the result that many amateurs have been misled into seeking low SWR for the wrong reason.

Let's consider a lossless transmission line having a perfectly matched load termination. The line is also matched to the generator or transmitter. Under these conditions, there is no reflected power in the line and therefore no reflection loss. Thus, the generator delivers what is defined as the maximum available matched power, and the load absorbs all the power delivered. If the load termination is now changed, creating a mismatch between the line impedance Zc and the terminating load, less power will be absorbed by the load. The amount of reduction in absorbed power resulting from the change in load impedance is the measure of the reflection loss. As the reflected power wave returns toward the generator, it causes a change in the line impedance from Zc to a complex Z = E/I all along the line. This change is as described in Chapters 3 and 4, and as shown for an SWR = 3.0 in Fig 3-2. When the reflected wave reaches the input terminals of the line, the generator is presented with a change in line-input impedance from the original Zc value to some new value determined by the complex E/I vector relationship appearing at the line-input terminals. This new impedance at the line input has exactly the same degree of mismatch to the line Zc as the mismatched terminating load that generated the reflection. Thus, the line is also now mismatched to the generator in the same degree, and in this condition the generator will automatically make less power available to the line in the amount determined by the resulting mismatch.

The reduction of power delivered to the line is exactly the same amount as the power reflected at the load. In other words, the reflection loss at the load is referred back along the line to the generator. Thus, reflection loss is simply a *non-dissipative* loss representing only the unavailability of power to the load because the generator makes less power available as a result of the impedance mismatch at the line input.

It will now become evident that reflection loss represents only the *unavailability* of power to the load, as we see that the load absorbs all the power the generator makes available to the line. On reaching the generator terminals and causing the mismatch to the generator, the reflected power adds to the reduced source power by exactly the same amount of power as the decrease in power made available by the generator. Since forward power now equals the source power plus the reflected power, the forward power reaching the mismatched load remains the same as before the generator reduced its power available for delivery. Hence, the reflection loss equals the amount of decrease in power made available by the generator. However, because the power reflected by the load is now a part of the forward power reaching the load, the forward power continues at the same level as that originally delivered by the generator prior to decreasing its delivery. Thus, the load continues to receive the original amount of power, and reflects the original amount of power, and therefore absorbs *all* of the decreased power delivered by the generator. If an impedance match is now provided anywhere along the line, even at the input terminals, the reflected power is prevented from traveling past the match point toward the generator, as

explained in Chapter 4. Thus, the line impedance between the match point and the generator is now unaffected by the reflected wave, and remains at its Z_C value at the input. Consequently, the generator no longer sees a mismatch and again delivers its *maximum available* power to the line. The impedance match has thus provided a negative reflection, commonly called "reflection gain," which exactly equals and cancels the reflection loss. Consequently, all the power delivered by the generator is absorbed in the load in either case—with or without the reflection gain. The generator simply made less power available before the reflection gain restored the matched condition between the generator and the line (*Ref 19 p 37*).

Therefore we now ask the question, how does this situation relate to the Houghton nomograph (*Ref 102*), where reflected power is stated to be "lost power," and to the "useful power" table from the *Knight* SWR indicator review (*Ref 103*).[1, 2] It is this: The nomograph simply converts SWR back to reflected power, ρ^2, which is what the SWR indicator actually measures but converts to SWR by means of its scale construction. As discussed in Chapter 3, ρ^2 is the measure of reflection loss or power reflected, which equals the decrease in power made available from the transmitter, calculated directly from the mismatch between the characteristic impedance Z_C of the line and the terminating load impedance Z_L. The reflected power is the square of the voltage (or current) reflection coefficient, ρ, from Eq 3-1 (also see Fig 3-2), but remember further that reflected power ρ^2 is a *non-dissipative* power, because it all eventually reaches the load and absorbed, as explained in Chapters 4 and 5.

The tabulated data in the SWR-indicator-review article correctly lists percentage of reflected power ρ^2 for corresponding values of SWR. However, the "useful-power" column is incorrectly labeled, and is therefore misleading because it is actually listing percentage values of $(1 - \rho^2)$, which is the portion of the maximum-available *matched* power the transmitter actually delivers, depending on the degree of mismatch it sees. In other words, the "useful power" column is simply specifying the amount of power the transmitter will deliver into the mismatch if first tuned to a line having a matched Z_C load, and is then switched to the mismatched load without the benefit of *retuning* or *re-matching* to the new impedance at the line input. However, we do not operate in this manner. We retune, thereby re-matching the transmitter to the new load, and consequently establishing the reflection gain as:

$$\frac{1}{1 - \rho^2}$$

which completely cancels the reflection loss ρ^2 and the effect of the load mismatch. The transmitter now returns to delivering *100%* of its matched available power to the line, whatever the SWR on the line may be! Thus, the two missing ingredients are: (1) understanding the concept of reflection loss and reflection gain; and (2) the discovery that the reflected power is totally re-reflected at the transmitter output terminals, either with or *without* the reflection gain.

It is now evident that the information presented by Houghton and Scherer is not specifying "lost" power at all, but only the non-dissipative *reflection loss*—the amount of power made unavailable by the transmitter until an impedance match provides the reflection gain, which cancels the reflection loss and permits the transmitter to again deliver its maximum-available matched power. Also, as stated on several previous occasions, the conjugate impedance match is automatically attained (sometimes unknowingly) either by proper tuning of the transmitter tank circuit to the complex line-input impedance E/I, or (knowingly) by use of a line-matching network if the pi-network tank of the transmitter lacks sufficient range to obtain the match by itself. How the tank performs the impedance match, and the effects of undercoupling, overcoupling, and possible reactive loading of the tank which can result in the absence of the impedance match are explained in detail in Chapter 7.

Sec 6.3 Reflection Gain

Refer now to Fig 6-1. This figure was developed to illustrate the concept of *reflection-gain*, in order to emphasize the effect of misinterpreting reflection loss to be "lost" or dissipated power. The impact of this single misunderstanding of transmission-line principles has been disastrous, because it is the principal cause of the prevalent "low-VSWR mania" (low-vis-war-ma'nya). It is the rea-

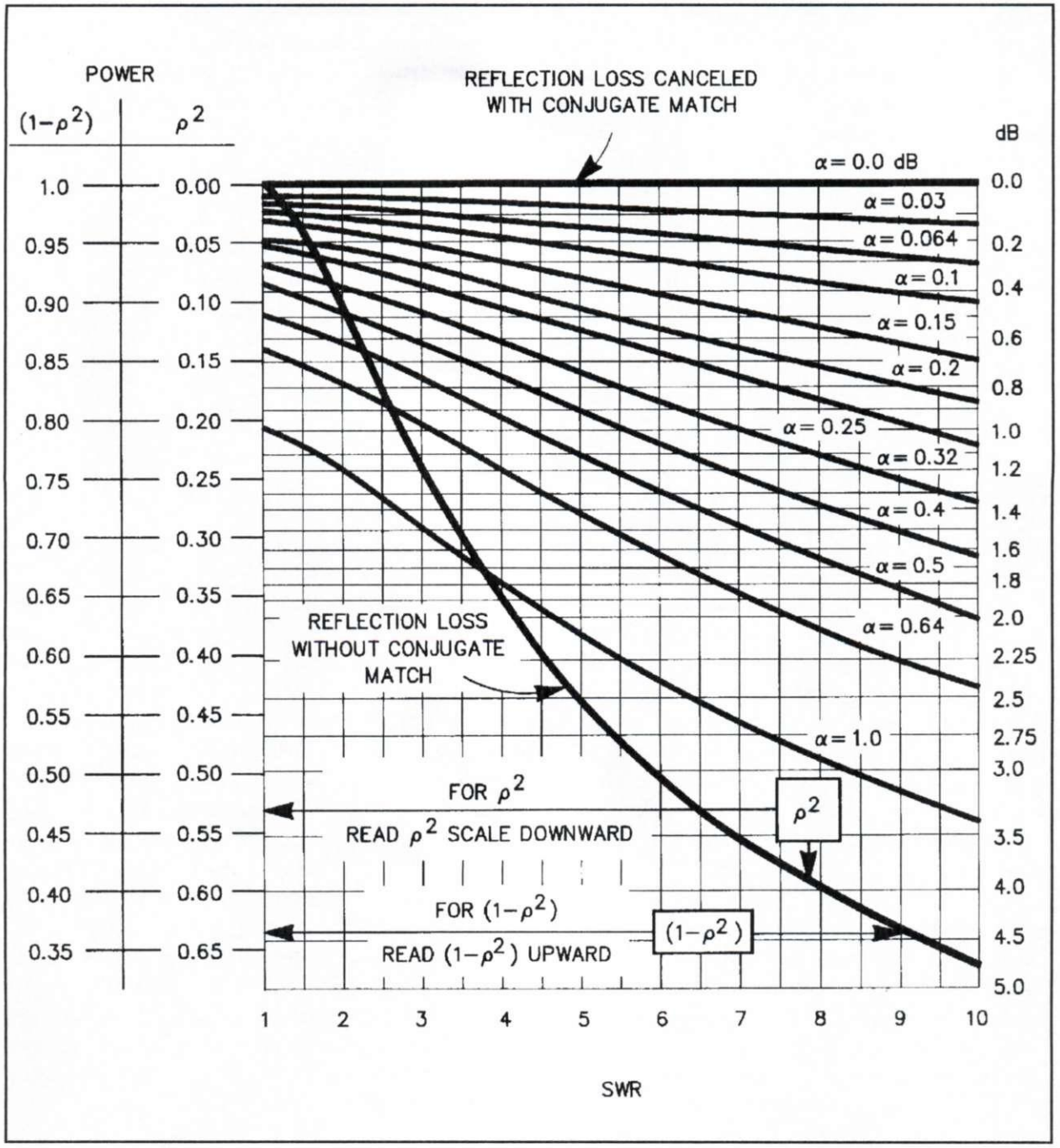

Fig 6-1. Reflection loss versus SWR and matched-line loss of RF transmission lines. Total attenuation in a line operating with SWR may be determined from the dB scale at the right of the chart. The calibration scales at the left are discussed in the text. The α alpha curves in the body of the chart represent the matched-line loss for any given transmission line. For example, the following types and lengths of line would exhibit the attenuation factors indicated at the frequency of 4 MHz: α = 0.03 dB for 100 ft of no. 12 open-wire line; α = 0.064 dB for 20 ft of RG-8; α = 0.1 dB, for 100 ft of Amphenol twin-lead, no. 214-022; α = 0.2 dB for 62.5 ft of RG-8; α = 0.32 dB for 50 ft of RG-59, 100 ft of RG-8, or 200 ft of RG-17; α = 0.5 dB for 87 ft of RG-59 or 175 ft of RG-8; α = 0.64 dB for 100 ft of RG-59 or 200 ft of RG-8; α = 1.0 dB for 119 ft of RG-58, 350 ft of RG-8, or 700 ft of RG-17. For mathematical derivations of Eqs 6-1 and 6-2 see Appendix 5. The curves are plots of Eqs 6-1 and 6-2.

Incident or Forward Power (multiply by source power delivered)			–	Power Reflected (by load)	=	Power Absorbed* (by load)	
Power at Match Point		Power at Load (after line attenuation)					
$\frac{1}{1-\rho^2\varepsilon^{-4\alpha}}$	→	$\frac{\varepsilon^{-2\alpha}}{1-\rho^2\varepsilon^{-4\alpha}}$	–	$\frac{\rho^2\varepsilon^{-2\alpha}}{1-\rho^2\varepsilon^{-4\alpha}}$	=	$\frac{(1-\rho^2)\,\varepsilon^{-2\alpha}}{1-\rho^2\varepsilon^{-4\alpha}}$	(Eq 6-1)

With lossless line $\alpha = 0$, therefore

$\frac{1}{1-\rho^2}$	→	$\frac{1}{1-\rho^2}$	–	$\frac{\rho^2}{1-\rho^2}$	=	1	(Eq 6-2)

where

ρ = magnitude of reflection coefficient (see Chapter 3, Sec 3.1)

α = line attenuation in nepers = dB ÷ 8.6859

ε = 2.71828, the base of natural logarithms

**Power Absorbed* = $\frac{(1-\rho^2) \text{ times one-way line-attenuation factor}}{(1-\rho^2) \text{ times two-way line-attenuation factor}}$ × source power

son why so many amateurs wrongly believe that "getting the SWR down" is the most important factor in "getting the power into the antenna." They fail to realize that whatever the SWR with a low-loss feed line, the reflection gain obtained inherently by the tuning and loading procedure has canceled the effect of the load mismatch if the transmitter can be made to tune and load properly into the line, and that all the available transmitter power is already being taken by the antenna. Therefore, as explained in Chapter 5, they have also been unaware that no more power of any significance reaches the antenna by achieving the lower SWR. They have also been unaware that line attenuation is the key to whether the SWR level has any *practical* effect on efficiency at all.

In Fig 6-1, the heavy curve marked ρ^2 and $(1 - \rho^2)$ is based on lossless-line conditions. It is also an exact replotting of the Houghton "lost power" nomograph (*Ref 102*), and indicates both the reflected and so-called "useful power" columns from the Scherer's SWR-kit review article (*Ref 103*). Reading downward from the top of the chart, the heavy curve represents reflected power ρ^2 versus SWR. Conversely, the power made available by the transmitter versus the mismatch it sees in terms of SWR, $(1 - \rho^2)$ is found by reading upward from the bottom of the chart. Thus, in reading upward, the curve represents the power being made available with the transmitter tuned for a perfect Zc match, but actually looking into an uncorrected mismatch. However, as explained earlier, when the reflection loss is canceled by the reflection gain obtained by re-establishing the impedance match by retuning the transmitter, a new curve, $\alpha = 0.0$ dB, which now represents the newly matched condition, follows *the heavy straight line horizontally across the top of the graph.* This indicates that 100% of the power is being made available, and is also absorbed by the load *regardless of the value of the SWR.* Suddenly the "lost" power is found! Since the curves we've just been discussing represent conditions on *lossless* lines, it is evident that neither Houghton nor Scherer was even considering line attenuation in their presentations.

As stated earlier, power can be "lost" in a transmission line only through line attenuation, alpha (α). If the attenuation is zero, lost power is also zero, as shown along the straight-line $\alpha = 0.0$ dB curve at the top of Fig 6-1. When the line has attenuation, power is lost, as shown by the various loss curves marked $\alpha = 0.03$ dB, etc. Since no allowance for the attenuation factor was made in either case in the material presented by Houghton and Scherer, we have still another reason why the terms "lost power" in one case and "useful power"

in the other are incorrect and misleading (*Ref 55*).

In Chapter 15 I deal in detail with attenuation effects and show how to perform some of the pertinent calculations based on Eqs 6-1 and 6-2, which are used as the basis for the loss curves appearing in Fig 6-1. However, these loss curves are in a form practical for visualizing the correct relationship between the losses actually encountered in feed lines of various lengths, values of attenuation, and values of SWR. From these curves we can determine the total loss encountered on the line arising from attenuation for the values of SWR indicated on the scale at the bottom of the chart. The curves represent the condition in which the transmitter is matched to the input of the line, and therefore signify that the effect of the load mismatch is canceled in each case. Each curve starts at the left, where the SWR is 1.0, thus indicating the actual attenuation encountered by a particular line when terminated in a perfectly matched load.

Continuing, the loss value along each curve is seen to increase logarithmically as the SWR on the line rises with increasing mismatch due to mis-termination of the line. Thus, the difference between the loss incurred with a 1.0 SWR compared to that for any other given SWR value on the same line indicates the amount of additional loss that will be incurred for that SWR. Hence, the graph in Fig 6-1 presents further evidence that when the line attenuation is low, the additional loss from reflection is surprisingly small, even when the SWR is quite high.

Examine the SWR region between 1:1 and 2:1. Do you see enough difference in power level on

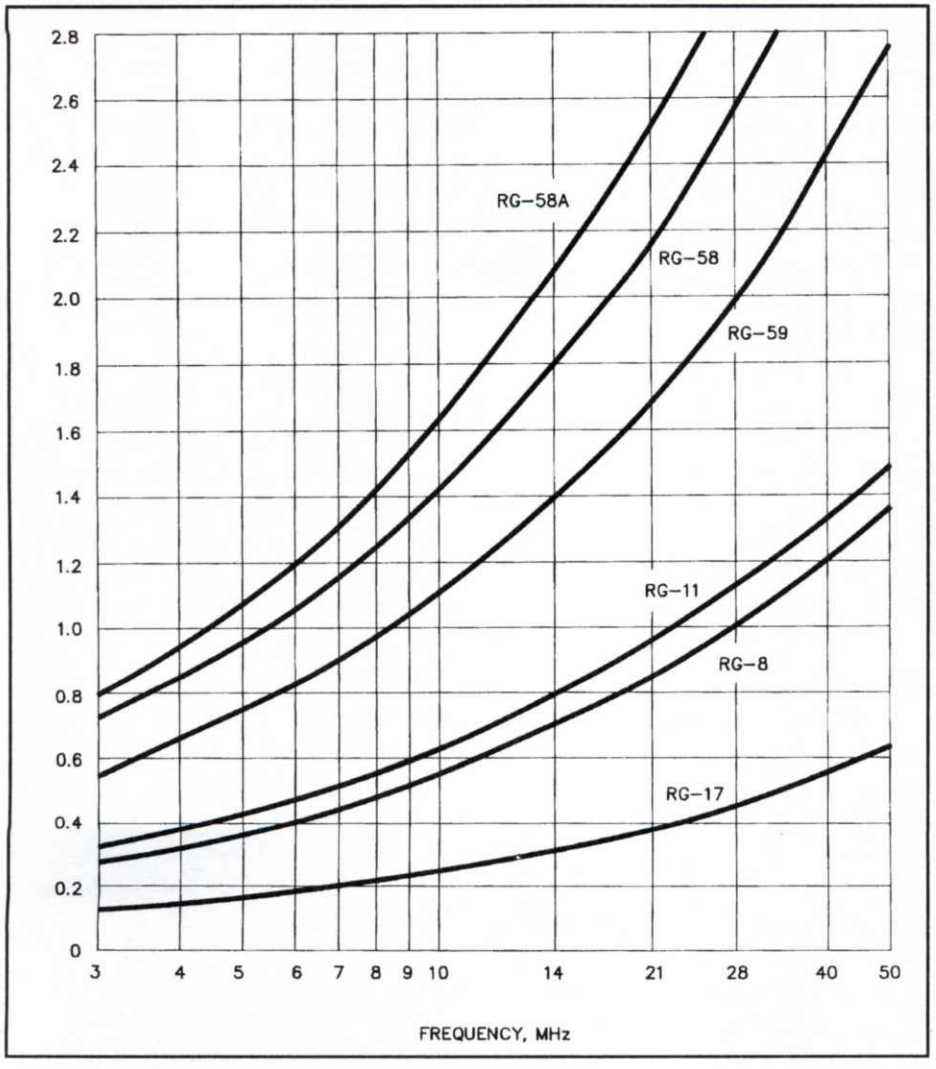

Fig 6-2. Attenuation in decibels per hundred feet for various coaxial cables.

any of these curves to justify any effort in reducing a 2:1 SWR to *any* lower value whatsoever? Do you still think you'll get out better by squeezing that SWR of 1.8 down to 1.2? A review of Chapter 1 is now appropriate to re-emphasize how the use of these concepts can broaden our design flexibility. It is also reassuring to check the efficiency values of both the TIROS and NAVSAT spacecraft feed-line examples from Chapter 1 in the Fig 6-1 graph. In the NAVSAT example, comparison of the 65% reflected power with only 1.04 dB actual line loss is especially revealing.

Fig 6-2 provides additional line-attenuation data, permitting us to extend the use of the Fig 6-1 curves to other frequencies and transmission lines. Fig 6-2 may also be supplemented with further data available in *The ARRL Handbook* and *The ARRL Antenna Book* (*Refs 1, 2, and 71*).

Sec 6.4 Radiation Resistance

In Chapter 2, statement 26 says, in effect, that with mobile whip antennas in the 80- through 10-meter bands, no significant amount of power is saved by using matching circuitry between the feed line and the antenna terminals. Also, statement 27 goes on to say that in the absence of such matching circuitry, more power is radiated from center-loaded mobile antennas that have a high feed-line SWR at resonance than those that have low SWR. The concepts involved in those two statements are also widely misunderstood, so this is an appropriate time to clarify both of these statements. These concepts also fit the category of "low SWR for the wrong reasons."

It is well known that the radiation resistance of the short whip-type mobile antenna is very low. Also, of all the HF amateur bands, the radiation resistance is the lowest at 80 meters, because the electrical length of the radiating portion is the shortest on this band. Depending on the exact length of the antenna and other factors, the radiation resistance of the center-loaded antenna is approximately 1 ohm at 80 meters, as shown by Belrose (*Ref 60*). The capacitive-reactance component in the terminal impedance of this short antenna ranges from $-j3000$ to $-j3500$ ohms in typical 80-meter models, as shown by Belrose and also confirmed by my own measurements using a General Radio 1606-A RF impedance bridge. This capacitive reactance is canceled by the equal $+jX$ inductive reactance of the loading coil.

However, it is not well known that there are two other resistances that become important for consideration in antennas of this type. These resistances, from loading-coil loss and ground loss, add to the radiation resistance to comprise the total resistive component of the impedance appearing at the antenna terminals. Thus, by ignoring these two resistances, it is erroneously thought by many amateurs that the 1-ohm radiation resistance alone comprises the entire antenna-terminal impedance, and also that it requires a matching device at the antenna to match what is thought would be about a 50:1 mismatch if fed directly with a 50-ohm feed line. Actually, the loss resistance in the loading coil and any ground-loss resistance both add to the radiation resistance, causing the terminal resistance of the antenna to be much higher than is commonly realized, although still lower than the 50-ohm feed lines that are normally used. Thus, the actual mismatch value is much lower than is usually realized.

While there are some who recognize that loading-coil loss appears as part of the total terminal impedance, only a few are aware that ground-resistance loss also exists, because, except for Belrose, most writers neglect to mention it or consider it in their system analysis. For example, see Swafford (*Ref 116*).

The *Mobile Handbook* (*Ref 117*) not only fails to recognize the existence of ground resistance, but misconstrues what is actually the combined ground and radiation resistances as radiation resistance alone. For example, in subtracting 6 ohms of terminal resistance, the 8-ohm difference is simply taken to be radiation resistance, with no mention of any ground resistance. Hence, the ground resistance, which cannot be ignored, is unknowingly and improperly being included as a portion of the radiation resistance instead of as a loss resistance in the expression for efficiency. This oversight might have been avoided if an analysis had been made of the increase in radiation resistance actually obtained by raising the loading coil from the base to the center of the whip, because the 6 ohms of coil resistance plus a 1-ohm radiation resistance subtracted from the 14 ohms of measured terminal resistance leaves 7 ohms, which requires an explanation of where those remaining 7 ohms of resist-

ance came from. Obviously, it is the ground resistance that was ignored.

From further study of the *Mobile Handbook* text, however, it is evident that an assumption of a greater amount of radiation from the coil than what is actually possible may have been the reason why such a high value of radiation resistance was considered plausible. But whatever the reason, we have been given the unrealistically high radiation resistance of 8 ohms and an impossible efficiency value of 8/14 = 58%. These values are fundamentally impossible to obtain in the center-loaded mobile antenna, and the true values have been obscured. In other words, a large portion of the power considered in the *Mobile Handbook* as being radiated is actually dissipated as heat in the ground. Belrose shows a proper analysis (*Ref 60*), which is supported by my own measurements.

It is practically impossible to obtain a mismatch of sufficient magnitude which requires any matching circuitry between the feed line and a properly resonated, conventional center-loaded mobile antenna for the purpose of conserving any significant amount of power. This statement is true, the many remotely controlled luggage-compartment tuning and matching arrangements notwithstanding. Now we will see why.

I have made measurements on loading coils and antennas using a Boonton 260-A Q meter and a General Radio 1606-A RF impedance bridge. Loading-coil loss resistances range from about 8 ohms for the better commercially available coils to as high as 31 ohms measured in poorer coils, depending on the Q and the self-resonant frequency of the coil. Ground-loss resistances encountered with conventional low-band mobile antenna installations range from about 5 ohms for low, wet ground to around 12 ohms for high, dry ground. Average ground yields about 7 ohms.

The ground-loss resistance in the mobile setup is less than that found in an antenna of a full $\lambda/4$ in physical height with no radials, because the radius of the circle where the minimum space-displacement currents return to the ground is shorter with the shorter antenna. Therefore, the return currents travel a shorter distance through lossy earth (see Fig 5-1). The current-flow pattern in the mobile system is also described by Belrose.

Consequently, from all of this we can see that the total terminal resistance of the mobile antenna is nowhere near the 1-ohm radiation resistance alone (which would produce an SWR of 50:1), but it also includes the ground-loss resistance and the coil-loss resistance, all three appearing in series. The absolute minimum resistance is 1 + 5 + 8 = 14 ohms, for an SWR of 3.5:1 at resonance when using the low-loss loading coils over good ground. The resistance can be as high as 1 + 12 + 31 = 44 ohms for an SWR of 1.1:1 when the higher ground loss and higher coil loss occur simultaneously. Hence, the actual resistance appearing at the antenna terminals lies in the range from 14 to 44 ohms, with corresponding SWR values of 3.5:1 and 1.1:1.

Thus, as strange as it may seem, the *higher* the minimum SWR attainable *at resonance*, the greater the power will be radiated for the same amount of power delivered to the feed line by the transmitter. It does not seem so strange, however, when we consider that the low radiation resistance of around 1 ohm is the only portion of the total terminal resistance that contributes to radiation, and this 1 ohm is constant, fixed by the radiator length. Therefore, by making the loss resistance lower through the use of a higher Q loading coil, less power is dissipated as heat in the coil, leaving more to be radiated. Conversely, if the lower Q coil is used simply to achieve a lower SWR, less power is radiated because more power is now being spent in heating the coil.

Many amateurs unknowingly select loading coils of low Q because "they produce a lower SWR than coils having a higher Q." Some lower Q coils, such as the Hustler manufactured by Newtronics, are advertised as producing a lower SWR and greater bandwidth. They do, indeed, produce a lower SWR and greater bandwidth because of their higher loss resistance, which results in a substantial loss of power. However, when using the higher Q, lower loss loading coil, even though its lower loss resistance results in a larger load mismatch and higher feed-line SWR, the resulting increase in radiated power with the higher Q coil is *still* proportional to the decrease in total resistance. Any additional loss from the higher SWR is so small that it can be neglected, because line attenuation in the short feed lines used in mobiles is extremely low. Remember, line attenuation is the only cause of power loss in the feed line, regardless of the SWR level.

I don't know whether it is through unawareness or by intent in the design that Hustler loading coils have close-wound turns (no space between turns). Close-wound turns result in higher distributed capacitance, which contributes to the high loss resistance that provides the low SWR and greater bandwidth of these coils. Let me digress here for a moment to examine the nature of coil resistance so that we may understand why some loading coils have high Q and low loss, while others have low Q and high loss, depending on their design.

The AC resistance loss in inductors is comprised of two separate resistance components, resistance from skin effect, related to wire size, and resistance from distributed capacitance, related to the spacing between turns. For a coil of given length, diameter and number of turns, there is an optimum wire size that yields minimum coil resistance and maximum Q. On one hand, the largest wire that will fit the given length (no space between turns) yields minimum resistance from skin effect. On the other hand, when the turns are closely spaced, the resistance from distributed capacitance is maximum. Spacing the turns apart (by using smaller wire for the same number of turns over the same length) reduces the resistance from distributed capaci-

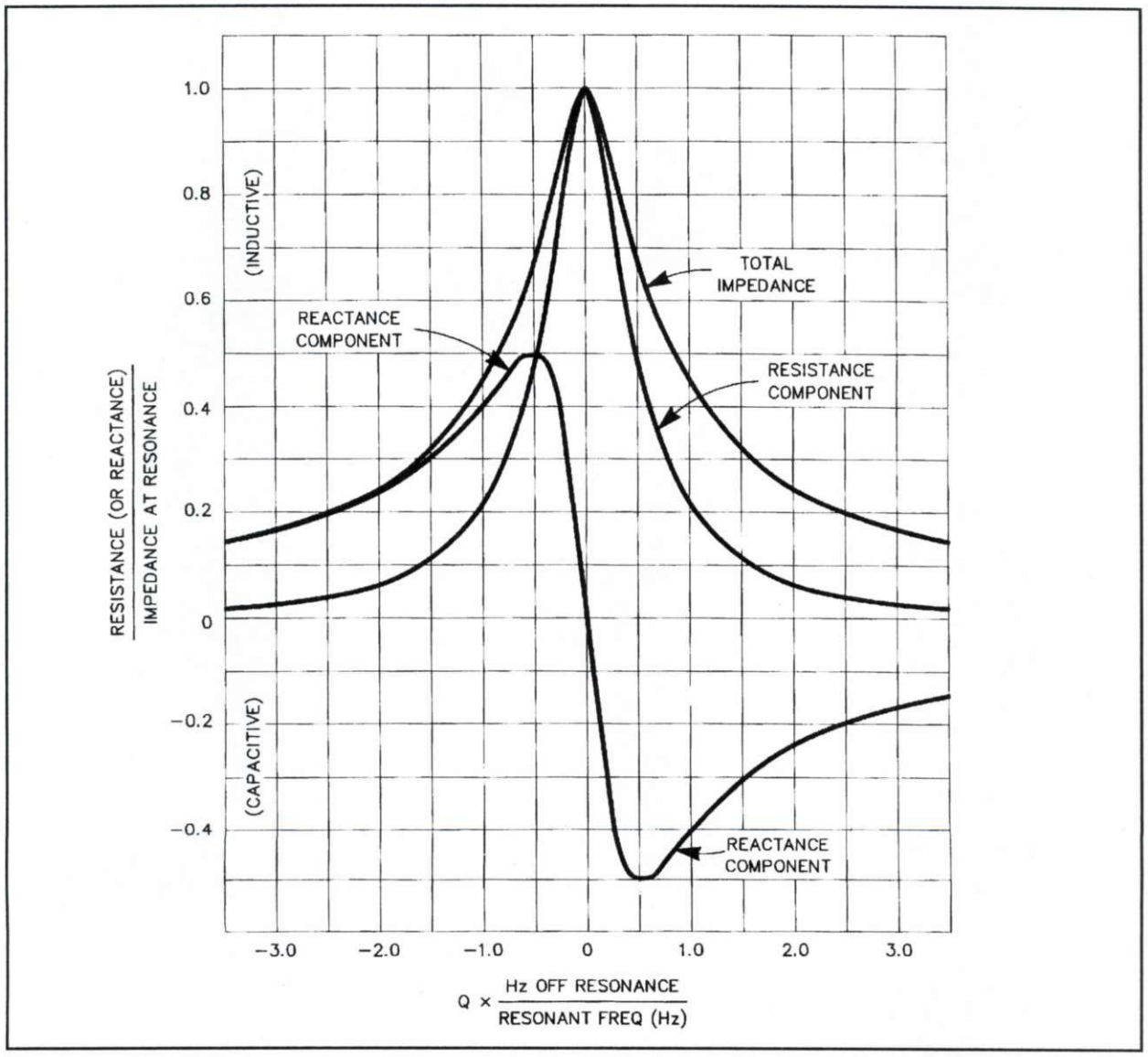

Fig 6-3. Universal curves giving the resistance and reactance components of the impedance of a high-Q parallel-resonant circuit as a function of frequency. ***After Terman (Ref 126, p 145).***

tance. Hence, the optimum wire size is a trade-off between a large wire that minimizes the resistance from skin effect and a small wire that minimizes the resistance from distributed capacitance because of the increased spacing between the turns.

The decrease in skin-effect resistance from increasing the wire size is obvious. However, the decrease in resistance from lower distributed capacitance with the smaller wire size is not obvious, so I'll now explain why this is true. It is well known that there is distributed capacitance between turns of an inductor. The closer the spacing between the turns, the greater the distributed capacitance, with maximum capacitance appearing when there is no spacing (except for insulation). The distributed capacitance appears inherently in parallel with the inductance of the coil. Consequently, there is a frequency (above the operating frequency of the coil) where the reactance of the distributed capacitance is equal to the inductive reactance of the coil, and the coil becomes self-resonant.

At the self-resonant frequency of the coil, the impedance appearing at its terminals is a very high, pure resistance (which we don't want in a loading coil), and the natural inductive reactance disappears. At this frequency, the coil no longer supplies any inductive reactance to cancel the capacitive reactance of the antenna. Instead, the coil simply introduces its high resistance in series with the antenna terminals, and the dipole portion extending above the coil effectively disappears.

The curves of Fig 6-3 show the relative impedance, resistance, and reactance components of the impedance versus frequency in parallel-resonant circuits, such as we have in the self-resonant inductor. For a given frequency, the resistance curve shows the amount of coil resistance relative to the maximum resistance that appears at the self-resonant frequency. We know that in a resonant circuit and with a given inductance, the smaller the capacitance, the higher the resonant frequency. Hence, in the loading coil, the lower the distributed capacitance (from increased turn spacing), the higher the self-resonant frequency and the lower the loss resistance for a given operating frequency. Certainly the design goal for obtaining minimum loss resistance in an inductor is to make its self-resonant frequency as high as possible relative to the operating frequency by optimizing the turn spacing. Because turn spacing (for a fixed winding length and number of turns) has no substantial effect on the amount of inductance in the coil, there is an optimum spacing versus wire diameter that yields the lowest resistance, and hence the highest Q.

It is interesting to note that of the commercially available 80-meter mobile loading coils I have measured, the Hustler coils having the loss resistance of 31 ohms at 4.0 MHz were self-resonant at 6.0 MHz. The better Webster KW-80 coils having 8 ohms of resistance at 4.0 MHz were self-resonant at 14.0 MHz. The windings in the Hustler coils are close spaced, while the spacing between turns in the Webster coils is approximately equal to the wire diameter. Need I say more?

Before leaving the subject of mobile loading-coil loss relative to distributed capacitance, here is some important information and a warning concerning the use of top-hat capacitance loading. When using an adjustable loading coil, the increased capacitance to ground afforded by top loading can reduce the coil loss, and thus improve the efficiency of the loading coil substantially. This is because the extra capacitance in the top loading reduces the amount of coil inductance required to obtain resonance, and hence reduces coil loss. However, to obtain the maximum improvement in efficiency, the top hat must be placed at the top of the radiator, not part way down. If the hat is large enough to be effective, any portion of the radiator protruding above the hat is ineffective.

Now the warning. I have seen many top-loading devices placed directly above the loading-coil inductor, with the entire top portion of the radiator extending above the top hat. This placement is incorrect, an absolute no-no! This incorrect placement of the hat causes an undesirable increase in the hat-to-coil capacitance. That capacitance adds to the already undesirable distributed capacitance of the coil, further reducing the Q and increasing the coil resistance as described earlier—just the opposite of the hat's intended purpose. Consequently, the coil performance is degraded by the hat, rather than enhanced. This incorrect placement of the hat does reduce the resonant SWR, as many have discovered, but this reduction in SWR is for the same wrong reason as explained earlier: It results from the increased resistance of the coil. For further information on capacitive loading, I

refer you to a section I wrote that appears in *The ARRL Handbook* on "Top-Loading Capacitance." It appears in Chapter 33 of all editions from 1986 through 1994 (*Ref 1*).

In Fig 6-1, the loss curve = 0.064 dB represents the loss characteristics of a typical mobile feed line—20 feet of RG-8 at 4.0 MHz. The curve shows a matched-line attenuation of 0.064 dB, plus an additional loss of 0.056 dB resulting from the 3.5:1 SWR, for a total loss of 0.12 dB. When this condition is accompanied by the 1:14 ratio of radiation resistance to total terminal resistance and a transmitter power of 100 watts, the difference in power radiated between matching at the antenna terminals and leaving the 3.5:1 SWR on the line and matching at the line input amounts to less than 0.1 watt!

It is also of interest to note that with the lower loss resistance ratio (1 to 14 ohms) while using the high-Q coil, the radiating efficiency is 7.14%, or 11.46 dB below the transmitter power delivered (excluding line loss). With the 1 to 44-ohm resistance ratio (with the higher loss coil and poor ground), the radiating efficiency is only 2.22%, or 16.53 dB below the transmitter power. We thus have a 5.07 dB loss in efficiency in return for lowering the SWR from 3.5 down to 1:1 by using a "low-SWR" loading coil. Contrast these actual values of efficiency with the 58% recited in the *Mobile Handbook* (*Ref 117*).

Therefore, contrary to statements found in numerous articles that have insisted that we believe otherwise, no significant improvement in efficiency can be obtained on the lower frequency bands by performing the matching function between the feed line and the mobile antenna terminals when a low-loss loading coil is already in use. The matching can be performed equally well at the input of the feed line, either by the transmitter output tank itself, or by a separate matching network if the transmitter tank lacks sufficient range, with the feed line connected directly to the antenna terminals! (*See Refs 4, 24, and 61.*) Thus, as emphasized in the opening paragraphs of Chapter 5, the important point here, again, is that a flexible, open choice is available in our system design.

The matching that is required to transfer maximum power to the load end of the feed line is a choice that should be determined according to personal preference of the operator. It should be based on convenience and accessibility to adjustment, and not on an arbitrary, low SWR dictated for the wrong reason by a decree of an "SWR King" who doesn't understand his "Subject"! However, wherever the matching is performed during operation, the antenna that will radiate the strongest signal is the one with the loading coil that is capable of producing the *highest SWR at resonance* with no matching at the antenna terminals, for the reasons explained above.

Now I'll again explain why loading coils of low Q have a high resistance that reduces the SWR, but also reduces the radiated power. A principal contributor to low Q in loading-coil inductors is the careless (or intentional?) lack of attention to coil design, particularly in relation to the spacing between turns. As is well known, there is distributed capacitance between every turn. The total distributed capacitance resonates with the coil inductance at some frequency, and at this frequency the coil becomes a self-resonant L-C tank circuit. As is also well known, the series AC resistance in a resonant tank circuit is very high. Insufficient spacing between turns results in a large distributed capacitance, which lowers the self-resonant frequency. Hence, the effective RF resistance of the coil will be high unless the operating frequency is substantially lower than the self-resonating frequency. On 80-meter coils, where I measured 31 ohms of series resistance at 4.0 MHz, the resonant frequency of the coils was around 6 MHz. On the higher Q coils that measured 8 ohms, the resonant frequency was around 14 MHz—a considerable difference!

Finally, here is a suggestion that may be helpful in tuning a mobile antenna. The use of a dip oscillator or a noise bridge in an attempt to determine the resonant frequency of the coil and radiator combination can rarely give the correct answer when you measure at the input terminals of the feed line. The reason is that when using these measuring devices in such a way, they are measuring the resonant frequency of the entire system, including the length of the feed line. As the length of the feed line is changed, the resonant frequency of the antenna system will also change. However, an SWR indicator connected directly at the input of the feed line provides an accurate indication of antenna resonance at the frequency of lowest SWR, providing the instrument is reliable and accurately calibrated for the impedance of the line (*Ref 59*).

This is because the minimum SWR for a given terminating load of the type we're discussing occurs at the resonant frequency of the load, regardless of the length of the feed line.

Sec 6.5 Low SWR for the Right Reasons

It is of interest to know that in TV broadcasting, where a long feed line is required to reach the antenna on a high tower, low SWR is an absolute necessity. However, the requirement here is primarily to avoid multiple, displaced ghost images from appearing in the received picture images which would result from reflections on the feed line caused by a mismatch. Similarly, low SWR on the feed line is a necessity in FM stereo broadcasting to avoid cross contamination between the two audio modulation channels. However, in amateur radio we do not have the problems encountered in TV and FM broadcasting. To summarize the discussions of SWR and reflections as they pertain to amateur radio operations, we have seen that *we do not need* a low SWR on the antenna feed line:

(1) to prevent reflected power from dissipating in the transmitter, because none dissipates in the properly coupled transmitter anyway, whatever the SWR;

(2) to prevent feed-line radiation or TVI, because a mismatched load on the feed line doesn't cause feed-line radiation or TVI;

(3) to attain proper coupling to the transmitter, because we can couple to or match the impedance at the input terminals of the line, whatever the SWR.

From examining Figs 6-1 and 6-2, it is evident that we do not need an SWR lower than 2:1 on any feed line to avoid any significant loss in efficiency, or with SWR values considerably higher than 2:1 when using feed lines having low attenuation. It seems that there aren't many reasons for needing a low SWR on amateur feed lines at HF, if an antenna tuner is used when required to obtain a satisfactory impedance match for the transmitter. (In fact, now would be an appropriate time to review statements 11 through 17 in Chapter 2.) Thus, let's see how we can briefly develop realistic SWR limits in relation to the attenuation values found in practical feed lines. Here are a few time-tested rules of thumb to use as guidelines:

(1) When operation is near the dipole-resonant frequency, either 50- or 75-ohm feed line may be used equally well. Depending on the height above ground, the antenna terminal resistance at resonance will fall somewhere between 40 and 80 ohms, so the resulting mismatch with either line impedance is so small as to be inconsequential, despite arguments to the contrary from those who are still afflicted with low "viswarmania." However, to obtain accurate readings with an SWR indicator, the impedance of the indicator must be compatible with the impedance of the line on which it's being used.

(2) An impedance-matching device placed anywhere on the feed line between a mismatched load and the transmitter compensates for the mismatch at the load, with the resulting effect that a match now exists everywhere on the line (*Ref 17, p 243*). In other words, if a mismatched load impedance, $Z_L = R + jX$, is conjugately matched anywhere on the line, the reflection generated by the complementary mismatch at the matching point causes the impedance looking into the termination end of the line to change from Z_C to $Z = R - jX$. *(See Chapter 4.)*

(3) Now let's take advantage of the increased usable bandwidth immediately available to us simply using our knowledge that nothing magical or miraculous happens in "bringing the SWR down" to 1.0. When we use coaxial line to center-feed a dipole, the operation is usually for one amateur band only. One exception is that satisfactory operation may be obtained on 15 meters with a 40-meter dipole. However, we now have the freedom *to operate anywhere within the entire band*, letting the SWR climb to whatever value it should as the antenna terminal impedance changes with frequency (but still staying within limits that are defined presently). To minimize the increase in mismatch and SWR resulting from the frequency excursion to either end of the band, the dipole should be cut to resonate near the center of the band. On the 75–80 meter band, where the percentage of frequency excursion is the greatest, the mismatch at the ends of the band will be somewhat less severe with a 75-ohm feed line than with a 50-ohm line. Of the smaller size coax, RG-59 is preferred over RG-58, because the combination of the somewhat lower maximum SWR and lower matched-line attenuation with the RG-59 permits either a greater frequency excursion away from the self-resonant frequency of the dipole, or a longer line for the same amount of loss. Of the larger size cable,

either RG-8 or RG-11 gives nearly equal results, because the matched-line attenuation of the RG-11 is a little greater than with RG-8, thus offsetting the gain resulting from its lower maximum SWR. However, the lower attenuation of the larger cables permits either a greater frequency excursion, or a longer line for the same loss than with the smaller cables, regardless of their relative power-handling capabilities.

(4) The smallest reduction in power that can just barely be detected as a change in level at the receiving station with the AGC disabled is 1 dB. Thus, to find the SWR that reduces the radiated power by 1 dB, we first use Fig 6-2 to find the attenuation per hundred feet of the correct feed-line type at the desired operating frequency. Then apply the correction for the length of the actual feed line to be used to determine the attenuation, α, of the line. Now go to Fig 6-1 and find the α-loss curve that most nearly corresponds to the value of the feed-line attenuation. Starting where that loss curve crosses the SWR = 1.0 line, follow the curve to the right until 1.0 dB additional loss is indicated on the dB scale on the right side of the graph. Read the SWR at this point from the scale on the bottom. This is the SWR that will reduce the radiated power by the "just barely noticeable" amount at the receiving station, compared with the signal that would be received if the line had been perfectly matched at the load. More exact data is presented later, but Table 6-1 shows SWR values to be expected for a dipole at the ends of the bands when the dipole is cut for resonance at the center of the band. Applying these data to Fig 6-1 readily shows that it requires feed lines of lengths substantially longer than the average to lose enough additional power from SWR ever to be noticed at the receiving station. In other words, a full 1 dB of additional loss will seldom be encountered, and therefore, no "pileup punch" will be sacrificed in obtaining the increased operating-bandwidth flexibility.

(5) At an SWR of around 4:1, the additional loss because of SWR just equals the perfectly matched line attenuation for any line. Thus, in effect, a 4:1 SWR multiplies the matched line loss by a factor of two. As an example, this statement means that the power lost in 350 feet of RG-8, or in 174 feet of RG-59, at 4.0 MHz with an SWR of 4:1 will have a "just barely noticeable" difference compared to a line having no attenuation loss whatsoever! This is because these lines each have a matched-line attenuation of 1.0 dB. However, also note that this "just barely noticeable" difference could not be noticed when the signal is well up on the S meter, because on many receivers it takes a *6-dB change in signal level for a change of one S unit.*

Frequency (MHz)	Max. SWR Value
3.5 to 4.0	5:1 or 6:1 (50-ohm line)
3.5 to 4.0	4:1 or 4.5:1 (75-ohm line)
7.0 to 7.3	2.5:1
14.0 to 14.35	2.0:1
21.0 to 21.45	2.0:1
28.0 to 30.0	3.0:1

Table 6-1. Approximate SWR values at band edges for wire dipoles cut to resonate at band center.

(6) The SWR on the feed line may be monitored to determine that the SWR is within the limit based on the line attenuation by placing the SWR indicator between the line-matching network and the feed-line input terminals. However, remember, *the SWR remains on the line even after the matching network has been properly adjusted.* The match between the transmitter and the matching network may be monitored with the SWR indicator placed between the transmitter and the network. The network is properly adjusted when the forward power is maximum and the power reflected from the network is zero. If the forward-power readings are the same as those obtained with a dummy load, and the reflected-power reading is zero in both cases, the input impedance of the network is the same as the impedance of the dummy load. If the SWR indicator shows some power being reflected from the matching network and the transmitter still loads properly, obtaining further reduction of the reflected power is probably unimportant. This indication of reflected power is not showing an "SWR," but only the degree of impedance mismatch remaining between the transmitter and the input of the network. If insufficient TVI rejection is obtained with the line-matching network alone, a conventional TVI filter may be used between the transmitter and the matching network with the same degree of effectiveness as when used in a line that is matched at the load.

As I have now shown, any required matching can be performed at the input to the feed line instead of

at the terminating load, such as an antenna. Therefore, no SWR bandwidth limit for amateur use (such as the commonly used, low arbitrary value of 2:1) is realistic unless it is based on the attenuation of the specified feed-line installation and the amount of total attenuation allowed. The arbitrary 2:1 SWR limit came into existence because the matching range of most amateur transmitters was thought to be limited to 2:1 by design, with economics being considered more important than operational flexibility. However, simple line-matching networks as described in the bibliography references can extend the inherent matching range of the transmitters to accommodate values of load impedance far beyond the limits defined by a 2:1 SWR. Line-matching networks are often built into modern transmitters, giving us amateurs back the matching range we were accustomed to having with the old swinging-link method of coupling. We weren't as conscious of SWR before the pi-net coupling replaced the swinging link. Matching at the line input in those days involved basically a simple adjustment of the adjustable link position to achieve the proper degree of coupling to match the resistive component of the load, and retuning the plate-tank capacitor to cancel the reflected reactance. Using this technique, we often loaded our transmitters into lines with high SWR values without even knowing about the SWR. However, with the appearance of the SWR indicators after the departure of the link, we "discovered" SWR and then learned how to misinterpret the meaning of the SWR readings.

In conclusion, if the feed-line loss is within your acceptable limits at a given SWR level, determined from consulting Figs 6-1 and 6-2, and if the transmitter can be adjusted to load and tune properly (either with or without an additional line-matching network), operate and don't worry about the SWR, because you are now using realistic SWR for the *right reasons!*

When the series of articles "Another Look at Reflections" originally appeared in *QST*, reader response was excellent. However, some readers told the author, "Your story is interesting, but you'll never convince me that I won't get out better with a perfect 1.0 SWR." Now I remind any reader who still entertains any skepticism of these entire proceedings concerning SWR that the information presented here is not simply a recitation of my own ideas or opinions, but has been taken directly from the professional scientific and engineering literature (note the extensive bibliography in Chapter 24), and paraphrased specifically for the radio amateur with great care not to change the meaning. Moreover, in striking contrast to the many differing opinions heard on the subject during amateur discussions, there *are no* such differing opinions among the professional sources, because among the professionals (including textbook authors) the principles involved are completely understood and are based on true, proven scientific facts that are not subject to divergent opinions such as we find in politics and religion.

Apparently, many have forgotten that this story was told for the amateur in *QST* no less than twice prior to the initial appearance of this series by two well-known experts in this subject area. They are the late George Grammer, W1DF, former engineer and Technical Editor of *QST*, and Dr. Yardley Beers, WØJF, formerly a professor of physics, Chief of the Radio Standards Physics Division, National Bureau of Standards (now the NTIA), and Senior Scientist, Quantum Electronics Division of the National Bureau of Standards. Their illuminating contributions, listed as Refs 3 through 6, 16, and 22 of the bibliography should be reviewed, even if it means a trip to the library. The trip will be very rewarding.

Notes

1. All references appear in Chapter 24.

2. Houghton *(Ref 102)* states that reflected power is lost, accompanied by a nomograph for converting SWR into percent reflected power "to make it easier to determine just how much power is lost." The reader is invited to read an excellent rebuttal to this nomograph presentation by Anderson *(Ref 55).*

3. Scherer *Ref 103)* erroneously shows data on page 90, where 100% minus the reflected power is given as "useful" power. The succeeding paragraph also states incorrectly that the SWR indicator must be placed at a multiple of $\lambda/2$ from the load to indicate the true SWR. This statement is simply *untrue*! The example demonstrates that the SWR indicator was either not properly adjusted to the impedance of the line, or that it was unreliable, or that no balun was being used to feed a dipole with an unbalanced feed line. See Chapter 2 (statements 21 and 23), Chapter 21, and *Ref 38, pp 25–26, and Ref 59.*

Chapter 7

My Antenna Tuner Really Does Tune My Antenna

(Adapted from QST, *August 1976)*

Sec 7.1 Introduction

Chapter 4 discusses conjugate matching and introduces the concept of wave interference as the basis for the mechanics of the matching. I used the transmission-line stub form of matching for the example because of the ease in describing the generation of the waves and the wave actions involved in the matching process. Chapters 5 and 6 discuss some of the reasons why many have been plagued with myths concerning mismatch and SWR, myths that have prevented an enlightened use of impedance matching in our daily operating procedures with antennas and transmission lines. In those chapters I also explained power loss caused by line attenuation, and presented both graphic and mathematical means for determining the additional loss resulting from SWR on the feed line. A detailed discussion of the conjugate match may be found in Chapter 19.

This chapter focuses on the use of line-matching networks formed with adjustable capacitors and inductors instead of stubs made from sections of transmission line. Here I show that the wave actions in both of these forms of matching are identical. I will also explain in detail how transmitters are matched to mismatched feed lines with an external matching network as shown in Fig 7-1, or by using the pi-network tank in the transmitter shown in Fig 7-2. However, first let's examine one last reason why so many have been reluctant to operate with an SWR greater than 1:1.

The principle that maximum efficiency is obtained when a feed line is perfectly matched to an antenna—no reflections on the feed line, and a 1:1 SWR—is so well known it hardly needs repeating. Even so, it is recited in practically every good textbook on the subject. Thus, it is important to appreciate that this book makes no statement which violates that principle, nor suggests any disagreement with it. The misconceptions to be clarified concerning lost reflected power simply stem from overuse, or misuse, of the perfect-match principle in its practical applications.

Ironically, textbooks may be a bit responsible for this misuse. While extolling the virtues of the perfect match, some authors fail to explain how much (or how little) one loses when the load is mismatched to the line, if compensated with a conjugate match at the line input. Those authors generally present the case for the ideal impedance match of the load in terms of single-frequency operation, and practically ignore the unique, multi-frequency operations of the radio amateur. We have frequency *bands*, not single, specific frequencies—and we want to operate anywhere within those bands.

Because the antenna impedance changes as we change frequency, relaxation of any feed-line-to-antenna matching restriction is necessary if we are to enjoy such operating freedom. Although many engineering textbooks discuss loss versus load mismatch, few texts discuss multi-frequency antenna-matching situations where line-input matching usually exists. Consequently, an overly rigorous application of the perfect-load matching principle has unwittingly been thrust upon us by dozens of misleading statements appearing in various amateur journals. Add to this a prevalent misconception of pi-network loading principles. The result? The "lost reflected power" syndrome and the mania for low SWR. Thus, providing guidance for the amateur concerning match quality and efficiency in his multi-frequency operation is the primary purpose of this writing. For example, Fig 6-1 is a graph that plots transmission loss in dB versus SWR for various values of line attenuation. The graph shows that maximum efficiency is indeed obtained with a perfect match. On the other hand, it also provides dramatic evidence that when using low-loss feed line that is matched at the line input, the difference

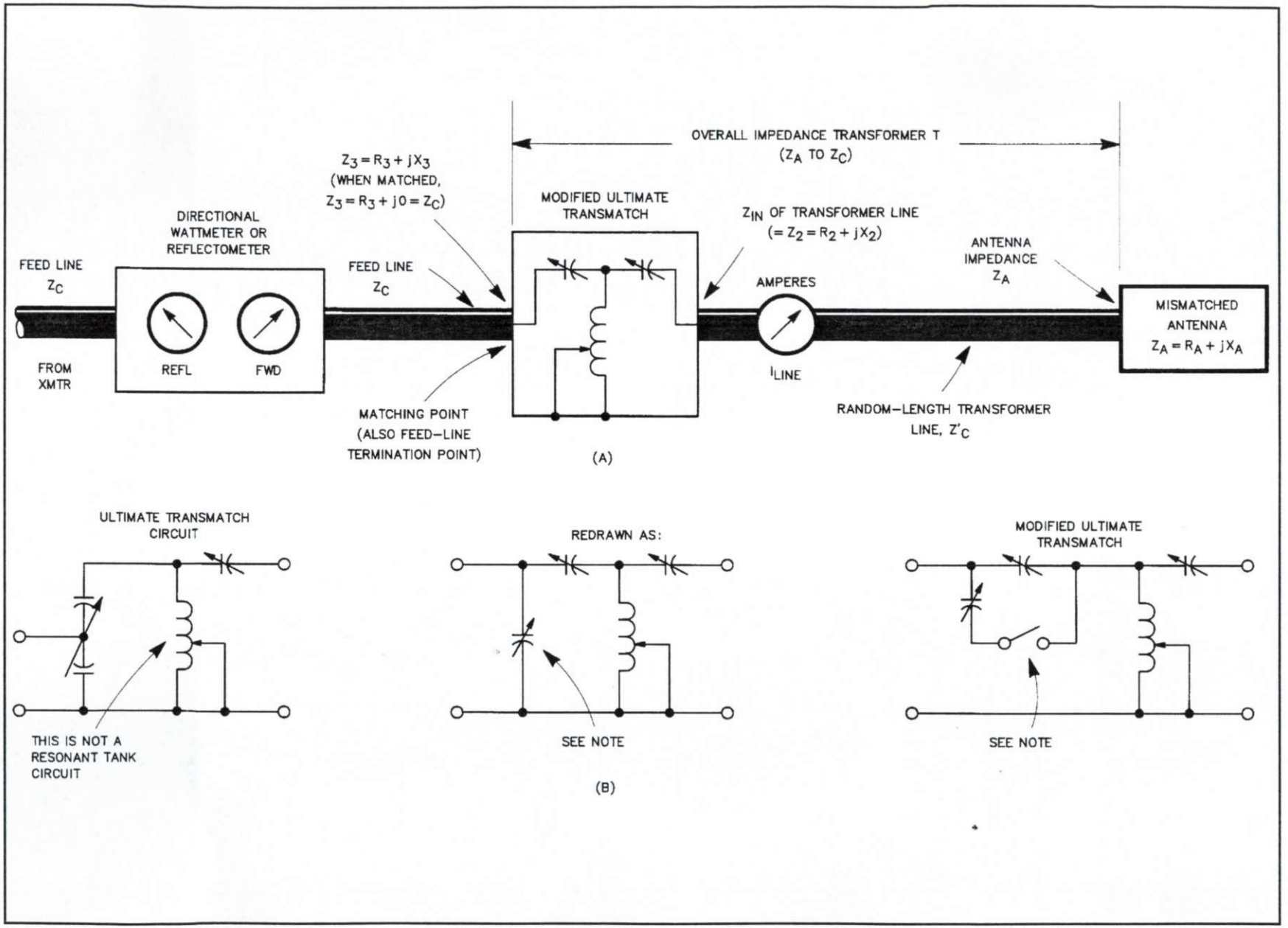
OVERALL IMPEDANCE TRANSFORMER T
(Z_A TO Z_C)
$Z_3 = R_3 + jX_3$
(WHEN MATCHED,
$Z_3 = R_3 + j0 = Z_C$)
MODIFIED ULTIMATE
TRANSMATCH
Z_{IN} OF TRANSFORMER LINE
($= Z_2 = R_2 + jX_2$)
ANTENNA
IMPEDANCE
Z_A
DIRECTIONAL
WATTMETER OR
REFLECTOMETER
FEED LINE
Z_C
FEED LINE
Z_C
AMPERES
MISMATCHED
ANTENNA
$Z_A = R_A + jX_A$
FROM
XMTR
REFL
FWD
I_{LINE}
MATCHING POINT
(ALSO FEED-LINE
TERMINATION POINT)
RANDOM-LENGTH TRANSFORMER
LINE, Z'_C
(A)
ULTIMATE TRANSMATCH
CIRCUIT
REDRAWN AS:
MODIFIED ULTIMATE
TRANSMATCH
THIS IS NOT A
RESONANT TANK
CIRCUIT
SEE NOTE
SEE NOTE
(B)

Fig 7-1. Impedance matching with a matching network external to the transmitter. The impedance of the feed line, Zc, is usually 50 or 75 ohms in most amateur applications, but the impedance of the transformer line, Z'c, may be any value, and may be of open-wire or coaxial type. The matching network at A is a simple "T" network, Lew McCoy's Ultimate Transmatch less the shunt capacitor (*Ref 41*), as shown at B. NOTE: In the redrawn circuit at B (center) the shunt input capacitor is not needed to obtain a match, and the capacitor range may be increased by reconnecting as shown at the right. The story of how this change came about and why commercial present-day antenna tuners now use the simple "T" *network is told in* Chapter 14, Sec 14.4.

between having either a perfect load match or a moderately high SWR is insignificant in terms of power transferred to the antenna. In other words, through the use of line-input matching, the antenna accepts the maximum available power from the transmitter, even when the feed line and antenna are mismatched, and with the antenna off resonance. Matching at the input terminals of the feed line allows us to tolerate this load mismatch because the reflection loss caused by the mismatch is compensated by the *reflection gain* provided by the input match. Consequently, the transmitter is properly coupled to its desired load impedance and the reflected power is conserved. It is *system resonance* that underlies these intrinsic characteristics of input matching involving the principles of the conjugate match, and system resonance compensates for the effect of the off-resonant condition of the antenna as we move around within a given frequency band. For the myth believer who is still unconvinced of the wondrous compensating powers of conjugate line-input matching, let me quote Everitt on the Maximum Power-Transfer Theorem from classical network theory (*Ref 17, p 49; Ref 69*). The application to feed-line antenna matching is indicated in parentheses: "The maximum power will be absorbed by one network (the antenna) from another (the feed line) joined to it at two terminals, when the impedance of the receiving network (the antenna) is varied, if the impedances of the two networks at the junction are conjugates of each other." Everitt then presents the proof of the theorem.

The expressions in Eqs 6-1 and 6-2, which are plotted in Fig 6-1, illustrate this theorem for the case where a feed line is the sending network. These expressions show that when the networks are conjugately matched, meaning when the transmitter is tuned to the line: (1) there is no loss at the terminals joining the networks; (2) there is no loss in the sending network, the feed line, when that network attenuation is zero; and (3) if the sending network has attenuation other than zero, the transmission loss results only from the line attenuation. For further discussion on the theorem, I invite you to review Chapters 2, 4, 5, and 19.

The way that conjugate matching and reflection gain are achieved is illustrated in Chapter 4, using the stub form of matching to develop the understanding of the wave action. The stub form was used for the illustration because it is easy to visualize. However, since it is not a practical form to use where we make frequent changes in frequency, let's see how conjugate matching is performed using devices that are easily adjusted to perform at any desired frequency. Such devices are the transmatch, a T network, L, pi, and other types of networks. I will show that these devices can perform the matching function at the *input* of a feed line, and that the feed line can be of *any* length instead of requiring it to be $\lambda/2$. I will also show how, in some instances, the transmitter tank circuit itself performs matching at the input of the feed line.

Sec 7.2 Matching at the Line Input

At this point you may ask, "Why match at the *input* of the feed line?" The answer is that without matching at the input, we have very little operating flexibility relative to changing frequency within a band. In the absence of a line-matching network we are restricted to operating in a narrow portion of a band (especially on 80 meters) unless effective measures for broad-banding the antenna itself have been taken. We are restricted because as we deviate from the resonant frequency of the antenna, the resulting increase in the impedance mismatch between the feed line and the antenna is transferred back to the input of the feed line as an increased mismatch between the transmitter and the feed line. As a result, the load impedance seen by the transmitter varies beyond acceptable limits; the transmitter fails to load properly, and it can be damaged by overloading or by arc-overs caused by underloading.

These phenomena (plus an lack of awareness of the remarkable performance capabilities of line-input matching) are largely responsible for the traditional low-SWR mania. On the other hand, simple impedance matching at the input of the feed line provides stupendous improvement in operating flexibility; the matching network compensates for the impedance changes at the line input terminals, and provides the correct load impedance for the transmitter at whatever frequency we select within an entire band. The correct load impedance for the transmitter is obtained simply by adjusting the network, conveniently located at the operating position.

Therefore, the next question is "Why not broadband the antenna and avoid having to retune a matching device when changing frequency?" The answer is that we can, but only to a limited degree. This is because, for example, broad-banding techniques that would permit coupling the average amateur transmitter directly into the feed line over the entire 80-meter band (with no adjustments other than retuning the transmitter) are not practical in the average amateur situation. This includes the coaxial dipole (sometimes called a Double-Bazooka), which, contrary to prevalent opinion, fails to deliver a reasonable improvement in bandwidth over that of a simple dipole when it is fed with the usual 50-ohm feed line.[1] While the above statement may appear a bit incredible, I wrote a revealing analysis of that antenna and published it in *Ham Radio* magazine (*Ref 62*). (A condensed version of that analysis appears here as Chapter 18.) However, there is a recent development worthy of your attention. In my analysis I presented information concerning the use of a feed line having an impedance Z_C higher than the usual 50 or 75 ohms (such as 144 ohms) for increasing the bandwidth with stubs in the coaxial dipole. Using my analysis, Frank Witt, AI1H, engineered a novel transmission-line impedance transformer that achieves the required effect of increasing the feed-line impedance. With Witt's transformer, the 2:1 SWR bandwidth of an 80-meter coaxial-stub dipole extends well beyond the range of 3.5 to 4.0 MHz (*Refs 122, 123, and 124*). Witt has presented a practical way of broad-banding the dipole that deserves serious attention. An explanation of how either a final tank network or an external line-matching network performs conjugate matching from the viewpoint of reflections is really a continuation of Chapter 4. However, to dramatize both the availability and the advantages of matching at the input of the feed line, we digressed in Chapters 5 and 6 to highlight some of the wrong and right reasons for using low SWR. These reasons show that in the search for obtaining low SWR on the feed line, we have often put misplaced emphasis on matching at the wrong end of the line. As stated earlier, the principles of wave reflection found in stub matching are the same as in other matching schemes, such as series λ/4 transformers, L, T, pi-networks, etc. As some of the concepts I discuss here were presented in detail in Chapter 4, you may wish to refer to them again.

Sec 7.3 The Intermediate Role of the λ/4 Transformer

How many amateurs remember the Johnson Q Match? And how many have used a λ/4 section of 70-ohm transmission line to match a 100-ohm resistive load to a 50-ohm feed line? Both are examples of series λ/4 line transformers. In addition to requiring an electrical length of 90°, impedance matching is accomplished in these transmission-line transformers because of a specific relationship between their characteristic impedance Z_C, their input impedance Z_I, and their output load impedance Z_L. To perform the matching, the ratio of Z_C to Z_I must be the inverse of the ratio Z_C to Z_L, that is:

$$\frac{Z_I}{Z_C} = \frac{Z_C}{Z_L} \qquad \text{(Eq 7-1)}$$

In other words, the impedance required of the transformer is the geometric mean value of the two impedances being matched, stated simply by the well-known expression:

$$Z_C = \sqrt{Z_I \times Z_L} \qquad \text{(Eq 7-2)}$$

Both the impedance and the length of the λ/4 line transformer play important roles in clarifying the principles underlying all forms of line-matching networks. Since these roles are not generally well understood, let's examine them. Chapter 4 shows that reflections play a necessary role in impedance-matching operations. We saw that impedance

matching is obtained by canceling the reflections from a load mismatch by wave interference. The interference is set up by new, separate reflections generated by a separate mismatch introduced at a desired matching point. The mismatch introduced at the matching point is tailored to complement the load mismatch so that the new reflection has the same magnitude and opposite phase (at the matching point) as the reflection generated by the load mismatch. The reflection generated by this complementary mismatch is called either a complementary or a canceling reflection. In stub matching, the complementary mismatch is introduced by the stub. While investigating complementary reflections generated by stubs, we observed the wave action through which the λ/4 transformer performs the matching (see Table 4-1 and Fig 4-2[D]).

In Chapter 4 we analyzed the effects of using various stub and transformer lengths to match a resistive load to various feed lines having different values of impedance. We found that when the feed-line impedance is equal to Z_I (relative to transformer impedance Z_C and load impedance Z_L in Eqs 7-1 and 7-2), the transformer length became 90°, and the stub length became zero. In this case the complementary reflection is generated by the mismatch appearing at the junction of the feed line and the input of the transformer. This mismatch results from the abrupt change in impedance (Z_I to Z_C) encountered by the forward wave as it propagates out of the feed line (Z_I) and into the transformer (Z_C). This mismatch is complementary to the resistive load mismatch in magnitude because the ratio between the feed line and transformer impedances (Z_I/Z_C) is the inverse of that appearing between the transformer and the load impedances (Z_C/Z_L), as in Eq 7-1. Thus, the reflections generated by both the load mismatch and the transformer-input mismatch are equal in *magnitude* (as required to obtain perfect cancellation), because both mismatches are equal in magnitude.

Because the input and output mismatches are physically separated by 90° (the electrical length of the transformer), they are also complementary in relation to the *phase* of the reflections appearing at the matching point (also required for cancellation). This is because the wave reflected by the input mismatch has zero distance to travel relative to the matching point, but the 90° length of the transformer results in a travel of 180° for the wave reflected by the load mismatch—90° from the input to the load, plus the 90° return trip. Thus, the load-reflected wave arrives at the matching point with a 180° phase difference relative to the input-reflected wave. We now have two complementary reflected waves—equal in magnitude but opposite in phase at the matching point. Consequently the two waves mutually cancel, resulting in total re-reflection of both waves into the transformer to propagate in the forward direction, as explained in the final paragraphs of Chapter 4. The voltage and current components of both re-reflected waves are in phase with their corresponding components of the source wave. Hence, an impedance match appears at the input terminals of the transformer, all of the power reflected from the load mismatch that reaches the input of the transformer is again on its way to the load, and no reflected wave appears on the feed line.[2]

This λ/4 line-transformer matching action deserves serious study. Why? Because it provides an intermediate step in understanding how matching can be achieved at the input of a line transformer of *any random length*, and that may have *any impedance* for its terminating load, such as the complex impedance $Z_A = R_A + jX_A$ of a mismatched, off-resonance antenna. This line transformer is none other than the feed line so many strive to operate with no reflections by simply restricting its *load* to a matched, resonant antenna!

Sec 7.4 Input Line-Matching Networks

Now let's examine external line-matching networks from the viewpoint of matching impedances with reflections. Referring to Fig 4-2(D), we replace the 90° transformer (T) with the combination of an adjustable matching network and a line of *random* length to connect the mismatched load (antenna) to the network. This arrangement is shown in Fig 7-1(A). The line connecting the matching network to the antenna will now be called the *transformer line*. The line connecting the transmitter to the matching network is the *feed line*, as in Chapter 4. The matching point is defined as the junction of the feed line and the input of the network.

In a manner which is explained later, the transformer line (which can have *any* value of imped-

ance Z'C) transforms the complex antenna impedance $Z_A = R_A + jX_A$, to a second impedance $Z_2 = R_2 + jX_2$ at the input of the transformer line. The network then transforms Z_2 to a third impedance $Z_3 = R_3 + jX_3$ at the matching point (the network input). When the network is correctly adjusted, Z_3 is a pure resistance R_3, equal to the feed-line impedance Z_C. In mathematical terms, $Z_3 = R_3 + j0 = Z_C$. Thus, the antenna impedance Z_A is matched to the feed-line impedance Z_C, which is a proper load for the transmitter (*Ref 17, p 243; Ref 69*). Without the matching network, the transmitter load would be impedance Z_2, which could deviate far beyond the range of matching capability for most transmitters. However, by adding the network, we obtain the impedance match by simply adjusting the network to transform R_2 to equal the feed-line impedance Z_C at the matching point, and to cancel any reactance X_2 appearing at the input of the transformer-line to zero at the matching point.

Let's now examine more closely the transformation of impedance Z_2, that which appears at the input of the transformer line. The variations of resistance R_2 and reactance X_2 of impedance Z_2 are dependent on three different factors: the antenna impedance Z_A, and both the length and the impedance Z'C of the transformer line. From Chapter 4 we know that for given antenna and transformer-line impedances, a length of line can be found that will make $R_2 = Z_C$, but will also yield reactance X_2. The reactance X_2 requires canceling to obtain a match, for example with a stub, as shown in Fig 4-2A or 4-2B. Another length of line can be found that will make X_2 become zero, but now R_2 will not equal Z_C (still no match). *There is no line length that will yield* $Z_2 = R_2 + j0 = Z_C$, *unless* Z_A *equals* Z'C.

This situation illustrates the typical endless cat-and-mouse game we play in trying to load the transmitter by changing line lengths. An elegant solution to this problem would be a line of *variable* length, plus a device for dumping the unwanted reactance. So how can we possibly solve the problem using a fixed, random-length line? Because, as we now discover, the line-matching network is the star performer! We know from elementary transmission-line theory that a transmission line is made up of an infinite number of tiny, distributed, series inductances and shunt capacitances. Therefore, it should not be surprising that we can adjust the *electrical* length of a line of a given *physical* length by adding lumped inductances or capacitances. Indeed, by a selection and adjustment of reactances arranged in an appropriate L, T, or pi configuration, we can simulate a line having *any desired electrical length* without specifying any physical length whatsoever! (*See Refs 8 through 13; 19, p 115; 21; 22; 24; 30; 31; 41; 61; and 63.*)

When a matching network is adjusted to obtain a match between the antenna and feed-line input impedances, it performs the following two feats. First, it creates the effect of stretching the *electrical* length of the transformer line to make it reach the matching point, so that resistance R_2 at the input of the *physical* transformer line is transformed to $R_3 = Z_C$. And second, it introduces reactance $-X_3$ to cancel reactance $+X_3$ of the *stretched*-transformer line appearing at the matching point, in the same manner as a stub would perform in stub matching.

The introduction of reactance $-X_3$ at the matching point provides the complementary mismatch which generates the canceling reflection having equal magnitude and opposite phase relative to the reflected wave arriving at the matching point from the mismatched antenna. The matching network has thus provided the proper *overall* transformer length to obtain both the required transformation of the resistance component from R_A to R_3, and a canceling-phase relation between the load-reflected wave and the canceling reflected wave provided by the complementary mismatch of reactance $-X_3$. Consequently, the network has also transformed a dream into reality by conjuring up the elegant variable-length line and a means for dumping the unwanted reactance.

An ideal arrangement for observing the action while performing the tuning adjustments of the network includes an RF ammeter in the transformer line to indicate line current (a meter in each conductor if using a balanced, two-wire line), and a dual-meter reflectometer or wattmeter to indicate forward and reflected power simultaneously in the feed line. It is important that the reflectometer be adjusted initially to indicate zero reflected power with the feed line terminated in a pure resistance equal to the feed-line impedance. The tuning adjustments are complete when we obtain maximum current in the transformer line simultaneously with maximum forward and zero reflected

power in the feed line. Of course, because of standing waves on the transformer line, we will obtain different values of line current depending on where along the line the ammeter is inserted. However, our only interest is in seeing *changes in relative current* to indicate when maximum network output occurs during the tuning adjustments. Hence, neither the absolute line current, nor where the meter is inserted, is important.

The simultaneous indication of maximum current in the transformer line and zero reflected power in the feed line is meaningful. This condition denotes four significant factors for comparing the wave actions involved in impedance matching with a line-matching network versus matching with the λ/4 line transformer described earlier. First, proper network adjustment establishes the complementary mismatch between the feed-line termination and the input of the network, which produces the canceling reflection at the matching point. Second, the canceling reflection at the matching point is equal in magnitude and opposite in phase relative to the load-mismatch reflection. Third, the canceling reflection and the load-mismatch reflection cancel each other at the matching point. Consequently, a purely resistive impedance equal to the feed-line impedance Z_C appears at the input terminals of the network, while reflections and a standing wave remain on the transformer line. And fourth, observing the transformer-line current rising to maximum while the reflected power in the feed line drops to zero provides visual evidence that the power reflected from the load mismatch is indeed re-reflected by the complementary mismatch at the matching point.

Incidentally, it is a good practice to have an ammeter permanently connected in the transformer line. Here's why. If your matching network effectively comprises more than one L section, you can generally obtain a match (zero reflected power in the feed line) with several different combinations of network L and C tuning. However, minimum network loss (which corresponds to highest maximum transformer-line current) usually occurs while using the maximum C and minimum L at which a match can be obtained. Monitoring the transformer-line current during tune-up lets you select the L-C combination that yields the highest output line current. To ensure quick resetability of the network, and to minimize on-the-air tune-up time, L and C settings for the best combination should be logged whenever the network is tuned to a new frequency. The transmitter should be tuned initially into a dummy load, then the network tuned into the antenna *using the lowest power* at which the reflectometer provides a satisfactory indication.

Sec 7.5 Pi-Network Tank-Circuit Line Matching

Let's now examine the case where the final amplifier tank circuit of Fig 7-2 performs the line-matching function. To differentiate from the external network, I will call this network the *tank network*. Comparing Figs 7-1 and 7-2, we see that in general, the transformations of impedance from Z_A to Z_3 are identical whether using the tank network or the external network. The principal difference is the range of the transformation that can be performed by the two networks. With the external network, impedance Z_2 is transformed to a value Z_3, matching the feed-line impedance Z_C. When the tank network is used alone, as shown in Fig 7-2, impedance Z_2 is transformed to directly match the load impedance Z_L of the final amplifier of the transmitter.

Now a requirement for an amplifier (tube or transistor) to deliver its maximum available power into a load (the loaded tank circuit) is for it to see an impedance which we call the *optimum load impedance*, Z_L. In practice, impedance Z_L is usually resistive, so that $Z_L = R_L + j0$. Thus, the amplifier is properly loaded when it sees impedance $Z_3 = R_L + j0$ (which is $R_3 + j0$) looking into the tank network. The amplifier is underloaded with R_3 *greater* than R_L, overloaded with R_3 less than R_L, and it will have higher than normal dissipation if Z_3 contains any reactance X_3.

When using the tank network alone to perform the matching, as in Fig 7-2, the impedance value of Z_3 is determined by two factors: the impedance value of Z_2 loading the network, and the impedance transformation ratio of the network. The transformation ratio is somewhat variable (using the tuning and loading capacitors, C1 and C2), thus providing a range of impedance-matching capability. The matching range allows impedance Z_2 to be any value that the network can transform to the impedance $Z_3 = R_L + j0$ by adjusting the tuning and load-

ing controls. Additional details on this point appear in Chapter 13.

Now we can summarize the principal operating conditions involving transformation of antenna impedances to the optimum load impedance for the output amplifier.

Case 1: The antenna impedance $Z_A = R_A + j0$ (resonant) is matched to the transformer line, and the tank network is used alone—no external matcher, Fig 7-2. Here, antenna impedance Z_A equals the impedance of the transformer line, Z'_C, the SWR on the line is 1:1, and impedance Z_2 is equal to the line impedance. If the transformer-line impedance Z'_C is the commonly used 50-ohm, then the tank network yields the proper amplifier load $R_L + j0$ with the same tank adjustment settings as obtained when tuning up with a 50-ohm dummy load.

Case 2: The antenna is operated somewhat off resonance. Its impedance, $Z_A = R + jX_A$, yields a mismatch to the transformer line so as to transform Z_A to an impedance Z_2 that is within the matching range of the tank network (for transformation to $Z_3 = R_L + j0$). Again, the tank network is used solo.

Case 3: The antenna is operated off resonance, beyond the matching range of the tank network. Here, the tank network is used in conjunction with an external network, as in Fig 7-1. An impedance $Z_3 = R_L + j0$ cannot be obtained with the tank network alone, and the amplifier would be either underloaded, overloaded, or reactively loaded. We remedy this situation by inserting an external line-matching network, which transforms impedance Z_2 to an impedance Z_3 that is within the range the tank network can transform to $R_L + j0$.

Case 1 needs no comment, so let's refer to Fig 7-2 and examine the action in the tank network as it performs the matching function under the conditions of Case 2. As described in Chapter 4, wave interference establishes an open circuit to reflected waves at the matching point. This interference exists between the wave reflected by the mismatched termination on the line and the wave gen-

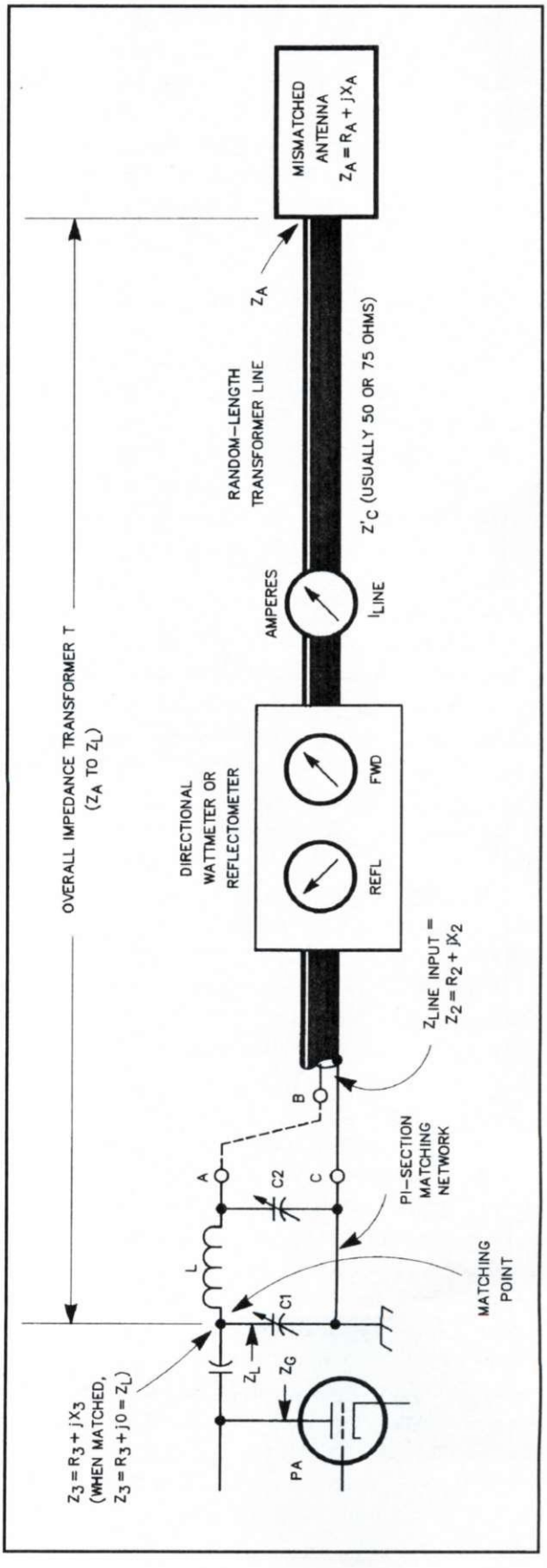

Fig 7-2. Impedance matching with the final-amplifier tank circuit of the transmitter. Z_L is defined as the optimum load impedance of the amplifier—the impedance into which it delivers its maximum available power.

erated by the complementary mismatch at the matching point in the matching network. Recall that the open circuit so established causes total re-reflection of the reflected wave returning toward the generator.

In the tank network, the open circuit to the reflected wave is established at the tank-network input terminals, fed by the plate of the amplifier tube. Consequently, waves reflected from a mismatched antenna, those causing impedance Z_2 to deviate from Z'_C, enter the tank network at its output terminals and become totally re-reflected on arrival at the open-circuited input of the tank.[2] When the network is tuned to resonance, voltage and current components of the reflected wave are re-reflected in phase with the corresponding source-wave components emanating from the amplifier tube. Thus, the amplifier sees a resistive load $Z_3 = R_3 + j0 = Z_L$ at the input to the tank circuit, and the reflected power reaching the input adds to the power from the amplifier. This is why a directional wattmeter indicates a higher forward power than the amplifier is actually delivering when reflections are present on the transformer line.

Optimum amplifier loading is obtained by adjusting the capacitance of the loading-control capacitor C_2 to the value that causes the network to transform R_2 to $R_3 = R_L$. When R_2 changes, following a change in antenna impedance Z_A, C_2 can then be varied to modify the network transformation ratio. This transforms the new value of R_2 to $R_3 = R_L$. The plate tuning capacitor, C_1, is then readjusted to return the network to resonance and we again have optimum amplifier loading. The range of R_2 values that can be transformed to $R_3 = R_L$ by varying C_2 is determined by the design parameters of the network (*Refs 4, 63, and 64*).

Now, what happens when the line-input impedance Z_2 which loads the network contains reactance X_2? This reactance shifts the available range of capacitance provided by the loading-control capacitor, C_2. This shift occurs because reactance X_2 appears in parallel with the reactance of the loading capacitor. Consequently, for proper setting of the loading capacitor where $X_2 = 0$, a capacitive X_2 increases the effective capacitance C_2 (decreasing loading), while an inductive X_2 decreases C_2 (and increases loading). Thus, to obtain a proper loading when X_2 is present, the setting of the loading-control capacitor must be shifted from the $X_2 = 0$ position to compensate for the additional line reactance X_2. If R_2 is within the matching range of the tank network, proper loading will be attainable. This is true as long as X_2 doesn't exceed the value which the loading-control capacitor range can accommodate to maintain the value of C_2 required to transform R_2 to $R_3 = R_L$.

If the line reactance X_2 is too large for the loading capacitor to compensate, we have the conditions described in Case 3. However, there are simple remedies for this condition if R_2 is within matching range of the tank network, but X_2 is not. Here we can simply add a compensating reactance in series with the RF output (between points A and B in Fig 7-2). The added reactance may either cancel the line reactance X_2, or merely bring it within the range the tank network can handle. On the other hand, if the resistance component R_{2P} of the equivalent parallel circuit of impedance Z_2 is within the matching range, the compensating reactance should be added in parallel across the RF output between points A and C.

Whether the compensating reactance should be capacitive or inductive can be determined experimentally by trying first one kind or the other to see whether loading is improved or worsened. The correct kind and value of compensating reactance has been found when proper loading can be obtained with a convenient setting of the loading-control capacitor. An excellent discussion of this subject by Grammer appears in *Ref 4, Part 3*. When using this matching technique with the tank network alone, an adjustment of the length of the transformer line can be of great assistance in obtaining values of impedance Z_2 which are most favorable to the matching range of the network. This subject of impedance transformation versus line length is discussed in Chapter 11.

When operating under the conditions of Case 2 (Fig 7-2), tuning up into a dummy load requires special care; it can be troublesome, since the actual load Z_2 at the input of the transformer line often differs widely from that of the dummy load. If the tank network is first tuned into the dummy load and then switched to the transformer line-input impedance Z_2, the tank network must be *retuned* to the new impedance Z_2! Failure to retune to the actual operating impedance Z_2 after tuning up into the dummy

load results in an improper load impedance Z_3 for the amplifier; it is no longer $Z_3 = R_L + j0$ because the loading of the tank network has changed. Without retuning, the amplifier is then either underloaded, overloaded, or reactively loaded.

In addition to the possibility of damaging the amplifier if operated in this mistuned condition, you also have less power available! Because of this mistuning, the amplifier *delivers less power* by the amount of the reflection loss resulting from the line mismatch. This power reduction is as shown in Fig 6-1, on the curve labeled *Reflection Loss Without Conjugate Match* and at the appropriate SWR ordinate. For example, if the line SWR is 3:1, the amplifier output will drop by 25% while it sees the improper load. On the other hand, retuning the network to the actual operating impedance Z_2 establishes a match to the line-input that restores the proper amplifier load impedance $R_L + j0$ and the amplifier again delivers its maximum available power. For additional discussion on this point refer to Chapter 6, Sec 6.3, and Chapter 19.

"But," you ask, "how do we determine when proper loading is obtained, or that impedance Z_2 is within the matching range of the network?" The answer is simply by completing a normal tuning and loading operation in which you obtain the same plate current, plate-current dip, and screen-current readings that you do with the dummy load. However, tuning- and loading-control settings, and the relative power (output voltage) generally will differ from those obtained with the dummy load, depending on how much Z_2 differs from 50 ohms. If normal plate current (and dip) cannot be obtained with any setting of the loading capacitor, Z_2 is outside the matching range of the tank network, and we have conditions as defined in Case 3. If proper loading cannot be obtained with the simple series- or parallel-reactance compensating technique described earlier in this section, then an external network is required. However, I want to emphasize that *any* value of $Z_2 = R_2 + jX_2$ can be transformed to a suitable value for loading the tank network by selecting the proper network configuration (*Refs 19, p 115; 30; and 61*).

The range of impedances Z_2 that the tank network will transform to the value equal to the load impedance $Z_L = R_L + j0$ of the amplifier raises an interesting point concerning the tuning procedure for the external network. The usual practice is to tune the tank network with the dummy load, and then switch in the external network and antenna and tune for zero reflected power in the feed line (not the transformer line). This procedure should be followed if there is a filter in the feed line. However, in the absence of a filter, it is necessary to adjust the external network only for a line-input impedance Z_3, which brings it within the matching range of the tank network. This can be a time-saving feature when changing frequencies during contest operation! If both tank and external networks are adjusted for optimum match at midrange of the intended frequency excursions, in most cases only the tank network needs retuning with changes in frequency. This is true providing the frequency excursions are within the range in which the external network yields a load impedance that the tank network can transform to $R_L + j0$.

Notes

1. The broad-banding effect of the coaxial dipole has been widely thought to be accomplished by the shunting of the short-circuited coaxial stubs across the antenna terminals to cancel the off-resonance dipole reactance that appears as the frequency deviates from the resonant frequency. However, a computer analysis performed by Frank Witt, AI1H, has shown that the broad-banding was actually obtained by the resistive conduction loss in the dielectric of the coaxial line. Also see Chapter 18.

2. See Chapter 23.

Chapter 8

The Reality of Reflected Power

(Adapted from Technical Correspondence, QST, *February 1983)*

Sec 8.1 Introduction

From time to time, articles concerning transmission-line principles and techniques have appeared in various amateur radio journals, promoting the erroneous notion that reflected power is fictitious. (*See Refs 65, 67, 97, and 98.*) Unfortunately, some amateurs are misled by these authors, who are misinformed on this subject, while specialists in wave and field propagation are dismayed at seeing this erroneous concept in print. The truth is, reflected power is as real as the power delivered to the line by the transmitter, or that radiated from the antenna.

While there are many analytical proofs that are unfailing, such proofs are often disbelieved by those who do not understand them. However, here's one easy laboratory proof with physical evidence that can't be denied: Energy reflected by a mismatched line termination can be entirely separated from the forward-traveling wave, and can then be dissipated in a temperature-calibrated resistor and accurately measured as I^2R heat.

If the power associated with the reflected energy were fictitious, no heat would be generated! Within the accuracy of the measuring equipment, the power measured as heat in the resistor equals the reflected energy calculated from the known relationship between the impedances of the mismatched load and the line. The power measured in the load equals the source power minus the reflected power, which provides the proof we're looking for. I have performed these measurements many times. (Also see Chapter 3.)

A semantic problem with the term *power flow* also fuels the erroneous belief that reflected power is fictitious. This brings us to the question "Does power flow?" To help us understand the answer, let's examine an analogy that involves current.

When we talk about *current flow*, we take the meaning for granted. However, does *current* really flow? The basic electricity sections of engineering textbooks (also *The ARRL Handbook*) say that current does not flow—*charge* flows. Current is defined as the quantity of charge flowing past a point per unit time. However, once we leave basic electricity and move on to circuit analysis, the term current flow is used almost exclusively, and yet we know exactly what is meant.

The same problem exists with the term *power flow*. Engineering textbooks define power as the "quantity of energy passing a point per unit time." Thus, power does not flow—*energy* flows. However, except when reciting the definition of power, textbooks and journals on wave propagation use the term power flow almost exclusively, with only an occasional use of energy flow. As with current flow, we know what is meant because of the common usage, which generally overshadows the strict definition.

Apparently unaware of the common usage, Woods rejects use of power flow, and its meaning has distorted its meaning in an attempt to show not only that reflected power is fictitious, but also to challenge proven textbook principles of transmission-line phenomena (*Refs 67, 97*). His definitions of power and energy are correct, but the remaining portions of his articles are not. In addition, Woods' criticism of my statements published in *QST* (repeated in Chapter 3 of this book) concerning directional wattmeters would have us believe that directional wattmeters don't prove the physical existence of waves on the transmission line (*Ref 67*).

Walter Johnson, the author of the graduate-level textbook *Transmission Lines and Networks* (*Ref 18*) gives us the facts. He was the chairman of the electrical engineering department at Princeton University when he authored his book. Johnson derived equations involving forward and reflected waves of voltage and current, equations that provide the means for calculating both forward and

reflected power from values of voltage and current obtained from specific points in the standing waves. These equations are the basis for understanding the operation of all directional wattmeters, and are repeated in Chapter 3 as Eqs 3-4 through 3-9. In his lack of understanding, Woods has called Johnson's Eq 3-9 "fallacious."

Another reason why some amateurs believe reflected waves contain no power is because they have misinterpreted certain characteristics of standing waves (*Ref 97*). First, let me state the facts: Because the voltage and current components of the forward wave are always in phase, and those of the reflected wave are always 180° out of phase, the resulting standing-wave plots of voltage and current are always separated on the transmission line by a *distance of 90°, not a difference in phase of 90°*, as shown in Fig 9-3. (Also see Chapter 3.) Line *voltage*, measured *across* the line, is the phasor sum of the forward and reflected voltages. Line *current*, measured *in series with the line*, is the phasor sum of the forward and reflected currents.

The 90° distance between the voltage and current standing-wave plots conveys no phase information, but at every point along the line where either the voltage or current standing wave is minimum, the phase angle between *line* voltage and *line* current is exactly 0°. At points along the line between the standing-wave minima, the phase angle may vary between 0° and plus or minus 90°, depending on the degree of mismatch. The phase angle reaches 90° only when the mismatch results in total reflection of power (an infinite SWR, as shown in Chapter 9. Fig 9-3).

Sec 8.2 Standing Waves versus Reflected Waves

Now for the classic misconception: The 90° distance between the voltage and current standing-wave plots has been misinterpreted as the phase angle between the voltage and current of the reflected wave. From this misinterpretation, the erroneous conclusion has been drawn by at least two authors that because the cosine of 90° = 0, reflected waves contain no power! (*See Refs 68 and 97.*) It is the *standing wave* that contains no power, not the reflected wave. The results have been disastrous, because the erroneous conclusions of these authors were published in amateur radio journals that enjoy wide circulation.

Further proof that reflected power is real comes from the *Poynting Vector Theorem*. Consider an imaginary unit-cube with its sides parallel to the X, Y, and Z axes, containing a quantity of energy, E. If this cube moves forward with a velocity v, the energy will be carried past a given point along the Z axis at the rate of Ev joules per second, which is equal to the power in watts per unit area XY.

In vector notation $E_X \times H_Y = P_Z$ (watts per unit area). E_X and H_Y are energy field vectors; E and H represent the magnitudes, and X and Y represent the mutually perpendicular directions of the electric and magnetic fields contained in the cube. The Poynting Vector P_Z represents the power passing the point in the Z direction, at right angles to the XY plane formed by the E and H field vectors. When a flow of energy encounters a change of impedance (a mismatch), the magnitudes of both the E and H fields change, causing a motor-generator effect on the circuit elements. As a result, the mismatch is converted to a virtual source generator (of the reflected wave) in series with a matched load (*Ref 69*).

According to Lenz's law on counter-electromotive force, in any energy not absorbed by (or transmitted past) the mismatch, the vector direction of either the E or the H field must reverse. Which field reverses depends on the character of the mismatch. When either the X or Y direction reverses, the Poynting Vector of the unabsorbed energy must also reverse to the –Z direction, launching the reflected wave. The energy now flowing in the –Z direction is a portion of that energy flowing earlier in the +Z direction, except its magnitude has changed and its direction reversed. An exact analogy is that of light energy reflected from a mirror.

Wave energy reflected from a mismatch can be totally separated from the energy traveling in the forward wave. After separation, the Poynting Vector, P_{-Z}, of the reflected wave is the cross product of the E and H field vectors of the reflected wave: $E_{\pm x} + H_{\pm y} = P_{\pm z}$ watts per unit area, again proving that reflected power *is* real power.

Chapter 9

Standing-Wave Development and Line Impedance

Sec 9.1 Introduction

So far in this book we have discussed the impedance-matching function of the antenna tuner, or transmatch, from the viewpoint of wave reflections. The wave (or power) reflected by the mismatch at the junction of the feed line and antenna is returned to the antenna because of re-reflection by the antenna tuner. We observed that because of the impedance match achieved by the antenna tuner, power reflected by the mismatch at the feed line and antenna junction adds to the source power in the tuner. This addition enables all the reflected power to be returned to the antenna and radiated, with the exception of that lost because of line attenuation.

The next few chapters explore the background for understanding matching from the viewpoint of impedance. There we will examine a concept that explains why impedance can exist in the absence of physical resistors, inductors, or capacitors. Once we understand this concept, we can apply it to a practical, mismatched transmission line. In doing so, we will learn why the impedance Z_{IN} appearing at the input of the mismatched line no longer equals the line's characteristic impedance, Z_C, when reflected waves generated by the mismatched load terminating the line arrive back at the input.

However, to fully appreciate the discussions that follow, you must clearly understand that reflected power traveling rearward along a transmission line is *real power*, not reactive power, as some would have us believe. If you are among those who have been misled to believe that reflected power is reactive power, then I suggest you review Chapters 3 and 8. You can learn the truth from those chapters, and thus dispel for yourself the reactive- vs. reflected-power myth. The myth has been perpetrated unwittingly by some writers who drew erroneous conclusions from a basic fact concerning standing waves (*Refs 67, 68, 97, 98*). That fact is this: Standing waves of voltage and current are always separated by 90° in distance along the line. This 90° distance has been misinterpreted to be a 90° phase difference between the reflected voltage and reflected current, which is not true. Those writers then drew the erroneous conclusion that what they thought was a 90° "phase difference" between reflected voltage and current meant that the reflected power is reactive. As explained in detail in Chapter 3, the phase difference between the reflected voltage and current is *always* 180°, *never* 90°, providing evidence that reflected power is real.

Other people have tried to persuade me that reflected power is not real power for another reason. They say that power cannot flow in both directions simultaneously on a transmission line for the same reason why water cannot flow in both directions in a pipe (*Ref 99*). This is a false argument. Using water analogies to explain electrical circuits is fine if the analogies fit, but this one doesn't fit. Water flow enclosed in a pipe is not a legitimate analogy for current flow on a transmission line.

The smooth surface of a pond, however, is a legitimate basis for an analogy. Consider this: A pebble dropped at the center of a pond causes ripples, or waves, to travel forward until they reach the edge of the pond. Unless the material of the pond edge totally absorbs the energy in the forward wave, reflected waves containing the unabsorbed energy will originate at the edge and travel back toward the point where the pebble was dropped. The resulting standing wave can then be observed on the surface of the water between the edge of the pond and the point where the pebble was dropped as the forward and reflected waves of water pass through each other. Much more is said later concerning the formation of standing waves, and waves traveling in both directions on a transmission line was discussed in detail in Chapter 3.

Before we proceed to the background study of matching from the viewpoint of impedance, let's

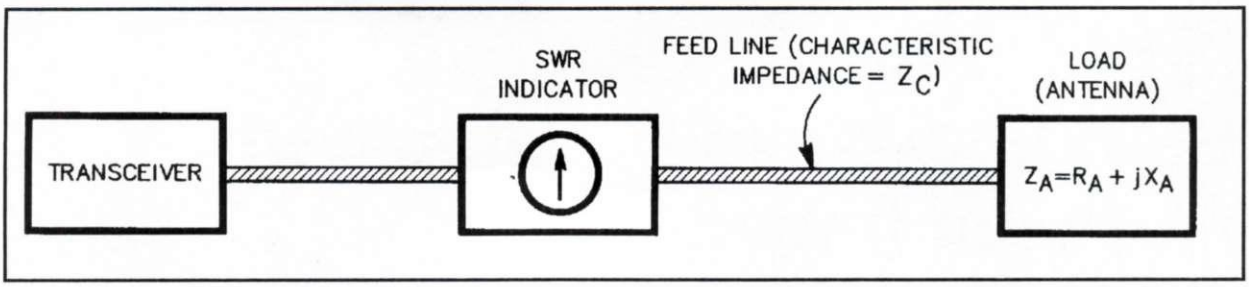

Fig 9-1. The conventional arrangement of connecting a transceiver to an antenna. The SWR indicator is inserted in the feed line near the transceiver. For the text discussion of input impedance, Z_C = 50 ohms.

take a final, summarizing look at matching from the viewpoint of wave action and reflections. Keep in mind that the wave actions described in this summary are responsible for *all impedance-matching operations*, regardless of the type of network used to perform them.

Whenever impedance matching is performed at any junction of transmission lines, components, or loads having different impedances, a wave reflection is set up from the mismatch at the junction. With whatever type of matching network is used, the matching is achieved because the network itself presents a complementary mismatch that generates another wave reflection complementary to that generated at the junction. These two complementary reflected waves are mirror images of each other, because they have the same magnitude but opposite phase (*Ref 35, p 58*).

The complementary nature of the waves generated by the network is obtained by selecting the appropriate values for the components in the network. When the two reflected waves of opposite phase join at the matching point in the network, they cancel each other. This cancellation creates either a virtual open or short circuit to the rearward traveling waves and causes their total re-reflection—a complete reversal of their rearward direction. The waves then add, producing a resultant wave traveling in the forward direction in phase with the source wave.

Because the network mismatch generated a wave having the same magnitude but opposite phase relative to the wave generated at the junction mismatch, the voltage and current components of the new forward-traveling wave resulting from the re-reflection emerge in phase with the corresponding components of the source wave. Hence, the power in the re-reflected resultant wave adds directly to the source power. Because the power contained in the wave reflected from the junction mismatch is now a portion of the forward-traveling wave, it is evident that the power reflected by the junction mismatch is added to the source power at the matching point, and that no reflected power travels beyond the matching point in the rearward direction. It is for this reason that the matching device transfers the maximum available power from a source to a load of different impedance.

Sec 9.2 Introduction to Line Impedance

Before we delve into the study of impedance encountered on transmission lines, let us first discuss briefly the nature of impedance to make certain that we have a clear understanding of what is meant by impedance. In the analysis of electrical networks we assign a pair of variables: *voltage* (an "across" variable) and *current* (a corresponding "through" variable). *Energy* is defined as the *product* of these two variables, voltage *times* current, and *impedance* is defined as the *ratio* of the variables, voltage *divided* by current.

Impedance has a component of resistance, R, and, depending on the phase relation between the voltage and current, it may also have a component of reactance, X, as well. Impedance may be dissipative or non-dissipative, depending on the type of resistance, which also may be dissipative or non-dissipative. A *non*-dissipative resistance? Yes, the *real* part Re of impedance is non-dissipative unless the resistance in the impedance is a physical resis*tor*, such as in a terminating load with its current flow converting energy to heat, or an antenna that converts the energy to radiation.[1] A non-dissipative impedance occurs, for example, between two terminals of a network, where the energy is transferred from one por-

tion of the network to the next, with no dissipation to heat except for the loss due to the inherent resistance in the components of the network. A network with lossless components would dissipate no energy to heat, but would simply transfer the energy on to the next component downstream. Therefore the voltage *across* the network terminals divided by the current *through* the terminals defines the impedance Z = E/I appearing at the terminals. This impedance appearing at the network terminals is *non*-dissipative for the reasons just explained. (A more in-depth examination of the nature of impedance appears in Appendix 10.)

The same is true at the input terminals of a transmission line. If we consider a lossless line, the input impedance of the line is simply Z = E/I, and it is a non-dissipative impedance because no dissipation to heat occurs either at the input or anywhere along the line. Any dissipation to heat occurs downstream where the energy encounters a resistive termination on the line that either converts the energy to heat there, or radiates it into space via an antenna.

Now let's begin our in-depth background study of the impedances encountered on transmission lines. This study will lead to an understanding of the impedance that appears at the input terminals of the line carrying RF power to the antenna. We know that widely differing values of impedance appear at the input terminals with various combinations of line length and antenna impedance. It is these large excursions of line-input impedance relative to the preferred 50 ohms that make loading of the transceiver difficult or impossible, and often require an antenna tuner to accomplish a satisfactory loading. Thus, in this study we'll want to see why these different impedance values appear. We will want to learn how reflected waves of voltage and current change the input impedance from its usual characteristic impedance, Z_C, of 50 or 75 ohms to any one of an infinite number of different possible complex values. I'll purposely omit any mention of antenna tuners for the present, but after we see why the input impedance changes (which makes the tuner necessary), I'll explain how the tuner transforms the line-input impedance to either 50 ohms, or to an impedance that will properly load the transmitter. Once this is understood, the earlier paragraph on network matching from the wave reflection viewpoint will come into sharper focus.

First we'll consider the conventional arrangement in which an SWR indicator is inserted in the feed line near the transceiver so that a short section of feed line connects the transceiver to the SWR indicator, and a longer section runs from the indicator to the antenna (see Fig 9-1). We'll assume that the transceiver is tuned to the resonant frequency of the antenna, and that the antenna resistance, R_A (the resonant impedance), is the same value as the characteristic impedance, Z_C, of the feed line. Under these conditions we can say that the antenna is matched to the feed line. We know that when the antenna is matched to the feed line, there are no reflections generated at the antenna end of the line, and the SWR indicator shows a reading of 1:1. However, do we really know what this reading of 1:1 means?

In answering this question, let's first make sure we really understand what SWR is—what the numbers in the standing-wave *ratio* tell us. The line voltage and line current vary with distance along the line. The numbers in the ratio tell us the relative amount of variation in line voltage (and current) between the minimum and maximum values that appear. To appreciate the significance of these variations, though, it is important that we also understand the reason why they occur. Therefore, at this point I'll digress to explain this very important concept.

Sec 9.3 Line-Voltage Variation and the Generation of Reflections

For ease in understanding, let's use numbers for the various impedances and voltages; we'll use 50 for the line impedance, and a source-generator voltage of 1 volt. Hence, from Ohms Law, the line current will be 0.02 amperes when the line is terminated with a matched load. We'll begin by continuing with the condition shown in Fig 9-1, in which the line is terminated with a matched load, except in this case we'll make the load a 50-ohm resistor instead of the antenna. This load gives rise to no reflection, because all the power carried by the line is dissipated as heat in the resistance of the load. Also, there is also no change in current, as the line current of 0.02 ampere becomes load current. This happens because there was no change in impedance in transferring the power from the line

into the load. This is an important point to remember. In this case there is no variation in either the voltage or current along the line, so the ratio between the maximum and the minimum of voltage or current is obviously one. We represent this in ratio form as 1:1.

Let's now replace the matched 50-ohm load resistance with a 150-ohm resistance. This new 150-ohm resistance causes a 3:1 mismatch to the line, resulting from the 3:1 ratio between the 150-ohm load impedance and the 50-ohm line impedance. Because of motor-generator action in the load (which was explained in Chapter 3, but which I reexamine shortly), the 3:1 mismatch causes the generation of a reflected potential of 0.5 volt. The reflected 0.5 volt adds to the 1 volt of the forward voltage wave at the load point and causes a new potential of 1.5 volts to appear across the load. Keep in mind that the voltage all along the line remains at 1 volt before the first voltage wave encounters the mismatch. As we will see, the line voltage changes after the forward voltage encounters the mismatch.

The constant forward line current of 0.02 amperes encountered an abrupt change of impedance in transferring from 50 ohms of line impedance to 150 ohms of load resistance. The current suddenly dropped to 0.01 ampere because of the increased resistance. The resulting change in the electromagnetic field caused by the change in current generated the new voltage—the 0.5 volts that is reflected. Thus, motor-generator action generates the reflected voltage.

Another way of visualizing the generation of the reflected voltage is from the viewpoint of a reflection generator connected in series with the load resistance. Because the changing current in the load resistor caused the field surrounding the resistor to change, a new voltage was generated within the resistor. This is because the resistor is a conductor immersed in the lines of force of the electromagnetic field surrounding it, which changed in the same way as if the resistor was a conductor in the rotating armature of a mechanical generator. The only difference is that in the mechanical generator the field is stationary and the conductor moves, while in the case of the load resistor the resistor (the conductor) is stationary and the field moves. The result is the same in either case: A voltage is generated.

We therefore may say that a mismatched load is a reflection generator. The voltage it generates is applied between the line terminals at the load end of the line in the same way the source generator applies the original source voltage between the terminals at the input of the line. Once the reflected voltage is applied to the load end of the line, it starts a new wave of voltage and current traveling rearward up the line in the same manner as the forward wave of voltage and current travel toward the load. The two waves slide past each other in opposite directions, as if the other didn't exist, except for one notable result: They produce the standing wave!

Before I go into detail on how the standing wave is formed, this is an opportune time for me to reintroduce rho (ρ), the magnitude of the reflection coefficient. This coefficient has an important relationship in the development of the standing wave. Rho first appeared in Chapter 3, Eq 3-1. It is directly related to the SWR, as shown in Eqs 3-2 and 3-3. Reflection coefficient ρ defines the size, or magnitude, of the reflected voltage (or current) relative to the forward voltage (or current). However, in practice, the reflected voltage is used more often than current when specifying ρ. The assigning of 1 volt for the forward-wave voltage in the earlier paragraph was for the express purpose of simplifying the understanding of the reflection coefficient, because with a forward-wave voltage of 1, the voltage of the reflected wave automatically becomes the value of the reflection coefficient. Thus, the reflected voltage of 0.5 in the example above signifies that the reflection coefficient magnitude, ρ, is also 0.5.

Reflection coefficient is a more specific term than SWR, because with the complete complex reflection coefficient, $\rho\angle\theta$, we can specify and define impedance, while with SWR alone we cannot. However, we need more than just the *magnitude* of the reflection coefficient to specify impedance. We also need *phase* or *angle*, which SWR does not contain. Sec 1 of Chapter 3 introduced this phase angle as theta (θ). The angle of the reflection coefficient in the example above is $\theta = 0°$ relative to the forward voltage, meaning the reflected wave is exactly in phase with the forward wave at the load. Hence, the 0.5 volt of reflected voltage adds to the 1.0 volt of forward-wave voltage to make the load voltage equal 1.5 volts. We saw in Chapter 3 that

the nature of the load determined the magnitude ρ = 0.5, but because the resistance of the load was larger than the line impedance Zc, the angle of the reflection coefficient is θ = 0°.

If the load resistance had been 16.667 ohms (one third the value of the line impedance, instead of three times the value), the magnitude would remain at 0.5, but the angle would be shifted to θ = 180°. In that case the polarity of the reflected voltage is reversed, so it is *subtracted* from the forward voltage, making the load voltage 1 – 0.5 = 0.5 volt. The reason for this change is explained in Chapter 3, and is also discussed in Chapter 11, which covers the use of the Smith Chart.

We can now make general statements concerning the relationship between the reflection coefficient and the nature of the mismatch which determines it. These statements apply when the load impedance is *purely resistive*:

(1) If the load current becomes less than the transmission-line current (because the load resistance, RL, is greater than the line impedance, Zc), the load voltage rises above the line voltage, and the angles of the voltage and current reflection coefficients are θ = 0° and 180°, respectively.

(2) Conversely, if the load current becomes greater than the line current (because RL is less than Zc), the load voltage becomes less than the

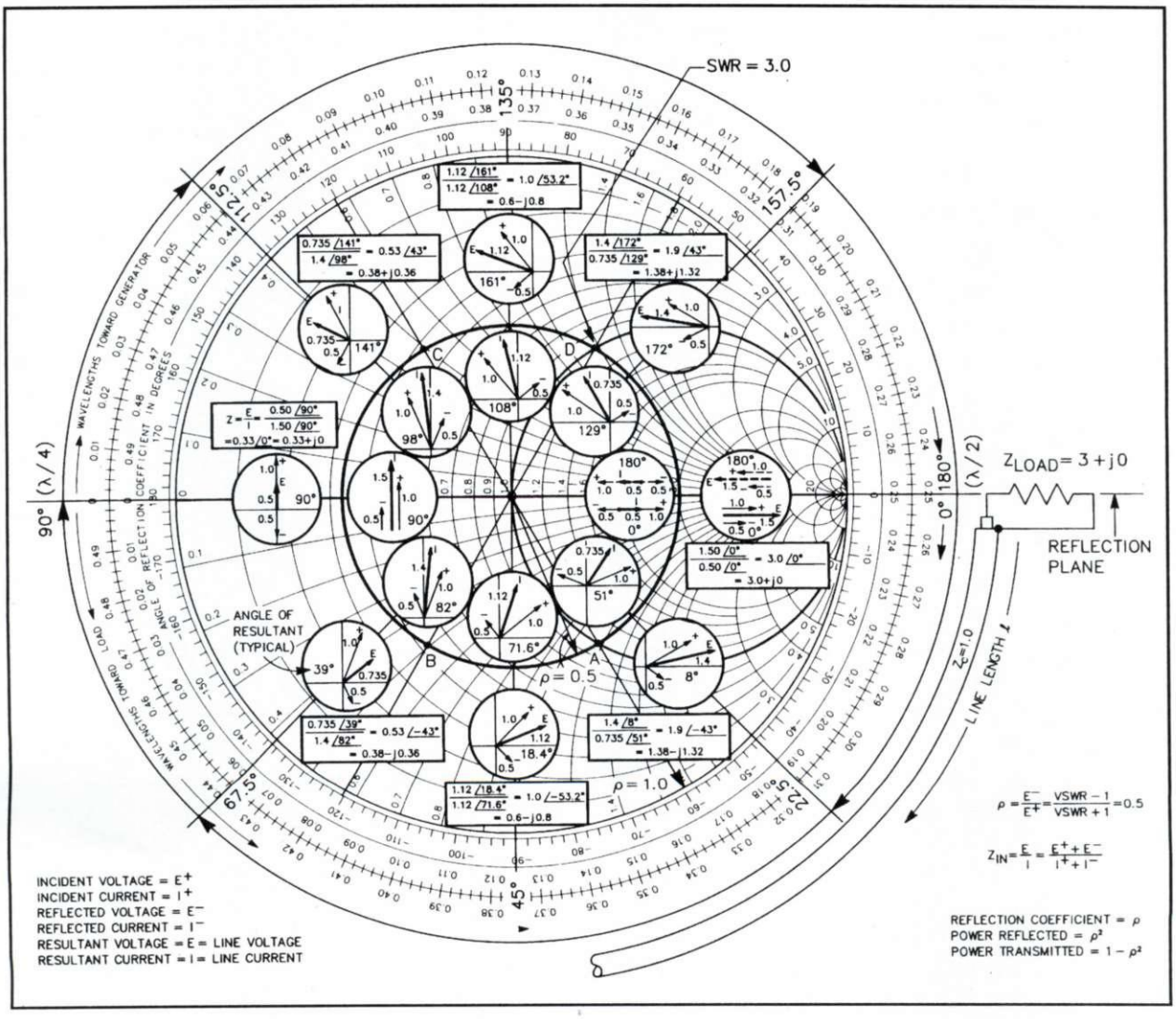

Fig 9-2. The W2DU Reflection Mechanics Vector Graph. This graph is presented as Fig 3-2 with a detailed description of its use in Chapter 3, but is reproduced here for convenient reference (enlarged version at back of book).

line voltage, and the angle of the voltage and current reflection coefficients are reversed, becoming 180° and 0°, respectively.

Angles other than 0° or 180° are obtained when the load contains reactance, but that's getting ahead of our story. We'll get into reactance concepts in detail later. Consequently, the concept contained in the above general statements form the basic reason why a standing wave is developed when reflected waves of voltage and current travel in the rearward direction along the line in conjunction with their respective forward-traveling components: While the phase relationship between the forward voltage and current is always 0°, the phase relationship between the reflected voltage and current is always 180°. The 180° phase difference is simply because of the opposite direction of wave travel of the forward and reflected wave. However, as we will see, the standing wave is born because of this seemingly small detail!

Sec 9.4 Development of the Standing Wave

We are now ready to examine the development of the standing wave. Our ultimate goal for this section is learning why the input impedance of the line changes in the presence of reflections from a mismatched load termination, but just be patient. We are still laying the groundwork that is essential to a clear understanding of the reason why the impedance changes. As we proceed, it will become evident that the impedance appearing anywhere on the line is directly related to the relative amplitudes of the voltage and current standing waves.

In Chapter 3, I stated that standing waves are formed by the alternate cancellation and reinforcement of the forward and reflected waves as they slide past each other while traveling in opposite directions. As we proceed in this section, I will prove this statement true with an analytic approach. I'll use the vectors appearing on the W2DU Vector Graph of Fig 3-2. These vectors, more properly called *phasors,* represent the values of the forward (incident) and reflected voltages and currents appearing on the transmission line, as described in Chapter 3 and as appearing on the graph itself.

As we now look into the development of standing waves, let's use the same values of impedances, voltages, currents, and reflection coefficients as in the earlier example. Refer again to Fig 9-1, and remember that the load is a 150-ohm resistor. It should be clear that the standing wave originates at the 150-ohm mismatched load terminating the 50-ohm line. To review briefly an earlier discussion, when the forward voltage wave having the amplitude of 1 volt encountered the 150-ohm mismatch, the line current of 0.02 ampere abruptly decreased to 0.01 ampere. This change in current caused a corresponding change in the electromagnetic field surrounding the load, which induced a new value of 0.5 volts appearing in series with the 150-ohm load resistance. Because the load resistance is greater than the line impedance, the new voltage is in phase with the 1-volt source potential, and adds to the line voltage to produce a total of 1.5 volts across the load resistance. This additional 0.5 volts applied to the terminals at the load end of the line launches a new voltage and current wave into line, which starts traveling in the reverse direction, toward the transceiver (generator).

Because phase plays a prominent role in our discussion of standing-wave development, I'll now digress for a brief discussion of phase for the sake of clarity. As we all know, the voltage and current waves we are discussing here are sine waves that travel with a finite velocity. Thus, the waves have a wavelength on the line that depends on the frequency of the wave, or the number of cycles completed in one second. One wavelength on the line is equal to one complete cycle of the sine wave, which is equal to 360° of phase. Therefore, $\lambda/4$ equals 90°, and $\lambda/2$ equals 180°, etc. Haven't we all heard how a $\lambda/2$ line repeats the load impedance at its input, but reverses the phase, changing it 180°? We will soon understand why. While the magnitude of the reflection coefficient, ρ, is the ratio of the reflected voltage to the forward voltage, as stated earlier, angle θ of the voltage reflection coefficient is equal to the difference in phase between the forward and reflected waves.

A phasor line having a length proportional to its magnitude and a direction representing the angle of the phase may represent both the magnitude and phase of either a voltage or current wave. These relationships, and those which follow, are clearly shown in the circular insets of "The W2DU Reflection-Mechanics Vector Graph," Fig 9-2. It

may be helpful here to review Chapter 3 for further study of these concepts, which are essential to the understanding of the impedance change at the input terminals of the line when the line is terminated in a mismatch. The phasors of Fig 9-2 (and Fig 3-2) are displayed on a Smith Chart, but don't let that scare you, as the explanation of how to interpret it is included. It is also explained in Chapter 10. The Smith Chart presentation actually enhances the appreciation of how the change in impedance occurs. It is important to note that the W2DU Vector Graph was drawn using normalized impedances, where Zc = 1 instead of 50. The values of resistance, reactance, and impedance appearing in the graph will conform to the present example simply by multiplying them by 50.

We established earlier for the above example that at the mismatched termination point (the reflection plane in Fig 9-2), the forward voltage and current and the reflected voltage are all in phase, while the reflected current is 180° out of phase. If we let the reflection plane be a zero-phase reference point, then the forward voltage and current and the reflected voltage appearing there are all at zero phase, and the reflected current is at 180°. Hence, we can assign phasor lines to represent the voltages and currents appearing at the zero-phase reference point as follows: Forward voltage and current phasors have length 1 at 0°, and because reflection coefficient ρ is 0.5, reflected voltage and current phasors are length 0.5 at 0° for voltage, and length 0.5 at 180° for current.

If we now move to different points along the line, we see from the phasors shown in the successive insets on the graph that the *magnitudes* of the forward and reflected voltage and current vectors remain constant, but the *relative phases* of all the voltage and current components change. These changes cause their phasors to rotate correspondingly, degree for degree, with changes in position along the line. As we move toward the generator, the phase of the forward wave *leads*, causing the corresponding phasors to rotate counterclockwise. Conversely, the phase of the reflected wave *lags* as we move, causing their phasors to rotate clockwise. It is therefore evident that for every degree of motion along the line, the phase relationship between the forward and reflected wave changes two degrees. Therefore, by definition, the angle θ of the reflection coefficient also changes two degrees for every degree of motion on the line.

It is now evident, as shown in the phasor plots, that if we move along the line from the 0° reference point to a point 90° toward the generator, the phase of the forward voltage is +90°, while that of the reflected voltage is –90°, for a resulting phase difference of 180°. Likewise, the phase of the forward and reflected current wave has also changed by the same amount. However, while the phase of the forward current changed from 0° to +90°, the phase of the reflected current changed from 180° to +90°, which means that the reflected current and the forward current are now in phase at the 90° point on the line. These phase relationships can all be observed in the phasor plots at the 0° and 90° points appearing in Fig 9-2.

These new phase relationships at the 90° point on the line are of great significance in the development of the standing wave and ultimately the line-input impedance. Note that the forward and reflected voltage waves are in phase at the zero-phase reference point (where ρ = 0.5 at 0°), and the voltages there add vectorially to form a maximum voltage of 1.5. However, at the 90° point (where ρ = 0.5 at 180°), the forward and reflected voltage waves are 180°*out of phase*, so by vectorial addition the 0.5 volt of the reflected wave subtracts from the 1 volt of the forward wave, forming a minimum line voltage of 0.5 volt. The maximum line voltage is thus 1.5, and the minimum, at a point 90° away, is 0.5 volt. The voltage standing-wave ratio is therefore 1.5 to 0.5, or 3:1.

Conversely, the current waves behave in the opposite manner. At the zero-phase reference point, the out-of-phase reflected current adds vectorially to the line current to *subtract* from the line current, resulting in a minimum load current of 0.01 ampere (one half of the 0.02 ampere original line current). However, at the 90° point on the line, the reflected current is in phase with the forward current, and adding. This raises the line current 0.01 ampere higher than the original 0.02 ampere, for a maximum line-current value of 0.03 ampere. Thus, we see the current is 0.03 ampere at the maximum, and 0.01 ampere at the minimum. The current standing-wave ratio is 0.03/0.01 = 3, also 3:1.

If we continue on toward the generator another 90° to the 180° point, we will have completed 180°

of travel along the line. Then we will have returned to the equivalent of the starting point, where the relative phase relationships are the same as they were at the zero-phase reference point, with the exception that the phase of *all* phasors has changed 180°. This is shown by the positions of the phasors in the insets of Fig 9-2. Hence, we have witnessed the alternate reinforcement and cancellation of the forward and reflected waves through the use of phasor representation of the waves.

Several general statements of great importance may now be made, which are verified by observing the relative positions of the phasors in Fig 9-2:

(1) At any point on the line where a voltage maximum and a current minimum occur, the angle of the reflection coefficient θ is 0°.

(2) Conversely, at any point on the line where a voltage minimum and a current maximum occur, the reflection coefficient angle θ = 180°.

(3) A voltage maximum and a current minimum always occur simultaneously at the same point, and vice versa.

(4) Points where voltage maxima and current minima occur are always separated by 90° along the line from points where voltage minima and current maxima occur.

(5) The SWR is the ratio of the maximum and minimum values of either the voltage or current.

These five statements may be interpreted graphically in Fig 9-2. Graphic illustrations of statements three through five appear in Fig 9-3, which is explained in more detail in Sec 9.6.

So far I have identified and explained the formation of the maximum and minimum points of the standing wave—the successive reinforcement and cancellation mentioned earlier. Now let's examine the smoothly changing voltage and current amplitudes appearing on the line between the maximum and minimum points—amplitudes along the line that form the standing wave.

The voltage standing wave is a pattern of successive amplitudes of voltage resulting from the *vectorial* addition of the forward and reflected phasor voltages at every point along the line, as the two waves slide past each other while traveling in opposite directions. The current standing wave is produced by similar action of the forward and reflected current phasors. Earlier we saw that when the phase was either 0° or 180° at the points of maximum voltage and minimum current, or vice versa, respectively, we could determine the amplitude of the standing wave by simple arithmetical addition or subtraction of the forward and reflected wave phasors. However, to find the standing-wave amplitude *between* these maximum and minimum points, we cannot simply add or subtract the phasors, because their respective reflected voltages and currents are no longer either exactly in or exactly out of phase. Consequently, *vectorial addition* is required to obtain the amplitudes for all the in-between values of relative phase along the line because the resulting impedances are complex.

Accordingly, eight vectorial additions were calculated at 22.5-degree intervals along a λ/2 line having a 3:1 SWR. The results of these additions are shown as insets in Fig 9-2. The voltage E and current I resultants of the additions are shown by the wider, darker vector lines in the enclosed circles. Both the lengths (magnitudes) and the phase angles of these resultants are indicated in the insets. The magnitudes of the resultants are plotted as the voltage and current amplitudes for the corresponding 22.5-degree intervals along the line to supply the points for forming the resulting smooth, continuous curves of the voltage and current standing wave shown in Fig 3-3.

Sec 9.5 Determining Impedance on The Mismatched Line

We should now be aware that the phasor resultants labeled voltage E and current I in Fig 9-2 represent both the magnitude and phase of the actual line voltage, E, and line current, I, appearing at the corresponding points on the line. The length of a phasor represents the magnitude, and the angle of direction represents the phase. *Voila!* The values that these resultant phasors represent are just what we need for determining the impedance appearing at those points on the line. Keep in mind that the line voltages and currents represented by these phasors result from the vectorial addition of the forward (incident) and reflected voltages and currents at each point as the waves slide past each other, traveling in opposite directions.

To determine the impedance at any point on the line, including the input terminals, we simply take the ratio of voltage to current appearing at the

desired point, thus Z = E/I. However, vectorial division is required here to obtain the impedance, because E and I are complex numbers, comprising both magnitude and phase angle, as shown in their phasor presentation in Fig 9-2.

Of course the resulting impedance is also complex, containing capacitive reactance at points where the angle of reflection coefficient is negative, and inductive reactance where the angle is positive. At points where the angle of reflection coefficient is either 0° or 180°, the resulting impedance is a pure resistance, because, as we found earlier, at these points (and only at these points) the line voltage and current are in phase. This means that the impedance contains reactance everywhere on the line except where the angle of reflection coefficient is 0° and 180°. (The relationship between the angle of the reflection coefficient

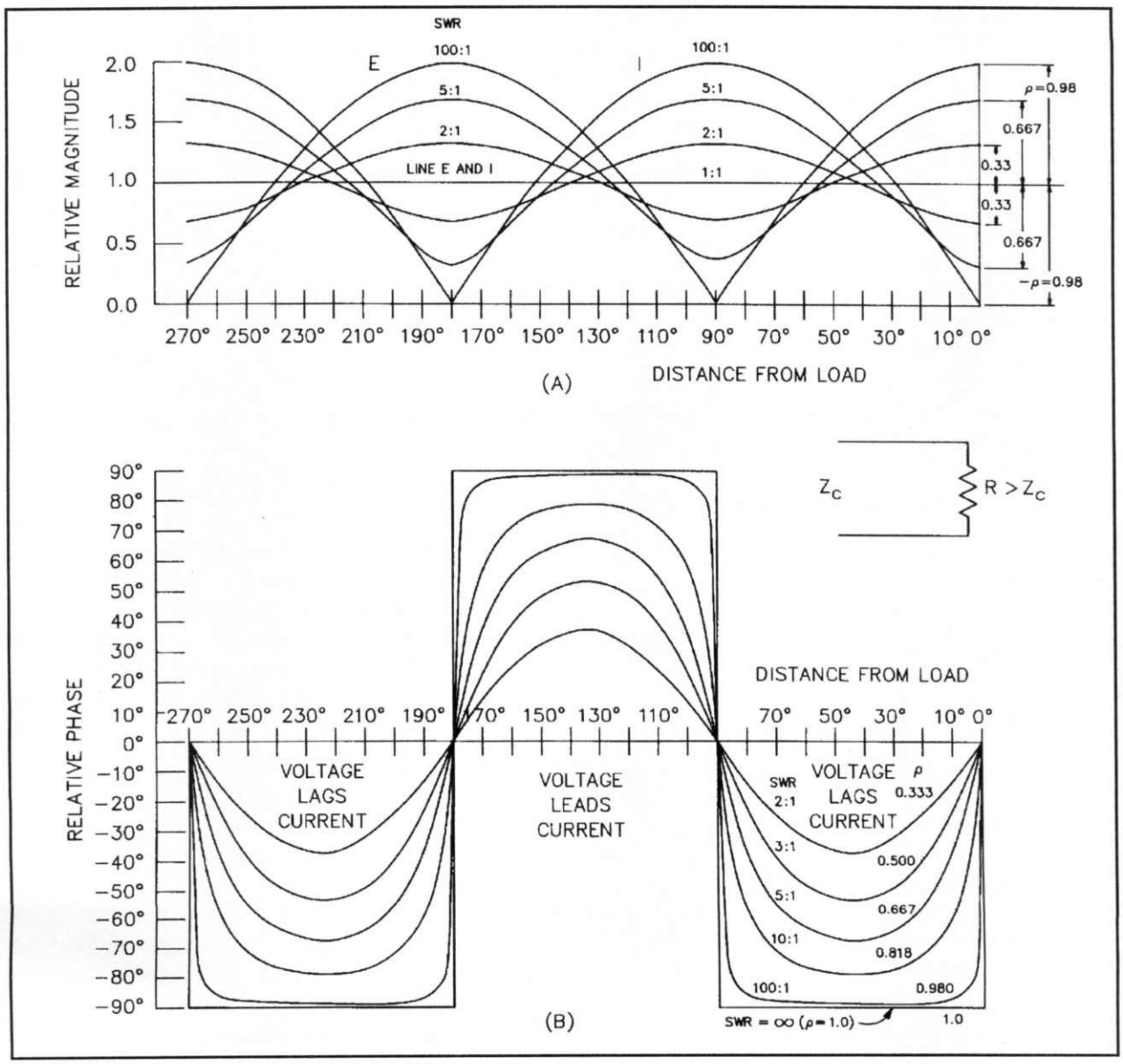

Fig 9-3. Plots of relative magnitude (A) and phase (B) between line voltage, E, and line current, I, versus position along a mismatched transmission line. Curves for different mismatch values are shown for resistive loads greater than Zc (no reactance). When the resistive load is less than Zc, the E and I plots will exchange positions and the *phase will reverse.*

and reactance is explained in Chapter 10.) To perform the vector division we divide the magnitudes, E/I, to yield the magnitude, Z, of the impedance. We then subtract the phase angle of the current, I, from that of the voltage, E, to yield the phase angle ϕ (phi) of the impedance.

I'll illustrate with an example from Fig 9-2. Using the resultant phasors of voltage, E, and current, I, appearing where the line length $\ell^\circ = 45^\circ$, and where the angle of the reflection coefficient is -90°, we see that the voltage phasor has a length of 1.12 normalized units at angle 18.4°, and the current phasor is also 1.12 units long, but at angle 71.6°. As stated above, to perform the vector division to obtain the impedance, we simply divide the magnitudes, 1.12/1.12 = 1.0, and subtract the angles, $18.4^\circ - 71.6^\circ = -53.2^\circ$. Thus, the normalized line-input impedance in polar form at a point 45° from the 3-ohm load termination is z = 1.0 at $\angle -53.2^\circ$. (This division is shown in the adjacent inset box in the graph.)

In a 50-ohm system we multiply the impedance by 50, making the de-normalized impedance Z = 50 ohms at $\angle -53.2^\circ$ Note that these impedances are in polar form. To obtain the resistance and reactance values we need to convert the polar impedances to the rectangular, or complex form, $r + jx$, using the simple trigonometric relationships:

$$r = z \cos \phi \qquad \text{(Eq 9-1)}$$

$$x = z \sin \phi \qquad \text{(Eq 9-2)}$$

where

z = the magnitude of the impedance
ϕ = the phase angle of the impedance
r = the resistance
x = the reactance

Solving these relationships for the example yields $1.0 \cos (-53.2^\circ) = 0.6$ ohms resistance, and $1.0 \sin (-53.26^\circ) = -0.8$ ohms reactance. De-normalizing these values to a 50-ohm system yields R = 30 ohms and X = –40 ohms. In other words, $Z = 30 - j40$ ohms, where the minus sign denotes a capacitive reactance. We are following the customary practice here in which symbols for normalized components are shown in lower case, while symbols for actual, non-normalized components are capitalized.

Summarizing for the 50-ohm system, we see that with a load resistance of 150 ohms terminating a 50-ohm line and producing a 3:1 SWR, the input impedance of the line of length 45° ($\lambda/8$) is $Z = 30 - j40$ ohms. These values can be seen in the W2DU Antenna-Impedance Feed-Line Transformation Graph, Fig 10-1, which is described in Chapters 10 and 12.

Sec 9.6 Development of Reactance on Transmission Lines

From elementary AC theory we know that impedance contains reactance when the voltage and current are not in phase. When the current lags the voltage, as when flowing through an inductor, the impedance looking into the inductor contains inductive reactance. Conversely, when the current leads the voltage, as when flowing through a capacitor, the impedance looking into the capacitor contains capacitive reactance. Therefore, at this point you are probably wondering, "How does a reactance originate when the load terminating a transmission line is a pure resistance?" You'll be happy to know that all the ingredients for obtaining the answer to this question have already been presented.

Recall the electrical configuration of two AC generators—the source generator and the reflection generator, one at each end of the transmission line. The line simply transfers the energy from each generator along the line simultaneously in opposite directions, but with a changing phase relationship with position along the line because of time delay.

Return to the example in Fig 9-2, at the point where the line length $\ell^\circ = 45^\circ$. Again observe that the voltage and current arriving from the source generator (the forward, or incident, voltage and current—the phasors with the plus signs) are both at +45°, and the reflected voltage and current arriving from the reflection generator (the phasors with the minus signs) are at –45° and +135°, respectively. These are the phase relationships between the voltages and currents from each generator as they arrive at this 45° point on the line. The transmission line has simply carried the energies from each generator to the $\ell^\circ = 45^\circ$ point on the line while accounting for the change in phase with the time of travel from each generator to this point. Hence, for purposes of analysis we can eliminate the line completely and simply connect the two generators in

series, while assigning the same phase relationships between them that previously appeared between the forward and reflected waves at the $\ell^\circ = 45^\circ$ point on the line.

With this phase relationship, we know the voltages and currents from the two generators connected in series are not in phase. Also, we know that reactance is developed whenever the voltage and current are not in phase. From the circular insets we see that the resultant phase of the voltages between the two generators is 18.4°, and the resultant phase of the currents is 71.6°, yielding an impedance phase angle of –53.2°, as explained earlier. This means the current leads the voltage by 53.2°, thus producing the 40 ohms of capacitive reactance at the $\ell^\circ = 45^\circ$ point on the line.

In Fig 9-3 we have a rectangular graph showing the amplitudes of the line voltage and current, E and I (the SWR curves), and the phase angle ϕ between voltage and current. Curves are shown for four different values of SWR versus distance from the load. Hence, the impedance in polar form at any point on the line for these four values of SWR may be obtained by dividing the voltage by the current obtained from the amplitudes in the SWR curves, and adding the phase angle from the corresponding phase curve. The polar form may then be converted to the rectangular form $R + jX$, as explained in Sec 9.5.

There is one further point concerning impedance on the line. We know that in the presence of reflections, the line impedance is a pure resistance at points on the line where the angle of reflection coefficient $\theta = 0^\circ$ and 180°. The point to note is that even though the reactance is zero at these two points, the resistance at these points is never equal to the line impedance Z_C in the presence of reflections. The resistance at $\theta = 0^\circ$ is always higher than Z_C, and equals $Z_C \times$ SWR, while the resistance at $\theta = 180^\circ$ is always lower than Z_C, equaling $Z_C \div$ SWR. However, there are points on the line where the resistance, R, does equal Z_C, but reactance is always present at these points, because, as stated previously, reactance is present in the line impedance everywhere on the line except at $\theta = 0^\circ$ and 180°. These points are covered again in Chapter 11 on the use of the Smith Chart.

Note

1. One of the most serious misunderstandings in the engineering community is in the lack of knowledge of the two different definitions of "resistance." The misunderstanding arose because the IEEE chose to call two different, mutually exclusive entities by the same name, *resistance*. One is dissipative and the other is not. The separate IEEE definitions of the two types of resistance appear in Appendix 10, along with additional explanation to clarify the misunderstanding that has wide implications.

Chapter 10

An Introduction to the Smith Chart

Sec 10.1 Introduction

In Chapter 9, with a fair degree of difficulty using vector arithmetic, we succeeded in calculating a few line-input impedances. We did this for only one SWR, 3:1, and for only eight different line lengths (those appearing in Fig 9-2). However, in amateur operation we know we'll encounter hundreds of different input impedances as we use different antennas, different lengths of transmission line, different bands, etc. Wouldn't it be great if we could determine, at least roughly, what impedances we might encounter with these different configurations when matching the rig to the feed line? Without a computer and a suitable program to run, the impedance-solving problem is tedious at best. There is a practical solution, however—the *Smith Chart!* In spite of its apparent complexity at first sight, the Smith Chart provides the best solution with the most vivid presentation of changes in line-input impedance as the line length changes.

With the brief explanation of the Smith Chart that follows, you will discover that although it initially looks quite formidable, the chart isn't really all that difficult to use. Also, once you see how beautifully it demonstrates impedances on transmission lines, you'll find the time spent becoming acquainted with the Smith Chart is well justified.

The W2DU Vector Graph, Fig 9-2, is a basic Smith Chart that I modified by adding vectors representing forward (incident), reflected, and resultant voltages and currents. These added vectors form the basis for developing an understanding of the standing wave and the impedance functions. (As mentioned in Chapter 9, what I earlier chose to call *vectors* should more correctly be called *phasors*.)

The W2DU Antenna-Impedance Feed-Line Transformation Graph, Fig 10-1, is another modification of the Smith Chart designed to enhance the presentation of feed-line impedance transformation. Fig 10-1 will help you understand the matching problem that exists when you attempt to tune and load your rig into a feed line when the SWR is not 1:1. This problem is discussed in detail in Chapter 12.

Fig 10-2 is a basic, normalized Smith Chart with a useful example drawn in. Normalizing is explained in Sec 4.2. For convenience, however, I'll repeat portions of the explanation here. Normalized impedances are obtained by dividing the values of all impedances by the system impedance, which is usually taken as the characteristic impedance of the transmission line, Zc being used. Normalizing an impedance by dividing it by Zc amounts to a change of scale such that the unit of impedance is 1 chart ohm, rather than Zc ohms. For example, in a 50-ohm system, 150 ohms becomes 3 chart ohms. Likewise, 50 ohms becomes 1 chart ohm, which appears at the center of the Smith Chart. To convert back to the 50-ohm system, simply reverse the process and multiply the normalized values by 50, or whatever the system impedance may be. For example, the normalized impedance $z = 0.6 + j0.8$ becomes $Z = 30 + j40$ in a 50-ohm system.

To normalize a chart to the impedance of any specific system or line, all impedances on the chart are divided by the system or line impedance. On a normalized Smith Chart, all values of resistance and reactance are normalized values. Smith Charts are available in both normalized and non-normalized forms. The normalized form of Fig 10-2 permits use with transmission lines having any and all characteristic impedances, and all impedance values entered or appearing on the chart are normalized to the line impedance. The non-normalized form is printed with the actual impedances based on the selected line impedance.

Sec 10.2 The Basic Smith Chart

Refer again to Fig 10-2. The basic Smith Chart has two sets of circular scales, one set representing constant resistances, and the other representing constant reactances. The diameter line running horizontally is called the resistance axis, or *real* axis, for reasons that will soon become apparent. The resistance axis represents resistance components

and is graduated in values of normalized resistance. The left end of the resistance axis represents zero resistance, and the right end represents infinite resistance. The center point of the axis on a normalized chart represents 1 chart ohm. Figs 9-2 and 10-2 are normalized charts, but the W2DU Antenna-Impedance Feed-Line Transformation Graph, Fig 10-1, is a 50-ohm chart. Thus, the center of the resistance axis on Fig 10-1 represents 50 ohms. The 50-ohm Smith Chart is explained in detail in Chapter 12.

The constant-resistance circles all are centered on the resistance axis and vary in diameter. The largest circle forms the rim of the graph, represent-

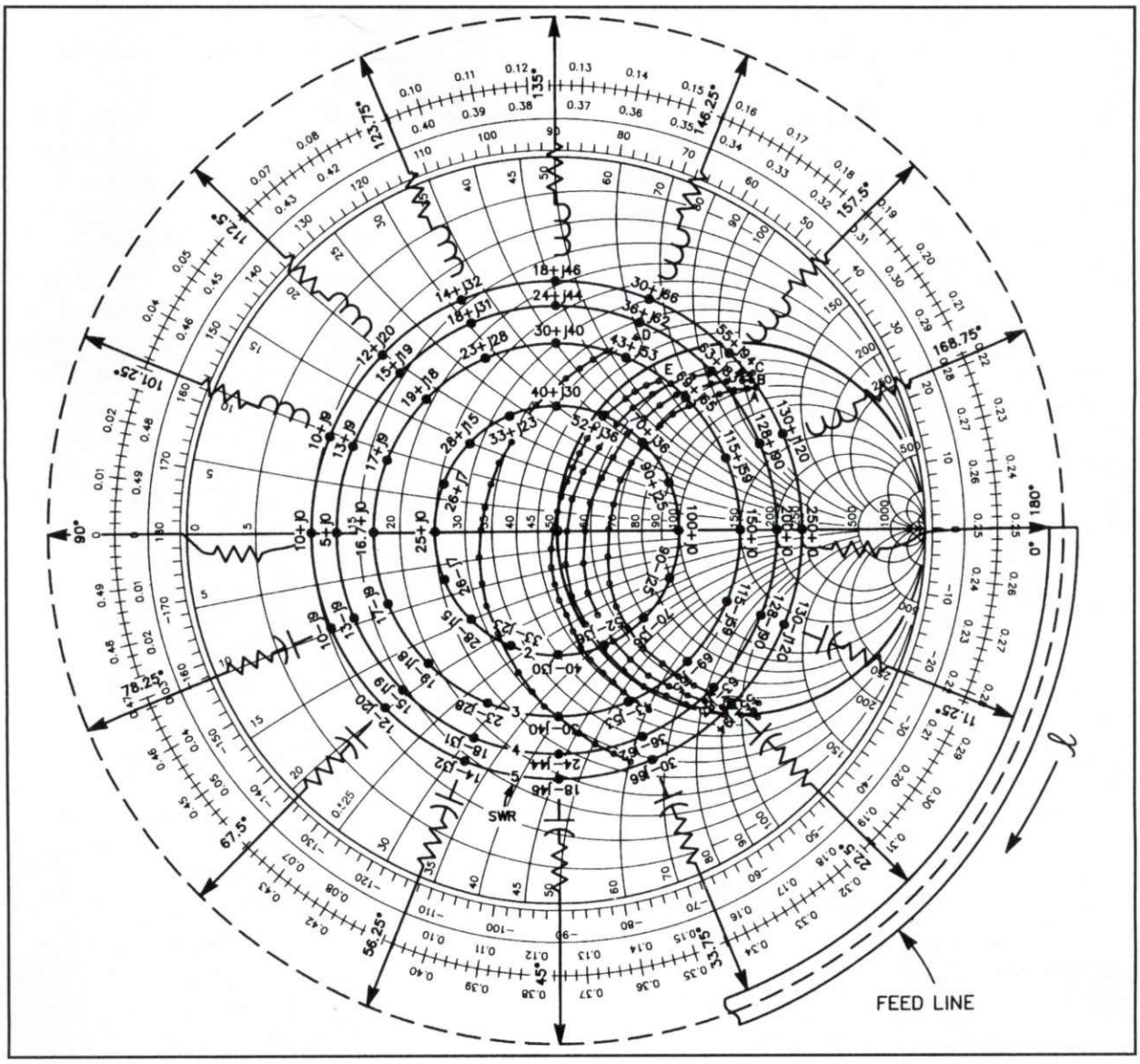

Fig 10-1. The W2DU Antenna-Impedance Feed-Line Transformation Graph. This is a 50-ohm chart. The curves show the impedance of various antennas versus length. Each dot represents a half-percent change from the resonant or center frequency. (For enlarged version see the back of the book.)
Curve A—Dipole in free space.
Curve B—Average of curves A and C.
Curve C—W2DU 80-meter dipole, 30 feet above ground, measured with a General Radio 1606-A RF impedance bridge.
Curve D—Vertical radiator over perfect ground (100 radials or more).
Curve E—Radiator of curve D with 16 ohms of ground-loss resistance (typical with 15 radials).

ing zero resistance. The smallest circle appears at the right end of the resistance axis, representing z = 50 chart ohms. The extreme right end of the resistance axis represents an infinite resistance. In addition, all of the resistance circles are tangent to the rim of the chart at the right end of the resistance axis. All points along a constant-resistance circle have the same resistive value as the point where it crosses the resistance axis.

The constant-reactance circles are superimposed on the resistance circles, and are all tangent to the resistance axis at the infinite resistance point at the right end of the resistance axis. The centers of the reactance circles are off the edge of the chart, but are on a line tangent to the rim at the right end of the resistance axis and perpendicular to the resistance axis. The outer rim of the chart is graduated in reactance, and is called the *reactance* axis. All points along a constant-reactance circle have the same reactance value as the point where it intersects the reactance axis on the rim of the chart. All points on the chart below the resistance axis contain components of capacitive reactance, and those above contain components of inductive reactance. Hence, it is evident that all points on the resistance axis have zero reactance, which is why it is also called the *real* axis.

Because both the resistance and reactance axes go from zero to infinity, any complex impedance can be plotted on the chart. A complex impedance, R + *j*X, may be defined at any intersection of a resistance circle and a reactance circle. The value of the impedance is the complex value of the resistance and reactance circles that intersect. However, remember that the *j* operator must precede the reactance value to denote trigonometric treatment of R and X, rather than simple arithmetical addition, which is a no-no.

There are two peripheral scales on the chart graduated in wavelengths. These scales indicate position along the transmission line. One scale indicates clockwise direction along the line, or *wavelengths toward the generator*, and the other indicates counterclockwise direction, or *wavelengths toward the load*. One complete length around the circumference of the chart represents exactly λ/2 length of line.

A third peripheral scale indicates angle θ (theta) of the reflection coefficient, which is the phase angle between the forward, or incident, and reflected voltage wave. Angle θ is directly related to the impedance, as well as to the position of the impedance on the line. Graduations on the lower half of the chart contain negative values of the angle of the reflection coefficient, from 0° on the right to 180° on the left. Negative values indicate capacitive reactance. The graduations on the upper half contain positive values from 0° to 180°, indicating inductive reactance.

If seeing 360° of reflection coefficient angle in traveling a 180° line is confusing (λ/2, or a complete travel around the chart), you must recall the discussions in Chapters 3 and 9 in which I explained why the angle of the reflection coefficient changes two degrees for every degree of motion along the line. Now for a word of caution: In modifying the Smith Chart in Figs 9-2 and 10-1, I added line-length scales around the chart that don't appear on the basic Smith Chart of Fig 10-2. For example, observe the *90°* appearing at the left, and the *0°* and *180°* at the right. Be careful not to confuse these *line-length* degree numbers with those from the *angle of reflections coefficient* scale.

Recall my discussion in Sec 9.4 of reflection-coefficient angles θ = 0° and 180° relative to the positions of voltage maxima and minima on the line. Now note that θ = 0° appears on the Smith Chart at the infinite resistance end of the resistance axis (voltage maximum), and that θ = 180° appears at the zero-resistance end of the resistance axis (voltage minimum). We will see later how the chart shows that the value of SWR determines the actual maximum and minimum voltage values.

I'll now explain the peripheral wavelength scales used to determine either the position of an impedance on a transmission line, or the length of a line. The scales are graduated in decimal values of a wavelength from 0 to 0.5 λ. Both scales start at the left of the chart, and end at the starting point after 0.5 λ of travel around the chart going in opposite directions. I'll explain their use with an example. We'll use Fig 10-2 to determine the electrical length of a transmission line in wavelengths from a measurement of impedance at the input terminals of the line. The electrical length of the line we've chosen is known to be less than 0.5 λ, so the entire line will fit within one revolution around the chart. How line lengths greater than 0.5 λ are handled is explained later.

The input impedance of the line was measured with a normalized load impedance $z = 1.38 - j1.32$ terminating the line. This is plotted in Fig 10-2 at point A. This load impedance places us at the angle of reflection coefficient $\theta = -45°$ as the starting point for determining the length of the line. To find the starting point on the wavelengths scale, we extend the radial line through the point where the load impedance appears, on out to the outer scale labeled "Wavelengths Toward Generator" at point B, where we read 0.313 λ. The measured impedance at the input of the line was found to be $z = 0.38 - j0.36$, normalized. This impedance value is plotted at point C. A radial line through this impedance point on the chart goes through reflection coefficient angle $\theta = -135°$. Extending this radial line to the same outer wavelengths scale, we read 0.438 λ at point D.

Hence, the electrical length of the transmission line is the difference between the wavelength values of 0.438 λ and 0.313 λ, which is 0.125 λ. This length is λ/8, which is 45° in electrical length and 90° of difference in position along the reflection angle θ scale. These values may be confirmed using Fig 9-2. We will discuss how to manipulate lengths of feed line and their impedances in Chapter 12.

A wealth of additional information concerning the construction and use of the Smith Chart is available (*Refs 19, 25 through 29, 70, and 71*). Chapter 28 of *Ref 71* by Hall, K1TD, is by far the best I've seen for the amateur.

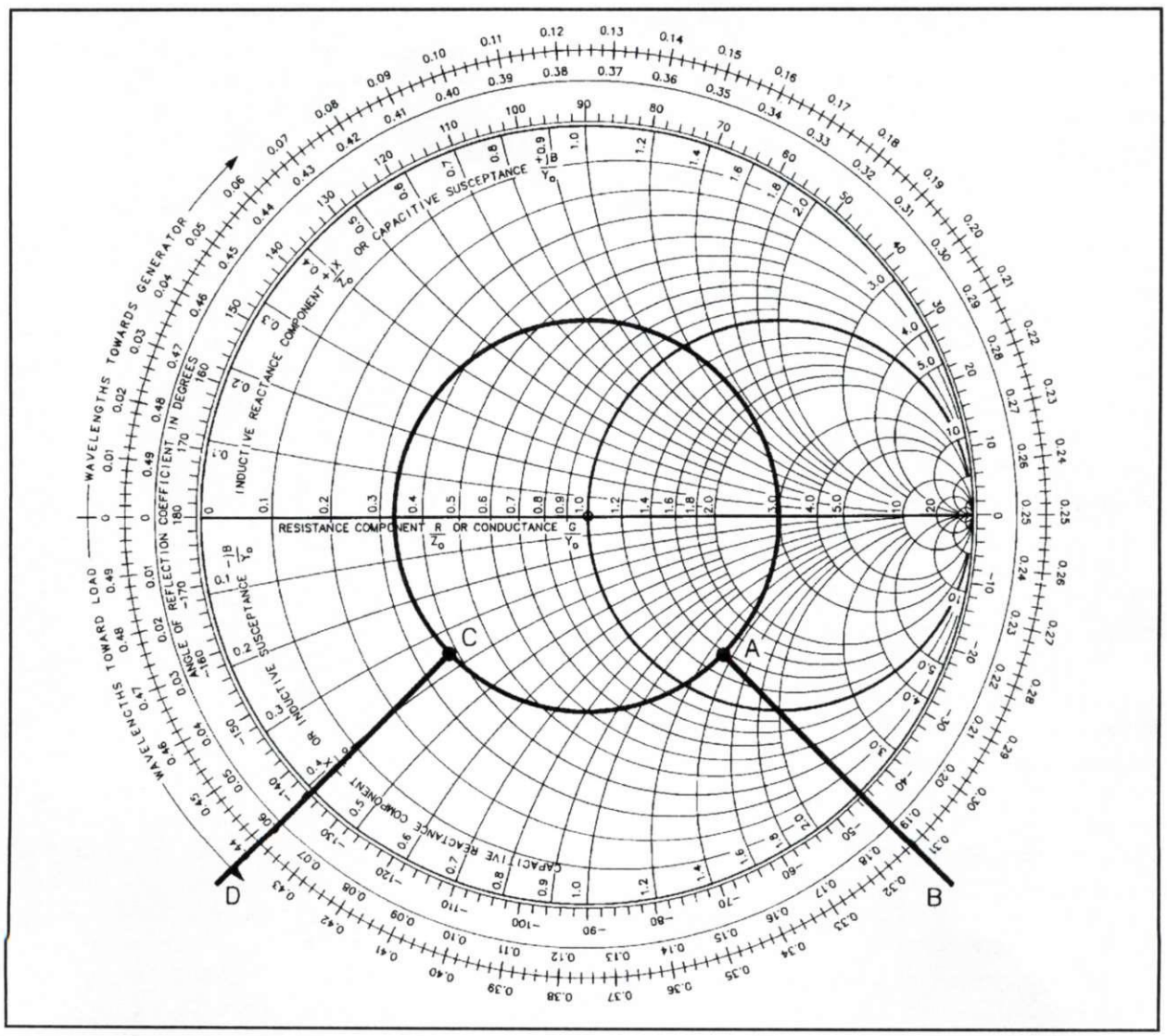

Fig 10-2. A basic, normalized Smith Chart with an example added.

Chapter 11

Using the Smith Chart

Sec 11.1 Introduction

Because impedance along a mismatched transmission line is so directly related to the standing-wave pattern, a logical place to begin discussing the use of the Smith Chart is with entering and plotting SWR data. SWR on a transmission line is represented on the normalized Smith Chart as a circle centered on the resistance axis at r = 1, which is also the center of the chart. The radius of the SWR circle is measured from the center of the chart along the resistance axis to the point where the normalized resistance equals the SWR. For example, as shown in Fig 11-1, a 2:1 SWR circle centered at r = 1 intersects the resistance axis at two points, where r = 2.0, and at 0.5, the reciprocal of the SWR. A 3:1 SWR circle intersects the axis at 3.0 and at 0.33. As stated earlier, the symbols for normalized values of impedance, resistance, and reactance are shown in lower case, while the symbols for the actual, non-normalized values are capitalized.

There are two very important points to learn about the SWR circle:

(1) One trip around the circle represents a movement of 180° along the transmission line, or λ/2.

(2) The constant radius of the SWR circles on the chart indicates that the SWR is *constant* all along the line. If you find this statement confusing because you've witnessed a change in SWR when changing the length of the line, there probably was RF current flowing on the outside surface of the coax from either an ineffective balun or no balun at all. This phenomenon is explained in detail in Chapter 21. (The SWR is constant on *lossless* lines, but decreases gradually toward the input on lines with loss, causing the SWR circle to spiral inward on the Smith Chart.)

Once drawn on the chart, an SWR circle of a given value represents the locus of all complex impedances that appear on a λ/2 section of line having that value of SWR. The impedance values are read from the chart at the points where the SWR circle passes through the intersection of constant resistance and reactance circles. Note, for example, in Fig 11-1 that the 2:1 SWR circle passes through the point where the 0.8 resistance circle intersects the –0.6 reactance circle, point A. The normalized impedance at this point is $z = 0.8 - j0.6$ ohms. As already stated, the 2:1 SWR circle also intersects the resistance axis at two points, where r = 0.5 and r = 2.0. The normalized impedances where it intersects these two points are $z = z_C \div SWR = 0.5 + j0$ and $z = z_C \times SWR = 2.0 + j0$ ohms, respectively. These are the *only two* impedances on the entire λ/2 of line that are purely resistive! All impedances everywhere else on the line are reactive—capacitive if below the resistance axis, and inductive if above.

If you haven't already guessed, I'll mention that the SWR-circle and impedance relationship is reciprocal. Not only can all impedances on the line be determined by an SWR circle on the chart, but the SWR of any impedance can also be determined by plotting the impedance on the chart and then measuring the radial distance from the chart center to the impedance point.

For example, assume that the 2:1 SWR circle in Fig 11-1 had not been drawn in. This time let's find the point representing the normalized impedance $z = 0.8 + j0.6$. Being inductive, it lies above the resistance axis, where the 0.8 resistance circle intersects the +0.6 reactance circle. This point is marked in Fig 11-1 as B. Place the centering pin of your drawing compass at the center of the chart, where r = 1, and place the pen of the compass on the $0.8 + j0.6$ impedance point. This determines the radius of the SWR circle. After swinging the compass for a complete circle, you'll discover that the SWR is 2:1, because the circle also intersects the resistance axis at 2.0. So you see, any impedance falling on the 2:1 circle can be used to determine the SWR as 2:1. Furthermore, if any one of those impedances appearing on the 2:1 circle is used to

terminate the line, it *will* produce a 2:1 SWR all along the line.

So far I have not mentioned the position of the standing-wave pattern and the distribution of impedance along the line, so now is the time to add

position to the puzzle. The first important point to note is that the position of both the standing-wave pattern and the impedances appearing on the line are determined *solely* by the load impedance that terminates the line. *Nothing* can be added at the

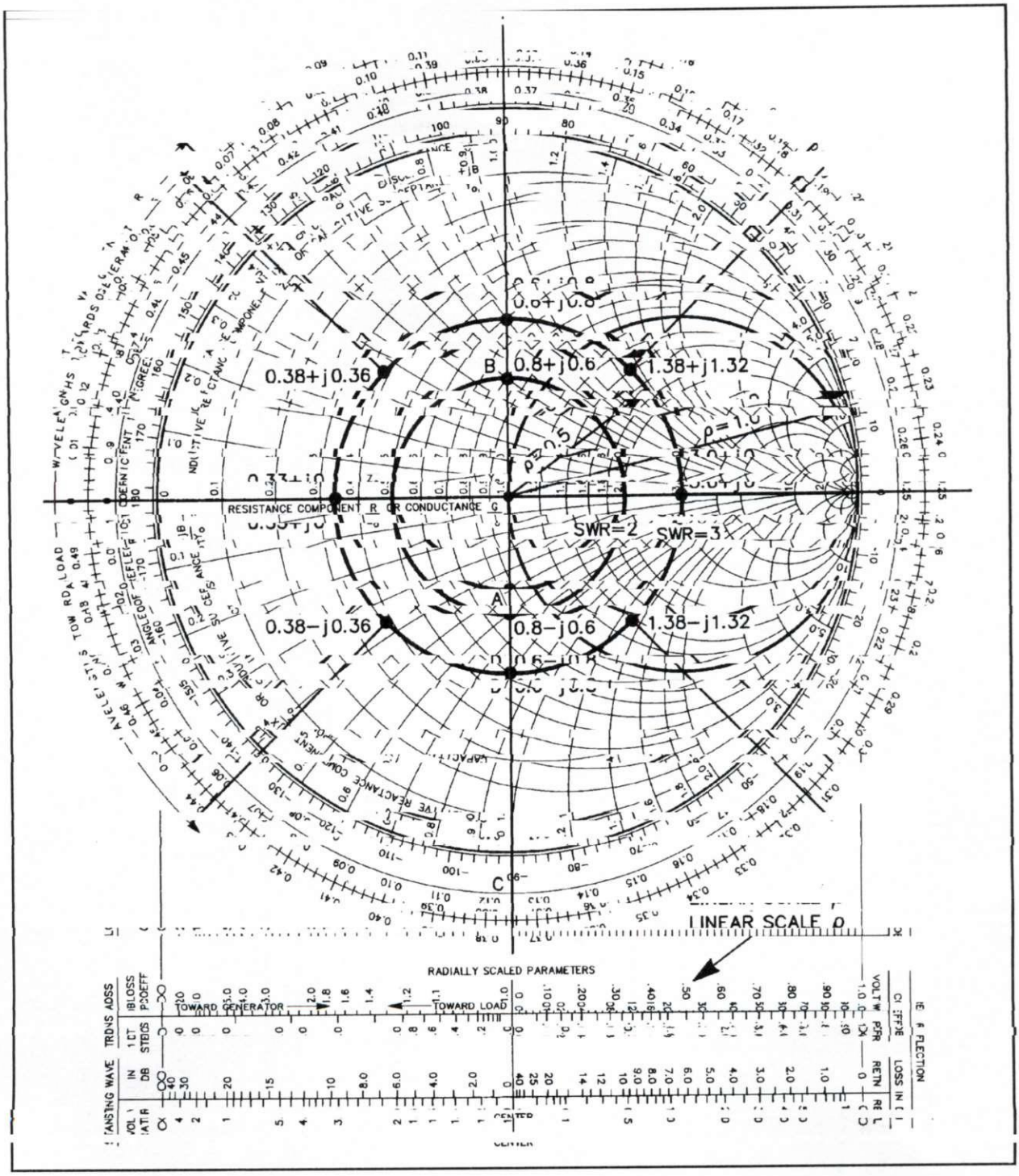

Fig 11-1. A normalized Smith Chart with examples added.

input terminals that will affect them in any way. Contrary to the belief of many amateurs, an antenna tuner at the line input *does not* reduce the SWR on the line; it only matches the line-input impedance to the source of the RF! The position of impedance on the line is determined by the angle of the reflection coefficient. We'll continue by examining the complete complex reflection coefficient.

Every impedance has its own unique complex reflection coefficient, comprising both magnitude ρ and angle θ. The magnitude is directly related to the SWR, as shown in Eqs 3-2 and 3-3. On the Smith Chart, ρ is equal to the radius of the SWR circle measured on a linear scale extending from zero at the center of the chart to 1 at the rim. The linear scale at the bottom of Fig 11-1 is for measuring the radial distances of magnitude on the chart. The decimal value of the magnitude ρ is read directly from this scale. At the center of the chart the radius is zero, indicating zero reflection and a 1:1 SWR. At the rim, or boundary of the chart, where the constant resistance circle is zero, $\rho = 1$, indicating total reflection of all forward traveling waves and an infinite SWR. In other words, the length of the radius extending to the rim of the chart indicates the magnitude $\rho = 1.0$.

We can also see from Eq 3-3 that when $\rho = 1$, the SWR is infinite, which occurs when the load contains zero resistance and any amount of reactance. On the other hand, we can find ρ from the SWR by using Eq 3-2. For example, a 3:1 SWR yields $\rho = 0.5$, or half the chart radius. A 3:1 SWR circle (also the $\rho = 0.5$ circle) is shown in Fig 11-1. Note the radial line labeled "$\rho = 0.5$" extending to the SWR circle that is also labeled "SWR = 3." Also observe the radial labeled "$\rho = 1$" extending from the center of the chart to the rim. (All of this information is also shown in Fig 9-2.) In summary, the magnitude of the reflection coefficient for any impedance is equal to the radial length from the center of the chart to the point where the impedance appears on the chart.

So much for magnitude ρ of the reflection coefficient. Now we come to angle θ. To use angle θ of the reflection coefficient for determining the position of an impedance on the line, we draw a radial line from the center of the chart through the point of the impedance, and extend it to the scale on the rim of the chart titled Angle of Reflection Coefficient in Degrees. The point where the radial line intersects this scale denotes angle θ. For example, Fig 11-1 shows a radial line through point D, the normalized impedance point $z = 0.6 - j0.8$ on the 3:1 SWR circle. This line is extended to reach the θ scale at point C, which shows the radial line at $\theta = -90°$. From Eq 3-2 we find that the 3:1 SWR yields $\theta = 0.5$, and hence the complex reflection coefficient of $z = 0.6 - j0.8$ is $\rho = 0.5$ at $\theta = -90°$. Either set of numbers completely defines the impedance, but angle θ at $-90°$ also identifies the relative position of the impedance on the line.

It is interesting to note that this radial line at $\theta = -90°$ also passes exactly through the normalized impedance $z = 0.8 - j0.6$, point A, which is on the *2:1 SWR circle*. However, magnitude ρ for an SWR of 2:1 is 0.333 on the magnitude scale. In other words, the impedances $0.6 - j0.8$ (for a 2:1 SWR) and $0.8 - j0.6$ (for the 3:1 SWR) both appear at the same location on the transmission line. This first occurs with a resistive load that produces a 2:1 SWR, and the second with a resistive load producing a 3:1 SWR.

I stated earlier in this chapter that the load impedance terminating the line determines the position of the impedances all along the line. Let's examine this concept as we direct our attention back to Fig 9-2. Here we see line impedances calculated vectorially at eight different points, each point separated by 22.5° in distance along the line. The radial lines extending from the 3:1 SWR circle at each impedance point to the angle of reflection coefficient scale indicate the angle of reflection coefficient, θ, associated with its corresponding impedance. Inspection of the θ angles reveals that the impedance appearing with every 22.5° of increase in distance along the line has a corresponding increase of 45° in angle θ. This serves to remind us that angle θ changes two degrees for each degree of change in position along the line.

Let's now examine the significance of these θ angles along the line. In determining why the position of impedances along the line is determined by the impedance terminating the line, we must first remember that the impedances anywhere on the line result from the division of the phasor voltage, E, by the phasor current, I. These impedances result from the phasor sum of the forward and reflected waves at each point on the line. In turn,

the phasor voltage and current resulting from each summation is determined by the complex reflection coefficient at each point—in other words, by the relative magnitude, ρ, and phase θ angle of the forward and reflected waves.

Because the reflected waves originate at the impedance terminating the line, we'll let the termination point be a zero-time reference point for the origin of the reflected waves. We know that magnitude ρ and angle θ of the reflection coefficient appearing at the zero-time reference point are determined by the impedance terminating the line. However, while magnitude ρ remains constant all along the line, angle θ changes two degrees for every degree of distance from the reference point, as stated above. Hence, the phase relationship θ between the forward and reflected waves occurring at the zero-time reference point determines all the other phase relationships occurring at a later time as the waves progress along the line.

For example, refer again to Fig 9-2. If we proceed to a point 22.5° along the line from the $3 + j0$ termination where $\theta = 0°$, the forward wave has advanced to +22.5°, and the reflected wave has retarded to –22.5°. This makes the phase of the reflected wave –45° relative to the forward wave, and produces the impedance $z = 1.38 - j1.32$ at the 22.5° point. In the same manner, at the 45° point on the line, the reflected wave is at –90° relative to the forward wave, producing the impedance $z = 0.6 - j0.8$. We can see these changes in phase (angle θ) between the forward (incident) and reflected wave in the phasor plots appearing in the circular insets of Fig 9-2. It should now be evident that the impedance at any point on the line is determined by the relationship between the forward and reflected voltages and currents. This explains why the terminating impedance, which determines the complex reflection coefficient, $\rho\angle\theta$, at the zero-time reference point, also determines the corresponding reflection coefficient angles and the impedances at all points along the entire line.

While the eight line impedances calculated by phasor arithmetic are shown in the circular and rectangular insets in Fig 9-2, the impedance points are shown in their correct respective graphic positions on the 3:1 SWR circle. However, because the reading of the values from the chart circles is difficult because of the intrusion of the insets, a 3:1 SWR circle and partial radials at the corresponding 45° angles of reflection coefficient are also shown in Fig 11-1 to allow reading of these normalized impedance values in true Smith Chart fashion.

Let's now see what happens to impedances along the line if we change the position and value of the terminating load impedance in Fig 9-2. Observe that at the $\ell° = 22.5°$ point, angle θ of the reflection coefficient is –45°, and the normalized impedance $z = 1.38 - j1.32$. It would be interesting to see what happens to impedances along the line if we were to cut it at this point where $\ell° = 22.5°$, eliminate the portion between $\ell° = 0°$ and 22.5° and then terminate the new end of the line with an impedance $z = 1.38 - j1.32$. Because the new load impedance with its own corresponding angle $\theta = -45°$ is the same as that which appeared at $\ell° = 22.5°$ with the $3 + j0$ load impedance at $\ell° = 0°$, the conditions of reflection at $\ell° = 22.5°$ are identical to those which existed there before cutting the line. Hence, the values of the reflection coefficient and impedance remain the same as before everywhere along the remainder of the line!

If we now return to the conditions as shown in Fig 9-2, we see that the line can be cut at any point and the impedance appearing at the input terminals of the portion terminated by the $3 + j0$ load will be the impedance indicated on the Smith Chart at the point where the cut is made. For example, if the line is cut at $\ell° = 45°$, the new normalized input impedance will be $z = 0.6 - j0.8$, and if cut at $\ell° = 67.5°$ the input impedance would then be $z = 0.38 - j0.36$, as shown in the rectangular insets of Fig 9-2.

As a result of this discussion, we may now make the following general statement: Any impedance appearing along a terminated line, as indicated on the SWR circle containing that impedance, may be used as a new terminating load at the point on the line where that value of impedance appeared with the original load, and all impedances appearing between the new load and the source will remain unchanged.

Sec 11.2 Four Distinctive Features of the Smith Chart

As we continue examining various uses of the Smith Chart, four interesting features emerge that merit explanation. Two of the four features involve the $\lambda/2$ line—first, its capability of repeating the

value of its terminating load impedance at its input terminals, and second, its phase-inverting action that reverses the polarities of the voltages and currents appearing at the opposite ends of the line. The third feature is the *impedance-inverting* action of the λ/4 line. The fourth feature involving the λ/4 line concerns the appearance of impedances having the same resistance but opposite signs of reactance simply by having opposite signs of their corresponding angles of reflection coefficient θ.

We'll first examine the impedance-repeating action of the λ/2 line, using Fig 10-1.[1] Select one of the impedance points printed out on any of the four SWR circles to represent a starting position on a transmission line. Recall an earlier statement that one complete trip around an SWR circle represents a movement of λ/2 along a line. With your eyes, trace all the way around the SWR circle you selected. No matter where you start, with one complete trip around the circle, the impedance at the starting position on a line (represented by the corresponding point on the SWR circle) is repeated λ/2 away in either direction. This means that if the length of a mismatched line is greater than λ/2, an impedance appearing at any point farther away than λ/2 from the terminating load will be the same as that appearing λ/2 from that point.

While the impedances repeat themselves *exactly* on lossless lines at intervals of λ/2, they do not repeat exactly on real lines having attenuation. So far, all of our calculations and statements have been made with the assumption that the lines are lossless. However, the lines we use in practice are considered *low loss,* so the error in assuming the lines to be lossless is relatively inconsequential. On lines having enough attenuation to make the impedance error significant, the error in the resistance at the input is to bring it closer to the value of the characteristic impedance Zc of the line, and the error in the reactance is to decrease it.

In addition to repeating the impedance, a λ/2 section of line also reverses the phase, or polarity, of the voltages and currents at opposite ends of the line. To see how the phase inversion is accomplished, it is informative to observe the rotation of the resultant phasors of voltage E and current I appearing in the circular insets in Fig 9-2 as we proceed around the chart. Start at the right of the chart where the resultant vectors point to the right, indicating a reference phase of 0° at the $3 + j0$ load end of the line. Now proceed clockwise around the chart in the 22.5° increments of the insets. Observe the counterclockwise rotation of the resultant phasors with each increment of travel. After completing one trip around the chart, note that the resultants are now pointing to the left, having rotated 180°. This signifies a change in phase of 180° relative to the starting point. Keep in mind that one trip around the chart represents a travel of λ/2 along the line.

Now we come to the third feature, the impedance-inverting action of the λ/4 line that makes it so useful as an impedance transformer. The wave actions that give this length of line its special impedance-transforming properties are described in detail in the final paragraphs of Chapter 4, and the impedance-inverting action is shown mathematically in Eq 7-1. On the Smith Chart, the impedance inversion is obtained numerically by observing the values of the impedances appearing on an SWR circle at the opposite ends of a diameter line. Opposite ends of a diameter line signify a trip *half way* around the circle, indicating 90°, or λ/4 of travel along the line. For example, in Fig 11-1 we find the normalized capacitive impedance $z = 0.8 - j0.6$ at point A on the radial line at the reflection coefficient angle $\theta = -90°$. However, if we follow the radial line up, crossing the $r = 1$ point in the center and continue until it reaches the 2:1 SWR circle *above* the center of the chart, we find the normalized *inductive* impedance $0.8 + j0.6$ at point B. This is the reciprocal of the initial capacitive impedance that appears below the chart center. Hence, by going half way around the SWR circle, corresponding to a change of λ/4 on a transmission line, we have inverted the impedance. It should be noted that the inverted normalized impedance is also the normalized *admittance* of the initial capacitive impedance.

It is now interesting to note that if we continue around the second half of the SWR circle and arrive back at the point of beginning, we have *reinverted* the inductive impedance back to the original capacitive impedance we had at the starting point. Hence, two λ/4 lines connected in series (forming a λ/2 line) can be likened to a seesaw.

Let's try another example, this time using Fig 10-1. At reflection coefficient angle $\theta = -135°$ on the

5:1 SWR circle, we see the impedance $Z = 12 - j20$ ohms. Diametrically opposite, at $\theta = +45°$ on the 5:1 SWR circle, we find the impedance $Z = 55 + j94$ ohms. The normalized values of these two impedances are also reciprocals of each other. If we used an impedance $Z = 12 - j20$ to terminate a 50-ohm, $\lambda/4$ line, the impedance at the input terminals would be $Z = 55 + j94$ ohms.

A special case of impedance inversion occurs along the resistance axis, where the reactance is zero. This is the condition that most often prevails when the $\lambda/4$ line is used as an impedance-matching transformer. In most cases the transformer is used to convert one purely resistive impedance to that of another purely resistive impedance. It is evident that both of these resistances will lie on the resistance axis.

Recall from earlier discussions that the right-hand portion of the resistance axis represents maximum resistance points on the line (where $\theta = 0°$), and that the left-hand portion of the axis represents minimum resistance points (where $\theta = 180°$). To illustrate, we can see that on any of the SWR circles the resistance appearing on the resistance axis to the right of the center of the chart is $R = 50 \times$ SWR, while on the same circle to the left of chart center, the resistance is $R = 50 \div$ SWR.

Let's now use this information to work out an example of impedance matching with a $\lambda/4$ section of transmission line. Assume that we have two transmission lines of different impedances, 25 and 100 ohms, respectively, and we want to couple them together with a matching-transformer section of line. From Eq 7-2, we find the geometric mean value between these two impedances to be 50 ohms, which means that a $\lambda/4$ 50-ohm transformer line will perform a satisfactory match with a 2:1 SWR on the transformer line. However, we may also observe in Fig 10-1 that based on a 50-ohm system, both 25 ohms and 100 ohms lie on the 2:1 SWR circle at opposite ends of a diameter that lies on the resistance axis. This is another way of telling us that the $\lambda/4$, 50-ohm line will provide a match between the 25-ohm and the 100-ohm lines, the impedance match we want.

Now we'll consider the fourth characteristic of transmission lines that appears as an interesting display on the Smith Chart. This concerns the points on the line where the magnitudes and both the resistance and reactance components of two different impedances are equal, respectively, except that the reactances are of the opposite sign. These impedances occur at two different points on the same SWR circle, with each point on opposite sides of the circle equidistant from either end of the resistance axis. In other words, this condition exists for any two points having the same angle θ of the reflection coefficient, but having the opposite sign of θ. For example, on the 3:1 circle of Fig 10-1 at $\theta = -135°$, the impedance is $Z = 19 - j18$, and at $\theta = +135°$ the impedance is $Z = 19 + j18$ ohms.

Sec 11.3 A Reader Self-Test and Minimum-SWR Resistance

Everyone knows that when a 50-ohm transmission line is terminated with a pure resistance of 50 ohms, the magnitude of the reflection coefficient, ρ, is 0, and the SWR is 1:1. Right? Of course! With that in mind, here is a little exercise to test your intuitive skill.

If we insert a reactance of 50 ohms in series with the 50-ohm resistance, the load becomes $Z = 50 + j50$. The SWR will be 2.618:1. Now for the question. With this 50-ohm reactance in the load, is the SWR already at its minimum value with the 50-ohm resistance, or will some other value of resistance in the load reduce the SWR below 2.618:1? You say the SWR is already the lowest with the 50-ohm resistance, because, after all, the line impedance, Z_C, is 50 ohms? Sorry, wrong. With reactance in the load, the minimum SWR always occurs when the resistance component of the load is *greater* than Z_C. In fact, the more the reactance, the higher the resistance required to obtain minimum SWR. For any specific value of reactance in the load there is one specific value of resistance that produces the lowest SWR. I call this resistance the "minimum-SWR resistance." Finding the value of this resistance is easy. First you normalize the reactance, X, by dividing it by the line impedance, Z_C. The normalized value of X is represented by the lower case x. Thus $x = X_C \div Z_C$. Then we solve for the normalized value of resistance, r, from Eq 5-1, which is repeated here:

$$r = \sqrt{x^2 + 1} \qquad \text{(Eq 5-1)}$$

Let's try it on the example above. The normalized value of 50 ohms of reactance, X, is x = 1. Substituting in Eq 5-1, $r = \sqrt{2} = 1.414$. Thus, the true value of the minimum-SWR resistance is 1.414 50 = 70.7 ohms. While the 50-ohm resistance yields a 2.618:1 SWR, the 70.7-ohm resistance in series with the 50-ohm reactance yields an SWR of 2.414:1. Not a great deal smaller, but still smaller than with the 50-ohm resistance.

Now let's try a more dramatic example, this time with a 100-ohm reactance, which has a normalized value x = 2.0. With a 50-ohm resistance, the SWR is now 5.828:1. However, with the normalized minimum-SWR resistance, $r = \sqrt{2^2 + 1} = r = \sqrt{5} = 2.236$. Multiplying by 50, we get R = 111.8 ohms. With this larger resistance in series with the 100-ohm reactance, the SWR is reduced from 5.828:1 to 4.236:1. The results of this exercise didn't turn out quite the way you expected, did it?

These results seem incredible, so how do we know they're true? By a simple demonstration using the Smith Chart. The Smith Chart provides an elegant way to demonstrate why the SWR is not at a minimum with 50 ohms of load resistance when reactance is also present in the load. I'll demonstrate using the values in the last example, but first let's normalize them. The 50-ohm resistance, R, becomes r = 1, and the 100-ohm reactance, X, becomes x = 2. This normalized impedance, 1 + *j*2, is plotted at point A in Fig 11-2. Next we draw a radial line from the center of the chart to the point on the 2.0 reactance-circle segment where a line perpendicular to the radial becomes tangent to the reactance circle. This point is identified as B in Fig 11-2. The minimum-SWR resistance is then found on the resistance circle to which the radial is tangent, 2.236 in this case. This resistance circle will have a normalized value greater than 1 (meaning greater than 50 ohms).

Here is the proof. We know the length of the radial from the center of the chart to the 2.0 reactance circle is proportional to the SWR. Therefore, for minimum SWR we're looking for the shortest possible radial that will reach the 2.0 reactance circle. The radial is shortest when it is perpendicular to a line tangent to the circle. To prove this, swing the radial in either direction from point B in Fig 11-2. The radial will no longer reach the 2.0 reactance circle, because the circle curves away from the point of tangency. Hence, the radial would require lengthening to again reach the 2.0 circle, which means an increase in SWR. Using the shortest length that will reach the 2.0 reactance circle, we see the radial is tangent to the r = 2.236 circle, for an SWR of 4.236:1. When the radial is swung and extended to reach the 2.0 reactance circle at r = 1 (point A), the length has increased to indicate an SWR of 5.828:1. Hence, the resistance yielding the lowest SWR with a reactance of 100 ohms is 111.8 ohms, and the case is proved.

Incidentally, the line tangent to the reactance circle is coincident with the radius of the minimum-SWR resistance circle. In Fig 11-2, that radius is line segment CB, where C is at the center of the minimum-SWR resistance circle. Hence, the radial line and the radius of the r circle are mutually perpendicular.

Using the Smith Chart, we have proved geometrically that the minimum-SWR resistance is greater than Z_C when the load contains reactance, and the Smith Chart is also seen to reveal the value of that resistance. In addition, Eq 5-1 is also seen to yield values of resistance that are in complete agreement with those obtained graphically with the Smith Chart. If you are interested in pursuing the subject further, I have performed a rigorous mathematical proof of the relationship shown in Eq 5-1 in Appendix 1. In addition, Appendices 2 and 3 include equations for determining the exact value of SWR produced on a line when terminated with any complex load R + *j*X. Appendix 4 includes a program listing for hand-held calculators that yields the SWR from R + *j*X. Another interesting relationship resulting from this exercise is shown in Eq 5-2, repeated here.

$$SWR_M = r + x \qquad \text{(Eq 5-2)}$$

where

SWR_M = SWR obtained with the minimum-SWR resistance

r = the normalized minimum-SWR resistance

x = the normalized reactance

Eq 5-2 shows that to determine the value of the SWR with the minimum-SWR resistance in the load, we simply add the normalized values of the resistance and the reactance in the load. I have

never seen a reference to the minimum-SWR resistance in relation to terminating loads in any of the engineering or academic literature. Therefore, I believe I am the originator of the relationships represented by Eqs 5-1 and 5-2 (which I first published in *QST* in April 1974), along with both the geometrical and mathematical proofs.

What is the significance of the minimum-SWR resistance? First, it relates directly to the shape of the SWR curve when you plot the SWR measured on your dipole feed line over a range of frequencies that includes the resonant frequency of the dipole. Of significance is the discussion in Sec 5.6 on loss resistance being separable from the radiation resistance in antenna terminal impedance, where Eqs 5-1 and 5-2 were introduced. In addition, the significance of the minimum-SWR resistance phenomenon is evident in the SWR plots of Figs 15-1, 20-2, and 20-3. Those plots of dipole SWR (without traps) show that the SWR values are asymmet-

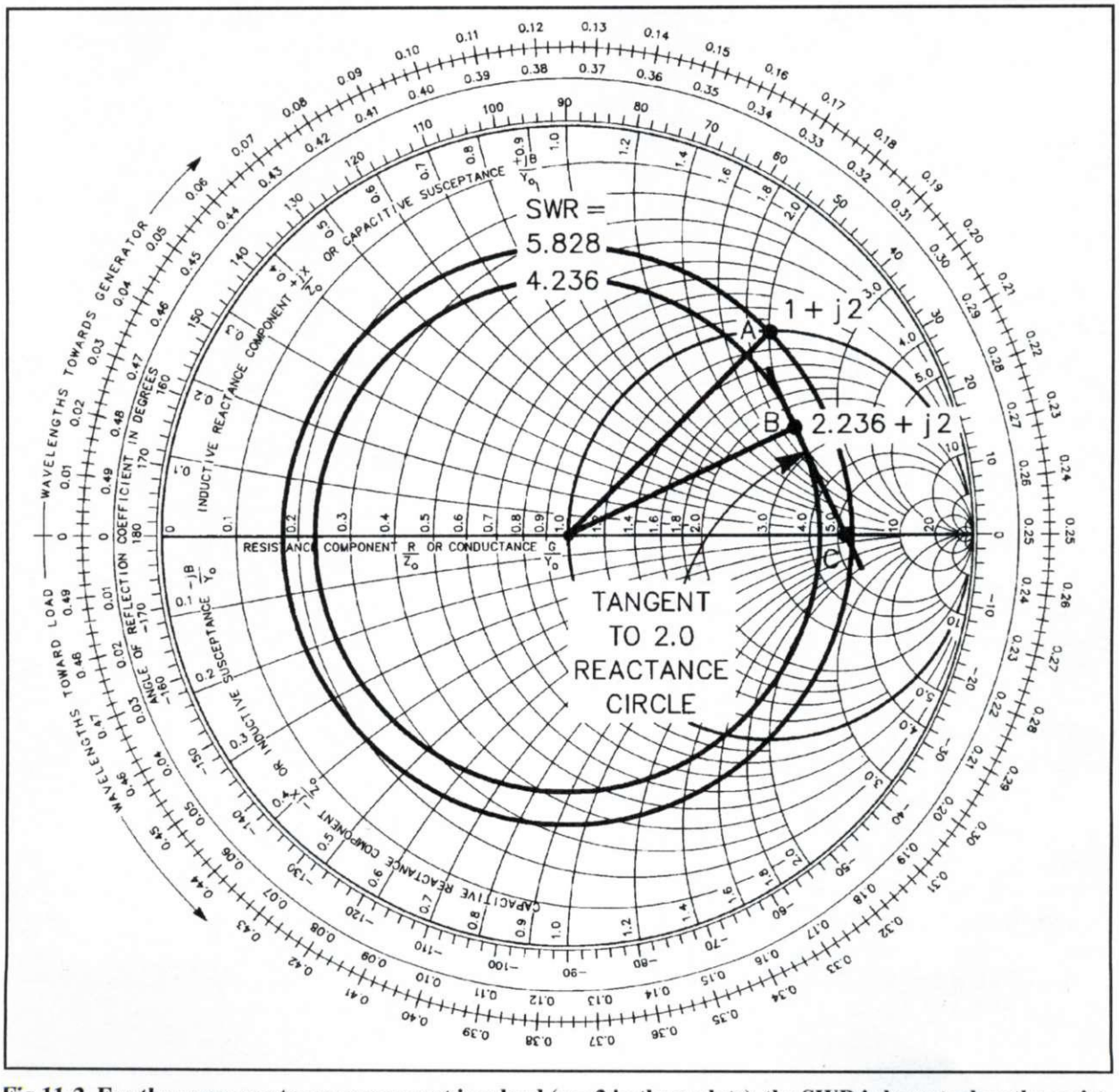

Fig 11-2. For the same reactance component in a load (x = 2 in these plots), the SWR is lowest when the resistance component is greater than the line impedance, Zc (r > 1). The minimum-SWR resistance is that value producing the lowest possible SWR.

rical with respect to the minimum value obtained at the resonant frequency; for the same amount of frequency excursion above and below resonance, SWR values above resonance are lower than those below resonance.

The reason for the asymmetry is that the resistance component R of the dipole terminal impedance increases with frequency (as also shown in the figures), and thus the resistance is higher above resonance than it is below resonance. On the other hand, the reactance values are seen to be nearly identical on opposite sides of the resonance point, except for the opposite sign. Hence, for a given frequency excursion off resonance in either direction, the SWR above resonance is less than that for the same excursion below resonance, because the resistance is higher above resonance. This effect follows directly from the minimum-SWR resistance phenomenon described above.

Note

1. In addition to Figs 9-2 and 11-1, the text in this section refers to Fig 10-1, which has not yet been described in detail. To enhance the clarity of the explanations, you may want to skip to Sec 12.1 and read the description of Fig 10-1 before proceeding.

Chapter 12

Antenna Impedance and the 50-ohm Smith Chart

Sec 12.1 The W2DU Impedance Transformation Graph

We are now ready to examine the W2DU Antenna-Impedance Feed-Line Transformation Graph, Fig 10-1, in more detail. This graph has three significant features that will help you use the antenna tuner in matching the rig to the feed line. First, the Smith Chart of Fig 10-1 is a 50-ohm chart, which means that all resistance and reactance components of impedance are shown as actual, non-normalized values. Note that the resistance scale at the center of the chart reads 50 instead of 1.0.

Second, Fig 10-1 has four SWR circles to assist in determining the range of impedances you might expect to encounter at the input terminals of the feed line. As shown in the lower section of the chart, separate circles have been drawn for SWR values of 2:1, 3:1, 4:1, and 5:1. The special feature of these SWR circles is that the actual values of impedance appearing on each circle are printed out at intervals of 22.5° in angle of reflection coefficient θ all around each circle. These are the impedances that will appear at every 11.25-degree interval along each λ/2 section of the feed line for each of the four values of SWR shown. For all practical purposes, these impedance values cover the complete range of impedances one is likely to encounter at the input terminals of a 50-ohm feed line of any length, and for all SWR values up to 5:1. These impedance values, along with their corresponding angles of reflection coefficient θ, also appear in Table 12-1.

Angle of Reflection Coefficient θ°	SWR 2:1	SWR 3:1	SWR 4:1	SWR 5:1
0	100 + *j*0	150 + *j*0	200 + *j*0	250 + *j*0
–22.5	90 – *j*25	115 – *j*59	128 – *j*90	130 – *j*120
–45	70 – *j*36	69 – *j*65	63 – *j*83	55 – *j*94
–67.5	52 – *j*36	43 – *j*53	36 – *j*62	30 – *j*66
–90	40 – *j*30	30 – *j*40	24 – *j*44	18 – *j*46
–112.5	33 – *j*23	23 – *j*28	18 – *j*31	14 – *j*32
–135	28 – *j*15	19 – *j*18	15 – *j*19	11.5 – *j*20
–157.5	26 – *j*7	17 – *j*9	13 – *j*9	10.3 – *j*9
180	25 + *j*0	16.7 + *j*0	12.5 + *j*0	10 + *j*0
157.5	26 + *j*7	17 + *j*9	13 + *j*9	10.3 + *j*9
135	28 + *j*15	19 + *j*18	15 + *j*19	11.5 + *j*20
112.5	33 + *j*23	23 + *j*28	18 + *j*31	14 + *j*32
90	40 + *j*30	30 + *j*40	24 + *j*44	18 + *j*46
67.5	52 + *j*36	43 + *j*53	36 + *j*62	30 + *j*66
45	70 + *j*36	69 + *j*65	63 + *j*83	55 + *j*94
22.5	90 + *j*25	115 + *j*59	128 + *j*90	130 + *j*120
0	100 + *j*0	150 + *j*0	200 + *j*0	250 + *j*0

Going from angle of reflection coefficient θ = 0° at the first line in the table through 180° to 0° at the bottom represents 180 (λ/2) of travel along the line. Impedance values are obtained from the SWR circles of Fig 10-1.

Table 12-1. Impedances along a 50-ohm λ/2 line for various values of SWR.

Third, Fig 10-1 shows curves labeled A through E, which plot impedance versus frequency for both dipole and vertical antennas. From these impedance plots you will be able to determine the approximate impedance at the input terminals of the feed line with various feeder lengths, and with various degrees of off-resonance operation of the antenna.

Sec 12.2 Antenna Impedance versus Frequency

We'll now examine the plots of antenna impedance versus frequency shown as curves A through E in Fig 10-1. The types of antennas represented in the curves are described in the figure caption. The reason for including these plots is to demonstrate how the impedance appearing at the input terminals of a feed line can be predicted with a fair degree of accuracy with the Smith Chart if the antenna impedance and feed-line lengths are known.

The dots in all five curves have a special significance because they represent both impedance and frequency. The impedance indicated at each dot is read from the Smith Chart in the conventional manner. However, the frequency corresponding to the antenna impedance for a given length of antenna is indicated by the spacing of the dots. The dots appearing on the zero-reactance axis (the resistance axis) represent the impedance of an antenna cut to its resonant length. In other words, the dots appearing on the resistance axis indicate the antenna impedance while operating at its resonant frequency, whatever that frequency might be. The spacing between each dot represents a 0.5% change from the resonant, or center, frequency.

Here's an example of how it works. Curve C represents data measured on an 80-meter dipole using a General Radio 1606-A RF bridge. The dipole was cut to resonate at 3.75 MHz, the center of the 80-meter band. The length is 125 feet, from the formula length = 468/f(MHz). Thus, the dot in curve C which lies on the resistance axis indicates an antenna-terminal impedance $Z_A = 52 + j0$ ohms at the resonant frequency. Let's now examine the frequency and impedance at the point on curve C ten dots below or in the downward direction from the *resonant*-frequency dot. First, ten dots at 0.5% per dot means the frequency is 5% below the resonant frequency of 3.75 MHz. The new frequency is thus f = 3.75 – 0.05(3.75) = 3.5625 MHz. The tenth dot was chosen to make the example easy, because it lies on the 5:1 SWR circle. This dot tells us that a typical 80-meter antenna cut to resonate at 3.75 MHz has close to a 5:1 SWR at 3.5625 MHz. The position of this tenth dot also indicates the impedance of this antenna to be approximately $Z_A = 50 - j90$ ohms at 3.5625 MHz. As this is the impedance appearing at the terminals of the antenna, it is also the impedance that our feed line sees as a terminating load impedance.

Sec 12.3 Determining Line-Input Impedance

To determine the impedance an antenna tuner must match at the *input* terminals of the feed line, we need to know only the electrical length and characteristic impedance of the feed line. Because we are working with a 50-ohm Smith Chart, it goes without saying that we're using a 50-ohm feed line. Also, for the purpose of making the example easy to solve, I'll select a line length that results in a line-input impedance that is easy to read from the chart. Therefore, let us select a line having a physical length of 113.0 feet. We'll use RG-8 coax, which has a velocity factor of 0.659, so the effective *electrical* length of the line is 113.0/0.659 = 171.5 feet.

We now need to find the decimal value in wavelengths of the electrical length of 171.5 feet in order to enter the wavelength scale on the chart. One wavelength at 1.0 MHz is 983.57 feet, so one wavelength at 3.5625 MHz = 983.57/3.5625 = 276.1 feet. To find the wavelength, λ, of the line, we divide its electrical length in feet by the number of feet in one wavelength at 3.5625 MHz. Therefore the wavelength of the line is 171.5/276.1 = 0.621 λ. Since 0.621 λ is greater than $\lambda/2$ (0.5 λ), we subtract 0.5 λ from 0.621 λ, thus 0.621 – 0.5 = 0.121 λ. We do this because 0.5 λ takes us completely around the chart with 0.121 λ left over.

We now draw a radial line from the chart center through the antenna impedance $Z_A = 50 - j90$, extending to the outer wavelengths scale, where we read 0.317 λ on the scale labeled "Wavelengths Toward Generator." This is the starting point for determining the distance along the wavelengths scale on the chart between the point representing the antenna impedance Z_A and the impedance Z_{IN} at the input terminals of the feed line. Thus, next

we add to 0.317 λ the effect of the electrical length of the feed line. Because the feed line is 0.121 λ longer than λ/2, we simply add 0.121 λ to 0.317 λ, which brings us to 0.438 λ on the wavelengths scale. To find the impedance at the input terminals of the feed line, we now draw a new radial line from the center of the chart to the 0.438 λ point on the wavelengths scale. The impedance we're looking for is at the point where the new radial crosses the 5:1 SWR circle, which we see is approximately $Z_{IN} = 12 - j20$ ohms. The 0.621-λ feed line has thus transformed the antenna impedance $Z_A = 50 - j90$ ohms to $Z_{IN} = 12 - j20$ ohms. This is the impedance the antenna tuner will then transform to 50 ohms for the line running to the transmitter.

With the procedure just described, the dipole-impedance data appearing in Fig 10-1 can be applied for general use to obtain the approximate input-terminal impedance of a feed line of any length used to feed any thin-wire dipole, within 6% of antenna resonance. Furthermore, this dipole impedance data can also be used with feed lines having any characteristic impedance simply by normalizing the antenna-impedance data obtained from the 50-ohm W2DU chart to the impedance of the line to be used, and then processing the normalized data on a normalized Smith Chart by following the procedure outlined above.

Turn your attention now to impedance curves D and E for the vertical radiators, and observe that the impedance $Z = 48 + j0$ appearing on curve E (where the curve crosses the resistance axis) comes very close to a perfect resistive match to 50 ohms. Note that this curve represents a radiator having only a few radials, resulting in a ground-loss resistance of around 16 ohms. Many amateurs using ground systems such as this one are apparently happy with the near-perfect match they get at resonance. However, they are blissfully unaware that the true radiating efficiency of this system is only about 67%, while believing the efficiency is close to 100% because of the near-perfect match.

Unfortunately this is not true. The radiation resistance of the resonant λ/4 vertical radiator is approximately $Z = 32 + j0$ ohms, as shown in curve D, which results in about a 1.5:1 mismatch. Consequently, the total load resistance of 48 ohms in curve E results from adding the 16 ohms of ground-loss resistance to the 32-ohm radiation resistance of the radiator. As a result, the power from the transmitter divides in a 2 to 1 ratio, with only 67% radiating from the antenna, and 33% lost in heating the ground, amounting to a 1.76 dB loss.

On the other hand, when the radiator with the good ground is properly matched at the input of the feed line, the power lost to any unwanted resistance from the 1.5:1 mismatch is negligible. It is interesting to note that even if one didn't match the 1.5:1 mismatch with an antenna tuner, the maximum loss would be only 0.177 dB more than the matched attenuation of the feed line. A more detailed discussion of this subject of ground loss with vertical radiators appears in Sec 5.4. I think you'll find it quite illuminating.

Before finishing this subject, let's now be completely candid. The ground-loss exercise just completed was straightforward engineering, pure and simple. No mention was made concerning the practical effect of the loss of radiated power from the ground resistance. From the point of view of the FCC in approving an AM broadcast tower radiator, the strict engineering approach would prevail. In fact, the FCC requires 90 radials for such systems, and most AM stations have installed 120 to optimize the efficiency. However, when we amateurs think of received signal levels in terms of 6 dB per S unit on the S meter, we see that a difference of 1.76 dB is insignificant when the signal level is already S8 or S9. This is, of course, the reason why it makes sense to operate with a vertical antenna even when it isn't practical economically to install more than a few radials. This is why there are so many amateurs who are completely happy with their verticals. On the other hand, the 1.76-dB difference does become significant when using the vertical for low-signal-level DX, with received signals below S1. Some avid DXers have the fortunate real-estate situation where they can squeeze every bit of radiation out of their verticals by having the radials in salty sea water. What a dream! Thus, now it's up to you to make your own informed decision on the number of radials you'll put down.

Chapter 13

The Line-Matching Problem

Sec 13.1 Introduction

In Chapter 12 we identified the range of impedances likely to be encountered at the input terminals of a 50-ohm feed line for any length of line, and with any antenna impedance that produces mismatches up to a 5:1 SWR. The next step is to provide the means for transforming the line-input impedances that are outside the matching range of the transmitter to an impedance that will be a satisfactory load for the transmitter. We don't need to look very far for such a device, because impedance-matching networks have been performing such transformations for as long as there have been radio transmitters.

We must keep in mind that the main goal is to permit the output stage of the transmitter to deliver all of its available RF power to the load, which in our case is the antenna. All that is required for the output stage to do this is for it to see its optimum load impedance. To avoid any misunderstanding, the optimum load impedance is, by definition, that impedance into which an amplifier will deliver its maximum available power, while staying within the limits of maximum rated plate current. As we will discover very soon, the matching device we are looking for is simply an extension of the tank circuit in the transmitter, if it has one. (For those that don't, there is further explanation in Sec 13.4.) Therefore, to achieve a better understanding of how the matching device performs, we must first digress briefly to discuss the role of the pi-network tank circuit used in transmitters with tubes in the final output stage.

Sec 13.2 Matching with a Pi-Network

In transmitters using tubes in the final output stage, the conventional pi-network tank circuit shown in Fig 7-2 performs two functions: It filters out harmonic energy delivered by the output stage, and it matches its output impedance to the tube load *impedance*. When the output of the network is terminated with an impedance within its matching range, and is properly tuned or adjusted, its input terminals present the optimum load impedance for the tubes to work into. Let's illustrate with an example.

The optimum load impedance of the commonly used pair of 6146 tubes in parallel is around 2000 ohms resistive. Let's initially place a 50-ohm resistive dummy load on the output of the pi-network. We use the relative power meter to indicate proper adjustment of the network while obtaining the optimum load impedance for the tubes. The relative power indicator on most commercial rigs is simply an RF voltmeter connected across the output terminals of the pi-network tank circuit. Using the conventional tuning procedure, we slowly advance the output loading control to increase the output power, while simultaneously rocking the plate-tuning control gently back and forth to maintain the dip in plate current and thus maintain resonance in the tank circuit. (Resonance occurs at the bottom of the dip. If it doesn't, check the neutralization.)

As we continue to advance the output loading control, we pass through a peak in the output power, after which the power *decreases* with any further advancing of the loading control. This means we have gone past the optimum load impedance. The plate current dip will also have become very broad and shallow. Before reaching the peak output, the tubes were underloaded because the load impedance presented by the input of the network was greater than 2000 ohms, and the plate current was also less than normal for the maximum availability of power. After we passed the peak output, the tubes were overloaded, because their load impedance was then lower than 2000 ohms, and the plate current was greater than normal, *most likely* exceeding the rated or normal value.

The optimum load impedance of 2000 ohms is obtained when the output loading control is adjusted precisely at the peak of maximum power output, and the plate current at the dip is the normal loaded value. Because our adjustment took us past

the point of peak output, we'll now readjust the controls for maximum output power (or for the maximum power available at the maximum rated plate current) with the network still terminated with the 50-ohm dummy load. With this condition, we note the positions of the plate tuning and output loading controls.

Next, let's replace the dummy load with a 50-ohm resistor in series with a 50-ohm capacitor, an impedance Z = 50 – *j*50 ohms, which produces a 2.618:1 mismatch. The impedance of this new load is higher than the 50-ohm dummy load, so for the same output power, the relative power indicator shows a higher level than with the dummy load. This is why it's called a *relative* power indicator. Remember, it's a voltmeter indicating voltage across an impedance, and not a true power meter.

The same maximum output power as with the dummy load will be indicated by obtaining the same loaded plate current as with the dummy load. On applying power with the new load impedance, the plate current is no longer at a dip minimum. Why? Because the capacitance in the new load reflects capacitance into the tank circuit so that it is no longer in resonance; the tank is now detuned. Resonance is restored by retuning the plate-tuning capacitor for the dip. The output loading-control capacitor (paralleling the output terminals) also requires readjustment to decrease its capacitance. This readjustment allows a higher RF voltage to appear across the increased load impedance, and again transfers the maximum available power into the 50-ohm resistance in the new capacitive load. When the maximum power output has again been obtained by following the same procedure as before, the tubes are again seeing their optimum load impedance of 2000. Further, the plate current at the dip is the same value as with the 50-ohm dummy load, and the actual power absorbed by the 50-ohm resistance in the capacitive load is the same as that with the dummy load. No power is absorbed by the 50-ohm capacitor.

The important message of this exercise is that the change in positions of the pi-network tank-circuit controls compensates for the change in the load *impedance* at the output terminals of the tank circuit. The output load impedance was changed from 50 ohms resistive to a capacitive 50 – *j*50 ohms, while the impedance compensation obtained by changing the plate tuning and loading of the tank circuit maintained the 2000-ohm input impedance required as the load for the tubes. This example shows that the pi-network can match impedances of widely differing values, and that by adjusting the variable components of the network, different values of impedance terminating the network can be transformed to the desired impedance at the input terminals.

Now to another important point that is not generally well understood, because the manufacturers of amateur transmitters imply in their instruction books that the input impedance of the feed line connected to the RF output terminals should be 50 ohms. (Some manufacturers allow for a range of impedances that would produce an SWR of 2:1, referenced to 50 ohms.) The important point is that most transmitters using tubes in the output stage have pi-network tank circuits with impedance-range adjustment capabilities, as just described above. Most often those capabilities can accommodate mismatches greater than 2:1. Many rigs will accommodate any impedance found on the 3:1 SWR circle, and even some impedances on the 4:1 circle.

Thus, whatever the load on the tank circuit might be, with even a 4:1 SWR, the tuning and loading control range may allow you to obtain a dip in plate current at the same value as with a 50-ohm dummy load. If so, the tubes are seeing their desired load impedance and are operating at the same temperature as with the 50-ohm dummy load; no overheating will result from the SWR on the feed line! The tubes are completely unaware of what impedance is loading the output of the pi-network tank circuit. Sec 7.5 contains additional information concerning matching with the tank circuit.

Sec 13.3 The Antenna Tuner

When the external load impedances are outside the range of those that can be matched by the transmitter's own pi-network, an additional matching network is all that is required to match the optimum load impedance of the tubes. Such a network simply extends the impedance range of the pi-network tank circuit. In ARRL publications, this additional matching network is called a *transmatch*, meaning to match the transmitter to the transmission line. The other popular name for the line-matching net-

work is *antenna tuner*. I rather like *antenna tuner* because this name is also descriptive of its performance. (You'll often see *ATU* in foreign publications, for *antenna tuning unit*.)

The antenna tuner really does tune the antenna to resonance, in spite of opinions to the contrary of those who are unaware of the principles of conjugate matching. The tuner obtains a match, by which all reactances throughout the entire antenna system are canceled, including that of the non-resonant antenna, thereby tuning it to resonance. It should also be noted here that when the pi-network in the transmitter alone matches the feed-line input impedance to the output-tube impedance, the pi-network performs the match in an identical manner, and again, the off-resonant antenna is tuned to resonance. If you are interested in the definition and other features of conjugate matching, I refer you to Chapter 19, based on information that I wrote earlier for the ARRL. That information appears on page 16-10 in all issues of *The ARRL Handbook* (*Ref 1*) starting with the 1986 edition (summarily deleted beginning with the 1995 edition) and on page 25-1 in the 15th edition of *The ARRL Antenna Book* (*Ref 71*). Also see Chapter 17. A review of Chapter 7 will also be informative.

From discussions both on the air and at hamfests, I know there are many amateurs who still refuse to use an antenna tuner because they are adamant in their belief that the tuner doesn't tune the antenna. Thus, before leaving the subject of conjugate matching, I'd like to make two more attempts to persuade nonbelievers into accepting the truth concerning tuning the antenna. First, they should also read "My Feed Line Tunes My Antenna" by Byron Goodman, W1DX (*Ref 7*). Second, there are thousands of AM broadcast stations throughout the world using vertical tower radiators for their antenna. The height of the majority of these towers is determined not by the height at which they are resonant, but by the height that obtains the desired vertical radiation pattern. Therefore, nearly all AM station towers are not resonant at their operating frequency, but have a reactance component in their input-terminal impedance. How are these antennas made resonant so they will radiate the total available power from the transmitter? You guessed it—by matching with an antenna tuner! Think about it.

Sec 13.4 Fixed-Tuned Rigs

Here's another item that should surely thrill the nonbeliever. So far we have discussed only transceivers using tubes and pi-network tank circuits. Keep in mind that with these transceivers, all reflected power reaching the tank circuit is conserved; it is totally re-reflected to the antenna, and the only power lost is in feed-line attenuation. Sadly, we now come to the newer solid-state rigs that have no adjustable tuning and matching components. The tuning is fixed. The manufacturers have eliminated adjustable components to reduce costs and to make room for more sophisticated circuits. The circuits containing the output transistors are designed to work only into a 50-ohm load, period!

Does the circuit have a feature that re-reflects the reflected power to conserve it, as does the pi-network? Hardly! Therefore, what happens to the reflected power reaching the output circuit if the feed line is mismatched? All reflected power is lost! The new design routes all reflected power into a circuit which reduces the RF output power in proportion to the amount of reflected power to protect the output transistors from overloading because of detuning. With too much reflected power (too high an SWR), the output stage shuts down almost completely! I'm sure you all understand what this means: If the amateur with a solid-state rig wants to retain the across-the-band operating flexibility he had with his conventional tube rig, he's forced to install an external matching unit—the antenna *tuner*. Didn't I tell you this would thrill the non-believer?

Chapter 14

Matching Networks

Sec 14.1 Development of the L Section

The antenna tuner, or transmatch, in amateur use is fundamentally the same type of matching network as the pi-network tank circuit of the transmitter. It uses the same circuit components—inductors and capacitors—and the circuital action is identical. The principal difference is in the circuital arrangement of the components, although some tuners also use the pi configuration. The circuital arrangement and component values in the tuner are determined primarily by the range of impedances the tuner is desired to accommodate, and the frequency response. All such matching networks have a common element—the simple L section, which is the building block for all of the more complicated networks. For example, the pi-network comprises two L sections with their series reactances connected together, and the T-network comprises two L sections with their parallel reactances connected together. However, what is an L section? What does it do? To answer these questions we begin with an examination of some relationships involving resistance and reactance that are pertinent to the circuit action in the L section.

The basis for matching impedances using L sections as building blocks lies in the equivalence between series and parallel circuits. For any circuit containing resistance and reactance in series, there is an equivalent circuit containing resistance and reactance in parallel that has the same impedance and phase angle when the circuits have an applied voltage of the same frequency. The basic series and parallel circuits are shown in Fig 14-1. Because the same principles apply whether the reactances are inductive or capacitive, the reactances are shown as blocks in the figure. However, the reactances in both circuits are the same kind—that is, if the series reactance, Xs, is inductive in A, the parallel reactance, Xp, in the equivalent parallel circuit in B is also inductive, and vice versa.

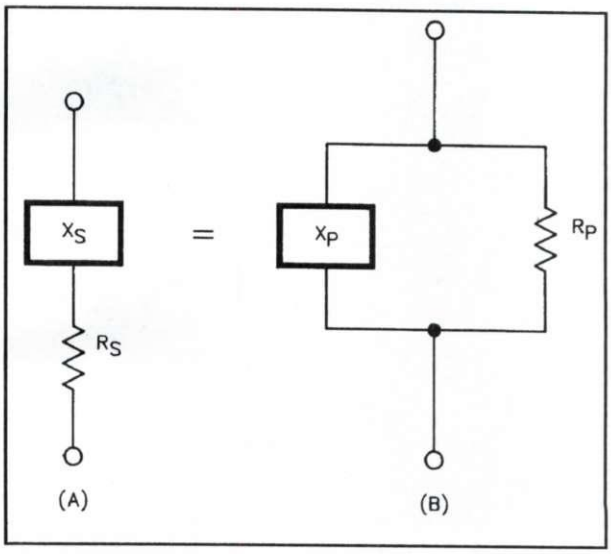

Fig 14-1. At A is the basic series circuit, and at B is the equivalent parallel circuit. Xs and Xp may be either inductive or capacitive, but they must be the same kind of reactance for circuit equivalence.

The value of Rp is always larger than Rs, and Xp is always larger than Xs. Herein lies the basis for impedance transformation: For a given Rs, the higher the value of Xs, the higher will be the values of Rp and Xp. Hence, Rp can be transformed to any value higher than Rs by selecting the proper value of Xs. Because the primary function in matching impedances is the transformation from one resistance level to another (and then canceling the reactance), we find that we can transform levels of resistance as desired by selecting the appropriate value of Xs in series with Rs.

Thus, how do we determine the component values in the two equivalent circuits? Evidently the actual values in the equivalent circuits are related by the quantity Q. When the series and parallel circuits are equivalent, the following equations involving Q provide the necessary relationships between the two circuits to determine all of the component values.

$$Q = \frac{X_S}{R_S} = \frac{R_P}{X_P} \qquad \text{(Eq 14-1)}$$

$$R_P = R_S (Q^2 + 1) \qquad \text{(Eq 14-2)}$$

$$\frac{R_P}{R_S} = Q^2 + 1 \qquad \text{(Eq 14-3)}$$

$$Q = \sqrt{\frac{R_P}{R_S} - 1} \qquad \text{(Eq 14-4)}$$

$$X_S = QR_S \qquad \text{(Eq 14-5)}$$

$$R_S = \frac{R_P}{Q^2 + 1} \qquad \text{(Eq 14-6)}$$

$$X_P = \frac{R_P}{Q} \qquad \text{(Eq 14-7)}$$

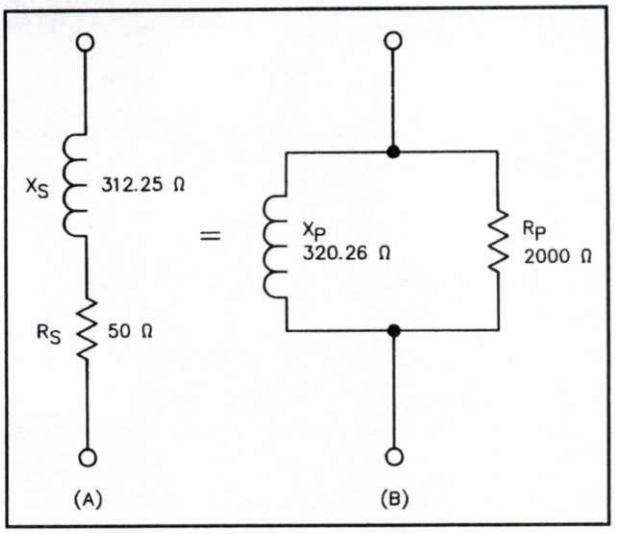

Fig 14-2. Equivalent series and parallel circuits. Component values are related by equations given in the text.

Let's now calculate some component values with an example.

This example is illustrated in Fig 14-2. We'll use the same values as used with the pi-network in matching a 50-ohm resistive load to the 2000-ohm load impedance of parallel 6146 tubes in Chapter 13. We want to transform the 50-ohm resistance to 2000 ohms, so we let R_S = 50 ohms and R_P = 2000 ohms. From Eq 14-4, we see that R_S and R_P determine the value of Q, so $Q = \sqrt{2000/50 - 1} = \sqrt{39} = 6.245$. Next, the series reactance, X_S, required to transform 50 ohms to 2000 ohms is found from Eq 14-5: $X_S = 6.245 \times 50 = 312.25$ ohms. To complete the calculations, we determine X_P from Eq 14-7: $X_P = 2000/6.245 = 320.26$ ohms. Thus, we can transform the 50-ohm resistance, R_S, to 2000 ohms by inserting a reactance, X_S, of 312.25 ohms in series with R_S. Are we finished? Not quite. Recall that we had to introduce a reactance X_S to obtain the transformation of resistance, and as we have done nothing so far to eliminate it, the resulting parallel reactance, X_P, is still present. However, it is a simple matter to eliminate X_P. By placing a reactance of the same value as X_P, but of the opposite kind ($-X_P$) in parallel with X_P, all of the reactance is canceled (eliminated) from the equivalent parallel circuit, and only the resistance, R_P, remains. This effect is illustrated in Fig 14-3.

Keep in mind that the series circuit in Fig 14-2A is the only physical circuit that exists. The parallel equivalent circuit of Fig 14-2B does not exist, although if it did, it would exhibit the same impedance and phase angle as the series circuit. With the $-X_P$ added to cancel the reactance, X_P, the resulting physical circuit is shown in Fig 14-4. R_P is now shown with an arrow to indicate the resistance that a source of power would see when looking into the terminals. The circuit of Fig 14-4 is an L section which evolves from the equivalence of the series and parallel circuits, but appears physically as the original series circuit of Fig 14-2 with the $-X_P$ canceling reactance added. As we can see, the L section of Fig 14-4 has transformed a pure resistance of 50 ohms to another pure resistance of 2000 ohms by means of a series reactance and a parallel canceling reactance. While X_S and X_P are shown as inductive, either inductive or capacitive reactances would perform equally from the viewpoint of impedance matching. The choice of which kind to use depends on the particular application of the circuit.

The L section can be used to match any two values of resistance. However, there is a limitation that sometimes restricts the practical usage of the single L section alone. The limitation is that the Q of the single L section is determined solely by the values of the load and input resistances, R_S and R_P, and in many instances the resulting Q may not be a satisfactory value. In such instances, more complicated circuits comprising two or more L sections may be used to remove the Q limitation, and also to

permit other factors to be considered in the design of a matching circuit.

Sec 14.2 Design of the T-Network

Now that we have the procedure and equations required to design L sections, we are ready to design T- and pi-networks. The step-by-step procedure is the same for any network calculation. We'll start with the T-network because we're interested both in extending the range of the pi-network tank circuit of the tube rig and in providing a matching unit for the solid-state rig that requires a 50-ohm resistive load, as initially discussed in Sec 13.4. The T-network is especially convenient for matching relatively low values of impedance in our range of interest, such as those appearing on the SWR circles of Fig 10-1. The T-network is also the choice of most tuner manufacturers for reasons that are discussed later.

As stated earlier, the T-network consists of two L sections with their parallel reactances connected together. This is shown in Fig 14-5. The impedance transformation in the T-network is performed in two steps. As drawn in Fig 14-5, the right-hand L section (section 1) transforms the resistance in the load up to a value higher than the load and input resistances. The left-hand section (section 2) then transforms that value down to the desired input resistance. The series arm of section 1 contains the load impedance that is to be transformed to the desired input resistance. Any reactance in the load becomes a part of series reactance Xs. The result-

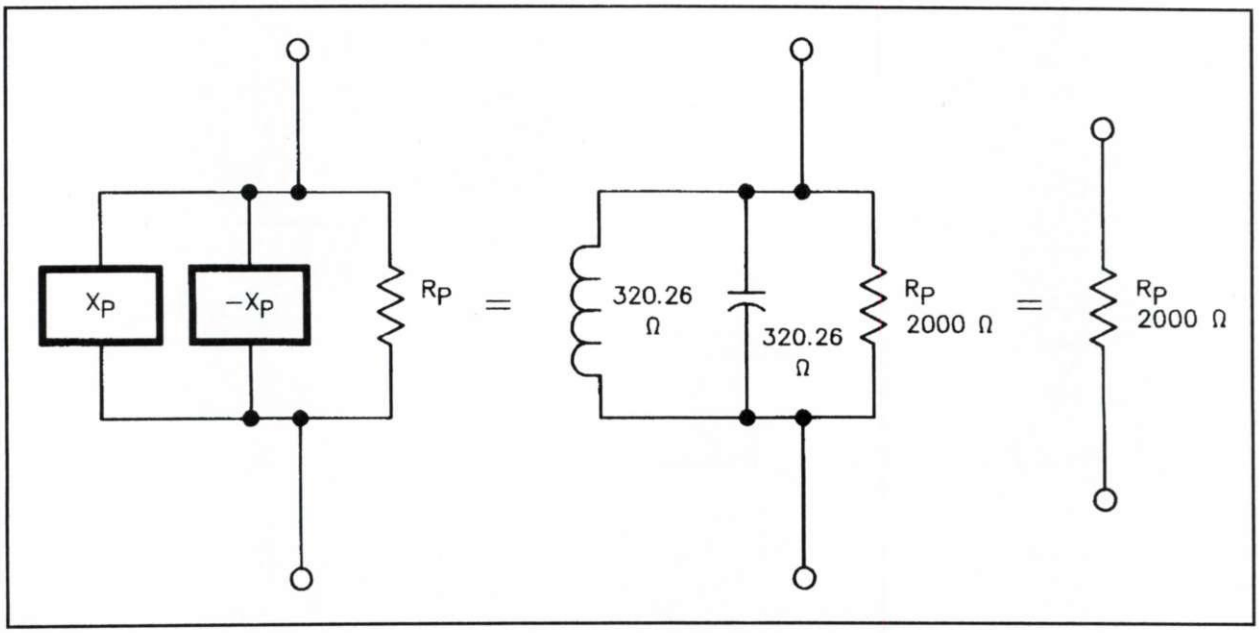

Fig 14-3. Reactance cancellation by adding a parallel reactance of the opposite kind.

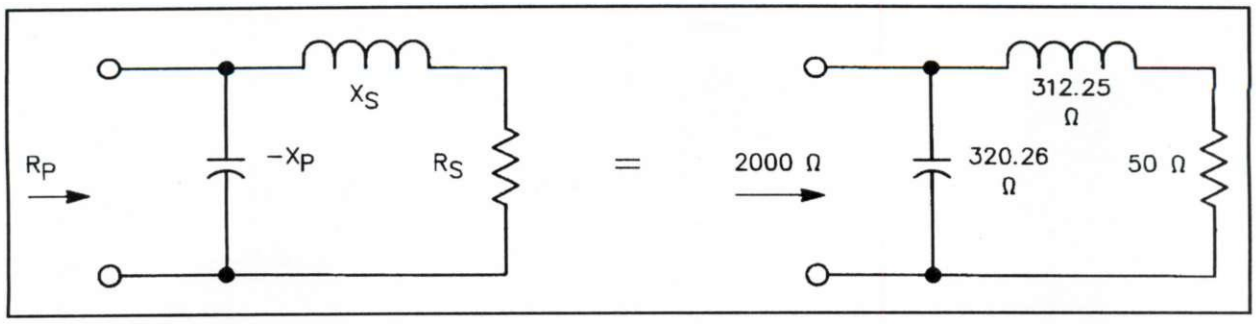

Fig 14-4. The resulting L-section matching circuit for the example given in the text. This circuit is developed from those of Figs 14-2 and 14-3.

ing series network reactance is calculated later. The resistance in the load, R_{S1}, is transformed in section 1 to R_P, which is required to be higher than both the load resistance, R_{S1}, and the desired input resistance, R_{S2}.

R_P is a virtual resistance, not a physical resistor, so it is shown as R_V in Fig 14-5. R_V is treated as RP in the equations, and is determined by R_{S1} and Q1 from Eq 14-2. Q1 can be any value that makes R_V higher than both R_{S1} and R_{S2}. Unless a high Q is desired for selectivity and harmonic rejection, Q is usually kept low to minimize losses from circulating currents. X_{P1} is determined by R_V and Q1 with Eq 14-7. The virtual resistance, R_V, becomes the load for section 2, where it is transformed down to the desired value of input resistance R_{S2}. X_{S1} is determined by R_{S1} and Q1 from Eq 14-5. If the reactance in the load is the same kind (same sign) as the series network reactance, the load reactance is subtracted from X_{S1} to obtain the network reactance; if of the opposite kind, the load reactance is added to X_{S1}. Because R_V and R_{S2} have already been determined, the Q of section 2 is also determined, obtained from Eq 14-4. X_{S2} is then obtained from R_{S2} and Q2 by using Eq 14-5. X_{P2} is determined by R_{P2} and Q2 from Eq 14-7.

Because X_{P1} and X_{P2} are in parallel (Fig 14-5A), a single reactance equal to the total value of the combination will suffice. This reactance is shown as X_{PT}, Fig 14-5(B). If the two parallel reactances

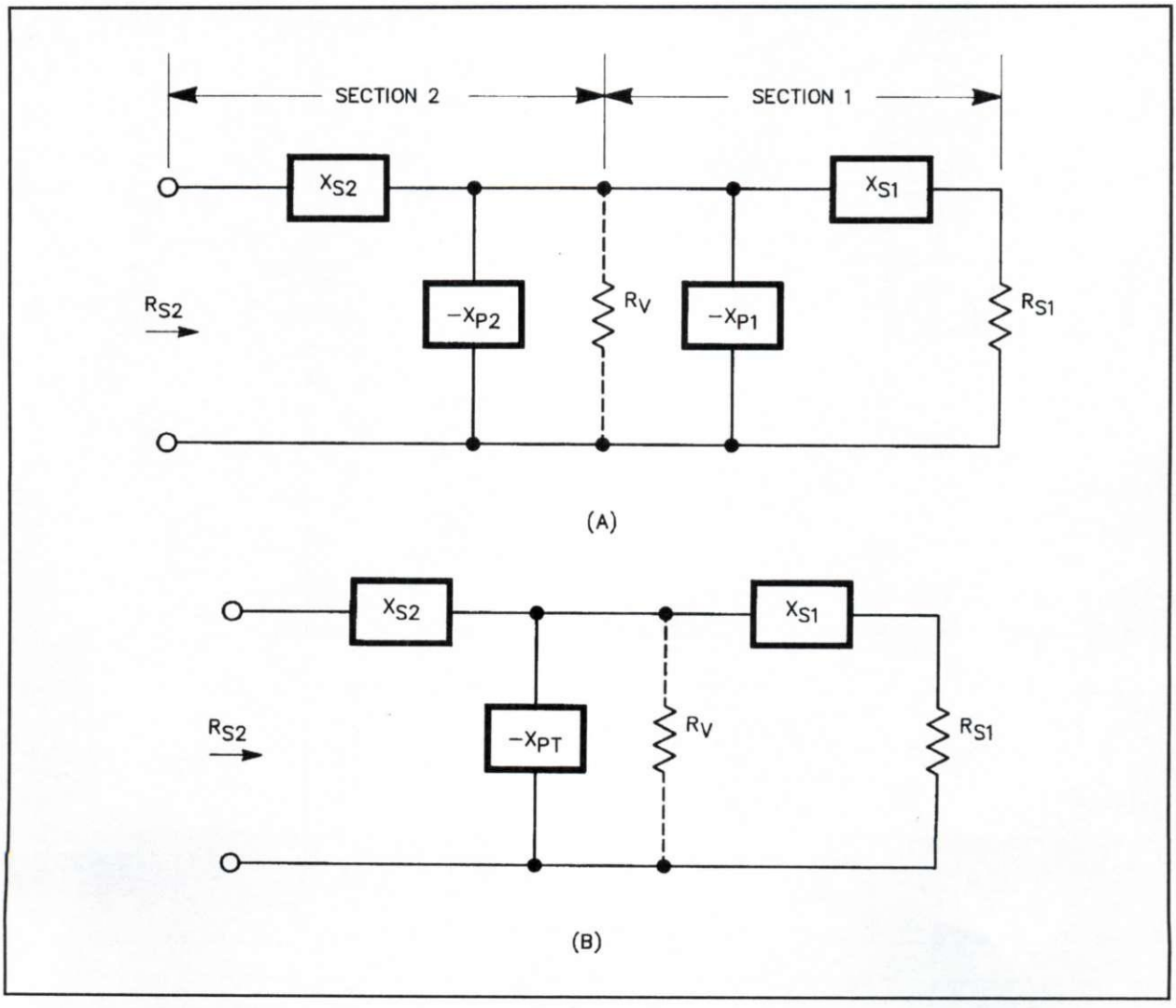

Fig 14-5. The T network, formed from two L sections. The circuits of A and B are equivalent.

of X_{PT} are of the same sign, the parallel value is equal to the product of the two reactances divided by their sum; if they have opposite signs, divide the product by their difference. If the signs of the two reactances X_{P1} and X_{P2} are opposite, the net reactance is of the same sign as the smaller reactance.

The completed network is shown in Fig 14-5(B). It is evident that there are several possible combinations of inductive and capacitive arrangements that may be used in a T-network. If the objectives of the T-network are to reject harmonics as well as to match impedances, the choice of reactances would be series inductors and parallel capacitors. Unfortunately, the opposite arrangement is most prevalent in amateur practice, even with the smaller amount of harmonic rejection available. However, one rule must be strictly followed for any combination of the network to perform correctly. This rule is that the two reactances in a single L section must be of the opposite sign.

Now let's work out an example using data from Sec 12.3. In the example there, the antenna impedance $Z = 50 - j90$ was transformed to $Z = 12 - j20$ through a 113-foot length of RG-8 coax. (We obtained the line-input impedance $Z = 12 - j20$ from the 5:1 SWR circle in Fig 10-1.) The line-input impedance, $12 - j20$, is the load to be matched to 50 ohms resistive. This load establishes $R_{S1} = 12$ ohms, and $R_{S2} = 50$ ohms. The results of this example are shown in Fig 14-6.

First we need to select a value for Q1 that makes R_V greater than R_{S2}, so we'll let Q1 = 5. From Eq 14-2, $R_V = 12 \times 26 = 312$ ohms. The reactance X_{S1} required to transform 12 ohms to 312 ohms is found from Eq 14-5: $X_{S1} = 5 \times 12 = 60$ ohms. We must now account for the 20-ohm capacitive line-input reactance appearing in the load. Because this reactance appears in the series arm of L-section 1, it is a part of X_{S1}. We may choose capacitive reactance for the series element X_{S1} in Fig 14-6. Then the capacitive reactance in the load must be subtracted from X_{S1} as calculated above to obtain the series reactance in the physical network. Therefore, the reactance of the capacitive series network element is $X_{S1} - X_{LOAD} = 60 - 20 = 40$ ohms. If the reactance in the load had been inductive (the opposite of the series network reactance we chose), it would have been added to the network reactance. Next, from Eq 14-7, we obtain $X_{P1} = R_V/Q1 = 312/5 = 62.4$ ohms. This completes the calculations for L-section 1.

The Q for section 2, Q2, is predetermined because R_V and R_{S2} are already determined. So from Eq 14-4, $Q2 = \sqrt{312/50 - 1} = \sqrt{5.24} = 2.29$. The series X_{S2} required to transform R_V, 312 ohms, down to 50 ohms is found from Eq 14-5: $X_{S2} = 2.29 \times 50 = 114.5$ ohms. From Eq 14-7 we obtain $X_{P2} = R_V/Q2 = 312/2.29 = 136.2$ ohms. For the total parallel reactance:

$$X_{PT} = \frac{X_{P1} \times X_{P2}}{X_{P1} + X_{P2}} = \frac{62.4 \times 136.2}{62.4 + 136.2} = 42.8 \text{ ohms}$$

Finally, one more step is needed to convert the reactances to the circuit constants of the components in a matching unit. The constants for the operating frequency may be calculated from Eqs 14-8 and 14-9. The results using 3.5 MHz are given in Table 14-1.

$$C = \frac{159{,}150}{f \times X} \qquad \text{(Eq 14-8)}$$

$$L = 0.15915 \times \frac{X}{f} \qquad \text{(Eq 14-9)}$$

where
C = capactiance, pF
L = inductance, µH
X = reactance, ohms
f = frequency, MHz

The circuit constants appearing in Table 14-1 are realistic values, and should be within the range consistent with most commercially made tuners. It is important to realize that the antenna impedance with the 5:1 SWR used in the example is a realistic impedance for operation around 3.55 MHz with an 80-meter dipole cut for resonance at 3.75 MHz. The example also demonstrates that match-

Circuit Designation	Reactance	L or C Value
$X_{S1} - X_{LOAD}$	–40 ohms	1136.8 pF
X_{S2}	–114.5 ohms	397.1 pF
X_{PT}	+42.8 ohms	1.95 µH

Table 14-1. Component values for the example of Fig 14-6 at 3.5 MHz.

ing the 5:1 SWR with a tuner is practical, and should be routine.

For the example, a lower value of Q1 could have been chosen to satisfy the requirement that RV be higher than R_{S1} and R_{S2}. However, some of the resulting reactances would have been lower than those found in practical tuners, so the more realistic Q was chosen. Because Q1 in the tuner is determined by R_{S1} and the setting of the output capacitor providing X_{S1}, here is a tip that will lead to the capacitor setting for the most efficient operation of the tuner. The minimum Q1 of the tuner (which is what we want) is obtained with the output loading capacitor set for its maximum capacitance. Try first to obtain a match with the maximum setting. If no match can be obtained, decrease the output capaci-

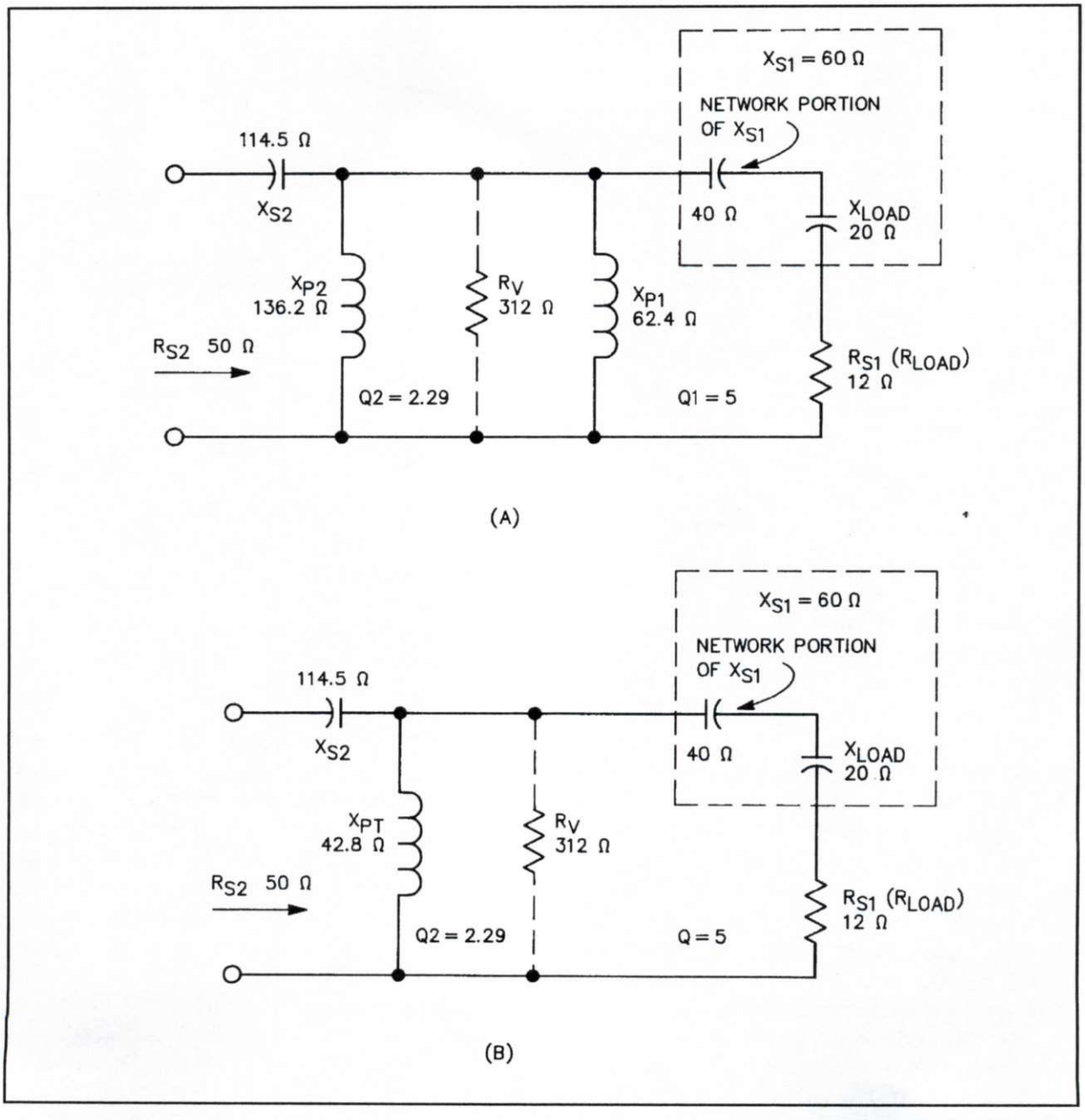

Fig 14-6. Two L sections combined to form a T network in a practical example. The circuits of A and B are equivalent, where the inductance X_{PT} is the resultant reactance of the two inductances X_{P1} and X_{P2} connected in parallel.

tor setting in small increments until a match can be obtained. The match that can be obtained with the maximum possible capacitance in the output loading capacitor results in the lowest Q and maximum efficiency of the tuner. This subject is also touched on in the final paragraphs of Chapter 16.

Sec 14.3 Roller Inductor or Tapped Inductor

There seems to be the notion that the antenna tuner must be adjusted for a perfect 1:1, 50-ohm input impedance. Of course if the transmitter has been tuned into a 50-ohm dummy load, it's nice to be able to switch directly into a 50-ohm tuner input impedance without having to retune the transmitter. However, the tuner does not need to be adjusted for a perfect 50-ohm input impedance to obtain the optimum performance. Any tuner input impedance that the transmitter can load into with the same plate current at the dip as obtained with a 50-ohm dummy load is satisfactory, and will result in the same output power as when the tuner has been adjusted for a 50-ohm input impedance. The point of this last statement is to focus on the issue of which is better, a roller inductor or a tapped inductor.

It is true that with the continuously variable roller inductor for X_{PT}, the parallel reactance in the tuner can be reduced exactly to zero for a perfect match. However, if a tapped inductor has taps at least at every other turn, obtaining a minimum reactance with a tapped inductor rather than zero reactance with the roller inductor will result in no difference in efficiency in the tuner. This is because any small residual reactance in the tuner is canceled by tuning for the resonant plate-current dip in the transmitter, and the indication of a small SWR at the input of the tuner is insignificant.

Let's return briefly to the subject of choosing which arrangement of reactances to use in the T-network. There is a dramatic difference in harmonic rejection between networks of series-L parallel-C circuits versus series-C parallel-L equivalents. This difference is shown graphically in Figs 16-2 and 16-3. Those figures show the frequency response of both arrangements of the C and L reactances, and clearly indicate the superiority of the series-L parallel-C arrangement for harmonic rejection. My personal thoughts concerning the manufacturers' use of the less desirable of the two arrangements is that they initially used McCoy's Ultimate Transmatch circuit (*Ref 41*) because it was popular. They probably didn't explore the use of T-networks. In 1976 I showed in *QST* that the Ultimate is simply a T-network with an unneeded capacitor—the shunt section of the split stator (see Fig 7-1). After that, the manufacturers dropped the split stator in favor of the single series input capacitor, probably without any engineering thought concerning which L-C arrangement would be best suited for amateur use.

BASIC computer programs were used to generate the frequency response data and input impedances shown in Figs 16-2 and 16-3, as well as Tables 16-1 and 16-2. The programs are presented in Chapter 15. These programs are for general use, enabling you to design or analyze T-networks with various values of Q and reactive elements.

Sec 14.4 The Ultimate Transmatch and the T-Network

Servicing or repairing one's transceiver these days is practically impossible for the average amateur because of its sophisticated high-tech design. Building one's own equipment anymore is almost out of the question. However, because of its relative simplicity, the antenna tuner remains attractive to those who still like to build their own. There are also many fine factory-built tuners on the market, so there is a choice of whether to build or buy.

There are a few different circuit arrangements available among manufactured tuners, but the majority now use the T-network. The T-network has been around in the commercial field for a long time, but only recently has it been the preferred form for amateur use in antenna tuners. From the amateur viewpoint, the T-network is an outgrowth of the well-known "Ultimate Transmatch" circuit introduced by Lew McCoy, W1ICP, in *QST* (*Ref 41*), and shown here in Fig 7-1B. McCoy's circuit included a split-stator capacitor for the input element, which has since been replaced with the single-element capacitor, as I have shown in Fig 7-1, for a reason that will soon become apparent. The Ultimate circuit was the favored arrangement among tuner manufacturers until I came along and upset the apple cart, with the result that most present-day tuners embrace the simpler T-network with the single-element input capacitor. How this

change came about involves a story I believe you'll find interesting.

While I was serving as editor of antenna and transmission-line articles for *Ham Radio* magazine during the 1970s, it became necessary to explain the operation of McCoy's Ultimate Transmatch to a would-be *Ham Radio* author who submitted a tuner circuit he claimed to be superior to the Ultimate. On analyzing the Ultimate circuit, I observed that the lower portion of the split-stator capacitor shunting the output of the transmitter contributes nothing to the matching function. Without the lower portion, the circuit becomes a simple T-network, as shown in Fig 7-1(B). An experiment using a General Radio 1606-A RF impedance bridge verified the analysis. I then notified Dentron, for whom I was a consultant. They were ecstatic because they were about to reorder a large batch of the more expensive split-stator capacitors. Shortly thereafter, during a trip to Newington, I demonstrated my experiment using the General Radio RF bridge in the ARRL Lab for some of the League staff, including Doug DeMaw, W1FB. Jim Fisk, then editor of *Ham Radio*, was also present. All were surprised to learn that the shunt section of the split-stator capacitor was unnecessary. I published my finding in *QST* in 1976 (Fig 7-1[B] here). Doug reported on my ARRL Lab demonstration in his product review of the Murch UT 2000-B antenna tuner in *QST* (*Ref 72*), and McCoy reported on the modification in *CQ* (*Ref 73*). Dentron was the first to go to the simple T-network, and others followed.

It is interesting to note that the Johnson MatchBox tuner has a situation somewhat similar to that of the McCoy Ultimate concerning the unneeded capacitor. The MatchBox uses a dual-differential capacitor in the output circuit, which the instruction book says is a balanced voltage divider, and therefore it is also said to be an impedance divider. Consequently, it is generally believed that the impedance-matching operation is achieved by simple impedance-divider action. However, in my opinion this is not true, because when the two capacitor sections shunting the balanced output terminals to ground are disconnected, the impedance match to the transmission line can be reestablished with a small readjustment of the capacitor. As will be seen later, this is somewhat similar to eliminating the shunt capacitor on the input side of McCoy's "Ultimate Transmatch."

We'll now examine the circuitry of the MatchBox, which is essentially a dual-balanced pseudo T-network. An internal semi-fixed tap-adjustable inductive coupling between the unbalanced input inductor and the balanced output inductor establishes the adjustable input component of the T, which achieves the transformation of the output-input resistance components of the corresponding impedances. The inductive coupling between the unbalanced input inductor and the balanced output inductor also performs the balun function. The inductance in the balanced output inductor, in combination with the two outer (series output) capacitors of the dual-differential capacitor, forms a dual-balanced L network that comprises the output circuit of the balanced T-network. The two inner capacitors of the dual-differential capacitor form a series capacitance connected between the output terminals, thus connecting this capacitance in parallel across the input of the balanced transmission line. The common connection between the two inner capacitors is connected to the tuner-chassis ground, thus balancing each side of the input of a balanced transmission line with respect to ground. However, the principal effect of this series capacitance shunting the input to the feed line is to place a variable capacitive load across the line input that decreases the effective input impedance of the line.

It is immediately obvious that all four individual variable capacitors of a dual-differential capacitor rotate simultaneously, because they are all mounted on a single shaft. This mechanical limitation presents a problem, because as the series output capacitors of the balanced T are adjusted to achieve matching to the input impedance of the transmission line, the capacitance of the two inner capacitors shunting the line varies simultaneously. Thus, the *effective* line-input impedance appearing at the output terminals of the tuner is constantly varying without any plan or reason as the tuner is being adjusted to match to the line input impedance. Therefore, this capacitive loading on the input to the transmission line plays no *direct* part in the matching process. After all, we are attempting to match to the input impedance of the *transmission line*, not to an input impedance that *varies* with

every adjustment of the capacitor. Thus, as we will see later, in certain cases it actually reduces the impedance-matching range of the tuner.

Now recall that after obtaining a match with the parallel capacitor sections connected, these sections can be disconnected, and the impedance match can be restored with only a small change in the capacitor setting. Then just what is the purpose of the two capacitors that shunt the input of the feed line? Apparently the designers at Johnson misunderstood their function. As long as these capacitors rotate simultaneously with the *series* capacitors of the L networks they serve *no* useful purpose and are in fact detrimental to the range of impedances the tuner can match. Recalling from our earlier statement, the reason is that as the series capacitors are varied to achieve the impedance match at the input of the transmission line, the effective input impedance at the input of the line is changing simultaneously, because the shunt-loading capacitance of the *parallel* capacitors is also changing. From this viewpoint the parallel capacitors are excess baggage.

However, from a broader viewpoint the effect of the shunt capacitance may be either good or bad, depending on the actual input impedance of the line at a given frequency or length of line. If the two line-shunting capacitors are disconnected from the circuit, the matching is performed directly to the actual input impedance of the transmission line. If the input impedance of the line is higher than the MatchBox can match without the shunting capacitors, then the shunting capacitors are beneficial in reducing the line-input impedance to allow the MatchBox to match the higher input impedance. If, on the other hand, the input impedance of the line is already approaching the lower limit of the matching range of the MatchBox with the shunting capacitors *disconnected,* then if connected the shunting capacitors will restrict the matching range on the low-impedance end of the range. The overall impedance-matching range of the MatchBox could be increased if a switch were added to allow the line-shunting capacitors to be either connected or disconnected, depending on the impedance condition of the actual input impedance of the transmission line.

However, the designers of the MatchBox could have come up with an even better solution. If the dual-differential capacitors were replaced with two split-stator capacitors, the capacitors shunting the input of the transmission line could be adjusted independently of the series output capacitors. With this arrangement the impedance-matching range could be extended dramatically when the line-input impedance is higher than what the tuner can match in its present form. This is because, as stated above, the input impedance of the line is reduced by capacitive shunt loading.

I have thus shown that the legend of the dual-differential capacitor in the Johnson MatchBox performing as an impedance divider is another of the many misconceptions prevalent among us.

Sec 14.5 The Pi-Network

The component values in the pi-network are calculated using the same procedure as with the T-network. The basic difference between the two networks is that while the parallel reactance arms of the L sections are connected together in the T-network, the series reactance arms are connected together in the pi-network. Also, because the virtual resistance is in the series arms of both L sections in the pi arrangement, R_V must be lower than both the input resistance and the load resistance.

The pi-network arrangement may be used in the antenna tuner, or for other general uses, but its most prevalent use is in the output tank circuit in rigs having tubes in the final amplifier. In output tank service, the pi-network must filter out the harmonic energy generated in the amplifier, in addition to providing a match between the output tube and the load. The requirement for harmonic filtering places two restrictions on the design: (1) the network must be a parallel-C series-L, low-pass configuration, and (2) the Q must be selected to achieve a predetermined value of harmonic rejection. In output tank service, a Q of 12 is generally considered appropriate.

We'll now calculate the values needed for a pi-network to match a 2000-ohm tube load resistance R_{P2} to an output load resistance R_{P1} of 50 ohms with an input Q (Q2) of 12. The results of this example are shown in Fig 14-7. With a Q2 value of 12, we find X_{P2} from Eq 14-7: $X_{P2} = 2000/12 = 166.7$ ohms. Because the virtual resistance R_V is in the series arms of the L sections, we treat it as R_S

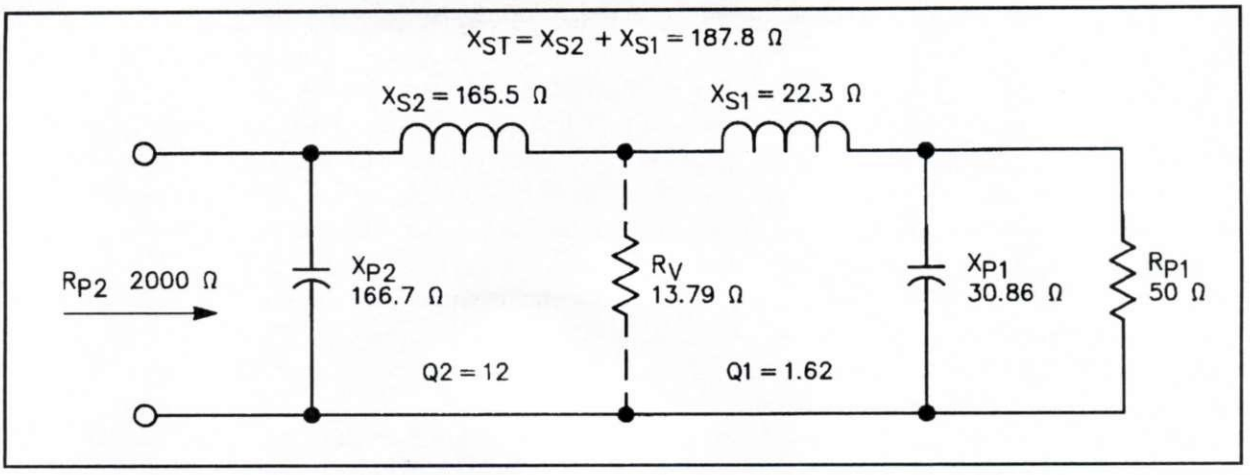

Fig 14-7. Two L sections combined to form a pi-network. The component values are calculated as described in the text.

in the equations. Therefore, we find R_V from Eq 14-6: $R_V = 2000/145 = 13.79$ ohms. X_{S2} is then found using Eq 14-5: $X_{S2} = 12 \times 13.79 = 165.5$ ohms. This completes the calculations for the input L section. Because Q2 is greater than 10, the two reactances in the input section are nearly equal, but of opposite sign. Hence, the input section is equivalent to the standard parallel resonant tank circuit having the same Q.

We begin the calculations for the output section by finding the output Q (Q1) from R_V and R_{P1} using Eq 14-4: $Q1 = \sqrt{50/13.79 - 1} = 1.62$.

We now find X_{S1} using Eq 14-5: $X_{S1} = 1.62 \times 13.79 = 22.3$ ohms. To complete the network calculations, we find X_{P1} using Eq 14-7; $X_{P1} = 50/1.62 = 30.86$ ohms. Because R_V is a virtual resistance, and does not appear as a physical resistor, the values of X_{S1} and X_{S2} can be added to determine the total series reactance X_{ST}, permitting use of a single reactor for the series element. Thus, $X_{ST} = 165.5 + 22.3 = 187.8$ ohms.

As stated earlier, if the network is designed for general application, any combination of capacitive and inductive elements may be used for the reactances as long as the one cardinal rule is followed: The two reactances appearing in a single L section must be of the opposite sign to obtain resonance. However, if the design is for output tank service, the parallel elements must be capacitive and the series element inductive to obtain the required low-pass circuit action.

Elmer Wingfield, W5FD, focused on an interesting aspect of pi-network design in an article he published in *QST* in 1983 (*Ref 74*). in the T- and pi-network calculations we made in the examples above, the total operating Q (Q_O) of the networks is the sum of Q1 and Q2. The equations we used to determine the component values have been in general use for years, and they are correct. However, as Wingfield points out, in some instances the equations have been applied incorrectly, notably in the use of the input Q (Q2) as the operating Q (Q_O). When the input Q is 10 or more, the error in misusing Q2 as Q_O is negligible. An example is in our design of the pi-network where we chose a Q of 12, but wound up with a total Q_O of 12 + 1.62 = 13.62. The error in this case is negligible, but when the ratio of the input to output resistance is less than 10, the error in using Q2 as Q_O becomes significant. For example, when the input and output resistances are equal, Q1 = Q2, so when taking Q2 as Q_O the error is 100%, because Q_O is twice the value of Q1 and Q2.

Wingfield derived equations for obtaining the component values of the pi-network based on the actual value of Q_O. You will find them useful when designing a pi-network where the ratio of the input to output resistances is less than 10. This is an excellent reference. He included in his *QST* article a computer program in BASIC programming for performing the calculations. If your copy of Wingfield's article is no longer available, you can obtain a photocopy from ARRL headquarters. However, I have included a copy of Wingfield's BASIC program in Chapter 15, along with my own

network programs in BASIC, using the old standard equations presented here.

Other references to the use of L sections in matching networks are found in *Refs 4, 61, 63, 64, and 74*. Particular note should be taken of the reference by Grammer, W1DF (*Ref 4*), because it is by far the most clear, concise, and illuminating treatise on network design that I've seen published. In three installments, Grammer presents not only the "whats," but also the important "whys," of the circuit functions in the various network combinations. For the reader who wants to learn the "whys" of what you're reading here, the Grammer articles are a must. If you can't find a library copy, photocopies are available from the ARRL.

Sec 14.6 Matching at the Load

One of the goals of this book is to provide enlightenment concerning the matching of impedances at the input of a feed line, in contrast to matching at the load, or antenna. However, in the discussion of inductively loaded HF mobile antennas in Sec 6.4, I stated that the matching could be performed either at the line input or at the load, depending on which was most convenient for the operator. Therefore, before leaving the subject of matching networks, I'll include a novel, yet simple method of providing L matching at the input terminals of inductively loaded HF mobile antennas. This method is not new. What follows is based on data that I contributed to *The ARRL Handbook*. It appears in Chapter 33 of all editions since 1986 (*Ref 1*).

With this method, which is especially adaptable to loading coils that have no means for either adjusting or tapping into the inductance, only one circuit element for the L-network is required, the shunt element. Let's assume we'll use a capacitance for the shunt element. All that is required to determine the value of the capacitance is a reasonably accurate measurement of the resonant SWR. By extending the whip slightly beyond its natural resonant length, the series inductance component of the L-network appears inherently in the feedpoint impedance. At the correct length, the resulting parallel reactance component, X_L, causes the parallel resistance component, R_A, to equal the feed-line characteristic impedance, Z_C ohms. The match is accomplished by canceling the parallel inductive reactance component, X_L, with the shunt capacitance of equal but opposite reactance.

To perform the matching operation, first resonate the antenna at the desired frequency by adjusting the whip length for minimum SWR without the capacitor. The approximate value of X_L with the whip lengthened to make R_A equal to Z_C may now be found from:

$$X_L = Z_C \frac{\sqrt{SWR}}{SWR - 1} \qquad \text{(Eq 14-10)}$$

where SWR is that obtained at resonance. The reactance, X_C, of the shunt matching capacitor is the negative of X_L. The capacitance may be determined for the desired frequency, f, from:

$$C(pF) = \frac{10^6}{2\pi f X_C} \qquad \text{(Eq 14-11)}$$

Form a capacitor from a parallel combination of fixed mica capacitors, and connect the combination across the input terminals of the antenna. Finally, increase the whip length in small increments until the minimum SWR is reached; it should be very low.

If a lower SWR is desired, a trimmer capacitor may be added to the fixed capacitor bank, and by alternate adjustment of the trimmer and whip length, a perfect 1:1 match can be obtained. Once the size of the capacitor has been established for a given band, the antenna can then be matched at other frequencies in the same band simply by adjusting the whip length for minimum SWR. If an inductive rather than a capacitive shunt element is preferred, replace the capacitor with an inductor having the same absolute value of reactance, and shorten the whip instead of lengthening it from the resonant length. The principle behind this matching technique is identical to the "hairpin" matching used in Yagi beams.

Chapter 15

Computer Programs for Impedance Matching

Sec 15.1 Introduction

This chapter was written to provide computer assistance in solving impedance-matching problems and for transforming transmission-line terminal impedances from one end of the line to the other. The chapter contains listings of nine programs written in the BASIC language. These programs will enhance your enjoyment of experimenting with impedance-matching circuitry.

Five program listings relate to the design of T and pi-networks, two of which include network input impedance versus frequency, and the resulting frequency response of the network. One additional program calculates transmission-line constants using data obtained from measurements made on the line. The three remaining programs transfer a known complex impedance from one end of a line to the other. The impedance-transformation calculations include the effect of line attenuation. With the detailed instructions provided here, these program listings should be helpful and easy to use. Two program listings for hand-held calculators are also included.

Sec 15.2 Designing T and Pi Matching Networks

T.BAS is listed as Program 1. This program is for designing or analyzing T-networks, using the conventional equations appearing in Chapter 14. The prompts ask for the input and output resistances to be matched, and the Q of the output L section. The screen output yields the Q of the input L section, and the reactance values of the components. The configuration can be either C-L-C or L-C-L. If it is desired to calculate using input Q instead of output Q, simply reverse the input and output resistances at the prompts, and then reverse the input and output series reactances when reading the screen output. The value of Q shown in the input Q column is the output Q.

PI.BAS, Program 2, is for designing pi-networks, also using the same conventional equations from Chapter 14. As in the T-network, the configuration can be either L-C-L or C-L-C. However, if the network is for a final-amplifier tank circuit, the configuration must be the low-pass C-L-C configuration to obtain the desired harmonic rejection. In this program, the input Q is called for in the prompts. However, if you desire to calculate using the output Q, the same reversal technique described for the T-network will yield the desired results.

The third and fourth network programs are listed as Program 3, T-CLC.BAS, and Program 4, T-LCL.BAS. Both programs are for designing and analyzing T-networks using the conventional equations, but with two added bonuses: calculation of the input impedance of the network versus frequency, and frequency response of the network in decibels. T-CLC.BAS is for the C-L-C configuration, and T-LCL.BAS is for the L-C-L configuration. Both configurations yield the same component values of reactance. However, because the C-L-C circuit is a high-pass filter and the L-C-L is low pass, the network input impedances are different, as are the frequency responses. These two programs were used to calculate the input impedances and frequency responses of the two T-networks shown in Figs 4 and 5 in my Technical Correspondence item, "Wave Reflections in Attenuators, Filters, and Matching Networks," *QST*, November 1981 (included in this book as Figs 16-2 and 16-3). However, I want to point out a printing error in the *QST* article: The frequency response data in Table 1 goes with Fig 5, and that of Table 2 goes with Fig 4. This correction appears in "Feedback," *QST*, February 1982.

The capability of a computer program to produce frequency response data is significant; this enables

us to determine the amount of harmonic rejection available with various values of Q in a network designed to provide a perfect match between the source and load at the fundamental frequency. Now you might ask, "What is the importance of knowing the input impedance of the network?" It is significant, because the key to harmonic rejection is mismatch. The network is designed to provide a match for delivery of the maximum available power, *but only at the fundamental frequency.* This is shown in Tables 16-1 and 16-2 as a perfect match only at the normalized frequency, f = 1. At all other frequencies, the input impedance is mismatched to the source, and the greater the difference in frequency relative to the fundamental f = 1, the greater the mismatch. Hence, the greater is the rejection of off-frequency power. Thus, the attenuation curves in Figs 16-2 and 16-3 are the direct result of the degree of mismatch occurring at each off-resonant frequency listed in the input-impedance tables. Note the dramatic difference in the attenuation of the high frequencies between the C-L-C and L-C-L configurations, as pointed out in Chapter 14. Further discussion appears in Chapter 16.

The last network program listing, Program 5, is W5FD.BAS. This program is for pi-networks in which the total operating Q (Qo) is used in the calculations. This program uses equations derived by Wingfield, W5FD (*Ref 74*), to yield exact values of reactance using Qo. It is especially important to use this program when the ratio of input to output resistances is less than 10, as explained in detail in Chapter 14.

Sec 15.3 Antenna Impedances from Measured Line-Input Impedances

Now we come to what for me is the most exciting and challenging aspect of impedance-matching exercises—the rapid transforming of complex impedances from one end of a transmission line to the other. It is exciting because the almost instantaneous calculation, either by computer or hand-held calculator, makes it practical to obtain antenna-terminal impedances covering a wide range of frequencies that would be impractical and too time consuming to perform manually on the Smith Chart. I'm referring to the determination of the resistance and reactance components of antenna terminal impedances at many frequencies across a band. These impedances are obtained by measuring impedances at the input of the feed line, and then transferring the measured impedances through the line to the antenna. It is challenging to obtain antenna-terminal impedance data that is sufficiently close to reality to be satisfying and rewarding. To do so requires an understanding of transmission-line principles, some math, the ability to take measurements with a good degree of precision, and the availability of impedance-measuring equipment that obtains acceptable precision in the measurement data.

With respect to the measuring equipment, I'm thinking in terms of RF bridges in the same league as the General Radio 1606-A impedance bridge. Perhaps there are noise bridges that have the precision required to obtain sufficient measurement accuracy, but at present I don't know of any that are qualified. Thus, if you have access to the proper equipment and have the desire to learn the impedance at the antenna terminals instead of just the line SWR, the computer listings that follow should give you a lot of pleasure. Tables 15-1 through 15-5, along with Fig 15-1, are examples of information you can obtain with these programs. So are Tables 20-1 through 20-5 and Figs 20-1 through 20-3.

Sec 15.3.1 Calibration of the Feed Line

To measure the terminal impedance of an antenna with acceptable accuracy requires that the measuring equipment be located at a sufficient distance from the antenna so as not to distort the RF field surrounding it. Hence, a feed line is required. To obtain a mathematical solution to the problem of transferring an impedance measured at the input terminals of the feed line to the impedance at its load terminals first requires calibration of the feed line. For the calibration, we need to know the true, measured characteristic impedance Zc of the line—not just the nominal value of 50 or 75 ohms as listed in the manufacturer's catalog. We also need to know the electrical length and attenuation of the line. These calibration data are obtained by first making short-circuit and open-circuit impedance measurements on the feed line alone—that is, measuring the impedance at the line input with the far end terminated first in a short circuit and then in an open circuit. Then the measured data is processed with TRANSCON.BAS, Program 6. This program yields characteristic impedance Zc, the electrical line

```
FREQUENCY =? 1.9
Rsc =? 2.0
Xsc =? 50.0
Roc =? 0.6
Xoc =? -48.5
          CHARACTERISTIC    ELEC.LINE     LINE      LENGTH     ATTENUATION
            IMPEDANCE         LENGTH     ATTEN.    PER MHZ    PER SQR FREQ.
  FREQ.       ZC      ANGLE    DEGREES      DB         PHI        DB    A
-------------------------------------------------------------------------
  1.900    49.266   -0.791    45.44678    0.11367    23.91936     0.08247

FREQUENCY =? 5.65
Rsc =? 2.1
Xsc =? -50.177
Roc =? 2.58
Xoc =? 47.778
          CHARACTERISTIC    ELEC.LINE     LINE      LENGTH     ATTENUATION
            IMPEDANCE         LENGTH     ATTEN.    PER MHZ    PER SQR FREQ.
  FREQ.       ZC      ANGLE    DEGREES      DB         PHI        DB    A
-------------------------------------------------------------------------
  5.650    49.020   -0.347   134.30580    0.20799    23.77094     0.08750
FREQUENCY =? 5.7
Rsc =? 1.9
Xsc =? -48.42
Roc =? 2.58
Xoc =? 49.47
          CHARACTERISTIC    ELEC.LINE     LINE      LENGTH     ATTENUATION
            IMPEDANCE         LENGTH     ATTEN.    PER MHZ    PER SQR FREQ.
  FREQ.       ZC      ANGLE    DEGREES      DB         PHI        DB    A
-------------------------------------------------------------------------
  5.700    48.994   -0.369   135.31610    0.19837    23.73966     0.08309
```

Table 15-1. Printout of feed-line calibration data from TRANSCON Program. This printout shows the results from three successive sets of data input. Measurement results are entered from the keyboard at the prompts (=?). See text for details.

length, and the line attenuation. An equivalent program listing for Hewlett-Packard hand-held calculators appears near the end of this chapter as Program HP1. When you run the computer program, supply the measured short- and open-circuit resistances and reactances at the prompts.

The short-circuit impedance measurement (Zsc) and the open-circuit measurement (Zoc) should be made on frequencies at which the electrical length of the feed line is fairly close to odd multiples of λ/8. Frequencies that make the line length close to λ/8 and 3λ/8 are preferable for obtaining the best accuracy. For a detailed discussion on this subject, refer to *Ref 70, p 134*.

For verification that the calibration data is accurate at the antenna operating frequencies, measurements should also be made at frequencies of two successive odd multiples of λ/8 bracketing the antenna frequencies. The reason for using lengths that are multiples of λ/8 is that at these lengths the Zsc and Zoc measurements yield reactances Xsc and Xoc that are of similar magnitude and are nearly equal to Zc. Acceptable accuracy will be obtained if the ratio between Xsc and Xoc does not exceed 3:1. However, the resistance components Rsc and Roc will be very low, with typical values as shown in Table 15-1, a feed-line calibration data printout from TRANSCON, Program 6. The lower these resistance values, the lower the line attenuation. The resistances would be zero on lossless line.

Mathematically, line reactance Xsc = Zc tan ℓ°, and Xoc = Zc cot ℓ° on lossless line, where ℓ° is the electrical line length. However, the measured values will differ slightly on real lines with attenuation. Note that Xc equals Zc when ℓ° is λ/8 (45°), because tan 45° = 1. An approximate value

of Zc may be found from the expression $Zc = \sqrt{Xsc \times Xoc}$. TRANSCON (Program 6) yields the exact value of Zc because the program includes the effect of resistances Rsc and Roc resulting from line attenuation.

A short explanation at this point concerning the sign of the reactances Xsc and Xoc may be helpful. A short-circuited line shorter than λ/4 is inductive, a positive reactance. An open-circuited line shorter than λ/4 is capacitive, a negative reactance. Adding a λ/4 section to lines shorter than λ/4 reverses the sign; inductive becomes capacitive, and vice versa. Therefore, short-circuited lines of lengths greater than λ/4 but less than λ/2 are capacitive, and open-circuited lines greater than λ/4 but less than λ/2 are inductive. Adding λ/2 to any length of line will not change the sign of the reactance, because, as we learned earlier, a λ/2 line simply repeats the impedance seen at its load. Knowledge of these facts will assist in understanding the results of your measurements. Note that the values and signs of the data entered for the Xsc and Xoc reactances appearing in Table 15-1 conform with the facts just outlined. Additional discussion on the circuital effects of shorted and open-circuited lines may be found in *The ARRL Antenna Book* (*Ref 71, p 24-11*).

We'll now examine the various data appearing in Table 15-1. The values shown there are typical. They result from open- and short-circuit impedance measurements on 41 feet of RG-214 coax plus a commercially made W2DU HF balun.[1] Real transmission lines have attenuation loss, so the characteristic impedance Zc of real lines has a reactance component (negative), as well as the resistance component. This information, shown in the second and third columns in the table (Zc), is in polar form. Moving to the right, we see the electrical line length in degrees, followed by the line attenuation in dB at the measurement frequency. However, for use with the impedance-transformation programs to be described shortly, we need the data converted to line length per MHz (PHI) and attenuation per square root of MHz (A). Using this data during the impedance transformation, the program multiplies PHI by the frequency of each antenna measurement, and multiplies A by the square root of each measurement frequency, so we have the resulting TRANSCON line-length and attenuation values corrected for each antenna-measurement frequency.

When collecting data, it is customary to take several measurements, rather than a single one, so that each measurement provides an accuracy check on the others. In this way, we can spot a wild error that might otherwise go unnoticed and cause much distress later. TRANSCON has an elegant way of spotting measurement errors. If our measurements were perfect, with zero error, all values in the PHI column in Table 15-1 would be identical for all frequencies of measurement, and so would the values of A. Hence, a substantial deviation in either of these two columns indicates either a measurement error or an equipment malfunction. However, note in the table that the difference in the values appearing in those two columns is very small, indicating good agreement between the successive measurements of Zsc and Zoc, even with large differences in measurement frequency.

Values of length per MHz, PHI = 23.7°, attenuation per square root of MHz, A = 0.082 dB, and the characteristic impedance, Zc = 49, obtained using program TRANSCON (as shown in Table 15-1) are the feed-line calibration data used in transforming impedances from one end of the transmission line to the other. Programs for this purpose are described in the next section.

Sec 15.3.2 Transmission-Line Impedance-Transformation Programs

LINTRNSM.BAS, LINTRNSA.BAS, and WRITE.BAS (Programs 7, 8, and 9), compute the unknown impedance appearing at one end of a transmission line when the impedance at the opposite end is known. The programs also yield the reflection coefficient and SWR at both ends of the line. The programs have built-in compensation to correct for the changes in electrical length and attenuation with changes in the frequency of the impedance measurements. The programs compute using the basic hyperbolic transmission-line equation shown in the heading box in the program listings. With LINTRNSM (the final letter M for manual), the impedance at a given frequency appearing at one end of the line is entered one line at a time from the keyboard, and the output is immediately sent to the screen and printer. With LINTRNSA

(the final letter A for automatic), multiple impedance and frequency data are taken from a data file, and the calculated data outputs are automatically sent to the screen and printer line by line in columnar form. Both programs operate from prompts.

Before using the impedance-transformation programs, you will need to determine the electrical length, attenuation, and characteristic impedance Zc of the feed line at some frequency, f, using the TRANSCON program to calibrate the feed line, as discussed in Sec 15.3.1. The first prompt appearing in the LINTRNSM program asks if the transformation is from the input to the load. Answer **y** if yes; **n** means the transformation is from the load to the input. If the answer is **n**, the program reacts to transform the impedance in the opposite direction. The next prompt asks for PHI, the electrical line length *per MHz* (from TRANSCON). The next prompt asks for A, the attenuation *per square root of MHz*. "A" is the dB value appearing in the right-hand column of the TRANSCON calibration printout (see Table 15-1). The program corrects for the electrical length and attenuation at the frequency of each antenna measurement by multiplying PHI

```
125' W2DU 80-m Dipole, Height 40', Calibrated RG-214 + W2DU HF Balun,
RF Bridge General Radio GR-1606-A, Receiver Kenwood TS-530, Signal
Generator Boonton 250A RX Meter. 80 METERS
23.7, 0.082, 49
3.45, 5.9, 6.9565
3.475, 6.7, 8.2014
3.5, 7.7, 9.4286
3.525, 9.0, 10.9220
3.55, 10.5, 12.3944
3.575, 12.25, 13.9021
3.6, 14.8, 15.1389
3.625, 17.9, 16.0
3.65, 22, 16.5753
3.675, 26, 15.7823
3.7, 30.9, 13.5676
3.725, 35, 9.7987
3.75, 37.2, 4.8533
3.76, 37.5, 1.8617
3.77, 37.8, -0.0398
3.775, 37.6, -1.457
3.78, 37.2, -2.5661
3.785, 37.2, -3.6988
3.79, 36.9, -4.7493
3.8, 35.6, -6.7105
3.825, 32, -10.8497
3.85, 28, -13.5065
3.875, 23.95, -14.4516
3.9, 20.6, -14.359
3.925, 17.5, -13.8854
3.95, 15.1, -12.9114
3.975, 12.95, -11.9497
4.0, 11.4, -10.375
4.025, 10.15, -9.2422
4.05, 9.1, -8.2716
4.075, 8.16, -6.9939
0,0,0
```

Table 15-2. Data file format for use with program LINTRNSA.BAS. No carriage returns are permitted inside the text description. Otherwise, a carriage return exists at the end of every line.

times the measurement frequency, and A times the square root of the measurement frequency.

The next prompt asks for Zc, which is printed out in the TRANSCON calibration printout. The next prompt asks for the frequency, f, of the first antenna measurement. The next two prompts ask for the measured impedance data, R and X, in that order, after which the program runs. After the calculated data of the first line is printed out, the next prompt asks for the frequency, f, and the data of the next antenna measurement, and so on. To enter calibration data for a new transmission line, type Control-C and *RUN*. The prompts will then ask for the new calibration data.

LINTRNSA runs from a data file you have stored on a disk, which includes the feed-line calibration data and a set of related impedance data at selected frequency intervals. The data file must be configured in the format shown in Table 15-2. The file begins with a text description of the test setup. The text is limited to 255 characters. No carriage returns are allowed until the end of this text description. A carriage return within the text will halt the program. The data begins on the line following the

```
FILE --> measured.dat <--
125' W2DU 80-m Dipole, Height 40', Calibrated RG-214 + W2DU HF Balun, RF Bridge
General Radio GR-1606-A, Receiver Kenwood TS-530, Signal Generator Boonton 250A
RX Meter. 80 METERS

TRANSFORMING Zi = Ri+jXi MEASURED AT LINE INPUT TO ZL = RL+jXL AT LOAD

FEEDLINE CALIBRATION:
LINE-LENGTH IN DEGREES/MHz, PHI = 23.7
LINE ATTENUATION IN DB/SQR(MHz), A = .082
LINE IMPEDANCE, Zc = 49
```

F	Ri	Xi	RHOi	SWRi	RHO L	SWR L	RL	XL
3.450	5.90	6.957	.7889	8.47	.8171	9.933	55.22	-147.31
3.475	6.70	8.201	.7653	7.52	.7927	8.649	56.21	-136.31
3.500	7.70	9.429	.7370	6.60	.7635	7.457	57.75	-125.48
3.525	9.00	10.922	.7026	5.72	.7279	6.350	58.16	-112.97
3.550	10.50	12.394	.6655	4.98	.6896	5.443	58.40	-101.44
3.575	12.25	13.902	.6256	4.34	.6483	4.687	58.15	-90.45
3.600	14.80	15.139	.5704	3.66	.5912	3.892	59.37	-78.39
3.625	17.90	16.000	.5084	3.07	.5271	3.229	60.58	-66.58
3.650	22.00	16.575	.4345	2.54	.4505	2.640	60.62	-53.76
3.675	26.00	15.782	.3640	2.14	.3774	2.212	61.86	-42.99
3.700	30.90	13.568	.2791	1.77	.2894	1.815	62.32	-30.65
3.725	35.00	9.799	.2021	1.51	.2096	1.530	62.64	-19.44
3.750	37.20	4.853	.1478	1.35	.1533	1.362	63.60	-9.32
3.760	37.50	1.862	.1346	1.31	.1397	1.325	64.36	-3.88
3.770	37.80	-0.040	.1290	1.30	.1339	1.309	64.14	-0.33
3.775	37.60	-1.457	.1327	1.31	.1376	1.319	64.46	2.26
3.780	37.20	-2.566	.1400	1.33	.1453	1.340	64.98	4.39
3.785	37.20	-3.699	.1433	1.33	.1487	1.349	64.63	6.49
3.790	36.90	-4.749	.1511	1.36	.1567	1.372	64.70	8.54
3.800	35.60	-6.711	.1766	1.43	.1832	1.449	65.74	12.93
3.825	32.00	-10.850	.2468	1.66	.2561	1.688	67.15	24.37
3.850	28.00	-13.507	.3194	1.94	.3314	1.992	67.87	35.86
3.875	23.95	-14.452	.3889	2.27	.4036	2.353	69.44	47.23
3.900	20.60	-14.359	.4478	2.62	.4648	2.737	71.15	57.90
3.925	17.50	-13.885	.5067	3.05	.5260	3.220	72.28	69.85
3.950	15.10	-12.911	.5548	3.49	.5760	3.717	74.00	81.09
3.975	12.95	-11.950	.6020	4.02	.6251	4.334	74.42	93.31
4.000	11.40	-10.375	.6365	4.50	.6610	4.899	78.61	105.24
4.025	10.15	-9.242	.6670	5.01	.6928	5.510	80.00	116.23
4.050	9.10	-8.272	.6943	5.54	.7212	6.175	79.96	126.62
4.075	8.16	-6.994	.7195	6.13	.7475	6.920	82.50	139.11

Table 15-3. Printout of LINTRNSA program for an 80-meter dipole. Input data is that shown in Table 15-2.

text description and contains three items of data per line. The first data line contains PHI (the electrical length per MHz), the attenuation factor A (the attenuation per square root of MHz), and Zc (the characteristic impedance of the line), in that order, obtained from the calibration data printout using TRANSCON. Each item of data must be separated by a comma, with a carriage return at the end of the line after the third data item. The second line, and all subsequent lines, each contain the measurement frequency, f, the line-input resistance, R_I, and the input reactance, X_I, in that order, with the same comma and carriage return sequence as in line 1. Spaces may follow the commas for easier readability of the data entries. The last data line must contain zeros—0,0,0.

Before you run LINTRNSA, select a file name and configure the test description and data in a disk file as instructed above. The first LINTRNSA prompt asks for the file name of the data file. It then asks if the transformation is from the input to the load. Answer **y** if yes; **n** means the transformation is to be from the load to the input. The program then takes the PHI, A, and Zc calibration data from the disk file, followed by the impedance data obtained at all the frequency points measured. The program continues to run until it reaches the last data line, containing the zeros. The format of the data printout is shown in Table 15-3. The values in this table result from using the input data file illustrated in Table 15-2. Input data can be seen in the data printout of Table 15-3: descriptive text at the beginning, data line 1 in the feed-line calibration section, and data in the remaining lines in the first three columns.

The printout format of LINTRNSA is the same for LINTRNSM, except that LINTRNSM prints out one line at a time as data is entered from the keyboard. The data in Table 15-3 results from line-input impedance measurements made at frequencies listed in the column headed F. Measured input impedance data are listed in Columns Ri and Xi. RHOi, RHO L, SWRi, and SWR L are the magnitude of reflection coefficient and the SWR values at the line-input terminals and at the load (antenna), respectively. RL and XL are the resistance and reactance components of the dipole antenna impedance obtained by transforming the measured line-input impedance along the line to the antenna.

As mentioned earlier, the data shown in Tables 15-1 through 15-5, and 20-1 through 20-5, and in Figs 15-1 and 20-1 through 20-3 were obtained using the computer programs TRANSCON and LINTRNSA. The input data was obtained by measuring 40- and 80-meter antennas at W2DU through a feed line calibrated in characteristic impedance, electrical length, and attenuation using the procedure described in Sec 15.3.1. The curves in the figures represent raw, unsmoothed data obtained directly from measurements using a General Radio 1606-A RF bridge. The smoothness of these curves attests to the quality of the results that can be obtained when using precision measuring equipment.

While LINTRNSA prints out the calculated data to hard copy, WRITE.BAS (Program 9) sends the output data to the screen and to a disk file. When you run WRITE, the program prompts you for the name of the data input file, and then for the name of the file in which you wish to save the calculated data. From there on, use the same procedure as for LINTRNSA.

Sec 15.4 Programs for Hewlett-Packard Hand-Held Calculators

If you prefer to use a hand-held calculator instead of a computer for solving the transmission-line problems, two calculator program listings are included that can substitute for the TRANSCON and LINTRNSM computer programs. They are written in reverse Polish notation for Hewlett-Packard calculators. I use HP-15C and HP-34C calculators. Other models may have different register designations than those shown in Programs HP1 and HP2.

The first is Program HP1, called Transmission-Line Constants. It yields the same line-calibration data as TRANSCON (except for PHI and A, where instead, the total line length and attenuation are yielded). The second, called Transmission-Line Impedance Transformation and listed as Program HP2, yields the same data provided by LINTRNSM and LINTRNSA, plus the angles of the reflection coefficient at both the input and output of the line, and the electrical length of the line at the frequency of each impedance measurement. The listings are written for calculators with twenty

registers, ten numbered 0 through 9 and ten more that are accessed by first pressing a decimal point and then numbers 0 through 9. In the text that follows they are designated as R_0 through R_9 and $R_{.0}$ through $R_{.9}$.

Sec 15.4.1 Program Transmission-Line Constants

First review Sec 15.3.1, "Calibration of the Feed Line." Second, load the calculator memory from the program listing. Next, load storage registers R_1 through R_4 with R_{SC}, X_{SC}, R_{OC}, and X_{OC} in that order, using data from TRANSCON, Program 6 (see Table 15-1), and then run the program. Remember that one of the reactance values must be negative. At the first pause (at program line 19), the line impedance Z_C appears. To check the accuracy of the program so far, compare the reading with the Z_C value printed in the TRANSCON calibration printout. Also compare the next two readings with the line-attenuation and line-length values appearing on the same calibration printout. If there are no program errors, the results will be identical to the values in the printout to at least seven significant figures. It should be noted that the computer and the calculator each run on two completely different algorithms. Because the computer and calculator programs yield identical answers, each answer verifies the other, and the accuracy of both programs is proved.

The program stops to pause during the run to allow inspection of pertinent data along the way. To continue after a pause press R/S. At the first pause (at program line 19) the characteristic impedance Z_C appears. At the second pause (line 75), the line attenuation in dB appears. At the third pause (line 82), the line length ℓ in degrees appears. If the sign of the number is positive and less than 90°, it indicates the correct length of the line if the actual line length lies between 0° and 90°. If the sign of the number is negative, press R/S one more time to add 180° to the reading of ℓ. The resulting number will be positive, and indicates the correct length if the *actual line* length lies between 90 and 180. Note that the vital line constants that appeared at the pauses remain available because they are stored in the memory registers: Z_C in R_5, line attenuation in $R_{.2}$, line length ℓ in $R_{.3}$, and $\ell + 180°$ in $R_{.4}$.

If the actual line length is greater than 180° ($\lambda/2$), there is more work to be done. As we know, a $\lambda/2$ line repeats its load impedance, so the line lengths indicated by the calculator are ambiguous if the line is longer than $\lambda/2$. Therefore, to obtain the correct reading we must first determine the approximate length in degrees from a physical measurement of the line.

To do this, first measure the physical length of the line in feet, and then divide by the decimal value of the velocity factor—0.659 for polyethylene dielectric, 0.695 for Teflon, or 0.775 for foamed polyethylene.[2] This yields the electrical length of the line in feet, ℓ_{FEET}. At 1 MHz, 360° = 1 λ = 983.57 feet. Now find ℓf, the length in feet of 360° at the frequency, f, of the line measurement: $\ell f = 983.57/f$. To find the electrical length of the line in degrees, $\ell°$, multiply the electrical length of the line in feet by 360 and divide by ℓf: $\ell° = (360 \times \ell_{FEET})/\ell f$. These calculations yield a length close enough to the true length to learn in which quadrant the real line length lies.

If the real length lies between 0° and 90°, the correct length is indicated by $\ell°$ at program line 82. If the real line length lies between 90° and 180°, the length indicated at program line 82 will be negative, and $\ell° + 180°$ (at line 88) will yield the correct answer. If the actual length lies between 180° and 270°, subtract $\ell°$ from 180°, observing the sign of $\ell°$. If the length exceeds 270°, set up a four-quadrant diagram and draw in a radius line at $\ell°$ from the reading at program line 82. Next determine which quadrant the real line length falls into from the calculation based on the physical measurement, noting the total number of degrees required to go around the four quadrants. Once you have found the correct quadrant, add 180° as needed to $\ell°$ to place the corrected $\ell°$ value in the same quadrant as that obtained from the physical length, and then add 360 to $\ell°$ for every complete revolution the line length made around the four quadrants.

After the true electrical length $\ell°$ has been determined, divide this length by the line-measurement frequency, f, to obtain PHI, the length in degrees per MHz. Next divide the line attenuation from register $R_{.2}$ by $\sqrt{f}$ to obtain the attenuation factor A, which is the attenuation per square root of MHz. We now have the required line calibration data—PHI, A, and Z_C—to be used with the program

Transmission-Line Impedance Transformation, in the same manner as the TRANSCON calibration data is used with LINTRNSM and LINTRNSA.

Sec 15.4.2 Program Transmission-Line Impedance Transformation

Before using this calculator program, it will be helpful to become familiar with Sec 15.3.2, the part explaining the computer program LINTRNSM. Although LINTRNSM computes from a different algorithm, it has the same purpose, achieves the same results, and operates from the same line calibration and input data. The algorithm used in this calculator program first converts the known impedance at one end of the line into its complex reflection coefficient, magnitude ρ at angle θ. It then modifies ρ in accordance with line attenuation factor A, the line attenuation per square root of MHz at the impedance measurement frequency f, and it modifies angle θ in accordance with PHI, the line length in degrees per MHz. It then converts the modified values of ρ and θ to the unknown impedance Z, appearing at the opposite end of the line. Consequently, as in LINTRNSM, the line length and attenuation are corrected for changes with frequency.

On lossless lines, magnitude ρ is constant all along the line. However, because of line attenuation, ρ is smaller at the input end of the line than at the load. Therefore, when transforming a known input impedance to determine the load impedance, input ρ is divided by the decimal attenuation factor A to enlarge it. Conversely, when transforming a known load impedance to determine the input impedance, the load ρ is multiplied by A to reduce it. Hence, the selection of multiplication or division by A is determined by which direction the impedance transformation is to be made. In LINTRNSM the selection is made at the prompt. In this calculator program the selection is made in the program at line 38. When going from the input to the load, key in division at line 38; when going from the load to the input, key in multiplication. Further, the value of the reflection coefficient angle θ increases when going from the input to the load, and vice versa. So for PHI to apply the proper correction to angle for the change in line length with frequency, load +PHI into the storage register $R_{.1}$ when transforming from the input to the load, and –PHI when going from the load to the input.

After loading the program into the memory, also load the remaining line-calibration data into storage registers—the attenuation factor A into register $R_{.0}$, and line impedance Z_C into register R_0. Next, load f_{MHz}, the frequency of each impedance to be transformed, into register R_1. Don't forget to reload the new value of frequency f with each new impedance. To run the program after the value of f is loaded, key in the resistance component R of the impedance to be transformed and press ENTER. Then key in the reactance component X and execute the program. When execution is completed, the output data will appear at the various storage registers as indicated in the program listing, and as follows: unknown R at register R_8, unknown X at R_9, input SWR at $R_{.3}$, load SWR at $R_{.4}$, input ρ at R_4, input θ at R_5, load at R6, load θ at R_7, and line length in degrees $\ell°$ at frequency f at $R_{.2}$.

To determine if the program is entered correctly, try it out using data from Table 15-3. Set program line 38 to multiply, and use +PHI. Load the PHI (ρ), A, and Z_C feed-line calibration data, and the f, R_1, and X_1 data from any of the lines in the table. After you run the program, the calculator output data should agree exactly with that of the printed computer output data appearing in Table 15-3.

Sec 15.5 Determining Antenna Measurement Accuracy

In most of the measurements we make on antennas, the accuracy of the results is generally taken for granted within the known accuracy of the measuring device. In some cases, the accuracy of the measuring device is overlooked, or even ignored. However, in the area of quantitative measurement there are often procedures for checking the results to determine whether they are correct, or whether unknown errors in either the measuring device or the measurement procedure are producing answers that are incorrect, or even completely unrealistic. Without some sort of check, one may never know that the results are not what they should be. Fortunately, there is an elegant procedure for determining the accuracy of the measurements when transferring an impedance measured at the input terminals of a feed line to the terminals of the antenna.

I stated earlier, in the description of the TRANSCON program, that in measuring antenna impedance through a feed line, the electrical length, characteristic impedance, and attenuation of the feed line must be determined before measuring the antenna impedance. Accuracy of the values of these feed-line parameters *is of utmost importance.* The elegant feature for determining the accuracy of the measurements lies in the fact that any error from incorrect feed-line calibration will become evident if the antenna is measured at least two times, using a different length of feed line during each measurement. If errors exist in the calibration of the feed lines, the maximum divergence of the errors in the resulting antenna impedances will be obtained if the lengths of the two feed lines differ by λ/4. In fact, the best spread in the error determination is obtained if one line is λ/4 and the other λ/2. In other words, the maximum difference in the indicated antenna impedances because of feed-line errors will appear when you measure with these two specific lengths of feed line. The correct value of antenna impedance

Freq	R_I	X_I	ρ_I	SWR_I	ρ_L	SWR_L	R_L	X_L
3.450	5.90	6.957	0.7889	8.47	0.8171	9.933	55.22	–147.31
3.475	6.70	8.201	0.7653	7.52	0.7927	8.649	56.21	–136.31
3.500	7.70	9.429	0.7370	6.60	0.7635	7.457	57.75	–125.48
3.525	9.00	10.922	0.7026	5.72	0.7279	6.350	58.16	–112.97
3.550	10.50	12.394	0.6655	4.98	0.6896	5.443	58.40	–101.44
3.575	12.25	13.902	0.6256	4.34	0.6483	4.687	58.15	–90.45
3.600	14.80	15.139	0.5704	3.66	0.5912	3.892	59.37	–78.39
3.625	17.90	16.000	0.5084	3.07	0.5271	3.229	60.58	–66.58
3.650	22.00	16.575	0.4345	2.54	0.4505	2.640	60.62	–53.76
3.675	26.00	15.782	0.3640	2.14	0.3774	2.212	61.86	–42.99
3.700	30.90	13.568	0.2791	1.77	0.2894	1.815	62.32	–30.65
3.725	35.00	9.799	0.2021	1.51	0.2096	1.530	62.64	–19.44
3.750	37.20	4.853	0.1478	1.35	0.1533	1.362	63.60	–9.32
3.760	37.50	1.862	0.1346	1.31	0.1397	1.325	64.36	–3.88
3.770	37.80	–0.040	0.1290	1.30	0.1339	1.309	64.14	–0.33
3.775	37.60	–1.457	0.1327	1.31	0.1376	1.319	64.46	2.26
3.780	37.20	–2.566	0.1400	1.33	0.1453	1.340	64.98	4.39
3.785	37.20	– 3.699	0.1433	1.33	0.1487	1.349	64.63	6.49
3.790	36.90	–4.749	0.1511	1.36	0.1567	1.372	64.70	8.54
3.800	35.60	–6.711	0.1766	1.43	0.1832	1.449	65.74	12.93
3.825	32.00	–10.850	0.2468	1.66	0.2561	1.688	67.15	24.37
3.850	28.00	–13.507	0.3194	1.94	0.3314	1.992	67.87	35.86
3.875	23.95	–14.452	0.3889	2.27	0.4036	2.353	69.44	47.23
3.900	20.60	–14.359	0.4478	2.62	0.4648	2.737	71.15	57.90
3.925	17.50	–13.885	0.5067	3.05	0.5260	3.220	72.28	69.85
3.950	15.10	–12.911	0.5548	3.49	0.5760	3.717	74.00	81.09
3.975	12.95	–11.950	0.6020	4.02	0.6251	4.334	74.42	93.31
4.000	11.40	–10.375	0.6365	4.50	0.6610	4.899	78.61	105.24
4.025	10.15	–9.242	0.6670	5.01	0.6928	5.510	80.00	116.23
4.050	9.10	–8.272	0.6943	5.54	0.7212	6.175	79.96	126.62
4.075	8.16	–6.994	0.7195	6.13	0.7475	6.920	82.50	139.11

Feed-line calibration:
Line length in degrees/MHz, PHI = 23.7 (λ/4 at 3.797 MHz)
Line attenuation in dB/√MHz, A = 0.082 (0.160 dB at 3.797 MHz)
Line impedance, Z_C = 49 ohms

Table 15-4. Measured antenna impedance data transformed through a quarter-wave calibrated feed line.

will then lie somewhere between the two spread values of the impedances obtained with the two different feed lines.

On the other hand, remember that the true antenna impedance cannot be found with an accuracy any better than that of the impedance-measuring device. So far, I have not become aware of any noise bridges that have the accuracy required to make satisfactory measurements of the type we've been discussing. I hope that RF bridges having the required accuracy, and within an acceptable price range for the amateur, will be available in the future.

I have included an example of this procedure, shown in the data of Tables 15-4 and 15-5, and in Fig 15-1, which plots the data. The details of the equipment used during the measurements are given below. The data in Table 15-4 was obtained using a feed line that is λ/4 at 3.797 MHz; the feed line in Table 15-5 is λ/2 at 3.782 MHz, close enough in frequency to obtain the desired results.

Freq	R_I	X_I	ρ_I	SWR_I	ρ_L	SWR_L	R_L	X_L
3.450	368.00	–76.232	0.7668	7.58	0.8118	9.627	53.17	–144.35
3.475	287.00	–131.799	0.7464	6.89	0.7904	8.541	52.49	–133.09
3.500	219.50	–140.286	0.7209	6.17	0.7636	7.459	53.13	–122.72
3.525	167.50	–132.340	0.6917	5.49	0.7327	6.483	52.91	–111.52
3.550	133.00	–117.042	0.6569	4.83	0.6960	5.579	53.30	–100.75
3.575	110.00	–100.000	0.6142	4.18	0.6510	4.730	54.34	–89.95
3.600	93.50	–84.028	0.5650	3.60	0.5989	3.987	55.13	–78.96
3.625	81.20	–69.241	0.5079	3.06	0.5385	3.334	55.52	–67.64
3.650	74.00	–55.890	0.4431	2.59	0.4699	2.773	57.09	–56.92
3.675	68.50	–43.265	0.3689	2.17	0.3913	2.286	58.30	–45.61
3.700	65.90	–31.622	0.2904	1.82	0.3081	1.891	60.49	–34.51
3.725	64.00	–20.993	0.2131	1.54	0.2261	1.584	61.93	–23.47
3.750	63.00	–10.533	0.1418	1.33	0.1505	1.354	63.01	–12.03
3.770	63.50	–2.782	0.1147	1.26	0.1217	1.277	64.31	–3.30
3.775	64.00	–0.927	0.1162	1.26	0.1234	1.281	64.92	–1.18
3.778	63.90	0.265	0.1152	1.26	0.1223	1.279	64.83	0.18
3.780	64.40	1.111	0.1194	1.27	0.1268	1.290	65.37	1.15
3.785	64.30	3.170	0.1214	1.28	0.1289	1.296	65.23	3.52
3.790	65.00	5.013	0.1308	1.30	0.1389	1.323	65.90	5.66
3.795	65.50	6.983	0.1406	1.33	0.1492	1.351	66.30	7.94
3.800	66.00	8.684	0.1503	1.35	0.1596	1.380	66.66	9.94
3.825	69.00	18.562	0.2152	1.55	0.2285	1.592	68.08	21.42
3.850	73.90	28.442	0.2872	1.81	0.3050	1.878	69.93	32.94
3.875	80.00	38.452	0.3548	2.10	0.3770	2.210	71.21	44.40
3.900	90.00	47.949	0.4171	2.43	0.4432	2.592	74.16	55.90
3.925	101.00	52.994	0.4547	2.67	0.4832	2.870	77.27	63.78
3.950	117.00	64.557	0.5150	3.12	0.5474	3.419	78.66	77.74
3.975	135.50	70.692	0.5543	3.49	0.5893	3.870	80.43	88.29
4.000	162.50	73.000	0.5925	3.91	0.6300	4.406	83.73	100.43
4.025	195.00	67.826	0.6255	4.34	0.6653	4.976	86.79	112.58
4.050	230.00	50.864	0.6533	4.77	0.6950	5.557	89.44	124.28
4.075	261.00	15.828	0.6757	5.17	0.7190	6.116	93.03	135.62

Feed line calibration:
Line length in degrees/MHz, PHI = 47.599 (λ/2 at 3.782 MHz)
Line attenuation in dB/√MHz, A = 0.1334 (0.259 dB at 3.782 MHz)
Line impedance, Z_C = 50.7 ohms

Table 15-5. Measured antenna impedance data transformed through a half-wave calibrated feed line.

For Table 15-4: 125-foot W2DU 80-meter dipole, height 40 feet. Feed line: λ/4 at 3.797 MHz, calibrated RG-214 plus W2DU HF balun. RF bridge: General Radio 1606-A. Receiver: Kenwood TS-530S. Signal generator: Boonton 250A RX Meter.

For Table 15-5: 125-foot W2DU 80-meter dipole, height 40 feet. Feed Line: λ/2 at 3.782 MHz, calibrated SF-214 plus W2DU HF balun. RF bridge: General Radio 1606-A. Receiver: Kenwood TS-530S. Signal generator: Boonton 250A RX Meter.

Compare the values of antenna terminal resistance R_L and reactance X_L of Table 15-4 with those appearing in Table 15-5. The same antenna was measured with the two different line lengths specfied above, λ/4 (results shown in Table 15-4) and λ/2 (results shown in Table 15-5). You will note only small differences in the antenna impedances obtained with the different lines at each frequency. These differences result from the total error present in the measurements of the feed lines during their calibration, plus any error in the line-input measurements and in the mathematical transfer of the measured data to the antenna terminals through the LINTRNSA computer program. After examining Tables 15-4 and 15-5, and Fig 15-1, I believe you will agree that the differences between the measured impedances of my 80-meter dipole using the two different lengths of feed line are indeed small, which proves that a high degree of measurement accuracy can be obtained using the computer programs and the procedures I've presented. These measurements also disprove the myth that a λ/2 length of feed line is required to obtain an accurate measurement of antenna terminal impedance.

Sec 15.5.1 Proof of Balun Effectiveness

The close agreement in the data obtained from the two different lengths of feed line shown in Fig 15-1 proves the effectiveness of the balun in eliminating antenna current from the outer surface of the coax shield. If substantial current was flowing on the coax shield because of an ineffective balun (or with no balun at all), the outer surface would be a part of the antenna radiating system. In that case, both the impedance and the SWR of the "antenna" would be affected by the length of the feed line. Also, if that were the case, there would be no agreement in the impedance or SWR data appearing in Fig 15-1, because the impedances and SWR values measured with the two different lengths of feed line would be drastically different.

This is the reason why many see a change in SWR when they change the length of the feed line! When a balun in the system is performing effectively, the *SWR will not change* when length of the feed line is changed. This is explained in more detail in Chapter 21.

Sec 15.5.2 Comparison of Data from Different Feed-Line Lengths

There are two more points that are of interest. It is often said that a λ/2 feed line is necessary to measure the impedance or SWR of an antenna. This is not true. I have proved this to be incorrect with the evidence shown in Fig 15-1. However, the first point of interest here appears in the resistance R_I and reactance X_I columns in Table 15-5. These are the values of resistance and reactance measured at the input terminals of the feed line with the antenna connected at the other end. The values of resistance R_L and reactance X_L are those appearing at the load end of the line, which are at the input terminals of the antenna. These values indicate the impedance of the antenna.

Compare the values of R and X between the input and load columns in the rows where the frequencies are close to 3.782 MHz, say from 3.770 to 3.800 MHz. Notice how closely they agree, as they should near the frequency where the feed line is λ/2. However, the reason the resistance values at the line input are slightly lower than at the antenna is because of line attenuation, which is 0.259 dB at 3.782 MHz (attenuation A times the square root of 3.782). When a mismatched transmission line has attenuation, the value of the input resistance is always closer to the characteristic impedance Z_C than it is when the line is lossless.

Now make a similar comparison of the values of line input and load around 3.5 MHz and 4.0 MHz. The differences between the input and output impedances on the line at these frequencies are seen to be very large, indicating that the impedance repeatability of a λ/2 line is valid only at the frequency where it is precisely a half wave in length.

The second point of interest is in the R_I and X_I columns in Table 15-4. At frequencies where this feed line is close to λ/4 at 3.797 MHz, we find

impedance values that demonstrate the impedance-*inverting* action of the λ/4 line. For example, at f = 3.775, R_I = 37.6 ohms and R_L = 64.46 ohms. Because of the impedance-inverting action of the λ/4 line, these two values of resistance lie equidistant geometrically on either side of the line impedance, Z_C. The proof is that the square root of the product of these two numbers is 49.2, while Z_C was found with TRANSCON to be 49 ohms. This is one way of *determining* the characteristic impedance Z_C of the feed line if it is λ/4 long. However, since Z_C in the feed-line calibration data is 49, and since the X_I and X_L values are nearly exact negatives of each other, the quarter-wave length of the

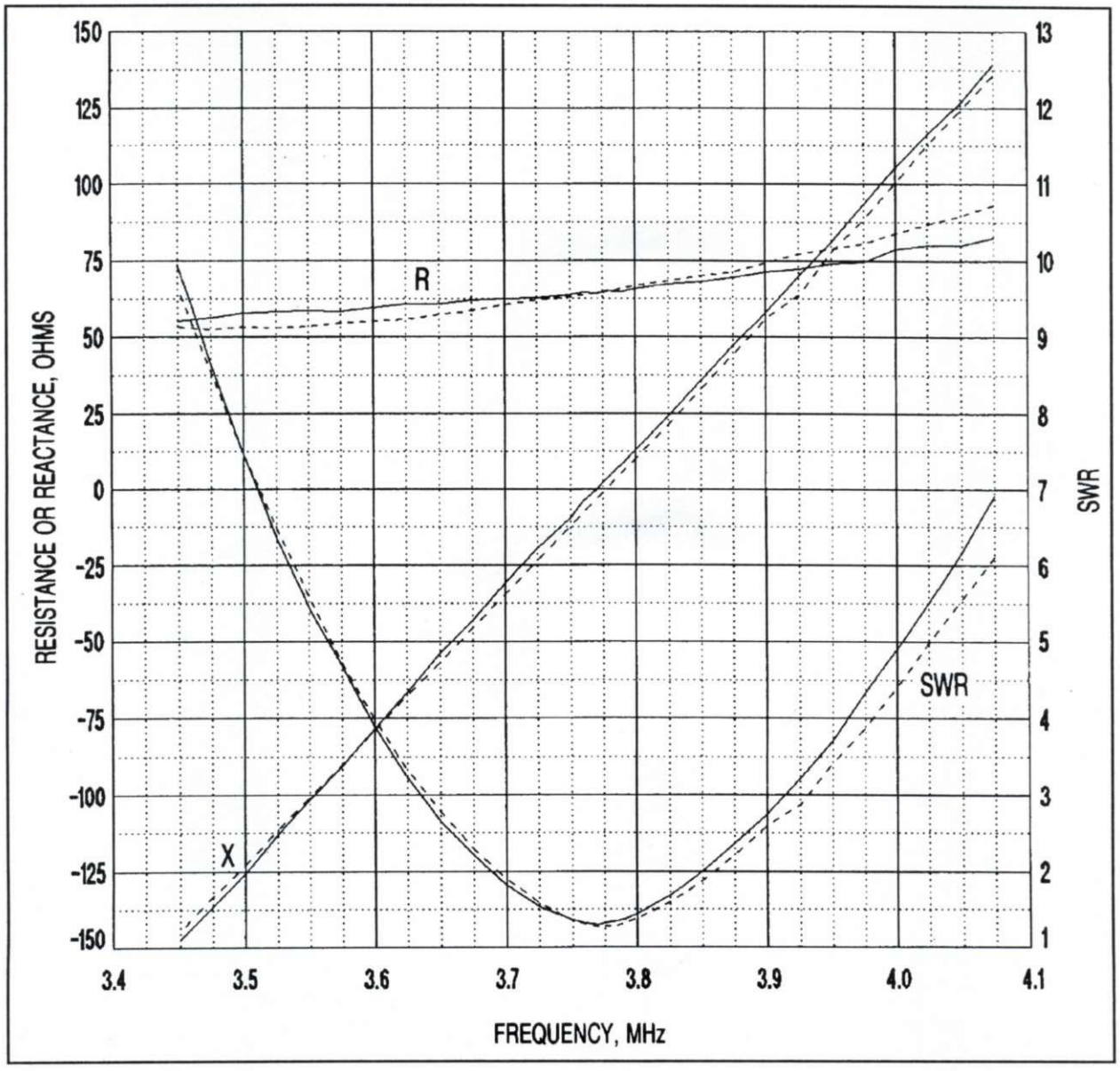

Fig 15-1. A comparison of resistance R, reactance X, and SWR of a 125-foot 80-meter dipole determined while measuring the impedances through different lengths of calibrated feed line. The solid lines indicate values obtained with a λ/4 line (data from Table 15-4), and the broken lines indicate values obtained with a λ/2 line (data from Table 15-5). The calibrated feed lines include the 10.5-inch length of RG-141 coax inside a commercially made W2DU balun. See note 2 at the end of the text in this chapter for balun description. (Computer-generated plot courtesy of Rick Maxwell, W8KHK, ex-WB4GNR)

line and the characteristic impedance Zc are both verified by the measurements.

In summary, the values of the antenna impedances appearing near the frequency at which the feed line is λ/4 are inverted from those measured at the input terminals of the feed line. This brings us to the point of recognizing that both the impedance and the SWR of an antenna can be measured with a *feed line of any length,* as long as the electrical length is known and used in the impedance-transformation equation as described in the discussion of the LINTRNSM and LINTRNSA computer programs. Finally, observe the large differences in the values of R_I and X_I obtained using a λ/4 line (Table 15-4) in contrast to those obtained using a λ/2 line (Table 15-5), with both lines terminated by the same antenna impedance.

Notes

1. The W2DU balun is a choke balun made of a 10.5-inch length of 50-ohm RG-141 coaxial line with 50 no. 73-mix ferrite beads surrounding the coax. This is a current balun, and contains no ferrite-core transformer, which would introduce serious errors in the impedance measurements. For details on the development of the W2DU balun, see Chapter 21. That chapter also explains why it is absolutely necessary to use a choke balun of the W2DU type if meaningful antenna impedance data is to be obtained. It tells why measurements on an antenna made either with no balun, or with a ferrite-core balun, yield erroneous data. For additional information concerning errors produced by ferrite-core balun transformers, see *Ref 118.*

2. The factor for foam polyethylene is between 0.75 and 0.81, depending on the amount of air in the foam material.

Program 1
BASIC Listing of T.BAS

```
0 ' ************************************************************************
10 '*                        "TEE" NETWORK CALCULATIONS                      *
15 '*                                                                        *
20 '*  CALCULATIONS EXECUTED USING STANDARD FORMULAS LISTED IN CHAPTER 14    *
25 '*                                                                        *
30 '*  BY WALTER MAXWELL          FILE NAME "T"              W2DU  1-05-89   *
40 '************************************************************************
45 '
50 PRINT "Ri =";  : INPUT RI '    INPUT RESISTANCE, Ri
60 PRINT "RL =";  : INPUT RL '    LOAD RESISTANCE, RL
70 PRINT "QL =";  : INPUT QL '    Q OF LOAD SECTION, QL
80 '
90 PRINT TAB(4)"Rp"TAB(15)"Xs in"TAB(25)"Xp in"TAB(36)"Q In"TAB(46)"Xs Load";
100 PRINT TAB(59)"Xp Load"TAB(71)"Xp Total"
110 '
120 RP = RL*(QL^2+1)      '      Rp, VIRTUAL RESISTANCE
130 XSL = RL*QL           '      Xs Load, SERIES REACTANCE, LOAD SECTION
140 XPL = RP/QL           '      Xp LOAD, PARALLEL REACTANCE, LOAD SECTION
150 QI = SQR((RP/RI)-1)   '      QI, Q OF INPUT SECTION
160 XSI = RI*QI           '      Xs In, SERIES REACTANCE, INPUT SECTION
170 XPI = RP/QI           '      Xp In, PARALLEL REACTANCE, INPUT SECTION
180 XPT = RP/(QI+QL)      '      Xp Total, TOTAL PARALLEL REACTANCE, TEE NETWORK
190 '                            QI + QL = TOTAL Q OF NETWORK
200 '
210 M$="#####.##    ####.##   ####.##   ####.##      ####.##      ####.##     ##
##.##"
220 PRINT USING M$;RP,XSI,XPI,QI,XSL,XPL,XPT
230 PRINT : RUN
```

Program 2
BASIC Listing of PI.BAS

```
0 ' ********************************************************************************
10 '*                        "PI" NETWORK CALCULATIONS                             *
15 '*                                                                              *
20 '*  CALCULATIONS EXECUTED USING STANDARD FORMULAS LISTED IN CHAPTER 14          *
25 '*                                                                              *
30 '*  BY WALTER MAXWELL          FILE NAME "PI"              W2DU  2-21-89       *
40 '********************************************************************************
45 '
50 PRINT "Ri ="; : INPUT RI '    INPUT RESISTANCE, Ri
60 PRINT "RL ="; : INPUT RL '    LOAD RESISTANCE, RL
70 PRINT "QI ="; : INPUT QI '    Q OF INPUT SECTION, QI
80 '
90 PRINT TAB(3)"Rs"TAB(12)"Xs in"TAB(23)"Xp in"TAB(35)"Q Out"TAB(47)"Xs Load";
100 PRINT TAB(61)"Xp Load"TAB(72)"Xs Total"
110 '
120 RS = RI/(QI^2+1)      '        Rs, VIRTUAL RESISTANCE
130 XPI = RI/QI           '        Xp In, PARALLEL REACTANCE, INPUT SECTION
140 XSI = RS*QI           '        Xs In, SERIES REACTANCE, INPUT SECTION
150 QL = SQR((RL/RS)-1)   '        QL, Q OF LOAD SECTION
160 XSL = RS*QL           '        Xs Load, SERIES REACTANCE, LOAD SECTION
170 XPL = RL/QL           '        Xp Load, PARALLEL REACTANCE, LOAD SECTION
180 XST = XSI + XSL       '        Xs Total, TOTAL SERIES REACTANCE, PI NETWORK
190 '                              QI + QL = TOTAL Q OF NETWORK
200 '
210 M$="####.##   ####.##   ####.##     ####.##       ####.##      ####.##
###.##
220 PRINT USING M$;RS,XSI,XPI,QL,XSL,XPL,XST
230 PRINT : RUN
```

Program 3
BASIC Listing of T-CLC.BAS

```
0 ' ************************************************************************
10 '*      T-NETWORK INPUT IMPEDANCE AND RESPONSE VS FREQUENCY              *
20 '*                                                                       *
30 '*                  SERIES C, PARALLEL L  (C-L-C)                        *
40 '*                                                                       *
50 '*                           FILENAME "T-CLC"            W2DU  1-25-89  *
60 '************************************************************************
65 '
70 PRINT "INPUT R =";: INPUT RI : PRINT "LOAD R =";: INPUT RL:
80 PRINT "INPUT Q =";  :  INPUT Q1
90 C1 = -RI*Q1  : RP = RI*(1+Q1^2) : L1 = Q1/RP : Q2 = ABS(RP/RL-1)^.5 :
100 L2 = Q2/RP : L = 1/(L1+L2) : C2 = -Q2*RL
110 L1 = 1/L1 : L2 = 1/L2
120 PRINT
130 PRINT "INPUT R =";RI"      LOAD R =";RL"     Q1 =";Q1"   Q2 = ";Q2
140 PRINT "L1 = ";L1;" OHMS   L = ";L;"  OHMS    L2 = ";L2;" OHMS
150 PRINT "C1 = ";C1;" OHMS       RP = ";RP;"        C2 = ";C2;"  OHMS"
160 PRINT : PRINT : PRINT "FREQUENCY": PRINT "FACTOR"; TAB(23);"INPUT Z";
170 PRINT TAB(48);"ATTEN, dB)" : PRINT
180 FOR F = .2 TO 5.5  STEP .2 : A = C1/F : B = F*L : C = C2/F : J = RL:
190 K = C : GOSUB 270
200 K = N+1/B : GOSUB 270
210 K = A+N : DB = ((J+50)^2+K^2)/(4*J*50) : DB = 4.34295*LOG(DB)
220 PRINT USING "#.#";F;: PRINT TAB(16)J;:IF K>=0 THEN PRINT "+J";: GOTO 240
230 PRINT "-J";
240 K = ABS (K):
250 PRINT USING "####.#";K;: PRINT TAB(48)DB
260 NEXT F
265 END
270 I = J^2+K^2 : M = J/I : N = K/I : J = M: RETURN
```

Program 4
BASIC Listing of T-LCL.BAS

```
0 ' ************************************************************************
10 '*       T-NETWORK INPUT IMPEDANCE AND RESPONSE VS FREQUENCY             *
20 '*                                                                       *
30 '*                   SERIES L, PARALLEL C  (L-C-L)                       *
40 '*                                                                       *
50 '*                           FILENAME "T-LCL"            W2DU  1-30-89   *
60 '************************************************************************
65 '
70 PRINT "INPUT R =";: INPUT RI : PRINT "LOAD R =";: INPUT RL:
80 PRINT "INPUT Q =";  :  INPUT Q1
90  L1 = RI*Q1  : RP = RI*(1+Q1^2) :  C1 = -Q1/RP : Q2 = ABS(RP/RL-1)^.5 :
100  C2 = -Q2/RP : C = 1/(C1+C2) : L2 =  Q2*RL
110  C1 = 1/C1 : C2 = 1/C2
120 PRINT
130 PRINT "INPUT R =";RI"       LOAD R =";RL"     Q1 =";Q1"   Q2 = ";Q2
140 PRINT "L1 = ";L1;" OHMS     RP = ";RP;"       L2 = ";L2;" OHMS
150 PRINT "C1 = ";C1;" OHMS    C = ";C;"  OHMS     C2 = ";C2;"  OHMS"
160 PRINT : PRINT : PRINT "FREQUENCY": PRINT "FACTOR"; TAB(23);"INPUT Z";
170 PRINT TAB(48);"ATTEN, dB)" : PRINT
180 FOR F = .2 TO 5.5  STEP .2 : A = L1*F : B = C/F : L = L2*F : J = RL:
190 K = L : GOSUB 270
200 K = N+1/B : GOSUB 270
210 K = A+N : DB = ((J+50)^2+K^2)/(4*J*50) : DB = 4.34295*LOG(DB)
220 PRINT USING "#.#";F;: PRINT TAB(16)J;:IF K>=0 THEN PRINT "+J";: GOTO 240
230 PRINT "-J";
240 K = ABS (K):
250 PRINT USING "####.#";K;: PRINT TAB(48)DB
260 NEXT F
265 END
270 I = J^2+K^2 : M = J/I : N = K/I : J = M: RETURN
```

Program 5
BASIC Listing of W5FD.BAS

```
0  ' ************************************************************************
10 ' *              Qo-BASED PI-NETWORK CALCULATIONS BY W5FD                 *
20 ' *                                                                       *
30 ' *   CALCULATING PI-NETWORK REACTANCES USING W5FD EQUATIONS BASED         *
40 ' *               ON ACTUAL CIRCUIT OPERATING Q (Qo).                     *
50 ' *                        SEE CHAPTER 14                                 *
60 ' *  FILE NAME: W5FD                              Edited by W2DU 2-21-89   *
70 ' *                                                                       *
80 ' *  SEE W5FD'S QST ARTICLE, AUGUST 1983, P23.  SEE ALSO CORRECTIONS,     *
90 ' *                 "FEEDBACK," QST, JANUARY 1984.                        *
100 '************************************************************************
110 '
120 X1=0:X2=0:XL=0:R1=0:R2=0:Q1=0:Q2=0
130 INPUT "R1";R1
140 INPUT "R2";R2
150 INPUT "Qo";QO
160 IF (R1*R2*QO)<=0 THEN PRINT "NOT A PI NETWORK" : GOTO 310
170 '  SPECIAL CASE WHERE R1 = R2
180 IF R1 = R2 THEN X1  = (2*R1)/QO : X2 = (2*R2)/QO : Q1 = QO/2
190 IF R1 = R2 THEN XL = (R1*QO)/(Q1*Q1+1) : GOTO 290
200 IF ABS((QO*QO+1)-(R1/R2))<.01 THEN PRINT "L NETWORK" : GOTO 310
210 IF ABS((QO*QO+1)-(R2/R1))<.01 THEN PRINT "L NETWORK" : GOTO 310
220 IF R1/R2>QO*QO+1 THEN PRINT "NO SOLUTION" : GOTO 310
230 IF R2/R1>QO*QO+1 THEN PRINT "NO SOLUTION" : GOTO 310
240 Q1=(R1*QO-SQR(R1*R2*QO^2-(R1-R2)^2))/(R1-R2)
250 Q2=QO-Q1
260 X1=R1/Q1
270 X2=R2/Q2
280 XL=(R1*QO)/(Q1*Q1+1)
290 PRINT TAB(3)"R1"TAB(14)"R2"TAB(23)"QO"TAB(33)"Xc1"TAB(45)"Xc2"TAB(57)"XL"
300 M$="####.#    ####.##      ##.#      ####.##     ####.##      ####.##"
310 PRINT USING M$;R1,R2,QO,X1,X2,XL
320 PRINT : RUN
```

Program 6
BASIC Listing of TRANSCON.BAS

```
  10 '   ************************************************************************
  20 '   *                          W2DU PROGRAM                                *
  30 '   *                                                                      *
  40 '   *              OBTAINING TRANSMISSION-LINE CONSTANTS                   *
  50 '   *                                                                      *
  60 '   *      FROM MEASUREMENTS OF OPEN- AND SHORT-CIRCUITED LINES            *
  70 '   *                                                                      *
  80 '   *              1. COMPLEX CHARACTERISTIC IMPEDANCE                     *
  90 '   *              2. ELECTRICAL LENGTH                                    *
 100 '   *              3. ELECTRICAL LENGTH PER MEGAHERTZ                      *
 110 '   *              4. ATTENUATION                                          *
 120 '   *              5. ATTENUATION PER SQUARE ROOT OF MEGAHERTZ              *
 130 '   *                                                                      *
 140 '   * REFERENCE: "Theory and Problems of Transmission Lines,"              *
 150 '   *              ROBERT A. CHIPMAN, PH.D.                                *
 160 '   *              SCHAUM's Outline Series, McGraw-Hill, NY.               *
 170 '   *                                                                      *
 180 '   *   BY WALTER MAXWELL     Filename:  TRANSCON          9-24-88        *
 190 '   ************************************************************************
 200 '
```

Program 6 ***Continued***

```
210 PRINT
220 A=B=C=D=0
230 PRINT "FREQUENCY ="; : INPUT F 'FREQUENCY AT WHICH MEASUREMENTS WERE TAKEN
240 PRINT "Rsc ="; : INPUT A 'LINE-INPUT RESISTANCE WITH LINE SHORT CIRCUITED
250 PRINT "Xsc ="; : INPUT B 'LINE-INPUT REACTANCE WITH LINE SHORT CIRCUITED
260 PRINT "Roc ="; : INPUT C 'LINE-INPUT RESISTANCE WITH LINE OPEN CIRCUITED
270 PRINT "Xoc ="; : INPUT D 'LINE-INPUT REACTANCE WITH LINE OPEN CIRCUITED
280 RAD = 57.2957795# 'NUMBER OF DEGREES IN ONE RADIAN
290 ZSC = SQR(A*A+B*B) 'ABSOLUTE VALUE OF SHORT-CIRCUITED LINE-INPUT IMPEDANCE
300 SCA = ATN(B/A)*RAD 'ANGLE OF SHORT-CIRCUITED LINE-INPUT IMPEDANCE
310 ZOC = SQR(C*C+D*D) 'ABSOLUTE VALUE OF OPEN-CIRCUITED LINE-INPUT IMPEDANCE
320 OCA = ATN(D/C)*RAD 'ANGLE OF OPEN-CIRCUITED LINE-INPUT IMPEDANCE
330 ZC = SQR(ZSC*ZOC) 'CHARACTERISTIC IMPEDANCE, ZC, OF MEASURED LINE
340 ANG = (SCA+OCA)/2 'ANGLE OF COMPLEX ZC OF LINE
350 ' INPUT ---> (A+JB)/(C+JD)
360 ' OUTPUT ---> R = REAL PART OF RESULT, I = IMAGINARY PART OF RESULT
370 R = (A*C+B*D)/(C*C+D*D)
380 I = (B*C-A*D)/(C*C+D*D)
390 M = SQR(R*R+I*I)
400 P = ATN(I/R)*57.29577950000001#
410 M = SQR(M)
420 P = P/2
430 IF P<0 THEN P=90+P ELSE P=-(90-P)
440 ' CONVERT POLAR TO RECTANGULAR COORDINATES
450 I = M*SIN(P/57.29577950000003#)
460 R = M*COS(P/57.29577950000002#)
470 ' DO COMPLEX NUMBER DIVISION
480 RN = 1+R
490 IN = I
500 RD = 1-R
510 ID = -I
520 R2 = (RN*RD+IN*ID)/(RD*RD+ID*ID)
530 I2 = (IN*RD-RN*ID)/(RD*RD+ID*ID)
540 'CONVERT RECTANGULAR TO POLAR COORDINATES
550 M2 = SQR(R2*R2+I2*I2)
560 LN = LOG(M2)/2
570 DB = LN*8.685889638#
580 P2 =(ATN(IN/RN)-ATN(ID/RD))*57.2957795#
590 IF RD<0 GOTO 600 ELSE GOTO 610
600 P2 = P2-180 : GOTO 610
610 P3 = P2/2
620 IF P3<0 GOTO 630 ELSE GOTO 640
630 P4 = P3 + 180 : GOTO 650
640 P4 = P3
650 P5 = P4/F
660 DBF = DB/SQR(F)
670 PRINT TAB(11)"CHARACTERISTIC"TAB(28)"ELEC.LINE"TAB(41)"LINE"TAB(49)"LENGTH";
680 PRINT TAB(59)"ATTENUATION"
690 PRINT TAB(13)"IMPEDANCE"TAB(29)"LENGTH"TAB(40)"ATTEN."TAB(49)"PER MHZ";
700 PRINT TAB(59)"PER SQR FREQ."
710 PRINT TAB(3)"FREQ."TAB(13)"ZC"TAB(20)"ANGLE"TAB(29)"DEGREES"TAB(42)"DB";
720 PRINT TAB(51)"PHI"TAB(61)"DB   A"
730 PRINT TAB(1)"------------------------------------------------------------
--------"
740 M$="###.###  ###.###  ##.###  ###.#####  ##.#####  ###.#####   ##.#####"
750 PRINT USING M$;F,ZC,ANG,P4,DB,P5,DBF
760 GOTO 210
```

Program 7
BASIC Listing of LINTRNSM.BAS

```
10 '   ************************************************************************
20 '   *                              W 2 D U                                 *
30 '   *       TRANSMISSION-LINE IMPEDANCE-TRANSFORMATION PROGRAM             *
40 '   *          Transforming Zi at line input to ZL at load                 *
50 '   *                        (or vice versa)                               *
60 '   *                                                                      *
70 '   *                           Zi - Zc TANH (A + jB)                      *
80 '   *                  ZL = Zc  ---------------------                      *
90 '   *                           Zc - Zi TANH (A + jB)                      *
100 '  *                                                                      *
110 '  *    To transform ZL to Zi answer "N" to prompt (ZL and Zi are          *
120 '  *    interchanged and (-) is changed to (+) in the equation).          *
130 '  *                                                                      *
140 '  *  WALTER MAXWELL     File Name: "LINTRNSM"  Rev. M     9-26-88         *
150 '  ************************************************************************
160 PRINT "PHI =";: INPUT P : PRINT "A =";: INPUT A : PRINT "Zc =";: INPUT Z1
170 PRINT "LINE-LENGTH CONSTANT IN DEGREES/MHz, PHI ="; P
180 LPRINT "LINE-LENGTH CONSTANT IN DEGREES/MHz, PHI ="; P
190 PRINT "LINE ATTENUATION CONSTANT IN DB/SQR(MHz), A ="; A
200 LPRINT "LINE ATTENUATION CONSTANT IN DB/SQR(MHz), A ="; A
210 PRINT "LINE IMPEDANCE, Zc ="; Z1
220 LPRINT "LINE IMPEDANCE, Zc ="; Z1
230 LPRINT
240 INPUT "TRANSFORMING FROM INPUT TO LOAD (Y,N) --> ";C$
250 IF C$="Y" OR C$="y" THEN Q=1 : C$="Y"  ELSE Q=-1 : C$="N"
260 IF C$="Y" THEN T$ = "TRANSFORMING Zi = Ri+jXi MEASURED AT LINE INPUT TO ZL =
 RL+jXL AT LOAD"
270 IF C$="N" THEN T$ = "TRANSFORMING ZL = RL+jXL AT LOAD TO Zi = Ri+jXi AT LINE
 INPUT"
280 LPRINT T$
290 LPRINT
300 P = P/57.29577910000001# : A = A/8.685889636000001#                    *
310 IF C$="N" THEN GOTO 350
320 LPRINT TAB(4)"F"TAB(12)"Ri"TAB(21)"Xi"TAB(29)"RHOi"TAB(37)"SWRi";
330 LPRINT TAB(45)"RHO L"TAB(54)"SWR L"TAB(65)"RL"TAB(74)"XL"
340 GOTO 370
350 LPRINT TAB(4)"F"TAB(12)"RL"TAB(21)"XL"TAB(28)"RHO L"TAB(36)" SWR L";
360 LPRINT TAB(46)"RHOi"TAB(54)"SWR i"TAB(65)"Ri"TAB(74)"Xi"
370 LPRINT "------------------------------------------------------------------";
380 LPRINT "-------------"
390 R1=X1=R=X=0
400 PRINT "FREQUENCY ="; : INPUT F
410 PRINT "Ri MEASURED ="; : INPUT RI
420 PRINT "Xi MEASURED ="; : INPUT XI
430 S = RI : I = XI
440 S = S/Z1 : I = I/Z1 : B = Q*P*F : A1 = Q*A*SQR(F) : T = TAN(B) : R1 = S*(1+T
^2)
450 R2 = 2*I+(I^2)*T+(S^2)*T : R1 = R1/(1+R2*T) : I2 = S^2+I^2-I*T-1
460 X1 = I+I2*T : X1 = X1/(1+R2*T) : H = (EXP(A1)-EXP(-A1))/(EXP(A1)+EXP(-A1))
470 R2 = R1*H-R1^2-X1^2-1 : R3 = 1-2*R1*H+H^2*(R1^2+X1^2) : R = (R1+H*R2)/R3
480 X = X1*(1-H^2)/R3 : R2 = R*Z1 : X2 = X*Z1 : R5 = R1*Z1 : X3 = X1*Z1
490 R4 = SQR((R-1)^2+X^2)/SQR((R+1)^2+X^2) : S3 = (1+R4)/(1-R4)
500 R6 = SQR((R1-1)^2+X1^2)/SQR((R1+1)^2+X1^2) : S4 = (1+R6)/(1-R6)
510  M$="##.### ####.##  ####.###   .####  ###.##    .####   ##.###   ###.##   #
###.##
520 IF C$="N" THEN GOTO 560
530 PRINT TAB(4)"F"TAB(12)"Ri"TAB(21)"Xi"TAB(29)"RHOi"TAB(37)"SWRi";
540 PRINT TAB(45)"RHO L"TAB(54)"SWR L"TAB(65)"RL"TAB(74)"XL"
550 GOTO 580
560 PRINT TAB(4)"F"TAB(12)"RL"TAB(21)"XL"TAB(28)"RHO L"TAB(36)" SWR L";
570 PRINT TAB(46)"RHOi"TAB(54)"SWR i"TAB(65)"Ri"TAB(74)"Xi"
580 PRINT USING M$;F,RI,XI,R6,S4,R4,S3,R2,X2
590 LPRINT USING M$;F,RI,XI,R6,S4,R4,S3,R2,X2
600 GOTO 390
```

Program 8
BASIC Listing of LINTRNSA.BAS

```
10 '   ************************************************************************
20 '   *                              W 2 D U                                 *
30 '   *       TRANSMISSION-LINE IMPEDANCE-TRANSFORMATION PROGRAM             *
40 '   *          Transforming Zi at line input to ZL at load                 *
50 '   *                        (or vice versa)                               *
60 '   *                                                                      *
70 '   *                           Zi - Zc TANH (A + jB)                      *
80 '   *                  ZL = Zc  ---------------------                      *
90 '   *                           Zc - Zi TANH (A + jB)                      *
100 '  *                                                                      *
110 '  *    To transform ZL to Zi answer "N" to prompt (ZL and Zi are          *
120 '  *    interchanged and (-) is changed to (+) in the equation).          *
130 '  *                                                                      *
140 '  *  WALTER MAXWELL      File Name: "LINTRNSA" Rev. N     9-27-88         *
150 '  ************************************************************************
160 INPUT "TYPE NAME OF DATA FILE --> ";A$
170 OPEN "I",1,A$
180 LINE INPUT #1,B$
190 FOR I = 1 TO LEN (B$)
200 MID$(B$,I,1) = CHR$(ASC(MID$(B$,I,1)) AND 127)
210 NEXT I
220 LPRINT "FILE --> ";A$;" <-- ";B$ : LPRINT
230 INPUT "TRANSFORMING FROM INPUT TO LOAD (Y,N) --> ";C$
240 IF C$="Y" OR C$="y" THEN Q=1 : C$="Y"  ELSE Q=-1 : C$="N"
250 IF C$="Y" THEN T$ = "TRANSFORMING Zi = Ri+jXi MEASURED AT LINE INPUT TO ZL =
 RL+jXL AT LOAD"
260 IF C$="N" THEN T$ = "TRANSFORMING ZL = RL+jXL AT LOAD TO Zi = Ri+jXi AT LINE
 INPUT"
270 LPRINT T$
280 INPUT #1,P,A,Z1
290 LPRINT
300 LPRINT "FEEDLINE CALIBRATION:"
310 LPRINT "LINE-LENGTH IN DEGREES/MHz, PHI ="; P
320 LPRINT "LINE ATTENUATION IN DB/SQR(MHz), A ="; A
330 LPRINT "LINE IMPEDANCE, Zc ="; Z1
340 LPRINT
350 P = P/57.29577910000001# : A = A/8.685889636000001#
360 IF C$="N" THEN GOTO 420
370 PRINT TAB(4)"F"TAB(12)"Ri"TAB(21)"Xi"TAB(29)"RHOi"TAB(37)"SWRi";
380 LPRINT TAB(4)"F"TAB(12)"Ri"TAB(21)"Xi"TAB(29)"RHOi"TAB(37)"SWRi";
390 PRINT TAB(46)"RHO L"TAB(54)"SWR L"TAB(65)"RL"TAB(74)"XL"
400 LPRINT TAB(46)"RHO L"TAB(54)"SWR L"TAB(65)"RL"TAB(74)"XL"
410 GOTO 460
420 PRINT TAB(4)"F"TAB(12)"RL"TAB(21)"XL"TAB(28)"RHO L"TAB(36)" SWR L";
430 LPRINT TAB(4)"F"TAB(12)"RL"TAB(21)"XL"TAB(28)"RHO L"TAB(36)" SWR L";
440 PRINT TAB(46)"RHOi"TAB(54)"SWR i"TAB(64)"Ri"TAB(74)"Xi"
450 LPRINT TAB(46)"RHOi"TAB(54)"SWR i"TAB(64)"Ri"TAB(74)"Xi"
460 LPRINT "------------------------------------------------------------------";
470 LPRINT "-------------"
480 R1=X1=R=X=0
490 INPUT #1,F,RI,XI
500 IF F=0 THEN END
510 S = RI : I = XI
520 S = S/Z1 : I = I/Z1 : B = Q*P*F : A1 = Q*A*SQR(F) : T = TAN(B) : R1 = S*(1+T
^2)
530 R2 = 2*I+(I^2)*T+(S^2)*T : R1 = R1/(1+R2*T) : I2 = S^2+I^2-I*T-1
540 X1 = I+I2*T : X1 = X1/(1+R2*T) : H = (EXP(A1)-EXP(-A1))/(EXP(A1)+EXP(-A1))
550 R2 = R1*H-R1^2-X1^2-1 : R3 = 1-2*R1*H+H^2*(R1^2+X1^2) : R = (R1+H*R2)/R3
560 X = X1*(1-H^2)/R3 : R2 = R*Z1 : X2 = X*Z1 : R5 = R1*Z1 : X3 = X1*Z1
570 R4 = SQR((R-1)^2+X^2)/SQR((R+1)^2+X^2) : S3 = (1+R4)/(1-R4)
580 R6 = SQR((R1-1)^2+X1^2)/SQR((R1+1)^2+X1^2) : S4 = (1+R6)/(1-R6)
590 M$="##.### ####.##  ####.###   .####  ###.##    .####   ##.###   ###.##  ###
#.##
600 PRINT USING M$;F,RI,XI,R6,S4,R4,S3,R2,X2
610 LPRINT USING M$;F,RI,XI,R6,S4,R4,S3,R2,X2
620 GOTO 480
```

Program 9
BASIC Listing of WRITE.BAS

```
10 '   ************************************************************************
20 '   *                                W 2 D U                               *
30 '   *       TRANSMISSION-LINE IMPEDANCE-TRANSFORMATION PROGRAM             *
40 '   *          Transforming Zi at line input to ZL at load                 *
50 '   *                        (or vice versa)                               *
60 '   *                                                                      *
70 '   *                          Zi - Zc TANH (A + jB)                       *
80 '   *                 ZL = Zc  ---------------------                       *
90 '   *                          Zc - Zi TANH (A + jB)                       *
100 '  *                                                                      *
110 '  *    To transform ZL to Zi answer "N" to prompt (ZL and Zi are          *
120 '  *    interchanged and (-) is changed to (+) in the equation).          *
130 '  *                                                                      *
140 '  *  WALTER MAXWELL      File Name: "WRITE"            4-28-89           *
145 '  *        To write calculated impedance data to disk file.              *
150 '  ************************************************************************
160 INPUT "TYPE NAME OF INPUT FILE ---> ";A$
165 INPUT "TYPE NAME OF OUTPUT FILE ---> ";D$
170 OPEN "I",1,A$
180 LINE INPUT #1,B$
190 FOR I = 1 TO LEN (B$)
200 MID$(B$,I,1) = CHR$(ASC(MID$(B$,I,1)) AND 127)
210 NEXT I
215 OPEN D$ FOR OUTPUT AS #2 LEN=3500
220 PRINT #2,A$
225 PRINT #2,B$
230 INPUT "TRANSFORMING FROM INPUT TO LOAD (Y,N) --> ";C$
240 IF C$="Y" OR C$="y" THEN Q=1 : C$="Y"  ELSE Q=-1 : C$="N"
250 IF C$="Y" THEN T$ = "TRANSFORMING Zi = Ri+jXi MEASURED AT LINE INPUT TO ZL =
 RL+jXL AT LOAD"
260 IF C$="N" THEN T$ = "TRANSFORMING ZL = RL+jXL AT LOAD TO Zi = Ri+jXi AT LINE
 INPUT"
265 WRITE #2,
270 PRINT T$
```

Program 9 ***Continued***

```
275 PRINT #2,T$
280 INPUT #1,P,A,Z1
290 WRITE #2,
295 PRINT #2,"FEED LINE CALIBRATION:"
310 PRINT #2,"LINE-LENGTH IN DEGREES/MHZ, PHI =",P
320 PRINT #2,"LINE ATTENUATION IN DB/SQR(MHZ), A =",A
330 PRINT #2,"LINE IMPEDANCE, ZC =",Z1
340 WRITE #2,
350 P = P/57.29577910000001# : A = A/8.685889636000001#
360 IF C$="N" THEN GOTO 420
370 PRINT TAB(4)"F"TAB(12)"Ri"TAB(21)"Xi"TAB(29)"RHOi"TAB(37)"SWRi";
375 PRINT #2,"   F       Ri        Xi     RHOi    SWRi     RHO L   SWR L     RL
      XL"
380 PRINT #2,"-------------------------------------------------------------------
-----------
390 PRINT TAB(46)"RHO L"TAB(54)"SWR L"TAB(65)"RL"TAB(74)"XL"
410 GOTO 480
420 PRINT TAB(4)"F"TAB(12)"RL"TAB(21)"XL"TAB(28)"RHO L"TAB(36)" SWR L";
440 PRINT TAB(46)"RHOi"TAB(54)"SWR i"TAB(64)"Ri"TAB(74)"Xi"
480 R1=X1=R=X=0
490 INPUT #1,F,RI,XI
500 IF F=0 THEN END
510 S = RI : I = XI
520 S = S/Z1 : I = I/Z1 : B = Q*P*F : A1 = Q*A*SQR(F) : T = TAN(B) : R1 = S*(1+T
^2)
530 R2 = 2*I+(I^2)*T+(S^2)*T : R1 = R1/(1+R2*T) : I2 = S^2+I^2-I*T-1

540 X1 = I+I2*T : X1 = X1/(1+R2*T) : H = (EXP(A1)-EXP(-A1))/(EXP(A1)+EXP(-A1))
550 R2 = R1*H-R1^2-X1^2-1 : R3 = 1-2*R1*H+H^2*(R1^2+X1^2) : R = (R1+H*R2)/R3
560 X = X1*(1-H^2)/R3 : R2 = R*Z1 : X2 = X*Z1 : R5 = R1*Z1 : X3 = X1*Z1
570 R4 = SQR((R-1)^2+X^2)/SQR((R+1)^2+X^2) : S3 = (1+R4)/(1-R4)
580 R6 = SQR((R1-1)^2+X1^2)/SQR((R1+1)^2+X1^2) : S4 = (1+R6)/(1-R6)
590 M$="##.### ####.##  ####.###   .####  ###.##    .####   ##.###   ###.##   ##
##.##"
600 PRINT USING M$;F,RI,XI,R6,S4,R4,S3,R2,X2
605 PRINT #2,USING M$;F,RI,XI,R6,S4,R4,S3,R2,X2
620 GOTO 480
```

Program HP1

Program Listing for TRANSMISSION-LINE CONSTANTS

This program is for hand-held calculators using reverse Polish notation. The program yields transmission constants line length ℓ° in electrical degrees, attenuation in dB, and characteristic impedance Z_C from line-input impedance measurements with the line terminated with impedances Z_{SC} and Z_{OC}. To find the attenuation factor A for use with the calculator impedance transformation program (Program HP2), divide by $\sqrt{f(MHz)}$, where f is the frequency of the line-input impedance measurements of Z_{SC} and Z_{OC}. Consult the text on how to find PHI from ℓ°. *(W2DU, 1-1-79)*

Line	*Key Entry*	*Comments*
1	H Label A	
2	RCL 2	
3	RCL 1	
4	g → P	
5	STO 1	|Z| of Z_{SC}
6	x ↔ y	
7	STO 2	Angle of Z_{SC}
8	RCL 4	
9	RCL 3	
10	g → P	
11	STO 3	|Z| of Z_{OC}
12	x ↔ y	
13	STO 4	Angle of Z_{OC}
14	RCL 1	
15	RCL 3	
16	×	
17	f → $\sqrt{\ }$	
18	STO 5	|Z_{OC}|
19	R/S	
20	RCL 2	
21	RCL 4	
22	+	
23	2	
24	÷	
25	STO 6	Angle of Z_C
26	RCL 1	
27	RCL 3	
28	÷	
29	f → $\sqrt{\ }$	
30	STO 0	
31	RCL 2	
32	RCL 4	
33	–	
34	2	
35	÷	

Store measured data into registers:

Data	*Register*
R_S	R_1
X_{SC}	R_2
R_{OC}	R_3
X_{OC}	R_4

Run program

Algorithm:

$$\tanh(\alpha + j)\ell^\circ = \sqrt{\frac{Z_{SC}}{Z_{OC}}}$$

Read registers at end of program:

R_1	|Z_{SC}|
R_2	Angle of Z_{SC}
R_3	|Z_{OC}|
R_4	Angle of Z_{OC}
R_5	|Z_C|
R_6	Angle of Z_C
$R_{.2}$	α in dB
$R_{.3}$	ℓ°
$R_{.4}$	ℓ° + 180°

ℓ° corrections for line lengths:

Actual Line Length	From Calculator
0° to 90°	ℓ° as is ($R_{.3}$)
90° to 180°	ℓ° + 180° ($R_{.4}$)

36	RCL 0	180° to 270° $180° - \ell^{\circ}$
37	f → R	
38	STO 0	
39	x ↔ y	
40	STO 7	
41	x ↔ y	
42	1	
43	x ↔ y	
44	−	
45	STO 8	
46	RCL 7	
47	RCL 0	
48	1	
49	+	
50	g → P	
51	STO 9	
52	x ↔ y	
53	STO .0	
54	RCL 7	
55	CHS	
56	RCL 8	
57	g → P	
58	STO 0	
59	x ↔ y	
60	STO .1	
61	RCL 9	
62	RCL 0	
63	÷	
64	f → LN	
65	2	
66	÷	α in nepers
67	1	
68	g → e^x	
69	f → LOG	
70	2	
71	0	
72	×	
73	×	
74	STO .2	α in dB (line attenuation)
75	R/S	
76	RCL .0	
77	RCL .1	
78	−	
79	2	
80	÷	
81	STO .3	ℓ° (line length, see text)
82	R/S	
83	1	
84	8	
85	0	
86	+	
87	STO .4	ℓ° + 180° (See text)
88	H Return	

Program HP2
Program Listing for TRANSMISSION-LINE IMPEDANCE TRANSFORMATION

This program is for hand-held calculators using reverse Polish notation. The program transfers a *known* impedance at one end of a line to the *unknown* impedance at the other end. *(W2DU, 7-20-80)*

Line	Key Entry	Comments
1	H Label A	
2	RCL 0	
3	÷	
4	STO 3	x (normalized)
5	x ↔ y	
6	RCL 0	
7	÷	
8	STO 2	r (normalized)
9	1	
10	+	
11	g → P	
12	STO 6	
13	x ↔ y	
14	STO 7	
15	RCL 3	
16	RCL 2	
17	1	
18	–	
19	g → P	
20	RCL 6	
21	÷	
22	STO 4	ρ At Known End
23	x ↔ y	
24	RCL 7	
25	–	
26	STO 5	θ At Known End
27	RCL 1	
28	f → $\sqrt{}$	
29	RCL .0	
30	×	
31	CHS	
32	1	
33	0	
34	÷	
35	g → 10^x	
36	RCL 4	
37	x ↔ y	
38	÷ or ×	
	(Use ÷ if going from input to load, × if going from load to input.)	
39	STO 6	ρ At Unknown End
40	RCL .1	
41	RCL 1	
42	×	

Store line calibration and Z measurement frequency data into registers:

Register	Data
R_0	Z_C characteristic impedance
$R_{.0}$	A attenuation factor (see p 13-14)
R_1	f_{MHz} (for each measurement frequency)
$R_{.1}$	± PHI

Use +PHI if going from input to load,
–PHI if going from load to input.

To run:

1) Key in R of R + *j*X
2) Press ENTER
3) Key in X of R + *j*X
4) Press Run

Algorithm:

Step 1) Z = R + *j*X to ρ∠θ
Step 2) $\rho\angle\theta_{IN}$ to $\rho\angle\theta_{LOAD}$ (or visa versa)
Step 3) ρ∠θ to Z = R + *j*X

Read registers at end of program:

Register	Data
R_4	ρ at known end
R_5	θ at known end
R_6	ρ at unknown end
R_7	θ at unknown end
R_8	Resistance at unknown end
R_9	Reactance at unknown end
$R_{.2}$	Line ℓ° at frequency f of measurement
$R_{.3}$	SWR at input
$R_{.4}$	SWR at load

43	STO .2	
44	2	
45	×	
46	RCL 5	
47	+	
48	STO 7	θ At Unknown End
49	RCL 6	
50	g → x^2	
51	STO 2	
52	RCL 7	
53	f cos	
54	RCL 6	
55	×	
56	2	
57	×	
58	−	
59	1	
60	+	
61	STO 3	
62	1	
63	RCL 2	
64	−	
65	RCL 3	
66	+	
67	RCL 0	
68	×	
69	STO 8	Resistance Answer
70	RCL 7	
71	f sin	
72	RCL 6	
73	×	
74	2	
75	×	
76	RCL 3	
77	+	
78	RCL 0	
79	×	
80	STO 9	Reactance Answer
81	RCL 4	
82	1	
83	+	
84	RCL 4	
85	1	
86	x ↔ y	
87	−	
88	÷	
89	STO .3	SWR at Input
90	RCL 6	
91	1	
92	+	
93	RCL 6	
94	1	
95	x ↔ y	
96	−	
97	÷	
98	STO .4	SWR at Load
99	H Return	

Chapter 16

Reflections in Attenuators, Filters, and Matching Networks

(Adapted from "Technical Correspondence," QST, November 1981)

Sec 16.1 Introduction

Network-type filters and attenuators have one thing in common: They both attenuate energy. However, this is just about the extent of their similarity; they operate on quite different principles and should not be confused with one another. Network-type *filters* attenuate energy at selected frequencies—for example, the harmonic and sub-harmonic energy appearing at the output of RF power amplifiers. Conversely, network-type *attenuators* usually comprise *resistive* elements to absorb and dissipate energy equally at *all* frequencies. See Fig 16-1 as an example of a network-type attenuator. The elements are well matched to the system impedance so as not to reflect any power back to the source.

Filters, on the other hand, comprise low-loss *reactive* elements. One such circuit is shown in Fig 16-2. Low-loss elements are used so as to absorb or dissipate a minimum of power, thereby conserving power at the frequencies to be passed through the filter. (An ideal filter would have lossless elements, and thus dissipate no power.) The reactive elements in the filter are selected and arranged so that the filter is well matched for minimum reflection at the frequencies to be passed, but mismatched for maximum reflection at all frequencies to be rejected. The rejection is accomplished by selectively reflecting back to the source all the power appearing at the unwanted frequencies, where, on return, the reflected power causes the source to be mismatched to the line at only the unwanted frequencies, and therefore fails to deliver power at those frequencies. Thus, attenuators attenuate *all* frequencies by *absorption* and *dissipation*, while filters attenuate only the *unwanted* frequencies by *selective reflection.*

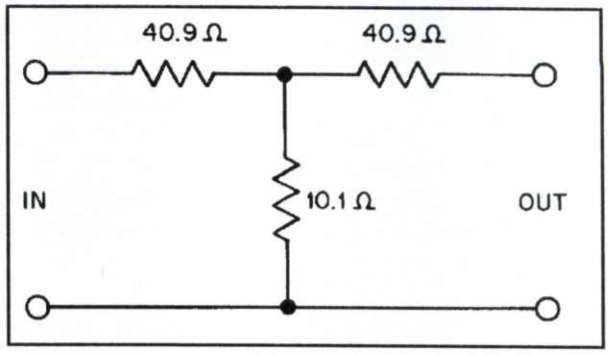

Fig 16-1. A network type of attenuator. The values indicated provide 20 dB of attenuation in a 50-ohm system. When terminated in 50 ohms, the input impedance of the network is 50 + *j*0, and the output energy is attenuated by 20 dB from that at the input, no matter what the input frequency, assuming the resistors have no reactance. Networks such as this may also be designed for unequal input and output impedances.

The primary purpose of a matching network is to couple circuits that have different impedance levels, such as a source of power and its load, so that the source will make its maximum power available to the load at the fundamental frequency. Low-loss reactive elements, as in the filter, are used to perform the matching function. See Figs 16-2 and 16-3. The distributed elements of transmission-line transformers and stub configurations may be used instead of lumped reactances, but the principles are the same.

The elements of the matching network are chosen so that it produces a mismatch at the fundamental frequency that is *complementary* to the mismatch that would arise if the source and the load were connected together directly without the matching network. Complementary mismatches produce complementary reflections, each mismatch producing a reflected voltage (and current) that is equal in magnitude, but of opposite phase, to that produced by the other.

Frequency	Input Z (ohms)	Frequency	Input Z (ohms)
0.4	1.8 – *j*1589.6	3.0	882.3 + *j*1811.7
0.6	8.4 – *j*814.4	3.2	996.5 + *j*1911.0
0.8	23.6 – *j*346.4	3.4	1111.9 + *j*1999.6
1.0	50.0 + *j*0.0	3.6	1227.6 + *j*2078.1
1.2	89.1 + *j*284.4	3.8	1343.1 + *j*2147.3
1.4	140.9 + *j*530.8	4.0	1457.6 + *j*2207.8
1.6	204.9 + *j*750.4	4.2	1570.8 + *j*2260.2
1.8	279.8 + *j*948.8	4.4	1682.1 + *j*2305.1
2.0	364.3 + *j*1129.1	4.6	1791.2 + *j*2343.1
2.2	456.9 + *j*1293.3	4.8	1897.9 + *j*2374.8
2.4	556.3 + *j*1442.7	5.0	2001.9 + *j*2400.8
2.6	661.2 + *j*1578.3	5.2	2103.0 + *j*2421.4
2.8	770.2 + *j*1701.1	5.4	2201.2 + *j*2437.2

Table 16-1. Frequency versus network input impedance for the C-L-C circuit of Fig 16-2. A fixed load of 5000 ohms and lossless circuit elements are assumed for all frequencies. The frequency is normalized to 1.0 for the fundamental.

When the matching network is inserted between the source and load of different impedances, complementary mismatches are produced, one between the source and the network, and its complement between the network and the load. The reflected voltages (and currents) of equal magnitude and opposite phase resulting from the mismatches combine in the network to produce a resultant voltage (and current) of zero phase relative to the voltage (and current) of the source wave. Thus, the resultants of the reflected voltages and currents add in phase to those of the source wave. These in-phase additions to the source wave have the effect of re-reflecting the reflected voltages and currents into the forward direction, resulting in the cancellation of all rearward-traveling waves. Thus, a 1:1 conjugate match is formed, and because the source now has its desired or optimum impedance for a load, it makes its maximum power available at the actual load of a different impedance.

Keep in mind that the "load" now seen by the source is the combination of the actual Zc-mismatched load and the matching network. Although it may seem difficult to appreciate that an additional mismatch is deliberately introduced to obtain a match (such as with a stub on a line), the mismatches described above must exist as Zc mismatches to produce the complementary reflections that are required to develop the conjugate match. However, no power is lost from the reflections, and, except for the small I^2R and E^2/R losses in the low-loss elements of the matching network, the maximum available source power is transferred to the Zc-mismatched, but conjugate-matched load. Details of the wave actions in developing the conjugate match are presented in Chapter 4 and further explained in Chapter 23.

As stated earlier, the principles of network and stub matching are identical. To emphasize the general concept that all conjugate matching is achieved by canceling one mismatch reflection with another, a few words concerning stub matching will be helpful. In stub matching, the stub introduces the deliberate mismatch, and thereby produces the complementary reflections that accomplish the conjugate match on the line. The stub is of the correct length and impedance Zc to produce amplitudes of reflected voltage and current equal to those reflected by the load mismatch. The stub is placed on the line where the voltages (and currents) reflected by the load mismatch are of opposite phase to those produced by the stub. The line is thus matched (no reflections) between the stub point and the source. By comparison, the network generates the same complementary-mismatch reflections as the stub, and simultaneously adjusts the effective electrical distance from the mismatched load so that its complementary reflections are placed at the same electrical position on the line as a correctly placed stub.

Sec 16.2 Harmonic Rejection in Matching Networks

Let us now consider the harmonic rejection capability of matching networks. The key to the rejection

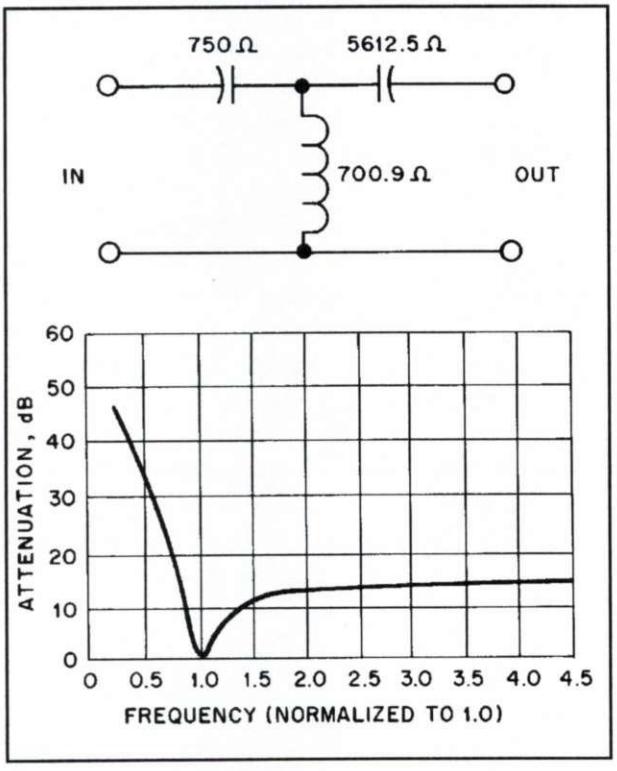

Fig 16-2—A T-network matching circuit of L and C elements, and a curve showing its attenuation versus frequency. The component reactances shown here provide a match for a 5000-ohm load to a 50-ohm source, with an unloaded input-section Q of 15. The attenuation curve is calculated for a 5000-ohm load of pure resistance at all frequencies, but the impedance of loads such as antenna systems are seldom if ever constant across such a frequency range. The input impedance versus frequency for the fixed 5000-ohm load is presented in Table 16-1. By changing the Q and component reactances in the circuit, many other combinations will provide the same 5000- to 50-ohm match, but the attenuation curve will assume a different shape.

is mismatch. As we know, the percentage of power that the source makes available to a load is proportional to the quality of the impedance match to the load. Conversely, and crucial to harmonic rejection, the amount of power the source *withholds*, relative to its maximum available power at a given frequency (such as a harmonic), is proportional to the impedance mismatch at that frequency.

Single-frequency matching networks are designed to provide *only one* complementary mismatch, compensating for the load mismatch appearing only at the fundamental frequency. Thus, the beauty of the network is that it inherently fails to provide complementary mismatches to compensate for the mismatches presented by the load at harmonic and other frequencies. Consequently, as in the filters described earlier, the source remains mismatched at the undesired sub-harmonic and/or harmonic frequencies, and delivers reduced power at these frequencies in the amount that the degree of match (or mismatch) dictates. Tables 16-1 and 16-2 indicate this effect by showing the input impedances for the networks of Figs 16-2 and 16-3, respectively, for a range of frequencies and a fixed load. Only at the fundamental frequency does a match occur.

The most common amateur use of a matching network is the antenna tuner. The tuner network increases operating flexibility by providing the conjugate match to compensate for the mismatch between the feed line and the antenna that arises when a coax-fed antenna is operated off resonance, or when the antenna is fed with open-wire line. In these cases, the load terminating the matching network is the impedance appearing at the input terminals of the feed line. As we know, when the antenna impedance is mismatched to the Zc impedance of the feed line, reflections from the mismatch cause the input impedance of the line to change from its resistive characteristic value Zc (usually 50 or 75 ohms) to some new complex value determined by the antenna impedance and the length of the feed line. (See Chapters 7, 9, and 12.) It is this new line-input impedance (which changes as we change frequency) that we match to the source with the antenna tuner at only the fundamental frequency.

Obviously, the antenna presents a drastically different impedance to the feed line at harmonic frequencies compared with that at its fundamental frequency, and consequently the input impedances to the feed line are vastly different at the harmonic frequencies than what the matching network sees as a load at the fundamental frequency. These changes in load impedance with frequency, as well as the effects described earlier in the paragraph on filter principles, create reflections from the uncompensated mismatches at the harmonic frequencies that are responsible for the harmonic rejection of the matching network. Thus, the mismatch between the

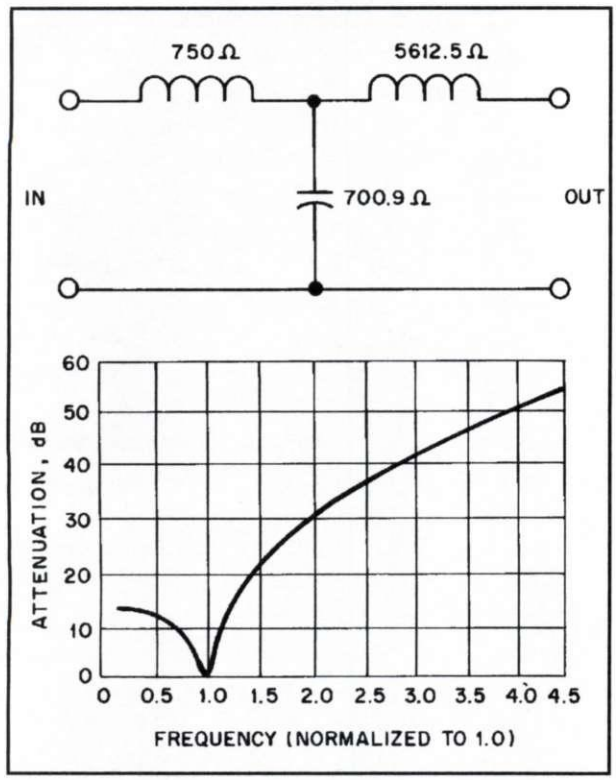

Fig 16-3—Another T-network matching circuit of L and C elements and its attenuation curve. The circuit is identical to that of Fig 16-2 except that inductances have replaced capacitances and vice versa; the reactance values remain the same for similar locations in the circuit. This network, too, will match a 5000-ohm load to a 50-ohm source. The input impedance versus frequency for a fixed 5000-ohm load is given in Table 16-2.

feed line and the antenna terminals also rejects harmonic energy, as well as the antenna tuner.

There are many arrangements and configurations of reactance elements that can be used equally well to generate a complementary mismatch for obtaining a conjugate match. However, there are vast differences among these various configurations concerning the severity of their non-complementary mismatches that are required to reject harmonics and other unwanted frequencies. Figs 16-2 and 16-3 illustrate this simply. Note that both circuits are T networks having identical reactance values in similar positions of the circuits; only the type of reactance differs, capacitive versus inductive. Both circuits will match a 5000-ohm load to a 50-ohm line at the fundamental frequency. The C-L-C circuit of Fig 16-2 is commonly called a high-pass configuration, and the L-C-L circuit of Fig 16-3 a low-pass configuration. Both circuits, however, attenuate frequencies both lower and higher than the fundamental, as shown by the frequency-response curves. Of course, as frequencies of the harmonic energy are higher than the fundamental, a matching network of low-pass configuration would be the most desirable, a circuit with series inductance and shunt capacitance arms. For a more detailed explanation of the role played by reflections in the technique of impedance matching and harmonic rejection, see Chapters 3, 4, and 23.

As a parting thought concerning the operational adjustment of antenna tuners, the amateur should be

Frequency	Input Z (ohms)	Frequency	Input Z (ohms)
0.4	608.1 – *j*1512.1	3.0	0.9 + *j*2013.4
0.6	228.7 – *j*818.7	3.2	0.7 + *j*2178.5
0.8	100.8 – *j*349.0	3.4	0.6 + *j*2341.8
1.0	50.0 + *j*0.0	3.6	0.4 + *j*2503.5
1.2	27.1 + *j*282.5	3.8	0.4 + *j*2664.0
1.4	15.8 + *j*526.1	4.0	0.3 + *j*2823.5
1.6	9.8 + *j*745.2	4.2	0.2 + *j*2982.0
1.8	6.4 + *j*948.3	4.4	0.2 + *j*3139.7
2.0	4.3 + *j*1140.2	4.6	0.2 + *j*3296.8
2.2	3.0 + *j*1324.2	4.8	0.1 + *j*3453.2
2.4	2.1 + *j*1502.3	5.0	0.1 + *j*3609.1
2.6	1.6 + *j*1675.9	5.2	0.1 + *j*3764.6
2.8	1.2 + *j*1846.0	5.4	0.1 + *j*3919.7

Table 16-2. Frequency versus network input impedance for the L-C-L circuit of Fig 16-3. A fixed load of 5000 ohms and lossless circuit elements are assumed for all frequencies. The frequency is normalized to 1.0 for the fundamental.

aware of the trade-off between optimum efficiency (minimum power lost in the network) and optimum harmonic rejection. There are usually several settings of the network that will yield a 50-ohm impedance at the input of the tuner. As far as the transmitter is concerned, all such settings are equivalent—the same as if you were feeding a 50-ohm dummy load. However, the 50-ohm input obtained with the lowest loaded Q has the optimum efficiency. At the other extreme, the 50-ohm input obtained with the higher loaded Q values offers increased rejection of unwanted frequencies, but with some increase in insertion loss. In either case, the loss is usually small, and is well worth the improved operation flexibility afforded by the tuner. In the circuits of Figs 16-2 and 16-3, higher Q values are obtained with greater reactances in the series-input arms (lower input capacitance in Fig 16-2, higher input inductance in Fig 16-3). This subject is also touched on in the final paragraph of Sec 14.2.

In conclusion, I would further point out that antenna tuner settings that yield a 50-ohm impedance at the input to the tuner do not mean the SWR is 1:1 on the feed line between the tuner and the antenna. It means only that a 1:1 SWR exists on a 50-ohm line preceding the tuner—i.e., between the tuner and the transmitter. You have not "brought down the SWR" on the antenna feed line by adjusting the matching network; you simply have a 50-ohm impedance looking into the input of the tuner.

The frequency response and input impedance data presented in this chapter for the two T networks were obtained by computer using the BASIC language. Two different computer programs were used, one for the C-L-C network of Fig 16-2, and one for the L-C-L network of Fig 16-3. Listings for these two computer programs are presented in Chapter 15, along with an explanation of how to use them for determining the frequency response and input impedance of these two network configurations in general applications.

Chapter 17

How Does a Transmatch Work?

(Adapted from "Technical Correspondence," QST, March 1985)

Sec 17.1 Introduction

In the "Technical Correspondence" column of *QST* for October 1984, Clifford Ward, WA5LVG, tells us there is confusion concerning the use of a Transmatch (*Ref 128*). Comments from amateurs I have encountered during my seminars on this subject confirm that he is correct. Unfortunately, his attempt to dispel the confusion fails because most of the remarks that follow his initial statement are simply not true. He tells us that with a transmatch:

(1) Only feed-line tuning is accomplished. (This is not true; the antenna is also tuned by the conjugate match that results from the correct transmatch adjustment.)

(2) Antenna system performance is increased only when the transmatch is located at the antenna feed point. (Not true.)

(3) We are providing a proper load only for the transmitter and not improving the antenna system efficiency. (Also not true.)

Many amateurs avoid using a transmatch because they misunderstand these points. Let us examine some aspects of impedance matching to understand why Ward's statements are incorrect, and learn the true advantage of using a transmatch.

It is appropriate to quote here two well-known network theorems that are pertinent to the subject of impedance matching. They are the Maximum Power Transfer Theorem and the Conjugate Matching Theorem. The Maximum Power Transfer Theorem states: "The maximum power will be absorbed by one network from another joined to it at two terminals if the impedances looking into the two networks at the junction are conjugates of each other." (*From Ref 17, p 49, and Ref 69, p 403.*) The Conjugate-Matching Theorem states: "If a group of four-terminal networks containing only pure reactances (or lossless lines) are arranged in tandem to connect a generator to its load, then if at any junction there is a conjugate match of impedances, there will be a conjugate match of impedances at every other junction in the system." (*From Ref 17, p 243 and Ref 69, p 407.*)

The same principles of transmission-line impedance matching apply, and the same wave actions and reflections occur, whether a match is achieved with a tuned stub or with a network of inductors and capacitors (see Chapter 4). In either case, the impedance match achieved is a conjugate match. Therefore, let us discuss the Conjugate-Matching Theorem as a basis for an evaluation of Ward's statements.

Sec 17.2 The Conjugate Match

The term *conjugate match* identifies a condition where the impedances on opposite sides of a junction have identical resistive components, and reactive components, if any, that are equal in magnitude but opposite in sign. For example, a conjugate match exists when a source impedance of $50 + j10$ ohms feeds a load impedance of $50 - j10$ ohms. When a conjugate match is accomplished at any of the junctions in a system, *all* reactances in the system are canceled, *including any reactance in the load.* This reactance cancellation establishes resonance in the entire system, and the generator delivers its maximum available power to the load. This means that *a non-resonant antenna* as the load is ***tuned*** *to resonance by the conjugate match.* Because the Conjugate Matching Theorem states that maximum power transfer occurs equally well with the matching operation performed at *any* junction in the system, it is clear that Ward's statements violate the theorem and are therefore incorrect.

I can illustrate the principles of the Conjugate Matching Theorem with an example. Imagine an ideal system in which a transmatch and transmission line that feed an antenna are both lossless. (It

is customary to assume lossless lines and components while discussing the principles, and then treat the effects of attenuation and loss later.) We'll assume that a Z_0 mismatch exists at the junction of the feed line and the terminals of a non-resonant antenna, meaning that the line impedance, Z_C, does not match the terminal impedance $R + jX$ of the antenna. (Z_C and Z_0 are the terms used to represent the characteristic impedance of a transmission line.) We'll also assume that the RF power source, or generator, is adjusted to deliver its maximum available power into the line impedance Z_C.

Case 1: Mismatched Antenna, No Matching

First we'll consider the case where the generator is connected directly to the input terminals of the mismatched line with no transmatch, and the feed line is also connected directly to the antenna terminals. In this case, there are two mismatches at the junction of the antenna and the feed line—both a Z_0 mismatch and a conjugate mismatch. The Z_0 mismatch causes a reflection loss that is transferred back along the line to the generator, presenting the same magnitude of Z_0 mismatch at the line input (*Ref 19, p 5*). This mismatch between the generator and input of the feed line causes the generator to deliver less than its maximum available power by an amount equal to the reflection loss. Considering that we've specified lossless line in this ideal case, there is no power lost to dissipation in the line—only a reduction in power delivered by the generator (*Refs 19 and 70, p 204*). (A point to remember: All power delivered to a lossless line is absorbed in the load, regardless of the degree of load mismatch. See Fig 6-1 and Eq 6-2.) Hence, the non-resonant antenna absorbs 100% of the reduced power delivered by the generator. I will now show why the non-resonant antenna absorbs the delivered power with 100% efficiency.

Case 2: Mismatched Antenna, Matched at Antenna Feed Point

Now we'll consider the case where a matching network placed at the antenna feed point is adjusted to obtain a conjugate match. By the Conjugate-Matching Theorem, an antenna input impedance of $R + jX$ is matched by a transmatch output impedance of $R - jX$. Thus, the initially reactive non-resonant antenna is now tuned to resonance, because the $+jX$ reactance of the antenna is canceled by the equal, but opposite $-jX$ reactance at the output of the transmatch. The input impedance of the correctly tuned transmatch is Z_0, which now provides the transmission line with a Z_0 match at the generator output: The reflection loss that previously was referred along the line to the generator is now zero; hence the generator sees both a conjugate match and a Z_0 match at the line input, and now delivers its maximum available power into the line. As before, the antenna absorbs 100% of the power delivered by the generator. However, the antenna current now flowing through the *resonant-antenna* resistance has increased to a maximum, in proportion to the square root of the increase in power delivered by the generator.

Case 3: Mismatched Antenna, Matched at Line Input

What happens when the matching network (antenna tuner or transmatch) is placed at the input of the feed line, with the feed-line output connected directly to the mismatched antenna terminals? If the length of the feed line is a multiple of an electrical half wavelength, the antenna impedance, $R + jX$, is repeated at the input of the line (we're still discussing lossless lines, remember?). The impedance looking back into the transmatch is $R - jX$ as before, and the transmatch needs no readjustment to again provide a conjugate match.

However, a line of any length other than a half wave (or multiple thereof) transforms the antenna input impedance to a new value, $R' + jX'$, at the input terminals of the line. Therefore, the transmatch must now be readjusted to again obtain a conjugate match. The result of readjustment: Because the antenna impedance is $R + jX$, the impedance looking back into the output terminals of the feed line is now $R - jX$. However, where the $+jX$ antenna reactance was previously canceled by the $-jX$ reactance at the output of the transmatch, the antenna reactance is now canceled by the $-jX$ reactance at the output of the feed line. Thus, the antenna is again tuned to resonance. The output impedance of the transmatch is now $R' - jX'$, the conjugate of the new line-input impedance. The input impedance of the transmatch is again Z_0, the generator delivers the same maximum available power into the transmatch as it previously deliv-

ered into the matched line with the transmatch at the antenna feed point, and the transmatch delivers this power into the line. Inasmuch as the line and transmatch have no losses (ideal case yet, remember?), the antenna still absorbs 100% of the power delivered by the generator. Hence, the same antenna current flows as when the transmatch was placed at the antenna feed point.

How can this be? Even though we have a conjugate match at the junction of the feed line and the antenna, don't we again have a Z_0 mismatch at that junction, producing the same reflection loss as without the transmatch? Indeed we do, so to obtain a better understanding of how the conjugate match transfers the maximum available power from the generator to the load, despite a Z_0 mismatch in the path, we must examine the wave actions and reflections resulting from Z_0 mismatches.

Sec 17.3 Wave Actions and Reflections with a Z_0 Mismatch

Whether a tuned stub or a lumped-constant network is used to perform the matching, the matching device itself (such as a transmatch) presents a mismatch to the line. When adjusted to achieve the conjugate match, the transmatch generates a new reflected wave having the same magnitude, but of opposite phase, as that of the reflected wave arriving from the antenna mismatch. These two waves combine in the transmatch to produce a resultant *forward* wave that is in phase with the voltage and current components of the source wave delivered by the generator. All of the power reflected by the Z_0 mismatch at the antenna *is now added to the source power at the matching point in the transmatch*, to be subtracted later when it again reaches the antenna. (*See Chapters 4, 5, and 6.*)

The re-reflection of power in the transmatch results in what is called reflection *gain*, which equals and cancels the reflection *loss* from the Z_0 mismatch. *(See Ref 19 and Chapter 6.)* This addition of the re-reflected power to the source power results in forward power between the transmatch and the antenna that exceeds the source power. When the reflected power is again subtracted by reflection at the antenna mismatch, the remainder, which is absorbed (radiated) by the antenna, equals the source power exactly. (*See Chapters 4 and 16.*) It may come as a surprise, but these same wave actions and reflection-loss cancellations also occurred in the matching network when it was placed at the antenna terminals. Indeed, it is the multiple reflections produced by the controlled mismatch of any matching device that form the basis for all impedance-matching operations. (*See Chapters 4 and 5, Eqs 6-1 and 6-2, the final paragraphs of Sec 9.1, and Chapter 16.*)

Sec 17.4 Attenuation and Power Loss

Now let's consider the effects of attenuation and power loss. In lines having attenuation, all power entering the line is absorbed in the load, except for that which is lost through line attenuation, regardless of the mismatch or SWR. (*See Chapters 5 and 6.*) Of course, the attenuation is greater when there is a load mismatch, because in addition to the attenuation of the forward power, the reflected power is also attenuated during its return to the transmatch. This is the *only significant* difference in performance between placing the transmatch at either the input end or the antenna end of the feed line—except for the obvious difference in convenience in tuning the transmatch.

The power lost to attenuation increases as the SWR on the line increases when the transmatch is at the line input. However, when the matched-line attenuation is low, as it is in typical amateur installations, the additional loss from a Z_0 mismatch is so small that the difference in radiated power cannot be discerned by a receiving station. The increase in line attenuation resulting from SWR can be determined from the graphs of Figs 1-1 and 6-1, or it may be calculated precisely from Eq 6-1. A study of these references shows that the logical place for a transmatch is on the operating desk, not at the antenna.

Chapter 18

The Broadband Double-Bazooka Antenna – How Broad Is It?

(Adapted from "Technical Correspondence," QST, September 1976)

Sec 18.1 Introduction

The increasing interest in using the coaxial dipole (sometimes called the Double-Bazooka antenna) for its questionable increased bandwidth is disturbing, especially in view of the results of an analysis and some experiments I performed and published some years ago (*Ref 62*). The antenna, with its inner section of coax and its end sections of open-wire transmission line (ladder line), was popularized for amateur use by Charles Whysall, W8TV, with an article in July 1968 *QST* (*Ref 129*). It appears in several editions of *The ARRL Handbook*, although it has never appeared in *The ARRL Antenna Book*. The results of my analysis and experiments indicate that the coaxial stubs in the coaxial-dipole configuration in general use by amateurs cannot provide the degree of bandwidth that users of the coaxial dipole appear to be measuring. Thus, it appears that features other than the shunt-compensating reactance provided by the coaxial stubs within the dipole must be responsible for achieving the bandwidth credited to the coaxial feature.

Here's why the shunt-reactance compensating feature cannot make any significant contribution to bandwidth when the feed-line impedance is the usual Z_C = 50 ohms. Depending on the height above ground, the input impedance of the average 40-meter or 80-meter amateur dipole generally runs from 50 to 80 ohms of resistance at resonance. Thus, at resonance, the mismatch on a 50-ohm line is generally quite low, from less than 1.1 to around 1.6 at worst. On either side of resonance, the mismatch increases rapidly because of the reactance appearing in the dipole impedance. With the addition of the coaxial reactance-compensating shunt stubs, the dipole reactance should be either canceled at best, or at worst reduced somewhat by the opposite shunt reactance provided by the stubs.

Sec 18.2 Reactance Cancellation

Although you'll see later why it can't be, let's first assume hypothetically that complete cancellation of the reactance can be achieved by the shunt reactance of the coaxial stubs. This means the cancellation is obtained by a *parallel*-connected reactance, which raises the series resistance of the dipole impedance to its equivalent parallel-circuit value, which is *much higher*. Here is the crucial point: When you use a feed line having an impedance that already matches the dipole terminal resistance rather well at resonance, the higher mismatch off resonance caused by the dipole reactance will not be significantly different, whether it is caused by the reactance of the uncompensated dipole or by the increased resistance received in exchange for the canceled reactance.

To illustrate with an example, consider an 80-meter dipole at a height that yields a resonant terminal impedance of 55 + *j*0 ohms at 3.75 MHz. The mismatch is 1.1 referred to 50 ohms. At 3.55 MHz, 200 kHz below resonance, the series impedance of the dipole is approximately 50 – *j*90 ohms, which yields a 5.04:1 mismatch. Now a 90-ohm inductive reactance placed in *series* with the dipole terminals *would* cancel the 90-ohm capacitive dipole reactance, and would leave the terminal resistance at 50 ohms. We would indeed have a perfect match.

Unfortunately, the reactance provided by the stubs in the coaxial dipole is in *parallel* with the dipole terminal impedance, *not in series*. And what a difference this makes! The values of the equivalent parallel-circuit components of the dipole impedance at 3.55 MHz (50 – *j*90 ohms) are R_P = 212, and X_P = –117.8 ohms, as shown in Fig 18-1(A). When the –117.8 ohms of capacitive dipole reactance is com-

pletely canceled by an equal inductive reactance in *parallel* with the dipole impedance, the resulting impedance is 212 + *j*0 ohms. Bad news! The terminal resistance of the dipole made resonant at 3.55 MHz by the shunt inductive reactance is now 212 ohms, raised from 50 ohms by the parallel connection! Canceling the dipole reactance with *parallel* circuitry has raised the resistive component by a factor of 4.24 from 50 ohms up to 212 ohms, and coincidentally, the mismatch is now 212/50 = 4.24:1. This is the lowest mismatch obtainable with any type of parallel compensation, because even though the dipole reactance has been completely canceled, we're still stuck with the 212-ohm dipole terminal resistance.

Obviously, a reduction in mismatch from 5.04:1 to 4.24:1 is hardly worthwhile, even if it could be accomplished, but it can't. Why? Because a canceling reactance of 117.8 ohms would require a coax having a characteristic impedance Zc of only 4.95 ohms for the stubs—impractical to build. Here's more bad news: Stubs made from 50-ohm coax yield a reactance ten times too high—useless. What about 75-ohm coax? That is 1.5 times worse. Incredible, you say? Example continues: A short-circuited stub, λ/4 resonant at 3.75 MHz made from 50-ohm coax, yields an inductive reactance of 595.4 ohms at 3.55 MHz, again 200 kHz *below* resonance. These values are calculated from the equations below at 3.55 MHz.

$$\text{Stub length } \theta = 3.55 \text{ MHz} \times 90^\circ = 85.2^\circ \quad \text{(Eq 18-1)}$$

Shunting reactance per stub

$$X = Z_C \tan \theta = 595.4 \text{ ohms} \quad \text{(Eq 18-2)}$$

when stub $Z_C = 50$ ohms, and $\theta = 85.2^\circ$

Stub impedance required, each stub

$$Z_C = \frac{X \cot \theta}{2} = 4.95 \text{ ohms} \quad \text{(Eq 18-3)}$$

when $X = 117.8$ ohms, and $\theta = 85.2^\circ$

The stubs in each dipole half (595.4 ohms each) are connected in series with each other through their center conductors, so the total inductive reactance of the series combination is twice the value of the single stub, or 1190.8 ohms. This is the value appearing in parallel with the dipole impedance when using 50-ohm stubs. (Stubs of 75 ohms would yield 1786.3 ohms.) The combined parallel components of the dipole impedance and shunt-stub reactance (R_P = 212 ohms and X_P = –117.8 ohms in parallel with stubs of +1190.8 ohms) yield total parallel-circuit component values of R_P = 212 ohms and X_P = –130.7 ohms. The series-equivalent dipole input-terminal impedance is now 58.4 – *j*94.7 ohms, also shown in Fig 18-1 at (B). The result? A whopping big reduction in mismatch from 5.04 without stubs, all the way down to 4.9:1 with stubs! Going still further, using the impractical 4.95-ohm stubs that would cancel all the dipole reactance, the resulting non-reactive dipole terminal impedance of 212 + *j*0 ohms would still yield a 4.24:1 SWR on the 50-ohm feed line. Conclusion? Isn't it obvious that the stubs are ineffective?

Thus, you ask what other features can be responsible for the lower mismatch values that appear to be measured by many coaxial-dipole users. I'll give you a number of possibilities.

First, the mismatch values shown here are those which appear at the junction of the feed line and the antenna, while values measured at the input of the feed line will be somewhat lower because of line attenuation.

Second, increased radiator thickness, especially when the stubs are constructed from RG-8, reduces the dipole characteristic impedance, resulting in less reactance than with the thinner wire dipole for the same frequency excursion away from resonance. (But who wants to hang 125 feet of RG-8?)

Third, the extensions for building out from the shortened, short-circuited ends of the coax stubs to obtain an *external* half wave are usually of multiwire construction such as ladder line, which further increases the effective radiator thickness. Such is especially helpful at the outer ends of the dipole, where the voltage and the electric field are high. This reduces the off-resonance reactance still further.

Fourth, the external dielectric material covering the stub coax increases both dipole capacitance (increasing the electrical length) and effective diameter of the radiator. However, indications under investigation suggest this increase in effective diameter is also accompanied by increased ohmic loss in the external dielectric, which decreases the Q, and thus increases the bandwidth at the expense of efficiency.

Fifth, in the range above 3:1, many SWR indicators show readings considerably lower than the true

value. If you are interested in pursuing the subject further, I invite you to read my paper entitled, "A Revealing Analysis of the Coaxial Dipole Antenna," appearing on page 46 of *Ham Radio* magazine, August 1976 (*Ref 62*).

Sec 18.3 Resistive Losses

Since I wrote the "Technical Correspondence" item on which the above information is based, the true reason for the increased dipole bandwidth obtained with the Double-Bazooka has been discovered. However, the reason is not a happy one. Frank Witt, AI1H (ex-W1DTY), with the aid of a computer, has discovered that the increased bandwidth of the Double-Bazooka obtained by many amateurs actually arises from the previously undetermined resistive loss due to the shunt conduction of the internal dielectric material in the coaxial cable used to form the stubs, and not by reactance cancellation

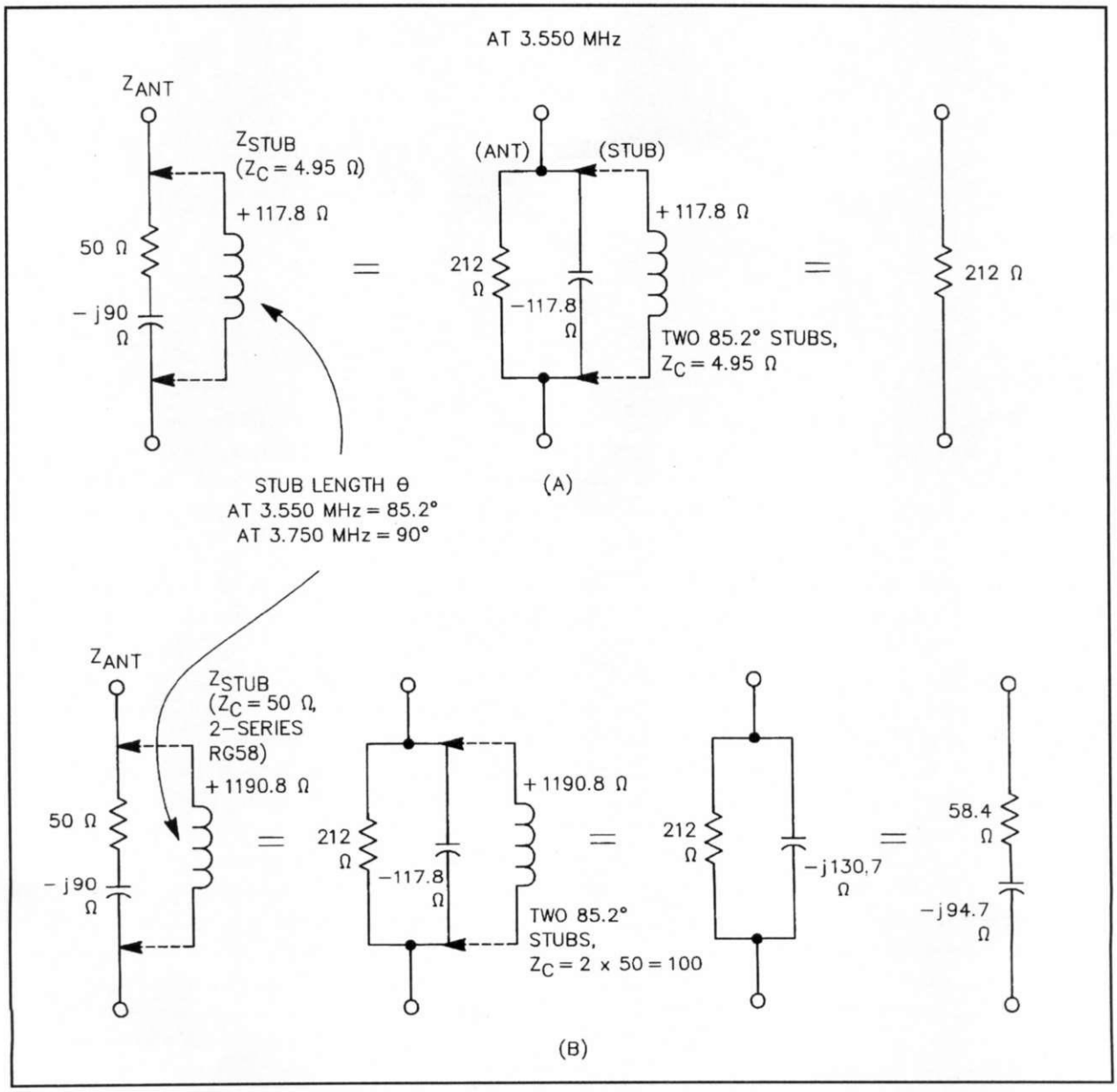

Fig 18-1. Showing the impedance transformation for (A) 4.95-ohm center coaxial section, and (B) 50-ohm center section. At both (A) and (B) the SWR without coaxial stubs is 5.04:1; with stubs at (A) it becomes 4.24:1, and in the practical case at (B), 4.9:1.

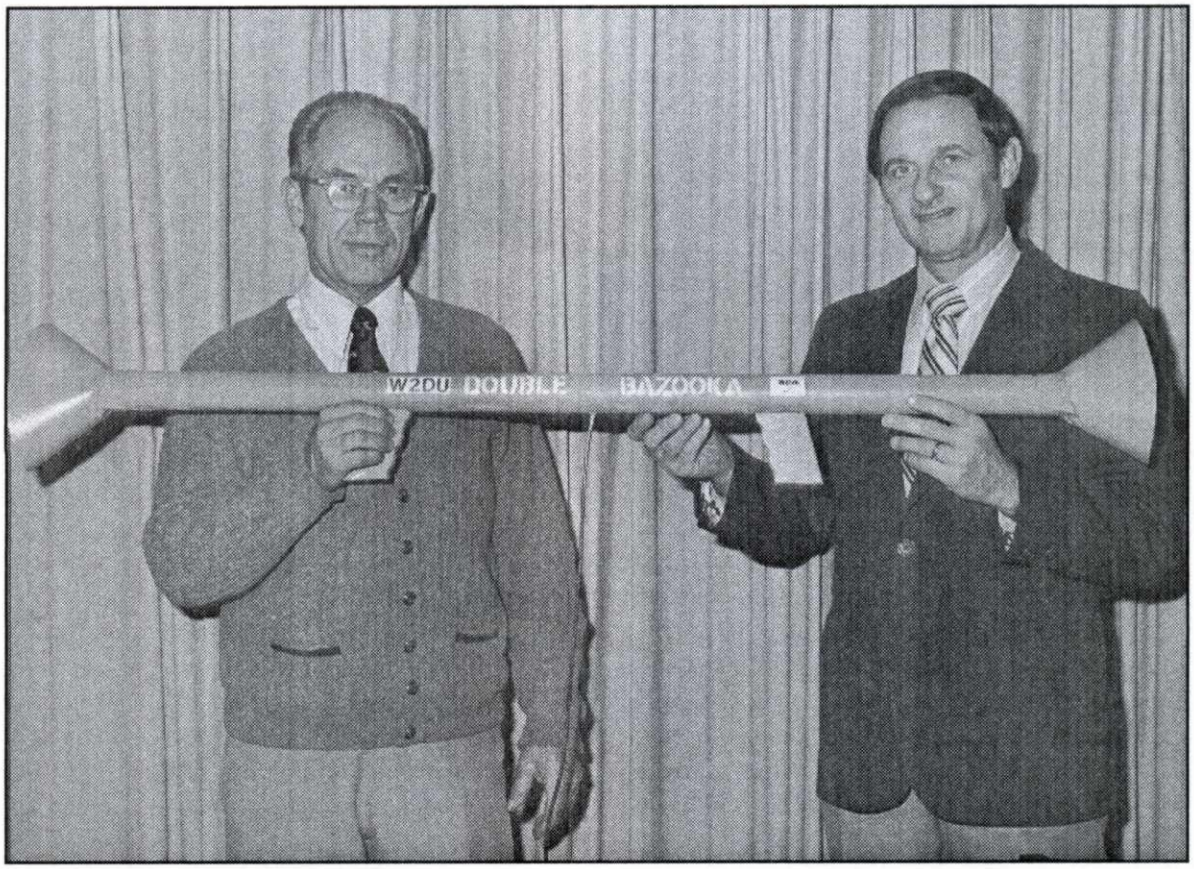

One-of-a-kind Double-Bazooka, RCA Model POW! POW! with double end-fire, narrow-beam, high-gain, heavy particle thuster, presented to the author by Tom Voorhis, K2EQU, at the dinner celebrating his retirement from the RCA Astro-Electronics Division's Space Center in November 1980, after 31 years with the company.

from parallel-connected coaxial stubs (*Ref 122*). In other words, the reduction in SWR obtained by those who use the Double-Bazooka is from lossy resistive loading and not from reactance cancellation. Unfortunately, the resistive loading results in a reduction in radiated power, power lost in heating the stubs. Thus, the users of this antenna are trading radiated power for a lower SWR on the feed line.

This turn of events is ironic for two reasons. First, as I showed earlier, the reactance available in the coaxial stubs in the Double-Bazooka is insufficient to obtain any practical amount of reduction in the SWR-producing antenna-terminal reactance, much less total cancellation. Second, even if the stubs could provide sufficient reactance to obtain complete cancellation, the improvement in bandwidth would still have been inconsequential as a result of the cancellation, as I proved mathematically.

Earlier in this chapter, and in my coaxial dipole analysis (*Ref 62*), I pointed out the reason *no bandwidth improvement is possible from parallel-circuit reactance cancellation when the feedline impedance is 50 ohms.* You'll remember, this is because the parallel-circuit form of the stub connection used in the cancellation raises the effective terminal resistance as the reactance is lowered, resulting in a negligible reduction of mismatch. I also pointed out in the analysis that an improvement in bandwidth could be achieved with parallel-circuit reactance cancellation by using a feed line having an impedance higher than the resonant terminal resistance of the dipole, and then accepting a corresponding increase in mismatch at the resonant frequency of the dipole. I showed that by using a 144-ohm feed line to feed a dipole having a resonant terminal resistance of 72 ohms (yielding a 2:1 SWR at resonance), the 2:1 SWR bandwidth could be improved from 165 kHz (on 50-ohm line with *no* stubs) to 565 kHz by canceling the off-frequency

dipole reactance with 19.7-ohm stubs. This results in a bandwidth improvement factor of 3.4. This arrangement is particularly appealing for the 80-meter band, because it achieves an SWR of less than 2:1 across the entire band, except at the center frequency, where it is exactly 2:1.

In my analysis I offered no concrete suggestion for practicing this arrangement, except to suggest the use of two 75-ohm coaxial lines side by side resulting in a 150-ohm balanced feedline. However, I considered using a lumped-constant capacitor and inductor at the feed point for an impedance transformer to obtain the required increase in feedpoint impedance and for reactance cancellation. However, I decided it was impractical to use, so I discarded the idea. On the other hand, Frank Witt came up with the same idea and made it work! (*See Ref 122.*) In addition, he also came up with a very clever method of using a shorted λ/4-stub impedance transformer to obtain both the required step-up of impedance and the reactance cancellation (*Refs 123 and 124*). His method uses the larger RG-8 or RG-213 coaxial cable for the λ/4 stub, ensuring optimum bandwidth improvement by reactance cancellation but with minimal loss in the cable stub. The Snyder dipole (*Ref 130*) uses a somewhat similar method of broad-banding, but with higher loss than with Witt's method, because the Snyder dipole uses the higher-loss RG-141 coax for the reactance cancellation. For anyone wishing to build a true broad-banded 80-meter dipole, the Witt articles referenced above provide all of the necessary details, plus the explanation of how it works.

Chapter 19

On the Nature of the Source of Power in Class B and C RF Amplifiers

(Based on data from Terman's Radio Engineers Handbook, *1943)*

Sec 19.1 Introduction

In this chapter we will discuss the nature of the source of power in Class B and C RF amplifiers. As in previous chapters that clarified misconceptions concerning SWR and reflected power, this chapter will be concerned with clarifying misconceptions prevalent among amateurs and professional electrical engineers alike concerning the operation of RF power amplifiers. In attempting to resolve the controversy concerning the Conjugate Matching Theorem in relation to these amplifiers, discussions with many of these people revealed an alarming number of misconceptions concerning the complex relationships of voltage and current that occur in the development of the source of power in these amplifiers, especially in relation to the coupling to their loads. Therefore, the focus of this chapter will be to highlight and clarify those misconceptions.

However, before discussing amplifier operation, two synonymous terms that play a vital role in amplifier operation need clarification, because they are widely misinterpreted in discussions relating to the source of power. The terms are *maximum available power* and *all available power*.

Maximum available power, or all available power, is simply the power available for delivery from the source to the load whenever the source is matched to the load. In Class B and C amplifiers it is the power delivered when the loading is adjusted for peak output *at any given level of drive*. It is *not* the absolute maximum power that can be obtained by overdriving, or using excess plate voltage or plate current, as many amateurs and engineers alike have been misled to believe.

Turning now to the discussion of amplifier operation, one misconception is that Class C amplifiers cannot support circuital analysis using general network theorems because of the nonlinearity[1] of the amplifier operation. In clarifying this misconception we will show that although the input circuit of the pi-network tank circuit in Class C amplifiers is nonlinear, the output circuit to the load is indeed linear, due to energy storage in the tank. Consequently, the linear relationship between voltage and current appearing at the output of the tank circuit does indeed support the application of theorems that require circuits to be linear for their application to be valid.

Another misconception concerns the relationship between the output and load resistances of these amplifiers. Because of speculations without verification by *valid* measurements, many people believe incorrectly that the output resistance is much greater than the load resistance, and thus proclaim that a conjugate match cannot be obtained between the amplifier and the load. However, when a *linear* source of power is delivering *all* of its available power to the load, there is a conjugate match by axiomatic definition, as explained in the following paragraph. *(Also see the references quoted in Appendix 9.)* An example from Terman is used in clarifying the misconception concerning the relationship between output and load resistances, shown in Sec 19.3. In addition, data obtained from my own measurements, shown in Sec 19.8, prove that after the amplifier has been adjusted to deliver all of its available power at any given drive level, the output and load impedances of the amplifier *are equal* and thus are conjugates of each other.[2] My measurements have been confirmed by Tom Rauch, W8JI, using identical measurement procedure.

Now to explain two axioms of the Conjugate Matching Theorem that are commonly overlooked, which has resulted in widespread confusion concerning its use. We know that when a load impedance differs from its source impedance, a matching device is required to allow delivery of all the avail-

able power from the source to the load. In this condition we say the load is *matched* to the source. The term *matched* has been used universally for many decades, and in the earlier days the term was used alone. However, when all the power available from the source is delivered to the load, the matching occurs because the source and load impedances are conjugates of each other. Consequently, during the last fifty years, the term "*conjugate* match" gradually came into use synonymously with "match" to describe the term more accurately. In other words, "match" and "conjugate match" are used interchangeably with no difference in meaning. Unfortunately, misinterpretation and misunderstanding of *conjugate* in the newer term has created confusion for many people when a routine impedance match is referred to as a "conjugate" match. To clarify the confusion, the following two axioms, which follow from the Maximum Power-transfer Theorem, accurately define a conjugate match:

Axiom 1. *There is a conjugate match whenever all of the available power from a source or network is being delivered to the load.*

Axiom 2. *There is a conjugate match if the delivery of power decreases whenever the impedance of load is changed in either direction.*

(Additional axioms and explanations appear in Appendix 9.)

We now return to clarify the misconception concerning output and load resistances. The term *source resistance, Rs,* of an RF power amplifier, as is often misused (and confused with R_P) in referring to the source of RF power delivered by Class B and C amplifiers, reveals still another prevalent misconception. This misconception is that the *entire source of power* in these classes of tube-type amplifiers is a *dissipative* resistance. In clarifying this misconception, we will use the example by Terman to demonstrate that the source of RF output power in a Class C amplifier is the combination of *two* resistances—a *non-dissipative* resistance related to the characteristics of the *effective* load line, and a *dissipative* plate resistance R_{PD}. Resistance R_{PD} is not plate resistance R_P, as determined from the well-known expression $R_P = \Delta E_P \div \Delta I_P$. From this expression it is evident that R_P is the result of a small change in plate current due only to a change in plate voltage, which is *not* the source of power in RF power amplifiers as is claimed by many who have misinterpreted the expression. The source of power is actually derived by a large change in plate current resulting from a change in ***grid*** *voltage*. This phenomenon will be discussed in more detail later.

One portion of the *non*-dissipative resistance is the reciprocal of the total conductance from both plate and power supply to the input of the pi-network tank circuit. At that point in the typical amateur pi-net Class B and C amplifier, the load is the tank input. The source is the combination of two parallel conductive paths to the tank: (1) the blocking capacitor in series with the active device, the tube(s),[3] and (2) the same blocking capacitor in series with the RF choke and the voltage of the power supply. These two conductance paths are paralleled at the input of the tank, operating at different, but overlapping times throughout the cycle. The other portion of the non-dissipative resistance is related to the operating load line, which will be discussed in Sec 19.3a.

Plate resistance R_{PD} is *dissipative*, and the value is determined by the power, P_D, dissipated as heat by the plate divided by the square of the average DC plate current I_{DC}, the current measured by the DC plate ammeter. Note in Terman's statement 3 in Sec 19.3 that dissipated power, P_D, is the product of *the instantaneous plate-to-cathode voltage and the instantaneous plate current*. We know that energy is transferred from the plate circuit of the amplifier to the pi-network by periodic pulses of plate current that flow during the conducting portion of the RF cycle. Knowledge of the *non*-dissipative portion of the source resistance will allow you to understand why Class B and C amplifiers can deliver all of their available power into a conjugately matched load with efficiencies greater than 50 percent. This concept is important, because the ability of these amplifiers to be conjugately matched has been incorrectly disputed due to three erroneous assumptions that have caused many amateurs and engineers alike to be misled.

If you experience difficulty appreciating the concept of a *non*-dissipative resistance, please refer to Appendix 10 for a detailed explanation and published references on the subject for clarification.

Sec 19.2 Erroneous Assumptions

The principal reason why many people have been misled is because they have incorrectly estimated the amount of the source resistance in the amplifier that is dissipative. This incorrect assumption led them to believe that half the power is dissipated in the source resistance, and thus, as in the *classical generator*, a conjugate match would limit the efficiency to 50 percent. However, this is not true, because as noted above the source of the power delivered to the pi-network tank circuit is non-dissipative, except for the dissipative plate resistance R_{PD}. Because dissipative plate resistance R_{PD} is generally less than the load resistance R_L, more power is delivered to the load resistance than that dissipated in the dissipative plate resistance, thus allowing efficiencies greater than 50 percent. The lower dissipative plate resistance occurs because plate current is allowed to flow only when the plate voltage is at the minimum of its sinusoidal swing, as explained in Terman's statement 7 in Sec 19.3. Repeating Terman's statement 3 for emphasis, dissipated power P_D is the product of *instantaneous* plate-to-cathode voltage and *instantaneous* plate current. (Keep in mind that plate current is zero except during the short conduction time, considerably less than 180 degrees.)

The second erroneous assumption is that the Conjugate Matching and Maximum Power-transfer Theorems don't apply to Class B and C RF amplifiers, because the operation of these amplifiers is nonlinear.[1] This assumption is also incorrect because they have failed to appreciate the isolating action of the vitally important pi-network tank circuit. The pi-network tank is *not* simply an impedance transformer, as many believe, but is also an *energy storage* device. The energy storage capacity of the tank isolates the pulsed nonlinear mode at the input from the smoothed *linear* mode at the output that delivers the nearly perfect sine waves. This widely overlooked and misunderstood concept will be discussed in depth later.

A third erroneous assumption concerns the misuse of the role *source* resistance, "R_S," plays in the delivery of power to the tank circuit. Because they say the value of R_S is as much as five times greater than load resistance R_L, a condition that violates the Conjugate Matching Theorem, some people assert this is why no conjugate match is possible in systems where the source is an RF power amplifier. However, to obtain R_S they erroneously used the expression $R_P = \Delta E_P \div \Delta I_P$, where R_P *is* greater than R_L. The reason the expression was used erroneously is because in this expression, I_P varies *only* with variation of plate voltage, not grid voltage, as explained earlier. Also, because the change in plate current due to a change in plate voltage is small compared to the change in plate current due to a change in grid voltage, R_P and the erroneous "R_S" are much greater than R_L. The crucial point here is that the source of power is derived from the much larger change in plate current due to the change in *grid* voltage, while the effect of the change in plate current due to the change in plate voltage is insignificant in relation to the output impedance of the amplifier. Consequently, as we proceed we will learn that both R_P and "R_S" are totally irrelevant to conjugate matching the output impedance of the amplifier to the impedance of its load, and thus impose no impediment to the conjugate match.

Sec 19.3 Analysis of the Class C Amplifier

The following discussion of the Class C amplifier, which reveals why the portion of the source resistance related to the charactersistics of the load line is non-dissipative, is based on statements appearing in Terman's *Radio Engineers Handbook*, 1943 edition, page 445, and on Terman's example of Class C amplifier design data appearing on page 449. Because the arguments presented in Terman's statements are vital to understanding the concept under discussion, I quote them here for convenience (parentheses and emphasis are mine):

1. The average of the pulses of current flowing to an electrode represents the direct current drawn by that electrode.

2. The power input to the plate electrode of the tube at any instant is the product of plate-supply voltage and instantaneous plate current.

3. The corresponding power (P_D) lost at the plate is the product of instantaneous plate-cathode voltage and instantaneous plate current.

4. The difference between the two quantities obtained from items 2 and 3 represents the useful output at the moment.

5. The average input, output, and loss are obtained by averaging the instantaneous powers.

6. The efficiency is the ratio of average output to average input and is commonly of the order of 60 to 80 percent.

7. The efficiency is high in a Class C amplifier *because current is permitted to flow only when most of the plate-supply voltage is used as voltage drop across the tuned load circuit R_L, and only a small fraction is wasted as voltage drop (across R_{PD}) at the plate electrode of the tube.*

Based on these statements, the discussion and the data in Terman's example that follow explain why the amplifier can deliver power with efficiencies greater than 50 percent while conjugately matched to its load, a condition that is widely disputed because of the incorrect assumptions concerning Class B and C amplifier operation as noted previously. The terminology and data in the example are Terman's, but I have added one calculation to Terman's data to emphasize a parameter that is vital to understanding how a conjugate match can exist when the efficiency is greater than 50 percent. That parameter is *dissipative plate resistance, R_{PD}.* (As stated earlier, dissipative resistance R_{PD} should not be confused with plate resistance R_P of amplifiers operating in Class A, derived from the expression $R_P = \Delta E_P \div \Delta I_P$.)

It is evident from Terman that the power supplied to the amplifier by the DC power supply goes to *only two places,* the RF power delivered to load resistance R_L at the input of the pi-network, and the power dissipated as heat in dissipative plate resistance R_{PD} (again, not plate resistance R_P, which is *totally irrelevant* to obtaining a conjugate match at the output of Class B and C amplifiers). In other words, the output power equals the DC input power minus the power dissipated in resistance R_{PD}. We will now show why this two-way division of power occurs.

First we calculate the value of R_{PD} from Terman's data, as seen in line (9) in the accompanying formulas. It is evident that when the DC input power minus the power dissipated in R_{PD} equals the power delivered to resistance R_L at the input of the pi-network, there can be no signifi-

Data from Terman's example on page 449 of the *Radio Engineers Handbook*

(1) E_b = DC Source Voltage = 1000 v

(2) $E_{min} = E_b - E_L = 1000 - 850 = 150$ v [See Terman, Figs 76(a) & 76(b)]

(3) I_{dc} = DC Plate Current = 75.1 ma = 0.0751 a

(4) $E_L = E_b - E_{min} = 1000 - 150 = 850$ v = Peak Fundamental AC Plate Voltage

(5) I_1 = Peak Fundamental AC Plate Current = 132.7 ma = 0.1327 a

(6) $P_{IN} = E_b \times I_{dc}$ = DC Input Power = $1000 \times 0.0751 = 75.1$ w

(7) $P_{OUT} = \frac{(E_b - E_{min})I_1}{2} = \frac{E_L I_1}{2}$ = Output Power Delivered to $R_L = \frac{(1000 - 150) \times 0.1327}{2} = 56.4$ w

(8) $P_D = P_{IN} - P_{OUT}$ = Power Dissipated in Dissipative Plate Resistance $R_{PD} = 18.7$ w

(9) $R_{PD} = \frac{P_D}{I^2_{dc}} = \frac{18.7 \text{ w}}{0.0751^2 \text{a}}$ Dissipative Plate Resistance $R_{PD} = 3315.6$ ohms

(10) $R_L = \frac{E_b - E_{min}}{I_1} = \frac{E_L}{I_1}$ = Load Resistance $= \frac{850}{0.1327} = 6405$ ohms [6400 ohms in Terman]

(11) Plate Efficiency = $P_{OUT} \times \frac{100}{P_{IN}} = 56.4 \times \frac{100}{75.1} = 75.1\%$

cant dissipative resistance in the amplifier other than R_{PD}. The antenna effect from the tank circuit is so insignificant that dissipation due to radiation can be disregarded. If there were any significant dissipative resistance in addition to R_{PD}, the power delivered to the load plus the power dissipated in R_{PD} would be less than the DC input power, due to the power that would be dissipated in the additional resistance. This is an impossibility, confirmed by the data in Terman's example, which is in accordance with the Law of Conservation of Energy. Therefore, we shall observe that the example confirms the total power taken from the power supply goes only to (1) the RF power delivered to the load R_L, and (2) to the power dissipated as heat in R_{PD}, thus proving there is no significant dissipative resistance in the Class C amplifier other than R_{PD}.

Note in line (10) that R_L is determined simply by the *ratio* of the fundamental RF AC voltage E_L divided by the fundamental RF AC current I_1 and therefore does not involve dissipation of any power. Thus, R_L is a *non*-dissipative resistance. (For more on non-dissipative resistance see Appendix 10.)

Referring to the data in the example, observe again from line (10) that load resistance R_L at the input of the pi-network tank circuit is determined by the ratio $E_L \div I_1$. This is the Terman equation that, prior to the more-precise Chaffee Fourier Analysis, was used universally to determine the approximate value of the optimum load resistance R_L. (When the Chaffee Analysis is used to determine R_L from a selected load line the value of plate current I_1 is more precise than that obtained when using Terman's equation, consequently requiring fewer empirical adjustments of the amplifier's parameters to obtain the optimum value of R_L.) Load resistance R_L is proportional to the slope of the operating load line that allows all of the available integrated energy contained in the plate-current pulses to be transferred into the pi-network tank circuit. (For additional information concerning the load line see Sec 19.3.1.) Therefore, the pi-network must be designed to provide the equivalent optimum resistance R_L looking into the input for whatever load terminates the output. The current pulses flowing into the network periodically deliver bursts of electrical energy to the network, in the same manner as the spring-loaded escapement mechanism in a pendulum clock periodically delivers mechanical energy to the swing of the pendulum.

In a similar manner, after each plate-current pulse enters the pi-network tank curcuit, the flywheel effect of the resonant tank circuit stores the electromagnetic energy delivered by the current pulse, and thus maintains a continuous sinusoidal flow of current throughout the tank, in the same manner as the pendulum swings continuously and periodically after each thrust from the escapement mechanism. The continuous swing of the pendulum results from the inertia of the weight at the end of the pendulum due to the energy stored in the weight. The path inscribed by the motion of the pendulum is a sine wave, the same as at the output of the amplifier. We will continue the discussion of the flywheel effect in the tank circuit later with a more in-depth examination.

Let us now consider the dissipative plate resistance R_{PD}, which provides the evidence that the DC input power to the Class C amplifier goes only to the load R_L and to dissipation as heat in R_{PD}. With this evidence we will show how a conjugate match can exist at the output of the pi-network with efficiencies greater than 50 percent. In accordance with the Conjugate Matching Theorem and the Maximum Power-transfer Theorem, it is well understood that a conjugate match exists whenever all available power from a linear source is being delivered to the load. Further, by definition, R_L is the load resistance at the tank input determined by the characteristics of the load line that permits delivery of all the available power from the source into the tank. This is why R_L is called the *optimum* load resistance. Thus, from the data in Terman's example, which shows that after accounting for the power dissipated in R_{PD}, all the power remaining is the available power, which is delivered to R_L and thence to the load at the output of the pi-network. *Therefore, because all* ***available*** *power is being delivered to the load, we have a conjugate match by definition.* In the Sec 19.4 we will show how efficiencies greater than 50 percent are achieved in Class C amplifiers operating into the conjugate match.

Sec 19.3a Examining the Operating Load Line

The finer details of the somewhat trial-and-error method of establishing the operating load line are

beyond the scope of this chapter. However, once established, the load line represents the non-dissipative load resistance R_L appearing at the input of the pi-network tank circuit. The slope of the load line is proportional to the ratio of the continuous fundamental RF voltage and current. When the network is terminated with the correct output load resistance (a resistance equal to the network output resistance as explained in Sec 19.8), the network transforms the output load resistance up to resistance R_L at the network input. Once established (and proven by measurements of network output impedance described in Sec 19.8), the slope of the operating load line remains constant with changes in output power resulting from changes in drive levels. Consequently, because R_L represents the slope of the load line, both the fundamental RF voltage-current ratio appearing along the load line and the network output impedance remain constant whatever the power level of the integrated current pulses enter the network. It should be clearly understood that because the operating load line and the optimum resistance R_L it represents are established solely by the *ratio* of the RF voltage and current, the load line and R_L are non-dissipative. As explained earlier, the entire dissipation to heat occurs only in the dissipative plate resistance R_{PD}.

When using the Terman equation to determine load resistance R_L, an approximate load line and average plate current are first estimated from the tube characteristic curves. The corresponding value of R_L is used as a trial value and the output power and efficiency are determined in a trial run. However, several trial runs with different load adjustments are necessary to converge toward the optimum value of R_L that will yield the desired conditions for operation, simply because the first estimation of average plate current is rarely the optimum value.

When the Chaffee Analysis is used to determine R_L in establishing the load line, the average value of plate current I_1 during the conduction period is obtained by first plotting the load line on a graph of constant plate-current characteristics of the tube. The load line is then marked off in several increments corresponding to successive angles of conduction of plate current. The plate current at each conduction angle is then found at the intersection of the load line and the constant-current curve. The plate voltage at each conduction angle is also found on the plate-voltage line directly below the above stated intersection. The averages of plate current and voltage are then determined using the trapezoidal rule. Load resistance R_L is then determined by dividing the average fundamental RF plate voltage by the average fundamental RF plate current, the Terman equation. Thus, the Chaffee method saves time compared to using Terman's equation alone, because the initial value of average plate current is closer to the optimum value than that estimated for use in the Terman equation.

Sec 19.4 Calculation of Efficiency Greater than 50 Percent

To show how efficiencies greater than 50 percent are obtained while the amplifier is conjugately matched, we will dissect the data in the Terman example to discover that load resistance R_L is greater than dissipative plate resistance R_{PD}, thus allowing more power to be delivered to the load than that dissipated in R_{PD}. Referring again to Terman's example in line (10), his calculation of load resistance R_L is 6400 ohms. From line (9) we find R_{PD} is 3315.6 ohms by dividing 18.7 watts dissipated in R_{PD} by the square of 75.1 ma. DC plate current I_{DC} flowing through R_{PD}. Correspondingly, line (7) shows the power delivered to R_L is 56.4 watts, and from line (8), power P_D dissipated in R_{PD} is 18.7 watts. With 56.4 watts delivered to R_L and 18.7 watts dissipated in R_{PD} we have accounted for the total input power, 71.5 watts, shown in line (6). The relative power distribution is 75.1 percent delivered to R_L, and 24.9 percent dissipated in R_{PD}. Earlier we showed that after accounting for the power dissipated in R_{PD}, all the remaining available power is delivered to the load R_L. Thus, this distribution of power clearly demonstrates why a Class C amplifier can deliver more than 50 percent of its input power to the load, because its load resistance R_L (6400 ohms) is greater than its *dissipative* plate resistance R_{PD} (3315.6 ohms).

These calculations are in accord with Terman's Statement 7 that "efficiency is high in the Class C amplifier, because current is permitted to flow only when most of the plate-supply voltage is used as voltage drop across the tuned load circuit R_L, and only a small fraction is wasted across R_{PD} at

the plate electrode of the tube." None is dissipated in the non-dissipative resistance related to the characteristics of the load line. As stated earlier, the non-dissipative portion of the source resistance is the reciprocal of the total conductance from both the plate of the tube and the power supply to the input of the pi-network tank circuit. It should be noted, however, that we are considering *only the power delivered to the tank*; we are not concerned here with inherent loss in the tank that results in some decrease in the power delivered at the output of the tank.

Sec 19.5 Evidence of Conjugate Match

The example has proven that a conjugate match exists, because all the available power has been delivered to the resistive load R_L, and thence to the load terminating the pi-network, in accordance with Conjugate Matching Axioms 1 and 2 recited in Sec 19.1 and again in Appendix 9. The example has also shown that more power has been delivered to the load than was dissipated, because 54.6 watts were delivered and only 18.7 watts were dissipated. Thus, we have shown that conjugate matching to a Class C RF amplifier does not limit its efficiency to 50 percent. The same reasoning applies to amplifiers operating in Class B.[2]

Now you ask: Do we have a conjugate match during SSB operation? The answer is yes, but it begs an additional question: Does the output impedance of the amplifier remain constant with SSB modulation, or does it change during the variations of drive and output power corresponding to the voice modulation? My measurements, described in Sec 19.8, show that the output impedance does not change significantly with voice modulation. This is because for a given load resistance R_{LOAD}, the operating load line related to the load resistance R_L appearing at the input of the tank circuit and the output resistance R_{OUT} are established during the tuning and loading procedure when the loading is adjusted to deliver maximum available power. During this procedure maximum available power is that power which is delivered to the load with the drive level set for obtaining the desired output power at the full modulation level. After the load line has been established in this manner it remains constant for all values of drive. I have made extensive measurements, described in Sec 19.8, which show that once the operating load line is established during this routine procedure, it remains constant during swings of grid voltage during SSB modulation as long as the plate supply voltage remains constant.

Now we ask, is the conjugate match of such importance that we should be concerned about it? Yes it is, if we are to understand why antenna tuners perform their intended task of matching the complex impedance appearing at the input of a transmission line that is Z_0 mismatched to an antenna, while also establishing a conjugate match that overrides the Z_0 mismatch at the antenna. *The principles of conjugate matching are fundamental to the matching function performed by the antenna tuner, and are indeed fundamental to all impedance matching obtained with any impedance-matching device that allows delivery of all available power from its source!* Additional material pertinent to understanding the matching function performed by the antenna tuner is presented in Chapter 24, "The Conjugate Match and the Z_0 Match."

Sec 19.6 The Vital Role of Energy Storage in the Tank Circuit in Providing Linear Operation at Output

We now return to conduct a close examination of the vitally important flywheel effect of the tank circuit. The energy storage (Q) in the tank produces the flywheel effect that isolates the nonlinear pulsed energy entering the tank at the input from the smoothed energy delivered at the output. As a result of this isolation the energy delivered at the output is a smooth sine wave, with linear voltage/current characteristics that support the theorems generally restricted to linear operation. We know that the widely varying voltage/current relationship at the tank input results in widely varying impedances, which precludes the possibility of a conjugate match at the input of the tank circuit. However, the energy stored in the tank provides *constant impedance at the output* that supports both the Conjugate Matching and the Maximum Power-transfer Theorems.[1]

The acceptance by many engineers and amateurs of the notion that the output of the RF tank is nonlinear is a reason some readers will have difficulty appreciating that the output of the RF tank circuit is linear, and thus can support the conjugate match.

Valid analogies among different disciplines are often helpful in clarifying difficulties in appreciating certain aspects of a particular discipline. Fortunately, energy storage in the mechanical discipline has a valid and rigorous analogous relationship with energy storage in LC circuitry that makes it appropriate to draw upon a mechanical example to clarify the effect of energy storage in the RF tank circuit. (A further convincing analogy involving water appears later in the chapter, in which the origin of the term *tank circuit* is revealed.)

The smoothing action of the RF energy stored in the tank circuit is rigorously analogous to the smoothing action of the energy stored in the flywheel in the automobile engine. In the automobile engine the flywheel smooths the pulses of energy delivered to the crankshaft by the thrust of the pistons. As in the tank circuit of the amplifier, the automobile flywheel is an energy storage device, and the smoothing of the energy pulses from the pistons is achieved by the energy stored in the flywheel. In effect, it is the flywheel that delivers the energy to the transmission. The energy storage capacity required of the flywheel to deliver *smooth* energy to the transmission is determined by the number of piston pulses per revolution of the crankshaft. The greater the number of pistons, the less storage capacity is required to achieve a specified level of smoothness in the energy delivered by the flywheel. The storage capacity of the flywheel is determined by its moment of inertia, and the storage capacity of the tank circuit in the RF amplifier is determined by its Q.

As stated earlier, the tank circuit in the RF amplifier receives two overlapping pulses of energy per cycle. However, if the effect of the overlapping pulses were considered to be a single pulse, we would have a condition that is somewhat analogous to an engine having only one cylinder. If we were to assume that the piston in the one-cylinder engine delivers one thrust of energy per revolution, it is evident that a large amount of energy storage is required to enable the crankshaft to deliver a smooth output during the entire rotation of the crankshaft. In this case, a very heavy flywheel is required to deliver a smooth output. This is also the case with the RF tank circuit, which requires a Q of 10 to 12 to yield a smooth sine-wave output with an acceptable minimum of harmonic ripple. Because the tank receives only one pulse of energy per cycle, it must store many times the amount of energy in comparison to the amount it passes through, to provide a continuous sine-wave output when supplied only with pulses of energy at the input. Thus, the energy storage capacity of the tank provides for the smoothed *linear* output to the load circuit despite the *nonlinear* pulsed input, which, for the purpose of analysis, allows the pulsed source and tank to be replaced with an equivalent Thévenin generator whose output impedance equals R_{Lout}. Although no conjugate match exists at the input of the pi-network tank, because of the large variation of impedance in the current pulses, the isolation derived from the flywheel action of the tank thus allows a conjugate match to exist between the output of the tank and its load, a concept that will become clear as we continue.

To further clarify the action, and the effect of the energy storage in the tank that achieves a linear voltage/current relationship at the output of the tank, parts of the following discussion are paraphrased from correspondence with Dr. John Fakan, KB8MU. It should be emphasized here that a conjugate match *can* exist between the output of the RF power amplifier and its load because of the linear voltage/current relationship at the output of the tank resulting from the energy storage in the tank.[1]

The tank circuit stores the energy by passing it back and forth cyclically between the L and C components, and passes only a fraction of that energy to the tank's load on each cycle. Because the amount passed on to the load is such a small fraction of the total stored in the tank, and because even that small amount is restored during the cycle, the tank can be considered to be an *active* source. Because it can be considered as an active source, we have no need for an interest in what is going on ahead of it in the overall system (as far as what the downstream devices see).

Consider that when designing to get energy from a power supply, our concern is only with the characteristics seen at the power-supply terminals. Our design does not depend on whether the line feed to the supply is single-phase or three-phase, 60 Hz or 400 Hz, or even if the power factor is unity or some other value. None of that matters once you know what shows up at the output connections of the supply. For our purposes the actual source of ener-

gy is the connection at the output of the supply, and the characteristics at that point will be determined by the components in the filter circuitry.

As a source of sinusoidal energy, our RF amplifiers are no different. The "source" of this energy that will be passed on to our antenna system is the *tank*. The load connected to the output port of the amplifier can only see the voltage swings and the impedance presented by the tank components. A properly designed tank (of any type) will not pass so much energy on each cycle that the relationship between its terminal voltage and current is affected enough to cause nonlinearity. Sometime during the cycle even that small amount of energy will be replaced, thus maintaining its operating levels.

Because this "new" source happens to present a linear impedance to its load (the first connection in our antenna system), we need have no concern about nonlinear processes occurring at points upstream of the tank. Once we have a linear active source in the cascade and we do nothing downstream to subsequently cause nonlinearities, we can take advantage of those theorems and ideas that depend on the linearity of the network.

My teachings in "Reflections" depend on the linear nature of the energy transfer from the amplifier's output port right on through to the last antenna element. Because the energy to this network is supplied by a linear source (the tank), everything in my teachings can be assured of sound scientific basis. Objections by others, based on nonlinearities ahead of the tank simply are not applicable.

The energy pulses supplied to the tank must be sufficient to "refill" the tank's energy store on each cycle. The connection where that energy transfer occurs is the one at the input to the tank. As stated earlier, at that point in the typical amateur pi-net class-C amplifier, the load is the tank input, and the source is the combination of two processes: (1) the blocking capacitor in series with the active device (the tube), and (2) the same blocking capacitor in series with the RF choke and the voltage of the power supply. These two sources are paralleled at the connection, but operate at different, but overlapping, times through the cycle.

The load resistance R_L appearing at the input to the tank is determined by the value required to accommodate the energy-transfer requirement to provide enough energy per cycle to make up for that being transferred by the tank to its load. Because of the lack of linear or even simple square-wave characteristics of the active device, the designs in this region have always been very empirical. Actual experience and a good "seat-of-the-pants" feel for the significance of active device data sheets have been the main tools for the design of tank circuits. The amount of energy delivered via the action of the active device (the tank) is dependent on a number of things, such as drive, feedback, supply voltages, etc. They all can play a role in providing for the right amount of energy transfer to allow the tank to function as a linear active source.

If the tank does not receive enough energy to sustain the power level it has established with its load, it will decrease in output accordingly. Malfunctioning of the upstream energy "bucket brigade" can result in linear operation at a lowered level, or in nonlinear operation depending on how well the tank design can handle the changes. The important point is that once conditions allow the tank to operate as a linear active source, everything else in the network downstream of the tank is linear and follows the Conjugate Match Theorem and other linear-system theories. Changing the conditions at the input to the pi-network (e.g., changing drive, feedback, etc.) affects the performance of the tank as a linear source of RF energy. If the tank is supplied with energy pulses having a different integrated average energy than that being supplied to the tank's load, the tank's output characteristics will change to fit the available energy. It will do this by changing its output impedance to whatever value is required so that at the new conjugate matching point the voltage-current product will equal the energy rate available. It has no choice, since the Conjugate Matching Theorem requires the change in output impedance if it is to continue to be a linear source. Consequently, the load impedance at the output must be changed accordingly to retain the conjugate match. If the changes are too extreme, it may not be able to accommodate the required impedance change in a linear manner, so wave-shape distortion could occur—e.g., flat topping.

The important point is that the design and operation of the circuitry providing energy input to the tank circuit involves a number of issues having to do with protection of the active device, stability,

efficiency, etc., as well as the amount of energy transferred to the tank during each cycle. It doesn't matter that the wave shape of the energy pulse is ugly and would be difficult to characterize mathematically because the tank circuit doesn't care.

Many people concede that amateur Class C amplifiers typically operate at greater than 50% efficiency. They will also agree that it is common to tune for a power peak. They then may avoid agreeing that the tuning process is simply matching the output and load impedances to a common conjugate. Their reason is that the internal "resistance" precludes the higher than 50% efficiency. The fact that there are two *independent* definitions for the word *resistance* doesn't seem to matter. They are completely ignoring Definition 2 of the IEEE definitions of *resistance*, the non-dissipative resistance—i.e., the real part of the impedance. To clarify the two independent definitions of resistance, Definition 1 and Definition 2, please refer to Appendix 10 for the IEEE definitions and an in-depth treatment of the two.

RF power amplifiers are necessarily designed to match to load impedances at or near the characteristic impedance of common coaxial transmission lines. No other design value would make sense. The Conjugate Match Theorem is simple and absolute: When the energy being transferred across any linearly behaving connection cannot be further increased simply by changing the impedance of either source or load, a conjugate match exists. Also, that is commonly the operating condition for amateur Class B and C RF amplifiers. From the tank circuit forward, the behavior is linear, because the voltage and current at the input of the tank are continuous and sinusoidal due to the energy storing ("flywheel"), smoothing action of the tank. There is really no wiggle room for debate.

Sec 19.7 Origin of the Term *Tank* Circuit

Let me digress for a moment to say that it is customary for an author of a chapter such as this to have his writing peer-reviewed to uncover possible errors that may have escaped him. Therefore, because this chapter is primarily concerned with presenting a convincing argument that a conjugate match does indeed exist in RF power amplifiers, I have attempted to make sure it contains no conceptual or substantive errors, or invalid statements. Consequently, I requested several professional RF engineers with unquestionable credentials and expertise to review and critique this chapter. All reviewers but one found my presentation accurate. This dissenting reviewer flat out rejected the concept that the pi-network tank circuit isolates the pulsed input from the output, and therefore he maintained that the output circuit of the pi-network cannot support or sustain linear operation, thus no conjugate match. It therefore occurred to me that others also might have difficulty in accepting the concept of energy storage in the tank circuit providing isolation between the input and output of the tank, allowing linear theorems, such as the Maximum Power-transfer Theorem and the Conjugate Matching Theorem, to be valid at the output. I have already presented two examples of the storage of mechanical energy that illustrate the smoothing function of energy storage and that are precisely analogous to energy storage in the tank circuit of the RF power amplifier. In addition, a valid water analogy where the operative word is *tank* in the literal sense might further clarify the issue. I also believe you'll find it interesting to learn how the term *tank* originated as an active description of the LC circuit used in the output coupling of all RF power amplifiers.

Legend has it that in the early days of RF amplifier development the "water tank" analogy was applied for the very purpose of explaining the energy-storage function of the LC output circuit. It goes like this: A water tank is filled to a specific depth, which causes a corresponding pressure applied on the bottom. A hole is made in the bottom with a size that allows one gallon per minute to flow with the specific applied pressure. Water is added at the top of the tank at the rate of one gallon per minute, thus maintaining the original level in the tank as the water flows smoothly out from the bottom. Let's now consider how the water is added at the top. It can be added in spurts, but the water flowing out from the bottom will still flow smoothly without ever knowing the nature of the spurts added at the top. The spurts can be added at a rate of one gallon dumped in every minute, a half gallon twice during the minute, or one-thirtieth of a gallon thirty times per minute, etc. You get the picture. As long as enough water is added to main-

tain the original level, thus maintaining the same constant pressure at the bottom, the water will continue to flow smoothly from the bottom at the rate of one gallon per minute, regardless of how the water is added at the top. It is the *energy stored in the tank* that isolates the intermittent addition of water at the top from the continuous flow at the bottom. If the tank is filled to a higher level (greater depth), the pressure at the bottom is increased, resulting in an increased rate of flow of water at the bottom in direct proportion to the increase in pressure.

It should be appreciated that the *fluid impedance* at the output of the tank (the ratio of the pressure to the flow rate), at which the energy contained in the water flowing from the bottom of the water tank, is established solely by the size of the hole and the height of the water above the hole. The same energy rate can exist with a tall tank and a small outlet hole (high output impedance) or shorter tanks with appropriate larger holes (low output impedance). However, the impedance and linearity of the *input* to the tank is irrelevant as long as it results in maintaining a constant water level. Thus, the action at the bottom is linear even though the action at the top is not.

The same is true in the *tank* circuit of the RF amplifier. The impedance at the output of the RF tank is the ratio of the voltage to current at which power is being delivered to the tank's load. The voltage and current appearing at the output of the pi-network tank circuit are analogous to the water pressure at the bottom of the tank (voltage) and the rate of flow of the water (current) out of the tank. As in the water tank, the shape of the current pulses entering the pi-network tank has no effect on the smooth sinusoidal voltage and current appearing at the output. If the average integrated energy of the current pulses entering the tank increases, the voltage and current at the output will increase in a linear relationship. Thus, it is shown that the output of a properly designed RF tank circuit is linear and the theorems associated with linear circuits are applicable.

Sec 19.8 Measuring Output Resistance of the RF Power Amplifier

Background

I have developed a test setup and procedure based on the standard IEEE load-variation method for measuring the source or output resistance ROUT of networks; they are described below. Measurements made with this setup and procedure show that output resistance ROUT equals the load resistance RLOAD when the amplifier is initially adjusted to deliver all of its available power to that load, thus proving the existence of a conjugate match. However, before proceeding further it will be helpful to obtain an appropriate perspective by reviewing some background concerning the issue.

There has never been a problem in determining the correct value of load resistance RL appearing at the input of the pi-network tank circuit of the RF amplifier. Resistance RL is routinely calculated using either the Terman equation or the more precise Chaffee analysis to determine the slope and other characteristics of the operating load line, as mentioned earlier. After the network has been adjusted to deliver its intended power into its terminating load, resistance RL appearing at the input of the network is easily and routinely measured with appropriate impedance measuring equipment with the amplifier powered down.

However, determining the *output* resistance ROUT appearing at the output of the pi-network has been daunting. Wild speculations abound, without measurements being made concerning the output resistance, because of the misunderstandings and incorrect assumptions concerning the actions of the tank circuit as described previously in Sec 19.2. The misconception that a conjugate match cannot exist at the output of RF power amplifiers has precluded logical reasoning that when the amplifier is delivering all its available power there is a conjugate match by definition. Consequently, it has been considered unthinkable that the output source resistance could possibly be equal to the load resistance.

I am not aware of any writings in the professional literature that discuss the measurement of ROUT. A probable reason for this lack of discussion is that knowledgeable people know that ROUT must equal the load resistance when all the available power is being delivered, and it would therefore be redundant to state it. However, it is now appropriate to describe the test setup and procedure that yields the correct value of source resistance ROUT, *the value that* ***equals*** *the load resistance.* Consequently, using the IEEE load-variation procedure described below, it will be seen that the data resulting from

my measurements (also shown below) prove the existence of the conjugate match at the output of RF power amplifiers.

It should be noted here that the data obtained from my measurements were verified by Tom Rauch, W8JI, who is an RF power amplifier design engineer for Ameritron.

The test setup I developed for measuring the output resistance R_{OUT} of RF power amplifiers is arranged to use the load-variation method of measurement, based on the IEEE expression for measuring the output resistance of networks. The IEEE expression is $R_{OUT} = \Delta E \div \Delta I$, where E and I represent the corresponding change in load voltage and load current, respectively, with each change in load resistance R_{LOAD} terminating the network. In the measurements described below all values of R_{LOAD}, (R_1 and R_2) are pure resistances, $R + j0$. In these measurements the output load resistance R_{OUT} (R_1) terminating the pi-network is selected and the parameters of the amplifier are then adjusted to obtain delivery of all the available power into that load at a given drive level. Then by varying the load resistance a small amount (to R_2), less than a 10% change from R_1, and then measuring the change in load voltage and current, the output resistance is obtained by substituting those voltage and current values in the IEEE expression for R_{OUT} shown above.

The equipment used in the measurements consisted of the following: A Kenwood TS-830S transceiver with two parallel 6146 tubes and pi-network tank circuit for the RF power amplifier. A Hewlett-Packard HP-4815A RF Vector Impedance Meter modified for digital readout, along with ESI 250-DA universal impedance bridge, for measuring RF and DC resistances of non-inductive load resistors R_1 and R_2. An HP-8405A Vector Voltmeter modified for digital readout for measuring voltages appearing across load resistors R_1 and R_2, and an HP-410B RF Voltmeter with HP-455A Coaxial Adapter, also modified for digital readout to indicate load voltage. The RF Vector Impedance Meter was used to confirm that the load resistors contained zero reactance. The experiments were conducted at 4.0 MHz.

Procedure

The pi-network output of the amplifier was initially terminated with R_1, then tuned and loaded to deliver a specific maximum available output power with a given level of grid drive. The load voltage E_1 was then measured with load R_1, and then the load was changed to R_2 and load voltage E_2 was measured. Load currents I_1 and I_2 were then determined by calculation of $I = E/R$, using the measured values of R and E. Finally, as stated above, $R_{OUT} = \Delta E \div \Delta I$, as shown in the data resulting from the measurements shown in Table 19.1.

Load Resistance	Load Voltage	Load Current	Output Resistance	Measured Power Out
51.2	75.9	1.482	52.7	112.5
44.6	70.6	1.583	111.6	
	Δ = 5.3	?=0.101		
51.2	76.9	1.502	51.2	115.5
44.6	71.6	1.605		114.9
	Δ = 5.3	Δ = 0.1034		
51.2	69.75	1.36	49.4	94.9
46.4	66.29	1.43		94.8
	Δ =3.46	Δ = 0.70		
51.2	62.5	1.22	51.7	76.25
46.4	59.4	1.28		76.0
	Δ =3.1	Δ =0.60		
51.2	77.8	1.519	47.8	118.2
46.4	74.1	1.597		118.3
	Δ =3.7	Δ =0.078		
51.2	77.5	1.514	47.4	117.3
47.75	74.9	1.569	**Average**	117.5
	Δ =2.6	Δ =0.0549	**50.3 ohms**	

Table 19-1. Using standard IEEE small-load-variation method to measure network output source resistance.

The amplifier was tuned and loaded with drive level set to deliver maximum available power of 120 watts. All adjustments remained undisturbed thereafter. The data in Table 19.1 was obtained using the Heathkit HW-100.

The reason for the variation, or scatter, in measured output resistance and output power seen in the data in Table 19.1 was found to be the short-term sag in output power between the measurement of R_1 and R_2. This problem was solved by changing the switching from R_1 to R_2 from manual to coaxial relay, thus reducing the time delay, and by waiting until the sag in power output bottomed out. However, the worst-case difference between the R_1 load of 51.2 ohms and the R_2 value that yielded R_{OUT} of 47.35 ohms is a mismatch of only 1.081:1, with a reflection coefficient of 0.039, for a conjugate mismatch loss of only 0.0066 dB.

After many more measurements similar to those above, except for adjusting the pi-network for delivery of maximum available power prior to each measurement, I found that with load R_L now at 51.0 ohms, the measured values of R_{OUT} varied randomly within 11 ohms on either side of the 51.0-ohm load with each measurement—i.e., from 40 ohms to 62 ohms. However, I discovered the variation results from the very small slope of the power output curve near the peak. Using only the analog output-power meter to observe the point at which the power was maximum, I found it impossible to find the true peak in output power where R_{OUT} equals R_L of 51 ohms, because the characteristics of the matching curve near its peak appear to be more like a "round-top hill" than a peak. Evidently, the adjustment for maximum output requires a method of indication that provides better resolution than that obtained with the analog output-power meter alone. On the other hand, the mismatch between 51 and 40 ohms, and between 51 and 62 ohms, is only 1.28:1, for a voltage reflection coefficient of 0.12, which results in a conjugate mismatch loss of only 0.066 dB at the maximum 11-ohm difference from 51 ohms.

The next step in the procedure yielded the required increase in resolution of the data required to find the exact point on the output curve where the output is maximum and R_{OUT} equals the load R_L. After the maximum output that could be obtained by observing the indication on the analog output power meter was reached, R_{OUT} was measured at that point. The pi-network was then readjusted in very small increments, measuring R_{OUT} after each readjustment until R_{OUT} became equal to 51.0 ohms. The increments were so small that the difference in output power at each increment was indiscernible on the analog power meter. Thus, it is shown that the output or source resistance R_{OUT} of an RF power amplifier is equal to the resistance of the load when the maximum available power of the source is being delivered to the load. It is therefore also evident that a conjugate match exists when the conditions just stated are present.

In addition to measuring R_{OUT} with the load resistance of 51.0 ohms, R_{OUT} was also measured with load resistances of 25 and 16.7 ohms. Using the same technique as described above, R_{OUT} measured 25 ohms when the load resistance was 25 ohms, and consistent with the measurement pattern already developed, R_{OUT} measured 16 ohms when the load resistance was 16.7 ohms. These measurements indicate that when the loading is initially adjusted to deliver maximum available power to any value of load resistance within the matching capability of the pi-network, R_{OUT} equals the load resistance.

There is more. So far we have only considered the condition in which the amplifier is delivering its maximum available power in the CW mode. However, we would also like to know what happens to output resistance R_{OUT} during SSB modulation after the amplifier is first tuned and loaded to deliver maximum available power with a specific drive level. The measurement data appearing in Table 19.2 shows that except for the two caveats stated below, once the operating load line and resistance R_{OUT} are established at tuning and loading, R_{OUT} remains substantially constant over the entire range of drive and output power encountered during SSB modulation. After setting the drive level for the pi-network to deliver maximum available power of 100 watts, and leaving all adjustments undisturbed thereafter, R_{OUT} was measured at power levels decreasing from 100 watts to 12.5 watts. This range of power levels, as shown in the table, corresponds to approximately the same range of output power prevailing during SSB modulation.

However, the two caveats are necessary to explain the changes in R_{OUT} that appears to conflict with the statement above that R_{OUT} is substantially constant. First, and most importantly, due to imperfect regulation of plate voltage E_P, the increase in E_P (as the plate current and output power decrease) causes a small change in the slope of the load line, resulting in an increase in R_{OUT} that would not occur with perfect regulation of E_P. Second, the scatter in the R_{OUT} data results from the measurements being taken prior to the improved setup and method of taking the measurements that yields more precise data.

As shown in Table 19-2, the maximum value of R_{OUT} is 80 ohms, appearing at the minimum output power level. The conjugate mismatch between the 80 ohms of output source resistance and the 51-ohm load resistance is 1.569, establishing a voltage-reflection coefficient $\rho = 0.2214$, a power-reflection coefficient $\rho^2 = 0.0490$, and thus a transmission coefficient $(1 - \rho^2) = 0.951$, which trans-

Output Power Watts	Network Output Resistance Rout Ohms	Plate Voltage Ep	Plate Current Ip, ma
100.0	48.4	800	270
75.0	58.3	810	240
50.0	57.3	820	190
25.0	74.0	840	140
12.5	80.0	860	110
0.0	NA	890	70

Note increase in network output resistance with increase in plate voltage, due to poor power supply regulation as plate current decreases with decrease in output power.

Table 19-2. Measured network output resistance vs output power, HW-100 transceiver. Also see Table 19-3 and Fig 19-1.

lates to a conjugate mismatch loss of –0.218 dB. This amount of loss is insignificant when considering that the purpose of the experiment was to establish proof that a conjugate match exists throughout the range of output power during SSB modulation.

It should be noted, however, that subsequent measurements using a more refined setup revealed scattering of less than ±10 ohms from the 51.2-ohm load impedance, a much smaller range of error in output resistance than those shown in the table. However, because a typo in the data required a verifying measurement that could not be made in time to meet publication schedule, this data has been omitted. On the other hand, a measurement showing an error in output resistance of 10 ohms relative to the 51.2-ohm load resistance results in a mismatch error of only –0.07 dB. In addition, the duty cycle of speech components during SSB modulation is shorter than the 100% duty cycle in the CW mode used during the measurements.

Therefore, it is reasonable to conclude that with the already insignificant loss in power due to the change in output resistance resulting from imperfect regulation of the plate voltage, the mismatch loss would be even less during the duty cycle encountered during speech transmission. Thus, we have proved that a *realistic* conjugate match prevails during all levels of SSB modulation, despite the imperfect plate-voltage regulation. We have also shown that the output of a properly designed RF tank circuit is linear, and that the theorems associated with linear circuits are applicable in the use of RF power amplifiers in the SSB mode.

However, the picture is even more optimistic when using the same measurement procedure with the Kenwood TS-830S transceiver. It can be seen from Table 19.3 and Fig 19.1 that the variation in output resistance with this transceiver is much less than with the HW-100 over the entire range of drive and output power. The reason for the nearly constant output resistance with the TS-830S is better plate-voltage regulation of the power supply. It should be especially noted that in the region of constant output resistance of the network with changes in power level from 102.3 to approximately 25 watts, the constant output resistance indicates a *constant slope* of the load line with changes in drive and power level, a point that has been in dispute in the absence of appropriate measurements. It is also important to observe that at the 10-watt output level, where the output resistance has increased somewhat due to imperfect voltage regulation (plate voltage increase with decrease in power), the mismatch between the 51.2-ohm load resistance and the 58.6-ohm output resistance is $58.6 \div 51.2 = 1.145{:}1$. This small mismatch results in a voltage-reflection coefficient $\rho = 0.0674$, a power-reflection coefficient $\rho^2 = 0.00454$, and thus a transmission coefficient $(1 - \rho^2) = 0.9955$ (99.55%), which translates to an insignificant conjugate mismatch loss of only 0.0198 dB with minimum speech level referenced to zero loss at maximum speech level.

Except for the lowest levels of speech that would result in output power less than 10 watts during SSB modulation, the data in Tables 19.2 and 19.3 and Fig 19.1 show that the output resistance of the RF amplifier remains sufficiently constant over the normal range of speech levels, ensuring a realistic conjugate match during SSB modulation. Additionally, extrapolation of the data extending the range of output power below 10 watts clearly indicates that further increase in output resistance dur-

Nominal Power Out	RLOAD	ELOAD	ILOAD	ROUT	Measured Power Out	Ep	Ip ma	Measured Power In
100 w	51.2	72.381	1.414	50.2	102.3	790	265	209 w
	43.5	66.548	1.530		101.8			
		ΔE = 5.833	ΔI = 0.161					
75 w	51.2	62.738	1.225	49.0	76.9	790	240	190 w
	45.3	57.738	1.327		76.6			
		ΔE = 5.000	ΔI = 0.102					
50 w	51.2	50.238	0.981	50.2	49.3	810	195	158 w
	43.5	46.190	1.062		49.1			
		ΔE = 4.048	ΔI = 0.081					
25 w	51.2	35.357	0.691	50.5	24.4	810	165	134 w
	43.5	32.500	0.747		24.3			
		ΔE = 2.857	ΔI = 0.057					
20 w	51.2	32.857	0.642					
	43.5	30.119	0.692	54.1	21.1	820	135	111 w
		ΔE = 2.738	ΔI = 0.051		20.8			
10 w	51.2	23.453	0.458	58.6	10.7	825	110	91 w
	43.5	21.429	0.493		10.6			
		ΔE = 2.024	ΔI = 0.035					

Note: ROUT = ΔE/ΔI

Table 19-3. Measuring output resistance of RF amplifier of TS-830S transceiver at 4.0 MHz at various power levels determined by drive level with all other adjustments undisturbed. See Fig 19-1 and Table 19-2.

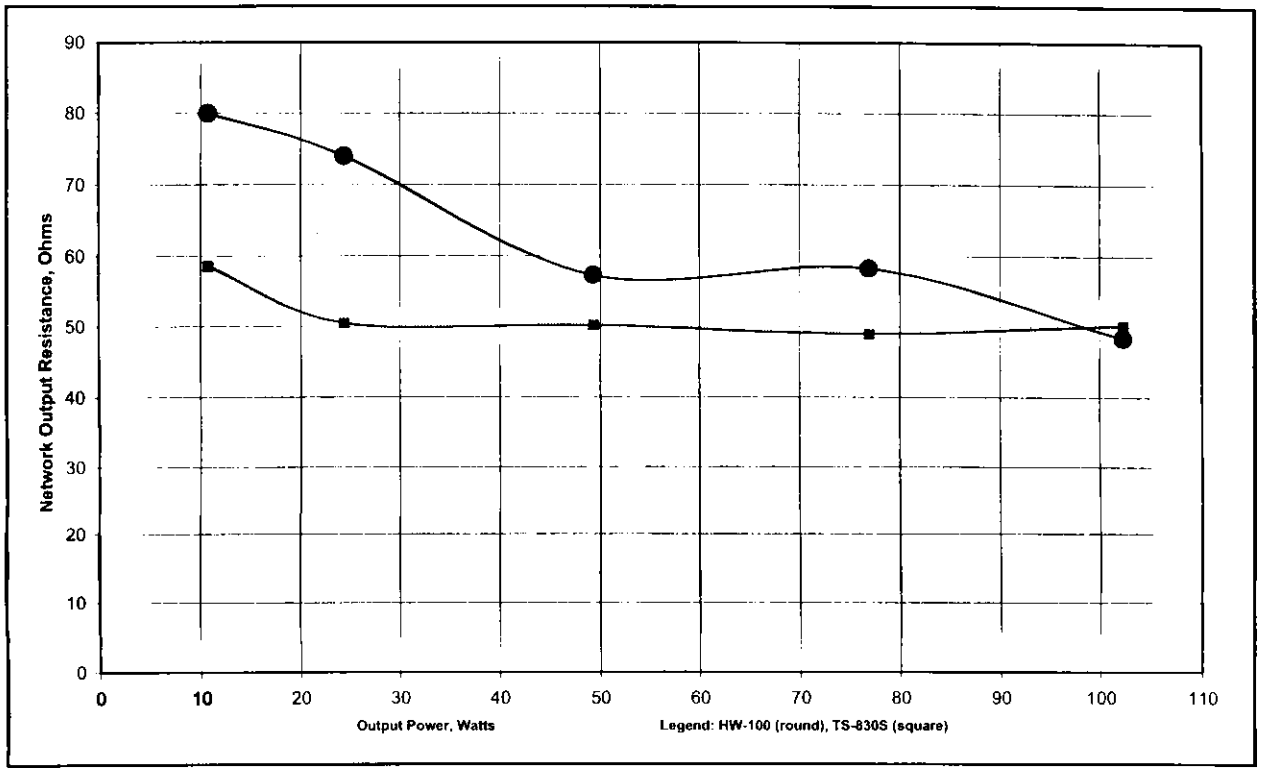

Fig 19-1. Measured network output resistance of Heathkit HW-100 and Kenwood TS-830S vs output power level set by drive level. See Tables 19-2 and 19-3.

ing the lowest practical levels of speech transmission is insignificant relative to load mismatch. Consequently, a realistic conjugate match exists over the entire range of speech levels.

Before concluding this subject, another way of explaining the action occurring in the amplifier during SSB modulation is that as the average integrated energy of the current pulses entering the tank changes with speech modulation, both the RF voltage and current at the output of the tank change linearly in proportion to the modulation level. Consequently, the ratio of output voltage to output current remains constant during speech modulation. Also, since the output resistance ROUT is determined by the ratio of current to voltage, the output resistance also remains constant and equal to the load resistance during modulation. Thus, all the available power from the source is delivered to its load at all levels of speech, satisfying the condition required for a conjugate match at the junction of the source and load during all levels of SSB modulation.

However, before concluding this section, let's discuss the conditions that would prevail assuming perfect regulation of plate voltage EP. With a constant plate voltage the slope of the load line would *remain constant* with changes in drive level proportional to SSB modulation, and consequently, the value of output resistance ROUT would also remain constant during modulation. This is because as the average integrated energy of the current pulses entering the tank changes with speech modulation, both the RF voltage and current at the output change in a linear relationship proportional to the modulation level. Consequently, the ratio of output voltage to output current remains constant, and thus the output resistance ROUT also remains constant. Thus, we have shown that when the output source resistance of an RF power amplifier equals its load resistance, all the available power from the source is delivered to its load, satisfying the condition required for a conjugate match at the junction of the source and load.

Sec 19.9 Justifying the IEEE Method for Determining Network Output Resistance

Recall that in the measurements described above to determine the network output resistance, the change in load resistance is *small*, around ±10% from the matched load resistance. The change in load must be small to avoid a significant change in the normal operation of the amplifier that would distort the results if the change in load resistance were relatively large. For example, a change in load that would result in a significant change in plate current would change the slope of the load line and the output resistance of the network. On the other hand, for examination and comparison, the data appearing in Table 19.4 and Fig 19.2 show the change in network output resistance (and magnitude of impedance) that results from somewhat larger changes in load resistance. Note that the magnitude of the output impedance changes linearly, but in indirect proportion to the load resistance. However, as seen in Fig 19.2, the output magnitude remains close to the load resistance when the load resistances are close to the value at which the network was adjusted for delivery of all available power. Thus, the questions are why are the changes in output impedance *in*directly proportional to the load resistance, and why does the measured output resistance equal the load resistance when the change in load resistance is small? The answer is in the amount of the resulting change in plate current with change in load, which directly affects the slope of the load line and network output resistance. As we will see, when the change in load is sufficiently small, the change in plate current is also so small that the resulting change in amplifier operation is insignificant in relation to causing error in the measurement of the network output resistance. Now let's examine the pertinent changes.

With the matched load (53.1ohms) the plate current was 260 ma; 280 ma with the 27.7-ohm minimum load resistance (network output impedance Z = 76.7 ohms) and 210 ma with the 85.7-ohm maximum load resistance (network output impedance Z = 22.5 ohms). However, when the load was changed from 53.1 to 49.0 ohms to obtain ZOUT = 52.7 ohms (see Table 19.4), any change in the 260 ma of plate current resulting from this small change in load was too small to be discernible on the 0–300 ma meter.

Observing Fig 19.2, it is interesting to note that in the range from the load resistance of 37.3 ohms (mismatch 1.42) to 63 ohms (mismatch 1.19) the square root of the product of the network output impedance and load resistance remains close to the

RLOAD (RL)	Load Mismatch	ELOAD (EL)	ILOAD (IL)	ZOUT (Zo)	Sq. Root RL x Zo	Power Delivered
53.1		71.0	1.34	76.7		94.9
27.7	1.92:1	46.0	1.66		46.1	76.4
53.1		73.0	1.37	67.6		100.4
37.3	1.42	59.0	1.58		50.2	93.3
53.1		72.0	1.36	56.1		97.6
43.9	1.21	65.0	1.48		49.6	96.2
53.1		75.0	1.41	52.7		105.9
49.0	1.08	72.0	1.47		50.8	105.8
53.1		74.0	1.39	41.35		103.1
61.1	1.15	78.5	1.28		50.25	100.9
53.1		73.0	1.37	39.0		100.4
63.0	1.19	78.2	1.24		49.57	97.1
53.1		74.0	1.39	31.95		103.1
66.6	1.25	80.1	1.20		46.13	96.3
53.1		74.0	1.39	29.1		103.1
73.3	1.38	82.0	1.12		46.13	91.7
53.1		74.5	1.40	22.5		104.5
85.7	1.61	84.0	0.980		43.95	82.3
					Average 48.0	

Table 19-4. Pi-network output impedance magnitude Z vs load resistance Kenwood TS-830S at approximately 100 watts output, 4.0 MHz.

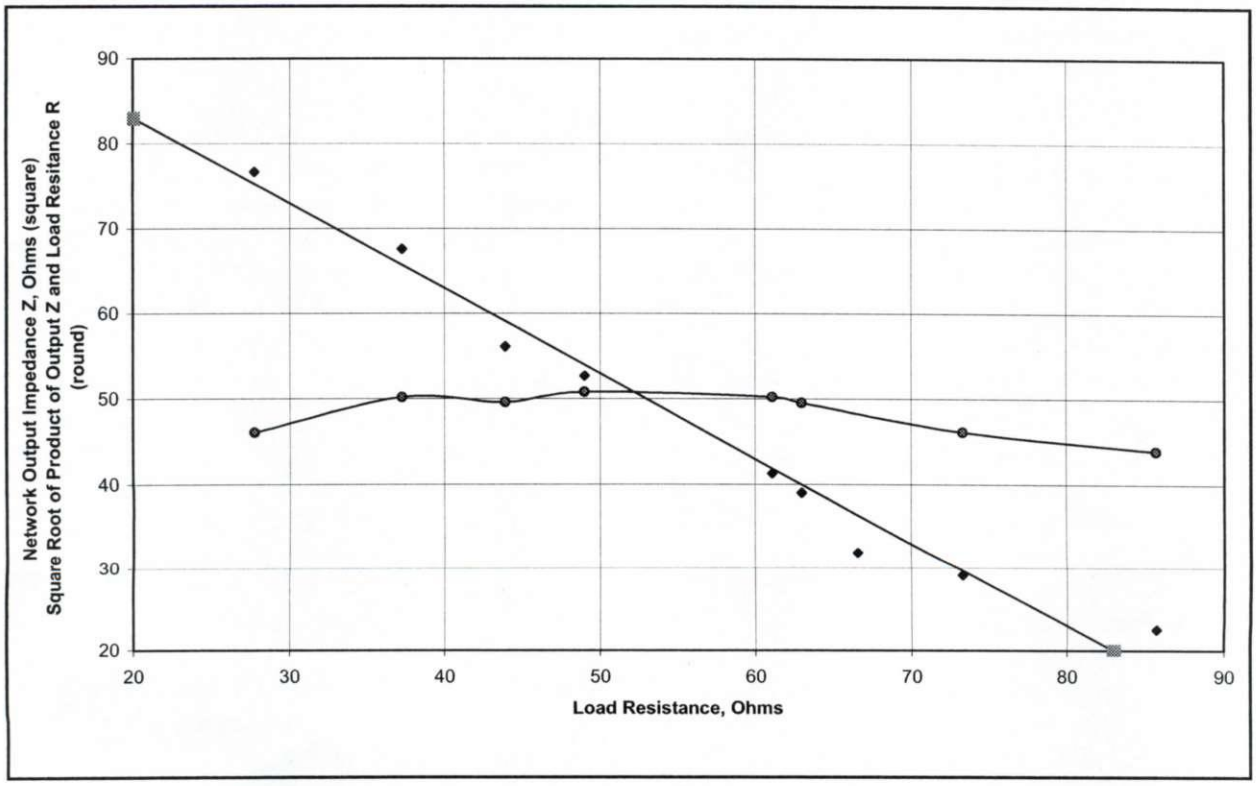

Fig 19-2. Kenwood TS-830S RF amplifier pi-network output impedance Z vs load resistance. All available power of approximately 100 watts delivered initially to 53.1-ohm load. All adjustments left undisturbed during measuring of other load values. See Table 19-4.

Network Load Ohms	Mismatch Re 52.0 Ohms	Network Input Z Polar	Network Input Impedance Rectangular (R + *j*X)
240.0	4.6:1	950@58°	503.4 + *j*805.6
160.0	3.17	980@48°	655.7 + *j*728.3
100.0	1.92	1060@32°	898.9 + *j*561.7
83.0	1.6	1150@20°	1080 + *j*393.3
52.0	1.0	1350@0°	1350 + *j*0
41.0	1.22	1580@–14°	1533 – *j*382.2
34.2	1.52	1630@–18°	1550 – *j*503.7
26.0	2.0	1780@–32°	1509 – *j*943.3
20.6	2.52	1900@–41°	1433 – *j*1245
17.5	2.97	2000@–48°	1338 – *j*1486

Table 19-5. Pi-network input impedance vs non-reactive load resistance HW-100 transceiver initially resonated with 52.0-ohm load at 100 watts output.

value of the load resistance that allows delivery of all the available power (≈50 ohms), but begins to decrease with increased load mismatch on either side of the matched condition. It will be shown later that the reactance introduced by the non-symmetrical network while transforming the non-reactive load resistances to the network input are responsible for the decrease as the mismatch increases in either direction away from the resonant condition.

Let's turn now to Table 19.5, where my measured data shows that impedance transformation through a non-symmetrical network is not the same as that through a perfect transformer having a linear ratio of transformation. Note that except for the 50-ohm load resistance that matches the network output, all other purely resistive load resistances transform through the network to obtain reactive impedances at the input. When plotted on a Smith chart normalized to 1350 ohms, the loci of these input impedances form a straight line at an angle of 64° clockwise from the resistive axis, intersecting the axis at the chart center where the impedance is 1350 + *j*0. Still in Table 19.5, note that when the load mismatch is approximately 2:1 on either side of the matched point, the angles of the impedances are numerically equal with respect to that at resonance, 32° with the high load resistance and –32° with the low load resistance. However, also note that with the high and low load resistances the magnitudes of the input impedances are 1060 and 1780 ohms, respectively. The differences between the matched input impedance (non-reactive) of 1350 ohms are thus 290 and 430 ohms, respectively. Let's now examine the significance of these *measured* input impedances.

First, the 1780 ohms input impedance obtained with the low-resistance load is 140 ohms further off the resonant value than the 1060 ohms with the high-resistance load, resulting in the higher off-resonance plate current with the low-resistance load than for the high-resistance load with same degree of mismatch (1.92:1 and 2.0:1, respectively).

Second, the measured input impedances resulting from two load resistances of ±5 ohms relative to 52 ohms were interpolated on the straight-line locus of all the impedances in Table 19.5. At the resulting two equal input mismatches of 1.12:1, the resulting input impedances normalized to 1350 ohms are 0.95 + *j*0.10 and 1.10 – *j*0.10, respectively, for real values of 1282.5 + *j*135 and 1485 – *j*135 ohms, respectively. With these mismatches of only 1.12:1on either side of resonance, the angle of the mismatched impedances is only ±6°, and the change from normal amplifier system performance of 1.0 only to 0.9968, (99.68%) amounts to a change of only 0.014 dB. Consequently, the small change in amplifier performance under these conditions is insignificant with respect to contributing to error while using the standard IEEE load-variation method in the measurement of network output impedance.

In conclusion, my measurements and discussion in this chapter prove that the output of a properly designed RF tank circuit performs with a linear relationship between output voltage and current. Consequently, the theorems associated with linear

circuits, such as the Conjugate Matching Theorem and the Maximum Power-transfer Theorem, are valid and applicable in both the analysis and practical operation of RF power amplifiers performing in both CW and SSB modes.

Sec. 19.10 Additional Experimental Evidence Proving the Existence of Conjugate Match and Non-Dissipative Source Resistance in RF Power Amplifiers

The additional data presented below was obtained through experiments performed since the 2nd edition of this book was published.

In general, R_S is greater than R_L, because plate current is zero for a portion of the cycle. Therefore, it is true that there can be no conjugate match at the *input* of the pi-network. This condition occurs *only at the input* of the pi-network tank circuit because of the non-linear plate voltage-current relationship appearing there. However, the effect of energy storage in the pi-network tank circuit isolates the non-linear condition at the input of the network from the *output* of the network, allowing the voltage-current relationship E/I at the output to be linear, thus supporting the conjugate match at the network output.

Furthermore, the *true* source resistance of the RF power amplifier is the dynamic resistance looking rearward toward the plate from the input of the pi-network which we shall call R_{LP}. It is *not* R_S, nor is it R_P, both of which will be defined later. Maximum available power is delivered into the pi-network tank circuit when the input resistance R_L of the pi-network at resonance equals R_{LP}, not R_S:

$$R_L = \frac{e_p}{i_p}$$

where e_p = peak RF fundamental plate voltage, and i_p = peak RF fundamental plate current during the conditions where the minimum RF plate voltage and maximum grid voltage are equal, the condition for delivering the maximum power into the load. R_L is represented by the slope of the load line, which can be determined using the Chaffee Analysis as described in Sec 19.3a.

However, the true *output source resistance* is a resistance we will call R_{OS} = E/I, the time-unvarying, linear voltage-current ratio that occurs at the *output* of the pi-network when the external load resistance $R_{LOAD} = R_{OS}$, and when the network is designed to transform resistance R_{OS} at the network output to resistance R_L at the network input. Therefore, R_{OS} is the correct resistance for use in the definition of the conjugate match, not R_S.

Consequently, the equality required for the conjugate match to exist at the output of the RF power amplifier is $R_{LOAD} = R_{OS}$, (not $R_L = R_S$), where R_{LOAD} is the load resistance external to the output pi-network. Thus, it is evident that there *can* be a conjugate match at the *output* of an RF power amplifier, while not at the input.

Sec 19.11 The Maximum Power-transfer Theorem

Before continuing, it may be helpful in appreciating the conjugate match to remind ourselves of the meaning of the Maximum Power-transfer Theorem, and its relation to conjugate matching, as stated by Everitt (*Ref 17*):

The maximum power will be absorbed by one network from another joined to it at two terminals, when the impedance of the receiving network is varied, if the impedances looking into the two networks are conjugates of each other.

A corollary of this theorem is *there is a conjugate match if the delivery of power decreases when the receiving impedance (the load) is either increased or decreased.*

It should be understood that this corollary is practiced whenever an RF power amplifier loading is being adjusted for delivery of all available power at any given drive level. This means that the amplifier is power limited at that drive level, and that when conjugately matched to its load, all the power available at that drive level is delivered to the load. In addition, when the load is initially adjusted to receive all the available power at the saturation level (when minimum plate voltage equals maximum grid voltage), output source resistance R = E/I increases slightly with decreasing RF grid-drive voltage. From an academic viewpoint this increase in resistance will cause a slight deviation from the perfect conjugate match that existed when the source and load resistances were equal at the saturation level of grid drive.

However, in practice, the shape of the peak of the output-power curve with a small change in either

the source resistance or the load resistance is so broad as to have little significance in the delivery of the available power at any given drive level relative to that delivered at the saturation level, where a conjugate match exists when all available power is being delivered to the load. As an example, for a –10% change in source resistance we get an *increase* of 0.012 dB in power delivered; for a +10% change we get a *reduction* of 0.012 dB in power delivered. Even for ±20% changes in source resistance we get corresponding changes of only 0.054 dB in power delivered. My measurements have shown that with power amplifiers using a pair of 6146 tubes in the output, when the drive level and load have been adjusted to deliver maximum power at 100 watts, the increase in source resistance is approximately 10% when the grid drive is reduced to deliver 25 watts. Consequently, when viewing the power-output meter while tuning and loading the transceiver for maximum delivery of power into a 50-ohm load, it is practically impossible to adjust the source resistance closer to 50 ohms than anywhere between 45 to 55 ohms (±10%), because it is impossible to detect a 0.012-dB change in the meter reading. In terms of lost power when considering a deviation from a perfect conjugate match, this amount of change is insignificant.

Sec 19.12 Non-Dissipative Source Resistance

In Sec 19.3 evidence was presented showing that the output source resistance of the RF power amplifier is non-dissipative. This new addition to Chapter 19 provides further evidence of this condition by reporting additional data resulting from measurements performed subsequent to those reported in Secs 19.8 and 19.9. However, before presenting this new evidence, the relationship among R_{LP}, R_L, R_P, and R_S needs to be put into a clear perspective. We will also present a clear definition of the term "Rs" as we proceed. This explanation is in addition to ignoring the effect of energy storage in the pi-network tank.

Sec 19.13 Examining R_P, R_S, R_{LP}, and R_L

We know that resistance R_P is the traditional term for plate resistance, but in Class B and C operation R_P cannot be considered the *source* resistance of the tube. Consequently, the nature of R_P relative to the operation of RF power amplifiers needs to be clearly understood to appreciate its effect on the operation of these amplifiers.

In a vacuum-tube plate resistance R_P is a measure of the ability of a change in plate voltage to produce a change in plate current when the grid voltage is held constant, and is represented by the ratio $R_P = \Delta E_P \div \Delta I_P$. Because of this resistance, plate current increases as plate voltage increases, and vice versa, in the same way current changes in a resistor with changes in voltage. However, we need to understand that plate resistance is not a *physical* resis*tor*, but is a *non*-dissipative resis*tance*, contributing to no loss of power to heat in the tube as the tube converts DC power into AC power. Resistance R_P is non-dissipative because it is simply a ratio as indicated above, and we know that a ratio cannot dissipate power.

To continue, we know that an increase in *grid voltage* also causes an increase in plate current, accompanied by a decrease in plate voltage due to the voltage drop across plate load resistance R_L appearing at the input of the pi-network tank circuit. Consequently, when plate voltage decreases, the effect of resistance R_P tends to retard the increase in plate current as it increases with the increase in grid voltage. The retardation of the increase in plate current is a form of negative feedback that prevents plate current from increasing to the level it would if R_P didn't exist. The greater the value of R_P the less its effect on the change in plate current. Although the lower plate current does result in a loss of deliverable power, it is not power that is dissipated, but only power that was not developed in the first place due to the lower plate current. However, the power lost due to R_P can be compensated for simply by increasing the grid drive to restore the plate current to the value it would have been in the absence of R_P.

To gain further perspective, we know that in triodes the plate current responsible for delivering power varies significantly with changes in plate voltage. Because the value of R_P is relatively low in triodes, the effect of R_P in these tubes results in a substantial opposition to any change in plate current in response to a change in grid voltage. (This is one of the reasons for low gain in triodes.)

However, in contrast to the triode, due to the shielding effect of the screen grid, plate current in tetrodes and pentodes varies *only slightly* with changes in plate voltage, and then only because of the imperfect shielding of the screen grid. Due to the shielding effect of the screen grid the value of R_P is very high in comparison to that of triodes, from five to ten times greater.

It must also be understood that the cathode-to-plate resistance R_{PD} in the tube that does dissipate energy to heat is completely separate from the non-dissipative resistance R_P, and that the dissipation to heat due to R_{PD} results only from the kinetic energy released as the electrons bombard the plate. The product of the instantaneous cathode-to-plate voltage and the instantaneous plate current determines the amount of the energy converted to heat in the tube. However, resistance R_{PD} is in no way associated with the output source resistance appearing at the output of the pi-network.

Now we'll examine the relationship between R_P and R_S. R_S is the effective R_P when the conduction angle θ of the plate current is less than 360°. When conduction angle is 360°, as in Class A operation, $R_S = R_P$. However, when angle θ is less than 360°, resistance R_S increases inversely with angle θ, because the plate current is flowing for a shorter time, at times being zero. For example, when conduction angle $\theta = 180°$, $R_S = 2R_P$, because plate current is zero half of the time. However, it will be helpful in perceiving the basis for our present problem to know the general expression for determining R_S relative to R_P for any value of θ. We first let:

$$R_S = \beta R_P$$

$$\text{where } \beta = \frac{\pi}{\theta_1 - \sin\theta_1 \cos\theta_1}$$

and where θ_1 is expressed in radians (*Ref 159*)

In determining the value of β, the half angle of θ is used, where $\theta/2 = \theta_1$, the angular extension of the conduction period on either side of the peak of the grid voltage and plate current.

In the example above, where $\theta = 180°$, it is obvious that the half angle of θ is $\theta_1 = 90°$. Thus, in solving the example in the above equation we get $\theta_1 = 1.570797$ (radian equivalent of 90°), $\sin\theta_1 = 1.0$, and $\cos\theta_1 = 0$. Because $\cos\theta_1 = 0$, the right-hand term of the denominator in the above equation is zero, reducing the equation to:

$$\beta = \frac{\pi}{\theta_1} = \frac{3.141593...}{1.570797...} = 2$$

verifying that $R_S = 2R_P$ when the conduction angle is 180°.

Now we present a more detailed explanation why the definition requiring that $R_L = R_S$ for a conjugate match to exist when the source is an RF power amplifier is invalid. To avoid confusion we must first be clear on how we view resistances R_{LP} and R_L. R_{LP} is the resistance looking rearward from the network input toward the plate, dependent on the following four independent variables: the DC plate voltage E_B; the DC grid bias E_C; the AC component of the grid voltage E_G (the input signal voltage); angle θ representing the period of plate-current conduction; and the AC plate voltage E_{LC}, the voltage appearing across the input to the LC pi-network tank circuit. In other words, R_{LP} is the average of the varying resistance appearing at the plate, upstream from the network input, during the current pulse. It is important to know that there is a single value of R_{LP} for each useful combination of these independent variables. (As stated earlier in this section, the optimum R_{LP} that allows delivery of the maximum output power is obtained when the minimum RF plate voltage and the maximum RF grid voltage are equal.) The procedure for determining the value of R_{LP} from the values of these variables is beyond the scope of this chapter and book. However, how the operating value of R_{LP} is obtained will be explained later, but it should be understood that all the available (or maximum) power delivered to the load occurs when $R_L = R_{LP}$.

Of the four independent variables listed above, the DC plate voltage usually is not readily available for adjustment; it is the voltage supplied by the power supply. On the other hand, adjustment of grid bias E_C is available to set the bias voltage that controls the resting plate current to the desired value. The grid bias adjustment determines angle θ of the plate-current conduction time, which in turn determines the value of R_S, as explained earlier. The grid drive level control adjusts the input signal grid voltage E_G, which determines the amplitude of the plate current. The final settings of these adjustments presets the value of R_{LP}, and thus determines

the value of R_L, equal to R_{LP}, required to deliver all available power into the pi-network, and finally into the external load.

What, then, is the importance of the value of R_{LP}, and its relation to R_S? First we need to know that there is a specific amount of RF output power available during any one combination of the independent variables. After grid bias E_C is set initially to the desired value, it usually is left undisturbed thereafter. Because the DC plate voltage is a given, the grid drive level is the only remaining adjustment for setting the value of R_{LP}. Next we are ready to adjust the output loading and plate tuning controls to couple the RF power into the feedline or external load. With the grid drive adjusted to the level that will cause the plate current to reach the maximum desired level, we increase the output loading to the point of maximum delivery of power, while keeping the network at resonance with the plate tuning control. At this point all of the power available for the value of R_{LP} set by that particular combination of the independent variables is being delivered. The reason is that with these settings of the loading and plate tuning controls, the load impedance at the output of the pi-network has been transformed to the resistance R_L appearing at the network input terminals, equal to resistance R_{LP} appearing at the plate looking upstream from the pi-network. In other words, when resistance R_L appearing at the input of the pi-network tank circuit equals R_{LP}, all the power available under the present conditions is delivered to the load, regardless of the value of R_S. *However, it must be understood that resistance R_{LP} is not constant over time, but is the average of the non-linear, time-variant, non-dissipative resistance resulting from the time-variant plate-voltage–current relationship throughout each cycle.* Consequently, even though they are equal, due to the cyclic dynamic condition of R_{LP}, there is *no* conjugate match between R_L and R_{LP} at the junction of the plate and the input of the pi-network.

R_L does not have to equal R_S for a conjugate match to exist, because the value of R_S does not appear as a condition responsible for achieving delivery of all the available power. As we know from the correct definition of the conjugate match, it exists when all the available power is being delivered to the load.

As stated in Sec 19.3, the value of R_{LP} during any of these conditions is found by applying a Fourier analysis on the plate-current waveform. The practical and most-used procedure for applying the Fourier analysis is the Chaffee analysis, from which the slope of the load line representing R_L is determined, as noted in Sec 19.3a. It is important to remember that R_L is simply the ratio of peak plate voltage E to peak plate current I, E/I, appearing at the input of the pi-network, when the all available power is being delivered to the load.

It is evident that the plate current flows through both R_S and R_L; thus the DC, fundamental AC, and all harmonic components appear across R_S. However, the high Q of the of the pi-network tank circuit at resonance provides a very low (near zero) impedance to the DC and harmonic components, but a relatively high resistance R_L to the fundamental. Thus, the tank circuit impedes the DC and high-order harmonic frequencies, but passes only the fundamental frequency and low levels of low-order harmonic frequencies, which is why the output of the tank circuit is essentially a sine wave. In other words, only the fundamental and low-level harmonic frequency current flows through R_L.

As explained earlier, R_S is a dynamic resistance occurring only as an inverse feedback to the plate current, not a resis*tor* that can be measured. In the discussion above which defines R_S as the value of R_P depending on the conduction angle θ of the plate current, it is evident that the value of R_S changes inversely with changes in angle θ. However, my own experimental data shows that R_L remains nearly constant over a wide range of power levels. Clearly, then, the difference between R_S and R_L cannot remain constant over a range of power levels.

It is now time to ask the question: "Is it really necessary to invoke R_S at all?" No, not really, because simply using R_L with its value determined by the length of the plate-current conduction period is sufficient.

Sec 19.14 Additional Experimental Data

The source resistance data reported in Secs 19.8 and 19.9 were obtained using the load-variation method with resistive loads. Note that of the six measurements of output source resistance reported in Table 19.1, the average value of the resistance is 50.3 ohms obtained with the reference load resistance of 51.2 ohms, exhibiting an error of only 1.8 percent. However, various critics assert that proof

of a conjugate match between the source and load requires the load to contain reactance. Accordingly, the experimental data reported below were obtained using both the load-variation method and an indirect method for determining the source impedance of the RF power amplifier, with a resistive load to obtain a reference source resistance and a complex load to determine the complex source impedance that is then proven to be the conjugate of the complex load.

We'll now examine the experimental data that resulted from measurements performed subsequent to those reported in Secs 19.8 and 19.9, new data that provides additional evidence that a conjugate match exists at the output terminals of an RF power amplifier when all of its available power is delivered into its load, however complex the load impedance. According to the definition of the conjugate match as explained in Sec 19.1, Axioms 1 and 2, if this condition prevails there is a conjugate match. In addition, the data presented below also provides further evidence that the output source resistance of the RF amplifier is non-dissipative. The following steps describe the experimental procedure I employed and the results obtained:

1. Using a Kenwood TS-830S transceiver as the RF source, the tuning and loading of the pi-network were adjusted to deliver all the available power into a 50 + *j*0-ohm load with the grid drive adjusted to deliver the maximum of 100 watts at 4 MHz, thus establishing the area of the RF power window at the input of the pi-network, resistance R_{LP} at the plate, and the slope of the load line. The output source resistance of the amplifier in this condition will later be shown to be 50 ohms. In this condition the DC plate voltage was 800 v and plate current was 260 ma. DC input power was therefore 800 v × 0.26 a = 208 w. Readings on the Bird 43 wattmeter indicated 100 watts forward and zero watts reflected. (100 watts is the maximum RF output power available at this drive level.) From here on the grid drive was left undisturbed, and the pi-network controls were left undisturbed until Step 10.

2. The amplifier was then powered down and the load resistance R_L was measured across the input terminals of the resonant pi-network tank circuit (from plate to ground) with an HP-4815 Vector Impedance Meter. The resistance was found to be approximately 1400 ohms. Because the amplifier was adjusted to deliver the maximum available power of 100 watts prior to the resistance measurement, the averaged resistance R_{LP} looking into the plate (upstream from the network terminals) was also approximately 1400 ohms. Accordingly, a non-reactive 1400-ohm resistor was then connected across the input terminals of the pi-network tank circuit and source resistance R_{OS} was measured looking rearward into the output terminals of the network. Resistance R_{OS} was found to be 50 ohms.

3. Three 50-ohm dummy loads (a 1500-watt Bird and two Heathkit Cantennas) next were connected in parallel to provide a purely resistive load of 16.67 ohms, and used to terminate a coax of 13.5° length at 4 MHz.

4. The impedance Z_{IN} appearing at the input of the 13.5° length of coax at 4 MHz terminated by the 16.67-ohm resistor of Step 3 was measured with the Vector Impedance Meter and found to be 20 ohms at ∠+26°. Converting from polar to rectangular notation, $Z_{IN} = 17.98 + j8.77$ ohms. ($Z_{IN} = Z_{LOAD}$ from the earlier paragraphs.) This impedance was used in Steps 5 and 6 to provide the alternate load impedance in the load-variation method for determining the complex output impedance of the amplifier, and for proving that the conjugate match exists.

5. With respect to 50 ohms, Z_{IN} from Step 4 yielded a 2.88:1 mismatch and a voltage reflection coefficient $\rho = 0.484$. Therefore, power reflection coefficient $\rho^2 = 0.235$, transmission coefficient $(1 - \rho^2) = 0.766$, and forward power increase factor $1/(1 - \rho^2) = 1//0.766 = 1.306$.

6. Leaving pi-network and drive-level adjustments undisturbed, the 50-ohm load was then replaced with the coax terminated with the 16.67-ohm load from Step 4, thus changing the load impedance from 50 + *j*0 ohms to 17.98 + *j*8.77 ohms, the input impedance Z_{IN} of the coax.

7. Due to the 2.88:1 mismatch at the load, neglecting network losses and the small change in plate current resulting from the mismatch, approximately the same mismatch appeared between R_{LP} and Z_L at the input of the pi-network. Consequently, the change in load impedance changed the network input resistance R_L from 1400 ohms to complex $Z_L \approx 800 - j1000$ ohms, measured with the Vector Impedance Meter using the method described in

Step 2. To verify the impedance measurement of Z_L the phase delay of the network was measured using an HP-8405 Vector Voltmeter and found to be 127°. Using this value of phase delay, the input impedance Z_L was calculated using two different methods—one yielding 792 – *j*1003 ohms, the other yielding 794.6 – *j*961.3 ohms, thus verifying the accuracy of the measurement. However, although grid voltage E_C and grid drive E_G were left unchanged, resistance R_{LP} of approximately 1400 ohms at the plate changed somewhat due to the small changes in plate voltage and plate current due to the change in the load, leaving a mismatch between R_{LP} and Z_L at the input of the pi-network. As stated above, this value of Z_L yielded substantially the same mismatch to plate resistance R_{LP} as that between the output impedance of the pi-network and the 17.98 + *j*8.77-ohm load—i.e., 2.88:1. This mismatch at the network input resulted in less power delivered into the network, and thus to the load, a decrease in the area of the RF window at the network input, and a change in the slope of the loadline. (It must be remembered that the input and output mismatches contribute only to mismatch loss, which does not result in power delivered and then lost somewhere in dissipation. As we will see in Step 8, the mismatch at the input of the pi-network results only in a *reduced delivery* of source power proportional to the degree of mismatch.)

8. Readings on a Bird 43 power meter then indicate 95 watts forward and 20 watts reflected, meaning only 75 watts were then delivered by the source and absorbed in the mismatched load. The 20 watts reflected power remained in the coax, and added to the 75 watts delivered by the source to establish the total forward power of 95 watts.

9. We next compared the measured power delivered with the calculated power, using the power transmission coefficient, $1 - \rho^2$. The calculated power delivered was: 100 w × $(1 - \rho^2)$ = 76.6 w, compared to the 75 watts indicated by the Bird wattmeter. However, because the new load impedance was less than the original 50 ohms, and also reactive, the amplifier was now overloaded and the pi-network was detuned from resonance. Consequently, the plate current increased from 260 to 290 ma, plate voltage dropped to 760 volts, and DC input power increased from 208 watts to 220.4 watts.

10. With the 17.98 + *j*8.77-ohm load still connected, the pi-network loading and tuning were next readjusted to again deliver all available power with drive-level setting still left undisturbed. The readjustment of the plate tuning capacitor increased the capacitive reactance in the pi-network by –8.77 ohms, canceling the +8.77 ohms of inductive reactance in the load, returning the system to resonance. The readjustment of the loading control capacitor decreased the output capacitive reactance, thus reducing the output resistance from 50 to 17.98 ohms. Thus, the network readjustments decreased the output impedance from 50 + *j*0 to 17.98 – *j*8.77 ohms, *the conjugate of the load impedance,* 17.98 + *j*8.77 ohms. The readjustments also returned the network input impedance Z_L to 1400 + *j*0 ohms (again equal to R_{LP}), returned the original area of the RF window at the network input, and returned the slope of the loadline to its original value. For verification of the 1400-ohm network input resistance after the readjustment, Z_L was again measured using the method described in Step 2 and was found to have returned to 1400 + *j*0 ohms.

11. Bird 43 power meter readings following the readjustment procedure then indicated 130 watts forward and 29.5 watts reflected, indicating 100.5 watts delivered to the mismatched load.

12. For comparison, the calculated power values were: Forward power = 100 × 1.306 = 130.6 w, reflected power = 30.6 w, and delivered power = 130.6 w – 30.6 w = 100 w, showing substantial agreement with the measured values. (1.306 is the forward-power increase factor determined in Step 5.) Plate current returned to its original value, 260 ma, and likewise, plate voltage also returned to the original value, 800 volts. Consequently, the DC input power also returned to its original value, 208 watts.

13. It is thus evident that the amplifier returned to delivering the original power, 100 watts, into the previously mismatched complex-impedance load, now conjugately matched, the same as when it was delivering 100 watts into the 50-ohm non-reactive load. However, *the reflected power, 30.6 watts, has remained in the coax*, adding to the 100 watts delivered by the amplifier to establish the 130.6 watts of forward power, proving that it did not enter the amplifier to dissipate and heat the network or the tube.

It must be kept in mind that impedance Z_{IN} appearing at the input of the 13° line connecting the 16.7-ohm termination to the output of the amplifier was the result of reflected waves of both voltage and current, and thus reflected power was returning to the input of the line and becoming incident on the output of the amplifier.

The significance of these measurement data is that for the amplifier to deliver all of its available power (100 watts) into the mismatched load impedance $Z_{IN} = 17.98 + j8.77$ ohms, the readjustment of the tuning and loading of the pi-network simply changed the output impedance of the network from $50 + j0$ ohms to $17.98 - j8.77$ ohms, *the conjugate of the load impedance*, thus matching the output impedance of the network to the input impedance of the coax. Consequently, there *is* a conjugate match between the output of the transceiver and its complex load, QED. The readjustments of the pi-network simply changed its impedance transformation ratio from 50:1400 to $(17.98 - j8.77)$:1400, returning the input resistance R_L of the pi-network to 1400 ohms, the value of R_{LP}. Thus, the plates of the amplifier tubes are unaware of the change in external load impedance.

14. We next made an additional indirect measurement of R_{OS} that proves the conjugate match statement above is true. Leaving the pi-network adjustments undisturbed from the conditions in Step 10, with the amplifier powered down we again connected a 1400-ohm non-reactive resistor across the input terminals of the pi-network tank circuit and measured impedance Z_{OS} looking rearward into the output terminals of the network. The impedance was found to be $Z_{OS} = 18 - j8$ ohms.

From a practical viewpoint, measured impedance $Z_{OS} = 18 - j8$ ohms is the conjugate of load impedance $Z_{LOAD} = 17.98 + j8.77$, proving that the amplifier is conjugately matched to the load, and also proving the validity of the indirect method in determining that the source impedance of the amplifier is the conjugate of the load impedance when all available power is being delivered to the load.

Thus, the data obtained in performing Steps 1 through 14 above proves the following four conditions to be true.

No reflected power incident on the output of the amplifier is absorbed or dissipated in the amplifier, because:

1. The total DC input power is the same whether the amplifier is loaded to match the resistive Z_0 load of $50 + j0$ ohms, with no reflected power, or to match the complex load of $17.98 - j8.77$ ohms with 30.6 watts of reflected power, while 100 watts is delivered to either the Z_0 load or the rematched complex load.

2. All the 100 watts of power delivered by the transmitter is absorbed in both the Z_0 load and the rematched complex load cases, with the same DC input power in both cases.

3. All the 30 watts of reflected power has been shown to add to the source power, establishing the total 130 watts of forward power in the case involving the rematched complex load.

4. All the reflected power is added to the source power by re-reflection from the non-dissipative output source resistance R_{OS} of the amplifier. Had the output source resistance of the amplifier been dissipative, the reflected power would have been dissipated there into heat, instead of being re-reflected back into the line and adding to the source power. In addition, the Bird 43 power meter would have indicated 75 watts of forward power, not 95. This proves that reflected power incident on the output of the amplifier does not cause heating of the tube.

It should also be noted that an accepted alternative to the load-variation method for measuring the output impedance of a source of RF power is the indirect method demonstrated above. As performed during the measurements described above, the procedure for this method is to first make the necessary loading adjustments of the output network to ensure that all of the available power is being delivered to the load. Next, the input impedance of the load is measured. It then follows that, as proven above, the source impedance is the conjugate of the input impedance measured at the input of the load, because when all available power is being delivered to the load, this condition conforms to the Conjugate Matching and the Maximum Power-transfer Theorems (*Ref 17*).

Additionally, I previously performed this same measurement procedure using a Heathkit HW-100 transceiver, using several different lengths of coax

between the 16.7-ohm load and the output of the transceiver in each of several measurements. The different lengths of coax provided different complex load impedances for the transceiver during each measurement. The same performance as described above resulted with each different load impedance, providing further evidence that a conjugate match exists when the amplifier is delivering all of its available power into its load. These results also prove that the single test with the Kenwood transceiver is not simply a coincidence.

Sec 19.15 Summary

More recent experimental evidence has been presented since that of Secs 19.8 and 19.9, adding further proof that a conjugate match can exist when the source is an RF power amplifier, and that the output source resistance of the amplifier is non-dissipative. It was also shown that R_{LP} looking toward the plate from the network input equals resistance R_L appearing at the input of the pi-network when a conjugate match is obtained, while there is no requirement that $R_L = R_S$ to obtain a conjugate match.

Notes

1. The use of "linear" and "nonlinear" relates to the voltage/current relationship at the output terminals of the amplifier tank circuit, or at the terminals of a network. This usage does not relate to nonlinearity between the input and output of an amplifier that results in generation of distortion products in the output signal.

2. In addition to the data in Terman's example, I have made measurements that determine the output impedance of RF power amplifiers which prove the existence of a conjugate match. The data show that when the amplifier is loaded to deliver all of its available power, the output impedance of the amplifier equals the load impedance, thus signifying a *linear* voltage/current relationship at the output of the tank circuit, and thus a *conjugate* match. The description of my measurement procedure and the resulting data showing the proof that follows appear in Sec 19.8.

3. The material discussed in this chapter pertains only to RF amplifiers used in the Amateur Radio Service with tubes and pi-networks in the output circuit. The material does not necessarily pertain to amplifiers used in various commercial services, or any amplifier using solid-state components.

Chapter 20

SWR with Multi-band and Non-resonant Antennas

Sec 20.1 Introduction

In Chapter 9, I departed from the study of impedance matching from the viewpoint of wave reflections and began an in-depth examination of matching directly from the viewpoint of impedance. During that examination I covered several pertinent subject areas, all of which have a direct bearing on matching antenna-terminal impedance to the transceiver.

I began with the assumption that the conventional setup included a transceiver, an SWR indicator, and a feed line running directly to the antenna. Subsequent discussion showed that flexibility in operating bandwidth is vastly improved when the matching capability of the pi-network tank circuit in the final amplifier is extended by the addition of an external matching unit—the antenna tuner, or transmatch.

Sec 20.2 Multi-band Dipoles

So far I have discussed only simple dipoles fed with coaxial transmission line. With the exception of 15-meter third-harmonic operation on a 40-meter dipole, the simple coax-fed dipole is limited to single-band operation, because the excessive antenna to feed-line mismatch precludes its use on even-harmonic frequencies related to the fundamental frequency for which it is designed. However, the simple dipole can be modified in different ways to extend its performance to multi-band operation. Let us now examine those different ways.

Sec 20.2.1 Trap Dipoles

One method of achieving multi-band operation from a dipole is to insert frequency-selective traps in the antenna. Traps allow operation at the lowest fundamental frequency for which the total electrical length of the dipole is λ/2, but which selectively disconnects dipole portions extending beyond traps designed to present a high impedance in series with the dipole at frequencies higher than the fundamental. Hence, the effective electrical length of the dipole is automatically shortened to λ/2 on the higher-frequency bands so that it maintains an acceptable match to a coaxial feed line.

Unfortunately, however, there is an undesirable penalty to be paid when using the trap method of multi-band operation. The penalty is that the operational bandwidth on all the bands on which the trap dipole operates is far narrower than that of separate simple dipoles cut to λ/2 for each band. In other words, the SWR rises much more rapidly with a trap dipole than with the simple dipole, as the operating frequency is moved away from the resonant frequency of the λ/2 section currently in use. Evidence of this sharp rise in SWR is shown in Figs 20-1 to 20-3, and in Tables 20-1 to 20-5, from which data the figures were plotted. These show antenna-terminal resistance, reactance, and SWR data measured with professional, precision laboratory equipment including a General Radio 1606-A RF bridge. The tables also include the corresponding reflection coefficient data, appearing in columns ρ_N and ρ_L. A more detailed explanation of trap operation may be found in *Ref 71, p 7-8.*

Sec 20.2.2 Stagger-Tuned Dipoles

There is a second method of obtaining multi-band dipole operation that does not have the undesirable bandwidth limitation of the trap dipole. This method uses multiple dipoles fed in parallel from the same feed line and is called stagger tuning. The length of each separate dipole is λ/2 for each band. Hence, each dipole presents a good impedance match to the feed line on the band for which it is intended and a poor match on all the others. It is an effective system, because none of the dipoles takes power from the feed line except the one that is λ/2 at the operating frequency, and thus it is the only one matched to the feed line at that frequency.

As an example, consider a two-dipole arrangement with one dipole cut to $\lambda/2$ on 80 meters and the other cut for 40 meters. With this arrangement, $\lambda/2$ dipole bandwidth is obtained on both 80 and 40, and in addition, the 40-meter dipole is also a center-fed $3\lambda/2$ radiator on 15 meters, which also presents a good match to coaxial feed lines. Here is how the frequency selection occurs. On 80 meters, the 80-meter dipole behaves in the conventional manner, but the 40-meter dipole is inactive because its terminal impedance at 80 meters is approximately $14 - j1300$ ohms. This impedance results in a mismatch of well over 2400:1 on 50-ohm line, assuring its inactivity. On 40 meters, the 40-meter dipole also behaves in the conventional manner, but the 80-meter dipole presents a terminal impedance

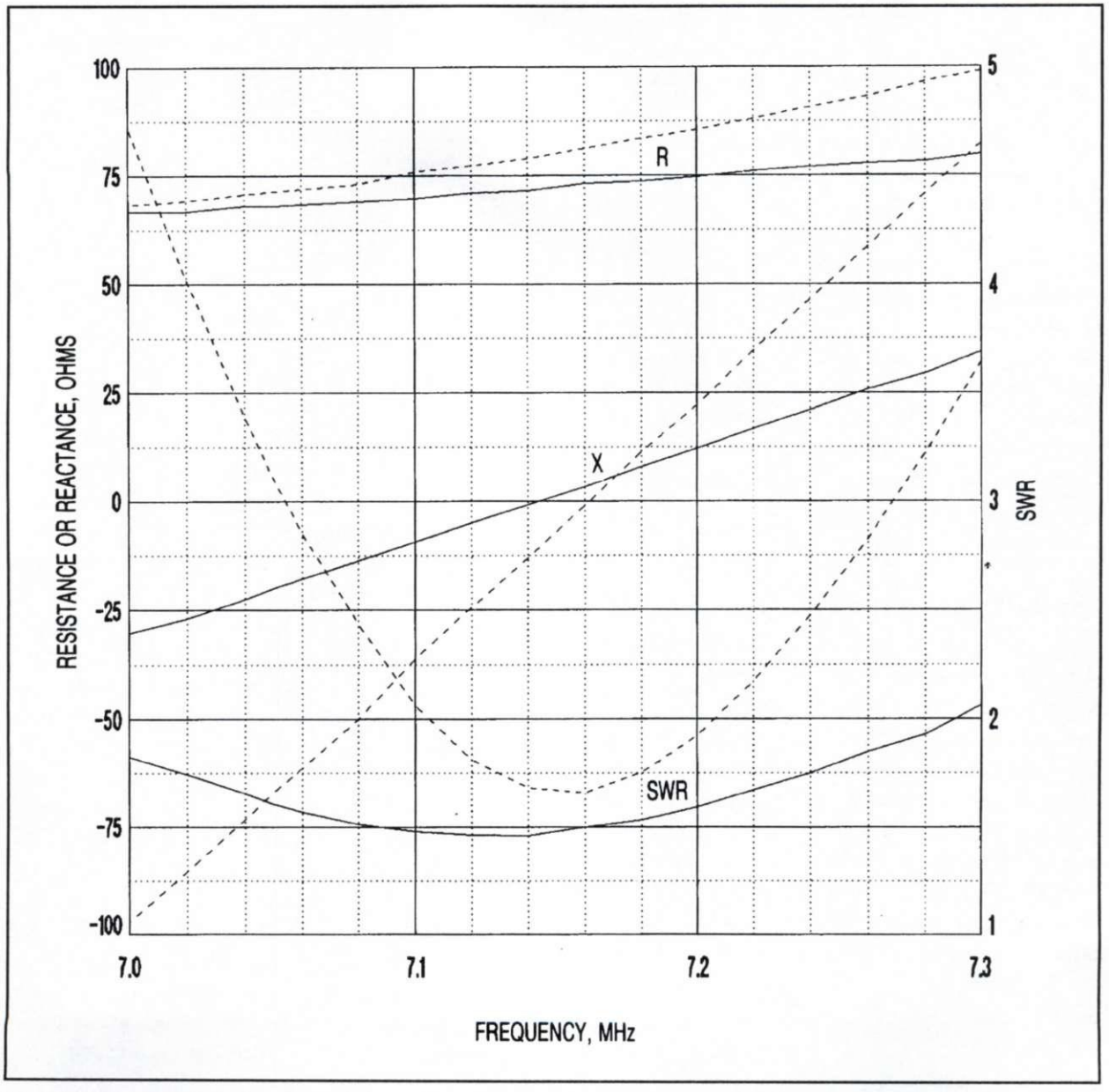

Fig 20-1. Measured feed-point resistance R, reactance X, and SWR versus frequency of 40-meter dipoles at a height of 40 feet. The solid lines show data for a 66-ft, 2-in radiator with no traps (data from Table 20-1). The broken lines show data for the same antenna but with 40-meter traps and 21-ft 5-in extensions added at each end to make the antenna usable on 80 meters (data from Table 20-2). (Computer-generated plot courtesy of Rick Maxwell, W8KHK, ex-WB4GNR)

of approximately 5000 ohms to the feed line at 40 meters, for a mismatch of 100:1. Consequently, this mismatch is also sufficiently severe to result in an inactive 80-meter dipole on 40 meters, especially since the 40-meter dipole is taking practically all the power from the line because of its good match. On 15 meters, the mismatch of the 80-meter dipole is in the same ballpark as it is on 40 meters, assuring inactivity on this band.

In practice, I have found that a good match results on 80, 40, and 15 meters when 80- and 40-meter dipoles are prepared for $\lambda/2$ operation using the standard length formula:

$$L_{FT} = \frac{468}{f\ MHz} \qquad \text{(Eq 20-1)}$$

When a 20-meter dipole is added to the 80- and 40-meter dipoles, there is a slight degradation in the impedance match of the 40-meter dipole on 15 meters. This results from a reactance component in the 20-meter dipole impedance when operating on 15 meters. There should be no serious problem in adding a 10-meter dipole, except that it may require a little trimming to obtain a satisfactory match at a particular frequency in the band. The bandwidth of each dipole is practically identical to that of a single-fed dipole, and hence the stagger tuning arrangement provides a multi-band antenna system far more satisfactory than a trap dipole. Each dipole in the parallel-fed combination may be supported from different directions if different directions of radiation are desired. Otherwise the shorter dipoles simply may be suspended from the longer ones. Additional information on multi-band dipoles in the parallel configuration may be found in *Ref 71, p 7-3.*

Measurement data: Z40 (no traps); see Fig 20-1. 66-ft 2-in 40-meter dipole, height 40 ft, resonant frequency 7.1439 MHz, calibrated RG-214 plus W2DU HF balun, RF bridge General Radio 1606-A, receiver Kenwood TS-530S, signal generator Boonton 250A RX meter.

Feed-line calibration:

Line length in degrees/MHz, PHI = 23.7
Line attenuation in dB/$\sqrt{MHz}$, A = 0.082
Line impedance, Zc = 49 ohms

Freq	R_{IN}	X_{IN}	ρ_{IN}	SWR_{IN}	ρ_L	SWR_L	R_L	X_L
7.000	83.00	–14.500	0.2783	1.77	0.2926	1.827	66.67	–30.19
7.020	80.00	–12.536	0.2580	1.70	0.2712	1.744	66.61	–26.96
7.040	77.50	–8.376	0.2343	1.61	0.2463	1.654	67.96	–22.38
7.050	75.80	–6.667	0.2210	1.57	0.2323	1.605	68.01	–19.98
7.060	74.50	–4.958	0.2102	1.53	0.2210	1.567	68.27	–17.77
7.080	72.50	–1.624	0.1939	1.48	0.2038	1.512	69.04	–13.60
7.100	71.00	0.999	0.1835	1.45	0.1930	1.478	69.61	–10.15
7.120	69.50	5.281	0.1785	1.43	0.1877	1.462	70.95	–5.09
7.140	68.00	8.473	0.1773	1.43	0.1865	1.459	71.45	– .81
7.145	68.00	9.517	0.1810	1.44	0.1904	1.470	72.04	0.31
7.150	68.00	10.499	0.1848	1.45	0.1944	1.483	72.59	1.38
7.155	68.00	11.321	0.1882	1.46	0.1979	1.493	73.05	2.31
7.160	67.70	12.011	0.1894	1.47	0.1993	1.498	73.12	3.29
7.180	66.50	15.390	0.2000	1.50	0.2104	1.533	73.62	7.88
7.200	66.00	18.750	0.2172	1.55	0.2285	1.592	74.63	12.20
7.220	65.80	22.299	0.2387	1.63	0.2512	1.671	75.88	16.70
7.240	65.70	25.553	0.2598	1.70	0.2733	1.752	76.90	20.94
7.250	65.50	27.586	0.2729	1.75	0.2872	1.806	77.35	23.64
7.260	65.50	29.201	0.2838	1.79	0.2987	1.852	77.79	25.78
7.280	65.50	31.868	0.3019	1.87	0.3177	1.931	78.26	29.43
7.300	66.10	35.890	0.3297	1.98	0.3470	2.063	79.83	34.52

Table 20-1. Measured antenna impedance data transformed through calibrated feed line.

With the trap dipole, the conventional pi-network tank circuit is unable to provide an acceptable match to the input impedance of the feed line except perhaps for a few kilohertz on either side of the resonant frequency of the trap. Hence, an antenna tuner is necessary if any wider frequency excursion is to be enjoyed. All solid-state rigs that have no internal antenna tuner require an external tuner in any case, except over very narrow frequency ranges away from dipole resonance where the input impedance of the feed line happens to be close to 50 ohms. Even in the case of the simple single dipole, there are some frequencies that will be out of range of pi-network tank circuits when using coaxial feed lines. This is especially true of the 80-meter band. If operation over the entire 80-meter band is desired when using coaxial feed line, the minimum band-edge SWR occurs when the dipole is cut to a length that resonates at 3.750 MHz, the center of the band. This length is usually 125 feet. With this length, the SWR is around 6.5:1 at 3.5 MHz and 5:1 at 4.0 MHz. Consequently, an external antenna tuner is necessary for operation out to the band edges. The point I'm making is that an antenna tuner is an indispensable part of any amateur station that operates in the HF bands. Anyone operating without one is operating with limited flexibility.

Sec 20.2.3 Random-Length Dipoles

Now I'm coming to the crucial topic concerning multi-band operation at HF. I hope I've convinced you of the necessity for an antenna tuner, so why not use it to the fullest advantage and achieve

Measurement data: Z40 with 40-meter traps; see Fig 20-1. 66-ft 2-in 40-meter dipole, height 40 ft, KW-40 traps (res. 7.150 and 7.160 MHz), 21-ft 5-in extensions, calibrated RG-214 plus W2DU balun, RF bridge General Radio 1606-A, receiver Kenwood TS-530S, signal generator Boonton 250A RX meter.

Feed-line calibration:

Line length in degrees/MHz, PHI = 23.7
Line attenuation in dB/$\sqrt{\text{MHz}}$, A = 0.082
Line impedance, Zc = 49 ohms

Freq	RIN	XIN	ρIN	SWRIN	ρL	SWRL	RL	XL
7.000	180.00	–68.714	0.6187	4.25	0.6504	4.721	68.18	–97.11
7.020	153.00	–61.396	0.5720	3.67	0.6014	4.017	69.11	–85.27
7.040	132.00	–50.710	0.5175	3.14	0.5440	3.386	70.64	–73.16
7.050	123.00	–45.106	0.4874	2.90	0.5124	3.102	71.27	–66.92
7.060	111.60	–39.518	0.4476	2.62	0.4706	2.778	70.37	–58.89
7.080	103.00	–29.520	0.3975	2.32	0.4179	2.436	72.96	–49.52
7.100	93.20	–16.620	0.3298	1.98	0.3469	2.062	75.73	–36.27
7.120	85.50	–6.461	0.2753	1.76	0.2895	1.815	77.22	–24.25
7.140	80.00	2.661	0.2411	1.64	0.2536	1.680	78.85	–13.09
7.145	79.00	5.178	0.2376	1.62	0.2499	1.666	79.60	–10.16
7.150	78.00	7.203	0.2349	1.61	0.2471	1.656	80.02	–7.59
7.155	77.00	9.790	0.2347	1.61	0.2469	1.656	80.73	–4.45
7.160	75.70	12.430	0.2350	1.61	0.2472	1.657	81.16	–1.00
7.180	72.40	22.006	0.2604	1.70	0.2739	1.754	83.63	11.39
7.200	70.00	28.333	0.2883	1.81	0.3033	1.871	84.43	20.53
7.220	68.30	38.920	0.3515	2.08	0.3698	2.174	88.00	34.81
7.240	67.50	47.238	0.4035	2.35	0.4246	2.476	90.71	46.58
7.250	67.20	51.448	0.4294	2.51	0.4518	2.649	92.01	52.69
7.260	67.00	55.510	0.4538	2.66	0.4775	2.827	93.20	58.66
7.280	67.50	63.874	0.5005	3.00	0.5267	3.225	96.52	70.74
7.300	68.00	71.781	0.5409	3.36	0.5693	3.643	98.94	82.48

Table 20-2. Measured antenna impedance data transformed through calibrated feed line.

multi-band HF operation with the simplest, yet most effective and efficient antenna? I'm speaking of a random-length dipole fed with either open-wire line or ladder line. By random length, I mean any length at least λ/4 long at the lowest frequency of operation.

A center-fed λ/4 dipole radiates with an effectiveness of approximately 95% relative to a λ/2 dipole, and has a terminal impedance of approximately 14 – *j*1300 ohms. This terminal impedance yields an SWR of 244:1 on 600-ohm line, 300:1 on 450-ohm line, and 424:1 on 300-ohm line. As would be expected, the tuning of the antenna tuner is quite sharp with these values of SWR. However, with the low-loss characteristics of lines of these impedances, the results are good. This is what I use for 160-meter operation—an 80-meter λ/2 dipole, which is λ/4 on 160 meters, and fed with 300-ohm

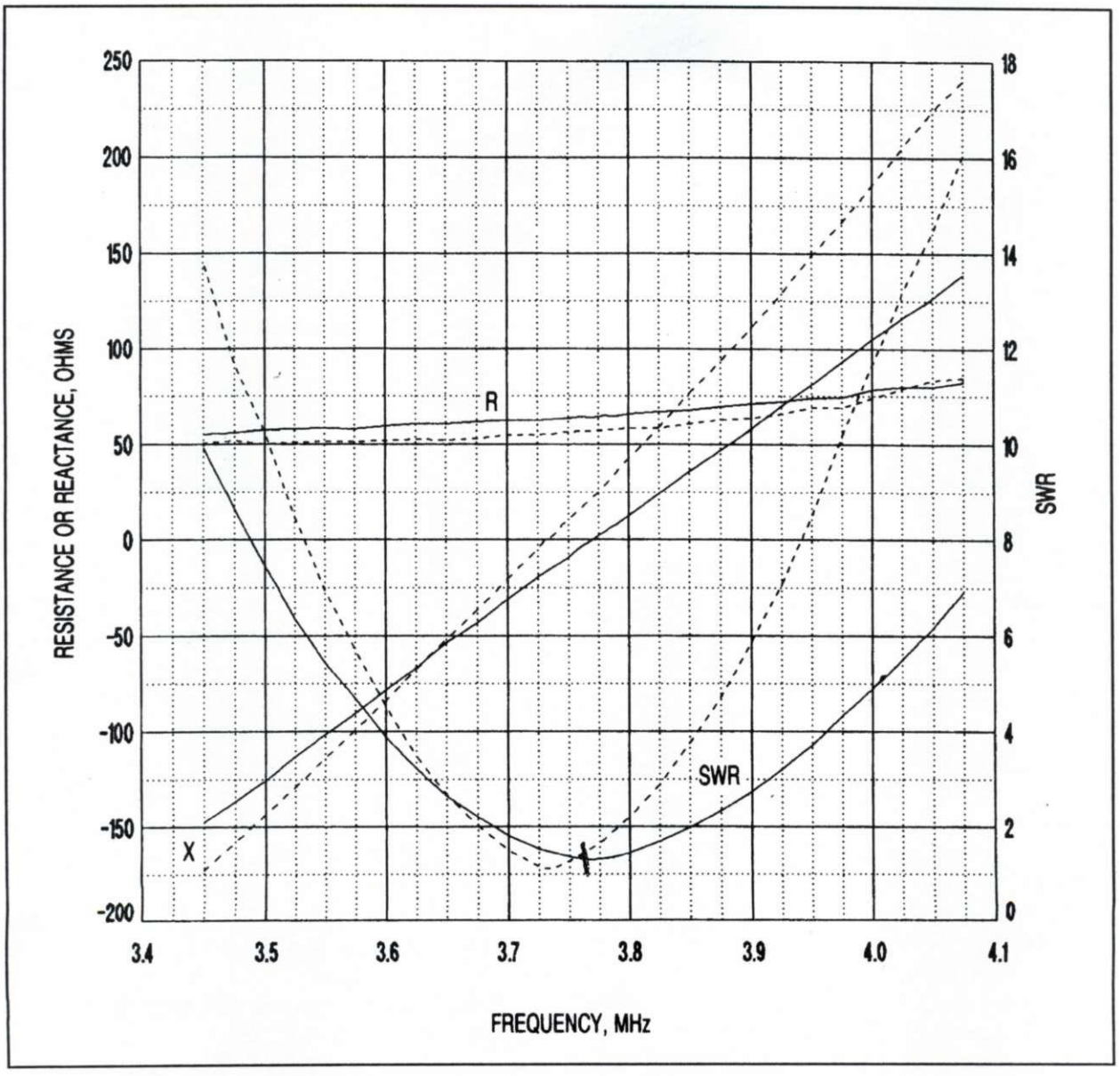

Fig 20-2. Measured feed-point resistance R, reactance X, and SWR versus frequency of 80-meter dipoles at a height of 40 feet. The solid lines show data for a 125-ft radiator with no traps (data from Table 20-3). The broken lines show data for a 109-ft radiator with traps (data from Table 20-4). (This is the 40-meter antenna of Fig 20-1 with traps and extensions added to make the antenna usable on 80 meters.) (Computer-generated plot courtesy of Rick Maxwell, W8KHK, ex-WB4GNR)

line. It works very well. I find it more satisfactory than the traditional method of tying the two wires of the parallel feed line together for a single-conductor feed to the resulting flattop. Tying the two wires together results in a single wire. A single wire that center-feeds both dipole halves feeds the halves in a phase relationship that causes current to flow in opposite directions in each dipole half. This opposite current flow results in no radiation from the flattop; the flattop is now only a capacitive-loading top hat, and *it is only the feed line that radiates as an antenna!*

I'm not suggesting that everyone use a dipole as short as λ/4, but I do recommend a length of about 3λ/8, halfway between λ/4 and λ/2, if you can't erect a full λ/2 on 80-meters. For general use, this antenna results in a little higher effectiveness than the λ/4 dipole, and it does not have such sharp tuning in the antenna tuner. A 3λ/8 dipole has an effectiveness greater than 98% relative to a λ/2 dipole, and has a terminal impedance of approximately 34 – *j*400 ohms. This impedance yields an SWR of 25.5:1 on 600-ohm line, 23.7:1 on 450-ohm line, and 24.6:1 on 300-ohm line, all very reasonable values for open-wire or ladder line. A 3λ/8 dipole at 3.5 MHz is approximately 100 feet long, which means that a random length from 90 to 100 feet will make an excellent radiator on all the HF amateur bands, 80 through 10 meters, including the WARC-79 bands. The length of a 3λ/8 dipole may be found using the formula

$$L_{FT} = \frac{351}{f\ MHz} \qquad \text{(Eq 20-2)}$$

If you don't have room for even 90 feet of straight wire for operation on 80 meters, a 10- to 15-foot portion of each end may be dropped vertically from each end support. There will be no significant change in radiation pattern on 80 and 40 meters. However, there will be a minor change in polarization in the radiation at higher frequencies, but the effect on propagation will be negligible. Although I work 160 meters with a 125-foot dipole, tuning of the antenna tuner would be less critical on 160 meters with a 200-foot dipole, and admittedly, the feed-line loss would be somewhat lower. However, the loss from feed-line attenuation is quite low, even at the high values of SWR. Your attention is invited to the loss versus SWR graph in Fig 6-1 to see just how little loss is incurred with open-wire feeders. The point I'm stressing here is that when using an antenna tuner with open-wire or ladder-line feeders, the dipole length is not critical, because the tuner provides the impedance match throughout the entire antenna system, whatever the dipole length may be.

Sec 20.2.4 The G5RV Antenna

With this background on random-length dipoles behind us, it seems appropriate to make a critical examination of a particular 102-foot dipole that is enjoying a great deal of popularity—Louis Varney's G5RV dipole. In spite of its popularity, its operation is not well understood among many amateurs, so I'll shed a little light on the G5RV. First of all, the reason for the 102-foot length for the G5RV is no secret, but it is not well known. Being unaware of certain antenna principles, many amateurs have come to believe that there is some sort of magic in the 102-foot length, and that their all-band success with this antenna is dependent on this specific length. Nothing could be further from the truth, because except for 20 meters (as I'll soon explain), any random length of at least 3λ/8 at the lowest operating frequency will perform equally well.

What is the significance of the 102-foot length? Unbeknownst to many amateurs who use it, Varney designed the antenna to be a resonant 3λ/2 radiator on 20 meters; that length is 102 feet. He had two specific reasons for selecting 3λ/2 on 20: He wanted a four-lobe radiation pattern and a low feed-point impedance. The 3λ/2 was a clever choice, because this length yields a four-lobe pattern, in addition to a low feed-point impedance that can be matched to a 50-ohm line with a line transformer without requiring an antenna tuner. As Varney also intended, this 102-foot length results in a strictly random length on all bands except 20, so except for the 20-meter considerations I've just described, there is no magic whatsoever to this length. The last comment in the previous paragraph should be taken seriously. It should be noted that the 102-foot length of the G5RV is almost exactly the length I recommended above for a random-length antenna, 3λ/8 at the lowest frequency of operation, because 100 feet is the length required for 3λ/8 at 3.5 MHz.

On 20 meters, the input impedance of the 3λ/2 G5RV radiator is low because the feed point is at

the center of the central λ/2 portion. Hence, the impedance (the resonant resistance) is only moderately higher than if the outer λ/2 sections were eliminated, leaving a single λ/2 dipole. At the frequency of mid-band resonance, the free-space feed-point impedance is approximately 100 + *j*0 ohms, which reduces to around 90 + *j*0 ohms at a convenient height above ground. This results in a mismatch of about 1.8:1 relative to 50 ohms. Varney's choice of the 34-foot line-transformer matching section, λ/2 on 20 meters, was to make a 1:1 impedance transformer that repeats the 90 + *j*0 antenna impedance at its input terminals. Thus, with a suitable choke balun to make a transition from a balanced to an unbalanced line, the low 1.8:1 mismatch makes connecting to a 50-ohm line

Measurement data: Z80 (no traps); see Figs 20-2 and 20-3. 125-ft 80-meter dipole, height 40 ft, calibrated RG-214 plus W2DU HF balun, RF bridge General Radio 1606-A, receiver Kenwood TS-530S, signal generator Boonton 250A RX meter.

Feed-line calibration:

Line length in degrees/MHz, PHI = 23.7
Line attenuation in dB/$\sqrt{MHz}$, A = 0.082
Line impedance, Zc = 49 ohms

Freq	R_{IN}	X_{IN}	ρ_{IN}	SWR_{IN}	ρ_L	SWR_L	R_L	X_L
3.450	5.90	6.957	0.7889	8.47	0.8171	9.933	55.22	–147.31
3.475	6.70	8.201	0.7653	7.52	0.7927	8.649	56.21	–136.31
3.500	7.70	9.429	0.7370	6.60	0.7635	7.457	57.75	–125.48
3.525	9.00	10.922	0.7026	5.72	0.7279	6.350	58.16	–112.97
3.550	10.50	12.394	0.6655	4.98	0.6896	5.443	58.40	–101.44
3.575	12.25	13.902	0.6256	4.34	0.6483	4.687	58.15	– 90.45
3.600	14.80	15.139	0.5704	3.66	0.5912	3.892	59.37	–78.39
3.625	17.90	16.000	0.5084	3.07	0.5271	3.229	60.58	–66.58
3.650	22.00	16.575	0.4345	2.54	0.4505	2.640	60.62	–53.76
3.675	26.00	15.782	0.3640	2.14	0.3774	2.212	61.86	–42.99
3.700	30.90	13.568	0.2791	1.77	0.2894	1.815	62.32	–30.65
3.725	35.00	9.799	0.2021	1.51	0.2096	1.530	62.64	–19.44
3.750	37.20	4.853	0.1478	1.35	0.1533	1.362	63.60	–9.32
3.760	37.50	1.862	0.1346	1.31	0.1397	1.325	64.36	– 3.88
3.770	37.80	–0.040	0.1290	1.30	0.1339	1.309	64.14	–0.33
3.775	37.60	–1.457	0.1327	1.31	0.1376	1.319	64.46	2.26
3.780	37.20	–2.566	0.1400	1.33	0.1453	1.340	64.98	4.39
3.785	37.20	–3.699	0.1433	1.33	0.1487	1.349	64.63	6.49
3.790	36.90	–4.749	0.1511	1.36	0.1567	1.372	64.70	8.54
3.800	35.60	–6.711	0.1766	1.43	0.1832	1.449	65.74	12.93
3.825	32.00	–10.850	0.2468	1.66	0.2561	1.688	67.15	24.37
3.850	28.00	–13.507	0.3194	1.94	0.3314	1.992	67.87	35.86
3.875	23.95	–14.452	0.3889	2.27	0.4036	2.353	69.44	47.23
3.900	20.60	–14.359	0.4478	2.62	0.4648	2.737	71.15	57.90
3.925	17.50	–13.885	0.5067	3.05	0.5260	3.220	72.28	69.85
3.950	15.10	–12.911	0.5548	3.49	0.5760	3.717	74.00	81.09
3.975	12.95	–11.950	0.6020	4.02	0.6251	4.334	74.42	93.31
4.000	11.40	–10.375	0.6365	4.50	0.6610	4.899	78.61	105.24
4.025	10.15	–9.242	0.6670	5.01	0.6928	5.510	80.00	116.23
4.050	9.10	–8.272	0.6943	5.54	0.7212	6.175	79.96	126.62
4.075	8.16	–6.994	0.7195	6.13	0.7475	6.920	82.50	139.11

Table 20-3. Measured antenna impedance data transformed through calibrated feed line.

feasible without requiring an antenna tuner. The SWR on a λ/2 matching section of 300-ohm line is around 3.3:1, while on a 450-ohm line it is about 5:1. Keep in mind that these considerations apply only to 20-meter operation. On all other bands, the G5RV antenna terminal impedance is much higher and reactive, resulting in a higher SWR and making the use of an antenna tuner imperative. Incidentally, the length of a 3λ/2 radiator may be found using the long-wire antenna formula:

$$L_{FT} = \frac{492\ (n - 0.05)}{f\ MHz} \qquad \text{(Eq 20-3)}$$

where n = the number of half wavelengths in the radiator

It is unfortunate that many amateurs believe that the balun should be omitted. Failure to include a balun between the balanced open wire and the unbalanced coax results in RF radiation in the shack from current flow on the outer surface of the coax shield.

In addition to the misunderstanding concerning the "magical" 102-foot length of the G5RV, there are also other areas of confusion focused on this antenna, some concerning the role of the feed line. There are some who believe that a particular combination of open-wire and coaxial feed line yields a perfect 1:1 match on all bands without a tuner. As stated above, this is true only on 20 meters. Others believe that because the 102-foot dipole length is shorter than λ/2 on 80 meters, a certain length of the feed line is a folded-up portion of the antenna to make up for the difference in length, and that the folded-up portion radiates along with the antenna. Still others believe certain lengths of feed line are to be avoided to prevent "antenna current" from flowing on the feed line because of line resonance. Patently untrue!

My own involvement with the G5RV antenna dates back to the early 1970s when I began lecturing on SWR and reflections on transmission lines. My lectures promoted the use of antenna tuners with open-wire feed line on random-length antennas as the best way to achieve all-band operation. I also promoted the concept that the correct length of feed line is that which is required to reach from the antenna terminals to the tuner, because regardless of the length of the feed line, both the feed line and the antenna are made resonant by the conjugate-matching action of the tuner. Hence, there is no reason to avoid certain lengths to prevent line resonance, because the tuner makes them resonant anyway.

I first heard of the G5RV when someone in my audience described his 102-foot antenna with open-wire and coax feed line. He claimed it gave him a 1:1 SWR on all bands without a tuner. I told him he must have a lossy coax to get 1:1, because I knew a 1:1 would be impossible with such an arrangement without some exceptionally high resistive loss somewhere in the antenna system. After hearing several more identical claims in later lecture sessions, I analyzed the antenna on all bands, observing it to be the 3λ/2 that it is on 20 meters, but a random length on all other bands, so I felt confident in rebutting the "1:1 on all bands without a tuner" claims. Incidentally, Varney published an update of the G5RV in *The ARRL Antenna Compendium, Volume 1* (*Ref 112*), in which he presented the same specifications for the antenna that I described above, confirming my earlier observation that his antenna is 3λ/2 on 20 meters, and a *random length on all other bands.*

Let's now examine the other myths and confusion concerning the G5RV that I mentioned earlier. First, we'll consider the feed-line combination believed to yield a 1:1 match on all bands. It has been written that the combination of 33 feet of open-wire line plus 68 feet of 50-ohm coaxial line will yield such a match. Don't believe it! A determination of the G5RV antenna-terminal impedance on all bands shows that there is no length of open-wire line of any characteristic impedance Z_C that will transform the antenna impedance Z_A to an impedance that is even close to presenting a match to 50- or 75-ohm coax, except on 20 meters. However, when fairly long lengths of coax follow a length of open wire, the high SWR appearing at the junction of the open wire and the coax will be reduced significantly at the input of the coax because of the attenuation loss in the coax, especially at the higher frequencies. The longer the coax, the lower the input SWR, but remember that this method of lowering the SWR is costly in terms of lost power. Because an antenna tuner is necessary anyway, except on 20 meters, it makes no sense to use any coax at all. Coax performs no useful function in the feed system, and it consumes power unnecessarily because of the high SWR. A more

sensible method is to run the open-wire line all the way to the tuner and eliminate the coax entirely.

Second, let's consider the length of feed line believed to be a folded-up portion of the antenna that radiates. Radiation occurs when the electromagnetic field developed by current flow on a conductor is not canceled by an opposing field developed by an equal current flowing in the opposite direction. Hence, radiation occurs as a result of current flowing on an antenna. However, antenna current ceases being antenna current at the antenna terminals, because once it enters the transmission line, the current becomes transmission-line current, with the current in the two conductors flowing in opposite directions. There is no radiation from any portion of the line, because the fields developed by the currents flowing in opposite directions in the two conductors oppose and cancel each other throughout

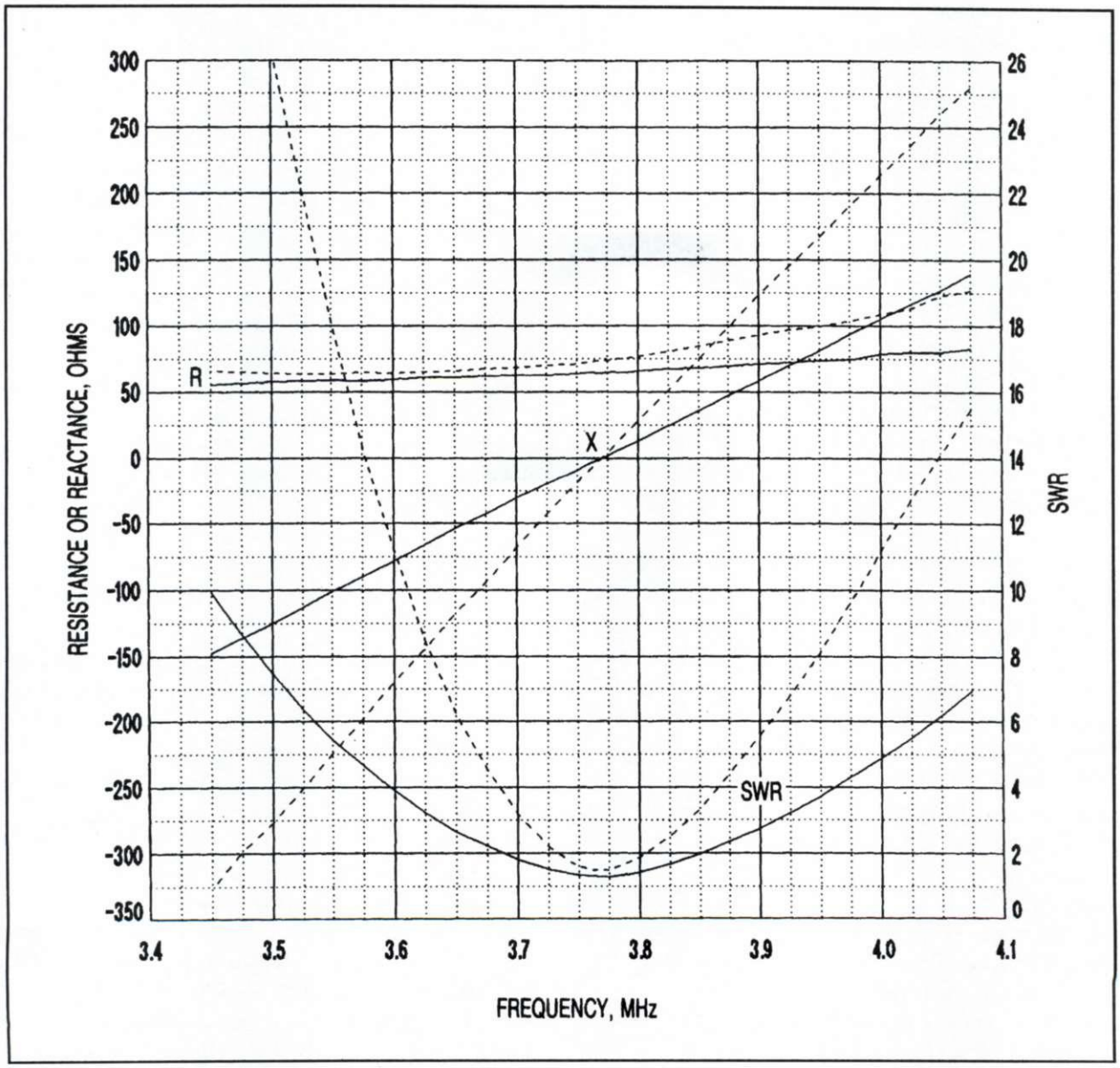

Fig 20-3. Measured feed-point resistance R, reactance X, and SWR versus frequency of 80-meter dipoles at a height of 40 feet. The solid lines show data for a 125-ft radiator with no traps (data from Table 20-3), the same as the solid-line curves in Fig 20-2. The broken lines show data for the same antenna with 80-meter traps and 42-ft extensions added at each end to make the antenna usable on 160 meters (data from Table 20-5). (Computer-generated plot courtesy of Rick Maxwell, W8KHK, ex-WB4GNR)

the entire length of the line. Therefore, no portion of the feed line becomes part of the antenna.

Sec 20.3 Antenna Currents on Feed Lines

We know there are times when the feed line does radiate in spite of the statement in the previous paragraph, so let's now examine this concept a little further to determine what conditions must exist to cause the feed line to radiate. Antenna currents and radiation can occur on a two-wire balanced line, but only when the currents in the two wires are unequal. Neither a resonant line nor a resonant combination of line and antenna length will cause the currents to be unequal. Nor will high SWR cause unequal currents or feed-line radiation. Never forget that whatever the length of the feed line (or the antenna), the antenna and feed-line combination is always made resonant by the conjugate matching action of the antenna tuner.

I'll now explain how antenna currents are developed, and it will become clear why feed-line length is not a factor in causing feed-line radiation. As stated earlier, equal transmission-line currents in the two wires of the line flow in opposite directions (push-pull). This mode of current flow is called the *differential mode*. The electromagnetic fields developed by these two currents are thus 180° out of phase and oppose each other. Because the separation between the wires is small in terms of a wavelength, the two opposing fields cancel each other, preventing radiation from the feed line. No antenna currents are generated. On the other hand, if the transmission-line currents in the two wires are unequal, their corresponding fields are also unequal, and thus do not completely cancel each other; hence, an antenna current is developed and radiation results. In this case the current resulting from the *difference* between the currents flowing in the two wires flows in the same direction on both wires. The uni-directional current flowing in this case is called the *common-mode* current.

The two main causes of transmission-line current imbalance that result in common-mode currents are (1) asymmetrical positioning of the feed line relative to the antenna, and (2) the antenna itself is unbalanced, either by unequal lengths relative to the feed point (as in the twin-lead off-center-fed, misnamed "Windom" antenna), or one portion of the antenna is closer to surrounding objects such as a metal roof. If the feed line is positioned symmetrically relative to the antenna, each half of the antenna induces an equal but opposite current flow on the feed line. This is because each half of the antenna is of opposite polarity. The result is zero induced current, regardless of line length.

If the feed line is *not* positioned symmetrically, the currents induced from each half of the antenna are unequal. The result is an induced current on the feed line traveling in the same direction on both wires as common-mode current. When the induced common-mode current joins the differential-mode transmission-line currents, the net current is increased in one wire and decreased in the other. The resulting difference in current now flowing in each wire, the common-mode current, constitutes the antenna current, which does cause the feed line to radiate. Therefore, I repeat, if the currents in the two wires of the feed line are equal, antenna current and radiation will be zero, regardless of the length or resonant condition of the feed line. Antenna current flowing on a coaxial (unbalanced) feed line resulting from not using a balun is another subject and is treated in depth in Chapter 21.

Although it is not pertinent to the G5RV, a strange example of asymmetrical feed-line positioning exists in the misnamed "Windom" antenna. This is a dipole antenna fed off-center with twin lead at the point where a true Windom would be fed with a single-wire feeder. This antenna is not a Windom, and the feed current paths are not the same. In this pseudo Windom, the go and return currents flow on the two wires of the twin lead. In the true Windom, the return path for the feeder current is in the ground-reflected image of the single-wire feeder. Yes, the Windom feeder does radiate, but not for the same reason the pseudo-Windom feeder radiates. The off-center twin-lead feeder of the pseudo-Windom radiates because it carries a common-mode antenna current in addition to the differential-mode transmission-line currents, because the currents induced in it from the asymmetrical dipole portions are unequal. There is a legitimate reason for moving the twin-lead feeder away from the center of the antenna, however, as discussed in Sec 21.10. In addition, for ease in matching a $\lambda/2$ dipole to a low-impedance line, a feed point one third of its length from one end exhibits low-impedance current loops on the even harmon-

ics of the fundamental frequency, while the center of the dipole exhibits low-impedance current loops on the odd harmonics.

Sec 20.4 Standing Waves and Feed-Line Radiation

It goes without saying that practically every amateur takes SWR measurements on his feed line to determine the condition of his antenna system. However, unless the SWR is 1:1, the results of the measurements are often misinterpreted, and the standing wave innocently becomes the culprit in an unfortunate scenario that leads to all sorts of needless effort to get the SWR down to 1:1. Many believe that standing waves produced by an impedance mismatch between the feed line and the antenna result in an energy field surrounding the feed

Measurement data: Z80 with 40-meter traps; see Fig 20-2. 66-ft 2-in 40-meter dipole, height 40 ft, KW-40 traps (res. 7.150 and 7.160 MHz), 24-ft 3-in extensions, calibrated RG-214 plus W2DU balun, RF bridge General Radio 1606-A, receiver Kenwood TS-530S, signal generator Boonton 250A RX meter.

Feed-line calibration:

Line length in degrees/MHz, PHI = 23.7
Line attenuation in dB/$\sqrt{\text{MHz}}$, A = 0.082
Line impedance, Zc = 49 ohms

Freq	R_{IN}	X_{IN}	ρ_{IN}	SWR_{IN}	ρ_L	SWR_L	R_L	X_L
3.450	4.45	5.507	0.8354	11.15	0.8652	13.840	51.11	–172.70
3.475	5.15	6.907	0.8132	9.71	0.8423	11.683	52.11	–157.90
3.500	5.81	8.571	0.7937	8.70	0.8223	10.252	50.20	–143.30
3.525	6.92	10.213	0.7617	7.39	0.7892	8.489	51.22	–128.76
3.550	8.40	12.113	0.7222	6.20	0.7484	6.948	51.59	–113.43
3.575	10.25	14.098	0.6770	5.19	0.7017	5.704	51.66	–99.06
3.600	13.00	16.250	0.6162	4.21	0.6387	4.536	51.91	–83.68
3.625	17.20	18.207	0.5337	3.29	0.5532	3.477	52.67	–67.38
3.650	22.80	19.589	0.4396	2.57	0.4557	2.674	52.56	–51.84
3.675	30.10	18.640	0.3266	1.97	0.3387	2.024	53.28	–36.53
3.700	37.90	12.973	0.1943	1.48	0.2015	1.505	54.99	–20.50
3.725	43.40	3.222	0.0699	1.15	0.0725	1.156	54.95	–4.63
3.730	43.50	0.268	0.0595	1.13	0.0617	1.132	55.40	–0.74
3.735	43.90	–1.071	0.0561	1.12	0.0582	1.124	54.95	1.07
3.740	43.20	–3.209	0.0718	1.15	0.0745	1.161	55.74	3.95
3.745	42.20	–6.008	0.0993	1.22	0.1030	1.230	56.41	7.97
3.750	41.50	–7.733	0.1186	1.27	0.1230	1.281	56.63	10.60
3.775	35.80	–15.364	0.2350	1.61	0.2438	1.645	57.26	25.32
3.800	27.60	–19.211	0.3641	2.15	0.3778	2.214	58.23	42.60
3.825	21.20	–19.739	0.4675	2.76	0.4851	2.885	58.26	58.56
3.850	15.90	–17.922	0.5591	3.54	0.5802	3.764	60.67	76.79
3.875	12.50	–15.871	0.6266	4.36	0.6504	4.720	62.69	93.92
3.900	10.00	–13.974	0.6833	5.31	0.7092	5.878	63.47	111.27
3.925	8.30	–11.975	0.7247	6.27	0.7524	7.077	66.00	128.79
3.950	6.95	–10.000	0.7605	7.35	0.7896	8.504	69.33	148.59
3.975	5.90	–8.554	0.7908	8.56	0.8212	10.184	69.10	166.25
4.000	5.40	–9.250	0.8077	9.40	0.8388	11.407	53.98	158.40
4.025	4.80	–8.944	0.8269	10.55	0.8588	13.163	46.67	160.29
4.050	4.35	–4.198	0.8380	11.35	0.8705	14.442	83.76	223.92
4.075	4.00	–3.190	0.8496	12.30	0.8827	16.044	85.07	239.80

Table 20-4. Measured antenna impedance data transformed through calibrated feed line.

line, causing it to radiate as an antenna. Is this true? No! This is not the case at all, and I'll explain.

A voltage standing wave is simply a variation in the line voltage appearing *between the feed-line conductors* at different positions along the line. A current standing wave is a corresponding variation in line current flowing through the conductors. Both voltage and current standing waves are illustrated in Fig 9-3. The variations in voltage and current that develop the standing wave result from the interaction between the forward and reflected waves of voltage and current, as explained in Chapter 9.

However, first let's consider the conditions prevailing on a matched, open-wire line with no standing waves. Here there is no variation in either the line voltage or line current as we move in position along the line. Also, we know from the discussion in the previous section that there is no radiation from the line, because the opposing fields produced by the oppositely flowing currents in the two conductors of the line cancel each other. In other words, there are actually two energy fields surrounding the feed line (open wire, not coax), but they cancel each other because they are of opposite polarity, resulting in no radiation.

Now consider the conditions prevailing on a mismatched line with standing waves. As stated above, we now have a variation in line voltage and current as we move in position along the line; at some points the current is higher and at other points it is lower. The crucial point is that no matter whether the current is higher at one point and lower at another, the current is *equal and opposite* in both conductors at any given point along the line. Therefore, the fields produced by the currents in the two conductors are also equal and of opposite polarity everywhere along the line, and cancel in exactly the same manner as in the line with no standing waves. Hence, there is no radiation from the line, standing waves or not.

So far I have been discussing open-wire lines, where there is nothing to contain the electromagnetic fields produced by the line currents. However, there is an additional reason why there is no radiation from *coaxial* lines because of standing waves. This is because the fields produced by the currents flowing through the conductors of coaxial lines are entirely confined within the coaxial shield surrounding the line. Hence, standing waves on transmission lines do not cause radiation from either open-wire or coaxial transmission lines.

Sec 20.5 The Extended Double Zepp and the 5λ/8 Vertical

There is another dipole type of antenna that is becoming popular with amateurs for its increased gain, and it is called the extended double Zepp, or EDZ for short. It is a collinear dipole, although it can't rightfully be called a dipole because each half of its length is greater than λ/2 (each half is actually 0.64 λ). This means it has a reversal of current flow in each antenna half, and therefore has more than two "poles." Hence, the EDZ rightfully belongs in the realm of the long wire. The EDZ is described in *The ARRL Antenna Book (Ref 71, p 8-34),* which shows the current distribution on the radiator and feed line, as well as the radiation pattern.

The reason for my mentioning the EDZ here is that it has a long history relative to AM broadcasting that is not well known, and I believe you will find it very interesting. In the early 1920s, antennas used in AM broadcasting were in their infancy. Many simply used a configuration similar to those used in long-wave, or LF, transmission. These antennas generally comprised a top-loaded vertical wire supported by two towers, one at each end of the top-loading wires. The vertical wire was usually much shorter than λ/4, and the radiation pattern in elevation was the same as the typical λ/4 vertical. However, the pattern was not uniform in all azimuth directions because of field distortion caused by the supporting towers. There is no radiation from the horizontal top-loading wires, because the currents in each opposing wire are flowing in opposite directions. The horizontal wires simply add capacitance to ground, electrically lengthening the short vertical portion. Consequently, the only radiation is from the vertical wire.

In 1923, Stuart Ballantine of the Harvard University Physics Department made an important discovery, which he published in 1924 (*Ref 115*). He discovered that there is an optimum height for a vertical radiator that produces the maximum radiation in the horizontal, broadside direction. That height is 0.64 λ. The increase in radiation in the horizontal direction is 3.03 dB relative to a λ/4 ver-

tical radiator. This increase in horizontal radiation arises from a corresponding decrease in the vertical components of the radiation in the major lobe. In other words, the fat half-doughnut pattern of the λ/4 vertical radiator is squashed down into a thinner doughnut, but one having a greater diameter. However, because this 0.64 λ is greater than λ/2, the current in the radiator reverses direction at a point λ/2 from the top, 0.14 λ above the ground. The reversal in current at this point produces a separate radiation field from the bottom 0.14-λ portion that is 180° out of phase relative to the field producing the major lobe of radiation. Consequently, this separate out-of-phase field produces a minor lobe of radiation at a high angle, with a deep null between the major and minor lobes.

I have performed a computer analysis of the 0.64-λ vertical radiator; a pattern integration yields 0.6346 λ (228.45°) as the true optimum height, furnishing a gain of 8.1898 dBi, or 3.029 dB over the λ/4 vertical. The maximum field in the minor lobe, which occurs at 58° in elevation, is 9.13 dB below that of the major lobe. The null between the major and minor lobes occurs in elevation at 35°. You may recognize by now that this vertical radiator is also the well-known 5λ/8 vertical.

Measurement data: Z80 with 80-meter traps; see Fig 20-3. 125-ft 80-meter dipole, height 40 ft, KW-80C traps (res. 3.770 MHz), 42-ft extensions, calibrated RG-214 plus W2DU HF balun, RF bridge General Radio 1606-A, receiver Kenwood TS-530S, signal generator Boonton 250A RX meter.

Feed-line calibration:

Line length in degrees/MHz, PHI = 23.7
Line attenuation in dB/$\sqrt{\text{MHz}}$, A = 0.082
Line impedance, Zc = 49 ohms

Freq	R_{IN}	X_{IN}	ρ_{IN}	SWR_{IN}	ρ_L	SWR_L	R_L	X_L
3.450	2.25	0.000	0.9122	21.78	0.9448	35.202	65.33	–325.75
3.475	2.50	1.094	0.9030	19.61	0.9353	29.915	65.11	–298.18
3.500	2.72	2.143	0.8950	18.05	0.9272	26.468	63.88	–276.56
3.525	3.10	3.404	0.8815	15.88	0.9133	22.081	63.65	–250.10
3.550	3.60	4.789	0.8643	13.74	0.8956	18.163	63.48	–224.14
3.575	4.35	6.294	0.8394	11.45	0.8699	14.371	64.88	–198.23
3.600	5.39	8.194	0.8067	9.35	0.8362	11.207	63.96	–170.03
3.625	6.90	10.069	0.7621	7.41	0.7900	8.524	65.36	–144.92
3.650	9.30	12.329	0.6976	5.61	0.7232	6.226	65.72	–117.68
3.675	12.60	14.150	0.6179	4.23	0.6407	4.566	67.39	–94.12
3.700	18.00	15.405	0.5035	3.03	0.5222	3.185	68.36	–68.17
3.725	25.40	13.691	0.3607	2.13	0.3740	2.195	70.05	–42.31
3.745	30.90	9.212	0.2525	1.68	0.2619	1.710	70.76	–23.41
3.750	31.90	7.387	0.2293	1.60	0.2378	1.624	71.33	–18.43
3.755	32.60	5.459	0.2114	1.54	0.2192	1.562	71.95	–13.61
3.760	33.20	3.723	0.1973	1.49	0.2046	1.515	72.03	–9.32
3.765	33.10	1.594	0.1946	1.48	0.2019	1.506	73.29	–4.49
3.775	33.00	–2.172	0.1968	1.49	0.2042	1.513	73.66	4.47
3.800	28.30	–9.921	0.2945	1.84	0.3056	1.880	76.45	28.10
3.825	22.00	–12.811	0.4142	2.41	0.4298	2.508	80.31	50.86
3.850	16.70	–12.987	0.5198	3.17	0.5394	3.343	84.02	74.38
3.875	12.75	–12.258	0.6078	4.10	0.6309	4.418	85.04	98.59
3.900	10.10	–10.205	0.6706	5.07	0.6960	5.580	93.16	123.32
3.925	8.40	–8.764	0.7153	6.03	0.7426	6.770	96.80	145.05
3.950	7.10	–7.418	0.7519	7.06	0.7807	8.120	99.61	167.06
3.975	6.10	–6.038	0.7816	8.16	0.8116	9.614	103.88	190.45
4.000	5.35	–4.750	0.8048	9.25	0.8358	11.178	108.65	213.97
4.025	4.80	–3.603	0.8224	10.26	0.8542	12.717	113.20	236.13
4.050	4.41	–2.395	0.8352	11.14	0.8676	14.103	122.57	260.19
4.075	4.10	–1.472	0.8457	11.96	0.8786	15.469	126.78	279.33

Table 20-5. Measured antenna impedance data transformed through calibrated feed line.

Getting back to Ballantine, his discovery formed the basis for the evolution of the vertical tower becoming the radiator in AM broadcasting, replacing the top-loaded vertical wire supported by two towers. There are two principal advantages in using the tower as the radiator. First, the cost for one tower is less than for two. The second very important advantage is that the single tower eliminated the radiation-pattern distortion caused by the two towers supporting the vertical radiator in the earlier arrangement. In addition, Ballantine's 1923 prediction of increased radiation in the horizontal direction was proved correct when single-tower radiators were erected at his predicted height. However, one unforeseen problem crept in: The radiation from the higher angle minor lobe returned to ground from the ionosphere at night and caused severe fading several miles from the antenna. At the distance where the minor-lobe signal from the ionosphere was the same strength as that of the direct ground wave from the major lobe, wave interference occurred between the two signals, causing the fading. The solution to the problem was the small reduction of the tower height to 0.528 λ (190°), which nearly eliminated the minor lobe, while reducing the radiation level by only 1.03 dB. Thus, the fading problem was solved. As a result, many of the AM broadcast stations throughout the world are still using 190° towers.

One other factor that resulted in increased radiation in the horizontal direction was the use of a more efficient ground-radial system that emanated from the experiments of my colleagues, RCA's Brown, Lewis (W2EBS), and Epstein in 1937 (*Ref 20*). The system they developed is still in use worldwide today. If you are interested in more detail concerning the evolution of the vertical radiator and the ground-radial systems in present use, I recommend reading *Radio Antenna Engineering* by the late Edmund A. Laport, also of RCA (*Ref 57*). Also see Chapters 1 and 5. In addition, Brown's analysis of the ground currents surrounding the base of the vertical antenna also makes interesting reading (*Ref 111*).

Let's now return to the EDZ. What is the connection between the EDZ and the vertical radiator used in AM broadcasting? Simply, its length. We must remember that the ground-reflected image of the vertical radiator supplies the missing half of the dipole. Consequently, a dipole having a half-length of 0.64 λ (0.6346 λ if we nit pick) yields the maximum possible radiation in the broadside direction from a single radiator, 3.03 dB greater than that of a λ/2 dipole. With further increases in length, the broadside radiation diminishes rapidly and becomes zero when the half-length is 360°. At 360° the radiation pattern forms two separate, equal lobes resembling a four-leaf clover when viewed on both sides of a pattern representing the radiation.

As stated earlier, the radiation pattern of the EDZ appears on page 8-34 of *The ARRL Antenna Book* (*Ref 71*), and for comparison, the pattern of the λ/2 dipole appears there on page 3-11. The difference in the widths of the lobes is remarkable. However, despite the 3-dBd gain obtained in the broadside direction from the EDZ, the narrower main lobe of the EDZ may work against you at angles away from broadside. Keep in mind that long-distance propagation at HF is via reflection from the ionosphere, so also remember to consider the takeoff angle from the antenna to the ionosphere for the station you are contacting. At angles away from broadside, a dipole may be radiating more energy at the higher wave angles than the EDZ.

I would be remiss if I neglected to discuss the terminal impedance of the EDZ, so for those who are thinking of feeding it directly with coax, guess again! From interpolating thin-wire antenna impedance data from King (*Ref 37*), the terminal impedance of a radiator with a half-length of 0.64 λ is 126.18 – *j*658.2 ohms. On a 50-ohm transmission line, the normalized terminal impedance is 2.5236 – *j*13.164, yielding an SWR of 71.57:1. (These impedances were interpolated from King's text book before Roy Lewallen's [W7EL] ELNEC and EZNEC were available.) However, on a more realistic approach, here are the values for three higher impedance transmission lines. On 300-ohm line the normalized impedance is 0.4206 – *j*2.194, SWR 14.17:1; on 450-ohm line the normalized impedance is 0.2804 – *j*1.4631, SWR 11.39:1; on 600-ohm line the normalized impedance is 0.2103 – *j*1.0907, SWR 10.59:1. These values of SWR are reasonable for the transmission lines involved, and the balanced output of your antenna tuner should be able to handle these mismatches very well! Just as an exercise, you might want to try calculating these SWR values using the hand-held calculator program listed in

F (MHz)	R 80	*j*X80	R 80–40	*j*X 80–40	SWR 80	SWR 80–40
3.5	55.25	–89.43	51.55	82.8	4.468	4.396
3.55	57.72	–68.84	55.2	–65.28	3.336	3.22
3.60	60.78	48.08	58.17	–43.86	2.359	2.221
3.65	64.53	–26.9	59.93	–22.77	1.688	1.556
3.70	67.06	–4.0	66.02	–1.35	1.334	1.303
3.75	69.69	16.7	71.34	20.61	1.526	1.617
3.80	75.08	40.91	77.04	44.4	2.125	2.237
3.85	79.32	64.34	82.56	68.75	2.887	3.043
3.90	84.61	87.34	90.73	92.84	3.782	3.97
3.95	91.02	111.4	99.89	121.13	4.835	5.182
4.00	98.49	135.18	109.62	149.02	5.949	6.466

Table 20-6. Impedance and SWR data for Figs 20-4 and 20-5.

Appendix 4. I should warn you, though, that program is in reverse Polish notation for Hewlett-Packard calculators. Sorry, but I couldn't include programs for the scientific-notation units.

I mentioned earlier that the 0.64-λ vertical is the same as the 5λ/8 vertical used in many VHF and UHF mobile applications. It is interesting to observe the ease with which this antenna can be matched to a 50-ohm transmission line. The terminal impedance of a vertical radiator over ground, or a ground plane, is half the impedance of the complete dipole having the same half-lengths. Therefore, half of the EDZ terminal impedance of 126.18 – *j*658.2 ohms is 63.09 – *j*329.1 ohms for the 5/8 vertical. However, this capacitive reactance of 329.1 ohms was determined for a *thin* radiator, while the whips used in our mobile applications are not thin for lengths

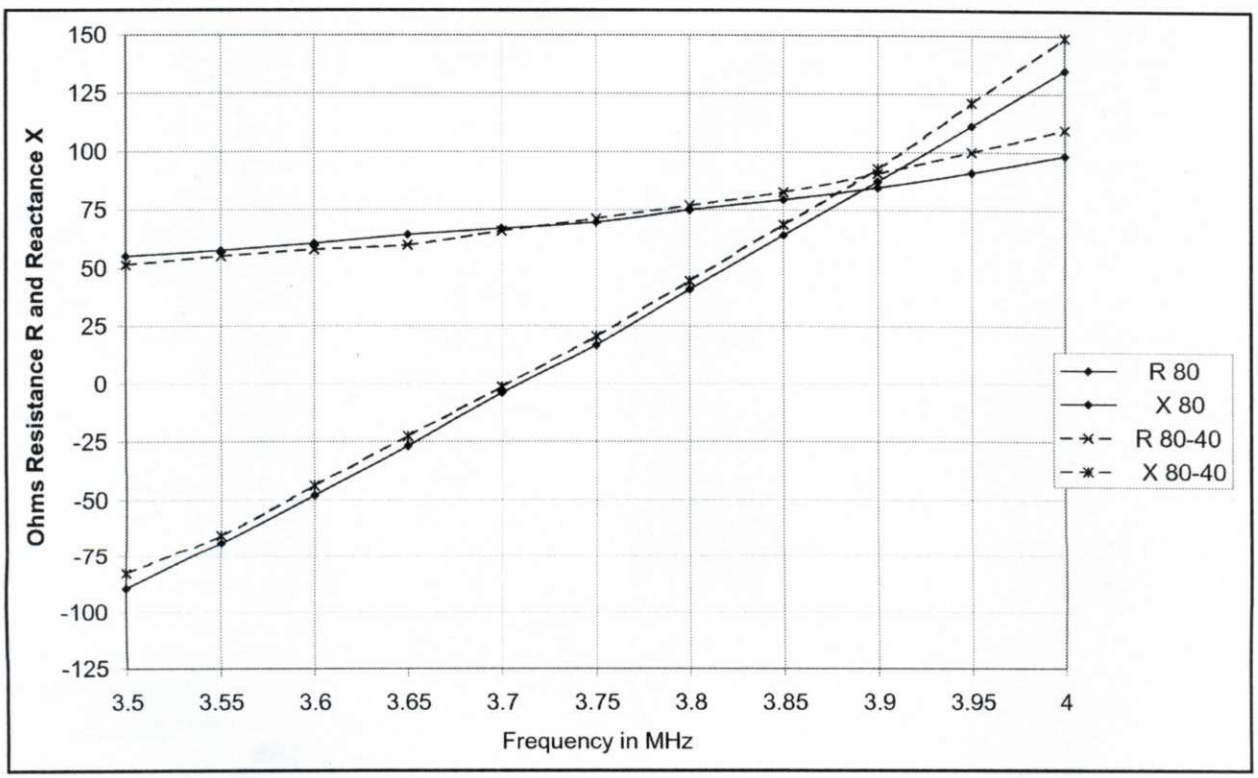

Fig 20-4. Comparing impedances (ohms R and X) of 80 meter with 80–40 meter stagger-tuned dipole spaced ~2 ft at 27 ft above sandy ground; 80 meter 125 ft, 40 meter 66 ft.

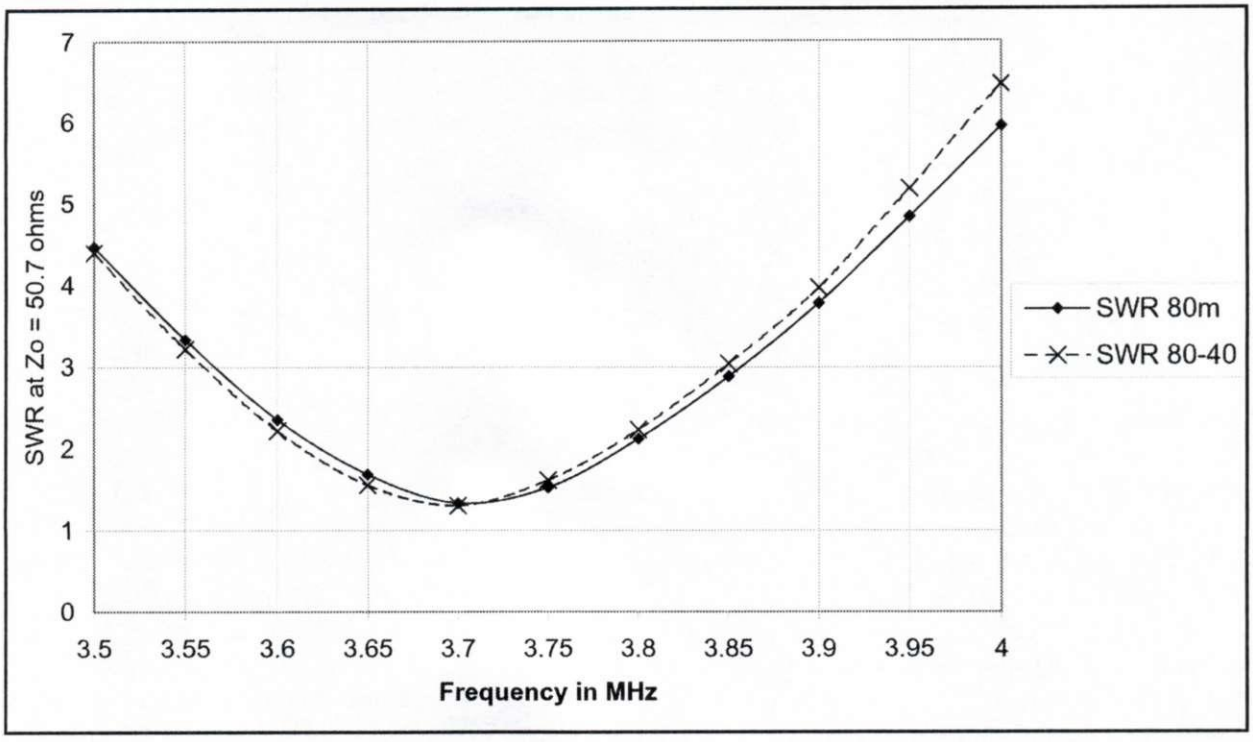

Fig. 20-5. SWR of 80 meter and 80–40 meter staggered dipoles spaced ~ 2 ft at 27 ft above ground; 80 meter 125 ft, 40 meter 66 ft.

and diameters we use at VHF or UHF. So the actual reactance at these frequencies will be considerably less than 300 ohms.

Common practice is to simply insert an inductor having a reactance equal to the capacitive reactance of the antenna in series with the antenna, thus canceling the antenna reactance, and leaving only the 63-ohm resistance component of the antenna terminal impedance to be fed with the 50-ohm line. The result is an SWR of only 1.26:1, which hardly needs any improvement. An alternative method of feeding the 5/λ8 vertical is to connect the inductor between the antenna and ground, and connect the center conductor of the feed line to one of the turns of the inductor. By trimming the length of the antenna and selecting the correct turn to tap onto the coil, an SWR of 1:1 can be achieved. With all of this said about the 5λ/8 antenna, perhaps you are now considering a change to a 5λ/8 vertical from λ/4. If so, there is a paper by Donald Reynolds, K7DBA, that is worth studying (*Ref 119*).

Sec 20.6 Stagger-Tuned Dipoles Revisited

Previously, in Section 20.2.2, we explored the action of two dipoles of lengths differing by one octave, specifically for operation on 80 and 40 meters, both dipoles fed in parallel from a single coaxial feedline. We learned there that the disparate impedances between the two frequencies provided sufficient isolation between the two dipoles to be connected in parallel to the same feedline with minimal adverse reaction.

However, since *Reflections II* was published several radio amateurs have reported having to trim or retune their 80-meter dipoles after adding the 40-meter section in parallel with the 80 meter section.

From my previous experience this procedure seems unlikely. Perhaps something else has intervened for those reporters to cause this reaction to occur. Consequently, for verification of my statements in Section 20.2.2, I measured 80- and 40-meter dipoles connected in parallel to the same coaxial feedline to determine whether the 80-meter dipole really needed retuning after the 40-meter dipole. The results of the measurements are shown in Table 20-6 and Figs 20-4 and 20-5, which indicate that very little change occurs in the impedance of the 80-meter dipole when the 40-meter dipole is added to the circuit.

Chapter 21

Some Aspects of The Balun Problem

(Adapted from QST, *March 1983)*

Sec 21.1 Introduction

Why all the mystery surrounding baluns? Here's some straight talk to dispel the rumors! The balun—to use, or not to use—is one of the hottest topics in amateur radio. Because certain aspects of the connection between a coaxial feed line and a balanced antenna have been ignored, misunderstanding still exists concerning the function of baluns. Many commercial baluns embody some form of impedance transformer, promoting our tendency to misconstrue them as little more than a matching device, while their primary function is to provide proper current paths between balanced and unbalanced configurations.

To help clarify the misunderstanding, this chapter explains some of the undesirable effects that occur when a balun is not used, and some that occur when baluns employing coupling transformers are used. In many cases, these effects cause significant errors in measurements of antenna terminal impedance and SWR. This chapter also describes a simple and inexpensive method of loading the *outside* of a coaxial feed line with ferrite, which effectively produces a well-balanced, wide-band choke balun. Because this configuration eliminates the coupling transformer (with inherent impedance-transfer ratio errors), the accuracy obtainable in antenna impedance and SWR measurements is greatly improved. In addition, antenna-matching networks may be used with this choke balun, because no mismatch limits are imposed by the balun.

Sec 21.2 Transformer Accuracy

Using the General Radio 1606-A precision impedance bridge and the Boonton 250-A RX meter, I have made measurements of transformer-type baluns which prove that with a 50-ohm resistive load, the transformers in typical 1:1 or 4:1 baluns do not yield a true 1:1 or 4:1 impedance transfer ratio between their input and output terminals. This is because of losses, leakage reactance, and less than optimum coupling. My findings have been substantiated by the work of the late John Nagle, K4KJ (*Ref 80*). Furthermore, the impedance-transfer ratio of such baluns degrades even further when used with an antenna that is reactive from operation away from its resonant frequency. This degradation of impedance transfer associated with transformer-type baluns poses no serious operational problems. However, SWR curves plotted from measurements of an antenna using such a balun differ significantly from those using a choke balun that has no impedance-transfer error. Thus, when a precision bridge is used to measure antenna impedance ($R + jX$), the data will be erroneous with either a transformer-type balun in the circuit, or with no balun at all.

Sec 21.3 Should SWR Change with Line Length?

We know that the feed-line input impedance changes with line length when the load (antenna) is not matched to the line. Sometimes trimming the length of the feed line helps to obtain a load impedance better suited to match the transmitter. Theoretically, the SWR should not change with line length—except for a barely perceptible change because of the corresponding change in line attenuation. Then why does the SWR sometimes change? If the SWR changes significantly with a change in line length, it means that the load impedance terminating the line is also changing. The load impedance can change with line length? *Yes.* If a balun is omitted when you feed a balanced antenna with coaxial cable, the load impedance will change when the line length is changed, and of course the

SWR will also change! To explain this commonly experienced phenomenon we must investigate how current flows in an antenna system.

To understand the functions of a balun, it is essential to be familiar with current paths at the feed point of the dipole. These paths are shown in Fig 21-1. Because of their symmetrical relationship, the dipole arms couple energy of equal magnitude and opposite phase onto the feed line, thus canceling induced current flow on the outside of the feed line (*Ref 81*). What is disturbing is the discovery that there are *three* paths for current flow in a coaxial feed line, instead of only two. How can there be three current paths in only two conductors? At RF, skin effect isolates the currents flowing on the inner and outer surfaces of the coaxial shield. This effect, which does not occur significantly at DC or low-frequency AC, prevents currents that flow on the inner braid surface from interacting with those on the outer surface, and vice versa.

As shown in Fig 21-1, while traveling within the transmission line, current I1 flows on the center conductor and I2 flows only on the inner surface of the outer shield. When antenna current is flowing

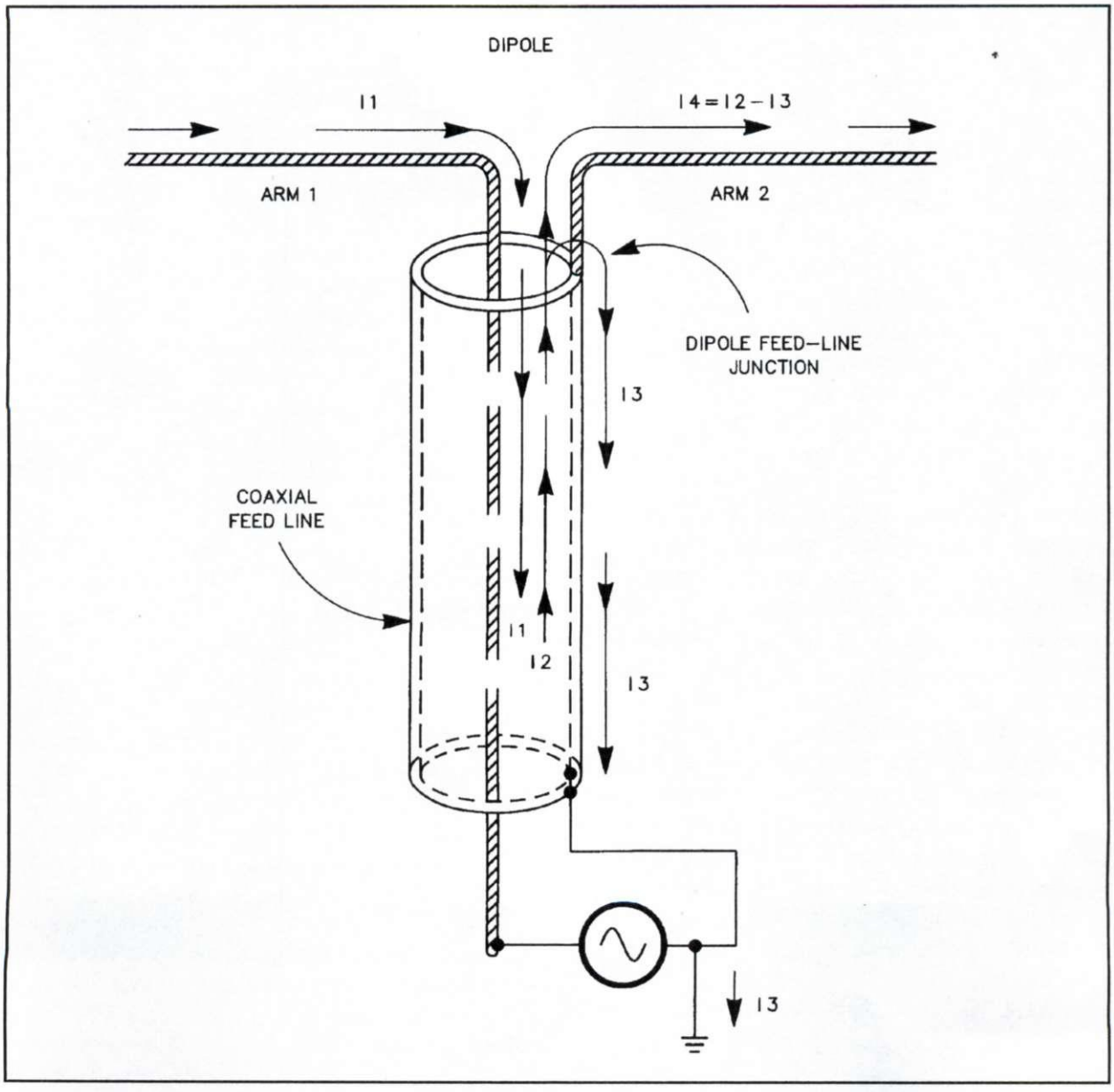

Fig 21-1. Illustration of the various current paths at a dipole feed point.

from left to right as shown, I1 flows out of dipole arm 1, downward onto the center conductor, and returns to the generator. Current I2, being of opposite phase and direction, flows upward along the inside surface of the feed-line shield until it reaches the junction of dipole arm 2. At this junction, I2 divides into two separate paths to form I3 and I4. Current I3 flows back down the *outside* surface of the feed line, and I4, which equals I2 – I3, flows to the right onto dipole arm 2. The magnitude of I3 depends on the impedance to ground provided by the outside surface of the coaxial shield.

If the effective path length to RF ground is an odd multiple of λ/4, the impedance to ground will be very high, making I3 negligible. In this case, I1 and I4 will be nearly equal. On the other hand, if the RF path to ground is a multiple of λ/2, the impedance to ground will be fairly low, and current I3 may be substantial. This results in unequal currents in the dipole arms and radiation from the feed line. In many instances, this RF path to ground includes the transceiver line cord and some house wiring, terminating at the power-line ground! Thus, the amplitude of I3 varies with changes in feed-line length because of changes in the impedance between dipole arm 2 and ground.

Keep in mind that transmission-line currents I1 and I2 *cannot* produce radiation because their fields are not only of equal magnitude and opposite phase, but their fields are also confined within the shield of the coaxial cable. However, the field developed by I3 *does radiate*, and thus, the outer surface of the coaxial braid effectively becomes dipole arm 3, which is connected in parallel with dipole arm 2.

To clarify this equivalent connection of radiators, I've simplified the circuit as shown in Fig 21-2. Since currents I1 and I2 do not interact with any other currents, we may hypothetically place the RF generator directly at the input terminals of the antenna. Now that the coaxial cable is no longer needed to transfer power from the generator to the antenna, the third conductor of the feed line (the outside surface) can be replaced with a single wire connected between arm 2 and RF ground. We have not changed the circuit electrically because I3, which previously flowed on the outside of the coaxial cable, still flows to ground—but now on the single wire shown.

We know that, depending on height, the impedance of a dipole at resonance is usually between 50 and 75 ohms, and is purely resistive. At frequencies above resonance, the resistance increases gradually and series inductive reactance appears; below resonance, the resistance decreases and capacitive reactance appears. The impedance of each dipole arm is half of the total dipole impedance. Since the far end of arm 3 is at RF ground, its impedance behavior follows that of a short-circuited transmission line, with the short appearing at ground. Thus, when the length of arm 3 is an odd multiple of λ/4, its impedance is a parallel-resonant maximum, a high resistance typically from 2000 to 3000 ohms. This high resistance in parallel with arm 2 has little effect on the total dipole impedance. However, as the effective electrical length of arm 3 departs from λ/4 (or odd multiples thereof), by changes in either its physical length or the generator frequency, the input resistance of arm 3 decreases, and reactance also appears in series with the resistance. This reactance is inductive when the length decreases and capacitive when the length increases. If the length of arm 3 is a multiple of λ/2, the resistance will be a series-resonant minimum value (but not zero, because of arm 3 radiation and ground loss). Thus, when arm 3 departs substantially from an odd multiple of λ/4, the net resistive and reactive components of the parallel combination of arms 2 and 3 are different than those of arm 1. Consequently, the dipole impedance is different than if arm 3 was not present.

Returning to Fig 21-1, we can now see that without a balun changing the feed-line length also changes the antenna length (arm 3), which in turn affects the impedance at the input end of the feed line. Therefore, the SWR measured at the input of the transmission line does change with line length when no balun is present to eliminate I3. This phenomenon explains a point that is often puzzling for the amateur who uses no balun, and who believes that he must trim his dipole each time the feed-line length is changed "to keep the SWR down."

It is evident that, in coupling an unbalanced line to a balanced load (such as a dipole), the *primary* function of a balun is to block the external current path between the inside and outside surfaces of the coaxial shield. With a balun in the circuit, I2 will not divide at the end of the feed line to form I3, but

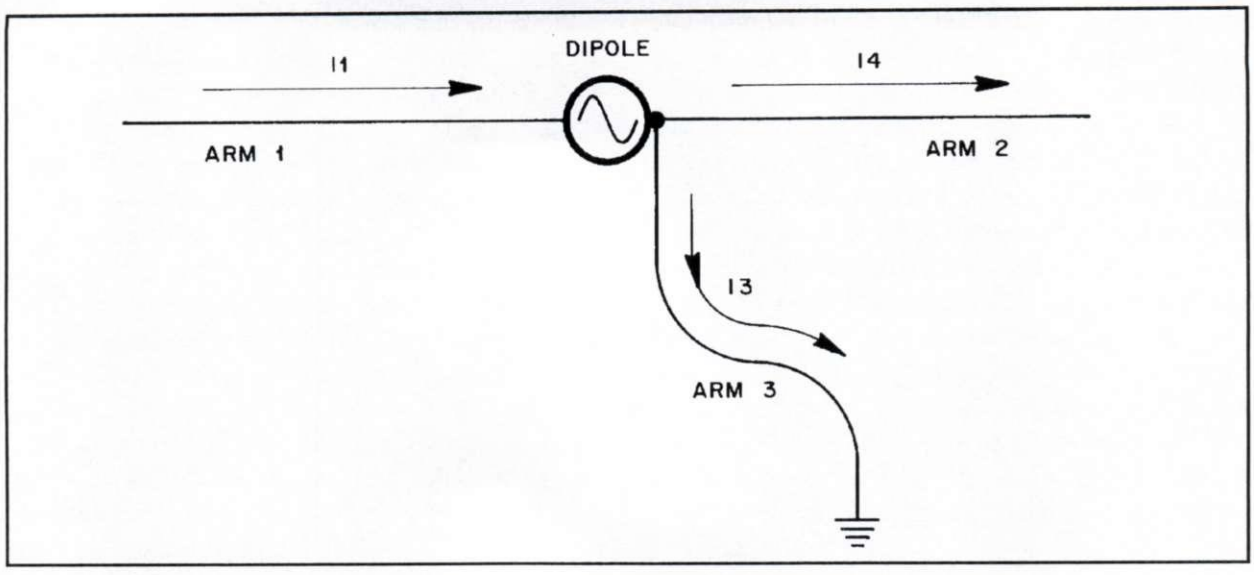

Fig 21-2. Simplified electrical representation of Fig 21-1.

instead will flow only onto dipole arm 2. Thus, when I3 is zero, I4 equals I1, and the currents flowing on dipole arms 1 and 2 are equal and therefore balanced.

After presenting all the above, let me stress that a balun at the antenna feed point will *not* prevent current from flowing on the outside of the coax shield when the coax is asymmetrically coupled to the antenna. When antenna currents on the feed line are caused by *asymmetrical coupling* to the antenna, a balun *will not* eliminate these currents, but will only change their phase and magnitude.

Sec 21.4 The Effects of Using No Balun

It should now be obvious that obtaining accurate impedance measurements of a dipole antenna is difficult. When a transformer-type balun is used to avoid errors caused by I3, impedance-transfer errors obscure the true impedance at the antenna terminals. If the balun is omitted, the true impedance is obscured by the impedance of arm 3 shunting half of the dipole. Since there is no practical way to determine the impedance of arm 3, the true antenna impedance and SWR cannot be calculated from the measured data (*Ref 83*).

Referring again to Fig 21-1, bear in mind that for any given physical length of feed line, the *electrical* length of the coaxial braid surface carrying I3 is not the same as that of the inside conductors carrying I1 and I2. This is because the dielectric constants and the propagation velocity factors are different for the internal dielectric material and the material of the outer jacket. For example, the velocity factors for polyethylene and Teflon™, the inner dielectric of various coaxial cables, are 0.659 and 0.695, respectively. The factor for foamed polyethylene is between 0.75 and 0.81, depending on the amount of air in the foamed material. If the outside surface of the coaxial cable is bare, the velocity factor for the outer shield carrying I3 approaches 0.95. However, the usually thin outer covering of polyvinylchloride (or sometimes Teflon™) reduces the antenna-current velocity factor to a value somewhat less than 0.95.

From an operational viewpoint, current I3 itself is usually not detrimental to the performance of simple dipoles for *160 through 40 meters*. In addition, I3 alone does not cause TVI, unless the feed line is much closer to the TV antenna than the transmitting antenna. However, radiation from external feed-line current can cause severe distortion in the radiation patterns of directive antennas, such as Yagis and quads. Unless a gamma match or other type of unbalanced input-matching scheme is used, all beam antennas with balanced input terminals require a balun if the optimum performance of the antenna system is to be achieved when fed with coaxial cable. For example, when a balun is not employed, the feed line and tower together become

a separate, non-directional vertical antenna. The tower then produces unwanted vertically-polarized radiation that fills in the rearward null in the beam pattern, destroying the front-to-back ratio. The tower radiates along with the feed line, because currents flowing on the outside surface of the line are induced in the tower through inductive and capacitive coupling between the feed line and the tower.

Sec 21.5 The Choke Balun

Although many baluns embody some form of coupling transformer, an alternative is to insert an RF choke in the outer conductor of the feed line. This presents a high impedance to I3 without affecting the internal line currents. Advantages of this method are the lack of limitations on either maximum SWR or power handling. In addition, there is no impedance-transfer error that plagues transformer types of baluns (which causes a skewing of SWR and impedance plots), because the choke balun has no coupling transformer; the feed line goes straight through to the antenna terminals!

The simplest choke balun is formed by coiling up a few turns of the feed line, starting where it connects to the antenna terminals. In the frequency range of 14 to 30 MHz, several turns of feed line coiled in a 6- to 8-inch diameter form an inductor with enough series reactance to minimize I3 and practically eliminate feed-line radiation. Unfortunately, this form of choke (with its air core) is not practical below 14 MHz, because too much coiled-up feed line would be required to reduce I3 to an acceptable level at the lower frequencies.

A word of caution is in order when the choke balun is used on tower-mounted antennas: The choke coil should be placed directly at the feed terminals of the driven element. If the coil is placed away from the feed terminals, any portion of feed line between the terminals and the coil is coupled to the boom or mast, which in turn is coupled to one arm of the driven element. This unbalanced coupling results in an imbalance of currents in the driven element, causing pattern skewing and tower radiation.

The frequency range of the choke balun can be extended to well below 2.0 MHz by using a core of high-permeability ferrite instead of air. With higher core permeability, the choke inductance increases dramatically, thereby retaining the high reactance needed to minimize I3 at the lower frequencies. Of great importance, no core saturation occurs at high power levels in the choke balun (a serious problem in transformer-type baluns), because the core excitation is low level, produced only by I3 and not by the high internal line current that feeds the antenna.

Sec 21.6 The W2DU Balun Constructed with Ferrite Beads

I have obtained greatly improved choke-balun performance by placing several ferrite beads or sleeves of even higher permeability *around* the coaxial feed line (*Ref 84*). For readers who wish to build this simple coaxial balun, bead materials of various size and RF characteristics are available that dramatically increase both the resistance and reactance of a conductor. (Adding resistance to the reactance in this circuit improves the operational bandwidth of the balun with no increase in loss.) In general, the impedance of the outer coaxial braid surface increases almost proportionately with the number of beads placed over it. A combination of 50-ohm Teflon™-dielectric RG-303 cable (or RG-141, with the fabric covering removed) and ferrite beads having an ID of 0.197 inch and a length of 0.190 inch form a superb, compact wide-band balun. While the two inner conductors of the coaxial cable remain unaffected, the beads introduce a high impedance in series with the outer surface of the braid. This configuration effectively isolates the external output terminal of the feed line from that at the input end.

I made a test balun by slipping 300 no. 73 beads (μ = 2500 to 4000) over a piece of RG-303 coaxial cable. The impedance of the outer conductor of the cable measured 4500 + j3800 ohms at 4.0 MHz; 15.6 + j13.1 was measured using a single bead. For practical baluns to be used from 1.8 to 30 MHz (less than 12 inches long, including connector), use 50 no. 73 beads (no. FB-73-2401).[1] For 30 to 250 MHz, use 25 no. 43 beads (μ = 950 to 3000, no. FB-43-2401). No. 64 beads (μ = 250 to 375) are recommended for use above 200 MHz, but I have not yet experimented with them. The coaxial cable need be only long enough to hold the beads and to access the end connectors. The plots appearing in the graph of Fig 21-3 show the measured values of series resistance R, reactance X, and impedance Z

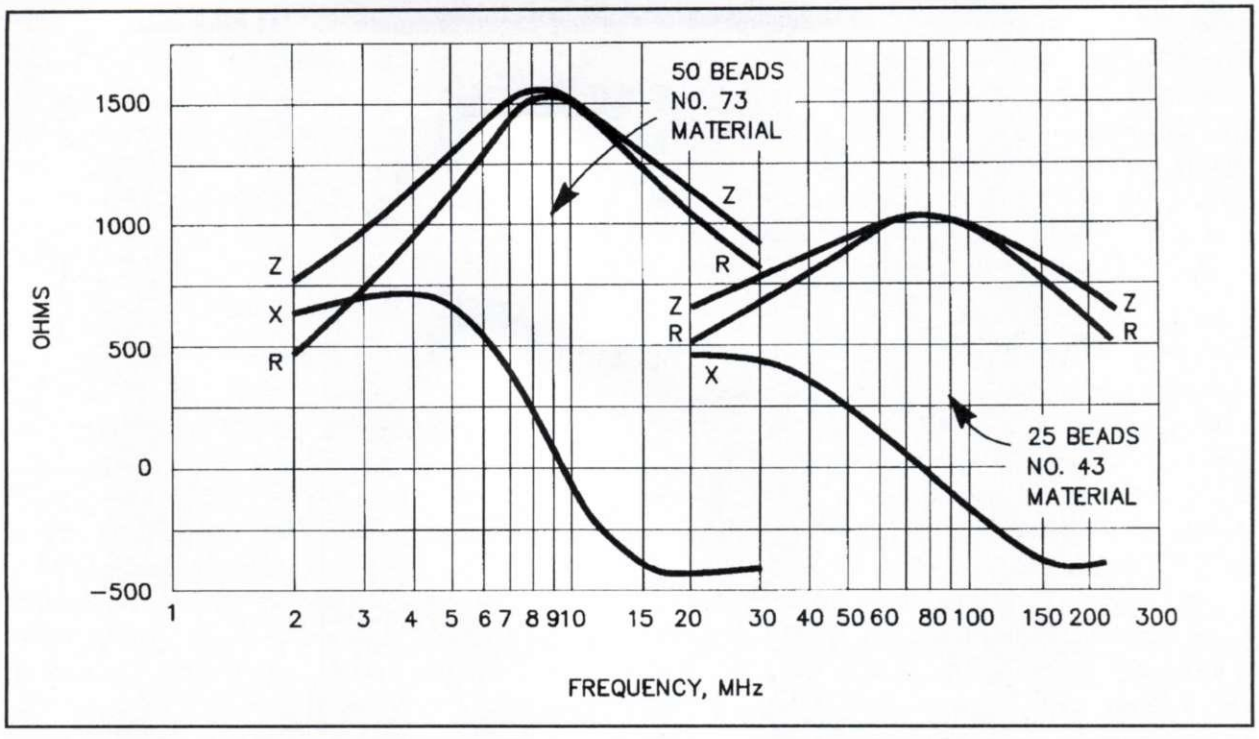

Fig 21-3. Graph of frequency versus series impedance of coaxial-balun shield outer surface.

versus frequency of the outer braid surface of a choke balun for both the 25- and 50-bead types. With either balun, I3 will be negligible over the frequencies indicated.

At full legal input levels, no power-handling problems will arise using these baluns, because the CW power-handling capability of the cable is 3.5 kW at 50 MHz, and 9 kW at 10 MHz *(Ref 87)*. Any suitable connector that will mate with the load end of your feed line can be used at the input of the balun coax, and the balanced-output terminals may simply be pigtails formed by the inner and outer conductors of the balun coax. Methods for connecting the output terminals of the balun to the antenna are left to your ingenuity.

To emphasize simplicity, what VHF antenna buff wouldn't delight in dumping his unwieldy, frequency-sensitive, λ/4 line balun? You can replace it simply by putting some ferrite beads on the last few inches of the coaxial feed line!

Sec 21.7 Analysis of Voltage and Current Baluns

Roy Lewallen, W7EL, performed extensive analysis and testing of imbalance on different circuit arrangements of both the choke balun and the ferrite-core transformer balun *(Ref 118)*. His analysis shows that while choke baluns are *current* baluns, bifilar-wound 4:1 and trifilar-wound 1:1 transformer baluns are *voltage* baluns. To the best of my knowledge, with the exception of the W2DU ferrite-bead balun (which is a current balun), all 1:1 baluns available on the commercial market that use trifilar transformer baluns are therefore *voltage* baluns.

Lewallen determined analytically that current baluns *force* equal currents into opposite halves of a dipole, independent of the impedance of either half. On the other hand, voltage baluns provide only equal voltage to the opposite halves, and thus do not provide equal currents in each half if the impedances of the two halves are not identical. His tests show overwhelmingly that choke-type current baluns provide the best balance of the dipole currents, and the least flow of antenna current on the transmission line. Lewallen's paper is a real eye-opener concerning balun design and use. Tests performed by Dr. John (Jack) Belrose, VE2CV, provide corroborating evidence of the validity of Lewallen's analysis and tests, which I describe in Sec 21.10.

In addition to Lewallen's work, Sabin also performed a detailed analysis concerning the actions

of the electric and magnetic fields in the operation of the 1:1 current balun, along with experimental evidence that prove his conclusions to be correct. *(Ref 136).*

Sec 21.8 Verifying Output-Current Balance in Current Baluns

As stated, the ferrite-bead choke balun is a current balun. I use a simple test technique that proves the balun is a current balun and that also determines the degree of current balance between the balanced output terminals. As illustrated in Fig 21-4A, mount the balun on a one-foot square aluminum plate, with the shield side of the unbalanced coaxial input terminal grounded to the plate. Connect a separate resistor between each of the coaxial output terminals and the plate. Fig 21-4B shows the electrical equivalent of this test setup. With an RF voltage applied at the unbalanced input terminals, measure the voltage appearing across each resistor with an RF voltmeter. (I use a Hewlett-Packard 410B.) When both resistors are of the same value, identical values of voltage will appear across each resistor, indicating equal current in each resistor, and signifying a balanced output.

Although equal current flowing in equal resistances signifies a balanced output relative to voltage, it does not yet prove we have a current balun. However, we can prove we have a current balun if we can show that equal currents flow in each terminating resistor when their resistances are *unequal.* Indeed, this is the case, because with this balun the voltages appearing across unequal values of terminating resistances are directly proportional to the values of the resistance, while the currents are equal. For example, say the two terminating resistors are 50 and 100 ohms, and the input voltage is adjusted so that 1 volt appears across the 50-ohm resistor. Then 2 volts will appear across the 100-ohm resistor. Applying Ohm's Law now proves that equal currents are flowing in the two terminations, even though their impedances are different.

The ferrite beads perform their task of isolating the output and input terminals of the coaxial-line outer conductor by inserting a high longitudinal impedance between them, which permits the balanced output from an unbalanced input. If you have any doubt about that, consider this: If the beads were not inserting a high resistance in series with the outer surface of the outer conductor, terminating resistor R1 in Fig 21-4 would be short circuited by the low resistance of the outer conductor and low resistance of the ground plane, thus the voltage appearing across R1 would be zero.

Sec 21.9 Baluns with Antenna Tuners

In providing a balanced output for feeding open-wire or ladder-line transmission lines, it is common practice among manufacturers of antenna tuners to place the balun in the output circuit of the tuner. In all manufactured tuners with which I'm familiar, the baluns used are transformer-type, 4:1 voltage baluns wound around ferrite cores, usually toroids. Unfortunately, the output circuit is not necessarily the ideal place for the balun, for reasons I'll explain shortly. Further, the voltage balun is vastly inferior to the current balun in obtaining balanced currents in the feed line. Sec 21.10 explains why it is that when you use balanced feeders, the ideal arrangement for an antenna tuner is to place the balun at the *input* of the tuner, and for the balun to be a choke-type *current* balun such as the W2DU balun.

Let's first examine some of the problems encountered when you use a ferrite-core, transformer-type voltage balun in the output circuit of the tuner. When a transformer balun has a ferrite core, the core is subjected to the total magnetic flux developed by the load current, and the resulting high magnetic flux density can cause the core to saturate. When the core saturates, the RF waveform in the output becomes distorted, creating undesirable harmonic signals. A transformerless choke balun made with coiled-up coax, or a short coax with external ferrite beads, has no core to saturate. In addition, the external beads are not subjected to the magnetic flux developed by the load current. The beads are subjected only to the flux developed by the small current flowing through the high impedance that the beads create on the outside surface of the outer conductor. Hence, no harmonics are generated with the ferrite-bead current balun.

Another problem encountered with the ferrite-core transformer-type voltage balun is the distributed capacitance between its windings, which causes current unbalance between the two output ports that feed the balanced feed line. The input impedance of a balanced feed line can range in value from low to very high, and generally has a

reactance component. The higher the line-input impedance, and the higher the operating frequency, the greater is the effect of the distributed capacitance in contributing to output current unbalance. On the other hand, output current unbalance is negligible with the ferrite-bead current balun.

Another undesirable feature of the 4:1 ferrite-core balun placed at the output of the tuner is that it easily can be permanently damaged. This can happen from overloading the balun when you operate with high power into a line having a high SWR that results in a high input impedance containing a large amount of reactance.

A still further undesirable feature of the 4:1 ferrite-core balun is its contribution to power loss. Typical losses with this type of balun range from around 0.5 dB at 2 MHz to 2 dB at 30 MHz. In contrast, the loss in the W2DU balun is minimal, only

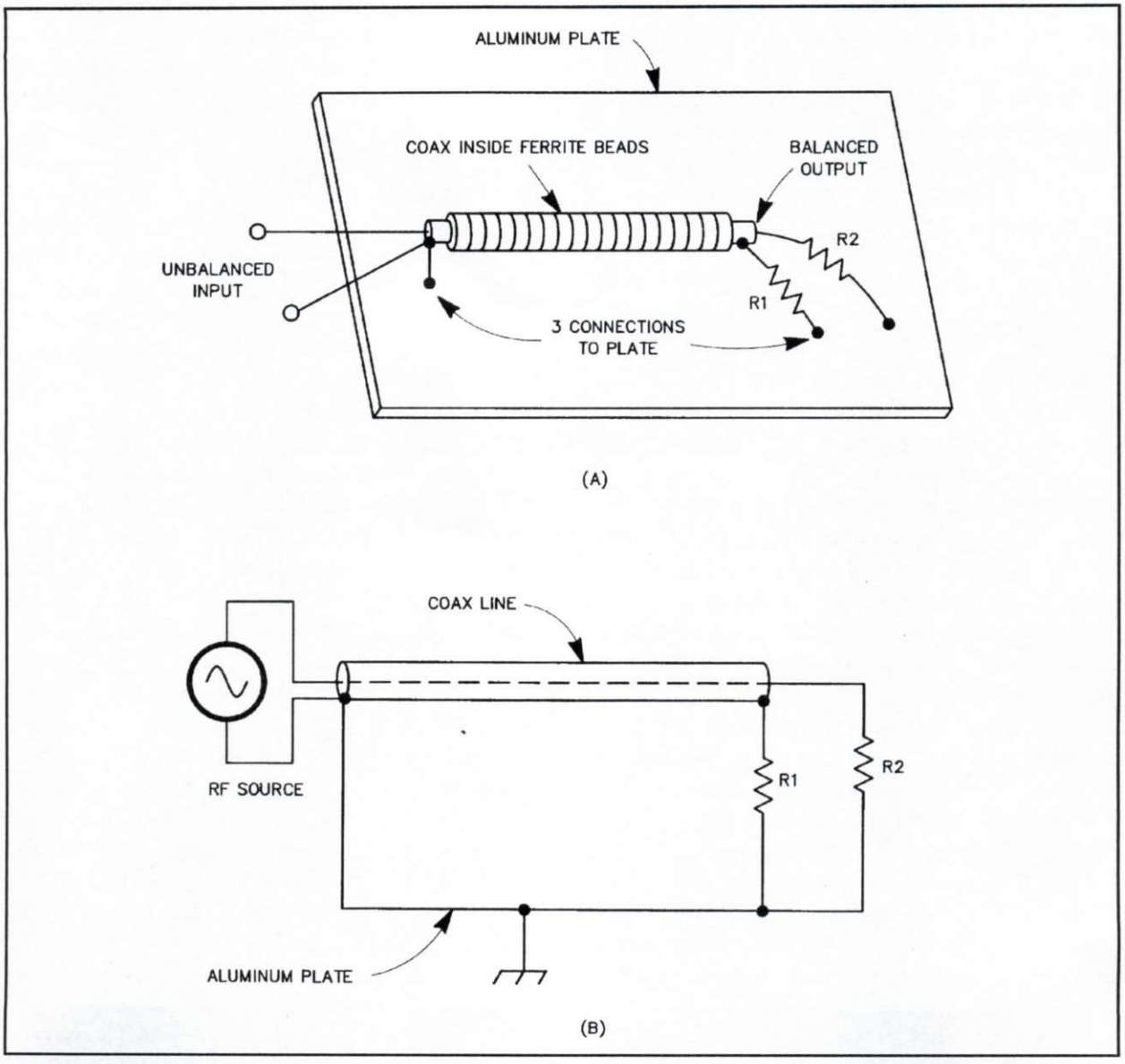

Fig 21-4. The drawing at A shows a test setup for measuring the degree of balance in a current balun, and B shows its electrical equivalent, with an RF source. With a perfect balun and an RF voltage applied at the unbalanced input, the voltage drops across R1 and R2 will be directly proportional to their resistances. This proves that equal current flows in the two resistors, and no current flows on the outside of the coax shield to short out R1, contrary to the way it appears in B.

from 0.1 to 0.2 dB across the band, because the only loss involved is in the attenuation suffered in a 10.5-inch length of coaxial line.

Sec 21.10 Placing the Balun at the Input of the Antenna Tuner

At least three writers published articles that advocate placing the balun at the *input* of the tuner, rather than at the output, for the same reasons I explained above. These writers are John Belrose, VE2CV (*Ref 132*), Albert Roehm, W2OBJ (*Ref 127*), and Richard Measures, AG6K *(Ref 133)*. Belrose (in 1981) showed a balanced T-network driven by a 4:1 voltage balun (but see the paragraphs that follow). Measures used a balanced L-network fed by a 1:1 choke, or current balun comprising a coiled-up section of coaxial line. To cover the range of 1.8 to 30 MHz, his balun is a rather bulky 20 feet of coax coiled on a 5-inch diameter ABS pipe. The bulkiness can be reduced by using the W2DU configuration—a 10.5-inch long coax section covered with external ferrite beads, which is just what Roehm did in his arrangement. However, the results of Roehm's and Measures' placing the balun at the input of the tuner are excellent.

Let me add a few words about the work of John (Jack) Belrose, PhD, VE2CV *(Ref 132)*. Jack conducted tests on a novel approach to the broadbanding of dipole antennas and published the results in *QST* (*Ref 134*). His antenna is asymmetrical with respect to the impedance seen relative to each wire of a balanced feed line. Consequently, he discovered that the currents in each wire of the feed line were severely unbalanced when using the 4:1 voltage balun to feed the balanced antenna tuner. He then substituted a commercially manufactured W2DU current balun and repeated the measurements. To his surprise, the feed-line currents were almost perfectly balanced when using the W2DU balun. Jack's feed line comprised two parallel coaxial lines; the outer conductors were connected together and grounded to the tuner, and the center conductors were used as the balanced feeders.

Jack's measurements also revealed that when he used the voltage balun, the current on the outer conductors was high, and varied widely over the frequency range from 2 to 30 MHz, also signifying poor balance. However, when using the W2DU current balun, the outer conductor current was very low, and nearly constant, verifying the good balance. These results of Jack's measurements offer additional verification of my own measurements that prove the W2DU current balun solves many of the problems experienced with the transformer baluns that I described earlier.

Jack prepared graphs that compare input impedance and attenuation versus frequency of a ferrite-core balun and the W2DU balun. The data in the graphs again confirm my measurements. They attest to the remarkable superiority of using ferrite beads around a coaxial line to form a current balun, compared to the ferrite-core transformer-type voltage balun. Jack has also devised a unique method of forming a 4:1 current balun by using two W2DU baluns, connecting them in parallel at the input and in series at the output.

Since the 1st edition of this book was published, Roy Lewallen performed an analysis concerning balun operation with antenna tuners, comparing the performance of 1:1 baluns placed at either end of the tuner. In private correspondence, he reported that there is an insignificant difference in performance of the balun, whether placed at the input or the output of the tuner.

Sec 21.11 The Labor Pains and Birth of the W2DU Ferrite-Bead Current Balun

It is interesting to know that the original design of the W2DU ferrite bead balun is a spin-off from the development of antenna systems designed for spacecraft built by RCA's Astro-Electronic Division, specifically the antenna system developed by the author for the world's first weather spacecraft, TIROS 1, and its successors.

Because the radiation patterns of the antenna system are vital to the successful operation of the spacecraft, many measurements of the patterns were required during the development stage to discover the correct physical and electrical properties of the antenna that would produce a satisfactory pattern while attached to the spacecraft.

To obtain realistic radiation patterns of the antenna it must be mounted on the spacecraft during the measurements, because the spacecraft is in the radiation field of the antenna, and therefore distorts, or modifies, the shape of the field that would be radiated from the antenna if it were oper-

ating in free space—i.e., without being mounted on the spacecraft.

Consequently, to measure the patterns from all angles around the entire radiation sphere of the antenna, the spacecraft was mounted on a revolving pedestal having a freedom of motion that allowed the spacecraft to be rotated on two separate quadrature-related axes—i.e., 90° between the axes.

In the measurement setup used at RCA's antenna test range, the entire spacecraft with its antenna was immersed in an electromagnetic field radiated from a ground-mounted log-periodic antenna aimed at the spacecraft. The field comprised an RF signal modulated by a 1-kHz audio tone received by the spacecraft antenna. The received audio signal tone was conducted down the pedestal through a coaxial downlead cable and routed to the control room where it was recorded during the rotation of the spacecraft, recording the RF signal level.

However, the vertically-oriented coax downlead distorted the radiation pattern when measuring either the vertical or circular polarization of the spacecraft antenna, but not when measuring with horizontal polarization. It was thus obvious that because the downlead was also immersed in the RF field, re-radiation from the downlead as a second source of RF was distorting the field illuminating the spacecraft antenna and thus distorting its radiation pattern. Proof that the downlead was the culprit was obtained when manually moving the downlead three or four inches in any direction caused a variation in pattern level greater than 3 dB in any antenna orientation where the pattern level was a few dB below the maximum. Unacceptable.

Consequently, to obtain true radiation patterns from the spacecraft antenna it was necessary to eliminate radiation from the downlead. I knew that a conductor of length $\lambda/4$ or less could not sustain an RF current, but at the VHF/UHF frequencies involved in the measurements the downlead was several wavelengths long. One way to solve the problem would be to break the downlead into individual lengths, $\lambda/4$ or shorter, and connect them with resistors that would effectively impede the RF, but allow the audio to travel. However, the mechanical construction for this solution seemed impractical.

During this era a new method of restricting flow of RF current on conductors was coming into vogue with the use of ferrites. Ferrite beads placed around a conductor allowed DC to flow, but restricted the flow of RF. I contemplated what would happen if I were to place an appropriate bead around the downlead at every $\lambda/4$ point along the coax at the measurement frequency. This arrangement would effectively break the coax into $\lambda/4$ RF sections electrically, but leave it intact physically. Therefore, I experimented with no. 43 bead material placed around the RG-58 cable at $\lambda/4$ intervals, and *voilá*—no more radiation from the downlead and thus no more distortion of the radiation pattern from movement of the downlead. Accurate radiation patterns from the spacecraft antennas at last!

Several months later, while listening to on-the-air discussions of problems that occurred when using wire-wound voltage baluns constructed around a ferrite core, a light bulb turned on in my mind. My immediate thought was if beads impeded current flow on the downlead in the radiation-pattern measurement setup, why wouldn't they also impede common-mode current flow on the outside of the coax feed line resulting from the *bal*anced input of the antenna terminating the *un*balanced coax? Why not indeed! I knew current was flowing on the outside of *my* feed line, because when measuring the impedance at the input terminals of the line using the General Radio GR-1606-A RF impedance bridge, the indicating null would disappear while running my fingers along the line. I knew from those symptoms that the common-mode current on the feed line was also destroying the accuracy of the impedance measurements.

I then reasoned that a bead resistance of at least ten times the impedance looking into one half of the dipole should reduce the current flow on the outside of the coax shield to one-hundredth of the power delivered to the dipole half connected to the shield, an insignificant amount.

After researching the various terminal impedances that would be encountered with dipoles throughout the HF bands the worst-case situation appeared to occur on the 75–80-meter band, when operating at the low end of the band at 3.50 MHz with the antenna resonant at 3.75 MHz. At 3.778 MHz the terminal impedance of my nearly resonant 125-ft dipole was $64.83 + j0.18$ ohms, for a 1.28 SWR. However, at 3.50 MHz the terminal

impedance was 53.17 – *j*144.35 ohms, for a 9.6 SWR. (These values can be seen in Table 15-5 and from Fig 15-1.) The magnitude of this impedance is 153.8 ohms at 69.8°. However, this is the total input terminal impedance of the dipole, while the dipole half fed by the shield, or outer conductor of the coax, is only one half of this value, or 76.9 ohms. Thus, a bead resistance of approximately 800 ohms should provide adequate reduction of common-mode current on the outside of the feed line in this worst-case situation.

After studying the specifications of several ferrite beads I ordered 300 no. 73 beads from The Wireman for experimentation. A brief report of some of the experimental data that led to the design of the commercial version of the W2DU balun is shown in Sec 21.6. Additional data can be seen in Fig 21-3, which shows the impedance, resistance, and reactance of 50 no. 73 beads versus frequency. Observe that the bead impedance at 3.50 MHz is slightly greater than 1000 ohms, amply sufficient to reduce the common-mode current on the feed line of the 80-meter dipole to insignificant.

In addition to showing the impedance plot of my 80-meter dipole from 3.45 to 4.075 MHz, the graph of Fig 15-1 provides evidence that the common-mode current on two different coaxial feed lines is insignificant when the 50-bead W2DU balun is inserted between the feed line and the antenna. As mentioned earlier, common-mode current on the outer surface of the coax will destroy the accuracy of any measurement of impedance at the input of the coax. When measuring the terminal impedance of an antenna by measuring the impedance at the input of its *calibrated* feed line, the same impedance reading will be obtained regardless of the length of the feed line as long as its calibration is accurate. However, if a common-mode current exists on the outer surface of the coax, different input terminal impedances will result if the impedance is measured using coax of different lengths, even though both are accurately calibrated. The greatest difference will prevail if the difference in lengths is λ/4.

Observe that in Fig 15-1 the solid lines represent measurements of the resistance, reactance, and SWR of my 80-meter dipole made with a λ/4 length feed line, while the dashed lines represent measurements made with a λ/2 length feed line. Observe also that the difference between the solid and dashed lines is almost non-existent, indicating insignificant errors in measurement, and showing negligible common-mode current flowing on the lines, thus proving the effectiveness of the W2DU balun in eliminating the common-mode current. Note that the dipole data measured with both the λ/4 and λ/2 length feed lines plotted in Fig 15-1 appears in Tables 15-4 and 15-5.

Thus endeth the story of the evolution of the W2DU ferrite bead balun.

Note

1. Ferrite bead material may be obtained from the following sources: The Wireman (Press Jones, N8UG), 261 Pittman Road, Landrum, SC 29356; phone 800-727-9473; website <www.thewireman.com>. The Wireman also has W2DU baluns available both in kit form and fully fabricated, ready for installation. Ferrite bead material is also available from Palomar Engineers, Box 462222, Escondido, CA, 92046; phone 760-747-3343; website <www.Palomar-Engineers.com>; and Amidon Associates, 240 Briggs Avenue, Costa Mesa, CA 92626; phone 714-850-4660; website <www.amidoncorp.com>. Fully fabricated W2DU baluns are also manufactured by the Unadilla Antenna Manufacturing Company, PO Box 4215, Andover, MA 01810; phone 978-975-2711; website <www.unadilla.com>, and are available at Amateur Electronic Supply (AES) outlets. (Note: W2**A**U baluns made by Unadilla are *trifilar 1:1, and bifilar 4:1, ferrite-core, transformer-type* ***voltage*** baluns.)

Chapter 22

The Quadrifilar Helix Antenna

Sec 22.1 Introduction

The quadrifilar helix antenna, shown in Fig 22-1, has seen use on commercial and military, as well as amateur spacecraft. For amateur applications it first saw use on AMSAT-OSCAR 7 in November 1974. I prepared the basic information in this chapter while I was employed as an antenna engineer at RCA's Astro-Electronics Division in Princeton, New Jersey. While working at RCA, I assisted in the development of the quadrifilar helix.[1] We consider this antenna to be an outstanding contribution to practical spacecraft antenna engineering from the viewpoint of flexibility in design. The quadrifilar helix provides a large range of radiation characteristics from a radiator of extremely small size and weight, from which we can select a pretested design to match the radiation requirements of any particular spacecraft. The quadrifilars shown in Fig 22-1 are flight-model units for operation at 1800 and 2200 MHz. I also assisted in the design of quadrifilars for 121.5, 243, and 1600 MHz, which flew on TIROS-N (NOAA 9 through 14) weather spacecraft in the worldwide Search and Rescue (SAR) Emergency Locator Transmitter (ELT) service. The service is primarily for downed or stricken aircraft, over either land or sea.

One reason for presenting details of the quadrifilar in this book is that it is an inherently excellent antenna for ground-station use in the Amateur Satellite Service. Once you study the following

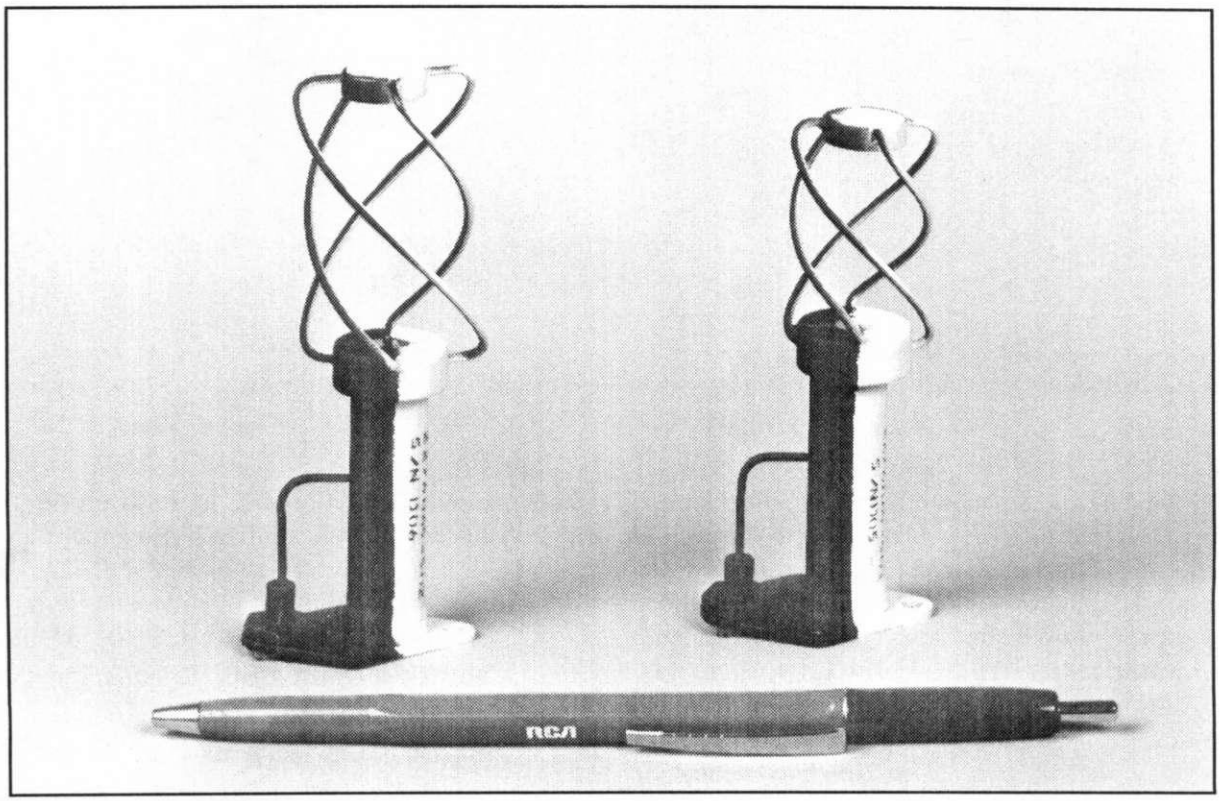

Fig 22-1. 1.8- and 2.2-GHz quadrifilar helix antennas.

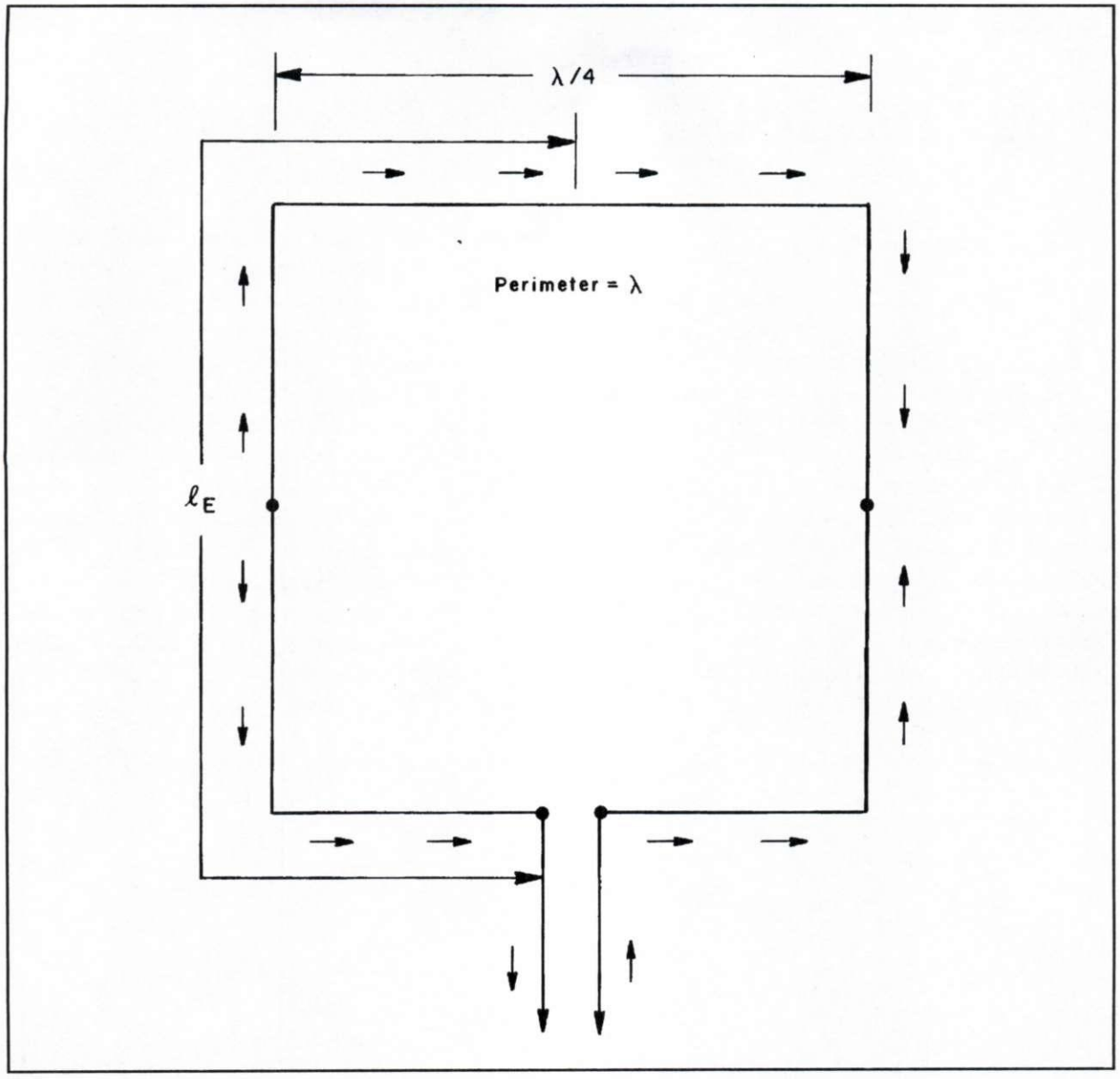

Fig 22-2. Horizontally polarized square loop radiator. The small arrows represent the direction of current flow.

engineering aspects of the quadrifilar, you will discover its advantages over other circularly polarized antennas, such as crossed Yagis. It is useful at 144 MHz, and up, and all the critical dimensions are included in this chapter. The dimensions are listed in wavelengths, so all you have to do is convert them to the desired frequency. The details of feeding, phasing, and infinite balun construction are given in the drawings and photos, long with sufficient explanation for you to construct your own quadrifilar.

Radiation from the quadrifilar helix antenna is circularly polarized and of the same screw sense everywhere throughout the radiation sphere. The antenna embodies a unique configuration and method of feeding loop elements to produce radiation having a controllable pattern shape. Refer again to Fig 22-1. The quadrifilar antenna comprises two bifilar helical loops oriented in a mutually orthogonal relation on a common axis. The terminals of each loop are fed 180° out of phase, and the currents in the two loops are in phase quadrature (90° out of phase).

By selecting the appropriate configuration of the loops, a wide range of radiation-pattern shapes is

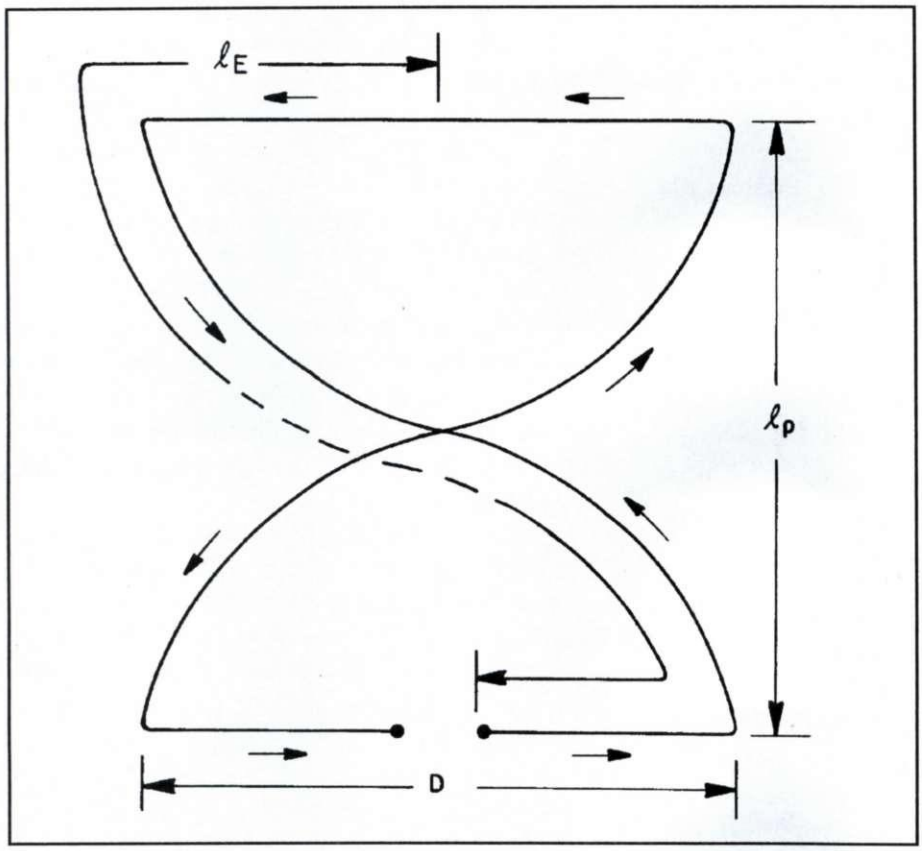

Fig 22-3. Half-turn bifilar helix loop. Distance len_E° equals the loop half-length.

available, with excellent axial ratio appearing over a large volume of the pattern. The basic form of the quadrifilar antenna was developed by Dr. C. C. Kilgus of the Applied Physics Laboratory, Johns Hopkins University, who published several papers that established the theoretical basis for its operation (*Refs* 88 through 96). The Brown and Woodward citation (*Ref 90*) is especially helpful in understanding the radiation characteristics of the quadrifilar. That paper describes radiation from the combination of a dipole and a circular loop sharing a common axis, and fed in phase, which produces radiation characteristics similar to the quadrifilar. This version of the quadrifilar helix uses a novel feed system that includes the infinite balun. The feed system also includes a means for attaining the required 90° differential current phase relationship without requiring additional components to achieve separate differential-phase excitations.

The quadrifilar antenna is applicable for general use in the frequency range above 30 MHz. It is especially attractive for certain spacecraft applications because it can provide omnidirectional radiation in a single hemisphere (a cardioid volume of revolution) without requiring a ground plane. This no-ground-plane feature affords a dramatic saving in weight and space. In addition, the inherent cardioid radiation characteristic that eliminates the need for the ground plane also affords freedom in the choice of a mounting position on a spacecraft. The profile of the volume beneath the antenna has relatively little effect on the radiation pattern, provided that the quadrifilar is mounted at least $\lambda/4$ above conducting surfaces which would form a reflective plane.

Quadrifilars designed to operate in the frequency range of 1800 and 2200 MHz can be extremely light, weighing only about 0.7 ounce. Developed by RCA Astro-Electronics, several of these antennas flew on U.S. Air Force satellites of the Defense Meteorological Support program, also built by RCA. A slightly smaller version of similar design (donated by RCA Astro-Electronics) is the 2304.1-MHz beacon antenna, which flew on AMSAT-OSCAR 7.

Quadrifilars having a somewhat different configuration from that shown in Fig 22-1 were also developed by RCA for use on RCA-built NOAA

TIROS-N weather satellites. The design differs because the radiation pattern requirements are different. The design of the quadrifilars for transmitting the principal video signals from the TIROS-N spacecraft is noteworthy because the radiation pattern was shaped to maintain a nearly constant signal level versus slant-range distance between the spacecraft and the ground station during the in-view portion of the spacecraft orbit. (RCA-built TIROS-N, or NOAA spacecraft launched around 1979 were still in service in April 1999.)

Sec 22.2 Physical Characteristics

There is a tendency to confuse the quadrifilar with the conventional helical antenna, probably because portions of the quadrifilar are helically shaped. As a result, the radiation characteristics of the quadrifilar antenna are sometimes misunderstood. Although the term quadrifilar is not incorrect, the term itself often fails to conjure up a true picture of the physical characteristics. Therefore, since several characteristics of the quadrifilar antenna differ radically from those of the conventional helical antenna (for example, opposite screw sense of circular polarization), the following paragraphs examine some aspects of both the physical and the radiation characteristics of the quadrifilar to clarify the confusion.

In describing the physical characteristics of the quadrifilar, I will concentrate on the simple half-turn $\lambda/2$ configuration. As I stated earlier, the quadrifilar helix is a combination of two bifilar helicals arranged in a mutually orthogonal relationship along a common axis, and enveloping a common volume.

What is a bifilar helix? One way of visualizing the half-turn $\lambda/2$ bifilar helix is to develop it from a continuous square loop of wire one wavelength in perimeter, as shown in Fig 22-2. As in the driven element of the conventional cubical quad antenna, each side of this square loop is $\lambda/4$, and the feed terminals are formed by opening the loop at the midpoint of the bottom side. We call this square-loop configuration a zero-turn, $\lambda/2$ bifilar loop. There is a half wavelength of wire radiator extending away from each feed terminal around the loop to the antipodal point on the opposite side of the square (loop half-length $len_E°$ equals $\lambda/2$). The drawing shows length $len°$ with a script letter L. This loop is a balanced input device, requiring a balanced, two-wire feed line with push-pull currents.

To visualize the development of the quadrifilar helix, imagine inserting an imaginary cylinder of diameter $D = \lambda/4$ inside the loop. Then, while holding the bottom side of the loop fixed, grasp the top side and give it a half turn of rotation with respect to the bottom. As a result, shown in Fig 22-3, each of the two vertical sides of the square loop becomes a half-turn helix as it curves around the surface of the imaginary cylinder. However, because of the curved paths of the once-straight vertical sides, the distance between the top and the bottom has shrunk, and the axial length, $len_P°$, is less than the $\lambda/4$ diameter.

With these particular proportions of the $^1/_2$-turn, $\lambda/2$ bifilar, some of the radiation characteristics are not particularly attractive. However, some physical parameters of the loop may be selected to obtain characteristics that make this antenna especially attractive. Such parameters include the electrical length of the conductors, the number of turns, the cylindrical diameter D, and length $len_P°$. In addition, for a given conductor length, the length-to-diameter ratio, abbreviated len/diam, of the cylinder is also an important variable, controlled by the diameter and number of turns. For example, the antennas shown in Fig 22-1 are $^1/_2$-turn, $\lambda/2$ quadrifilars. However, by reducing the diameter from 0.25 λ to 0.18 λ for this model, the axial length is inherently increased to 0.27 λ. This results in vastly improved radiation characteristics.

Sec 22.3 Electrical Characteristics

Let's take a short qualitative look at some basic changes in the radiation pattern that result from the $^1/_2$-turn twist of the square loop. First, recall that the square loop having a perimeter $P = \lambda$ is basically a broadside array of two dipole elements, with the top element being voltage fed from the bottom element. In this loop the currents in the top and bottom sides flow in the same direction, as shown in Fig 22-2. The horizontally polarized fields produced by the currents in both top and bottom sides are therefore in phase. The two fields add to form the conventional figure-8 broadside radiation pattern. The bidirectional lobes in the pattern are at right angles to the plane of the loop. The null in the pattern appears bidirectionally on a horizon-

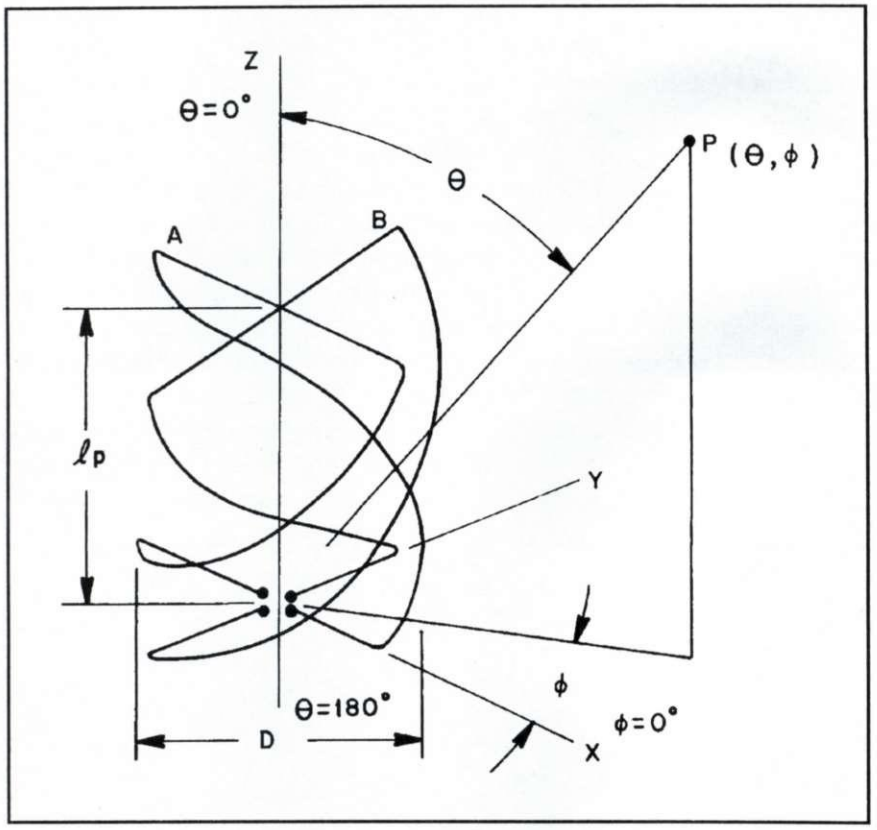

Fig 22-4. Half-turn quadrifilar (two half-turn bifilar loops.

tal line that is in the plane of the loop midway between the top and bottom sides.

In the vertical sides of the loop, the current in the top half of each side flows in the direction opposite to that in the corresponding bottom half. Consequently, the vertically polarized fields produced by both halves of each vertical side are mutually out of phase, and add to zero in all directions. This cancellation of the vertical fields results in zero net vertically polarized radiation.

On the other hand, in the bifilar helix loop having the half-turn twist, the currents in the top and bottom sides flow in opposite directions because of the physical half-turn rotation of the top side. This current relationship is shown in Fig 22-3. Thus, the fields produced by the currents in the top and bottom sides are now out of phase with each other, forming an end-fire array relationship.

In the direction broadside to the plane formed by the top and bottom sides, the fields now cancel completely. As in the ordinary end-fire array, this results in zero radiation in the broadside direction, where maximum radiation appeared with the square loop. The conventional lobes of end-fire radiation contributed by the top and bottom sides now occur toward the top and bottom of the antenna as drawn in Fig 22-3. This radiation is horizontally polarized.

The currents flowing in the helical portions of the loop retain the same current-flow pattern as in Fig 22-2. However, the physical positions of each current segment, or element, in the twisted vertical wires have now been shifted to a new position, and to a new orientation in the helical paths. This results in a corresponding different position and vector direction for each elemental field produced by the helical current elements. As would be expected, the addition of all these elemental fields now results in a composite field consisting of both horizontally and vertically polarized fields.

Sec 22.4 Difference Between Quadrifilar and Conventional Helix

Before further considering the radiation characteristics of the bifilar helix, it may be helpful to mention some critical distinctions between the Kilgus bifilar helix and the conventional helical antenna configurations. In the conventional helical antenna having more than one radiating element,

the elements are generally fed in phase. However, Kilgus found that interesting results were obtained with a helical antenna that has two elements spaced radially at 180° when the two elements are fed 180° out of phase. This finding led Kilgus to his further investigation of the bifilar helical antenna having out-of-phase feed, and still further to the quadrifilar configuration. Thus, an alternative way of visualizing the bifilar helix is as a conventional helical antenna with two elements radially spaced at 180°, but with the outer ends radially connected to each other, and with the elements fed *out of phase.*

Dr. Kilgus's analyses provide a more complete theoretical basis for the functioning of both the bifilar and the quadrifilar helix. He shows the current distribution and radiation characteristics of the half-turn, λ/2 bifilar helix to be similar to those of a loop-dipole combination described by Brown and Woodward *(Ref 90).* Brown and Woodward analyzed a combination horizontal loop and vertical dipole sharing a common axis. They show that while both a loop and a dipole produce identical toroid-shaped radiation patterns, the electric field produced by the dipole current in this arrangement is vertical, and the electric field produced by the loop current is horizontal. When the currents in the loop and dipole are in phase, their fields are in phase quadrature, a requirement for circularly polarized radiation. When the vertical and horizontal fields are also equal in magnitude, the resulting radiation is circularly

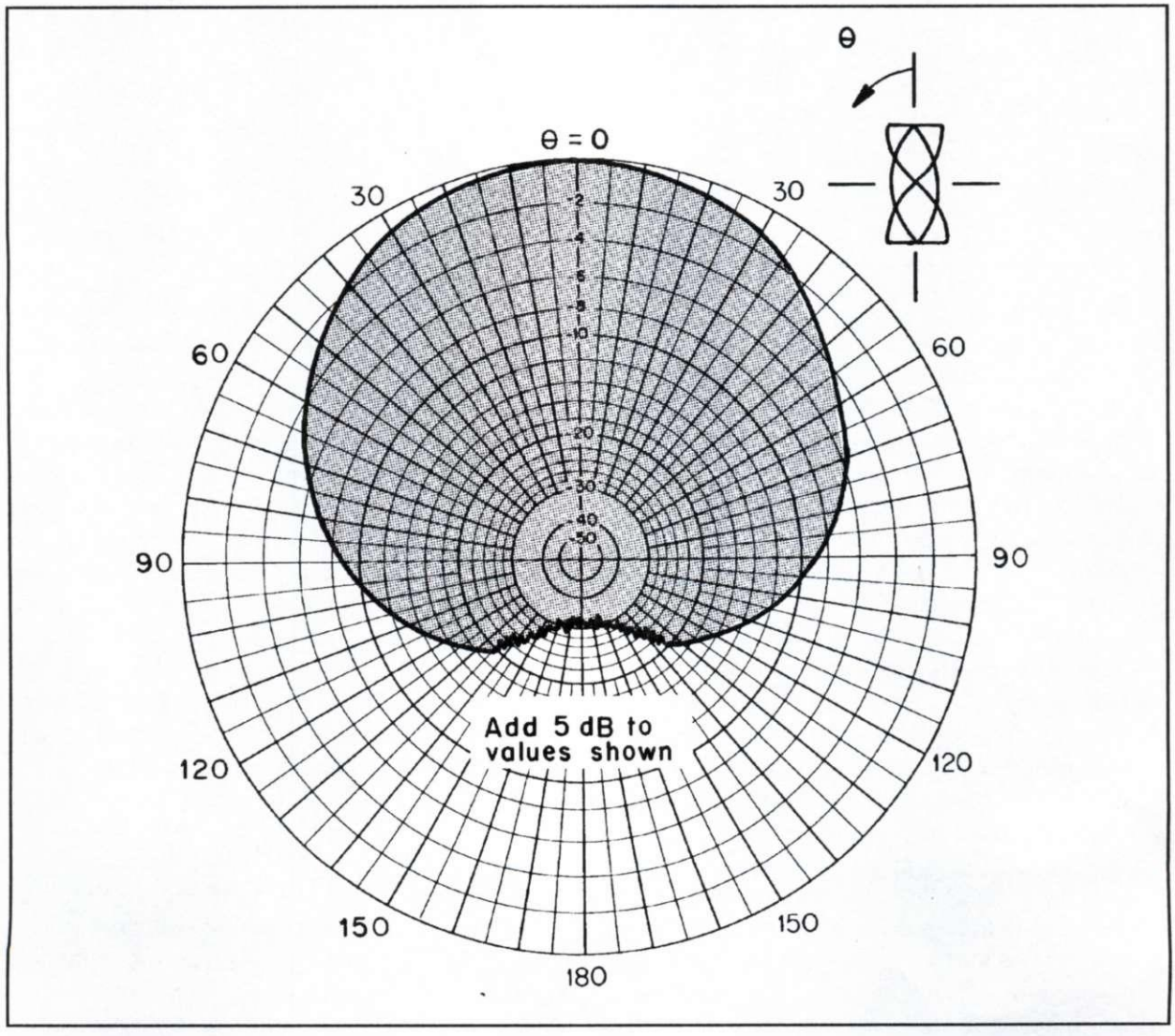

Fig 22-5. Radiation pattern of the half-turn λ/2 quadrifilar antenna when illuminated with a circularly polarized source.

polarized, with the same screw sense everywhere throughout the radiation sphere.

Experimental data obtained by Kilgus support his theoretical analysis, and confirm the similarity of radiation characteristics between the half-turn, $\lambda/2$ bifilar helix and the loop-dipole combination. For the purpose of obtaining additional data pertinent to the development of quadrifilar antennas for use on the TIROS-N spacecraft, I performed extensive measurements of pattern shape, polarization, axial ratio, and terminal impedance on more than a thousand different bifilar and quadrifilar helix configurations. The data obtained from these measurements agree with the Kilgus data, adding further validity to the earlier findings as well as extending them.

Sec 22.5 Development of the Quadrifilar Helix Antenna

In this section we examine the intrinsic cardioid, or omnidirectional hemispheric, radiation characteristic of the quadrifilar. In doing so, the toroidal radiation pattern of the bifilar helix becomes of initial primary interest. Recall that in the toroidal radiation pattern of the loop-dipole, maximum radiation occurs broadside to the axis, with the null on the axis. On the other hand, as mentioned earlier, maximum radiation from the bifilar loop occurs bidirectionally along the axis of the loop, while the null appears in the direction perpendicular to the plane formed by the top and bottom sides, or radials of the loop. Except for this 90° rotation of the axes, the radiation characteristics of the two antennas are similar.

We may develop a quadrifilar helix from the bifilar (which I will call bifilar A) by adding a second bifilar, B, on the same axis and enclosing the same space, but rotated 90° relative to bifilar A. This arrangement is shown in Fig 22-4. The fields radiated by bifilar B are identical to those of bifilar A, except that the entire radiation pattern of bifilar B is rotated 90° relative to that of bifilar A. Consequently, the null of bifilar A and the maximum radiation of bifilar B appear at the same point in space, and vice versa. On the other hand, in the axial directions the radiation fields from both bifilars are equal.

This field relationship is the key to the cardioid radiation characteristic of the quadrifilar. When both bifilars are fed in a 0–180° and 90–270°-phase relationship, respectively (excited simultaneously with a mutual 90° current-phase relationship), the cardioid radiation pattern appears in the far field. This is because the fields of both bifilars are in phase in one axial direction. In this direction, the two fields add, while in the opposite direction, the fields are out of phase and cancel. As the cancellation is not perfect off axis, the result is a cardioid-shaped pattern of revolution about the axis. In the broadside direction normal to the axis, the respective nulls and maxima of the two individual bifilars compensate each other to produce a uniform omnidirectional radiation pattern around the axis.

Sec 22.6 The Quadrifilar Shape Factor

As I stated earlier, the radiation pattern shape and the axial ratio of the polarization can be controlled. This is done by tailoring both the length of wire and number of turns in the loop, and the length-to-diameter ratio, len/diam, of the formed cylinder. Kilgus's data shows these relationships graphically for certain ranges of the parameter values. However, let us now examine how the Air Force 5D, the amateur AMSAT-OSCAR 7, and the TIROS-N quadrifilar designs were tailored to obtain the radiation characteristics required for their particular missions.

When using bifilars having a diameter $D = 0.25\ \lambda$, formed by placing a half twist in the square loop of Fig 22-2, the len/diam ratio is less than one, which yields poor front-to-back and axial ratios. By decreasing the diameter to $D = 0.18\ \lambda$ while retaining the half-turn, $\lambda/2$ loop, the axial length increases to $len_{\rho}° = 0.27\ \lambda$. The resulting ratio, len/diam = 1.5, yields a vast improvement in both front-to-back and axial ratios. These are the design values used in the Air Force 5D and AMSAT-OSCAR 7 quadrifilars. The radiation patterns obtained with this design are shown in Figs 22-5 and 22-6. The patterns are presented in the standard IEEE spherical-coordinate system of notation, and the orientation of the antenna relative to the coordinate axes is shown in Fig 22-4.

The θ radiation pattern shown in Fig 22-5 was measured while using circularly polarized illumination of the quadrifilar. This pattern shows an on-axis gain of 5 dBic (decibels relative to isotropic, circular) and a front-to-back ratio greater than 20 dB. The radiation at any angle θ is uniform for all values of ϕ around the Z axis. Thus, the single θ

pattern (at any value of ϕ) represents the shape of the envelope of the volume of revolution about the Z axis, which defines the solid radiation pattern in all directions.

The pattern shown in Fig 22-6 was obtained by using a spinning dipole to illuminate the quadrifilar to obtain axial-ratio information. The periodic ripple appearing in the pattern results from the rotation of the dipole. The maxima and minima, respectively, correspond to the times when the dipole is parallel to the major and minor axes of the polarization ellipse. The axial ratio may be determined from the difference between adjacent maximum and minimum values. Thus, the axial ratio of this design is seen to be less than 2 dB over a beamwidth of ±30°.

As mentioned earlier, the shape-factor parameters for the TIROS-N configuration were determined empirically from the results of my research measurements. I took measurements on more than a thousand combinations of quadrifilar configurations in which each physical parameter was separately varied in small increments while holding the other variables constant. Hundreds of shape-factor combinations were measured, which provided families of patterns from which to select the parameters for the desired pattern shape. The TIROS-N mission required a radiation-pattern shape which

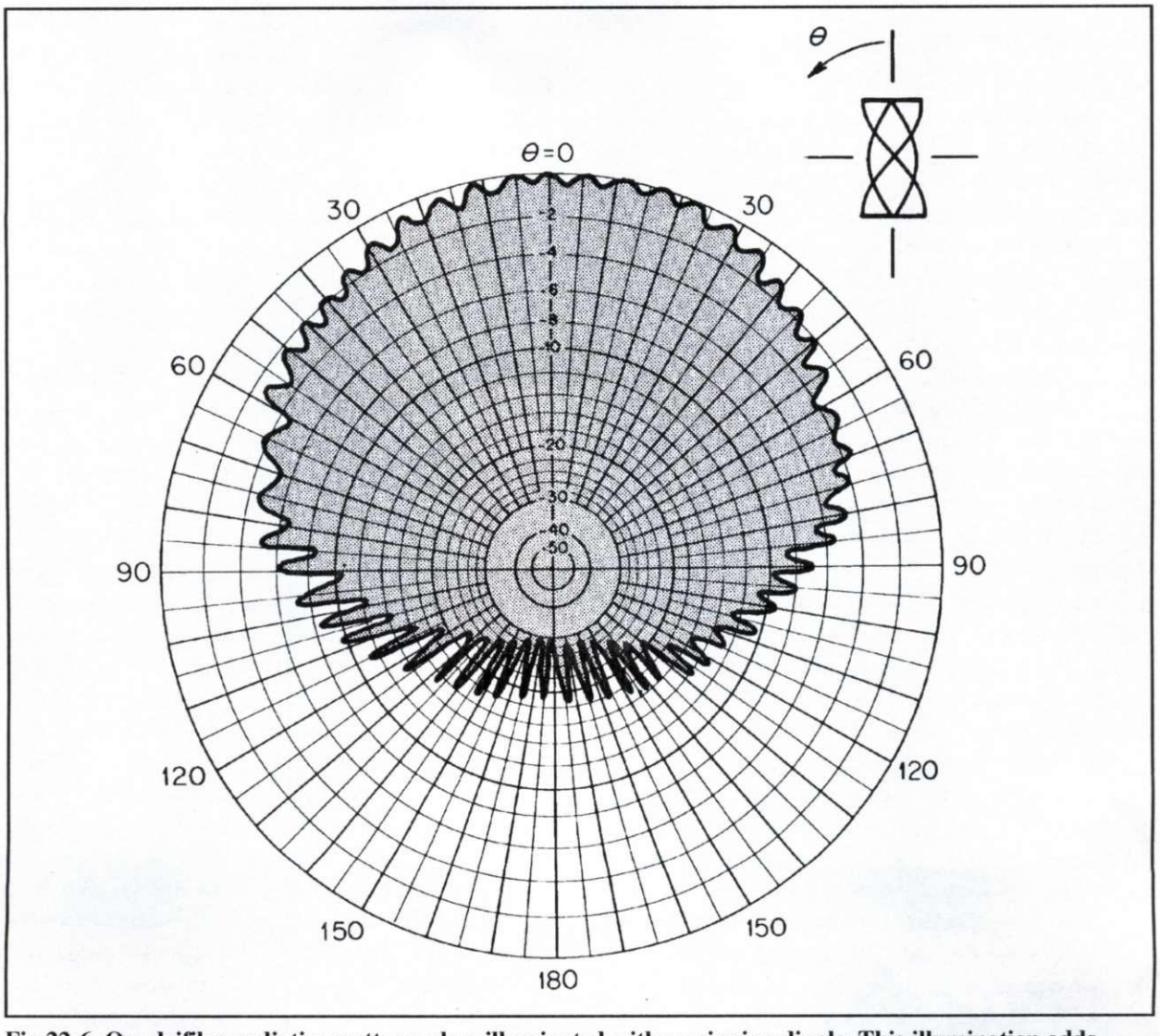

Fig 22-6. Quadrifilar radiation pattern when illuminated with a spinning dipole. This illumination adds axial-ratio data, represented as the difference between adjacent maximum and minimum of a ripple wave.

provides a nearly constant signal level to the ground station during in-view time. This pattern shape is shown in Fig 22-7. The configuration that yields this radiation pattern was one of the hundreds measured during my research. All that was required to determine the configuration that would satisfy the radiation-pattern requirements was to search through the hundreds of patterns obtained during the research to find the one that fit the requirements. The bifilar parameters which yield this pattern shape were found in to be $1^1/2$ turns, 1.25-λ loop, D = 0.1 λ, $len_p{}^o$ = 1.0 λ, and len/diam = 10.0. These quadrifilars, on TIROS-N, are for transmitting weather and other data in the 1600-MHz region, completely separate from the 121.5-, 243-, and 1600-MHz SAR-ELT quadrifilars flown on the same spacecraft.

Sec 22.7 Methods of Feeding the Quadrifilar Antenna

Feeding the quadrifilar with a single, unbalanced coaxial line requires special attention. Because the individual bifilar loops are balanced-input devices, some form of balun is required to provide balanced push-pull currents to the terminals of each bifilar. In addition, to obtain the unidirectional radiation characteristic of the quadrifilar, the two bifilar

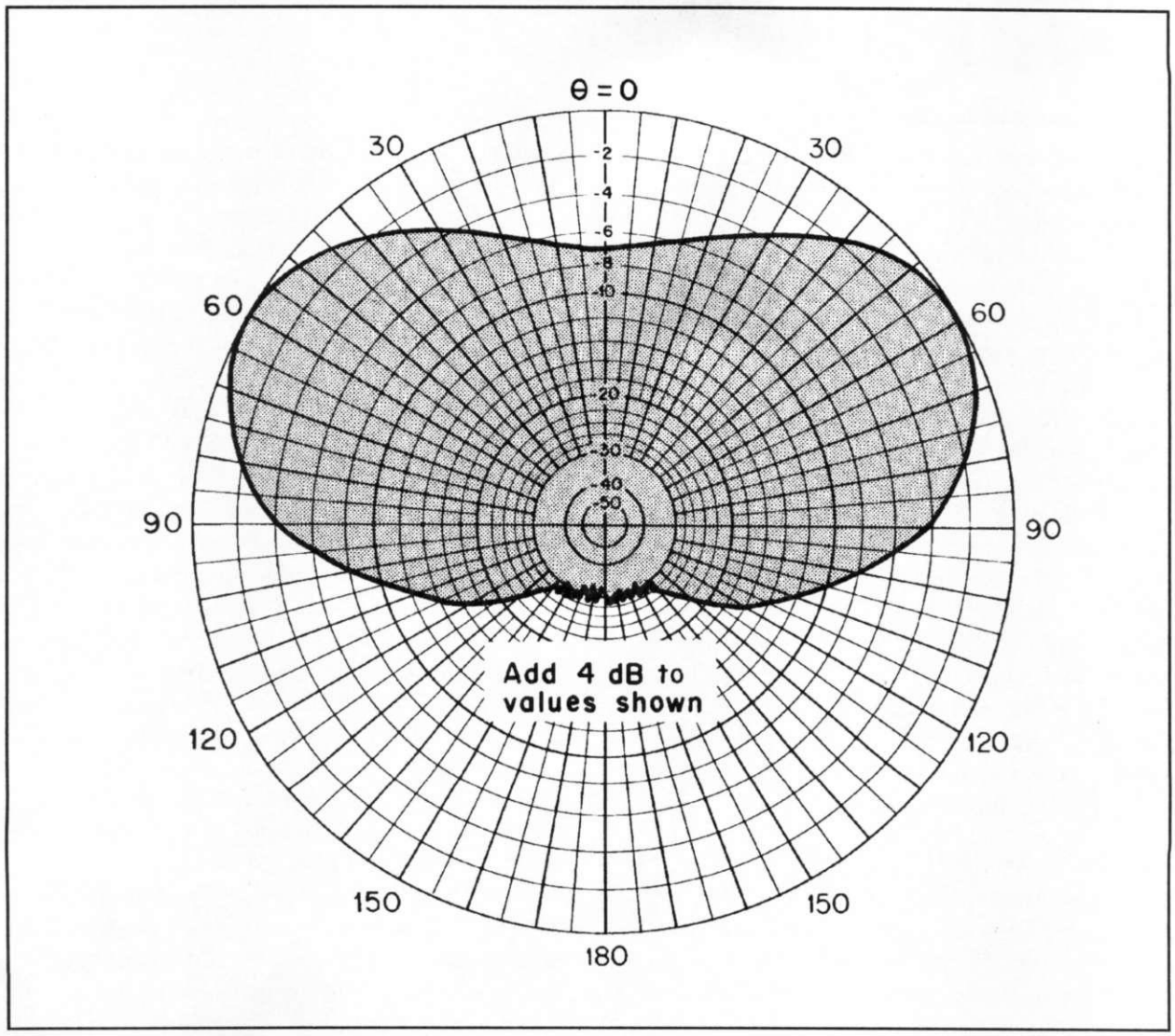

Fig 22-7. Radiation pattern of the $1^1/2$ turn, 1.25λ quadrifilar antenna.

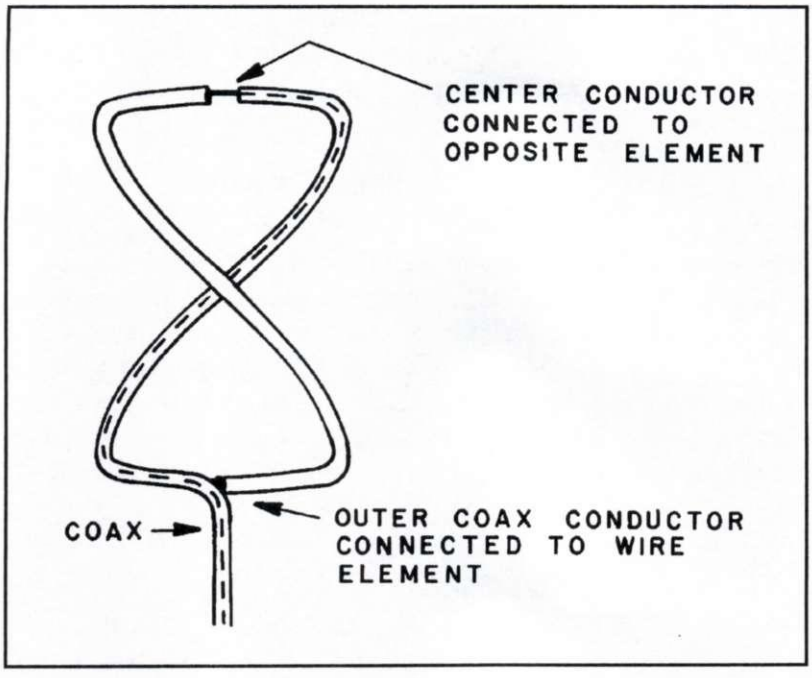

Fig 22-8. Half-turn bifilar loop with infinite balun feed.

loops require separate excitations having a relative phase difference of 90°. Further, the sense of the 90° phase relationship determines from which end the quadrifilar radiates.

Several different balun and quadrature-phase circuit arrangements are available for feeding the quadrifilar, such as the folded balun, the split-sheath balun, or a combination of 90° and 180° hybrids, and so forth, as described by Bricker and Rickert *(Refs 88, 89)*. However, to save weight and to effect simplicity in the construction, a unique feeding arrangement is used. This technique features the infinite, or inherent, balun combined with a novel method of self-phasing the two bifilar loops to achieve the 90° differential current relationship between the loops. The constructional simplicity is apparent in Fig 22-1, which illustrates the quadrifilar configuration used on both the TIROS-N and Air Force 5D satellites, and on the amateur satellite AMSAT-OSCAR 7.

Sec 22.8 The Infinite or Inherent Balun

In the infinite balun, shown in Fig 22-9, we see the coaxial feed line extending into the loop and shaped to form the first half of a bifilar loop. At the end of the coax, the inner conductor is connected to the opposite or second half of the bifilar loop to form the feed point. The other end of the second half of the loop is connected to the outside surface of the coax feed line. Thus, the loop is closed at the antipodal point of the loop, where the feed line enters. The second half of the loop is a solid wire of the same diameter as the outer diameter of the coax.

In operation, current flowing on the inner conductor of the coax emerges at the feed point to flow onto the second half of the loop. For current flowing on the inside of the outer conductor of the coax, on its arrival at the end of the coax, the only path for current flow is around the end and onto the outside of the outer conductor. Now such external feed-line current is the desired antenna current, because the outside portion of coax extending from the feed point to the antipodal point is the radiator. Externally, the antipodal point demarks the end of the feed line and the beginning of the loop radiator. Because of skin effect, the transmission-line currents flowing inside the coax portion of the loop are completely divorced from the antenna currents flowing externally on the loop. Their only relationship is that the internal transmission-line currents emerge at the feed point, where they become the external antenna currents.

As the feed line is dressed away from the antipodal point symmetrically relative to the loop, currents induced on the feed line because of coupling from each half of the loop are equal and flow in opposite directions. The opposing currents on the line thus cancel each other, decoupling the feed line from the loop. In other words, from the exter-

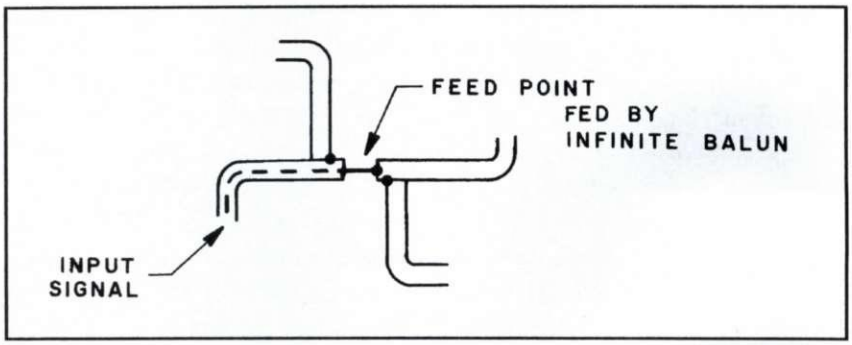

Fig 22-9. Feed arrangement for 90° self-phasing of loops.

nal viewpoint of the loop radiator, the source generator can be considered to exist directly between the two input terminals of the loop at the feed point, and the feed line effectively disappears. Thus, the current-mode transition in the coaxial-line portion of the loop—from an internal unbalanced mode entering at the antipodal point, to an external balanced mode emerging at the feed point—constitutes an inherent balun device. Such a device is called an "infinite balun."

Sec 22.9 Self-Phased Quadrature Feed

As stated, a quadrature-phase current relationship is required between the two bifilar loops of the quadrifilar array. This requirement is met by using the self-phasing method. The orthogonal bifilar loops are designed such that one loop is larger relative to the desired resonant frequency length and therefore inductive, while the other loop is smaller and therefore capacitive. Using this method, the two loops are fed in parallel by connecting the terminals of both loops together at the feed point, as shown in Fig 22-9. This self-phasing method requires only one coaxial feed line, and any of the balun arrangements mentioned earlier (shown by Bricker and Rickert, *Ref 88*) may be used. It is evident that one loop half is the coax feed line, while the other three half loops are simply solid wire.

The larger inductive loop is designed such that, at the operating frequency, the reactive component X_L of the loop terminal impedance is equal to the resistive component, R. Similarly, the smaller capacitive loop is designed so its reactive component X_C equals R at the operating frequency. The $\pm X = R$ relationship is important because to obtain a relative current phase of 90° between the two loops, the larger loop current must lag by 45° and the smaller must lead by 45°.

For the current phase of the larger loop to lag, or the smaller loop to lead by 45°, the phase angles must be 45°, or have an arc tangent of ±1. This occurs only when $\pm X = R$. When the two loops are fed in parallel, the relative lag and lead currents in the loops differ in phase by 90° without requiring any additional components to obtain separate differential phase excitations. Dimensions that yield the correct phase relationship with a loop wire diameter of 0.0088 λ are as follows.

Smaller loop:
D = 0.156 λ
$len_p°$ = 0.238 λ
Perimeter = 1.016 λ

Larger loop:
D = 0.173 λ
$len_p°$ = 0.260 λ
Perimeter = 1.120 λ

where:
D = diameter of imaginary cylinder on which bifilar is wound
$len_p°$ = axial length, as shown in Fig 22-3

The resultant impedance versus frequency response of the parallel-loop combination is shown in the Smith Chart, Fig 22-10. The formation of the cusp in the impedance locus is the design goal that signifies that the 90° phase relationship exists between the loops.

See 22.10 The Quadrifilar in Space

As I've indicated above, the quadrifilar antenna was developed for spacecraft use. Fig 22-11 shows the comparative size between an experimental S-band quadrifilar and the flight-model system of a

circularly polarized crossed-dipole antenna over a ground plane, which the quadrifilar replaced. The two antennas have identical radiation characteristics. Four of the crossed-dipole ground-plane units flew on ITOS (TIROS-M). They were replaced with quadrifilars on the newer TIROS-N to save space and weight, but accomplished the same communications tasks on the same frequencies. Using the same technique as described in Sec 22.9 for the quadrifilar, the required 90° dipole phasing to obtain circular polarization in the crossed-dipole array was accomplished by using the short and long dipole elements shown in the picture. The short elements are capacitive, causing the dipole currents to lead by 45°, and the long elements are inductive, causing the currents to lag 45°, resulting in a differential phase of 90°. The balun is a split tube.

Before the launch of OSCAR 7, AMSAT publicized the quadrifilar antenna in the "AMSAT Newsletter" for March 1975 (*Ref 131*). The cover picture for that issue is included here as Fig 22-12. The quadrifilar helix antenna is shown mounted on

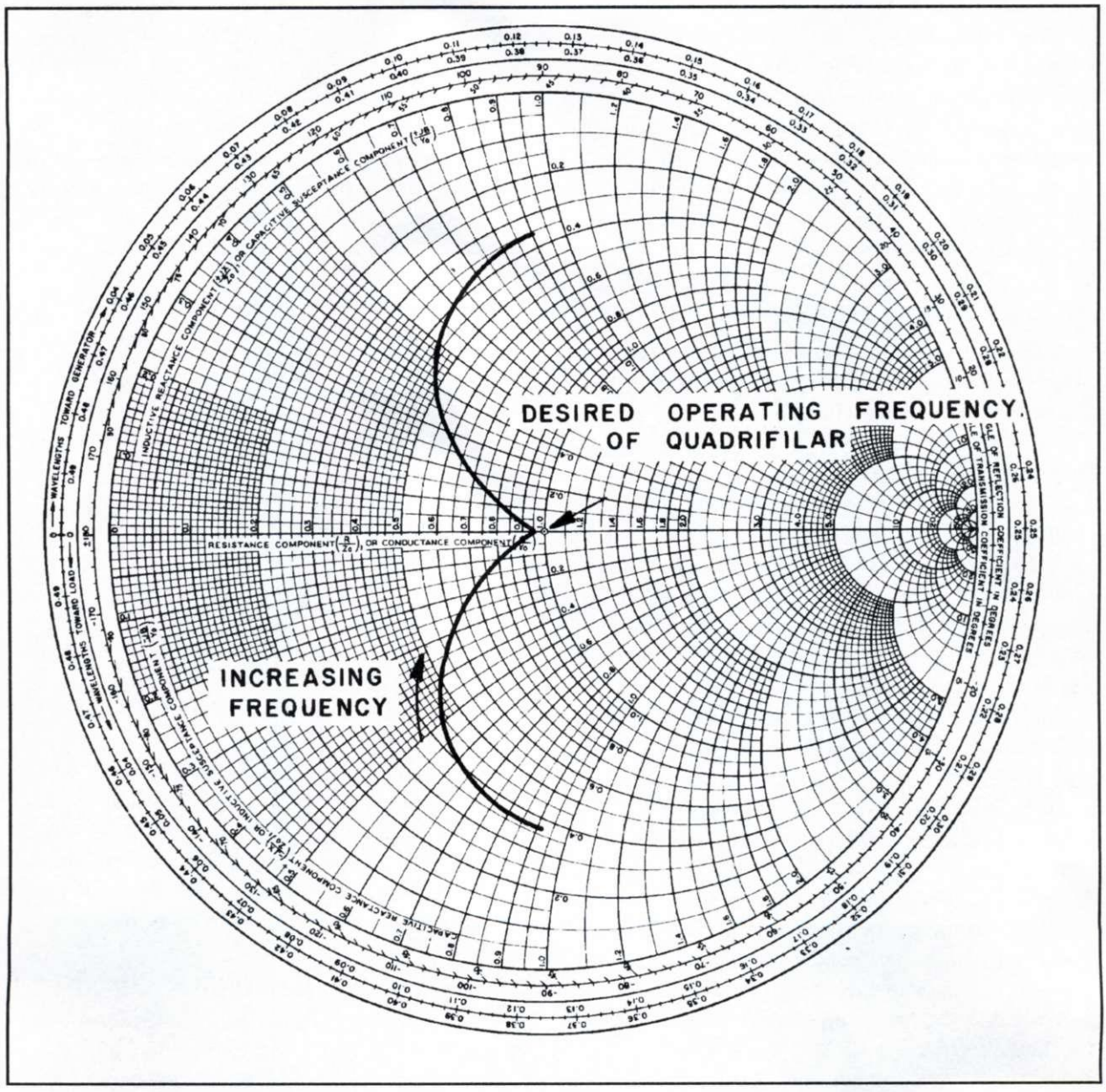

Fig 22-10. Impedance vs frequency plot of self-phased quadrifilar antenna.

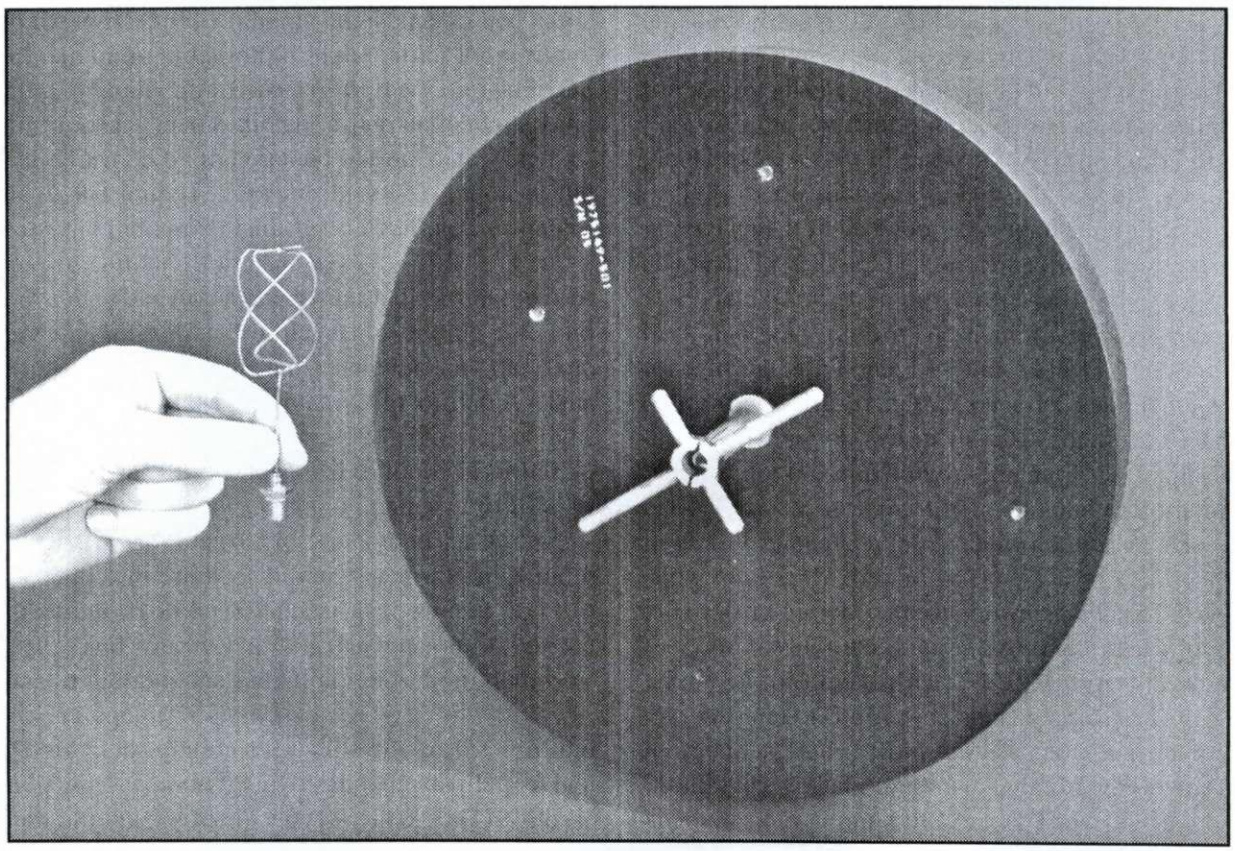

Fig 22-11. Comparing the size of a TIROS-N test-model quadrifilar helix antenna with a TIROS 9 flight-model crossed dipole over ground plane, both operating at frequency 1.6 GHz.

an OSCAR 7 test model at the RCA Space Center, attached to an ITOS weather satellite (TIROS-M) in the piggyback launch configuration. Fig 22-13 shows another view of the test model, while Figs 22-14 and 22-15 show the quadrifilar mounted on the OSCAR 7 spacecraft as it is being readied for flight. In spite of its small size (0.7 ounce), the quadrifilar antenna boasts tremendous performance for spacecraft use. RCA Engineers Randy Bricker, Herb Rickert, and myself developed the original design for use on the highly successful USAF spacecraft, the Block 5-D Meteorological Satellite, which was built by the RCA Astro-Electronics Division of Princeton, New Jersey.

The OSCAR 7 antenna is circularly polarized, radiates hemispherically without requiring a ground plane, and has a gain of 5 dBic on axis going down smoothly to 0.0 dBic 90° off axis over the entire 360° around the edge of the hemisphere, with good polarization circularity at the hemisphere edges. It is fed with an infinite balun, and has elements phased at 90° with no phasing line. With a modification I devised to operate at the 2304.1-MHz beacon frequency, this antenna was fabricated under the direction of Bricker and myself specifically for the OSCAR 7 amateur spacecraft and was presented to AMSAT by RCA, which designed and built the TIROS-ESSA-ITOS-TIROS-N weather satellite series. (After being accepted by the U.S. Weather Bureau, these RCA-built spacecraft became known as NOAA, with a number designation to determine the specific spacecraft of the series.) I also served as consulting engineer for all antenna systems on AMSAT OSCAR 7. RCA Technicians Walt Ozmon, W2WGH, and Joe Rovenski, W2HLO, performed many of the impedance and radiation pattern measurements during the final testing of the OSCAR 7 quadrifilar antenna.

Scaled up for lower frequencies, the quadrifilar has similar performance characteristics. At 146 MHz, the quadrifilar would form a cylinder

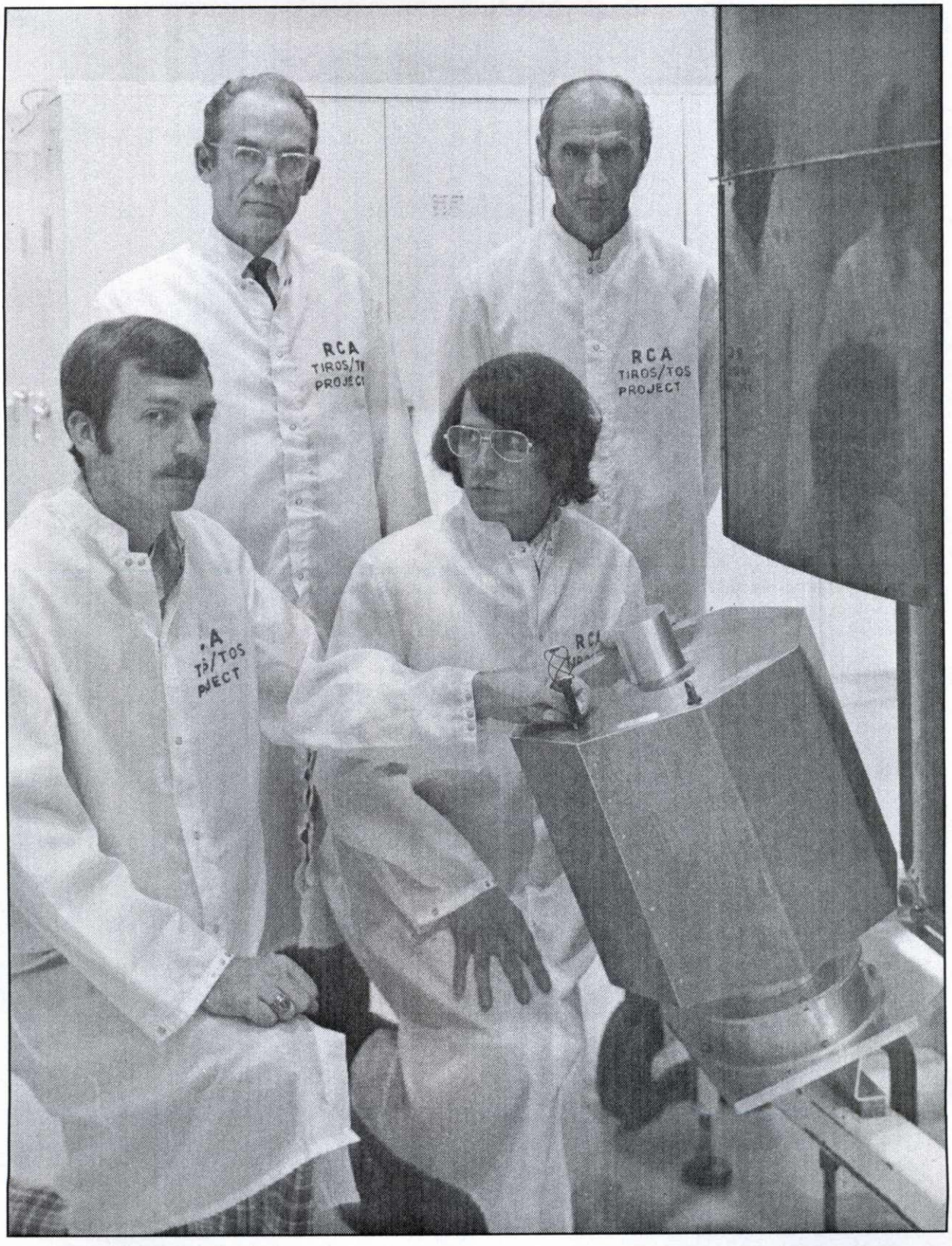

Fig 22-12. Cover picture for March 1975 issue of the "AMSAT Newsletter" showing test model OSCAR 7 in launch configuration with TIROS 9 spacecraft, with which it was launched from Cape Canaveral.

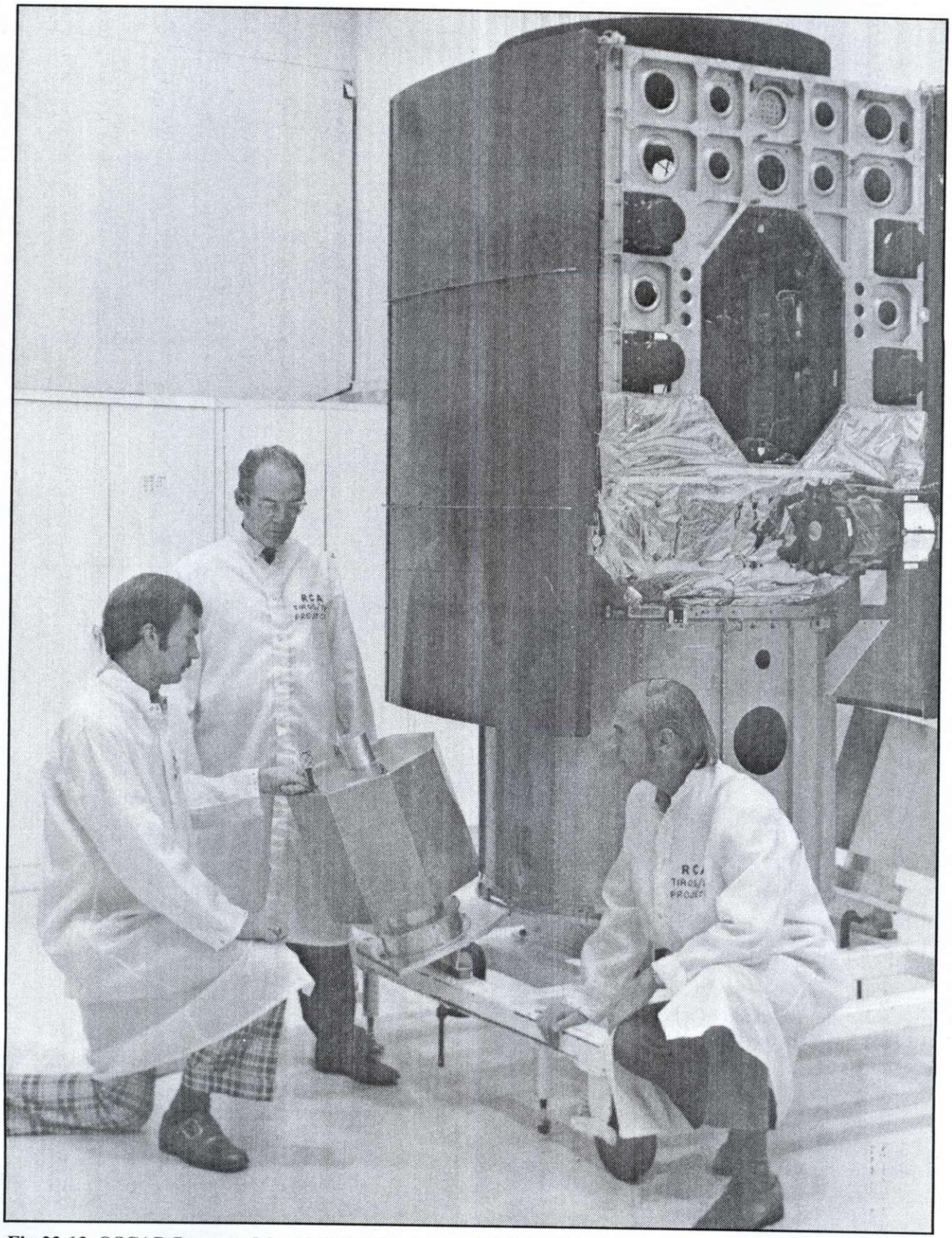

Fig 22-13. OSCAR 7 test model with TIROS 9 spacecraft while under construction at RCA Space Center, Princeton (Hightstown), New Jersey.

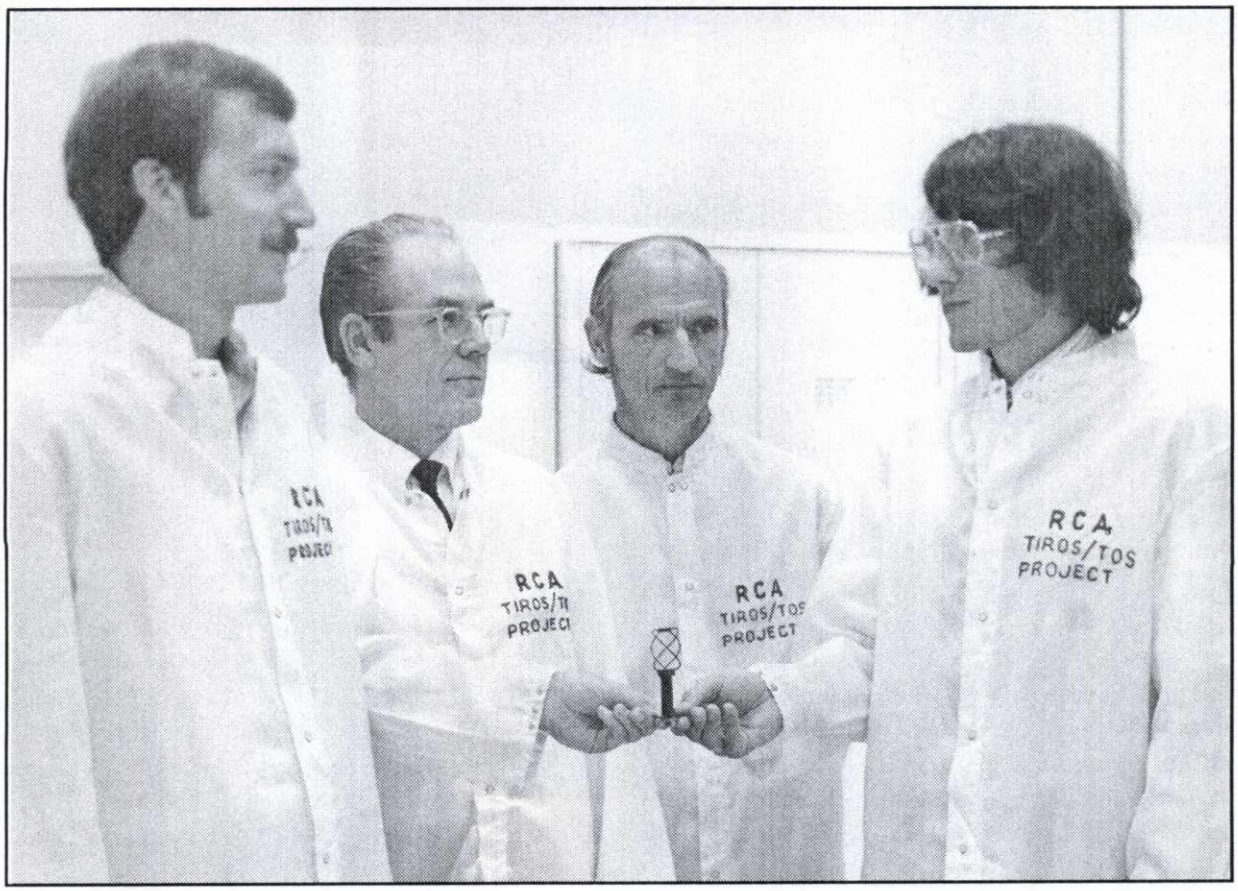

Fig 22-14. With author Maxwell and Walter Ozman, W2WGH, looking on at center, RCA engineer Randy Bricker (right) presenting to NASA engineer Jan King, W3GEY, the W2DU-designed 2304-MHz quadrifilar helix beacon antenna that flew on OSCAR 7.

approximately 13 inches in diameter and 20 inches high, while at 432 MHz, the diameter and height would be 4.4 inches and 6.8 inches. At 29 MHz the dimensions would be 5.5 feet and 8.4 feet, respectively. The circular polarization reduces polarization fading caused by Faraday rotation of the electric field vector, especially on the 10-meter downlink. The quadrifilar scaled for use at 137 MHz is used quite extensively by weather buffs for receiving APT weather pictures, with excellent results on both 137.5 and 137.62 MHz. One note is of particular importance for those intending to build the quadrifilar: The diameter of the conductors in the bifilar loops is especially critical. The reason is that the 45° leading and lagging currents in the respective bifilar loops, which obtain the required 90° differential phasing between the two loops, are derived by the corresponding capacitive and inductive reactances in the loops. The distributed inductance in each loop determines the reactance in the loop. When the length of the loop is less than the resonant length, the reactance is capacitive, causing the current to lead the voltage. When the loop length is greater than the resonant length, the reactance is inductive. Now the critical point: To make the leading current precisely +45° and the lagging current precisely –45°, the distributed inductance of the conductors must also be of precisely the correct value. To obtain the correct value of distributed inductance the length-to-diameter ratio of the conductor also must be correct. The optimum radiation pattern and gain of the antenna requires the leading and lagging currents to be 45°. It therefore behooves the builder of the quadrifilar to carefully observe the conductor-diameter requirement to obtain successful operation of the antenna. Using the λ dimension data listed earlier, it may be helpful for the 137-MHz builders to know that 3/4-inch

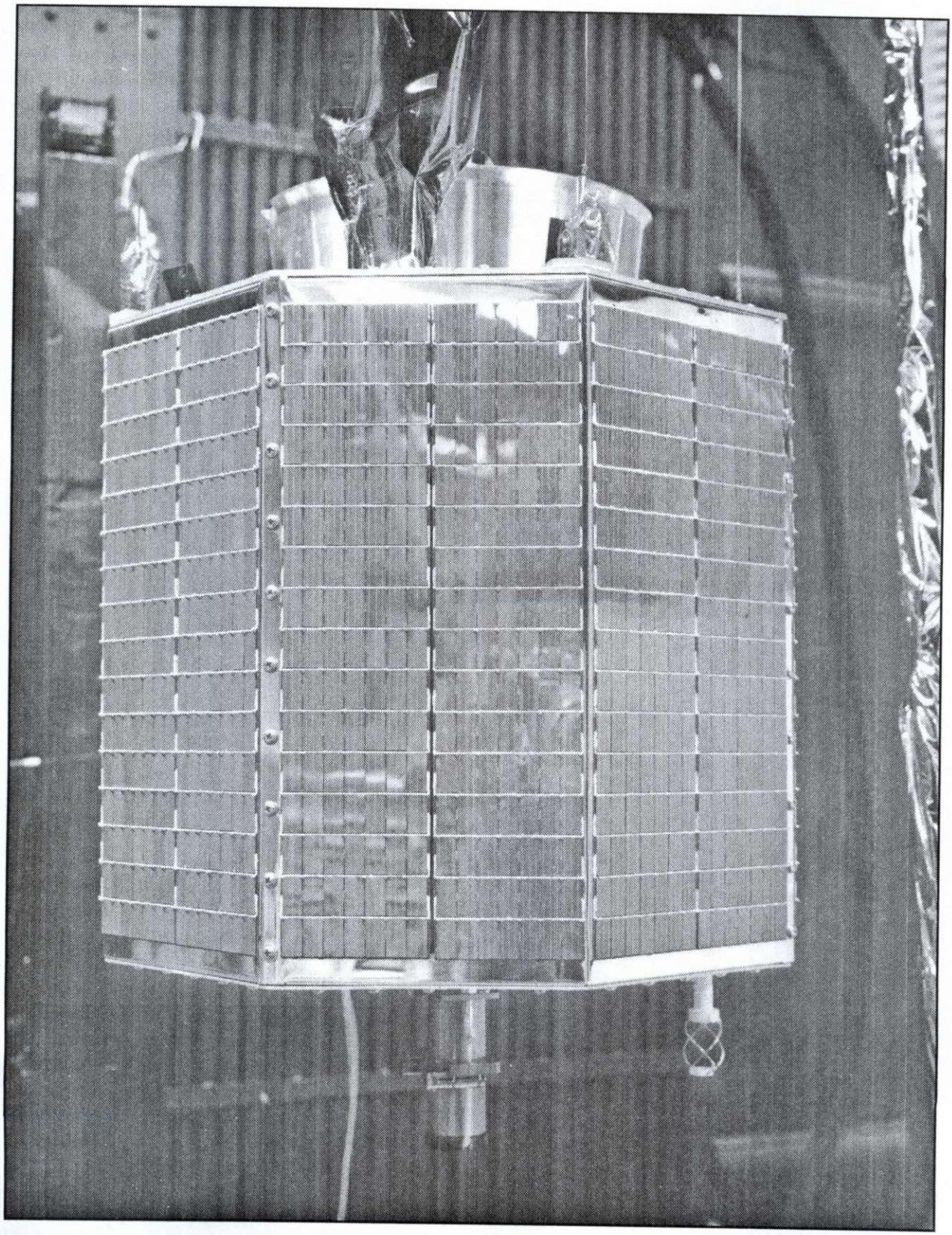

Fig 22-15. OSCAR 7 showing RCA-donated 2304-MHz quadrifilar helix beacon antenna mounted at bottom of spacecraft.

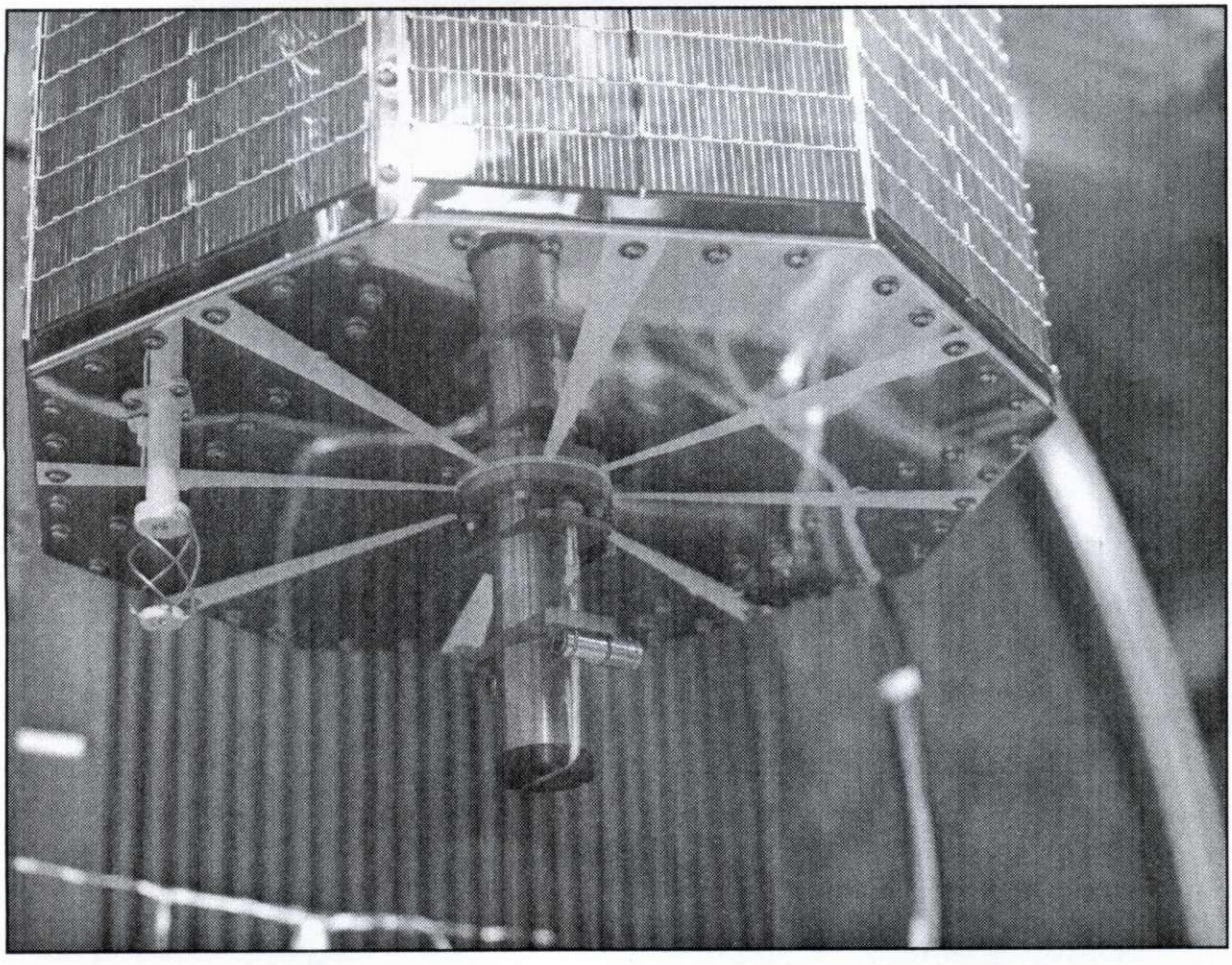

Fig 22-16. Bottom view of OSCAR 7 showing close-up view of the RCA-donated quadrifilar helix beacon antenna designed by the author.

soft copper tubing works very well. Generally, the 137 MHz will allow access of a NOAA weather spacecraft signal at between 5° and 10° in elevation with no nulls during an entire pass, with continued contact until between 5° and 10° in elevation at the end of the pass. The beauty of the performance of this antenna is that it needs to be no more than $\lambda/4$ above the ground, requires no manipulation or positioning to follow the orbital path of the spacecraft, but it does appreciate a clear shot to the orbital path of the spacecraft. NOAA spacecraft 9 through 13 are presently available for receiving APT pictures in the 137-MHz band.

In summary, the quadrifilar helix antenna differs significantly from the conventional helical antenna. Control of pattern shape and other radiation characteristics are available by selecting appropriate dimensional parameters. A novel balun for feeding this balanced-input device from coaxial feed line is used, as is a method of self-phasing the loop radiating elements to obtain a quadrature current relationship between the loops. The quadrifilar helix is a durable antenna, one that is seeing use on both amateur and commercial satellites, as well as on ground stations for receiving APT weather information transmissions on 137.5 and 137.62 MHz from the TIROS-NOAA weather satellites. The satellites presently transmitting on these APT frequencies are TIROS-N NOAA 9 through NOAA 14.

Note

1. Among other tasks on the quadrifilar project, I performed the R & D research on more than 1000 different configurations of the quadrifilar helix, which led to the development of the six quadrifilar antennas flying on the polar-orbiting TIROS-N NOAA weather spacecraft. A copy of my research report appears in Chapter 27.

Chapter 23

Examining the Mechanics of Wave Interference in Impedance Matching

(Newly revised for Reflections III)

Sec 23.1 Introduction

The purpose of this chapter is to examine a powerful, but relatively unused treatment of wave-reflection mechanics as an aid in understanding how the matching of impedances is achieved through the use of networks and transmission lines. This treatment focuses directly on the fundamental actions of four reflected waves, the voltage and current reflected waves that result from two mismatches, the mismatched load, and the mismatch introduced by the matching device. As we proceed *it will become evident that* ***all*** *impedance-matching operations are achieved through the superposition of these four reflected waves at the matching point, regardless of the type of matching device.* By wave interference resulting from this superposition, the reflections from the mismatched load are canceled by the conjugately-related reflections generated by the matching device (*Ref 35*). The cancellation of reflections at the matching point simultaneously creates a totally-reflecting virtual open or short circuit to all the reflected waves at the matching point. Consequently, no reflected waves travel rearward past the matching device, but are reversed in direction, again traveling toward the load. Thus, a matched condition exists between two previously mismatched impedances.

However, this newly revised edition of Chapter 23 clarifies certain statements that appeared in the 2nd edition of *Reflections* which were somewhat confusing, especially in the section pertaining to the quarter-wavelength ($\lambda/4$) transmission-line transformer. Since that chapter was written I have made a more in-depth analysis of the $\lambda/4$ transformer which has enhanced my viewpoint of the reflections mechanics responsible for achieving its matching function. In the original analysis I gave insufficient attention to the reflections occurring during the first few cycles of the period between the initial applied voltage and the achievement of the steady-state condition. The confusing statements resulted. Consequently, to clarify the confusion the recent analysis prompted the development of a more detailed description of the wave actions that occur during the first three full cycles of the initial period leading up to the steady-state condition are discussed in Sec 23.4. The results of the cycle-by-cycle analysis are shown mathematically in Figs 23-7, 23-8, and 23-9 and will be discussed later.

23.2 Background

Before presenting the discussion, however, it seems wise to acquaint the reader with some background on the subject. During the 1970s I published a series of *QST* articles (*Ref 138*), and the first edition of this book in 1990 (*Ref 139*), both aimed at dispelling prevalent misconceptions concerning wave propagation on transmission lines. One of the most serious misconceptions concerned reflected power reaching the tubes in the RF amplifier of the transmitter. The prevalent, but erroneous thinking was that the reflected power enters the amplifier, causing tube overheating and destruction. However, I dispelled this misconception in the above-mentioned publications (repeated in this book as Chapters 1 through 7), using wave-mechanics treatment, discussed here in greater detail, by showing that when the pi-network tank is tuned to resonance, a virtual short circuit *to rearward traveling waves* is created at the input of the network. Consequently, instead of the reflected power reaching the tubes of the amplifier, it is

totally re-reflected toward the load by the virtual short circuit appearing only to reflected waves at the network input.

23.3 Discussion

To begin, it must be understood that whenever there is a mismatch of impedances that introduces reflected waves that require cancellation by a matching device, it is fundamental that the cancellation of the undesired reflections is achieved through wave interference by introducing and superposing new reflections that are conjugately related to the undesired reflections. Introducing a new mismatch tailored to produce reflections

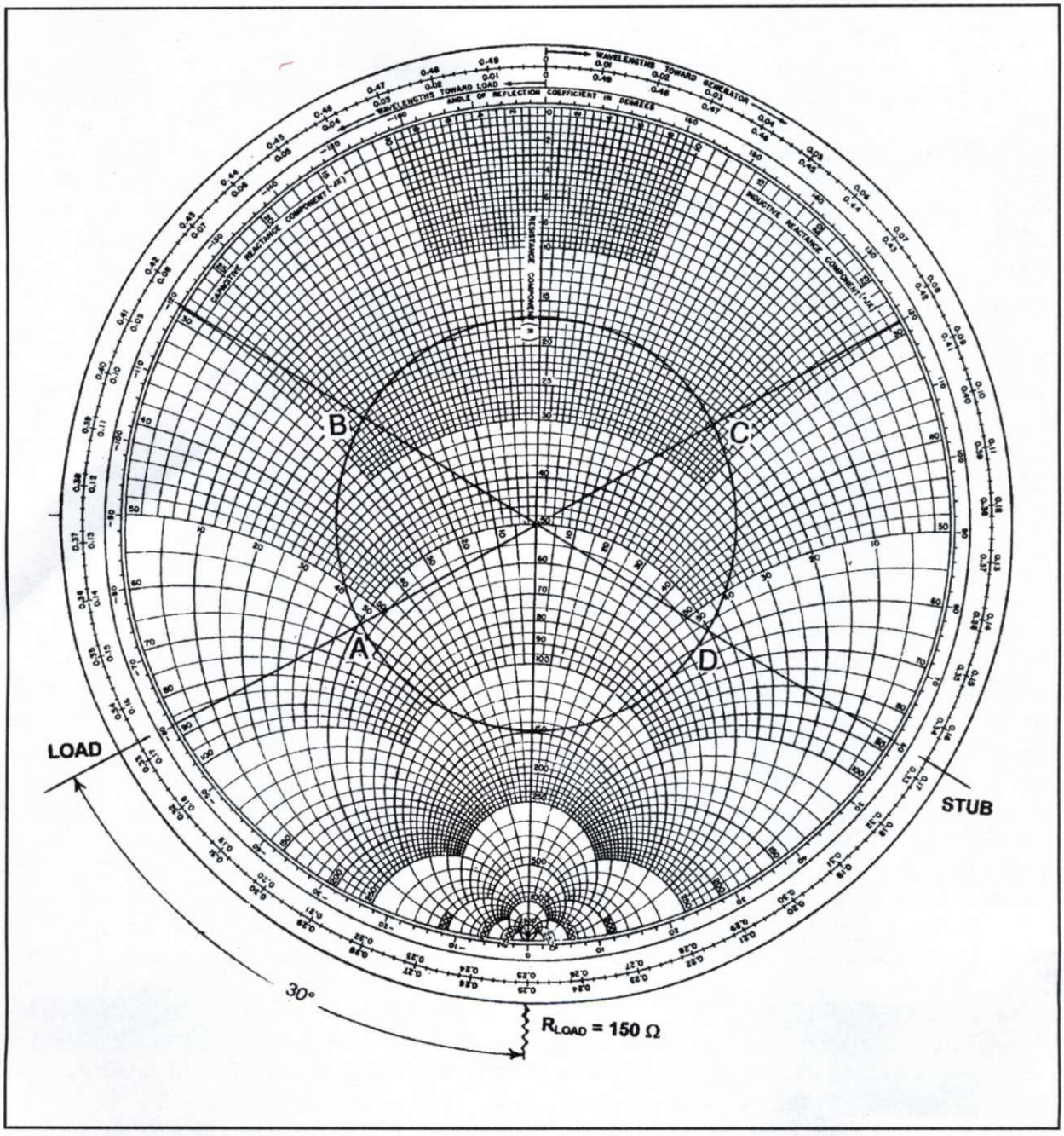

Fig 23-1. Smith Chart showing angles of voltage and current reflection coefficients of load and stub.

whose complex reflection coefficients are conjugates of the coefficients of the waves being canceled generates the new reflections. By conjugates we mean coefficients that have identical magnitudes, and equal angles with opposite signs. The new tailored mismatch may be established using any appropriate network or a transmission-line configuration that will achieve the match. However, cancellation of the reflected waves does not mean cancellation of the energy contained in the waves, because to conform to the Law of Conservation of Energy, energy cannot be canceled or destroyed. It means only that the energy in the reflected waves ceases traveling in the rearward direction and becomes totally re-reflected in the forward direction. It also means that when the reflected energy is totally re-reflected, the voltage and current in that energy are in phase with the voltage and current, respectively, in the energy supplied by the source, and thus add to the energy supplied by the source.

23.4 Impedance Matching with Stubs on Transmission Lines

The first analysis uses a model that focuses directly on the actions of four reflected waves: two sets of reflected voltage waves and two sets of reflected current waves, each set resulting from one of two mismatches; one set resulting from the mismatched load terminating the line, and the other, a new canceling mismatch introduced by the matching device, the stub. As we proceed, it will become evident that certain impedance-matching functions can be explained through the superposition of the voltages and currents of these four reflected waves at the matching point. In this analysis the reflections from the mismatched load are canceled by reflections introduced by the stub, which are conjugately related at the match point to those introduced by the mismatched load. Once the steady-state condition is reached at the end of the transient period, the wave interference resulting from the superposition establishes a totally-reflecting virtual open or short circuit to all the reflected waves arriving at the stub point. Whether a virtual open or short circuit is established will be explained later. Consequently, while in the steady state condition, all reflected waves are then totally *re*-reflected at the stub point, to travel only in the *forward* direction toward the load, and no reflected waves travel rearward past the stub, resulting in an impedance match on the line at the stub point. As we proceed we will discover how the virtual open and short circuits are established.

The technique of stub matching on a transmission line provides the first simple, but elegant model for analyzing the wave-interference mechanism, with the stub establishing the new mismatch. However, before analyzing the wave-interference treatment, it will be a study in contrast to review briefly the traditional treatment of matching with transmission-line stubs. To solve a matching problem in the traditional manner, engineering handbooks and texts provide equations and graphs to determine the length ℓ and characteristic impedance Z_0 of the stub and its position on the line, based on the characteristic impedance Z_0 of the line, the impedance of the load terminating the line, and the resulting SWR. Although the matching is achieved because the series reactance (or parallel susceptance) of the stub cancels the line reactance (or susceptance) at the stub point, the handbooks and texts do not explain the multiple wave reflections which achieve the reactance cancellation that results in the matching, or why the reflected waves produced by the mismatched load do not travel rearward beyond the stub. Thus, let's now examine an analysis that *does* reveal what the handbooks and texts do not. In this analysis we'll use a series stub that inserts a canceling reactance in *series* with the line. In this condition we'll be using *impedance* treatment instead of the more traditional admittance treatment.

The stub in series with the line is seen as a discontinuity that produces reflections to incident waves arriving from both directions along the line; it reflects waves rearward toward the source as well as re-reflecting forward those waves previously reflected rearward by the mismatched load. Because the 3:1 mismatch produced by the stub discontinuity causes only a partial reflection, a portion of initial energy incident on the stub is transmitted forward past the stub toward the load and dissipated there, while the remaining portion is reflected rearward toward the source. At this point the mismatched load becomes a virtual energy source as it reflects the portion of the incident energy that it doesn't dissipate. Also, again, because the

stub causes only a partial reflection, a portion of the energy reflected from the load is re-reflected forward toward the load, while the remaining portion is transmitted rearward past the stub toward the source. However, the energy initially transmitted past the stub toward the source occurs only during the initial transient period preceding the steady state, and is thereafter totally re-reflected at the stub by the virtual open circuit established by the wave interference initiated by the stub. It is this re-reflection that achieves the impedance match.

To analyze the wave-interference that establishes the open circuit we'll use a mathematical model of stub-matching circuitry. Assume a 50-ohm lossless line terminated with a pure 150-ohm resistance, yielding a reflection coefficient of magnitude 0.5, for a 3:1 SWR on the line, as shown in Figs 23-1 and 23-2.

By placing a series stub of the correct length at the correct position on the line, a 50-ohm impedance match is obtained at the stub point, resulting in a 1:1 SWR on the line between the source and the stub, but leaving the 3:1 SWR between the stub and the load, as shown in Fig 23-3.

This we already knew, so now we make a change that will provide a fresh perspective of how the stub achieves the impedance match. Leaving the stub in place, we replace the mismatched 150-ohm load with a 50-ohm matched resistance, as shown in Fig 23-4.

Now there is no reflection from the load, resulting in a 1:1 SWR between the stub and the load. The effect of this condition is the same as if the line were terminated at the stub by the stub in series with the 50-ohm resistance. In this condition, the stub that initially reduced the 3:1 SWR to 1:1 now

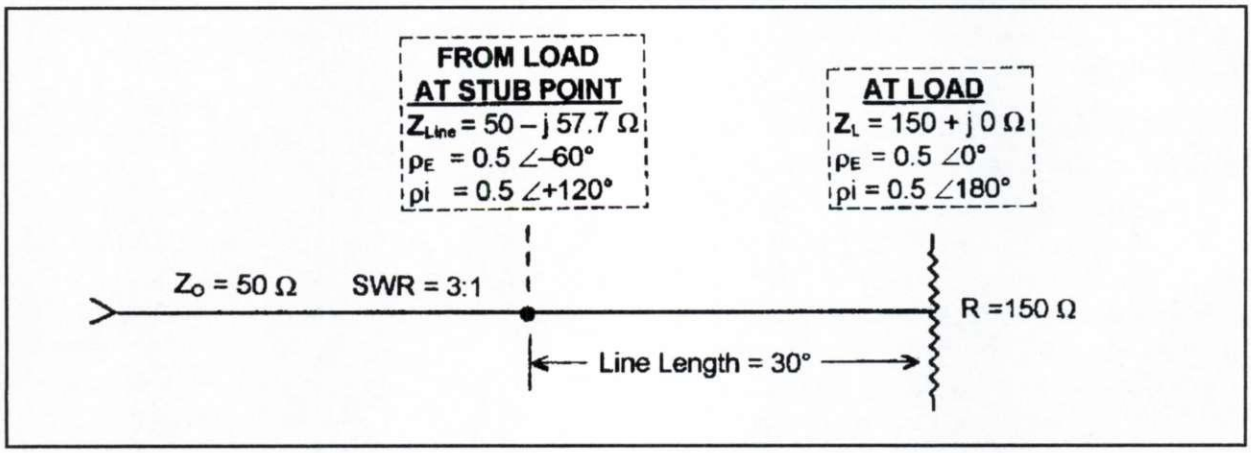

Fig 23-2. A 50-ohm transmission line terminated with a 150-ohm load, creating a 3:1 mismatch along the entire line.

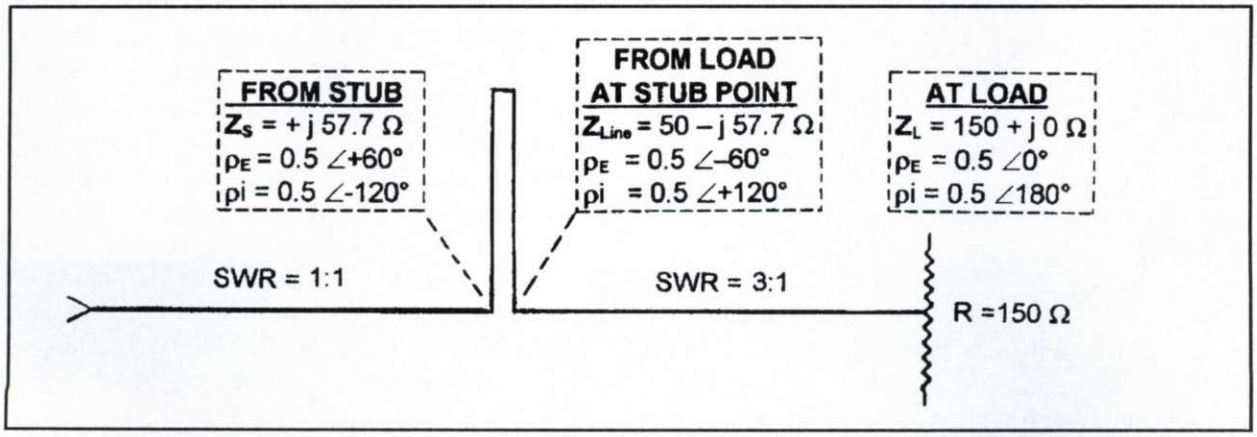

Fig 23-3. A 50-ohm line terminated with a 150-ohm load matched with a series stub, reducing the SWR to 1:1 from the stub to the source, leaving a 3:1 SWR from the load to the stub.

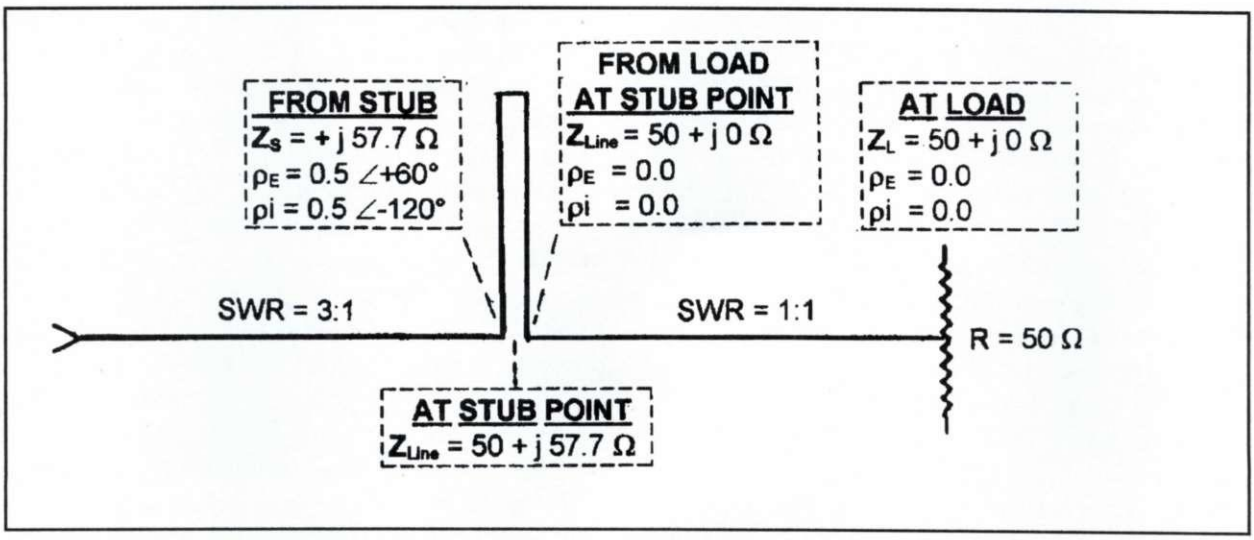

Fig 23-4. Series stub on matched line, generating a mismatch conjugately related to load mismatch generated by 150-ohm load in Figs 23-1, 23-2, and 23-3.

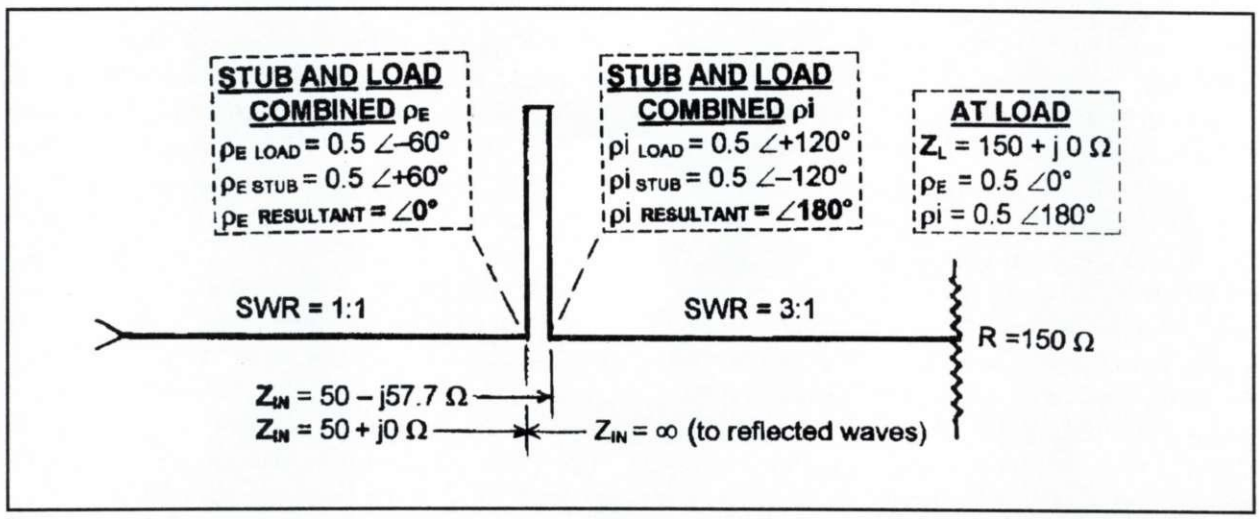

Fig 23-5. Showing how resultant angles of voltage and current reflection coefficients $\rho_e\theta = 0°$ and $\rho_i\theta = 180°$ at the match point establish a virtual open circuit at the match point to waves reflected by the load.

presents a reactive 3:1 mismatch to the 50-ohm line and produces a rearward-traveling reflection also of magnitude 0.5. Thus, with the 50-ohm matched load terminating the line, the stub alone now produces a 3:1 SWR on the line between the source and the stub. Then how does the stub achieve an impedance match with the 150-ohm resistance at the load? Because, in this analytic model, the reflection coefficients of magnitude 0.5 for both voltage and current produced by the stub reflections at the stub point are conjugates of those appearing at the stub point resulting from the reflections developed by the 150-ohm mismatch at the load. Now you ask: Why are there no reflected waves on the line between the source and stub with the 150-ohm load terminating the line? *This is the crucial point of the discussion.* It is because the superposition of the voltage and current components of the two sets of reflected waves at the stub point, each set generated by the *load* mismatch and the *stub* mismatch, respectively, creates a *totally–reflecting open circuit to all reflected waves arriving at the stub point.* These reflected waves are then totally *re*-reflected by the *open-circuit* condition at the stub point, reversing their direction to travel only in the *forward* direction toward the load; they cannot travel rearward past the open

circuit provided by the stub. This phenomenon is explained below and illustrated in Fig 23-5.

Let us now examine the wave-interference mechanism that produces the totally–re-reflecting condition at the stub, or match point, *which is the basis for all impedance-matching operations.* Then following, we'll discuss how the same phenomenon occurs in λ/4 transformers, as well as in pi-networks comprising lumped components, which, when resonant, behave as tapered λ/4 impedance transformers. After this discussion the reason for the virtual short circuit to rearward traveling waves appearing at the input of the pi-network in RF amplifiers will become clear.

However, as we will see, more action occurs at the stub point in preventing reflected waves from traveling rearward past the stub than simply canceling the reactances. To discover how the stub causes a wave interference that establishes the open circuit, and cancels rearward-traveling waves at the stub, we examine the reflection coefficients produced by both the load and stub mismatches. With the pure resistance of 150 ohms terminating the 50-ohm line, the voltage and current reflection coefficients at the load are $\rho_{EL} = 0.5$ at 0° and $\rho_{IL} = 0.5$ at 180°, respectively. Keep in mind that for every electrical degree of travel along a mismatched transmission line, angle θ of the reflection coefficient changes *two* degrees. Thus, the angle of the voltage reflection coefficient for the load mismatch appearing at the stub point 30° rearward from the resistive load resulting from the 3:1 mismatch is $\theta_{EL} = -60°$, as indicated on the reflection coefficient-angle scale at its intersection with the radial line extending from point A in Fig 23-1. Also, because reflected current is always 180° out of phase with its corresponding reflected voltage, the angle of the current reflection coefficient at the stub point for the load mismatch is $\theta_{IL} = +120°$, as indicated by the radial extending from point C.

Next, we examine the reflection coefficients of the stub mismatch. Keep in mind that in examining the stub mismatch separately from the load mismatch, we replaced the 150-ohm mismatched load with a 50-ohm matched load, as shown in Fig 23-4. With the stub in place, and the line terminated in a match, the reactance component of the line impedance at the stub point, normalized to Z_0, is seen as $+j1.1547$ at point D in Fig 23-1, along with the angle of the voltage reflection coefficient $\theta_{ES} = +60°$, as indicated by the radial extending from point D. Thus, $+j57.735$ ohms of inductive stub reactance in series with the 50-ohm matched line results in a line impedance of $50 + j57.735$ ohms at the stub point. Also, again, since reflected current is always 180° out of phase with the reflected voltage, the angle of the current reflection coefficient of the stub reflection at the stub point is $\theta_{IS} = -120°$, as indicated by the radial extending from point B. Because the load and stub both yield 3:1 mismatches, the *magnitudes* of all four reflection coefficients are identically 0.5, thus satisfying the first of two requirements for the total cancellation of the load-reflected wave by wave interference, and creation of the virtual open circuit at the stub. It should be noted that with the two voltage angles θ at +60° and –60°, respectively, to obtain the resultant magnitude, the superposition of their equal 0.5 magnitude coefficients involves the cosine of the angles, where cos 60° = 0.5. Consequently, the magnitude of each of the two voltage coefficients is cos 60° × 0.5 = 0.25, for a resultant sum of 0.5, corresponding to the magnitude of the load mismatch.

To summarize, the ρ magnitudes and θ angles of all four voltage and current reflection coefficients ($\rho_{\theta E}$ and $\rho_{\theta I}$) appearing at the stub point, we have $\rho_{EL} = 0.5$ at –60° and $\rho_{IL} = 0.5$ at +120° for the load mismatch, and $\rho_{ES} = 0.5$ at +60° and $\rho_{IS} = 0.5$ at –120° for the stub mismatch. By examining the wave interference at the stub resulting from the superposition of the voltages and currents represented by these coefficients, we will discover that the correlation of the magnitudes and angles of the coefficients are responsible for establishing the totally-reflecting open circuit. Later, using a different mathematical model, we'll examine the wave interference mechanism that occurs in λ/4 transformers.

Next we consider the two *voltage* angles at the stub point; $\rho_{\theta EL} = -60°$ for the load reflection, and $\rho_{\theta ES} = +60°$ for the stub reflection, with their resultant $\rho_{E\text{-}RES} = 0°$. With $\rho_{\theta EL}$ and $\rho_{\theta ES}$ canceling to zero we have a clue that the conjugate relationship between the two mismatches results in the $+j57.753$ohms of stub reactance canceling the $-j57.357$-ohm line reactance appearing at the stub point on the line. Next we consider the two *current*

angles at the stub point; $\rho_{\theta IL} = +120°$ for the load reflection, and $\rho_{\theta IS} = -120°$ for the stub reflection, with their resultant $\rho_{I\text{-}RES} = 180°$. The basis for establishing the virtual open circuit to reflected waves at the stub point lies in these two resultant angles, voltage 0° and current 180°, as explained below, and illustrated in Fig 23-5.

From universally known transmission-line theory, when the terminating load on a line is a physical open circuit (or an impedance greater than Z_0), the angles θ of the reflection coefficients are 0° for voltage and 180° for current (the conditions obtained in the example above). Conversely, when the terminating load is a physical short circuit (or an impedance less than Z_0), the θ angles are reversed, 180° for voltage and 0° for current. Now for the crucial factor in establishing the *virtual* open (or short) circuit at the stub. In both cases these conditions are reciprocally related; an open-circuit termination yields 0° and 180° for voltage and current, respectively, but conversely, if by some means we *establish* reflection coefficients of equal magnitude, with angles of 0° for voltage and 180° for current at any given point on a line (as we have in the example above), that combination of reflection coefficients establishes a virtual open circuit at that point to waves traveling rearward. The means for establishing these reflection coefficients of equal magnitude, and angles 0° for voltage and 180° for current, is illustrated in Fig 23-5. Continuing, if we *establish* reflection coefficient angles of 180° for voltage and 0° for current at a given point, that combination establishes a virtual short circuit to waves traveling rearward at that point, *but not to waves traveling forward.* Thus, having already established the resultant voltage and current θ angles of 0° and 180°, respectively, with equal magnitudes of 0.5 at the stub point in the present example, we have demonstrated that a virtual *open* circuit to rearward traveling waves has been established there, causing the waves to be totally re-reflected toward the load at the stub point. Consequently, if there are no reflected waves on the line between the stub and the source, that section of line must be matched, with an SWR of 1:1 between the source and the stub.

In the example described above, the action of the stub established an open circuit to rearward-traveling reflected waves at the stub point (but *not to forward* traveling waves). However, the stub can establish either an *open* circuit or a *short* circuit, depending on the relation between the terminating load impedance Z_L and the characteristic impedance Z_0 of the line. When the load impedance Z_L is *greater* than the line impedance Z_0, as in the illustration above, the reflecting condition at the match point is an infinite impedance to reflected waves, a virtual *open* circuit; when Z_L is *less* than Z_0, the reflecting condition is a zero impedance, a virtual *short* circuit to reflected waves. To avert any misunderstanding concerning the conditions just described, I repeat for emphasis, *these open- or short-circuit conditions apply only to the* ***rearward****–traveling waves, not to the forward-traveling waves,* which see ***only*** the characteristic impedance Z_0 of the line.

At this point it should be understood that there have been unwarranted objections to the concept that conjugately-related waves traveling in the same direction can produce reflections. This concept is explained in depth in Chapter 25 in Sec 25.3, "Virtual Open and Short Circuits Established by Wave Interference." For convenience, a portion of that section is repeated below to dispel the objections:

> Wave interference between two sets of reflected waves traveling in the same direction within a transmission line or network that are conjugately related at the matching point establishes either a one-way *short* circuit or a one-way *open* circuit to the rearward-traveling reflected waves. We'll now show from a different perspective how two sets of reflected waves (of both voltage and current) traveling in the same direction are established in the impedance-matching process, and how they also establish the one-way short or open circuit that prohibits any further rearward travel of the reflected waves, in other words, total re-reflection at the match point.
>
> In general, the impedance-matching process involves three harmonically-related traveling waves arriving at the match point: a forward wave delivered by the source (Wave 1), and two conjugately related rearward-traveling reflected waves (Waves 2 and 3) developed by two conjugately related physical discontinuities. Wave 2 is the wave reflected from a mismatched line termination that requires cancellation, and Wave 3 is the canceling wave reflected by the matching device at the match point, its input connection to the source line. Because of their conjugate relationship, Waves 2 and 3 are mirror images of each other.
>
> First, with waves traveling in opposite directions on a transmission line, we know that reflected waves pass through forward waves unimpeded, and the interference between them establishes only a standing wave—no open or short circuits are established. However, when two sets of voltage and current

reflected waves are traveling in the *same* direction and are conjugately related at the matching point in an impedance matching device, the interference between these two sets of reflected waves establishes either a virtual open or short circuit to the reflected waves at the matching point. Whether an open or short circuit is established depends on the boundary conditions of the mismatched load and the distance from the load to the matching point. When the match point at the normalized unity-resistance point using a *series* shorted stub of less that a quarter wave in length on the line occurs within the first quarter-wavelength from the load, an open circuit to reflected waves occurs at the match point when the resistive component R of load $Z_L > Z_0$. A short circuit to reflected waves occurs when the resistive component R of load $Z_L < Z_0$. The reasons for these phenomena will become clear as we proceed.

In learning how one-way open and short circuits are established through wave interference, it is helpful to first understand what happens to an electromagnetic field on encountering a physical open or short circuit. It is universally known that when an electromagnetic field encounters an open circuit, the electric field (or voltage wave) is totally reflected with 0° change of phase, and the magnetic field (or current wave) is totally reflected with a 180° change of phase. Conversely, when an electromagnetic field encounters a short circuit, the electric field (or voltage wave) is totally reflected with 180° change of phase, and the magnetic field (or current wave) is totally reflected with a 0° change of phase. *It is of vital importance to the issue of total re-reflection to understand that these relationships are reciprocally related.* Consequently, when the resultant voltage and current angles established by wave interference are 0° and 180°, respectively, an open circuit to the reflected waves is established. Conversely, when the resultant voltage and current angles are established at 180° and 0°, respectively, a short circuit to the reflected waves is established. Thus, when either an open or a short circuit is established at the matching point by wave interference between the two sets of conjugately-related reflected waves traveling rearward, the direction of the voltages, currents, and energies in both sets of reflected waves is reversed. That results in total re-reflection of the reflected waves.

Let us now determine why virtual open or short circuits are developed by wave interference. From King (*Ref 37*) we know that voltage and current traveling along the line can be represented by individual generators placed at any point along the line. King called those generators "point generators." For the purpose of analysis, King defines a point generator as an impedanceless EMF that can represent or replace the voltage and current on the line equal to the voltage and current actually appearing at that point on the line, without disturbing the wave action on the line.

To simulate and analyze interference between two waves of equal magnitude and opposite phase traveling in the same direction, such as the two sets of reflected waves generated by the load mismatch and the stub mismatch, we can connect two point generators together in either of two different configurations. Each generator replaces the voltage and current of each individual wave at the point of interference, the match point. In the first configuration, the two generators are connected *in phase*. Because their voltages are equal and in phase, the differential voltage is zero, resulting in no current flow. This connection is equivalent to an *open* circuit between the generators. In the second configuration, the generators are connected with their terminals reversed. Their voltages are now *in opposite phase* at the interference point and the resulting voltage is the *sum* of the voltages delivered by each generator—i.e., twice the voltage of each generator. This connection results in a *short* circuit between the two generators.

Identical wave-interference phenomena establishing a short circuit also occur in free space in the same manner as in guided-wave propagation along transmission lines. For example, when the fields emanating from two radiators in an array of antennas are of equal magnitude and 180° out of phase at a point in space, a virtual short circuit is established by destructive wave interference, resulting in a null in the radiation pattern at that point. Following Poynting's Theorem, the energy in the combined fields propagating is reversed in direction at that point; and with the constructive interference that follows, that energy adds to that in the fields propagating in the opposite direction, thus achieving gain in the that direction."

Does anyone now question the validity of the concept that two sets of voltages and currents that are conjugately related and traveling in the same direction along a transmission line can produce reflections, and believe that only physical open and short circuits can produce reflections? If you do still harbor such thoughts, please consider this: No reflected waves travel rearward beyond the match point where the stub is positioned, signifying that all voltage and current waves previously traveling in the rearward direction toward the match point are totally re-reflected there. Where are the *physical* open or short circuits? There are none, only two sets of superposing conjugately-related voltages and currents. Consequently, when you hear people claim that only physical open and short circuits can produce reflections, ask them to show you the "physicals" that "must be" at the stub-matching point on the transmission line to produce the reflections.

Before proceeding to discuss the corresponding conditions of matching with $\lambda/4$ transmission lines, let us first examine what happens to the phase of the reflected waves on re-reflection at the stub point that permits the energy contained in the reflected waves to be added to that delivered by the source. On re-reflection at the virtual open circuit appearing at the stub point, the resultants of the voltage and current components of the load- and stub-re-reflected waves emerge in the forward direction *in phase* with the corresponding compo-

nents of the source waves. Why do the re-reflected resultant waves emerge *in phase* with the source waves? Keep in mind that just prior to the re-reflection, the reflection angles θ of the resultants were 0° and 180° for voltage and current, respectively. Also keep in mind that on reflection from an open circuit, angle θ for voltage remains unchanged, while angle θ for current changes by 180°. Therefore, on re-reflection the voltage angle remains at 0°, and the current angle reverses from 180° to 0°, bringing both in phase with the forward voltage and current from the source. Consequently, the energy contained in the fields of the reflected waves adds directly to those of the source waves at the stub point, which accounts for the forward power in the transmission line between the stub and the load being greater than that supplied by the source by the amount of the power reflected. Of course, it is understood that the power reflected at the load is then subtracted from the sum of the source and reflected powers (the forward power), leaving the source power to be totally absorbed by the load. (We're considering only lossless lines here.) This same total-reflection phenomenon occurs at the input of a correctly tuned antenna tuner, which is why no reflected power is observed on the line between the transmitter output and the input of the tuner.

23.5 Impedance Matching with the Quarter-Wavelength Transmission Line

There is an important consideration concerning reflection coefficient angles of which one should be aware when discussing impedance matching with λ/4 transmission-line impedance transformers: When a traveling wave in a transmission line encounters either an open-circuit termination, or a change in line impedance from low to high at a junction, reflection angle θ is 0° for voltage and 180° for current, when the higher-impedance line is terminated in a matched load. Conversely, when the wave encounters a short-circuit termination, or a change in line impedance from high to low at a junction, angle θ is 180° for voltage, and 0° for current, when the lower-impedance line is terminated with a matched load.

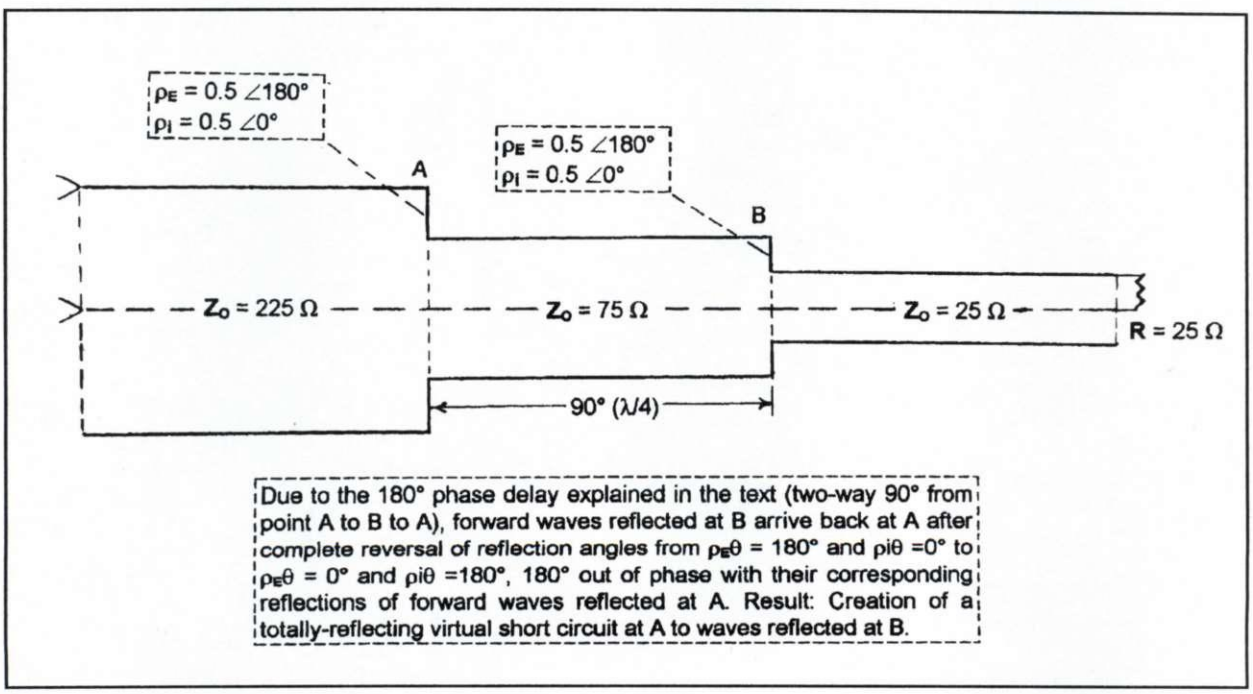

Fig 23-6 Impedance matching with a 90° (λ/4) transmission-line transformer. Due to the 180° phase delay explained in the text (two-way 90° from point A to B to A), forward waves arriving at B are reflected back to A after complete reversal of reflection angles from $\rho_e = 180°$ and $\rho_i = 0°$ to $\rho_e = 0°$ and $\rho_i = 180°$, 180° out of phase with their corresponding reflections of forward waves reflected at A. Result: Creation of a totally-reflecting short circuit at A to waves reflected at B.

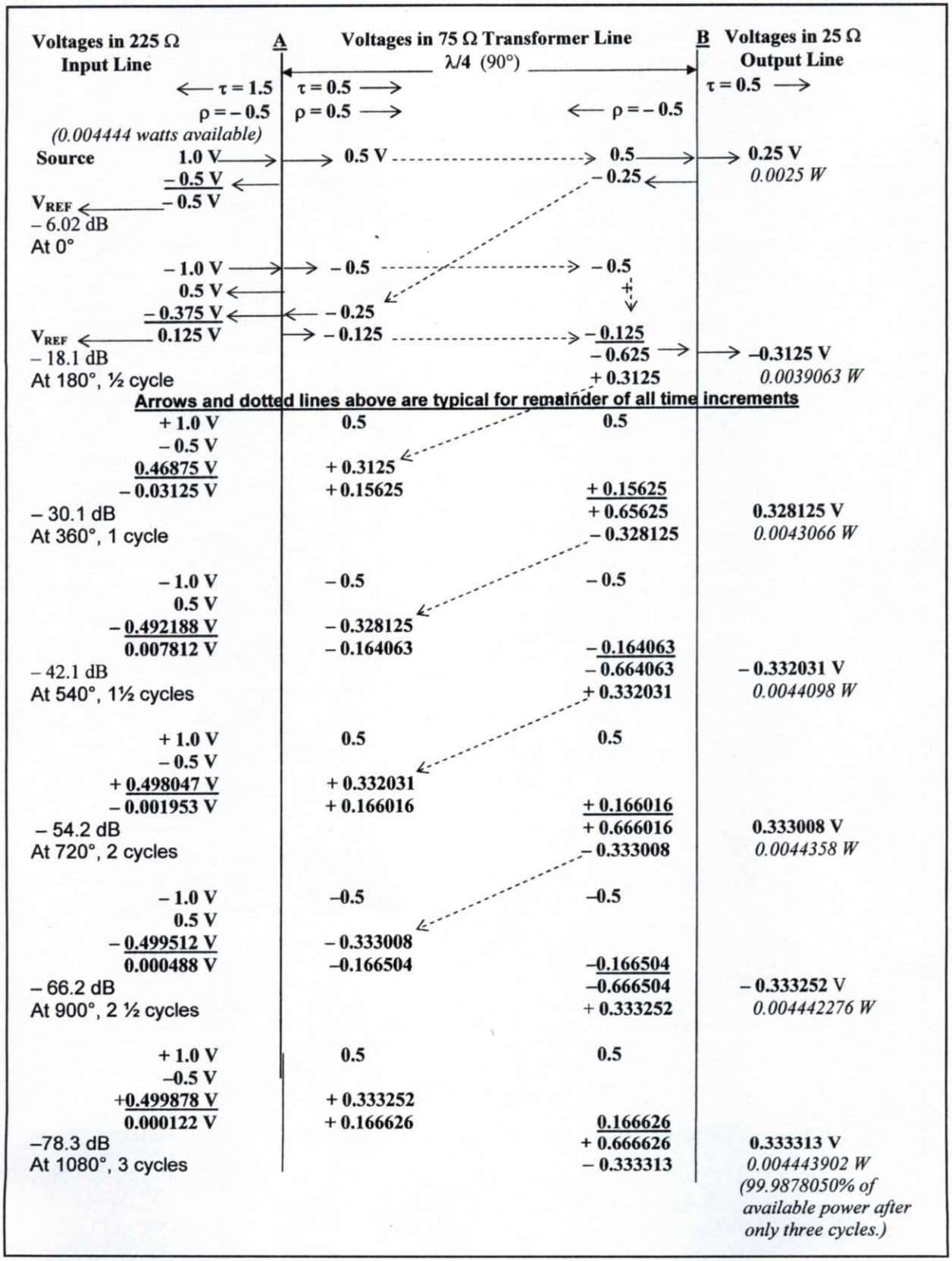

Fig 23-7 Initial to steady-state voltages in quarter-wavelength impedance transformers.

In explaining the wave action in the λ/4 line-matching transformer, let's assume that the transformer is to match two transmission lines having characteristic impedances Z_0 of 225 and 25 ohms, respectively, as shown in Fig 23-6. A source feeds the input 225-ohm line, and the 25-ohm line is terminated in resistance R = 25 ohms. To match the two differing Z_0 impedances the impedance Z_0 of the matching line must be equal to the geometric mean of the two impedances, which in this case is 75 ohms. The 75-ohm matching line is inserted between the 225- and 25-ohm lines at points A and B, also shown in Fig 23-6. In the steady-state condition with the matching line in place there are no wave reflections on either the 225-ohm line or the 25-ohm line, but there are reflections on the matching line, with a 3:1 SWR resulting from the 3:1 mismatches appearing at both ends of that line. To eliminate reflections on the 225-ohm line from the 3:1 mismatch at junction point A, and thus establish an impedance match at A, we must consider the wave interference between two oppositely phased reflected waves appearing simultaneously at A. To establish these two reflected waves we must consider three waves: (1) waves approaching junction A from the left, (2) waves approaching junction A from the right, and (3) waves approaching junction B from the left. Since there are no reflections from the matched termination on the 25-ohm line, there are no waves approaching junction B from the right. Because the reflection coefficient $\rho = 0.5$ is less than $\rho = 1$ at the discontinuities at the junctions, the waves incident on the junctions are partially reflected and partially transmitted through the junctions. Consequently, we must be concerned with both the reflection and transmission coefficients at the junctions to determine the characteristics of the three waves.

Because impedance Z_0 changes from high to low at both points A and B for waves traveling in the forward direction, the reflection coefficients at both A and B are $\rho_E = 0.5$ at $\theta = 180°$, and $\rho_I = 0.5$ at $\theta = 0°$ for voltage and current, respectively. Conversely, in the reverse direction impedance Z_0 changes from low to high at both A and B. Thus, for waves traveling in the rearward direction the reflection coefficients at A are $\rho_E = 0.5$ at $\theta = 0°$, and $\rho_I = 0.5$ at $\theta = 180°$. Correspondingly, voltage transmission coefficients tau are $\tau = (1 - \rho)$ for the forward waves traveling into a lower Z_0, and $\tau = (1 + \rho)$ for the rearward waves traveling into a higher Z_0. The corresponding current transmission coefficients have the opposite sign, respectively. These coefficients are shown at the top of Fig 23-7. As in the previous discussion concerning stub treatment, all lines are considered lossless.

There are advanced-level mathematical equations that describe precisely the wave actions occurring in the λ/4 transmission-line transformer which we could present here. The problem with this approach is that it requires an advanced-level mathematician to understand them. Consequently, to make the problem somewhat more palatable for those not inclined toward advanced-level mathematics, let's consider a simplified example aided by the diagram shown in Fig 23-7. This diagram is patterned after one using a similar approach to explain the wave action in the λ/4 transformer (*Ref 157*). In this figure we show the voltages appearing at the end of each half cycle through the first three cycles of the successive reflections and re-reflections recurring in the transformer. Voltages on the input line appear in the left-hand column, voltages on the λ/4 transformer line appear in the center column, and voltages in the output line appear in the right-hand column. The following describes the action of the voltages as they progress through the transformer. From Ohm's Law, the currents corresponding to the voltages are inherent, determined from the characteristic impedance Z_0 of the transmission line in which they are propagating.

Assume 1 v is applied to the 225-ohm input line; thus 0.0044444... watts enter the line. With the transmission and reflection coefficients as stated above, 0.5 v is transmitted through A into the transformer line and –0.5 v is reflected at A back into the input line, leaving –0.5 v of reflected voltage remaining in the input line until the end of the first half cycle 180° later. (Keep in mind that according to the signs of the reflection and transmission coefficients, voltage and current are in phase when traveling A to B, but are out of phase when traveling B to A due to reflection at the high-to-low impedance change at B.) Because $\tau = 0.5$ is in the forward direction, when the 0.5 v from A wave arrives at B, 0.25 v is transmitted through B into the 25-ohm output line, and 0.0025 w is dissipated in the 25-ohm termination ($0.25^2/25 = 0.0025$).

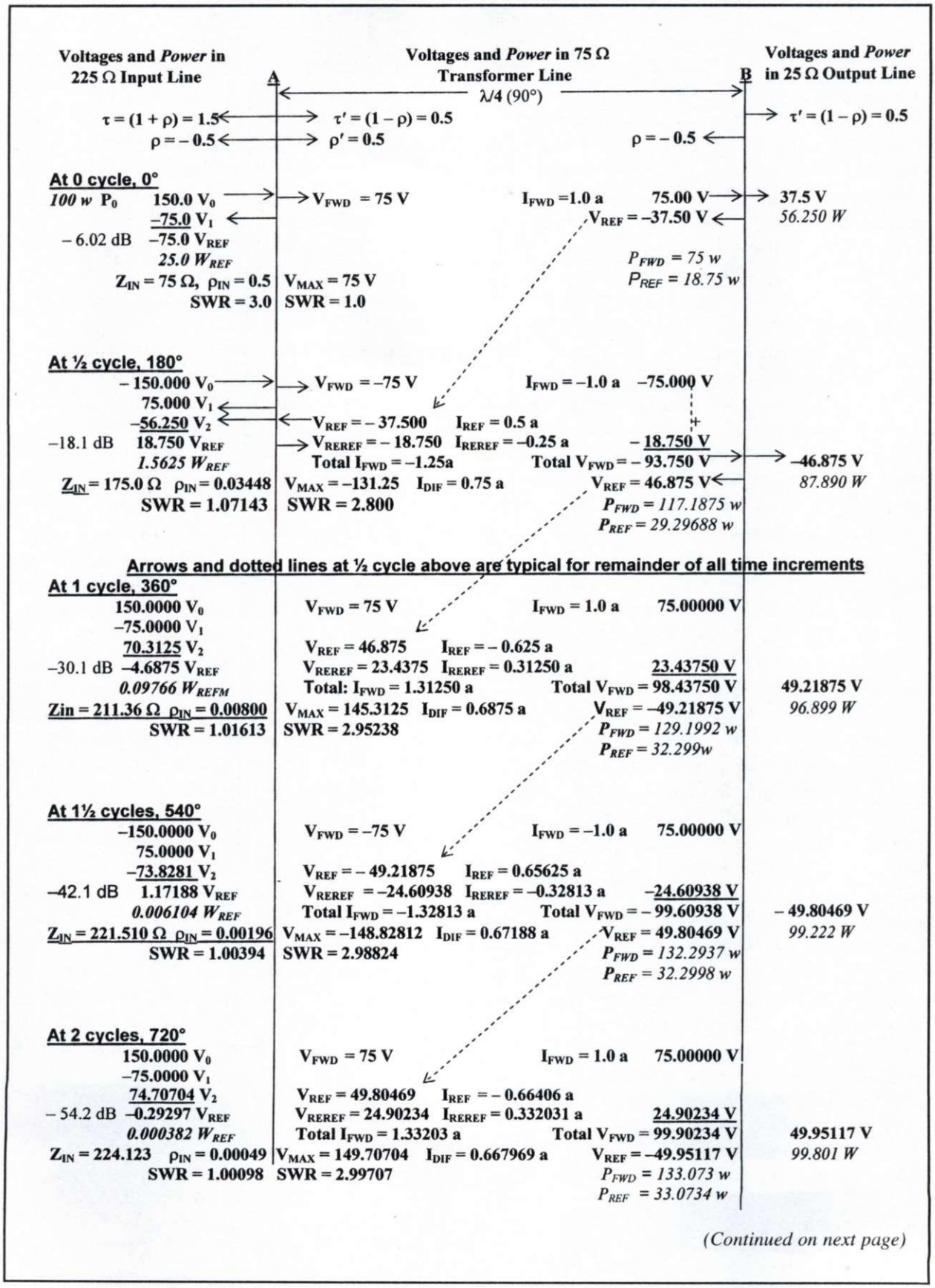

(Continued on next page)

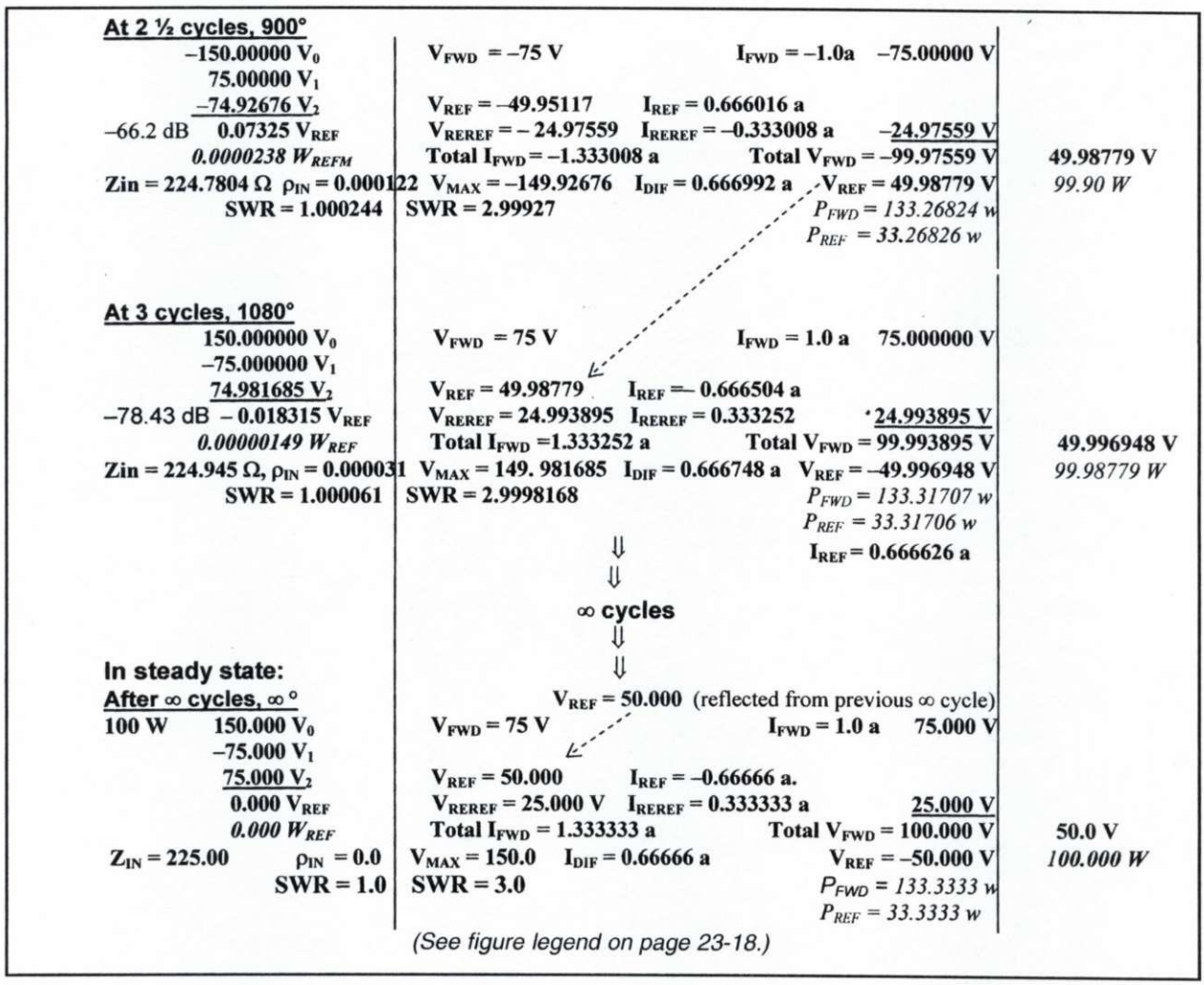

(See figure legend on page 23-18.)

Fig 23-8 Initial to steady-state voltages and *power* in a quarter-wavelength impedance transformer.

However, because $\rho = -0.5$ in the reverse direction, –0.25 v is reflected back into the transformer line and becomes incident on A 180° later, at the end of the first half cycle. During this time the polarity of the source voltage has changed from positive to negative, and the reflected voltage at A has changed from negative to positive.

Because $\tau = 1.5$ in the rearward direction, the reflected –0.25 v reflected rearward at B is transmitted through A into the input line and becomes –0.375 v, which subtracts from the +0.5 v now reflected back into the input line at A, reducing the voltage remaining in the input line from –0.5 v to +0.125 v. In addition, because $\rho = +0.5$ in the forward direction the polarity of the reflection coefficient at A remains the same. Thus, –0.125 v of the reflected –0.25 v is re-reflected forward, becoming incident on B.

Also during this first 180° period, the polarity of the source has changed from positive to negative. Consequently, –1 v from the source has now entered the input line, –0.5 v is transmitted through A into the transformer line, and +0.5 v is reflected back into the input line. However, the –0.125 v *re*-reflected at A adds to the –0.5 v transmitted through A, resulting in –0.625 v incident on B, where –0.3125 v is transmitted through B into the output line and +0.3125 v is reflected back to A. Note here that on reaching A the +0.3125 v transmitted through A becomes +0.46875 v in the input line, where it subtracts from the –0.5 v, now leaving only –0.03125 v remaining in the input line.

We have thus described the succession of events recurring during the first two half cycles of operation in the $\lambda/4$ transmission-line impedance-matching circuit. However, it is instructive to observe

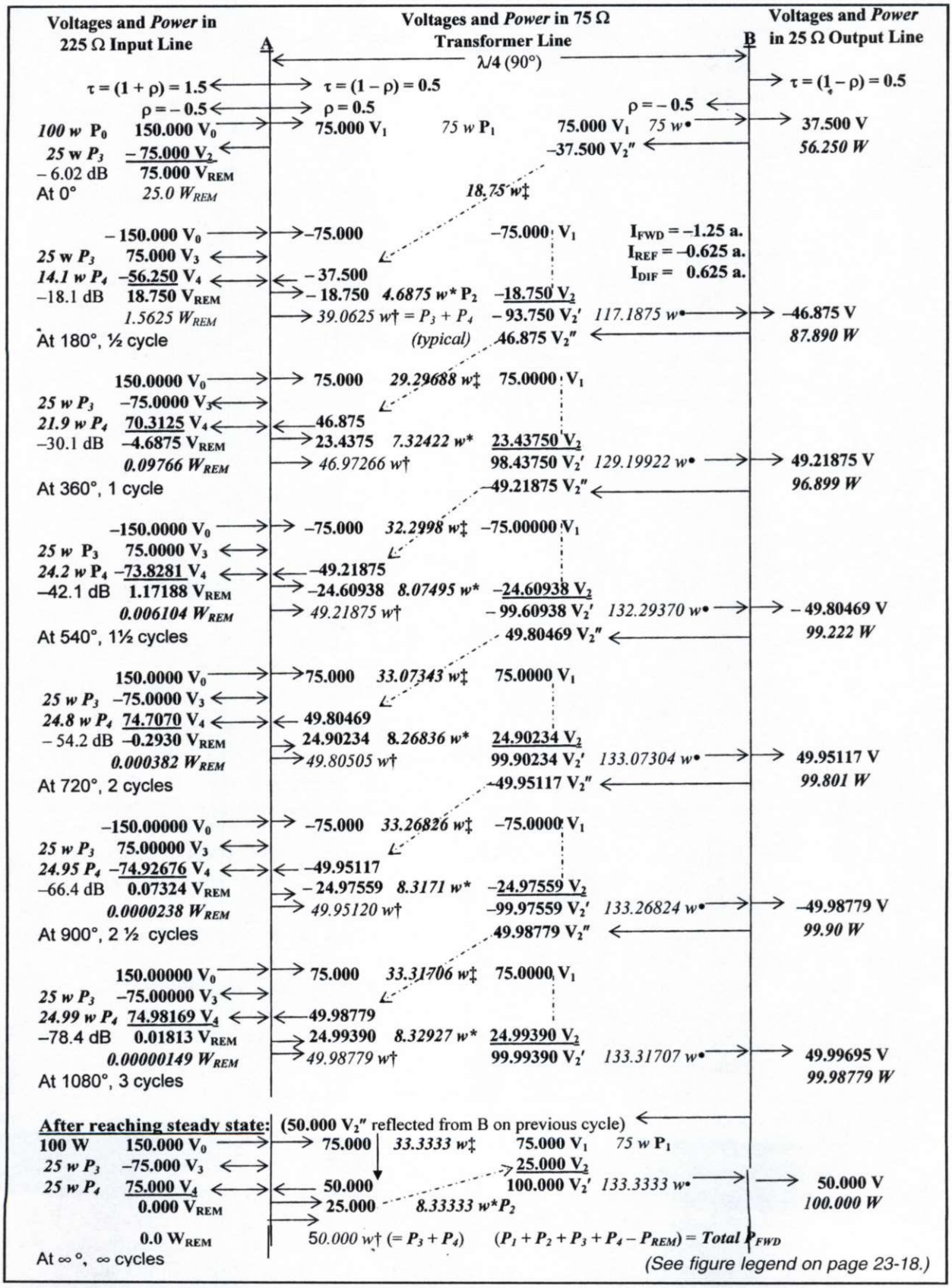

(See figure legend on page 23-18.)

Fig 23-9 Initial to steady-state voltages and *power* in a quarter-wavelength impedance transformer.

each following half cycle to observe the voltage incident on B and entering the output line increasing logarithmically toward the steady-state condition, while the reflected voltage remaining in the input line is decreasing exponentially during each half cycle. Fig 23-7 shows that after only three cycles has elapsed the voltage reflected into the input line has reduced from –0.5 v to +0.000122 v (–78.3 dB), and the voltage in the output line has increased from 0.25 v to 0.333313 v (0.25 w). While 1 v in the 225-ohm input-line represents 0.004444444 watts of available power, the 0.333313 v in the output line represents 0.004443902 watts dissipated in the 25-ohm terminating resistor, 99.9878050% of the input power, only 0.00192 dB lower than the input power. This indicates that we have almost reached the steady-state condition after this short period of only three cycles. This reflection and transmission process continues indefinitely until the final steady-state condition is reached, at which time both voltage and current reflected back into the input line approach zero. The currents corresponding to their respective voltages above are treated in the same manner as the voltages. Consequently, while the current traveling rearward in the source line decreased, the current traveling forward into the output line has increased (*Ref 157*).

While having presented the reflection mechanics basic to the impedance-matching function of the quarter-wavelength transformer with 1 v input, we'll now present some additional insight concerning the mechanics occurring there using values of transmitted and reflected voltages at a somewhat more practical level. Referring to Fig 23-8, note that the values of the transmission and reflection coefficients are identical to those appearing in Fig 23-7. (To appreciate the notes accompanying Figs 23-8 and 23-9, please refer to the legend for Figs 23-8 and 23-9.) However, note also that the input applied to the 225-ohm input line is changed from 1 volt to 150 volts to illustrate the corresponding voltages when delivering 100 watts into the line, an appropriate value for a practical example. Consequently, the various values of transmitted and reflected voltages appearing in Fig 23-8 are more realistic than those appearing in Fig 23-7.

In addition to the voltages appearing in Fig 23-8, the corresponding currents are also shown to provide the basis for determining the instantaneous values of input resistance of the transformer line at various half-wavelength intervals. The full expansion of the infinite number of terms of the convergent power series that appears in advanced mathematical equations has been abbreviated in Figs 23-7 and 23-8 to the RMS values of the instantaneous voltage and current terms appearing in the advanced equations. The voltage/current ratio using such terms can be interpreted in the usual way as instantaneous resistances for the purpose of better visualizing the changes in resistance at these selected times during the transient phase. However, the classic definition of resistance is, strictly speaking, only defined in the steady state. In other words, while it is generally understood that values of resistance are only considered valid during the steady-state condition, the input resistance appearing at the end of each half cycle is presented only to afford a better appreciation of the change in the condition appearing at the input of the transformer with each successive half wave. These values of input resistance are then those which would be seen if time were arbitrarily frozen at the end of each corresponding half cycle.

Refer now to Fig 23-9. While duplication of data will be observed between Figs 23-8 and 23-9, there are important differences that could not conveniently be shown in the space available in one figure. Note that voltages in the figures are shown in regular font, while powers are shown in italics.

To summarize the analysis of the data concerning the quarter-wavelength transmission-line transformer appearing in Figs 23-8 and 23-8, the following events that occurred *during only the first 3 cycles* should be noted and kept in mind:

1. In the case where the input voltage is 150 volts, the input resistance of the transformer increased logarithmically from the initial value of 75 to 255 ohms in the steady state.

2. The input SWR of the transformer decreased from the initial 3:1 to 1:1 in the steady state.

3. The SWR inside the transformer increased from the initial 1:1 to 3:1 in the steady state.

4. The voltage reflected back into the 225-ohm input line decreased exponentially from –75 v to –0.018315 v, –78.3 dB.

5. The power reflected back into the input line decreased exponentially from 25 w to 0.0000011149 w.

6. The output voltage increased logarithmically from the initial 37.5 v to 49.996948 v out of 50 at the steady state, with a corresponding power increase from 56.25 w to 99.98779 w out of 100 at the steady state.

7. In the case where the input voltage is 1.0 v, the voltage reflected back into the 225-ohm input line decreased exponentially from –0.5 v to 0.000122 v, decreasing –78.3 dB.

8. Similarly, the reflected power decreased, also exponentially, from 0.0044444 w to 6.62×10^{-11} w.

9. The output voltage increased logarithmically from the initial 0.25 v to 0.333333 v, with a corresponding power increase from 0.0025 to 0.004443902 w, 99.9878050% of the available power.

10. In the steady state the output voltage increased to 0.333333...v and 0.0044444...w, with reflected voltage zero and reflected power also zero.

To achieve utmost clarity in understanding the incremental increase in energy storage in the transformer occurring during the transient period, it also seemed important to display all values with at least eight significant figures, especially during the time periods approaching the steady-state condition, where utmost precision is necessary to achieve the desired result. It is hoped that the presentation of Figs 23-7, 23-8, and 23-9 and the legend has succeeded in improving the understanding and appreciation of the concept and operation of the quarter-wavelength transmission-line transformer as an impedance matching device. For their valuable help and inspiration on this section, the assistance of Robert Lay, W9DMK (*Ref 158*), James Kelley, AC6XG (*Ref 155*), and William Klocko, N3WK (*Ref 156*) is greatly appreciated. Their peer review and support assured me that I was headed in the right direction in the analysis of the quarter-wavelength transformer.

23.6 On the Input Impedance of Open- and Short-Circuited Transmission-Line Stubs

After having examined the wave mechanics that are basic in establishing the impedance-matching phenomenon in λ/4 transmission-line transformers, we would be remiss if we did not extend the examination to the wave mechanics that establish the input impedances of open- and short-circuited transmission-line stubs. In this discussion all lines are considered lossless for ease in understanding the principles.

Let us first consider the λ/4 *open*-circuit stub. On arrival at the input of the stub the source voltage and current are in phase, at which point we assign a reference phase of 0°. On arriving rearward at the input, the voltage and current waves reflected from the open-circuit termination of the stub have traveled 180° relative to those arriving at the input, 90° in traveling from the input to the open-circuit termination, and another 90° in returning to the input. However, keep in mind that on reflection from an open circuit, angle θ of the voltage reflection coefficient experiences no change, while angle θ for current changes 180°. Thus, on return to the input, angle θ of voltage waves reflected from the open-circuit termination is now 180°, a complete reversal in phase relative to the source. Consequently, the reflected voltage appearing at the input of the stub is of the *opposite polarity* to that arriving from the source. Continuing, with the 180-angle change in current on reflection at the open-circuit termination, plus the 180° travel on the stub line, on return to the input, angle θ for the reflected current is 0°, *in phase* with the source current. Therefore, we have two equal voltages of opposite polarity at the input, the source voltage and the stub voltage, with their currents *in phase*. The result? Maximum current flow—zero impedance—*a virtual short circuit.* A perfect DC analogy is two batteries connected in series, plus to minus, and plus to minus—short circuit—maximum current.

Let us now consider the λ/4 *short*-circuited stub. The only differences relative to the conditions prevailing in the open-circuit stub are the θ angles of the voltage and current reflection coefficients of the waves reflected from the short-circuit termination that appear on return to the input. On reflection from a short circuit, angles θ of the reflection coefficients for both voltage and current are opposite to those reflected from an open circuit—i.e., on reflection from a short circuit the voltage angle θ changes by 180°, while the current angle θ does not change. Consequently, on return to the input, the θ angles of the voltage and current waves reflected from the short-circuit termination of the stub are 0° and 180°, respectively, *opposite* to those returning

at the input of the open-circuit stub. As a result, the source and stub voltages are equal and of the *same polarity* at the input, while the currents are now *out of phase.* The result? Zero current flow—an infinite impedance—an *open circuit.* A perfect DC analogy is two batteries (of equal voltage) connected in parallel, plus to plus, and minus to minus—open circuit—zero current.

So far we have considered only stubs of λ/4, the length which yields zero reactance, because the stub-reflected voltage with stub length λ/4 is either exactly in phase, or 180° out of phase, with the source voltage. However, as we know, *capacitive* reactance is present in a circuit when current leads the voltage, and conversely, *inductive* reactance is present when voltage leads the current. Thus, let us examine the wave mechanics of stubs having lengths that do yield reactance by causing the voltage and current at the input of the stub to be out of phase.

Let us begin with stubs that provide *capacitive* reactance by causing current to lead the voltage. These are *open*-circuit stubs having lengths *less* than λ/4. When the open-circuit stub length is less than a λ/4, the stub *current leads the voltage* at the input of the stub, because the current reflected from the open-circuit termination has traveled *less* than 180° relative to the waves arriving from the source. As a result (while including the 180° phase reversal on reflection from the open circuit), the reflected current arrives back at the input of the stub *ahead* of the source voltage. Because of this *current-leading-voltage* phase relationship between the source voltage and the reflected current arriving at the input of the stub, a *capacitive* reactance $-jX$ is developed at the stub input.

For this knowledge to be useful we need to establish the relationship between stub length and the resulting reactance obtained from the superposition of the source and reflected waves at the input of the stub. First, the phase relationship between the source and reflected waves at the stub input is determined by angle θ of the reflection coefficient of the reflected waves. Angle θ is directly related to the stub length by the expression $Ls = \theta/2$, where Ls is the stub length. Both Ls and θ are in electrical degrees. The stub length in wavelengths may be found using the expression $Ls_\lambda = Ls°/360°$. And finally, the capacitive reactance at the stub input may be found using the expression $-jX = Z_0 \cot Ls$.

As an example, let us find the capacitive reactance obtained with an open-circuit stub having a measured current reflection coefficient angle θ of 90°, and where the characteristic impedance Z_0 of the stub line is 50 ohms. From angle θ the stub length in degrees is $Ls = \theta/2 = 90°/2 = 45°$. The length Ls_λ in wavelengths is $45°/360° = 0.125\lambda$, or λ/8. Capacitive reactance $-jX = Z_0 \cot Ls = 50 \cot 45° = 50 \times -1.0 = -j50$ ohms. The stub length required to obtain a given capacitive reactance may be found by reversing the above procedure.

Having examined the open-circuit stub for its capability of obtaining *capacitive* reactance, let us now examine the short-circuit stub for its capability of obtaining *inductive* reactance. Keeping in mind that in the open-circuit stub, angle θ of the voltage reflection coefficient remains unchanged on reflection, and angle θ for current reverses 180°, while the reverse is true with the short-circuit stub; angle θ for voltage reverses 180°, and angle θ for current remains unchanged.

When the short-circuit stub length is *less* than a λ/4, the stub *voltage leads the current* at the input, because the voltage wave reflected from the short-circuit termination has traveled *less* than 180° relative to the waves arriving from the source. As a result, while including the 180° phase reversal on reflection from the short circuit, the reflected voltage wave arrives back at the input of the stub *ahead* of the source current wave. Because of this *voltage-leading-current* phase relationship between the source current and the reflected voltage arriving at the input of the stub, an *inductive* reactance $+jX$ is developed at the input of the stub. Borrowing from the open-circuit expressions above, the stub length is obtained in the same manner, and the inductive reactance at the stub input may be found from the expression $+jX = Z_0 \tan Ls$. (Note that the tangent function is used for short-circuit stubs, yielding $+jX$, and the cotangent is used for open-circuit stubs, yielding $-jX$.)

As an example, let us find the inductive reactance obtained with a short-circuit stub having a measured voltage reflection coefficient angle θ of 90°, and where the characteristic impedance Z_0 of the stub line is 50 ohms, as in the open-circuit case above. From angle θ the stub length is $Ls = \theta/2 = 90°/2 = 45°$. The stub length Ls_λ in wavelength is

45°/360° = 0.125λ, or λ/8. Inductive reactance $+jX = Z_0 \tan Ls = 50 \tan 45° = 50 \times 1 = +j50$ *ohms.*

It is of interest to observe that because tan 45° = 1.0, and cot 45° = –1.0, the ±*j*X reactance obtained with short- or open-circuit stubs of length 45° (λ/8) always equals the value of the characteristic impedance Z_0 of the stub line.

23.7 Conclusion

This discussion has revealed four basic fundamentals concerning the phenomenon of impedance matching. They are:

1. The cancellation of mismatch-generated reflected waves is achieved through wave interference produced with the superposition of new mismatch-generated reflected waves that are conjugately related to the waves to be canceled.

2. The mechanism of wave interference is fundamental to all impedance matching operations; matching with transmission-line stubs, with λ/4 transmission-line transformers, as well as with impedance-matching networks comprising lumped elements.

3. Reflected waves cannot travel rearward beyond the matching point in the matching device because they are stopped by the virtual open or virtual short circuit to rearward-traveling waves that appear at the matching point.

4. The virtual open or short circuit results from wave interference between two sets of reflected waves, one set produced by the load mismatch, and the other set produced by the matching device tailored to produce reflected waves that are conjugately related to those produced by the load mismatch.

Finally, this discussion has also examined the capabilities of open- and short-circuit transmission-line stubs to obtain capacitive and inductive reactances.

Legend for Figs 23-8 and 23-9

The following is the legend for both Fig 23-8 and 23-9. While duplication of data will be observed in the two figures, there are important differences that could not conveniently be shown in the space available in one figure. Note that voltages in the figures are shown in regular font, while powers are shown in italics.

V_0 = Voltage delivered by the source
V_1 = Portion of source voltage transmitted through A into transformer from input line
V_2 = Portion of voltage V_2" reflected rearward from B and re-reflected forward from A
$V_2' = V_1 + V_2$, total voltage incident on B
$V_2'' = V_2' \times \rho$, total voltage reflected rearward from B becoming incident on A
V_3 = Portion of source voltage reflected rearward from A into input line
V_4 = Portion of voltage V_2" reflected rearward from B and transmitted through A into input line
$V_{MAX} = V_0 - V_{REM}$, voltage at A after reflection from B at each interval
V_{MIN} = Voltage incident on B at each interval
V_{REM} = Voltage remaining in 225-ohm input line during the transient period
$I_{MIN} = I_{FWD} - I_{REF} = I_{DIF}$, currents flowing on the line pertinent to determining input impedance of the transformer line
τ = voltage transmission coefficient tau
$\tau = (1 + \rho)$ when traveling from low to higher impedance
$\tau = (1 - \rho)$ when traveling from high to lower impedance
ρ = voltage reflection coefficient rho
ρ^2 = power reflection coefficient
$(1 - \rho^2)$ = power transmission coefficient
$1/(1 - \rho^2)$ = forward power increase factor
SWR in transformer at each interval = V_{MAX}/V_{MIN}
P_0 = Power delivered by the source
P_1 = Power transmitted through A into transformer from input line
P_2 = Power w* re-reflected forward from A toward B
P_3 = Portion of source power reflected rearward from A into input line
P_4 = Portion of power reflected rearward from B and transmitted through A into input line
P_{REM} = Power remaining in input line
$P_{FWD} = (P_1 + P_2 + 2\sqrt{P_3 \times P_4})$ = total forward power incident on B
$w\bullet = P_{FWD} = (P_1 + P_2 + P_3 + P_4 - P_{REM})$ = total forward power incident on B
w‡ = Power reflected rearward from B toward A $(= w\bullet \times \rho^2)$
w* = Portion of power w‡ re-reflected from A toward B $(= w‡ \times \rho^2)$
$w† = P_3 + P_4$
$Z_{IN} = V_{MAX}/I_{DIF}$

Chapter 24

The Conjugate Match and Z_0 Match

Sec 24.1 Introduction

Some of the material appearing in this chapter was originally written for the 1986 *ARRL Handbook*, and also appears in all subsequent editions through 1994, as well as in the 15th edition of *The ARRL Antenna Book* and the first edition of this book. This chapter is an edited and revised version of the original.

The primary purpose of matching impedances is to enable a power source having a specific output impedance to deliver its maximum available power to a load having a different impedance. A conjugate match exists by definition when the maximum available power is being delivered from the source to the load. In typical amateur antenna systems the impedance appearing at the input terminals of the antenna is rarely the same as that of the output impedance of the source, or transmitter, or that of the transmission line delivering the power to the antenna. Thus a matching device is required if all the available power is to be delivered. Various matching devices may be used for matching the input impedance of an antenna system to the output of a transmitter. The matching device may be a stub on a transmission line, a $\lambda/4$ line transformer, or a group of lumped reactances, such as a pi- or T-network often found in antenna tuners, or in the pi-network tank circuit of a transceiver. The same principles apply, and the same wave actions and reflections perform the matching function, whichever device is used. The wave actions underlying the matching process are discussed in detail in Chapters 4, 7, and 23. However, for those readers who are not yet acquainted with the principles of conjugate matching, before going further you may find it helpful to first refer to Sec 24.4 and Appendix 9.

Sec 24.2 Discussion

To aid in understanding the principles of matching, we shall first consider transmission lines and the inductive and capacitive reactance components of networks as *lossless* elements, and then treat the effects of attenuation loss later. We will be discussing two specific cases of impedance match and mismatch, one on a conjugate basis and the other on a Z_0 basis. If the power delivered to the load is compared with the maximum power available from the source, the comparison is on a *conjugate* basis. If the comparison is made with the power that the source will deliver to a Z_0 load, the comparison is on a Z_0 basis. Considerable confusion has arisen over the use of the terms "match" and "mismatch," as it is not always clear just what basis is intended (*Ref 120*). R. W. Beatty of the NTIA, formerly the National Bureau of Standards, has set forth a complete set of specific terms and definitions which eliminate this confusion (*Ref 121*). *(See also Ref 137 and Appendix 9.)* Beatty's terms and definitions are as follows:

1. Conjugate match: The condition for maximum power absorption by a load, in which the impedance seen looking toward the load at a point in a transmission line is the complex conjugate of that seen looking toward the source.

2. Conjugate mismatch: The condition in the situation above in which the load impedance is not the conjugate of the source impedance.

3. Conjugate mismatch loss: The loss resulting from a conjugate mismatch.

4. Z_0 match: The condition in which the impedance seen looking into a transmission line is equal to the characteristic impedance of the line.

5. Z_0 mismatch: The condition in which the impedance seen looking into a transmission line is not equal to the transmission-line characteristic impedance Z_0. In general, a conjugate match is a case of Z_0 mismatch.

6. Z_0 mismatch loss: The loss resulting from a Z_0 mismatch, which is canceled by the reflection *gain* obtained when the Z_0 mismatch is matched with a conjugate matching device (*Ref 19, Sec 4.1.3).*

7. Conjugate available power: *Maximum* available power.

8. Z_0 available power: The power a source will deliver to a Z_0 load.

It is well understood that if there is a difference of impedances at a junction of terminals in a series of networks, the mismatch between the impedances gives rise to reflections at the junction, resulting in a reflection loss. A reflection loss is not a dissipative loss; it means only that not all of the available power from the source will be delivered. However, if a matching device inserted between the mismatched components at the junction affects a conjugate match of impedances at the junction, the reflection loss occurring at the output of the device is canceled by the reflection *gain* resulting from the re-reflection at the input of the device. In this condition, *all* of the power from the source will be delivered in accordance with the Conjugate Matching Theorem. *(See Appendix 9; Ref 19; Sec 4.1.3)*

Let's now assume we have a source of RF power, an ideal lossless transmission line, and a load terminating the line, all of which have the same impedance, Z_0. Under these conditions, both a conjugate match and a Z_0 match exist, and the source delivers its maximum available power to the line. The line transfers all of the power from the source to the load, where it is completely absorbed.

If the Z_0 load is now replaced by a mismatched load, such as an antenna having an impedance $Z_A = R + jX \neq Z_0$, we have two mismatches at the load, a Z_0 mismatch and a *conjugate* mismatch. The Z_0 mismatch arises because the output impedance of the line, which is now the source, is Z_0. The conjugate mismatch arises because the Z_0 mismatch prohibits delivery of all the available power. The Z_0 mismatch creates a complex reflection coefficient ρ having a magnitude ρ and angle θ, determined by the line impedance Z_0 and load impedance Z_L in accordance with Eq 3-1 (from Chapter 3) below.

$$\bar{\rho} = \rho\angle\theta = \frac{Z_L - Z_0}{Z_L + Z_0} \qquad \text{(Eq 3-1)}$$

The magnitude ρ of the voltage reflection coefficient causes a power reflection loss ρ^2 to be referred back along the transmission line to the source. This reflection now causes the source to see a complex impedance at the line input having the same magnitude ρ^2 of Z_0 mismatch as at the line output. This mismatch at the input in turn causes the source to deliver less than its maximum available power by the amount equal to the reflection loss ρ^2. *(See Secs 4.1 and 6.2 herein, and Refs 19, Sec 1.8, and 70.)*

Because the transmission line we are discussing is considered to be lossless, there is no power lost in the line due to the reflection—only a reduction of power delivered by the source because of the mismatch to its new complex load impedance at the input of the line resulting from the return of the reflected power. However, under these conditions, the reflected power returned to the source adds to the reduced power delivered by the source, and thus the same amount of forward power is still delivered to the line as was delivered prior to the returning reflection. Consequently, all of the reduced power delivered by the source is absorbed by the load terminating the line, because the power absorbed equals the forward power minus the reflected power, as described in Chapter 4.

If a matching device is now inserted at the junction of the transmission line and the load (the antenna) the matching device establishes a conjugate match at that junction. The matching device achieves the conjugate match by introducing a reflection *gain* (*Ref 19*) that cancels the reflection loss and presents an output impedance $Z_{OUT} = R - jX$ to the antenna, the conjugate of the antenna input impedance $Z_A = R + jX$, and presents an input impedance $Z_{IN} = Z_0$ to the output of the line. Hence, the line now also sees a Z_0 match at the input of the matching device. Because the line is now terminated in a Z_0 match, the source again sees a Z_0 match at the input of the line, and again delivers its maximum available power into the line, to be completely absorbed by the load, the Z_0 ***mismatched***, but *conjugately* ***matched*** antenna.

However, if the matching device is inserted at the junction of the source and line instead of at the junction of the line and load (the antenna), the matching device now establishes a conjugate match at the *input* of the line, where before there was a Z_0 mismatch prior to inserting the matching device at the antenna. Thus the source still sees a Z_0 match at the input of the matching device, and again delivers its maximum available power as before, but this time it is delivered directly to the input of the matching device. However, the conju-

gate matching of the Z_0 impedances at the output of the source and the input of the matching device, which allows the source to deliver all its available power into the matching device, has also established a conjugate match throughout the entire system. This is in accordance with the Conjugate Matching Theorem, which states that once a conjugate match is established at *any* junction of components in the system, there is a conjugate match at *all* other junctions in the system. Although a Z_0 mismatch still remains at the junction of the transmission line and the antenna, and at the junction of the output of the matching device and the input of the line, a conjugate match exists at both of those junctions. The Z_0 mismatches at both junctions produce reflection losses that are referred back to the input of the line as before. However, with the matching network now located at the input of the line, the reflection *gain* supplied by the network (which cancels the resultant reflection loss from both junctions) shields the source from seeing the referred Z_0 mismatch that remains at the input of the line. Once again, the source delivers its maximum available power, all of which is absorbed by the antenna and radiated, in spite of the Z_0 mismatches that remain at the two junctions, the input to the line and at the antenna.

Sec 24.3 A Practical Example

At this point you ask, "What's so important about conjugate matching?" Is there really anything to be gained by an application of this phenomenon that would make it worth my while to try to understand the concept? Indeed there is! Here's a practical example that will demonstrate why knowledge of conjugate matching is important.

Let's say we want to construct an antenna that will perform well on 80 meters and also on all the remaining HF bands through 10 meters, including all the WARC-79 bands. We have a roll of antenna wire, which shows a paced-off measurement of approximately 120 feet, plus or minus two or three feet, suitable for a random-length center-fed dipole with which you can work all bands. In the junk box we find three short lengths of balanced feed line, one each of 300-ohm, 450-ohm, and 600-ohm impedances, none of which will reach between the antenna and the transceiver. However, the three lines connected together in series will reach. Lines of *different impedances* connected together in cascade? Yes. However, there will be three Z_0 mismatches, one at the antenna terminals and one at each junction of the lines of differing impedances. This arrangement is practical? Yes, *the resultant of the individual reflections from all of the cascaded Z_0 mismatches yields a single complex impedance* $Z_{IN} = R + jX$ at the input terminals of the composite line. However, the mismatch of the impedance at the line input to the 50-ohm Z_0 source impedance will prohibit delivery of all the available power from a transceiver tuned to deliver all its available power into 50 ohms unless some form of impedance matching is performed. The solution? *One* impedance-matching circuit (the antenna tuner) inserted between the transceiver and the line input will establish a conjugate match in the *entire transmissiom-line system*—i.e., a conjugate match at every Z_0 mismatched junction in the line, e.g., at the Z_0 mismatched junction of the line and the antenna, and at the junction of the transceiver output and the line input. The result? If the lines were lossless, *all* of the power available from the transceiver would be absorbed and radiated by the antenna in spite of all the Z_0 mismatches in the line and at its termination, all in accordance with Articles 1 and 2 of the Conjugate Matching Theorem stated earlier. The conjugate match throughout the system *overrides* all of the individual Z_0 mismatches in accordance with Article 3 of the Conjugate Matching Theorem. Thus, conjugate matches are established at every Z_0-mismatched junction (including at the output of the amplifier), allowing all the available power to be delivered to the load, according to Article 1. *Without the conjugate match, delivery of all available power would be impossible with transmission lines of different impedances in series transferring power to the antenna.* From this discussion it must be clearly understood that the conjugate matching accomplished by the matching network also tunes the antenna to resonance during operation at frequencies away from its self-resonant frequency.

Now you ask: If there is a conjugate match throughout the entire system when the amplifier is delivering all of its available power at tune up with full power, is there still a conjugate match throughout the system during SSB operation when the

power output is lower than full output during voice modulation? Yes, the match still exists. The conjugate match still overrides the individual Z_0 mismatches appearing at the junctions, and the load, or antenna, still absorbs and radiates all the instantaneous power delivered by the amplifier at the various levels corresponding to the levels of modulation, in accordance with Article 1 of the Conjugate Matching Theorem.

Sec 24.4 The Conjugate Matching Theorem

To understand how a conjugate match is created at the load with the matching network at the input of the line, we need to examine the Conjugate Matching Theorem and especially the wave actions that produce the conjugate match. As explained above, it is the conjugate match which enables the load to absorb the maximum available power from the source despite the Z_0 load mismatches. The Conjugate Matching Theorem was introduced in Chapter 17, and is presented in several different forms as separate Articles in Appendix 9. However, one form (Everitt's) is repeated here for convenience in appreciating the conditions in the example where three lines of different impedances were connected in series.

"If a group of four-terminal networks containing only pure reactances (or lossless lines) are arranged in tandem to connect a source to its load, then if at any junction there is a conjugate match of impedances, there will be a conjugate match of impedances at every other junction in the system." *(From Ref 17 and Ref 69)*

To expand on this definition, "conjugate match" means that if in one direction from a junction the impedance has the dimensions $R + jX$, then in the opposite direction the impedance will have the dimensions $R - jX$. Further paraphrasing of the theorem, when a conjugate match is accomplished at any of the junctions in the system, any reactance appearing at any junction is canceled by an equal and opposite reactance, which also includes any reactance appearing in the load, such as a *non-resonant antenna.* This reactance cancellation results in a net system reactance of zero, establishing resonance in the entire system. In this resonant condition the source delivers its maximum available power to the load. This is why an antenna operated away from its natural resonant frequency is tuned to resonance during operation by a matching network connected at the input to the transmission line.

It must be understood that there is a conjugate match if the delivered power decreases when the load impedance is either increased or decreased.

All conjugate matching of impedances is obtained through controlled wave interference between two sets of reflected waves combining in the matching network, *regardless of the type of matching device being used.* For further explanation of how the matching is performed by wave interference, a detailed discussion of the subject is presented in Chapters 4 and 23.

Sec 24.5 The Effects of Line Attenuation

In real transmission lines having attenuation, all power entering the line is absorbed in the load, except for that dissipated as heat and lost due to line attenuation. When the matching is performed at the line input, the loss from line attenuation increases as the Z_0 load mismatch increases. This happens because in addition to the attenuation of the forward power, the reflected power is also attenuated in the same proportion on its return to the source.

Should this concern us as amateurs? Probably not, if we are using a typical antenna system at HF. When the matched-line attenuation is low, as it is in typical amateur installations, the additional loss because of Z_0 mismatch is small, as explained in Chapters 1 and 6. The additional losses are so low that even with moderate to high SWR values, the difference in power radiated compared to that with a 1:1 SWR is too small to be discerned by the receiving station. The additional power lost versus SWR may be determined from Figs 1-1 or 6-1, or may be calculated using Eq 6-1. The additional power may also be determined by following the procedure outlined in Appendix 8, and by hand calculator using a program designed for it appearing in Appendix 8A.

Sec 24.6 Delivery of Power to a Mismatched Load

The amount of forward power flowing on a lossless transmission line and delivered to a mis-

matched load termination is determined by the expression:

$$P_{fwd} = \frac{1}{1 - \rho^2} \times P \qquad \text{(Eq 24-1)}$$

where

ρ = voltage coefficient of reflection
ρ^2 = power coefficient of reflection
P = power delivered by the source
P_{fwd} = forward power in the line

On a real line with attenuation, forward power at the conjugate matching point in the matching device is the source power multiplied by the expression:

$$P_{fwd} = \frac{1}{1 - \rho^2 e^{-4\alpha}} \times P \qquad \text{(Eq 24-2)}$$

where

α = line attenuation in nepers = dB/8.6859
e = 2.71828 . . ., the base of natural logarithms

The power arriving at the mismatched load with attenuation in the line is the source power multiplied by the expression:

$$\frac{e^{-2\alpha}}{1 - \rho^2 e^{-4\alpha}} \qquad \text{(Eq 24-3)}$$

The decimal value of the power reflected at the mismatched load is

$$\frac{\rho^2 e^{-2\alpha}}{1 - \rho^2 e^{-4\alpha}} \qquad \text{(Eq 24-4)}$$

and the decimal value of the power absorbed in the load is

$$\frac{(1 - \rho^2) e^{-2\alpha}}{1 - \rho^2 e^{-4\alpha}} \qquad \text{(Eq 24-5)}$$

See Eqs 6-1 and 6-2, in Chapter 6, and see Appendix 5 for their derivation.

Sec 24.7 The Conjugate Match—Is it Real, only Theoretical, or is it a Myth?

Along with the myth that no conjugate match can exist when the source of power is an RF power amplifier, another myth concerning the conjugate match has re-emerged. This myth has it that the conjugate match exists only in theory, because the assertion is that it can occur only in a lossless environment that doesn't exist. The claim is that any resistive loss in a circuit containing real reactive elements introduces additional reactances that destroy the true conjugate match. This is true to a point, but it is only the beginning of the story.

To appreciate what's really happening we'll first examine a lossless network and proceed from there. When a network comprised of lossless reactive elements connecting a source to a load is tuned to resonance, a conjugate match exists everywhere in the network—at the input and output terminals, and in both directions, forward and reverse. Figs 24-1 and 24-2 are Mathcad worksheets that illustrate these conditions in a CLC pi-network. (Figs 24-1 through 24-9 appear at the end of this chapter.) Fig 24-1 shows the input resistance of the network is 2000 + *j*0 ohms when the load terminating the network is 50 + *j*0 ohms, and Fig 24-2 shows the input resistance is 50 + *j*0 ohms when the load terminating the opposite end of the network is 2000 + *j*0 ohms. Now let's replace the lossless elements with real elements, but with the reactance values of elements, X_A, X_B, and X_C remaining unchanged. This condition is illustrated in Fig 24-3, where loss resistances R_A, R_B, and R_C in the elements result from a capacitor Q of 1000 (both capacitors) and an inductor Q of 200. In this case the loss resistances have detuned the network away from resonance. With the 50-ohm load, the input impedance is now reactive, having changed from 2000 + *j*0 ohms to 1889.6 – *j*21.958 ohms; the perfect, academic conjugate match has been destroyed, resulting in a conjugate mismatch. Unfortunately, this is where the myth originated, because not knowledgeable of the practical aspects of conjugate-matching principles have assumed incorrectly that the story ends here, without attempting to learn that both resonance and the conjugate match are restored simply by making small adjustments to the element reactances.

Consequently, let's assume the real network with resistive losses we just created is on our test bench. Reactive elements X_A, X_B, and X_C shown in the diagram of the pi-network in the figures all are adjustable. By adjusting these reactances individually to compensate for the reactances introduced by their loss resistances, we can return (tune) the network to resonance, thus eliminating the reactances appearing at the input of the network, and returning

the conjugate match that was initially destroyed by the losses in the individual elements. This procedure, called "tuning to resonance," is what we do when we tune our transmitter for delivery of the available power into its load. This condition is illustrated in Fig 24-5, where we see that the input impedance is now 2000 ohms with only an insignificant amount of reactance. Further adjustment of the reactances (arithmetical manipulation in the Mathcad calculations) would reduce the reactance to zero.

However, we must be careful to understand that during the conditions described above, although the conjugate match exists everywhere in the real network, it exists in only one direction—forward. To appreciate what is occurring here, let's return the reactances to the original values that appeared before retuning. If we remove the 50-ohm load and place a new load of 2000 + *j*0 ohms at the terminals at the left-hand end of the network, and look at the input impedance appearing at the terminals at the right-hand end of the network, we have reversed the direction of power flow. Again, with the original reactance values of the lossless elements unchanged, the input impedance is now 49.82903 – *j*2.88367 ohms, as shown in Fig 24-4. But a new readjustment (retuning) of the reactances of the network elements again brings the network into resonance with the input impedance 50 + *j*0.000007412, and the conjugate match again exists everywhere in the network, but in the reverse direction, as shown in Fig 24-6.

Pi-Network Analysis

CLC Pi-network Analysis with Lossless Elements

To match between impedances Z = 2000 ohms and Z = 50 ohms

Forward Direction, network terminated in 50 ohms

Tuning 130° pi-network to resonance. Zin = 2000 ohms, Zload = 50 ohms. Initial network parameters at resonance with lossless elements: Xa = - 219.89571936 ohms, Xb = 242.24452283 ohms, Xc = - 47.82388655 ohms

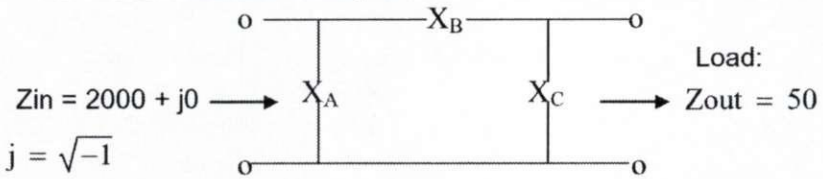

$j = \sqrt{-1}$

$Xa = -j \cdot 219.89571936$ $\quad Xb = j \cdot 242.24452283$ $\quad Xc = -j \cdot 47.82388655$

$Za = Xa$ $\quad Zb = Xb$ $\quad Zc = Xc$

$$Z1 = \frac{1}{\frac{1}{Zout} + \frac{1}{Zc}}$$

$Za = -219.89571936j$

$Zb = 242.24452283j$

$Zc = -47.82388655j$

$Z1 = 23.88828935 - 24.97526976j$

$Z2 = Z1 + Zb$

$Z2 = 23.88828935 + 217.26925307j$

$$Zin = \frac{1}{\frac{1}{Z2} + \frac{1}{Za}}$$

$Zin = 2 \times 10^3$

With lossless elements Zin is a purely resistive 2000 + j0 ohms when the network is resonant.

Fig 24-1.

It is now time to examine the effect of the apparent "conjugate mismatch" that occurs without retuning to obtain the perfect conjugate mismatch. The inductor in the network we're examining has a Q = 200, which is realistic for both the output tank circuit of the tube-type RF power amplifier and the inductance in an antenna tuner. The Q of the capacitors is 1000, which for practical applications their loss resistance can be neglected. Except for the slight mistuning of the amplifier output circuit that remains without retuning, we note that the conjugate mismatch is only 1.0596:1 in the forward direction and only 1.0594:1 in the reverse direction. Although the resistive loss in the network with Q = 200 is 0.2228 dB, the loss due to the conjugate mismatches is only 0.0036 dB—a loss so small that is practically immeasurable, and therefore insignificant. We have a practical conjugate match.

Let's take the network examination one step further. Let's return to the condition where the network is tuned in the forward direction and then we reverse the direction without changing the reactance values of the elements. In Fig 24-7 we observe that with a 2000-ohm load the input impedance is 49.14 – *j*5.844 ohms, compared to 49.829 – *j*2.8837 ohms, as shown in Fig 24-4 when going in the forward direction with the same reactance values as in the lossless condition. The conjugate mismatch is slightly greater, as we would expect. However, we again have a practical working conjugate match.

CLC Pi-network Analysis with Lossless Elements

To match between impedances Z = 2000 ohms and Z = 50 ohms

Reverse Direction, network terminated in 2000 ohms

Tuning 130° pi-network to resonance. Zin = 2000 ohms, Zload = 50 ohms. Initial network parameters at resonance with lossless elements: Xa = - 219.89571936 ohms, Xb = 242.24452283 ohms, Xc = - 47.82388655 ohms

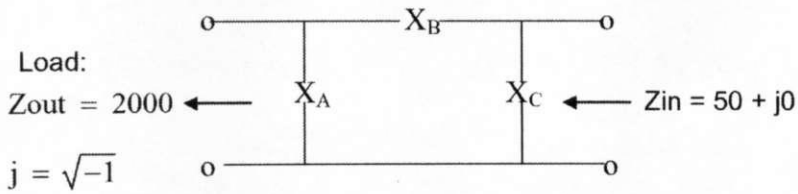

Xa = −j·219.89571936 Xb = j·242.24452283 Xc = −j·47.82388655

Za = Xa Zb = Xb Zc = Xc

$$Z1 = \frac{1}{\frac{1}{Zout} + \frac{1}{Za}}$$

Za = −219.89571936j

Zb = 242.24452283j

Zc = −47.82388655j

Z1 = 23.88828935 − 217.26925307j

Z2 = Z1 + Zb

Z2 = 23.88828935 + 24.97526976j

$$Zin = \frac{1}{\frac{1}{Z2} + \frac{1}{Zc}}$$

Zin = 50

With lossless elements Zin is a purely resistive 50 + j0 ohms when the network is resonant.

Fig 24-2.

Now let's reverse the above conditions: The network is tuned in the reverse direction and then we reverse the direction to forward, again without changing the reactance values of the elements. In Fig 24-8 we observe that with a 50-ohm load the input impedance is 1799 – *j*40.359 ohms, compared to 1889.6 – *j*21.958 ohms, as shown in Fig 24-3 when going in the reverse direction with the same reactance values as in the lossless condition. Again, as expected, the conjugate mismatch is slightly greater, but we still have a practical working conjugate match.

However, to learn how little these small values of conjugate mismatch affect the transfer of power

CLC Pi-network Analysis with Real Elements, Untuned

To match between impedances Z = 2000 ohms and Z = 50 ohms

Capacitor Q = 1000, Inductor Q = 200

Forward Direction, Network Terminated in 50 ohms

Reactance values unchanged from those during calculations with lossless elements

Tuning 130° pi-network to resonance. Zin = 2000 ohms, Zload = 50 ohms. Initial network parameters at resonance with lossless elements: Xa = - 219.89571936 ohms, Xb = 242.24452283 ohms, Xc = - 47.82388655 ohms

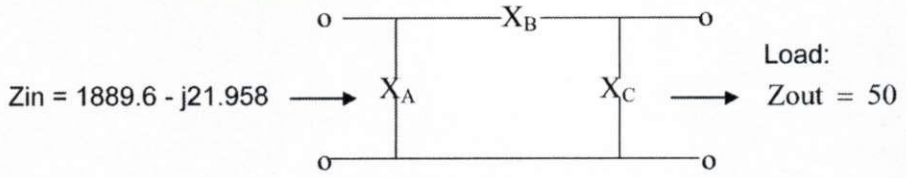

$Qc = 1000$ $\quad QL = 200$ $\quad j = \sqrt{-1}$

$Xa = -j \cdot 219.89571936$ $\quad Xb = j \cdot 242.24452283$ $\quad Xc = -j \cdot 47.82388655$

$$Ra = \frac{-Xa}{j \cdot Qc} \qquad Rb = \frac{Xb}{j \cdot QL} \qquad Rc = \frac{-Xc}{j \cdot Qc}$$

$Za = Ra + Xa$ $\quad Zb = Rb + Xb$ $\quad Zc = Rc + Xc$

$$Z1 = \frac{1}{\frac{1}{Zout} + \frac{1}{Zc}}$$

$Z1 = 23.88941 - 24.95033j$

$Z2 = Z1 + Zb$

$Z2 = 25.10063 + 217.29419j$

$$Zin = \frac{1}{\frac{1}{Z2} + \frac{1}{Za}}$$

$Zin = 1.88956 \times 10^3 - 21.95809j$

Element Loss Resistances

$Za = 0.2199 - 219.89572j$ $\quad Ra = 0.2199$

$Zb = 1.21122 + 242.24452j$ $\quad Rb = 1.21122$

$Zc = 0.04782 - 47.82389j$ $\quad Rc = 0.04782$

Note that with lossy elements, and with the reactance values of the original lossless elements left unchanged, the resistive input impedance is now somewhat less than 2000 ohms, and academically, a significant amount of capacitive reactance has been introduced by the resistive loss in the elements, indicating that a perfect conjugate match no longer exists. However, from a practical viewpoint, the conjugate mismatch is so small as to be negligible with respect to loss in delivery of power to the load, and can be ignored. Resistive loss due to Rb = 0.2228 dB.

Conjugate Mismatch SWR	Reflection Coefficient RHO (ρ)	Conjugate Power Delivered	Conjugate Mismatch Loss
1.0594	0.0288	0.9992	0.0036 dB

Fig 24-3.

compared to a perfect conjugate match, observe the values of SWR, RHO, Power Transfer, and Loss in dB shown at the bottom of Figs 24-3, 24-4, 24-7, and 24-8, with a summary in Fig 24-9. These values are indeed remarkable in proving that the principles of conjugate matching are alive and well.

Thus, from the information presented above, and after reviewing the Fig 24-9, when looking into the network *in either forward or reverse direction without retuning*, it is evident that the true conjugate match occurs only with *lossless* reactances in the network.

CLC Pi-network Analysis with Real Elements, Untuned

To match between impedances Z = 2000 ohms and Z = 50 ohms

Capacitor Q = 1000, Inductor Q = 200

Reverse Direction, Network Terminated in 2000 ohms

Reactance values unchanged from those during calculations with lossless elements

Initial network parameters at resonance with lossless elements: Xa = - 219.89571936 ohms, Xb = 242.24452283 ohms, Xc = - 47.82388655 ohms

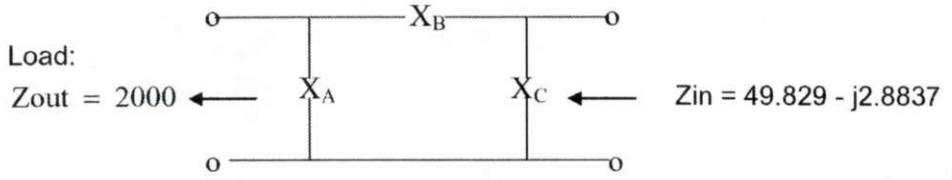

$QC = 1000$ $\quad QL = 200$ $\quad j = \sqrt{-1}$

$Xc = -j \cdot 219.89572$ $\quad Xb = j \cdot 242.244523$ $\quad Xa = -j \cdot 47.823887$

$$Ra = \frac{-Xa}{j \cdot QC} \qquad Rb = \frac{Xb}{j \cdot QL} \qquad Rc = \frac{-Xc}{j \cdot QC}$$

$Za = Ra + Xa$ $\quad Zb = Rb + Xb$ $\quad Zc = Rc + Xc$

$$Z1 = \frac{1}{\frac{1}{Zout} + \frac{1}{Zc}}$$

$Z1 = 24.10035 - 217.22206j$

$Z2 = Z1 + Zb$

$Z2 = 25.31157 + 25.02247j$

$$Zin = \frac{1}{\frac{1}{Z2} + \frac{1}{Za}}$$

$Zin = 49.82903 - 2.88367j$

$Za = 0.04782 - 47.82389j$

$Zb = 1.21122 + 242.24452j$

$Zc = 0.2199 - 219.89572j$

Element Loss Resistances

$Ra = 0.04782$

$Rb = 1.21122$

$Rc = 0.2199$

Note that with lossy elements, and with the reactance values of the original lossless elements left unchanged, the resistive input impedance is now somewhat less than 50 ohms, and academically, a significant amount of capacitive reactance has been introduced by the resistive loss in the elements, indicating that a perfect conjugate match no longer exists. However, from a practical viewpoint, the conjugate mismatch is so small as to be negligible with respect to loss in delivery of power to the load, and can be ignored. Loss due to Rb = 0.2228 dB.

Conjugate Mismatch SWR	Reflection Coefficient RHO	Conjugate Power Delivered	Conjugate Mismatch Loss
1.0596	0.0289	0.9992	0.0036 dB

Fig 24-4.

However, when we put these principles in perspective with respect to actual operation, we see that when the values of the real reactances are adjusted to compensate for the inherent resistances in the inductors and capacitors, such that all the available power is delivered to the load in the forward direction, there is a true conjugate match to the load. (This is true whether the load is purely resistive or reactive.) The match results because with the reactances adjusted as described above, the source impedance appearing at the output of the network is the conjugate of the load impedance. There is also a true conjugate match in the forward direction at any other junction in the system. If this condition did not occur, all of the available power would not be delivered.

Conversely, it is also true that if this same network is now operated with the source and load reversed (power now flowing in the opposite direction), a true conjugate match does *not* occur

CLC Pi-network Analysis with Real Elements, Retuned

Capacitor Q = 1000, Inductor Q = 200

To match between impedances Z = 2000 ohms and Z = 50 ohms

Forward Direction, Network Terminated in 50 ohms

Reactances retuned to resonance after inserting real elements

Tuning 130° pi-network to resonance. Zin = 2000 ohms, Zload = 50 ohms. Initial network parameters at resonance with lossless elements: Xa = - 219.89571936 ohms, Xb = 242.24452283 ohms, Xc = - 47.82388655 ohms

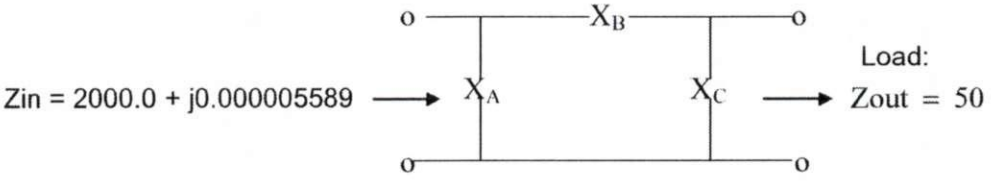

$QC = 1000$ $\quad QL = 200$ $\quad j = \sqrt{-1}$

$Xa = -j \cdot 219.9787443$ $\quad Xb = j \cdot 242.24453156$ $\quad Xc = -j \cdot 45.1905$

$$Ra = \frac{-Xa}{j \cdot QC} \qquad Rb = \frac{Xb}{j \cdot QL} \qquad Rc = \frac{-Xc}{j \cdot QC}$$

$Za = Ra + Xa$ $\quad Zb = Rb + Xb$ $\quad Zc = Rc + Xc$

$$Z1 = \frac{1}{\frac{1}{Zout} + \frac{1}{Zc}}$$

Element Loss Resistances

$Za = 0.21998 - 219.97874j$ $\quad Ra = 0.21998$

$Z1 = 22.4827 - 24.84795j$ $\quad Zb = 1.21122 + 242.24453j$ $\quad Rb = 1.21122$

$Z2 = Z1 + Zb$ $\quad Zc = 0.04519 - 45.1905j$ $\quad Rc = 0.04519$

$Z2 = 23.69392 + 217.39658j$

$$Zin = \frac{1}{\frac{1}{Z2} + \frac{1}{Za}}$$

$Zin = 2 \times 10^{3} + 5.58927j \times 10^{-6}$

Note that readjustments to the reactance values of each element from those of the lossless case compensate for the reactances introduced by the loss resistance appearing in the real elements, returning (retuning) the network to resonance. As a result, a conjugate match has been re-established in the forward direction. Resistive loss due to Rb = 0.2228 dB.

Fig 24-5.

without retuning. This condition occurs because when the flow of power is in the opposite direction *without retuning the network reactances for the opposite direction,* one sees a network input impedance where what was formerly the network output that is slightly different than the source impedance seen at the network output when the power flow was in the forward direction. However, if the network reactances are retuned to permit all the available power to be delivered in the reverse direction, a conjugate match is again achieved.

In summary, we have thus demolished the myth that the conjugate match can exist only in theory, and therefore has no place in real, practical operation. Let it rest in peace.

CLC Pi-network Analysis with Real Elements

Capacitor Q = 1000, Inductor Q = 200

To match between impedances Z = 2000 ohms and Z = 50 ohms

Reverse Direction, Network Terminated in 2000 ohms

Reactances retuned to resonance after inserting real elements

Initial network parameters at resonance with lossless elements: Xa = - 219.89571936 ohms, Xb = 242.24452283 ohms, Xc = - 47.82388655 ohms

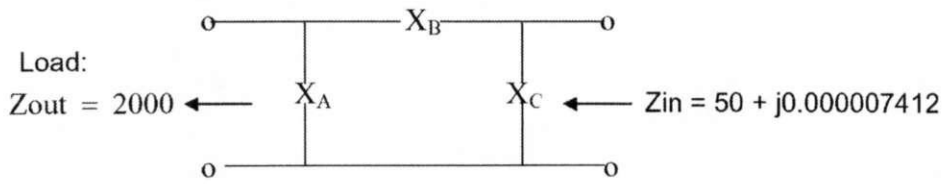

$QC = 1000$ $\quad QL = 200$ $\quad j = \sqrt{-1}$

$Xa = -j \cdot 228.6958996$ $\quad Xb = j \cdot 250.613483$ $\quad Xc = -j \cdot 54.7973$

$$Ra = \frac{-Xa}{j \cdot QC} \qquad Rb = \frac{Xb}{j \cdot QL} \qquad Rc = \frac{-Xc}{j \cdot QC}$$

$Za = Ra + Xa$ $\quad Zb = Rb + Xb$ $\quad Zc = Rc + Xc$

$$Z1 = \frac{1}{\frac{1}{Zout} + \frac{1}{Za}}$$

$Z1 = 26.03328 - 225.69324j$

$Z2 = Z1 + Zb$

$Z2 = 27.28635 + 24.92024j$

$$Zin = \frac{1}{\frac{1}{Z2} + \frac{1}{Zc}}$$

$Zin = 50 + 7.4119j \times 10^{-6}$

$Za = 0.2287 - 228.6959j$

$Zb = 1.25307 + 250.61348j$

$Zc = 0.0548 - 54.7973j$

Element Loss Resistances

Ra = 0.2287

Rb = 1.25307

Rc = 0.0548

Note that readjustments to the reactance values of each element from those of the lossless case compensate for the reactances introduced by the loss resistance appearing in the real elements, returning (retuning) the network to resonance. As a result, a conjugate match has been re-established in the reverse direction. Loss due to Rb = 0.2228 dB.

Fig 24-6.

CLC Pi-network Analysis with Real Elements

To match between impedances Z = 2000 ohms and Z = 50 ohms

Capacitor Q = 1000, Inductor Q = 200

Tuned in Forward Direction, Network terminated in 50 ohms, then ReCalculated in Reverse Direction Terminated in 2000 ohms

Initial network parameters at resonance with lossless elements: Xa = - 219.89571936 ohms, Xb = 242.24452283 ohms, Xc = - 47.82388655 ohms

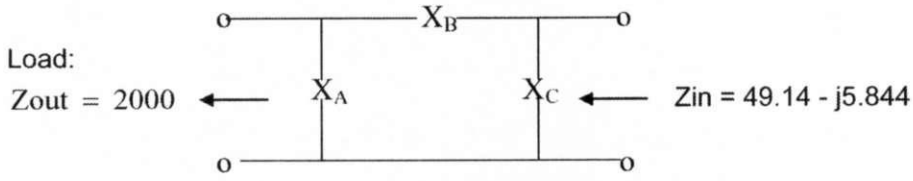

$QC = 1000$ $\quad QL = 200$ $\quad j = \sqrt{-1}$

$Xa = -j \cdot 219.979330045$ $\quad Xb = j \cdot 242.244503$ $\quad Xc = -j \cdot 45.2$

$$Ra = \frac{-Xa}{j \cdot QC} \qquad Rb = \frac{Xb}{j \cdot QL} \qquad Rc = \frac{-Xc}{j \cdot QC}$$

$Za = Ra + Xa$ $\quad Zb = Rb + Xb$ $\quad Zc = Rc + Xc$

$$Z1 = \frac{1}{\frac{1}{Zout} + \frac{1}{Za}}$$

$Z1 = 24.11837 - 217.30266j$

$Z2 = Z1 + Zb$

$Z2 = 25.3296 + 24.94185j$

$$Zin = \frac{1}{\frac{1}{Z2} + \frac{1}{Zc}}$$

$Zin = 49.13959 - 5.8441j$

Element Loss Resistances

$Za = 0.21998 - 219.97933j$	$Ra = 0.21998$
$Zb = 1.21122 + 242.2445j$	$Rb = 1.21122$
$Zc = 0.0452 - 45.2j$	$Rc = 0.0452$

Network first tuned to resonance in forward direction, and then calculated to show amount of conjugate mismatch when going in reverse direction without retuning. Mismatch loss increased to 0.0154 dB from 0.0036 dB when going in reverse direction with reactance values of lossy elements unchanged from being tuned to resonance in forward direction. Total loss, combination of mismatch and resistive losses = 0.2382 dB

Conjugate Mismatch SWR	Reflection Coefficient RHO (ρ)	Conjugate Power Delivered	Conjugate Mismatch Loss
1.1265	0.059	0.9965	0.0154 dB

Fig 24-7.

CLC Pi-network Analysis with Real Elements

Capacitor Q = 1000, Inductor Q = 200

To match between impedances Z = 2000 ohms and Z = 50 ohms

Tuned in Reverse Direction, Network Terminated in 2000 ohms, then ReCalculated in Forward Direction Terminated in 50 ohms.

Initial network parameters at resonance with lossless elements: Xa = - 219.89571936 ohms, Xb = 242.24452283 ohms, Xc = - 47.82388655 ohms

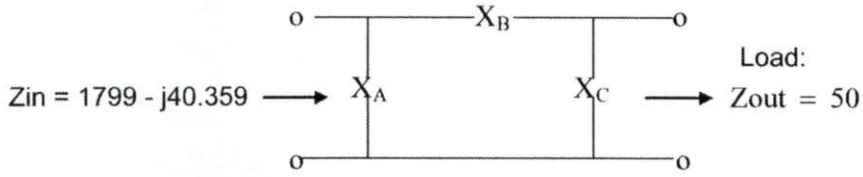

$QC = 1000$ $\quad QL = 200$ $\quad j = \sqrt{-1}$

$Xa = -j \cdot 228.6959$ $\quad Xb = j \cdot 250.61345$ $\quad Xc = -j \cdot 54.7973$

$$Ra = \frac{-Xa}{j \cdot QC} \qquad Rb = \frac{Xb}{j \cdot QL} \qquad Rc = \frac{-Xc}{j \cdot QC}$$

$Za = Ra + Xa$ $\quad Zb = Rb + Xb$ $\quad Zc = Rc + Xc$

$$Z1 = \frac{1}{\frac{1}{Zout} + \frac{1}{Zc}}$$

$Z1 = 27.2818 - 24.87066j$

$Z2 = Z1 + Zb$

$Z2 = 28.53487 + 225.74279j$

$$Zin = \frac{1}{\frac{1}{Z2} + \frac{1}{Za}}$$

$Zin = 1.79923 \times 10^3 - 40.35882j$

$Za = 0.2287 - 228.6959j$

$Zb = 1.25307 + 250.61345j$

$Zc = 0.0548 - 54.7973j$

Element Loss Resistances

$Ra = 0.2287$

$Rb = 1.25307$

$Rc = 0.0548$

Network first tuned to resonance in reverse direction, and then calculated to show amount of conjugate mismatch when going in fprward direction without retuning. Mismatch loss increased to 0.0127 dB from 0.0036 dB when going in reverse direction with reactance values of lossy elements unchanged from being tuned to resonance in forward direction. Loss due to resistive loss Rb = 0.2228 dB. Total loss, combination of mismatch and resistive losses = 0.2355 dB

Conjugate Mismatch SWR	Reflection Coefficient RHO (ρ)	Conjugate Power Delivered	Conjugate Mismatch Loss
1.1141	0.0540	0.9971	0.0127 dB

Fig 24-8.

Fig 24-9.

Comparison of Lossless vs Real Elements and Forward vs Reverse Directions in Pi-Networks

(CLC) Capacitor Q = 1000, Inductor Q = 200, Phase Delay 130 Degrees

Pi-network with Lossless Elements
Forward Direction, 50-Ohm Load
Zin = 2000 + j0.0000357787 (Fig 24-1)

Pi-network with Real Elements, Untuned
Forward Direction, 50-Ohm Load
Reactance values unchanged (Fig 24-3)
Zin = 1889.6 - j21.958
SWR = 1.0594, 0.0036 dB Conjugate Mismatch Loss

Pi-network, Real Elements, Retuned
Forward Direction, 50-Ohm Load
Reactances retuned to resonance (Fig 24-5)
Zin = 2000.0 + j0.000005589

Pi-network, Real Elements
Tuned in Reverse Direction with 2000-ohm Load, then ReCalculated in Forward Direction with 50-ohm Load
Zin = 1799 - j40.359 (Fig 24-7)
SWR = 1.1141, 0.0127 dB Conjugate Mismatch Loss

Pi-network with Lossless Elements
Reverse Direction, 2000-ohm Load
Zin = 50 + j0.0000002428 (Fig 24-2)

Pi-network with Real Elements, Untuned
Reverse Direction, 2000-ohm Load
Reactance values unchanged (Fig 24-4)
Zin = 49.829 - j2.8837
SWR = 1.0596, 0.0036 dB Conjugate Mismatch Loss

Pi-network, Real Elements, Retuned
Reverse Direction, 2000-ohm Load
Reactances retuned to resonance (Fig 24-6)
Zin = 50 + j0.000002021

Pi-network, Real Elements
Tuned in Forward Direction with 50-ohm Load, then ReCalculated in Reverse Direction with 2000-ohm Load
Zin = 49.14 - j5.844 (Fig 24-8)
SWR = 1.1265, 0.0154 dB Conjugate Mismatch Loss

Chapter 25

Dispelling New Misconceptions Concerning Wave Interference in Impedance Matching

(Adapted and revised from QEX, *July/August 2004)*

Sec 25.1 Background and Introduction

The first seven chapters of this book were written to dispel various myths and misconceptions that were prevalent at the time they were originally published in my 1970's series of *QST* articles, "Another Look at Reflections." However, new misconceptions have appeared recently that need to be proven wrong and corrected.

In a three-part article appearing in *QEX* (*Ref 148*) Dr. Steven Best, VE9SRB, wrote about the wave mechanics involved in impedance matching. In that article, he disputes the treatment of wave mechanics appearing in the writings of Slater (*Ref 35*) and Alford (*Ref 39*), in all editions of *Reflections* (*Refs 149, 150, 151, 152*) and my article in *QEX* (*Ref 153*). By his own statements, Steve's express purpose for publishing his article was an attempt to prove the explanation of impedance matching appearing in *Reflections* is wrong. Unfortunately, his concept of the wave mechanics occurring at the matching point in an impedance-matching device is flawed, and the results are incorrect and misleading. Therefore, this chapter was written to prove his statements and contradictions wrong.

Most of the errors in Steve's article are due to his misunderstanding of the concepts, and others follow from an invalid premise revealed in his Eqs 6, 7, and 8 of his Part 1 that precipitated a domino effect on additional misconceptions throughout the article. All three of these equations are invalid because of a misinterpretation of the universally known equations for determining the amplitude of voltage E of the standing wave as the equations for determining forward voltage V_{FWD}. These two separate voltage values, voltage E of the standing wave and forward voltage V_{FWD}, resulting from these three equations differ significantly. As we know, the amplitude of the voltage standing wave is the phasor sum of the forward and reflected voltages, which varies alternately between maximum and minimum with varying distance along the line. However, on lossless lines, the amplitude of forward voltage V_{FWD} is *constant* throughout the entire length of the line. The forward voltage can be determined using the correct expression $V_{FWD} = \sqrt{P_{FWD} \times Z_0}$ where P_{FWD} is the total forward *power*, and Z_0 is the characteristic impedance of the line. That expression is proven correct through the following mathematical exercise:

$$\text{Forward Current } I_{FWD} = \sqrt{\frac{P_{FWD}}{Z_0}}$$

$$\text{and } V_{FWD} \times I_{FWD} = P_{FWD}$$

A numerical example presented later verifies it. In addition, contrary to Steve's assertion, P_{FWD} equals the sum of the source and reflected *powers*, not the voltages, which will also be proved later. The derivation of the familiar equations for determining standing-wave voltages E along the line that Steve misinterpreted to obtain his Eqs 6, 7, and 8 can be found in Johnson (*Ref 18 Sec 4.3, pp 98 and 99*). Steve's Eq 6 is a misquote of Johnson's Eq 4.23 appearing on page 100.

Steve's Eq 6 in Part 1, the expression shown below for forward voltage V_{FWD}, is invalid due to the misquote, because the left-hand term of the equation V_{FWD} does not equal the sum of the terms on the right-hand side of the equation. The left-hand term in Johnson's Eq 4.23 that Steve misquoted is "E," not "V_{FWD}."

$$V_{FWD} = V1 + V1\,(\rho_S\rho_A e^{-2\gamma L}) + V1(\rho_S{}^2\rho^2{}_A e^{-4\gamma L}) + V1(\rho_S{}^3\rho^3{}_A e^{-6\gamma L}) + \ldots \qquad \text{Steve's Eq 6}$$

The terms on the right-hand side of the Eq 6 yield the voltage E of the standing wave, not the forward voltage V_{FWD} as shown. His Eqs 7 and 8 are also invalid for the same reason. So let's demonstrate that his Eq 8 is invalid, which will also prove Eqs 6 and 7 invalid.

$$V_{FWD} = V1\left(\frac{1}{1 - \rho_S\rho_A e^{-2\gamma L}}\right) \qquad \text{Steve's Eq 8}$$

where:

V1 = source voltage

S = reflection coefficient looking back into the source

A = voltage reflection coefficient of load (antenna) mismatch

First, using a lossless line, we let S = 1, and A = 1, representing total reflection at both ends of the transmission line. In this case the denominator is zero, thus $V_{FWD} = \infty$, which is an impossibility. Second, we let $\rho s = 1$ remain as total re-reflection at the source, but change ρ_A to 0.5 resulting from a 3:1 mismatch at the antenna. In this case the denominator is 0.5 and $V_{FWD} = V1 \times 2$, which is also impossible. We will show later that when the load reflection coefficient $\rho_A = 0.5$, the forward voltage increase factor caused by the integrated reflections added to the source voltage is 1.1547. Therefore, the forward voltage in this case is $V_{FWD} = V1 \times 1.1547$. Consequently, we have shown that Steve's Eqs 6, 7, and 8 do not yield the correct forward voltage V_{FWD}, as claimed; they only yield the standing-wave voltage E, where L in the exponents of his Eqs 6 and 8 specifies the position on the line.

As we'll also prove later, forward current I_{FWD} equals source current I1 × 1.1547. Thus, since forward power $P_{FWD} = V_{FWD} \times I_{FWD}$, the power increase factor is $1.1547^2 = 1.3333$ when $\rho_A = 0.5$ which is a well-known result. The derivations of the voltage, current, and power increase factors, which prove this treatment to be true, will also be presented.

Sec 25.2 VE9SRB's Fallacy

At the opening of his Part 3, Steve calls total re-reflection a fallacy. He states: "... it is a misconception that total re-reflection of reflected power occurs at a match point as the result of an impedance match being established there."

Then, after attempting to prove total re-reflection doesn't exist, he concludes, "... the concept of total re-reflection is inconsistent with generally accepted transmission line theory, basic circuit theory, and network theory." Then from his summary, "It was demonstrated that the concept of total power re-reflection is inconsistent with both transmission line and circuit theories."

On the contrary, his mathematical treatment did not demonstrate any inconsistency in the concept of total re-reflection. Also, an additional claim in his conclusion is also untrue: "A total re-reflection of power at the match point is not necessary for the impedance match to occur." His conclusion is untrue, because, as we will show, without total re-reflection the impedance match would not be accomplished. Furthermore, Steve has it backward: the impedance match *results* from total re-reflection, not the other way around.

To show that total re-reflection is not a fallacy, let's first examine the implications of his Eq 2, Part 3:

$$P_{FWD} = P_{DEL} = \frac{1}{1 - k^2|\rho_A|^2}$$

which he states, "... develops the relationship between delivered and forward power." He continues, writing: "Eq 2 is independent of whether an impedance match occurs at the T-network input.... Eq 2 does not support the concept of total re-reflection of power when an impedance match is established at the T-network input."

Of course it doesn't, because a vital term is missing in his Eq 2: the reflection term ρs, which determines the reflective condition seen by the reflected waves on return to the network input, and thus determines the amount of energy in the reflected waves will be re-reflected. Consequently, with term ρs missing, both the amount of re-reflection and the increase in forward power are undeterminable using his Eq 2. However, the complete *correct* equation:

$$P_{FWD} = \frac{1}{1 - k^2|\rho s\rho_A|^2}$$

derives the forward-power increase factor based on the reflection coefficients at *both* ends of a transmission system, not just at the load end. The term k^2 represents the decimal value of power lost to line attenuation, the term ρ_A represents the reflectivity of the load, or antenna mismatch, and the term ρs represents the reflectivity to the power in the reflected waves on their return to either the network input or the source. When $\rho s = 0$, the reflected power is totally absorbed in the source, thus *no* re-reflection and *no* increase in forward power, as in the classical generator. On the other hand, when $\rho s = 1$, which is the prevalent condition at both the network input and at the source when adjusted to deliver all the available power, there is *total* re-reflection and maximum increase in forward power, indicating an impedance match at the input. *Without total re-reflection there would be no match.* This issue appears to be the crux of the problem concerning total re-reflection: the wave activity that occurs at the network input, the matching point in the network. How the reflective condition $\rho s = 1$ to reflected waves is established at the network input will be explained later while discussing the establishment of open and short circuits by wave interference.

Steve created another misconception: that the forward traveling source and re-reflected voltage waves are vectorial in nature. He asserts, "The forward traveling voltage in the transmission line is a complex phasor that can be written in the general form of a vector $V = x + jy = V\angle\theta$." Thus, citing his Eq 9, Part 3:

$$P_F = \frac{|V_1 + V_2|^2}{Z_0}$$

he asserts incorrectly that phasors V_1 and V_2 are added vectorially to obtain the forward power in a mismatched transmission line, where P_F = forward power, and V_1 and V_2 are the phasors of the source and re-reflected voltages, respectively.

Steve's Eq. 9 is an invalid expression for use on a line with re-reflections for two reasons: (1) because for superposition of V_1 and V_2 to be valid, as used in his Eq 9, the voltages must be delivered by two separate sources, not the single source of the transceiver (reflections due to a mismatched line are not delivered by a second source), and (2) because on a lossless line the phase angles for both V_1 and V_2 are $\theta = 0°$ everywhere on the line when the re-reflections result from matching at the input of the line. Keep in mind that on a lossless line, voltage and current in the forward wave are always *in phase,* while voltage and current in the reflected wave are always 180° *out of phase.* Consequently, reflected power is real, not reactive power. To be reactive, the phase relation between voltage and current would need to be other than 0° or 180°. As will be explained in the section discussing open and short circuits established by wave interference, the wave action on re-reflection brings *all* re-reflected voltages and currents into zero phase relative to the source waves, regardless of their phase relationship prior to re-reflection. Consequently, Steve's lengthy dissertation on the different values of forward power that could result from various θ angles of V_1 and V_2, and Eq 9 itself, is irrelevant. As stated above, *Voltages V_1 and V_2 are never at other than 0° phase relative to the source phase at any time on lossless lines when matched at the input of the line.* Although V_2 is the resultant of two reflected waves whose magnitudes are equal, with equal but opposite phase angles, phase angle θ of the *re-reflected* resultant voltage V_2 following re-reflection is always zero on lossless lines.

As mentioned earlier, Steve failed to recognize that the addition of the source and reflected voltages establishes the *standing wave,* not the forward voltage V_{FWD}, which has a *constant* value everywhere along the line. So let's examine what happens when we perform this addition using his Eq 9.

Steve's Fig 1, Part 3 shows a 100-watt, 50-ohm source feeding a T-network connected to an antenna of impedance $Z_A = 150$ ohms through a lossless 50-ohm, 1 wavelength transmission line. Quoting from his example, source voltage $V_1 = 70.71$ V; forward power incident on the antenna, $P_{FWD} = 133.33$ W; and power reflected $P_{REF} = 33.33$ W. For $P_{FWD} = 133.33$ W, the total forward voltage V_{FWD} must be 81.65 V, and with reflection coefficient $\rho_A = 0.5$, reflected voltage $V_2 = 40.825$ V. In addition, the source current is $I_1 = 1.414$ A, total forward current $I_{FWD} = 1.633$ A, and reflected current $I_{REF} = 0.8165$ A. Each of these values is correct as stated in his article; the article also states correctly that the re-reflected voltage must equal the reflected voltage.

However, Eq 9 is invalid because it states *incorrectly* that re-reflected voltage V_2 adds directly to

source voltage V_1 to establish forward power; *it does not,* as we will prove. Steve does state correctly that the in-phase 40.825 V re-reflected voltage V_2 and 70.71 V source voltage V_1 cannot be added together such that the total voltage will be 81.65 V. This should have been a clue that source and reflected voltages add only to establish the voltage *standing wave, not forward voltage* V_{FWD}, because $V_{FWD} \times I_{FWD} = 133.33$ W. We prove his Eq 9 for forward power, P_{FWD} erroneous by showing that his:

$$P_{FWD} = \frac{(V_1 + V_2)^2}{Z_0} = \frac{(70.71 + 40.825)^2}{50} = 248.8 \text{ W}$$

not the correct 133.33 W

However, as stated earlier, Eq 9 is valid when there are *two separate and independent sources,* such as two generators. And it must also be kept in mind that the power in the reflected waves is delivered by only *one* source, the transceiver. Apparently, this anomaly, and believing incorrectly that the relationship between forward and reflected voltages is vectorial, are what led to the erroneous concept of a vectorial relationship between the forward and *re-reflected* voltages.

Recall that Steve asserts emphatically that forward power is not established by adding reflected power to the source power. However, contrary to Steve's incorrect assertion we'll now reveal the correct mathematical expression for obtaining forward power from V_1 and V_2 that proves source and reflected powers do indeed add to establish the total forward power. The universally known reciprocally related equations for determining either forward power P_{FWD} or delivered power P_{DEL} in a mismatched transmission line are:

$$P_{FWD} = \frac{|V_1|^2 + |V_2|^2}{50} = \frac{|70.71|^2 + |40.825|^2}{50} = 133.33$$

where:
V_1 = source voltage
V_2 = reflected voltage
V_{FWD} = forward voltage

The terms in the numerators are power terms; thus either of the two equations above indicates that forward power equals source power plus reflected power. Steve disagrees that forward power equals source power *plus* reflected power, so it's ironic that he somehow agrees that power delivered to the load is equal to the forward power *minus* the reflected power. See *Reflections,* Chapter 3, Eq 3-9, and Johnson (*Ref 18 p 150, Eqs 6.14 through 6.17*) for the derivation of those equations. To verify that the correct forward power is 133.33 watts, we'll now use an alternate method to determine that value. Using the standard equation for calculating the forward-power increase factor from the earlier example:

$$\frac{1}{1 - |\rho s \rho A|^2} = 1.333$$

where:
$\rho s = 1$
$\rho A = 0.5$
with source power 100 W

we have shown that the total forward power is 133.33 watts on a lossless line.

Let's now carry the math in this exercise a little further to provide additional proof that the exercise has been performed correctly. From Ohm's Law, we know that when forward power on a 50-ohm line is 133.33 W, the forward voltage must be 81.65 V and the forward current must be 1.633 A. Also from Ohm's Law, when resistance is constant in a circuit, voltage equals the square root of power. Thus we'll now take the square root of the P_{FWD} equation to establish both the forward voltage and current increase factor:

$$V_{IF} = I_{IF} = \sqrt{\frac{1}{1 - |\rho s \rho A|^2}} = \sqrt{1.333} = 1.1547$$

where, as above:
$\rho s = 1$
$\rho A = 0.5$

As before, source voltage $V_1 = 70.71$ V, and source current $I_1 = 1.414$ A. Thus, $V_1 \times V_{IF} = 70.71 \text{ V} \times 1.1547 = 81.65 \text{ V} = V_{FWD}$, the forward voltage determined earlier, and $I_1 \times I_{IF} = 1.414 \times 1.1547 = 1.633$ A, I_{FWD}, the forward current. Now, $V \times I = P$, 81.65 V × 1.633 A = 133.33 W, thus proving our case.

Note that the forward voltage V_{FWD}, 81.65 V, is an increase of only 10.94 V from the 70.71 source voltage V_1, and the forward current 1.633 A is an increase of only 0.219 A from the 1.414 A source current. However, these small increases in voltage and current represent the corresponding increase in forward power from 100 W to 133.33 W, prov-

ing that it is the reflected power adding to source power that establishes the forward power, *not the addition of the reflected voltage to source voltage.*

We can now show that the steady-state forward voltage V_{FWD} *plus* the reflected voltage V_2 establishes the maximum of the voltage standing wave (81.65 v. + 40.82 v. = 122.47 v.) and V_F *minus* V_2 establishes the minimum of the voltage standing wave (81.65 v. – 40.82 v. = 40.82 v.). Note also that the ratio of the max and min voltages of the standing wave is 122.47 ÷ 40.82 = 3.0, verifying that the values above are correct. We have thus disproved the assertion that adding source and reflected powers to establish the forward power is a fallacy.

Sec. 25.3 Virtual Open and Short Circuits Established by Wave Interference

In another quote from Part 3 of Steve's article he asserts that open and short circuits to reflected waves *cannot* be established by the wave interference involved in impedance matching. He writes, "For a total re-reflection of voltage, current, or power to occur at a T-network, transmission line theory requires that the physical or measurable impedance seen looking rearward into the matching network be a short circuit, open circuit or purely reactive. Since this generally would not be the case with a practical T-network impedance matching circuit, the concept of total power re-reflection contradicts this fundamental aspect of transmission-line theory."

That is fundamentally incorrect and also disputes Slater (*Ref 35*) and Alford (*Ref 39*). Those authors have shown that a physical short or open circuit is not what accomplishes total re-reflection of the reflected waves. Wave interference between two sets of reflected waves traveling in the same direction within a transmission line or network that are conjugately related at the matching point establish either a one-way *short* circuit or a one-way *open* circuit to the rearward-traveling reflected waves. We'll now show how two sets of reflected waves (of both voltage and current) traveling in the same direction are established in the impedance-matching process, and how they also establish the one-way short or open circuit that prohibits any further rearward travel of the reflected waves, in other words, total re-reflection at the match point.

In general, the impedance-matching process involves three harmonically-related traveling waves arriving at the match point: a forward wave delivered by the source (Wave 1), and two conjugately related rearward-traveling reflected waves (Waves 2 and 3) developed by two conjugately related physical discontinuities. Wave 2 is the wave reflected from a mismatched line termination that requires cancellation, and Wave 3 is the canceling wave reflected by the matching device at the match point, its input connection to the source line. Because of their conjugate relationship, Waves 2 and 3 are mirror images of each other.

First, with waves traveling in opposite directions on a transmission line, we know that reflected waves pass through forward waves unimpeded, and the interference between them establishes only a standing wave—no open or short circuits are established. However, when two sets of voltage and current reflected waves are traveling in the *same* direction and are conjugately related at the matching point in an impedance matching device, the interference between these two sets of reflected waves establishes either an open or short circuit at the matching point. Whether an open or short circuit is established depends on the boundary conditions of the mismatched load and the distance from the load to the matching point. When the match point at the normalized unity-resistance point using a *series* stub on the line occurs within the first quarter-wavelength from the load, an open circuit to reflected waves occurs at the match point when the resistive component R of load $Z_L > Z_0$. A short circuit to reflected waves occurs when the resistive component R of load $Z_L < Z_0$. The reasons for these phenomena will become clear as we proceed.

In learning how one-way open and short circuits are established through wave interference, it is helpful to first understand what happens to an electromagnetic field on encountering a physical open or short circuit. It is universally known that when an electromagnetic field encounters an open circuit, the electric field (or voltage wave) is totally reflected with 0° change of phase, and the magnetic field (or current wave) is totally reflected with a 180° change of phase. Conversely, when an electromagnetic field encounters a short circuit, the electric field (or voltage wave) is totally reflected with 180° change of phase, and the magnetic field

(or current wave) is totally reflected with a 0° change of phase. *It is of vital importance to the issue of total re-reflection to understand that these relationships are reciprocally related.* Consequently, when the resultant voltage and current angles established by wave interference are 0° and 180°, respectively, an open circuit to the reflected waves is established. Conversely, when the resultant voltage and current angles are established at 180° and 0°, respectively, a short circuit to the reflected waves is established. Thus, when either an open or a short circuit is established at the matching point by wave interference between the two sets of conjugately related reflected waves traveling rearward, the direction of the voltages, currents, and energies in both sets of reflected waves is reversed. That results in total re-reflection of the reflected waves.

Let us now determine why open or short circuits are developed by wave interference. From King, (*Ref 37*) we know that voltage and current traveling along the line can be represented by individual generators placed at any point along the line. Those generators are called "point generators." For the purpose of analysis, a point generator is an impedance-less EMF that can represent or replace the voltage and current on the line equal to the voltage and current actually appearing at that point on the line, without disturbing the wave action on the line.

To simulate and analyze interference between two waves of equal magnitude and opposite phase traveling in the same direction, such as the two sets of reflected waves generated by the load mismatch and the stub mismatch, we can connect together two point generators in either of two different configurations. Each generator replaces the voltage and current of each individual wave at the point of interference, the match point. In the first configuration, the two generators are connected *in phase.* Because their voltages are equal and in phase, the differential voltage is zero, resulting in no current flow. This connection is equivalent to an *open* circuit between the generators. In the second configuration, the generators are connected with their terminals reversed. Their voltages are now *in opposite phase* at the interference point and the resulting voltage is the *sum* of the voltages delivered by each generator—i.e., twice the voltage of each generator. This connection results in a *short* circuit between the two generators.

Identical wave-interference phenomena establishing a short circuit also occur in free space in the same manner as in guided-wave propagation along transmission lines. For example, when the fields emanating from two radiators in an array of antennas are of equal magnitude and 180° out of phase at a point in space, a virtual short circuit is established by destructive wave interference, resulting in a null in the radiation pattern at that point. Following Poynting's Theorem, the energy in the combined fields propagating is reversed in direction at that point; and with the constructive interference that follows, that energy adds to that in the fields propagating in the opposite direction, thus achieving gain in the that direction.

Stub matching on a mismatched transmission line provides an elegant model to illustrate the mechanism in wave interference that establishes one-way open or short circuits to reflected waves on transmission lines. When placed at the matching point on the transmission line, the stub is designed to introduce a mismatch. That produces a canceling reflection having the same magnitude as the reflection from the mismatched load terminating the line, but with the opposite phase angle. The following example illustrates this condition.

Assume a lossless line of $Z_0 = 50$ ohms terminated in a pure 150-ohm resistance, Z_L, yielding a 3:1 mismatch for a voltage reflection coefficient $\rho = 0.5$. An appropriate point to place a series stub on the line is at a normalized point of unity-resistance. When $\rho = 0.5$, the first point of unity-resistance appears at 30° rearward from the load toward the generator. The line impedance at this point is $50 - j57.7$ ohms. Traditionally, a $+j57.7$-ohm inductive reactance inserted in series with the line at this point cancels the $-j57.7$-ohm capacitive line reactance, achieving a Z_0 impedance match at this point, leaving a 1:1 flat line between the inductance and the source, and 3:1 mismatch on line between the inductance and the load. However, it makes no difference whether a series lumped inductor or a series stub, each presenting $+j57.7$ ohms, supplies the inductive canceling reactance. Either one establishes the impedance match.

However, there is more occurring here than a simple cancellation of reactances. The matching process is actually performed by the mechanics of wave interference at the matching point that gener-

ates either an open or short circuit to the reflected waves, preventing them from traveling rearward past the stub point. To examine the wave action, we focus mainly on the reflection coefficients of the reflected voltage and current waves that appear at the stub point, and to a lesser extent of those at the load, as shown below, where voltage and current coefficients are indicated by V and I, respectively. The remaining nomenclature is self-explanatory.

$\rho_{VLoad} = 0.5, \theta = 0°$
$\rho_{ILoad} = 0.5, \theta = 180°$
$\rho_{Vline\ at\ 30°} = 0.5, \theta = -60°$
$\rho_{Vstub} = 0.5, \theta = +60°$ Resultant $\angle\theta_{RV} = 0°$
$\rho_{Iline\ at\ 30°} = 0.5, \theta = +120°$
$\rho_{Istub} = 0.5, \theta = -120°$ Resultant $\angle\theta_{RI} = 180°$

Note that the magnitudes of all reflections are equal at $\rho = 0.5$. Note also that the voltage angles for the line and stub are equal but of opposite sign, as are the corresponding current angles. In addition, note that the resultant angles of the voltage and current are $\theta_{RV} = 0°$, and $\theta_{RI} = 180°$, respectively. We learned from the earlier detailed discussion above that when the magnitudes of the reflections are equal, and the resultant voltage and current angles established by wave interference are 0° and 180°, respectively, as they are in this case, an open circuit to the reflected waves is established. Consequently, the open circuit prevents any further rearward wave travel beyond the matching point—*total re-reflection*—resulting in a Z_0 match at the stub point.

Sec 25.4 An Analysis of Steve's T-Network Tuner

Refer to Steve's section, "The T-Network Tuner,"(*Ref 1*) in Part 3, where he analyzes the wave actions in a system comprising a 50-ohm, 100-watt source; a lossless tuner feeding a 1.20 λ, transmission line; and a 50-ohm lossless line terminated in a 150-ohm load (the antenna). As stated earlier, the load mismatch at the antenna establishes reflection coefficient $\rho = 0.5$, SWR = 3:1. The line then transforms the 150-ohm load impedance to impedance $Z_L = 18.213 - j14.237$ ohms, $\rho = 0.5$ at the main line input connected to the output of the source. The object is to match Z_L to the 50-ohm source. However, in examining the analysis, we find errors, such as:

1. The mathematical model is inconsistent with realistic wave activity in the steady state,
2. The setup is treated using mostly initial-state conditions, not the steady state,
3. Reflected voltages are added incorrectly, as described earlier, to determine forward power,
4. Forward and reflected powers determined from his Eqs 5 and 6 are using either incorrect voltages or incorrect values of Z_0.

The mathematical model used in Steve's analysis begins correctly, showing 133.33 watts of incident or forward power arriving at the antenna and 33.333 watts reflected because of the 3:1 mismatch at the antenna. Using that model, however, his analysis shows *incorrectly* that useful re-reflection occurs at the output of the network and none at the input, while in fact, *all useful* re-reflections occur at the input, the matching point, as we will prove.

Steve's article states that on encountering reflection coefficient $\rho = 0.5$ at the tuner output, 25 percent (8.33 watts) of the 33.333 watts reflected at the antenna is re-reflected back to the antenna and 75 percent (25 watts) "... [is] the level of rearward power delivered back into the T network." He further states: "... the rearward-traveling voltage delivered back into the main transmission line, V_{BACK} is $-32.940 + j12.843$ V." It is significant to note that after traveling rearward through the network, the 25 watts of the 33.33 watts reflected from the antenna mismatch—which *must* arrive at the network input—is totally ignored. However, Steve then writes: "This rearward-traveling voltage is the exact negative of the reflected voltage created at the input of the T network ($+32.940 - j12.843$ volts). Therefore the total steady-state rearward-traveling voltages within the main transmission line is 0 v. This cancellation of all rearward-traveling waves is the mechanism that causes the effective steady-state input impedance to be 50 ohms at the input to the T network."

Cancellation of *all* rearward traveling waves? This is a huge stretch from simply canceling the reflected *voltages*. Our earlier explanation of the matching process proves that it is not that simple. Does canceling the rearward-traveling waves also cancel the energy carried in those waves? In addition to not accounting for the 25 watts of reflected

power, he also neglected the rearward-traveling *current,* which is a component of the 25 watts that returned from the tuner output mismatch to the tuner input. Consequently, he did not incorporate the resultants of the reflection coefficients of both voltage *and current* at the network input to determine their necessary participation in the wave interference process that accomplishes total re-reflection. Failure to consider the currents involved, and believing that re-reflection does not occur at the network input, led to an inappropriate development of the equations with erroneous results.

Now let's analyze the T network from Steve's article, using the same network parameters as shown below, but with a different mathematical model that will show that *all* re-reflections pertinent to impedance matching occur at the network input. C_1 and C_2 are the input and output capacitors, respectively.

Beginning at the input of the network, recall that the initial input impedance $Z_{in} = 117.810 - j57.061$ when the initial load impedance $Z_{LOAD} = 50$ ohms, verified by the equations below.

$X_{C1} = -j269.496$
$X_L = j104.216$
$X_{C2} = -j150.146$
$Z_0 = 50$

$$Z_{in} = \left[\frac{1}{\left(\frac{1}{Z_{LOAD} + X_{C2}} \right) + \frac{1}{X_L}} + X_{C1} \right]$$

$$Z_{in} = 117.809 - j57.061$$

Initially the source delivers 100 watts into impedance $Z = 50 + j0$ at the input of the main line connecting the source to the network. Source voltage $V_S = 70.71$ V. On encountering the initial impedance $Z_{in} = 117.809 - j57.06$ ohms at the network input, where $\rho_{IN} = 0.466 - j0.182$ ($|\rho| = 0.5$, SWR = 3:1), 75 watts enter the network and 25 watts are reflected toward the source. The initial reflected voltage equals $V_S \times \rho_{IN} = 32.94 - j12.843$ V. On reaching the source, the 25 watts reflected rearward from the network input creates an initial 3:1 mismatch between the source and the line input, thus reducing the initial source delivery to 75 watts. However, on reaching the steady state the load impedance at the network output changes from 50 ohms to $18.213 - j14.273$ ohms, the steady-state impedance appearing at the input of the transmission line connected to the antenna. Consequently, the impedance appearing at the network input changes from the initial $117.809 - j57.06$ ohms to its steady-state value of $50 + j0$ ohms. Thus, the source returns to delivering 100 watts, and the 25 watts initially reflected toward the source is now transmitted through the network in the forward direction, along with the original 75 watts. However, on reaching the steady state, the reflected voltage increases to $38.036 - j14.830$ V. As explained in the earlier math example, we showed that in the steady state the forward voltage increased by the forward-increase factor 1.1547, from 70.71 V to 81.65 V. However, Steve states incorrectly that "... the total voltage at the network input is equal to the sum of the source and reflected voltages, $103.651 - j12.843$ V." These voltages *cannot* be added directly, as we proved earlier. However, we will also see that in the steady state the voltage reflected at the input will have increased to $38.036 - j14.830$ V, only to be canceled later by its conjugate returning from the load mismatch as the reflected power becomes re-reflected.

Steve's account of the wave actions described in his analysis is incorrect for the same reasons that the steady-state voltage created at the network input is not $+32.940 - j12.843$, but is really $+38.036 - j14.830$. Consequently, it is evident that the voltage returning from the antenna is *not* the exact negative of what he believes is reflected at the network input. Instead, it is its *conjugate*. This same oversight also resulted in using an incorrect mathematical model of the system.

As explained earlier and in Refs 35, 37, 149, 150, 151, and 152, undesired reflections from a load mismatch are canceled by the conjugately related mirror-image reflections generated by the mismatch established by the matching device—in this case, the T network. We'll now show how the conditions described above have set the stage for total re-reflection at the input of the network.

Using terminology set forth earlier, Wave 1 is the source wave, Wave 2 is the wave reflected from the load mismatch (the antenna), and Wave 3 is the canceling wave established by reflection of Wave 1

at the network input. The voltage and current of Wave 1 initially see impedance Z = 117.810 – j57.060 ohms at the network input, establishing reflection coefficients of Wave 3: ρ_{Vin} = 0.466 – j0.182 = 0.5, θ_{Vin} = –21.333°, and ρ_{Iin} = 0.5, θ_{Iin} = +158.666°, respectively. Also, on arrival rearward at the network input, Wave 2 "sees" impedance Z = 117.810 + j57.060 ohms, the conjugate of the impedance seen by Wave 1. Wave 2 thus establishes reflection coefficients ρ_{Vref} = 0.466 + j0.182 = 0.5, θ_{Vref} = +21.333°, and ρ_{Iref} = 0.5, θ_{Iref} = –158.666°. Note that coefficients of Wave 2 are mirror images, or conjugates, of those of Wave 3, because the impedances appearing at the network input from opposite directions are conjugates of each other. Consequently, steady-state voltages and currents at the network input are:

Wave 2 = 38.036 + j14.83 V = 40.825 V, θ_{V2} = +21.3°)
Wave 3 = 38.036 – j14.83 V = 40.825 V, θ_{V3} = –21.3°) . . . resultant $\angle\theta_{RV}$ = 0°
Wave 2 = 0.7607 – j0.2966 A = 0.8165 A, θ_{I2} = –158.666°
Wave 3 = 0.7607 + j0.2966 A = 0.8165 A, θ_{I3} = +158.666° . . .resultant $\angle\theta_{RI}$ = 180°.

Note that the voltage magnitudes are equal and their resultant phase θ_{VR} = 0°, while the corresponding current reflection coefficients are 180° out of phase with the voltage coefficients. The magnitudes of current are equal and their resultant phase θ_{IR} = 180°. Thus, in accordance with the principles described earlier, when resultant voltage and current phases are θ_{VR} = 0° and θ_{IR} = 180°, an open circuit to rearward traveling reflected waves is established and total re-reflection is achieved.

In general, when the equal but opposite phase angles of the two reflected voltages are between 0° and ±90°, the resultant phases of voltage and current are θ = 0° and 180°, respectively, establishing an open circuit. Conversely, when the equal but opposite voltage phase angles θ are between ±90° and 180°, the resultant phases of voltage and current are 180° and 0°, respectively, establishing a short circuit.

We'll now examine the reason the phases of the reflected waves change to zero for both voltage and current relative to the source waves after re-reflection. Because the resultant voltage phase at the open circuit is already at 0° prior to re-reflection, there is no change in phase of voltage on re-reflection. Thus, the resultant voltage component of the powers re-reflected from both the network input and the antenna mismatch is now traveling forward in phase with the source voltage wave as part of the total forward-traveling voltage wave. Because the resultant current phase is 180° prior to re-reflection but encounters a 180° change in-phase on re-reflection at the open circuit, the resultant current component of the re-reflected powers is now also traveling in phase with the source current wave as part of the total forward-traveling current wave. Consequently, the ultimate result is that all of the power reflected at the load mismatch and transmitted rearward through the network output is totally re-reflected at the network input.

Sec 25.5 Power Loss Through Use of Steve's Eq 13

Let's now examine Steve's Eq 13, Part 3:

$$P_F = \left(\sqrt{P_1} + \sqrt{P_2}\right)^2$$

derived from his Eq 9. He used Eq 13 in the section "The T Network Tuner," with the manipulation 75 W + 8.33 W = 133.33 W, with P_1 = 75 W of source power and P_2 = 8.33 W of reflected power. Using this equation led him to overlook 50 watts in his power budget, necessary to correct the error in the power equation above. Substituting P_1 and P_2 in Eq 13 does indeed yield 133.33 watts, but this answer itself proves the equation invalid. The reason for this error is in incorrectly adding V_1 and V_2 as vectors with phases other than zero. Why would such an error be made? On discovering that the sum of the in-phase re-reflected and source voltage waves did not yield the correct forward voltage, 81.65 volts, he evidently assumed that the two voltage waves must then be added vectorially to obtain the correct 81.65 volts. Had he considered that forward voltage and current travel in phase on a lossless line, thus making both V_1 and V_2 travel at zero phase, the analysis likely would have come right.

Continuing the discussion concerning the missing 50 watts mentioned above, we'll now examine what happened to the 25 watts that reached the network input (at –32.940 + j12.843 volts, Steve

asserts) after traveling rearward from the network output. This brings us directly to the cause of the error concerning the missing 50 watts. In Steve's example, the power source initially delivers 100 watts into impedance $Z = 50 + j0$ at the input of the line connecting the network to the source. Repeating earlier statements for convenience, on encountering the initial impedance $Z = 117.81 - j57.06$ ohms at the network input, where, $\rho = 0.5$, there are 75 watts transmitted through the network and 25 watts reflected toward the source. Note that the voltage reflected at the network input is $32.94 - j12.843$ volts, the negative of the voltage he claims arrived rearward from the network output. On reaching the source, the 25 watts reflected rearward from the network input creates an initial 3:1 mismatch between the source and the network input, thus reducing the initial source delivery to 75 watts. However, on reaching the steady state, the network input impedance has changed to $Z_{IN} = 50 + j0$; thus the source again delivers 100 watts, and the 25 watts initially reflected toward the source is now re-reflected in the forward direction at the network input. This is the first 25 watts of the missing 50 watts that Steve overlooked.

Further, observe that although the values are incorrect, the voltage initially reflected rearward from the network input appears to be the exact negative of the voltage at the input in his model because of the rearward-traveling 25 watts returning through the network. Seeing this relationship, he reached the incorrect conclusion because these voltages appeared to cancel and there could be no further rearward travel of voltage into the source line. In the steady state, the 25 watts initially reflected rearward from the network input toward the source actually becomes re-reflected forward at the input, and the 25 watts that traveled rearward through the network is also re-reflected forward at the input. Those two 25-watt packets of power comprise the 50 watts of power overlooked. That is why he considered the source was delivering only 75 watts, where he states, "The fact that the forward source power is 75 W, rather than 100 W, is significant in correctly interpreting the steady-state conditions and the relationship between the total steady-state forward and re-reflected powers." We earlier proved the above statement to be untrue, and that Steve's Eq 13 is invalid when there is only a single source. We have also proven that in the steady state, the source is delivering 100 watts, not 75 watts as Steve stated; and we have also found the missing 50 watts.

Sec 25.6 Conclusion

To conclude, we have stated, analyzed, and corrected the significant misconceptions appearing in Best's *QEX* article (*Ref 148*), proving his claims that my material appearing in *Reflections* and *QEX* is incorrect are unfounded. Furthermore, additional evidence that Best's assertion that open and short circuits cannot be established by wave interference is incorrect appears in the next section.

Sec 25.7 A Look Inside the Elegant Rat Race

The knowledge of all imaginable forms of wave mechanics in transmission-line propagation has been around for more than 100 years. However, from discussions I've had with several otherwise knowledgeable RF engineers, and from material appearing in the three-part article by Steve Best, VE9SRB (*Ref 148*) that is rebutted earlier in this chapter (and in *QEX* [*Ref 154*]), it seems that a short refresher course on the subject might be appropriate. The case in point focuses on whether or not wave reflections, and virtual open and short circuits, can be established on transmission lines by wave interference. Steve Best, for one, asserts in his article that they cannot, and that open and short circuits on transmission lines can only be achieved with *physical* opens or shorts. Nevertheless, contrary to Steve's assertion, I have shown in earlier in this chapter that these phenomena can be, and are, established by simple wave interference between certain combinations of waves, even though those waves result from physical discontinuities elsewhere in the system. The importance of this issue, also contrary to Steve, is that virtual open and short circuits are inherently established by wave interference as the basis for all impedance-matching operations, whether in transmission lines or networks. The virtual short or open circuit established at the matching point achieves the match by re-reflecting all the power reflected by a mismatched termination downstream.

I'll now address a specific transmission-line circuitry having such wave mechanics that will sur-

prise some of you, which proves a physical discontinuity is not necessary to achieve virtual open and short circuits in the wave mechanics of transmission-lines. Many otherwise expert RF engineers, in addition to Steve Best, also swear that wave interference cannot possibly establish virtual open and short circuits.

One of the gems of all transmission-line circuitry is the seemingly magical ring diplexer, otherwise known as hybrid ring or "rat race," as shown in Fig 25-1. Its apparent magic is used traditionally to isolate two signal sources closely related in frequency that deliver power into dual loads. It uses only wave interference to obtain isolation between the sources. It seems like magic because wave interference is established in the diplexer with *no physical discontinuities anywhere.* It is an elegant circuit to drive crossed dipoles to obtain circular polarization (CP) simply by adding baluns at the terminals of the dipoles, plus an additional λ/4 line section in one of the two lines. Right-hand CP is developed from one transmitter and left-hand CP from the other.

Observe that the diplexer comprises nothing more than a continuous loop of transmission line having four terminal ports: two inputs (A and C) and two outputs (B and D)—no physical discontinuities whatsoever. Note that both lines AB and BC on the left-hand side are each λ/4 in length, for a total of 180°; on the right-hand side, line AD is λ/4 and line DC is 3λ/4, for a total length of 360°. The differential line length between the two sides is therefore 180°, which is the magic number for the diplexer to perform the isolation between the two sources. Here is how it works.

Current induced by voltage applied at A splits at A and travels to C along both sides of the diplexer, through B and D. Because of the 180° difference in length between the two sides, equal voltages arrive at C 180° out of phase, establishing a short circuit at C. The reverse is true also: Current induced by voltage applied at C travels to A in a similar manner, where two equal voltages from C arrive at A 180° out of phase, thus establishing a short circuit at A. Consequently, the short circuit at C prevents current from A from entering the source at C; similarly, the short circuit at A prevents current from C from entering the source at A. However, the short circuits are like *one-way mirrors*; for example, the

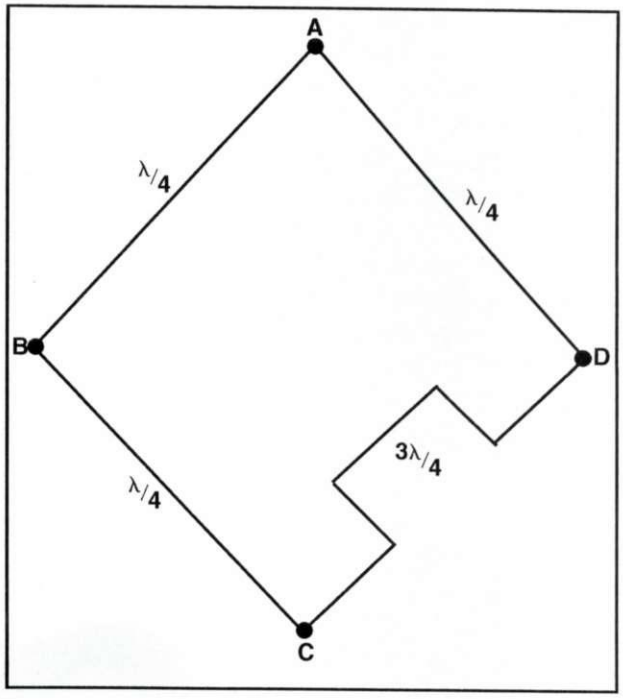

Fig 25-1. Circuit diagram of the ring diplexer, hybrid ring, or "rat race."

short circuit at C is transparent to current from C, but opaque to current from A; likewise, the short circuit at A is transparent to current from A, but opaque to current from C.

With Z_0 loads placed at B and D, current applied at A will enter both loads, but will not enter lines BC and DC (except in the amount required to overcome resistive loss to maintain the short circuit at C). Similarly, current applied at C will enter both loads but will not enter lines BA and DA (except enough to maintain the short circuit at A). Why? Here's where the apparent magic continues.

Observe that the lengths of all the lines are odd multiples of a quarter wavelength, λ/4 and 3λ/4. Short circuits have been established at both A and C. Terminated in a short circuit, lines whose lengths are odd multiples of λ/4 see an open circuit at their input terminals. Consequently, in traveling to loads at B and D, current from A sees an open circuit looking into lines BC and DC because of the short circuit at C. Similarly, in traveling to loads B and D, current from C sees an open circuit looking into lines BC and DC because of the short circuit at A. Consequently, there are two open circuits looking in opposite directions from both B and D. With

the open circuits at B and D between A and C, in tandem with the short circuits at A and C, we have two frequency-dependent filter sections providing mutual isolation between A and C.

In practice, the degree of isolation depends on the exactness of the line lengths and the uniformity of the dielectric constant of the insulating material. By measurements of diplexer circuits I've fabricated in stripline printed-circuit boards, with Teflon™-fiberglass GB-112T as the insulating material, I've obtained 40 dB of isolation between A and C.

In systems where the source and load impedances both equal Z_0 the characteristic impedance Z_{0DL} of the diplexer lines must account for the parallel circuitry at the source ports. Therefore:

$$Z_{0DL} = \sqrt{2Z_0^2}$$

Thus, where $Z_0 = 50$ ohms, $Z_{0DL} = 70.71$ ohms, which allows two parallel 100-ohm line-input resistances appearing at both A and C (from lines AB and AD in parallel at A, and from lines BC and DC in parallel at C) to present a 50-ohm load to the sources at A and C, respectively.

Therefore, it's not really magic, but simple wave mechanics that establish virtual open and short circuits in the absence of any physical discontinuities. Pretty neat, eh?

Chapter 26

On the Fundamentals of Impedance Matching

(Written especially for this book by John C. Fakan, Ph.D. E.E., KB8MU)

Sec 26.1 Considerations for Electrical Matching

The concept of matching is concerned with transferring energy from one entity to another. Energy, by definition, is the ability to do work. Of interest to this discussion is that energy is conserved. We rely on the principle that the amount of energy that is transferred cannot exceed the amount available. It can be less than the available amount, but not more. In electrical networks we consider electrical energy that is converted to thermal energy to be *dissipated*. When calculating electrical efficiency such dissipated energy, it goes into the *loss* column.

To permit mathematical analysis of electrical networks a consistent pair of variables is defined—namely, voltage (an "across" variable) and current (a corresponding "through" variable). Energy level is defined as the product of these two variables, and the entire system of units is chosen and defined so that, within this model, the principle of *conservation of energy* is assured.

It is a mathematical fact that any specific value can be the product of an infinite number of pairs of multipliers. Thus, a specific energy transfer rate will not be completely defined without a statement of the value of at least two of the three variables involved—voltage, current, and power (the rate at which energy is transferred—the product of voltage and current); or a statement that includes any other combination of the variables and/or new variables from which at least two of the original variables can be uniquely determined. Also, since the "law" of conservation is always true (at any instant in time), we also must account for any time-dependent variations of the variables.

Other applicable nomenclature includes the terms *source* (to label the entity from which energy is being transferred) and *load* (the entity to which the energy is being transferred). In the usual configuration a source and a load are connected together so that energy transfers at some rate from the source to the load. All of the energy that is transferred passes through the connection.

Note here that we can expand on the idea of source to include entities within which transformation from other forms of energy takes place and those that only pass on electrical energy. For analyzing the rate at which either type will transfer energy to a load, it is irrelevant to consider which type of source is involved. We need only know about the characteristics of the available energy at the point of connection.

In one of the most common engineering models, at each connection in a serial network of entities passing energy we have both a source and a load. For purposes of analyzing the rate of energy transfer at a specified connection, we need to know sufficient information about the source and the load. Traditionally, in electrical engineering, for the source we specify the maximum power level and the mathematical ratio of the voltage and current at which that power level is available. The ratio has been given the name *impedance*. For the load side of the connection, we specify the impedance at which the load will accept energy.

Of considerable interest, but of no relevance to the determination of the rate of energy transfer, is how the impedances of source and load are established. A simple resistor, for example, will present an impedance numerically equal to its electrical resistance. That is, a specific voltage will exist across it for a given value of current passing through it. Thus, the instantaneous ratio of voltage to current, which is defined by its electrical resistance, is also identical to the ratio of voltage to the

current it presents as a load when connected to a source. In most cases, however, the situation is not nearly as simple. The load impedance presented by a transmission line is established by factors such as the impedance of the load connected at the other end (at points of connection the line serves as a source) and perhaps also on the length of the line for situations in which the variables are time variant.

Sources of the type where transformations from other forms of energy take place are particularly interesting. An electrical battery cell transforms chemical energy into electrical energy, which is then transferred to the battery's electrical load. The chemical processes within the cells and the number and the connection combination of the cells determine the voltage level and impedance at which the rate of power (or current) at which the chemical energy is available from the battery. Note that the available voltage (or current) at which the energy is available is not necessarily due to dissipative processes. In the case of common battery cells, the chemical processes that determine the impedance are primarily non-dissipative.

Getting back to the analysis of energy transfer at the connections in a network, we should be able to identify some simple consequences of our model that are intuitively obvious. The standard model tells us that a load that presents a less-than-infinite voltage/current ratio to the connection will respond to any applied voltage with a current flow. If the relationship between voltage and current is linear (i.e., current and voltage are proportional to one another) and known (for both the source and the load), and we know one other value (such as the no-load voltage of the source), we have sufficient information to determine the rate of energy transfer across the connection. (Note that instead of the no-load source voltage we could use the source's short-circuited current, or we could use the power level established with any other known load connected.)

For any source with a proportional voltage/current relationship, the product of voltage and current (power level) will have a maximum. (This is a characteristic of the mathematics and has nothing to do with things such as limits imposed by the components used in the network. Good engineering design assures that the practical limits exceed the mathematical limits.) Therefore, if a particular load results in a combination of voltage and current that differs from the specific values that result in the maximum power level, the energy transferred to the load will be less than the maximum available.

Consider a source with the simple relationship that the voltage varies linearly from 10 to 0 volts when the current varies linearly from 0 to 10 amperes. In other words, a characteristic of this source is that when current is drawn from its terminals, the voltage across those terminals will decrease in proportion to the instantaneous value of the current. At either extreme the product of voltage and current is zero (i.e., $0 \times 10 = 10 \times 0 = 0$). At 5 volts and 5 amperes we have a product of 25 (25 watts), which turns out to be the maximum value for all possible mathematical products of the voltage and current. All other combinations result in a product less than 25 watts. This is still the case even if the voltage and current vary in time. The instantaneous results must still be the same. The mathematics will just be more complicated. If the variation is sinusoidal, the mathematics will again be relatively simple. In any event, the maximum rate of energy transfer from source to load occurs at one specific operating point for any system in which the variables are proportionally related.

Another way to look at this principle is to consider that in order to take all possible energy from the source the load must simultaneously make use of all of the voltage *and* all of the current at the operating point where the source is at its maximum power level.

For the single path, series-connected networks we have been discussing, the source and load voltages and current levels will always be equal in magnitude at the connection. To keep the mathematics consistent we need to do something about the arithmetic sign for the through variable current. The common convention is to define currents flowing into an entity as positive. Thus, the load current will be positive when the source current is negative. The mathematics then tells us that when the voltage applied to a simple load is increased, the current will also increase in proportion—the constant of proportionality being the load's voltage/current ratio (impedance). Using this same convention for the source, we have a negative proportionality (the source's impedance) that says the voltage decreases with increasing current. Further convention is to differentiate the two simply by calling

them the *source impedance* or *load impedance* without use of the sign. Note that a given device can exhibit a source impedance that is completely different from its impedance as a load. A primary chemical battery cell is just one example. A diode is another.

Now let's take a careful look at the condition where the load is such that the source is operating at the point where maximum energy transfer is taking place. The voltages and currents are the same magnitude for both source and load, and the voltage-current product is at the maximum for the source. Since the current level is determined by the load as a function of the source voltage, it must be that the characteristic voltage/current ratio for the load is the same as that for the source. Using the simple source described above as an example, if the load is such that an applied 5 volts results in a 5-ampere current, then the power level in the load is 25 watts. Since that is also the maximum power level for that source, it must be that any other load condition will result in a lower power level.

However, what if the source voltage and current are time varying and not in phase? Let's assume our simple source is operating as a sinusoidal source (AC) and the values expressed for the variables are RMS values. The mathematics still produces the same results. We can cause a phase difference between the source voltage and current by introducing a reactive element (say a capacitor in parallel with the output terminal). This will result in a different instantaneous voltage/current ratio for the source (i.e., the source impedance is now different because of the introduced phase shift). For the same load connected to the source, the instantaneous product of voltage and current will be less than the original 25 watts because of the phase difference. If the phase difference can be reduced or eliminated, the instantaneous product can be increased up to the maximum 25-watt level. This can be accomplished simply by placing an appropriate inductor across the load's terminals.

I find it interesting to note that if the two reactive elements (the capacitor attached to the source and the inductor attached to the load) are considered together, they form a simple parallel LC circuit across the connection. Because the reactance of each is the same value, this LC circuit is resonant at the operating frequency and thus takes no energy from the connection. It also draws no net current from the connection at any voltage, so it effectively displays an infinite impedance to the connection. Thus, we can eliminate it from consideration and we are right back to the simple case.

However, what about the impedances for the modified source and load? They are not the same because of the differences caused by the two different reactive elements. The convention is to state the out-of-phase voltage/current ratio as a complex number with the imaginary part of the number representing the reactive part. Because the reactances for the source and load are equal in magnitude but opposite in direction, their impedances are simply the conjugates of one another.

Thus, we can conclude that to design a load to operate at the mathematical maximum power level when connected to a specific source, the impedance of the load must be the complex conjugate of the source impedance. Any other value results in a lower power level.

Conversely, if the maximum available power level (as determined by the math, not the component ratings) is realized through adjustment of the load impedance, then it follows that the source impedance must be the complex conjugate of that load impedance.

If the characteristics of a source are such that it behaves approximately in a linear fashion, the conditions for matching to obtain maximum energy transfer will also be approximately the same.

Determining the output characteristics of a non-simple device, such as an RF amplifier using a pulsed active component as a part of its circuitry, is not a simple process. The usual RF amplifier also includes parallel energy transfer paths that further complicate rigorous analysis. The non-linear action of the active device in class-B and class-C circuits is hidden from the output terminal through the combined effects of the parallel energy paths and the energy storage capabilities of the tank circuit.

It has been my experience that the output characteristics of even class-C amplifiers are very close to those of ideal linear sources, and I thus conclude that there is no valid reason to preclude use of the various theorems for analyzing energy transfer to loads connected to these devices. Determination of an amplifier's output impedance is probably best accomplished by finding the load that results in the

maximum power level and then using the Complex Conjugate Theorem to define the impedance of the source. If the amplifier's output is reasonably linear, it is not even necessary to find the point of maximum power. Simply determining two operating points may be sufficient to extrapolate to the impedance.

Suggestions that the theorems don't apply because of non-linear activity somewhere within the bowels of a device makes no logical sense. For purposes of analyzing energy transfer from one entity to another, the only things that matter at all are the characteristics displayed at the terminals.

Chapter 27

Investigation of the Shaped-Beam Capabilities of the Quadrifilar

(By M. W. Maxwell, Advanced Development Final Report IR&D Project Quadrifilar, RCA Astro-Electronics, Princeton, New Jersey, March 31, 1977. Note that in prior editions of Reflections, *this was Appendix 13.)*

Sec 27.1 Introduction

The quadrifilar type of antenna has been proven useful in many spacecraft applications. It is particularly attractive because certain of its radiation characteristics can be tailored to meet the requirements of various specific spacecraft applications simply by selecting the proper relationship between the electrically significant physical dimensions. Other attractive features are its relatively small volume and light weight, plus its capability of providing unidirectional, end-fire radiation without requiring a ground plane.

This report describes the experiments performed and the data obtained from measurements made on a quadrifilar antenna that was uniquely constructed to permit selective, incremental dimension variation of the physical parameters that critically affect the electrical performance of the antenna. This experimental quadrifilar antenna model is shown in Fig 27-1.

Through a complex parametric measurement program, the radiation patterns and terminal impedances, plus corresponding physical design information pertinent to literally hundreds of different dimensionally incremented configurations, were obtained and catalogued. From this catalog of pattern and design data, the antenna engineer can select the quadrifilar configuration that will satisfy his performance requirements simply by searching the collected pattern data and finding the radiation pattern that matches those requirements. In other words, the

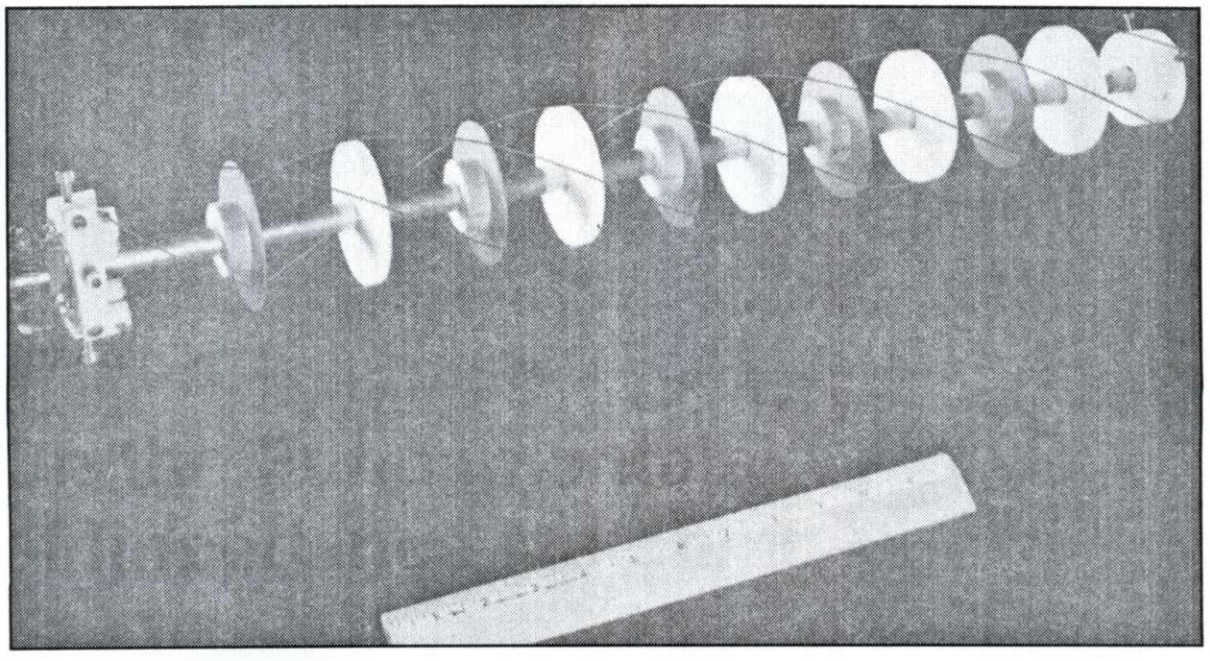

Fig 27-1. Experimental model of a quadrifilar antenna.

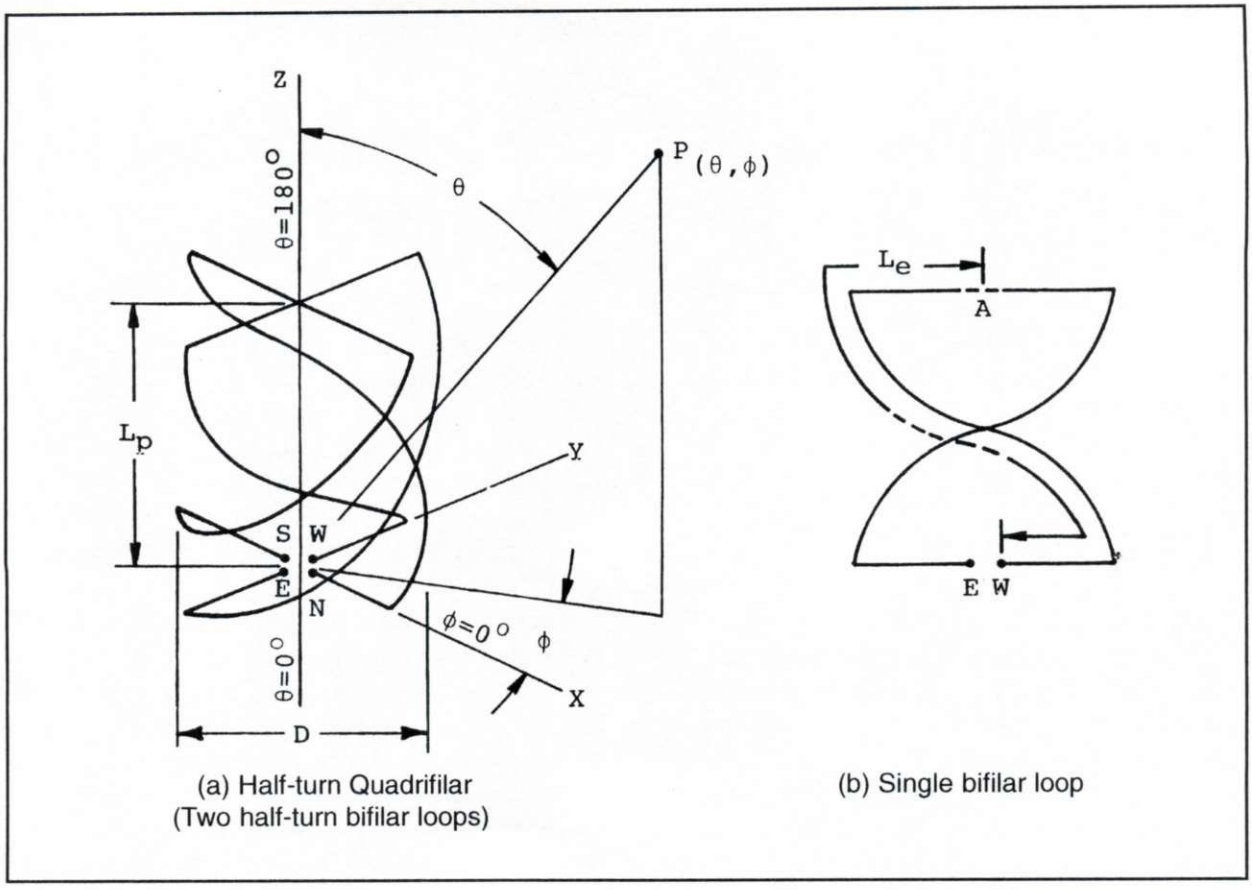

Fig 27-2. Quadrifilar and bifilar loops.

ultimate goal of this experiment was the generation of a catalog of design data covering a wide range of quadrifilar configurations from which the engineer can obtain complete design information concerning the physical parameters required to yield the electrical performance he desires. This report also contains directions on how to make effective use of the data catalog described herein.

Two important advantages were realized by the approach taken in this experiment: First, a search through the data catalog provides a quick, but thorough, overview of the scope and range of performance capabilities and design possibilities that are available with the quadrifilar configuration; second, a reduction in time required for setting up the equipment to perform the experiment is realized, because only one set-up time was necessary for obtaining the voluminous set of data families by the incremental-measurement approach used in this experiment. In contrast, without the data catalog obtained during this experiment, a different set-up time for each separate, similar experiment would be required on a per-inquiry basis.

Sec 27.2 Brief Background of Quadrifilar Antenna Development

As illustrated in Fig 27-2, the quadrifilar antenna comprises two sets of bifilar helices oriented mutually orthogonal on their common axis. A bifilar helix consists of two identical, parallel helical elements in 180-degree radial opposition (on a common axis) and connected radially as shown in Fig 27-2. In discussing quadrifilar antennas, the bifilar helix (one half of the quadrifilar) is often referred to as a *bifilar element*. Kilgus (*Ref 91*) reported that when the windings of a bifilar helix are fed in anti-phase, in contrast to the commonly-used parallel connection, the radiation characteristics are vastly different. Kilgus compared the radiation characteristics of a bifilar helix having one-half turn (fed in anti-phase) with those of the loop-dipole combina-

tion of Brown and Woodward (*Ref 90*), where loop and dipole symmetrically share a common axis. This comparison showed that their radiation characteristics are identical, except for a 90-degree shift in the entire toroidal pattern relative to the physical axis. While the two nulls in the loop-dipole pattern occur on the dipole axis, the two nulls in the otherwise identical pattern of the half-turn bifilar helix occur bi-directionally on a line normal to a plane formed by the radial elements at each end of the bifilar helix. The loop-dipole combination yields a toroidal radiation pattern in space with the same envelope shape as that of either the loop or the dipole radiating separately. However, the radiations from the loop-dipole combination are *circularly* polarized with the same screw sense everywhere in space, whereas the radiation from the dipole and loop separately are both *linearly* polarized. However, the dipole polarization is parallel with the axis, while the loop polarization is orthogonal to the axis. Consequently, a single bifilar element radiates circularly polarized waves bi-directionally along its axis.

However, by exciting two mutually orthogonal bifilar elements in a 90° phase relation (as obtained by connecting the feed terminals according to the circuitry of Fig 27-3), the fields of both elements add vectorially, canceling radiation in one direction while radiating the sum of the two fields in the opposite direction. Thus, we have the quadrifilar antenna, which obtains substantially hemispherical radiation *without requiring a ground plane*; the radiation is still circularly polarized with the same screw sense everywhere in space. This is an appealing radiator configuration for two reasons: (1) the weight and space required for a ground plane are eliminated; and (2) since the quadrifilar can be mounted so that its substantially unidirectional radiation is directed away from the spacecraft, the radiation pattern of the antenna when mounted on a spacecraft becomes relatively independent of the spacecraft environment in the area underneath the antenna. As a result, the problems of finding an acceptable mounting position for the antenna on a spacecraft are greatly reduced.

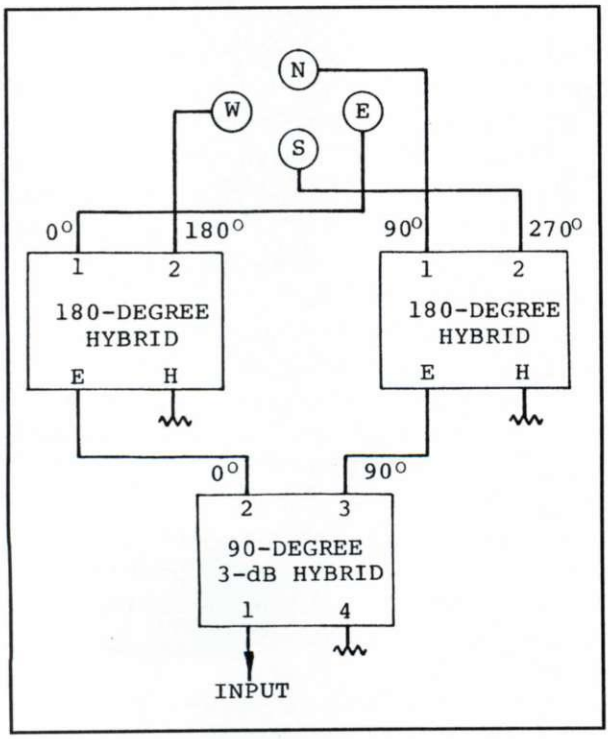

Fig 27-3. RF feed circuitry.

Kilgus also reported that different values of length and radius, and number of turns, yield different radiation patterns (*Refs 91, 92, 93*). Therefore, a logical application of end-fire array theory indicated that quadrifilar experimentation with various combinations of critical physical and electrical parameters beyond the dimensional range of those reported by Kilgus should yield a method of controlling the radiation-pattern shape to meet antenna requirements for various spacecraft orbital parameters. Consequently, the extensive measurement program described here was performed using a quadrifilar antenna designed to be adjustably pre-set to any combination of a variety of dimensional parameters, such as diameter, length, number of turns, etc. I systematically measured the radiation characteristics of this experimental model to create families of pattern plots that indicate the relationship between changes in a given parameter and the resulting radiation pattern. Thus, when a given set of antenna requirements is known, a search through the families of measured pattern plots provides a quick choice of quadrifilar design parameters that will satisfy these particular requirements. This technique has the advantage of using a single controlled setup to obtain many incrementally related measurement observations, in contrast to the former need of setting up measuring equipment each time a pattern investigation for a particular set of conditions is

required. Furthermore, because there are instances in which different parameter relationships have been found to yield similar radiation characteristics, a choice is readily available based on parameters that are most favorable to other than radiation-pattern considerations.

Sec 27.3 Description of the Quadrifilar Antenna

(A) Electrical Construction

The experimental model of the quadrifilar antenna comprises two separate, adjustable-length bifilar helical loops positioned in the mutual 90-degree axially-rotated relationship as shown in Fig 27-2(a). A hollow axial mast supports the loops and houses four separate coaxial transmission lines that feed the loops. Each bifilar loop comprises a continuous conductor that is open at the radial center of one end. The two open-conductor ends provide the feed terminals for the loop. (An alternate configuration in which the loop is also open at the radial center at the opposite end [Fig 27-2b, Point A] for impedance control will be described later.)

The input feed terminals of the loops are located at the top end of the mast, opposite the base-mounting end. By respectively connecting to opposite ends of the four separate coaxial feed lines housed by the mast, each of the two input terminals of each loop is fed separately from its own respective hybrid-balun output port in a 0° to 180° relative phase relation, as shown in Figs 27-2a and 27-3. The four coaxial transmission lines feeding the loop terminals are of 50-ohm semi-rigid construction dressed in a contiguous, parallel relationship down the inside of the support mast. The hybrids that feed each bifilar loop are nominal 50-ohm devices. As stated above, a separate 50-ohm coaxial feed-line is connected to each hybrid output port. The center conductor of each feed line is terminated in each of the balanced two-terminal input ports of each bifilar loop, respectively, while the outer conductors of the coax feed lines are soldered together at their terminating ends; no other connection is made to the outer conductors at the terminating end. This arrangement of the feed-line termination results in the two 50-ohm feed lines being effectively connected in a series relationship with respect to the input terminals of the bifilar loop. The effect of this series relationship of two 50-ohm lines is to produce a 100-ohm feed-point source for the loop-input terminals. Therefore, the normalized impedance data, which will be described later, will be presented in Smith chart form with values that are normalized to a *100-ohm system*.

In addition to being physically positioned 90 rotational degrees apart, the two bifilar loops are fed 90° out of phase in the standard quadrifilar. This 90-degree phase relationship is accomplished by feeding the 180-degree hybrid for each loop from the 0- and 90-degree output ports of the 3-dB hybrid, respectively. The hybrids are connected as shown in Fig 27-3.

(B) Adjustable Parameters

The critical parameters that determine or control the radiation characteristics of the quadrifilar antenna are as follows:

- L_e, which is one half of the electrical length of the radiating conductor of each bifilar section in wavelength A (total loop length between the input terminals is $2L_e$, see Fig 27-2b).
- D, which is the diameter of the radiating structure (see Fig 27-2a).
- L_p, which is the length of the radiating structure (see Fig 27-2a).
- T, which is the number of turns in the helical portion (determined by the number of rotations of the unfed radial element relative to the radial element containing the feed terminals).
- The electrical size of parameters L_e, L_p, and D.

The physical construction of the experimental antenna was designed so that these parameters can be varied to obtain the various different (or desired) radiation characteristics:

Parameters L_e, D, and T are physically variable and mutually independent.

For any given physical sizes of L_e, L_p, and D, the electrical sizes of these parameters are variable (in a mutually-fixed relation) using the technique of proportional frequency scaling.

Parameter L_p is physically variable, but not independently; it is completely dependent on the particular values of L_e, D, and T. L_p is a fixed value for any specific combination of L_e, D, and T. However, for any given combination of L_e and D, structure length L_p varies inversely with the number of turns T. In other words, since the wire in the loop is fixed for any given dimensional configura-

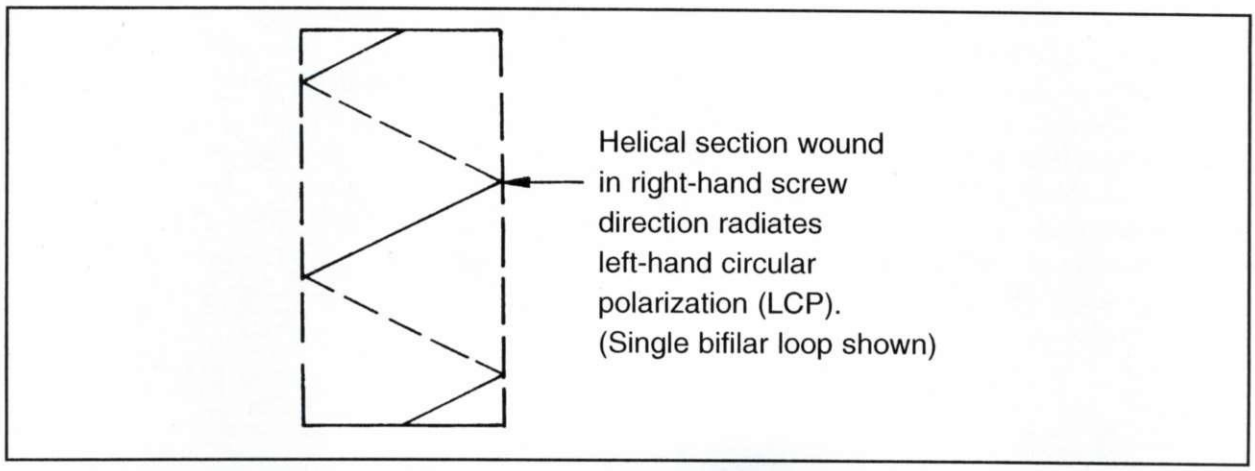

Fig 27-4. Relationship between radiation screw sense and winding direction.

tion, the overall end-to-end physical length of the antenna decreases as the number of turns of the loop increases.

The measurement program used was developed to obtain both maximum amount of useful data and optimum resolution of the data for achieving a practical degree of interpolative accuracy. To realize these objectives, the measurement techniques described in Sec 27-4 were used to determine the radiation characteristics and input-terminal impedances of the quadrifilar antenna designs.

Sec 27.4 Measurement Techniques

(A) Measurement of Radiation Patterns

The variable-parameter quadrifilar antenna model was initially assembled with the smallest of four available diameters D; the shortest of four available conductor lengths L_e; and a minimum number of turns T (for example, D = 0.06 λ , L_e = 0.46λ , and T = 1/2). Separate pattern plots of approximately thirty different electrical sizes were then measured using this configuration by making separate measurements at about thirty different frequencies. The frequencies were changed in increments of 25 MHz (usually) over the range from around 300 to 1000 MHz. The number of turns T was then increased in increments of 1/4-T from the 1/2-T starting condition to as many as 3 1/2 turns. The same thirty-frequency increments in this size-measurement procedure were then repeated at each successive 1/4-turn position. After completing the measurements at each 1/4-T increment, length L_e was then increased one increment at a time, and the entire frequency and turn increment procedure repeated for each of the three remaining L_e increments.

The whole procedure was again repeated for each of the three remaining increments of parameter D. Thus, these iterations ultimately included approximately thirty different electrical sizes of all possible combinations of four different conductor lengths L_e, four different diameters D, and all 1/4-turn increments of T, from T = 1/2 to as many turns as possible, depending on length L_e and diameter D.

The radiation-pattern measurements were made using a Scientific Atlanta pattern positioner at the AED (RCA Astro-Electronics Div.) outdoor antenna test range, together with suitable absorber material on the ground for control of ground-reflected energy. Circularly-polarized illumination (both right- and left-hand) was obtained from a Scientific-Atlanta log-periodic crossed-dipole antenna. This illuminating antenna was fed with appropriate hybrids to obtain proper amplitude and phase relation of RF signal energy to radiate either right-hand (RCP) or left-hand (LCP) polarization, as desired (see Fig 27-4). Thus, during this experiment, the quadrifilar structure was used as a receiving antenna.

To correlate the pattern displays with the physical orientation of the antenna during each measurement, the position of the antenna in relation to the standard spherical coordinate system of notation used during the measurements is shown in Fig 27-2a. The question now arises concerning the number

of pattern measurement cuts required for each configuration to obtain adequate radiation data. The minimum number of cuts was determined to be one for each polarization (LCP and RCP) for each different configuration and electrical size. This number is consistent with conventional pattern-measurement practice, which is based on a well-known principle of solid-geometry.

When the power radiated from an antenna at any given angle θ is constant for all values of angle ϕ (see Fig 27-2a), the shape of the radiation pattern obtained in the θ plane at any angle ϕ follows the contour of an axial slice taken through the volume generated by rotation of the θ pattern around the Z-axis. Under these conditions, a single θ pattern measurement at any ϕ angle represents θ cuts for

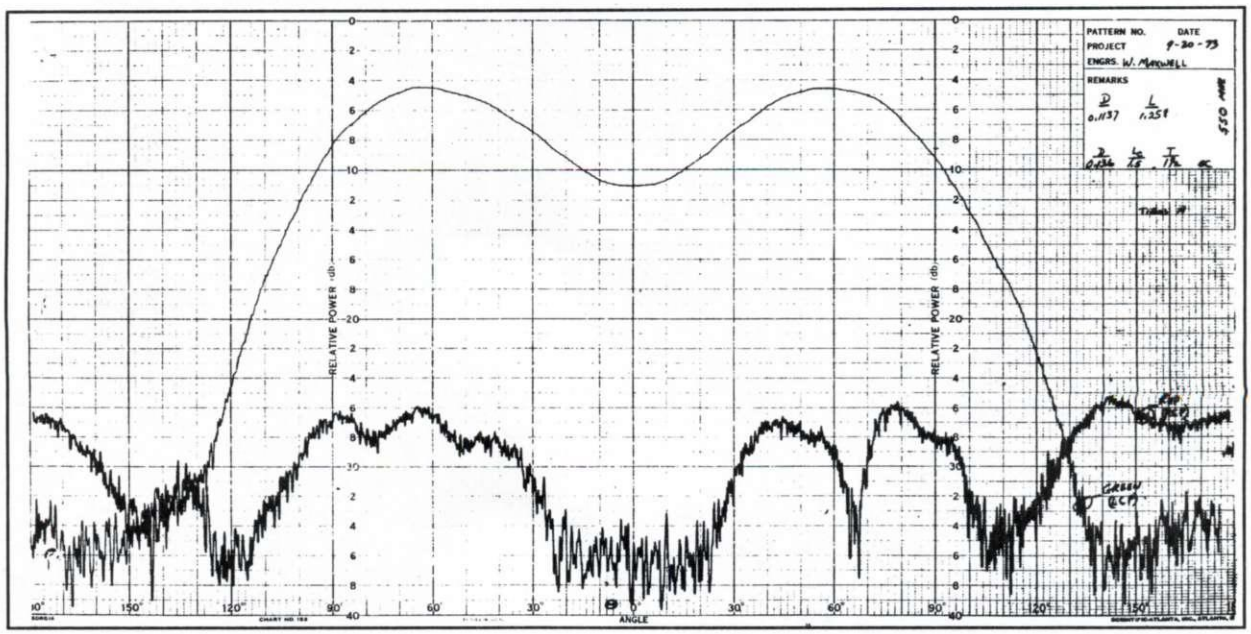

Fig 27-5. Typical measured antenna radiation patterns, example 1.

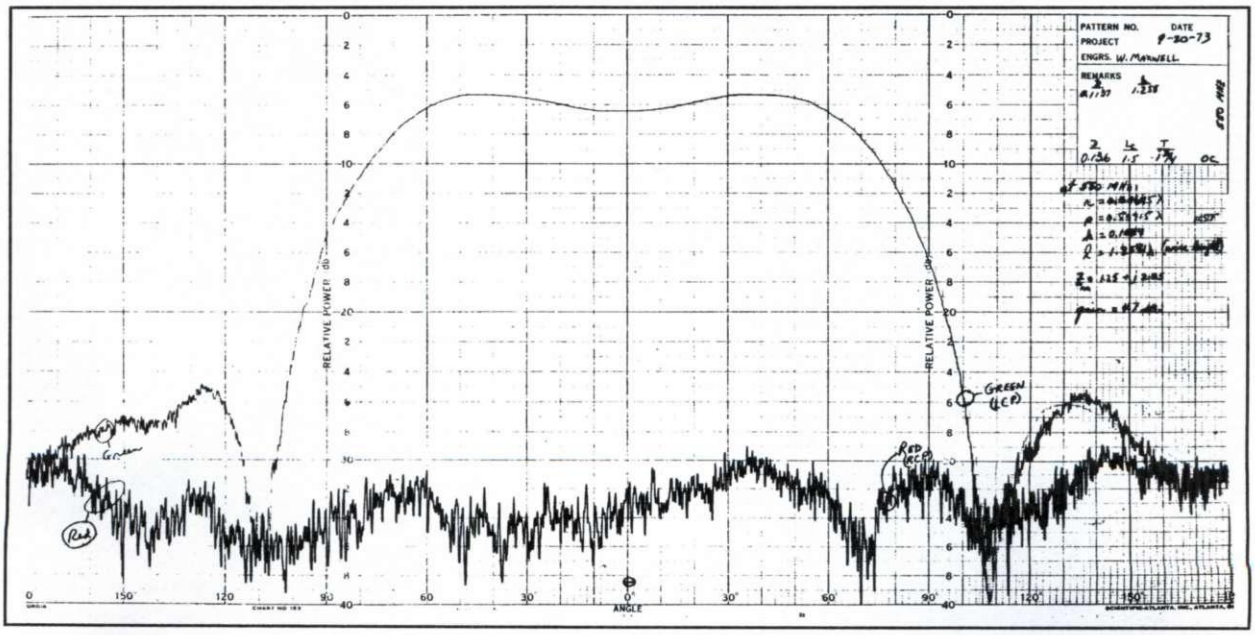

Fig 27-6. Typical measured antenna radiation patterns, example 2.

all ϕ angles, because θ cuts through all ϕ angles are identical. Experience has shown that radiation from symmetrical quadrifilar configurations is uniformly omni-directional, or constant, relative to rotation about the Z-axis of the antenna ($\phi = 0°$ to 360°), because of the geometrical symmetry. Based on this experience, the quadrifilar is seen to qualify under the principle just described. Consequently, one θ-pattern cut was measured at the $\phi = 0°$ position for each polarization screw sense of illumination (RCP and LCP) for each configuration and size combination; both LCP and RCP pattern cuts were plotted on the same pattern sheet. The plot of the principal response (co-polarized LCP) is recorded in green, and the cross-polarized RCP response is recorded in red on the original recording plots. In view of the principle explained above, each pattern represents the envelope shape of the volume of revolution generated by rotating the pattern on its axis, and therefore each pattern represents the particular radiation characteristics of each respective quadrifilar-antenna configuration in all directions in space. Typical measured patterns are shown in Figs 27-5, 27-6, and 27-7.

On these copies, the green (LCP) plot transferred as the lighter trace, while the red (RCP) plot is the darker trace. Three samples of the plots of typical patterns are included as Figs 27-5, 27-6, and 27-7.

(1) Quadrifilar Helix versus Conventional Helix. Since a portion of the quadrifilar is of helical form, it is tempting to classify it with conventional helical antennas. However, this should be avoided, because the screw sense of the circular polarization radiated by both the quadrifilar and its bifilar elements is opposite of that radiated by a conventional helical antenna wound in the same screw direction. In other words, a quadrifilar having the helical portion wound with a right-hand screw direction radiates a left-hand polarization screw sense (LCP). The principal response of the experimental quadrifilar is LCP, because the winding of the helical portion is in the right-hand screw direction (see Fig 27-4).

Although the helical portion of the quadrifilar used in this experiment was wound so that its principal response is to left circular polarization, this antenna is not a perfect LCP radiator. Consequently, it will also respond in some degree to right-circular polarization. Thus, there are two basic purposes for measuring the amplitude response of the antenna to illumination of both left- and right-hand circular polarizations:

1. To permit accurate determination of antenna directivity—i.e., to collect all the power incident on the antenna so that when both LCP and RCP power responses are separately integrated and then

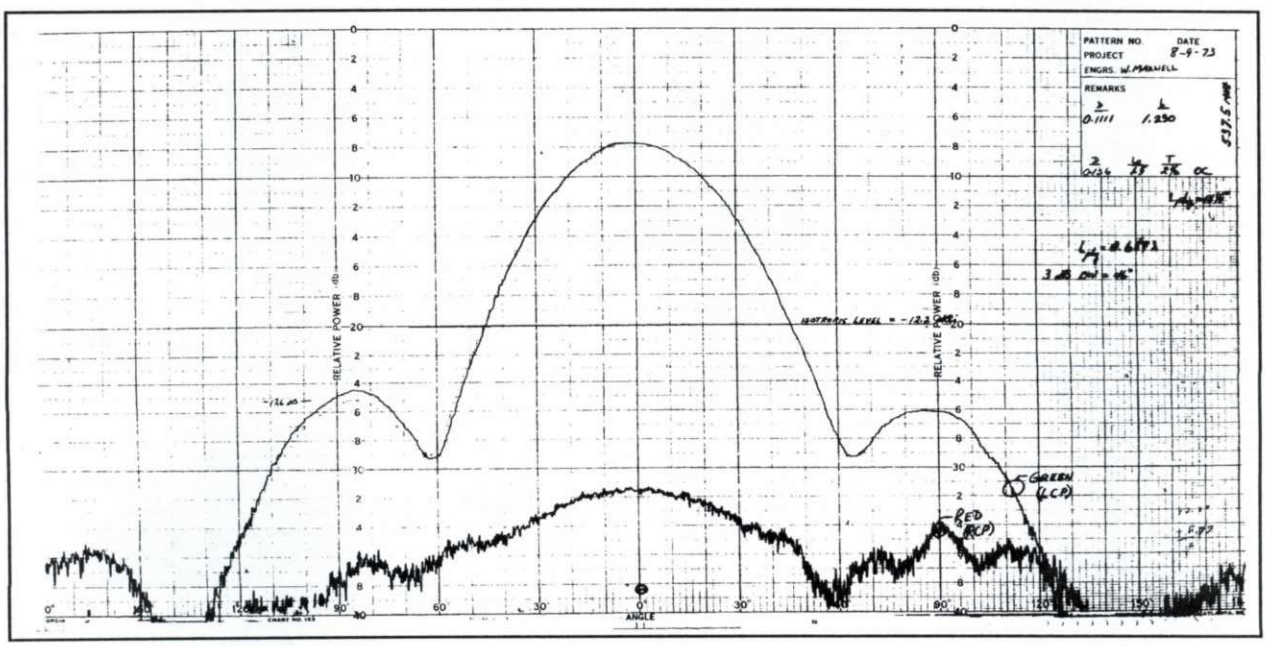

Fig 27-7. Typical measured antenna radiation pattern, example 3.

summed, an accurate calculation of antenna directivity can be performed.

2. To permit determination of the axial ratio (AR), or ellipticity of the radiation from the antenna. The ellipticity of the wave polarization can be calculated directly from the difference in the amplitude response measured between the two opposite senses of polarization.

(2) Incremental Change Size of Radiator. To establish a frame of reference for the electrical size of the various parameters with changes in the measurement frequency, the antenna was constructed so that λ is equal to 1.0 for a physical dimension (in air) of 18 inches. This particular physical size was selected because of the frequency where λ = 18 inches lies approximately at the center of the frequency range of the hybrids available for use in the feed system illustrated in Fig 27-3. Thus, 1.0 λ is equal to 18 inches at 655.714 MHz. Accordingly, the four diameters D used during the measurements were 2.44 inches (0.136 λ), 3.6 inches (0.20 λ), 5.4 inches (0.30 λ), and 7.2 inches (0.40 λ). The four conductor half-lengths L_e were 18 inches (1.0 λ), 27 inches (1.5 λ), 36 inches (2.0 λ), and 45 inches (2.5 λ). The λ values (indicated in parenthesis) represent the nominal sizes of the respective wavelength parameters at the reference frequency of 655.714 MHz.

The main purpose of these reference-frequency values is to establish a means for identifying the physical dimensions and configurations of the antenna during each measurement. For example, when the physically adjustable parameters were set so that D = 0.136 λ and L_e = 1.0 λ (at 655.714 MHz), and T = 2, measurements were then made for many different electrical sizes that are inversely proportional to the frequency used at each frequency increment in the range from 300 to 1000 MHz. (Some sets begin at frequencies somewhat higher than 300 MHz.) Therefore, the separate pattern plots for each measurement frequency in the group having the D, L_e, and T parameters of this example all are identified by these same parameter dimensions. In addition, in order to identify the electrical size of the structure during each measurement, the frequency at which each respective measurement was made is also indicated on the plot. Thus, the actual electrical size determined by the relationship between the physical parameter sizes and the frequency used during each measurement is obtained by multiplying the electrical size at the reference frequency (655.714 MHz) by the ratio of the measurement frequency to the reference frequency. (The electrical and physical sizes are identical at 655.714 MHz.) The actual electrical sizes of parameters L_e and D have been calculated for each measurement and are appropriately recorded on each pattern plot. Some of the patterns will be seen to have a statement of directive gain with respect to an isotropic radiator. These patterns have already been found to be of interest for specific spacecraft applications and thus have been integrated to obtain the gain information. (The pattern appearing in Fig 27-5 is the one that satisfied the requirements for the S-band antennas to be used on NOAA TIROS-N, to replace the crossed-dipole over ground plane used on TIROS-M for a saving of weight and space. Thus, the quadrifilar configuration that achieved the pattern of Fig 27-5 was used directly as the final configuration for the S-band quadrifilars used on all models of TIROS-N.)

(3) Significance of Peak-Level Value of Recorded Patterns. As stated earlier, during this experiment the adjustable quadrifilar antenna was used as a receiving antenna, and the input signal for the pattern recorder was obtained from a crystal detector connected to the feed terminals of the antenna (see Fig 27-3). As will be explained later in the section describing the impedance measurements, the input-terminal impedance of the antenna exhibits large variations as the measurement frequency is changed in accordance with the size-scaling operation. Since hundreds of incremental frequency changes were required during the course of the pattern measurements, time did not permit the luxury of continually rematching the varying antenna impedance to the load impedance of the detector. Consequently, no attempt was made to establish any power-level relationship between the pattern plots obtained at different measurement frequencies, or between differing configurations. As a result, the differences in reflection loss corresponding to the changes in mismatch between the antenna terminals and the detector account for the variation between values of successive plots measured at different frequencies for a given configuration. However, the accuracy of the pattern *shape* appearing on each separate sheet is unaffect-

ed by the antenna-terminal mismatch as long as sufficient detected power was available to establish adequate signal-to-noise ratio in the pattern-recording system over the entire dynamic range of the pattern amplitude. Thus, each separate pattern sheet provides accurate information concerning vital radiation characteristics such as directivity, beamwidth, axial ratio (ellipticity), cross polarization, etc., for the particular configuration and electrical size of the antenna while the patterns appearing on that sheet were being recorded. For patterns that showed promise for practical operation, the directivity was determined by integration.

(4) Definition of Legend Used in Identifying the Variable Parameters. It is now appropriate to explain the legend of the terms used in the data

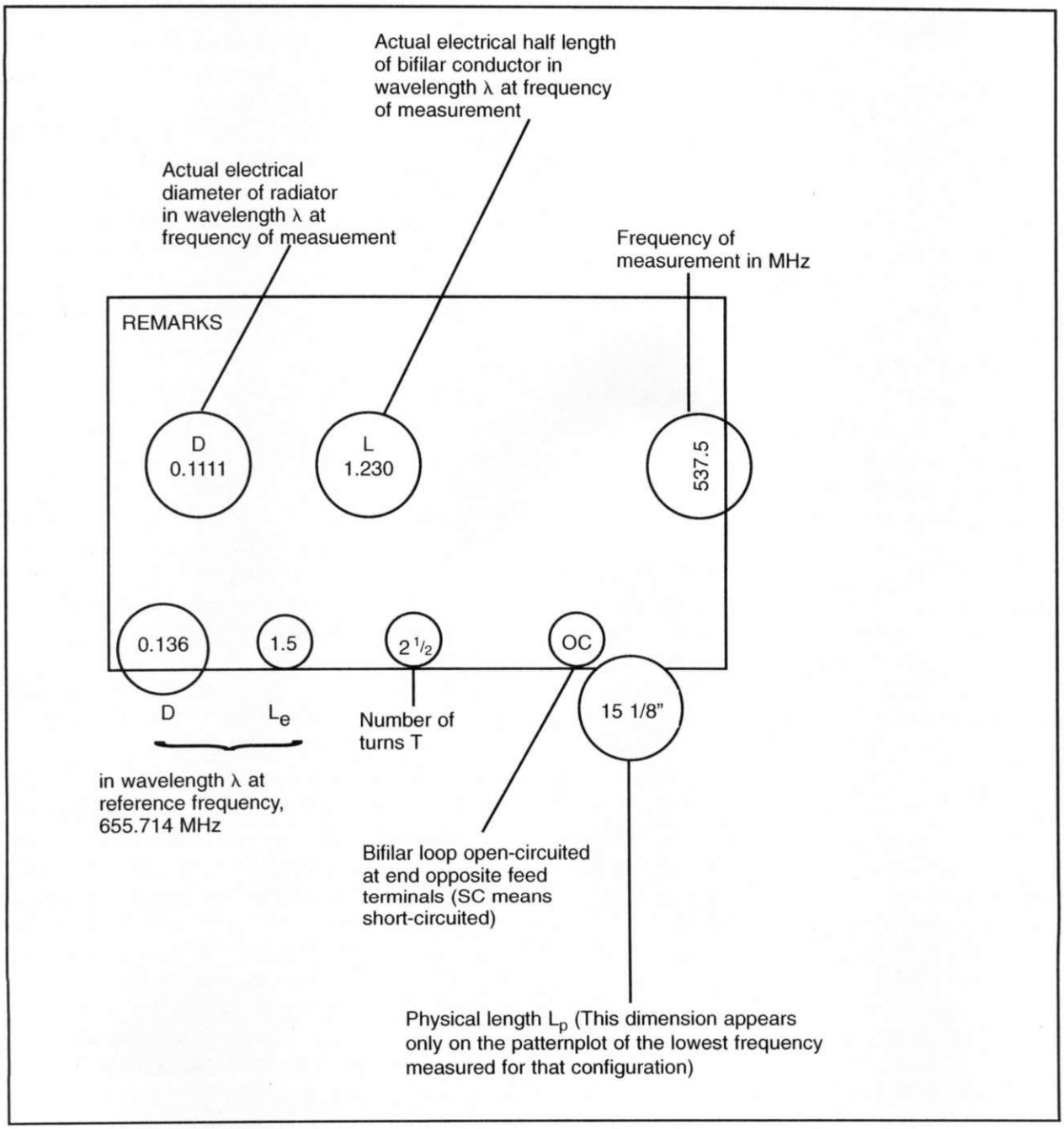

Fig 27-8. Description of entries appearing in legend box on all pattern-recorded sheets.

block appearing on each pattern plot. Refer to the sample data block (Fig 27-8) for identification of the individual parameters.

To determine the actual physical dimensions *in wavelength* λ required in designing this particular quadrifilar configuration for use at any desired frequency, the following procedure should be adopted:

Step 1. Find the physical length of 1.0 λ in the desired units at the design frequency f_{MHz}.

$$\frac{299.7924563}{f_{MHz}} \text{ meters,}$$

$$\frac{11802.85261}{f_{MHz}} \text{ inches, or}$$

$$\frac{993.5710508}{f_{MHz}} \text{ feet.}$$

Step 2. Multiply the λ dimension obtained in Step 1 by the wavelength dimension of the parameter taken from the legend box. The product is the physical dimension of the parameter appropriate for the design frequency.

To determine the actual physical length L_p at the desired design frequency, multiply the dimension found on the pattern plot by the ratio $655.714/f_{MHz}$, where f is the design frequency.

The radiation-pattern sheets are arranged in sets, or groups, with each set containing all of the patterns obtained from measurements of one specific parameter configuration at each of the many discrete frequencies in the range from 350 to 1000 MHz. With the patterns so arranged, as one leafs through a given set page-by-page starting with the lowest-frequency plot, the resulting effect of increasing the electrical size of the antenna in small increments is similar to looking at successive frames of a movie film. This feature has important value during a search through the data when seeking specific radiation characteristics, such as beamwidth, angle off-axis to peak, axial ratio, etc. This feature is an important searching tool, because these various characteristics can be seen changing dramatically as the effective size of the antenna changes with the appearance of each new successive pattern plot within the set.

(B) Measurement of Terminal Impedance

The design-data catalog generated during this experiment is invaluable to the design engineer; in addition to the collection of radiation patterns of hundreds of sizes and configurations of the quadrifilar antenna, the catalog also includes a measurement of the input-terminal impedance of the antenna for every size and configuration for which a radiation pattern was measured.

The impedance data were obtained by outputting the measurements from a Hewlett-Packard HP-8410 RF Network Analyzer to a hard-copy Smith-chart display by means of an HP X-Y pen plotter. Samples of typical impedance plots are included as Figs 27-9 and 27-10. A separate Smith chart plot was made for each antenna configuration; each plot is a continuous locus of impedance obtained by sweeping the applied RF-input frequency between approximately the same minimum-to-maximum limits as those used in the measurements of the radiation patterns. The RF feed circuit used during pattern measurements was also used during the measurements of impedance (see Fig 27-3). *It is important to observe that all impedance plots are referenced to 100 ohms.*

A very interesting and valuable impedance feature of the quadrifilar became known during this experiment. Both pattern and impedance measurements initially were made with each bifilar of the quadrifilar combination connected in a continuous, conductive condition. In this condition, the impedance versus frequency variation was as expected—a continuous locus spiraling around the 100-ohm match point, with a varying radius depending on the radiation resistance.

It subsequently was discovered that if each bifilar loop conductor is opened midway between the feed terminals (at the opposite end of the structure from the input terminals (Fig 27-2b, Point A), the impedance loci are inverted relative to frequency, as compared with the closed-loop condition. In other words, a low -impedance resonance obtained with the closed-loop condition inverts to a high-impedance anti-resonance when the loop is opened. In general, however, the radiation patterns were found to be substantially unaffected by this change in loop conditions. As a result of this fortunate change in impedance occurring between the closed- and open-loop conditions, an additional degree of freedom is available to the engineer in designing circuitry for matching the antenna impedance to suitable feed lines. The separate

closed- and open-loop conditions which existed during the measurements are indicated in the data sheets (both pattern and impedance) by the legend Sc (Short Circuit) and Oc (Open Circuit), respectively. Data obtained prior to the discovery of the dual impedance situation was measured in the closed (Sc) condition. Since the dual conditions were not known at that time, no Sc or Oc indications were included on those data. Thus, any data sheet not containing either "Sc" or "Oc" in the legend box represents a measurement made in the closed (Sc) condition.

Sec 27.5 Successful Use of the Data

This data catalog has already been proven a success from the viewpoint of its stated objectives described earlier in this book. The catalog provided useful design data for three different spacecraft antenna requirements. In one of these applications (NOAA TIROS-N, see *Ref 88*), the data obtained

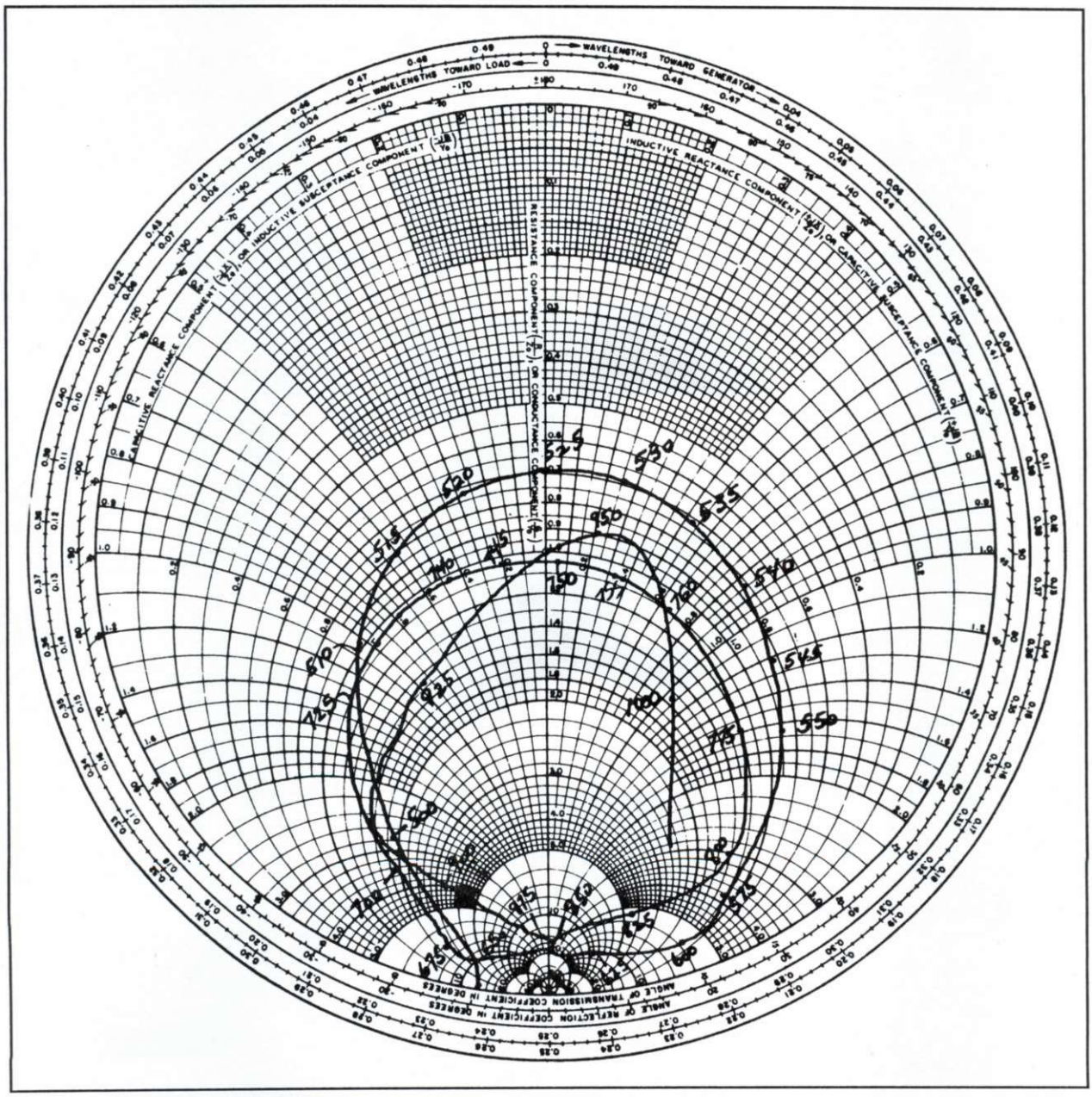

Fig 27-9. Smith Chart impedance plot, example 1.

from searching the catalog for an appropriate design was used with only minor refinements in the dimensions of the flight-component antennas compared with those of the experimental model used in generating the size-scaled data in the catalog. For additional evidence as to the utility of the catalog, both pattern and impedance measurements taken on the final flight units produced data that substantially agreed with that which appeared on the catalog sheets selected for the task. The original measurement data was obtained using the frequency scaled experimental model.

The quadrifilar antenna which was designed and fabricated for NOAA TIROS-N has replaced the ground-plane-mounted crossed-dipole antenna used on the ITOS (TIROS-M) spacecraft, because: (1) the radiation requirements for both spacecraft are similar; and (2) this quadrifilar provides the same radiation characteristics as the crossed-dipole, but without requiring the ground plane. The result of this re-

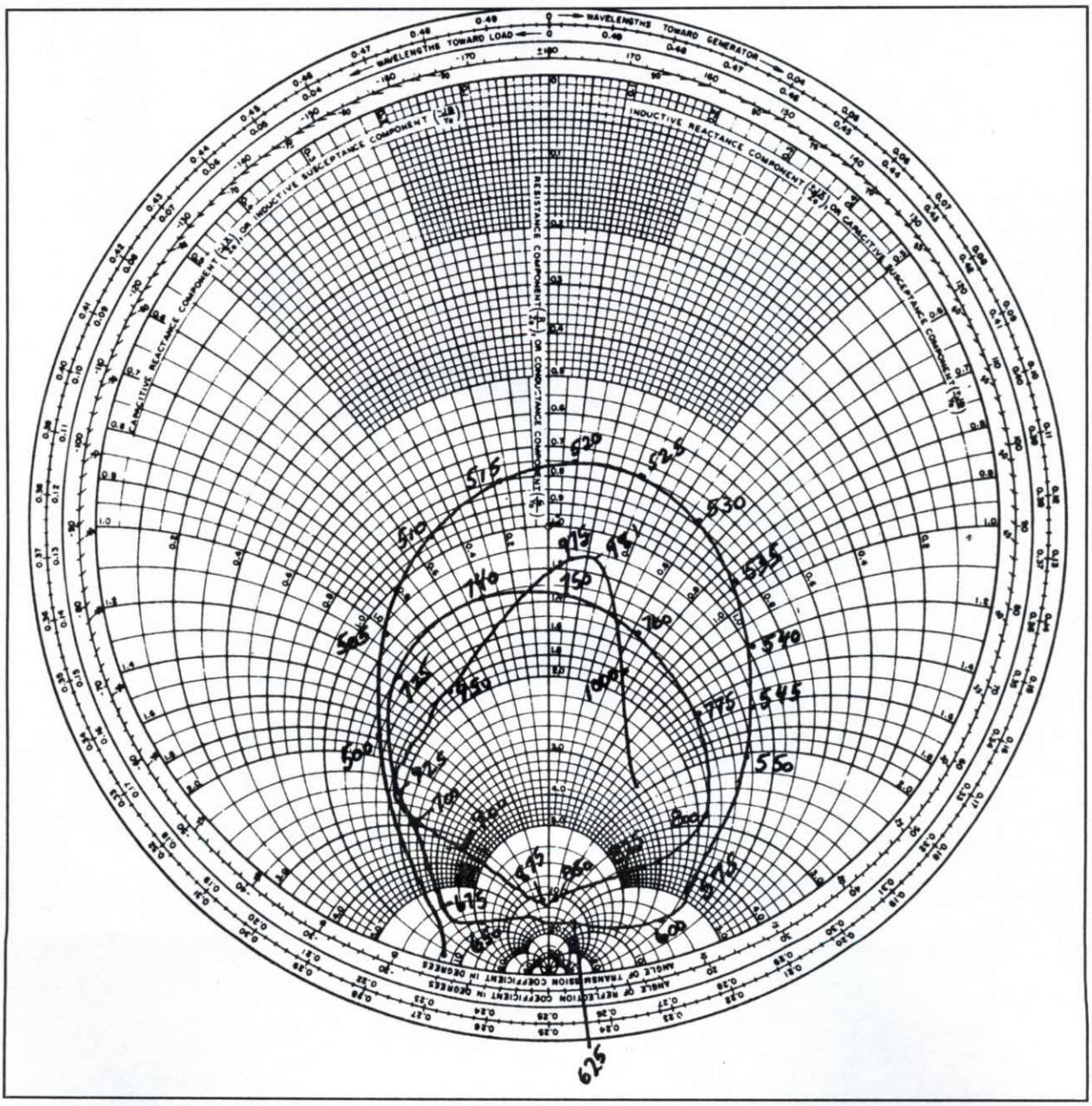

Fig 27-10. Smith Chart impedance chart, example 2.

placement is a considerable saving of space and weight by obviating the need for a ground plane.

The 70-P Block 5D spacecraft has radiation requirements similar to those of TIROS-N and ITOS, and uses a ground-plane-mounted crossed-dipole similar to that used on the ITOS spacecraft. In order to take advantage of the space and weight saving by omitting the ground plane, replacement of the crossed-dipole antenna with a quadrifilar configuration similar to the one fabricated for TIROS-N has been being contemplated for the S-band requirements on the Block 5D spacecraft.

Another search of the data catalog yielded two quadrifilar configurations which would have provided a satisfactory solution for the radiating requirements of the SATRACK project. No follow-up design effort was undertaken in this case, however, because the antenna responsibility was ultimately assumed by another vendor.

For the convenience of anyone wishing to use the data catalog described herein, a copy is available in the AED Library, and an additional copy in care of the Antenna Group of the Communications Systems Section at AED.

Chapter 28

Antennas in Space from an Historical and Archival Perspective

This chapter chronicles the series of events leading up to the launch of the world's first Earth-orbiting communications satellite. The project was known as SCORE, the acronym for Signal Communication by Orbiting Relay Equipment.

Sec 28.1 The SCORE Chronicles

Background

The SCORE project was secret until the launch occurred, with only 88 people on the "need to know list" which included the author. This chapter also tells of the vital part I played in the project. The communications-relaying equipment was carried as payload on an Air Force ATLAS B ICBM (Intercontinental Ballistic Missile) rocket, launched into orbit from Cape Canaveral on December 18, 1958. Among other firsts, it was also the first rocket-propelled missile to be launched into Earth orbit instead of following the usual down-range trajectory and landing in the Atlantic Ocean. At this early stage of the world's space programs, the Russian Sputniks 1 and 2 had been launched only a little over a year earlier, on October 4 and November 3, 1957.

The successful orbiting of the Sputniks was a shocking development, a huge surprise to everyone worldwide, and especially to the agencies in the United States that had been striving unsuccessfully to launch a satellite into orbit before the Sputniks appeared on the scene. Except for the grapefruit-size Vanguard 1 and the slightly larger Explorers 1, 2, and 3 launched in 1958 after the Sputniks, all other attempts to place a satellite in orbit failed. It was a depressing situation for the US agencies to have been outperformed by the Russians during the height of the Cold War. In the meantime, President Dwight D. Eisenhower had directed the establishment of the Advanced Research Projects Agency (ARPA) within the Department of Defense. He then directed ARPA to come up with a plan for the US to recover from the embarrassment caused by the Sputniks.

The Deception Surrounding the ATLAS Rocket

The ATLAS rocket was a product of Convair Aircraft (formerly Consolidated-Vultee) in San Diego, California. Several months earlier, ARPA Chief Roy W. Johnson had visited the Convair plant, and while there he heard that the ATLAS was capable of being launched into orbit. The wheels in his brain suddenly started turning; putting ATLAS into orbit could be just what the doctor ordered to dispel the nation's embarrassment. Johnson immediately flew to San Diego to consult with Convair's chief design engineer, who drew some pencil-sketch design changes to the ATLAS that would allow it to go into orbit. As of that moment the project became cloaked in melodramatic secrecy to avoid the kind of premature publicity that had turned some of the failed launchings into embarrassments. No one else at Convair was to know of the plan, and no formal design drawings were to be made, ensuring that no draftsman could leak the information. In fact, it was to be understood that if knowledge of the project became public it would be scrapped, the reason being that since such an attempt had never been tried there was the possibility of another failure.

Johnson took the pencil sketches to Senior Convair Engineer Travis Maloy at Cape Canaveral to have him perform the required changes to the ATLAS II that was selected for the project. However, the secrecy of the mission required that only those at Cape Canaveral with the need to know were told what was to happen to the rocket in the way of changes in the design that would allow

it to go into orbit. Maloy handed the sketches to Convair's head mechanical technician at the Cape, outlining the changes to be made on the rocket. However, because they were only informal drawings, and not signed off by Convair's chief design engineer, he refused to comply with the change orders called for in the sketches. Maloy couldn't give the technician the reason for the changes, because he was not on the need-to-know list. Maloy then telephoned Convair's chief design engineer in San Diego and told him of the problem. The chief design engineer told Maloy to put the technician on the phone, who then told the technician to make every change detailed in the pencil sketches or the technician would have to find a new job starting immediately. The technician then complied without question.

So as to not arouse suspicion, Maloy himself made many of the changes. He would also assemble some components needed for a normal down-range trajectory, but then would remove them at night when no one else was around. Another script was that a blockhouse test indicated that the fuel cutoff mechanism for the main engine was operating. If this had really been so, the engine would have stopped working too soon for the ATLAS to achieve orbit. Actually, the cutoff switch was not working at all, but the man who was checking it thought it was. One of Maloy's accomplices disconnected a wire, and at the moment when the cutoff light normally would have flashed on the panel, he instead sent in a charge that caused the light to flash on schedule. Even the blockhouse was rigged!

The ultimate irony in the deception came shortly after the launch key on the program console was pressed, initiating the launch of the ATLAS carrying the communications payload. Following standard procedure, engineers down range in the Bahamas who monitored the progress of each missile launch by radar, but not knowing of the plan to place the ATLAS into orbit, immediately signaled the Range Safety Officer for destruction of the rocket because it was going way off course, constituting a safety hazard. The Safety Officer was on the need to know list, ignored the signal, and allowed the ATLAS to continue. As we know, the ATLAS orbited successfully, and the communications system riding aboard performed brilliantly as it relayed President Eisenhower's "Christmas Message from Space" for everyone in the world to hear. For Roy Johnson the success of the communications system was the icing on the cake.

Developing the Communications System Payload

Now it's time to tell of the events relating to the development of the communications package that delivered the President's Christmas Message from Space, which was the first-ever radio-relay and repeater system operating from an Earth-orbiting platform in space. ARPA Director Roy Johnson decided that although the orbiting of an entire rocket the size of the ATLAS would in itself be a humungous display of recovery from the scientific doldrums, he considered the effect would be significantly more dramatic if an additional feature were to accompany the orbiting ATLAS. After consulting with people at the Army Signal Corps' Signal Research and Development Laboratory (SRDL) at Ft. Monmouth, New Jersey, it was decided that a first-time ever two-way communications system operating in outer space would enhance the project dramatically. SRDL was then directed to develop such a system. The system was not intended to be just a cosmetic attraction, but what turned out to be the forerunner and prototype of the practical operation of a satellite radio relay system with intercontinental capability.

SRDL and the Media Misleading the Country

At this point, speaking from first-hand knowledge, I take a contradictory position with the myriad of misleading reports on the SCORE Project dished up by SDRL and the media, reports that can be viewed on the internet by typing "SCORE" into either the Google or Yahoo search engines. One aspect appearing in all the reports is simply not true. Those reports state incorrectly that the communication system was developed and built by SRDL engineers in the SDRL laboratory at Ft. Monmouth. In addition, quoting from an article in *Life Magazine*, January 1959: "Scientists of the Army Signal Laboratory at Fort Monmouth, N.J., painstakingly adapted standard equipment, rearranged components, and hand built the final system for this specific task."

This did not happen as told in *Life Magazine* and as also reported in newspapers across the country. On the contrary, SDRL had no such equipment available, but contracted out the entire communications package that flew on the ATLAS to the RCA Laboratories in Princeton, N.J., for the design and fabrication, while SDRL engineers watched over our shoulders. Indeed, even the modification of the standard off-the-shelf receivers and transmitters used in the SCORE ground stations were performed by RCA engineers at both the RCA Laboratories and at the new RCA Astro-Electronic Products Division plant in Hightstown, N.J. The contract with RCA for both the payload package and the ground stations was signed in late June 1958. The entire RCA portion of the project was completed and delivered to SRDL around the first of September, slightly less than three months from start to finish. During the time between the RCA delivery to SRDL and the launch of the ATLAS on December 18, 1958, SDRL engineers and technicians installed the payload communications components in the ATLAS rocket at Cape Canaveral, installed additional operational-related equipment in the vans, trained technicians in the operational ground station procedures, and moved the vans to the various ground station locations.

RCA's Development of the Communications Payload and Ground Stations

The engineer who led the entire Project SCORE operation at RCA was Sidney Metzger. Working under Metzger were Seymour (Sy) Roth, who directed the design, construction, and modification of the receiver, transmitter, tape recorder, and control system that flew on the ATLAS, and author Walter Maxwell, who was responsible for the design and construction of the ground stations. Five ground stations were assembled, each built into a standard Army type V-51 van and trailer combination and each driven to a specific location across the country, at Cape Canaveral; Fort Stewart, Georgia; Fort Sam Houston, Texas; Fort Hauchuca, Arizona; and Fort MacArthur, California.

Because the goal of the project was to alleviate the embarrassment to the agencies in the US space program as quickly as possible, the activity at RCA proceeded with extraordinary expedition. After determining the components required to build the systems, it was decided to first explore the shelf inventory to determine whether there were existing components that could be used with a minimum of redesign and rework. Fortunately, a large percentage of the components that would fit the requirements with a minimum of rework were already available.

The Communications System that Flew Aboard the ATLAS as Payload

For starters, RCA was already well along in the development of the communications components —the receiver, transmitter, and tape recorder—for the TIROS weather satellite program, which began a few months earlier. The principal modification to a TIROS receiver required to ready it for the SCORE project was the change in input frequency from the 148-MHz TIROS frequency to 150-MHz SCORE frequency, a minor change. The original design and the modification to the receiver were performed by Harold Goldberg. A nearby supplier for the transmitter offered to deliver it on short notice in conformance with the required specifications. Finally, the tape recorder developed for TIROS needed only minor modifications to ready it for use with SCORE. However, an entirely new control system was developed by RCA engineer Al Aronson for remotely controlling the operation of the communications equipment in the ATLAS from the ground stations.

Modification and Assembly of Available Components for the Ground Stations

The RF engineers at RCA studied the propagation paths that would occur between the ATLAS satellite and the ground stations, and concluded that only a small amount of RF power transmitted from the ground stations would be required to obtain a high signal-to-noise ratio at the input of the receiver aboard the ATLAS. A power of 100 watts into a moderate-gain antenna was considered sufficient to provide a large margin for error. However, because these propagation paths were virgin territory, the engineers at SDRL were skeptical. Because so much emotion was riding on the success of the mission, the SDRL engineers insisted on using much higher power to be transmitted from the ground stations than that considered sufficient by the engineers at RCA.

The Army Signal Corps at Fort Monmouth made available five sets of trailer-mounted helical antennas called "Radiquads" that consisted of four helical elements, each mounted on a corner of a square horizontal ground plane. Each helical element had a gain of approximately 10 dB at the SCORE-assigned frequency of 150 MHz. Consequently, the total gain of the array of the four helical elements was approximately 16 dB, for a power gain of approximately 40 times. The Signal Corps furnished five Radiquads, one for each ground station. The SDRL specifications called for 1000 watts delivered to the Radiquads. With 1,000 watts from the transmitter along with a 16 dB gain in the antenna, the effective radiated power amounted to approximately 40 kilowatts—40,000 watts. These conditions required by the SDRL engineers gave me, this author, the information I needed to start thinking about how to develop the 1000 watts for the ground station transmitter.

I first checked with the RCA Broadcast Division to determine whether there were any 1000-watt FM broadcast transmitters on the shelf. Unfortunately, there were none available in finished condition. However, a manufacturer in Philadelphia had several 1000-watt amplifiers available that were built for the 88- to 108-MHz FM broadcast band. These would be satisfactory if they could be modified to operate at 150 MHz. However, these amplifiers needed from 10 to 50 watts of excitation power to deliver 1000 watts. I then checked with RCA's mobile communications division and discovered CarFone was the mobile unit available in quantity. CarFone was the name RCA assigned to its two-way FM mobile radios used in police cars, taxis, etc., with both receivers and transmitters operating in the 160–165 MHz band. However, the frequencies assigned to the SCORE project were 150 MHz for the uplink and 132 MHz for the downlink. Consequently, to use the CarFones both the receivers and transmitters required modification to operate on the frequencies assigned to SCORE. Three technicians from the RCA Service Company were made available to perform the modifications to the five sets of CarFone units, modifying the input frequency of the receivers to 132 MHz and the output frequency of the transmitters to 150 MHz. When the modifications were completed the CarFone transmitters, with a pair of 6146 tubes in the output delivered approximately 100 watts, more than enough to excite the 1000-watt amplifiers. The FM modulation characteristics of the CarFone transmitters also satisfied the requirements of the SCORE mission.

However, modifying the RF frequency-determining components in the plate and grid circuits of the amplifiers was quite another matter. The VHF plate tank circuit accompanying the two 4–400 push-pull amplifier tubes was a variable-length transmission line tunable only between 88 and 108 MHz. Consequently, the line was too long to resonate at the SCORE frequency of 150 MHz, requiring the fabrication of a new transmission line to operate at 150 MHz. However, when the attempt was made to operate at this frequency the amplifier was unstable. I fabricated and installed the new transmission line, but I also provided the expertise to tame the instability of the amplifier that resulted in satisfactory operation at the new frequency. Under my direction five sets of the CarFone and amplifier combination were installed in the five Signal Corps vans.

While the flight hardware was still in the RCA laboratory, the complete system was tested with each of the ground station equipments to assure that all components were operating correctly prior to delivering any portion of the system to SDRL.

The Radiquad Helical Antenna Array

Now we come to the antenna system described earlier. The stability of the 1000-watt transmitter required the load impedance to be very close to a non-reactive 50-ohm resistance. The impedance presented by the four helices connected in parallel was miles away from 50 ohms, thus requiring an impedance-matching network inserted between the antenna array and the transmitter to ensure the stability of the transmitter. Using data I obtained from measuring the impedance of the antenna array, I then designed and constructed the transmission-line stub matching network that provided the required 50-ohm impedance appearing at the input of the transmission line connecting the transmitter to the four-helix Radiquad antenna array. The array was mounted on a searchlight base atop the trailers attached to the V-51 vans. The receivers, with their input tuned to 132 MHz, operated satisfactorily, oblivious to the input impedance mismatch appear-

ing at that frequency, while the transmitter was matched to the 150-MHz transmitter frequency.

The Final Operation

The SCORE package worked perfectly, responding to 78 real-time and store–and-forward voice and teletype transmissions between ground stations located at Cape Canaveral, and in Georgia, Texas, Arizona, and California. On December 19, the day after the launch, President Eisenhower's recorded Christmas Message from Space was broadcast from the satellite:

This is the President of the United States speaking. Through the marvels of scientific advance, my voice is coming to you from a satellite traveling in outer space. My message is a simple one: Through this unique means I convey to you and all mankind, America's wish for peace on Earth and goodwill toward men everywhere.

After 12 days the batteries failed. On January 21, 1959, the satellite re-entered the Earth's atmosphere and burned up.

Dr. Hans K. Ziegler, writing in 1960 when he was chief scientist of US Army Signal Research and Development Laboratory, characterized SCORE as the first prototype of a communications satellite, and the first test of any satellite for direct practical applications. According to him, the significance of the experiment lay in the fact that it effectively demonstrated the practical feasibility of worldwide communications in delayed and real-time mode by means of relatively simple active satellite relays. During the 12-day life of its batteries, the satellite was interrogated by Signal Corps ground stations 78 times, using voice and teletype messages for the communications tests with excellent results. The project provided valuable information for the design of future communications satellites. An exact copy of the communications package that flew on the ATLAS can be seen in the Smithsonian Institution Museum in Washington, D.C.

It seemed only fitting that all RCA personnel who were involved with the project, including myself, were invited to the Smithsonian to participate in the ceremony sponsored by the State

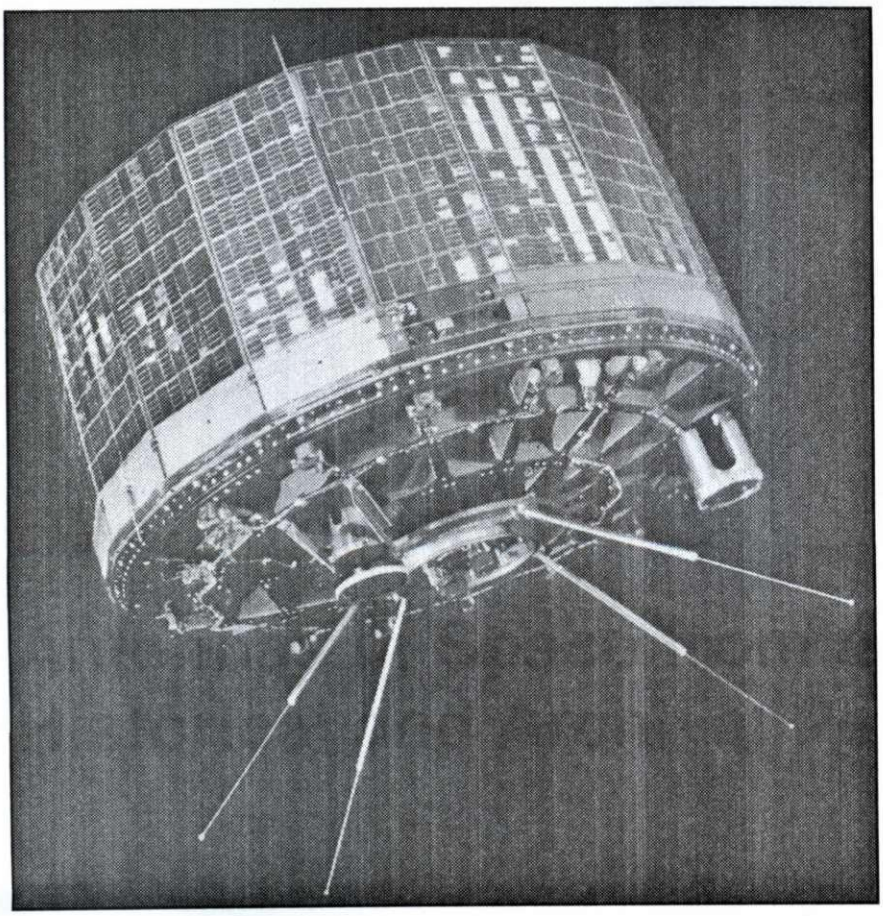

Photo 28-2.1. TIROS 1 weather satellite showing solar cells, cameras, and the author's multi-frequency transmitting antenna array.

Department, the U.S. Army Signal Corps, and the Advanced Research Projects Agency, dedicating the communications package to the museum.

Sec 28.2 The TIROS Weather Spacecraft

On the Design and Development of the Antenna System Used on the World's First Weather Satellites, TIROS 1–8, performed by the Author

Preface

In the first and second editions of this book we tossed in a few tidbits concerning the multi-frequency antenna system developed by the author that flew on the world's first weather satellite, TIROS 1. These tidbits appeared in Chapter 1, and again earlier in this section. This third edition of *Reflections* appears to be an appropriate place to archive for posterity a detailed description of the design and development of the TIROS 1 antenna system. However, I believe it is appropriate for the reader to have some historical background concerning the development of this antenna system that makes this new section seem especially important to me, and hopefully of interest to the reader.

Historical Background on the Origin of the World's First Weather Satellite, TIROS 1

In 1957, people from the U.S. Army's Advanced Research Projects Administration (ARPA) in Huntsville, Alabama, who included the eminent rocket scientist Werner von Braun, approached us at the RCA Laboratories in Princeton, N.J., concerning the possibility of designing and building an orbiting spacecraft that could photograph the geographic environs of the Soviet Union. After a short study we found that we could, and we subsequently received a performance contract to build it. My assignment was to develop the antenna system for receiving commands from the ground stations and also for transmitting the pictures obtained by the cameras on-board the spacecraft back to the ground stations. After progressing with the project to the point of being close to testing the prototype, our contract was suddenly terminated. It seems that Congress had just learned of this project, which had been classified as top secret, and ordered it stopped, because due to the timing, it was considered a politically dangerous undertaking. The timing was considered crucial diplomatically, because at that time the State Department was in the throes of quelling the fallout from Gary Francis Powers' U2 reconnaissance plane having been shot down over the Soviet Union.

During the few weeks that followed, the Washington, D.C. rumor mill spread the news that RCA had built a spacecraft capable of photographing the Earth from an orbiting platform. People at the U.S. Weather Bureau learned of it and came to us with the question: "Could you redesign the spacecraft to perform as an orbiting weather station?" We replied that we could, and then entered into a contract to build TIROS 1. (TIROS is the acronym for **T**elevision **I**nfra **R**ed **O**bservational **S**atellite.) During the next few months we completed the redesign of the new spacecraft. My new assignment was to redesign the antenna system for the new spacecraft. The completed spacecraft TIROS 1, the world's first weather satellite, was launched from Cape Canaveral on April 1, 1960, after which the first pictures of Earth and clouds ever taken by cameras in an orbiting weather satellite were transmitted back to Earth on my antennas during the first orbit. All systems were GO!

Photo 28-2.1 shows a flight model of the TIROS 1 weather satellite including solar cells, cameras, and my multi-frequency crossed dipoles.

Overview of the Spacecraft RF System

The transmitting antenna system designed by the author for TIROS 1, used for transmitting data obtained from the TV and IR cameras, comprised a multi-frequency array of two crossed-sleeve dipoles consisting of four monopoles mounted on the bottom of the spacecraft. The antenna array was fed by four transmitters operating simultaneously on different frequencies in two frequency bands, 108 and 235 MHz; the TV transmitter on 235.0 MHz; the infrared transmitter on 237.5 MHz; and two telemetry transmitters, one operating on 108.0 and the other on 108.03 MHz. The TV transmitter is shown in Photo 28-2.2 and the telemetry transmitter is shown in Photo 28-2.3.

The transmitters were coupled to the antenna array by a complex impedance matching network designed by me comprising ring diplexers, baluns, frequency-selective filters, open- and short-circuit stubs, and phasing lines, all fabricated in 25-, 50-,

and 70-ohm printed-circuit, sandwich-form stripline transmission lines. The network provided four outputs, one for each monopole, with progressive relative phases of 0, 90, 180, and 270° for feeding the two crossed dipoles in quadrature phase to obtain circular polarization in the 108-MHz telemetry band and the 235-MHz video band. (In later models the telemetry transmission frequencies were changed from the 108-MHz band to the then new 136-MHz band.) The two telemetry transmitters each delivered 30 milliwatts to the network, and each of the two video transmitters delivered 5 watts.

The well-known technique of scale modeling was used during the development of the antenna array for measuring both the radiation patterns of the antenna array and the terminal impedances. Taking many impedance measurements of various sleeve configurations at different frequencies in the experimental process leading toward the final con-

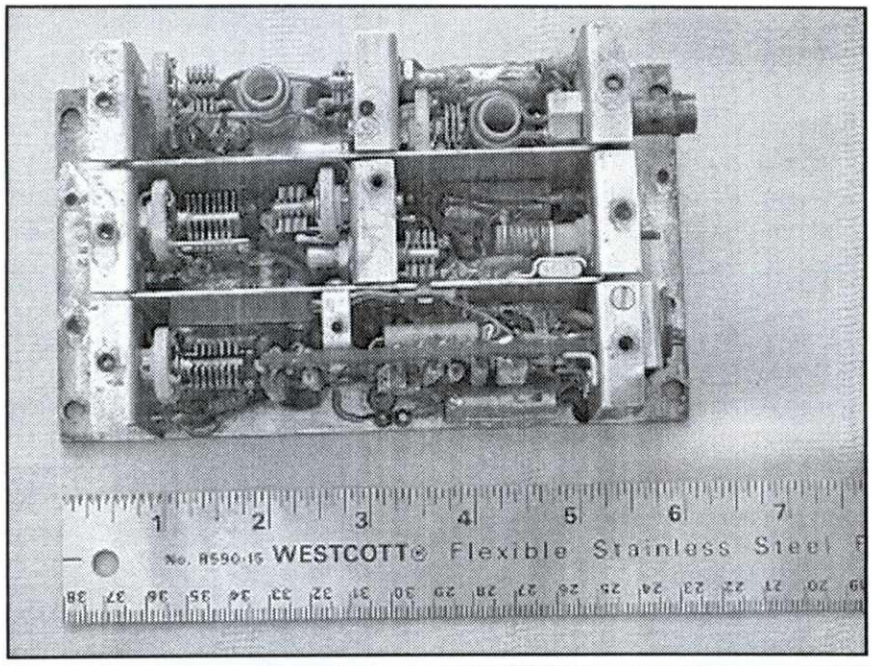

Photo 28-2.2. 235-MHz, 5-watt video transmitter (pencil tubes, no solid state).

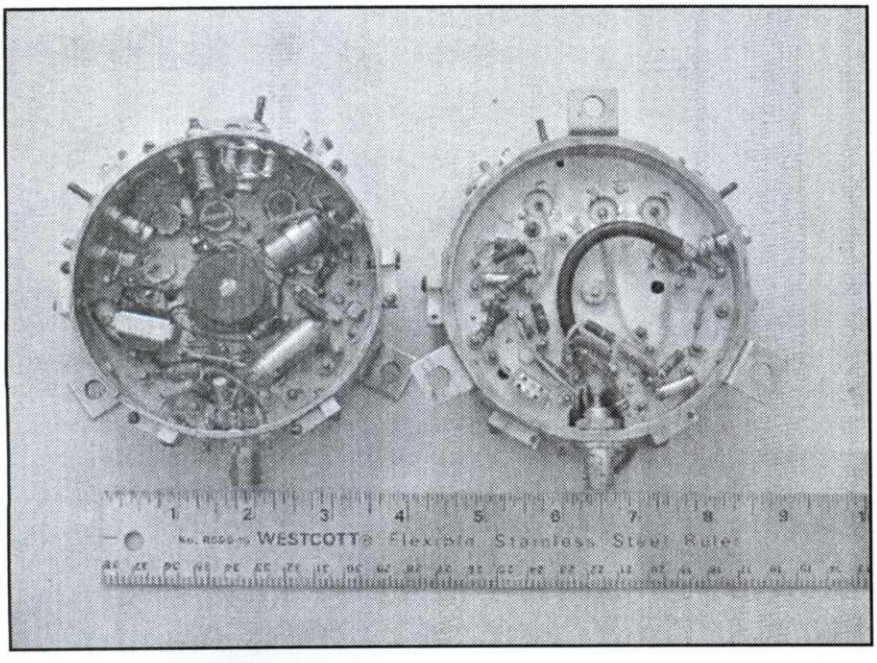

Photo 28-2.3. 108-MHz, 30-milliwatt beacon and telemetry transmitter, (L) top view, (R) bottom view.

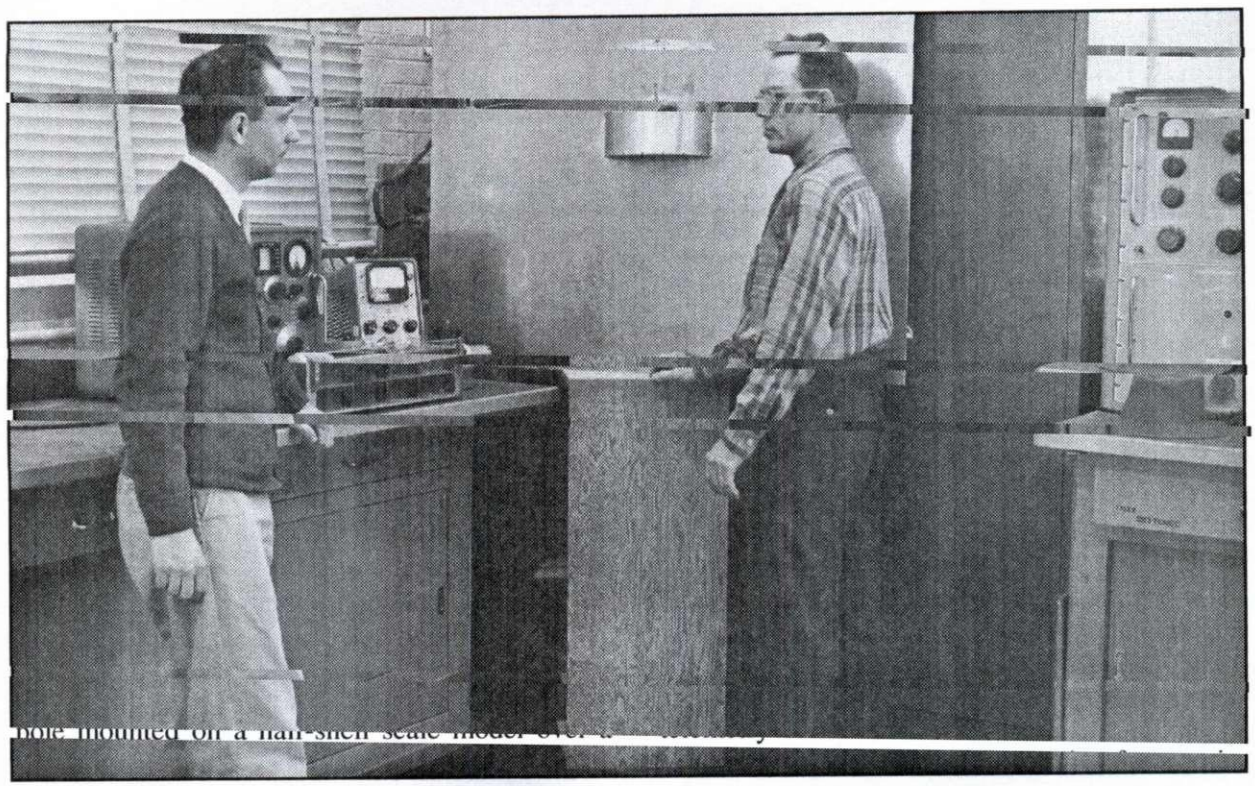

Photo 28-2.4. Author Maxwell with technician John Luzansky (L) viewing the half-shell 1:4 scale model of TIROS 1 mounted on ground plane for obtaining antenna impedance data during development of the antenna system. Note the HP-805 slotted line near Luzansky's left hand, used for obtaining the impedance measurements.

figuration was simplified by using only one monopole mounted on a half-shell scale model over a ground plane, because it avoided the difficult obstacles involved in measuring through a complex feed system that would be required if two dipoles or four monopoles had to be fed simultaneously. Only one monopole was needed for obtaining valid impedance measurements during the development, because its image and that of the half-shell model of the spacecraft both were formed in the four-foot-square aluminum ground plane on which the model was mounted. I used the arrangement shown in Photo 28-2.4 to make slotted-line impedance measurements during the experimental development. The tiny sleeve monopole is just barely visible projecting upward from the top of the half-shell model. Using the techniques of scale modeling and ground-plane imaging achieves the same results as with a full-scale model. However, scale modeling was preferred here because it permitted using smaller components and a smaller work space for conducting the experiments. The model was scaled down four-to-one from the full size. Hence, the test frequencies were 430–440 MHz for the telemetry band and 930–950 MHz for the video band, four times the actual operating frequencies. The equipment used in the impedance measurements were Hewlett-Packard HP-608C and HP-612A signal generators, an HP-805A slotted line, and an HP-415B SWR indicator, seen located on the bench at the left of the ground plane in the photo. A slide rule and a Smith Chart were used for correlating the impedance data obtained from the measurements. Hand calculators had not yet been developed.

It should be noted that radiation pattern and impedance measurements obtained for the earlier spy satellite that was scrapped were also made using scale models, but with 5-to-1 scale. The scale models for the spy satellite appear in Photo 28-2.5, and the scale model for TIROS 1 appears in Photo 28-2.6.

Photo 28-2.7 shows the author at the RCA Laboratories working on the crossed-dipole transmitting antenna system of TIROS 1. The spacecraft mockup in this photo is a full-scale electrical

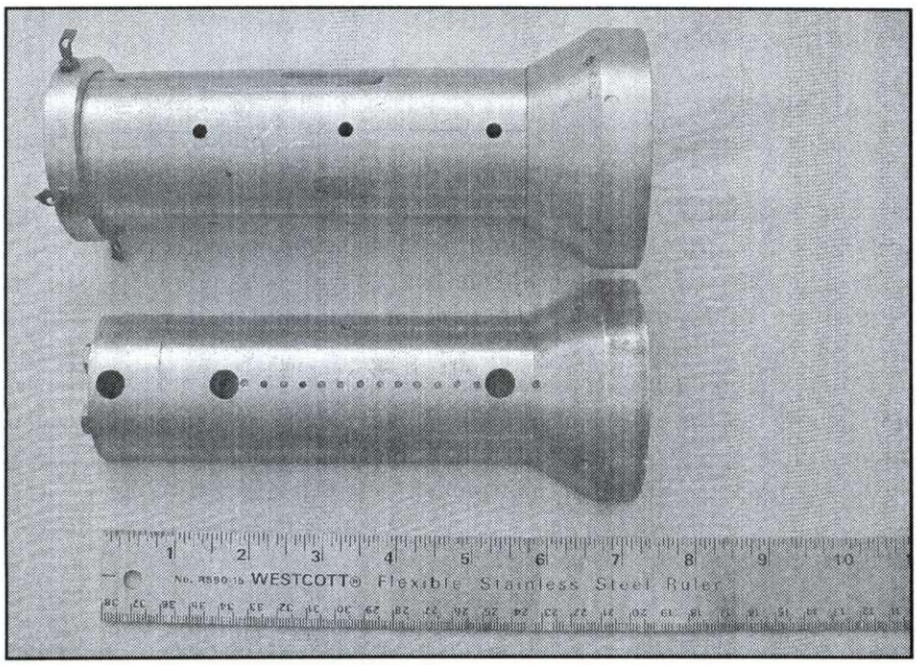

Photo 28-2.5. 5:1 scale models of unfinished spy satellite that preceded TIROS. Cylindrical model at top was used for obtaining radiation pattern measurements of various antenna configurations. Half-cylindrical model below was used for impedance measurements of various antenna configurations while mounted on 4 ft × 4 ft aluminum ground plane shown in Photo 28-2.4.

model constructed of sheet aluminum over a wood frame, used for full-scale testing all of the spacecraft antenna systems during the design phase. The model was constructed to be electrically identical to the flight models to obtain valid measurements of impedance and radiation patterns as various antenna configurations emerged during the design phase. The makeshift mounting for the model was used temporarily while the antenna test laboratory was being constructed at RCA for the TIROS project. An unused flight model of TIROS 1 with the my antennas attached is on display in the spacecraft museum of the Smithsonian Institution in Washington. The writing that follows describes in detail the progress of the design of the revised antenna system.

The General Approach to the Design of the Antenna System

There were two separate, but related projects in the development of the antenna system: the physical radiators of the antenna array required to radi-

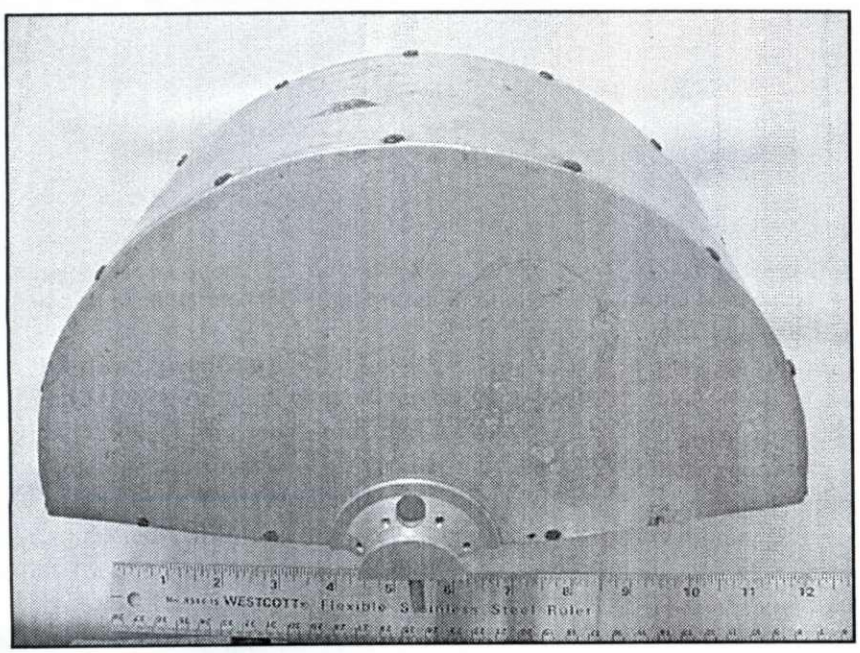

Photo 28-2.6. Half-shell 4:1 scale model of TIROS 1, seen mounted on 4 ft × 4 ft aluminum ground plane in Photo 28-2.4. Used for impedance measurements during development of transmitting antenna at 432 MHz (108 MHz × 4) and 940 MHz (235 MHz × 4).

and the coupling and impedance-matching networks

ate on four different frequencies simultaneously, and the coupling and impedance-matching networks to couple four transmitters to the antenna array, with all transmitters operating simultaneously on different frequencies without mutual interference. We will first discuss the requirements and development of the physical radiators of the antenna array.

The requirements:

1. The array must radiate efficiently on four specifically assigned frequencies in two frequency bands, 108 and 236 MHz. The specific frequencies are 108, 108.03, 235, and 237.5 MHz.

2. The array must radiate on all four frequencies with a radiation pattern shape that assures a reliable signal level received at the ground stations, regardless of the attitude of the spacecraft while spinning on its axis.

3. To satisfy requirement 2, all radiation from the array must be of circular polarization.

To obtain circular polarization from the array

the basic configuration of two orthogonally positioned dipoles was determined to be the correct choice—i.e., two dipoles with each half in the same plane, mounted on the bottom side of the spacecraft. However, because the third-stage rocket is attached to the spacecraft at the center of the spacecraft, to accommodate the rocket each half of the two dipoles was separated radially into four separate monopoles attached to a mounting ring surrounding the rocket-mounting location. Thus, the antenna array comprises four monopole radiators extending from the bottom section of the spacecraft at a downward angle of 45° spaced equally around the spacecraft. Each

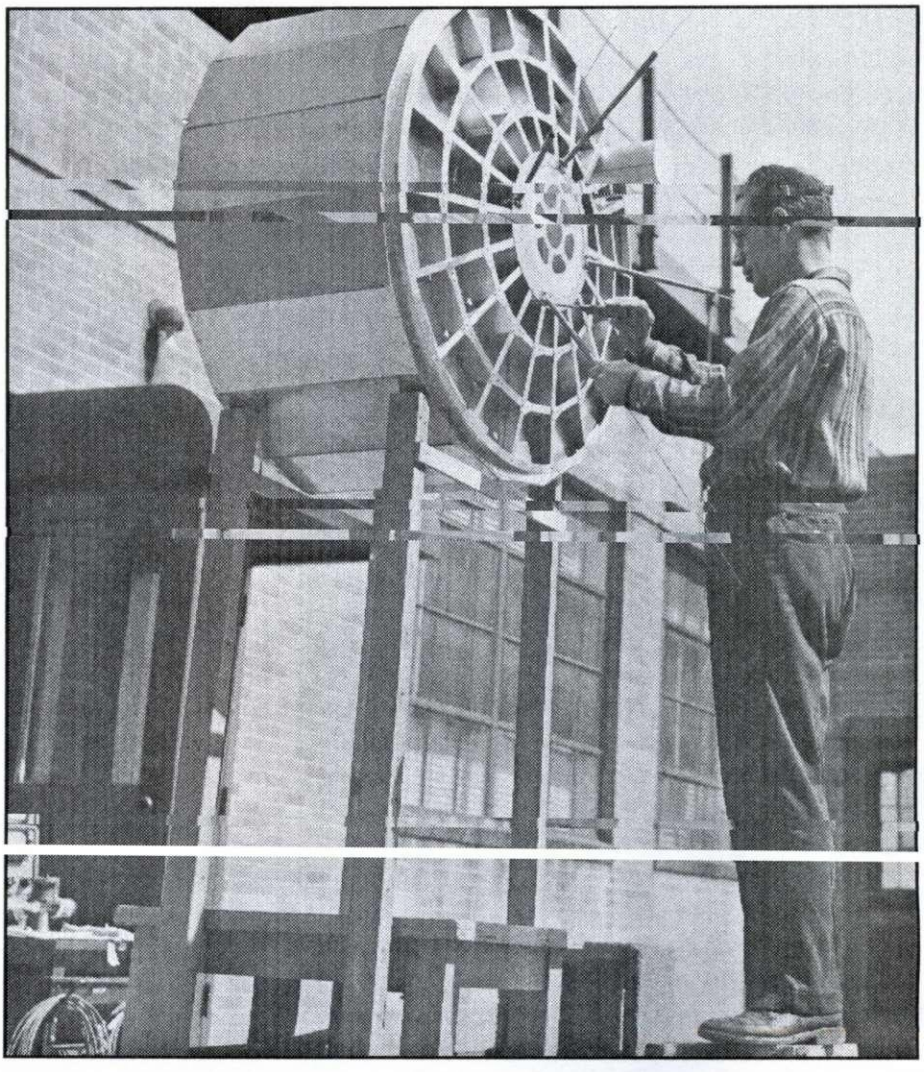

Laboratories (David

Photo 28-2.7. This picture, taken in 1959 at the Antenna Lab of the RCA Laboratories (David Sarnoff Research Center, Princeton Research Center), shows the full-scale TIROS 1 electrical-test model, with author Maxwell working on the four-monopole transmitting antenna array during its development.

radiator comprises a sleeve section with a coaxial rod extension. The sleeve section is the primary radiator for the frequencies in the 236-MHz band and the combination of the sleeve and rod extension is the radiator for the frequencies in the 108-MHz band. The layout diagram for the physical diagram ofthe sleeve and rod radaiator can be seen in Fig 28-2.9. The four monopoles can be seen pictorially in Photos 28-2.1 and 28-2.9. In Fig 28-2.9 the number 2 balloon indicates the mounting ring that supports the monopoles; number 4 indicates the BNC connector; number 5 indicates the Teflon™ insulator that separates the monopole base from the mounting ring; number 14 indicates the Teflon™ slug that tunes the inner section of the sleeve, which isolates the rod extension at the 236-MHz frequency; number 16 is the threaded screw brazed to the rod extension, screwed into the mounting base for adjusting the length of the rod extension.

The effort in the development of the four monopoles was greatly simplified by knowing that all four in the array can be identical, thus allowing the impedance-measurements during the design phase to be focused only on a single monopole. Attempting to feed all four development monopoles simultaneously and making design changes in four instead of one would have been foolhardy and practically impossible. Further, the mutual coupling between two opposing monopoles in the array must be considered, because these two monopoles comprise a dipole whose input terminals are separated by a distance greater than in a normal dipole configuration. Consequently, additional simplification was achieved by eliminating the opposing monopole and simulating it with a single monopole appropriately positioned on a half-shell portion of the spacecraft mounted on an extensive ground plane. The mirror image of the single monopole appearing in the ground plane substituted for the opposing mono-

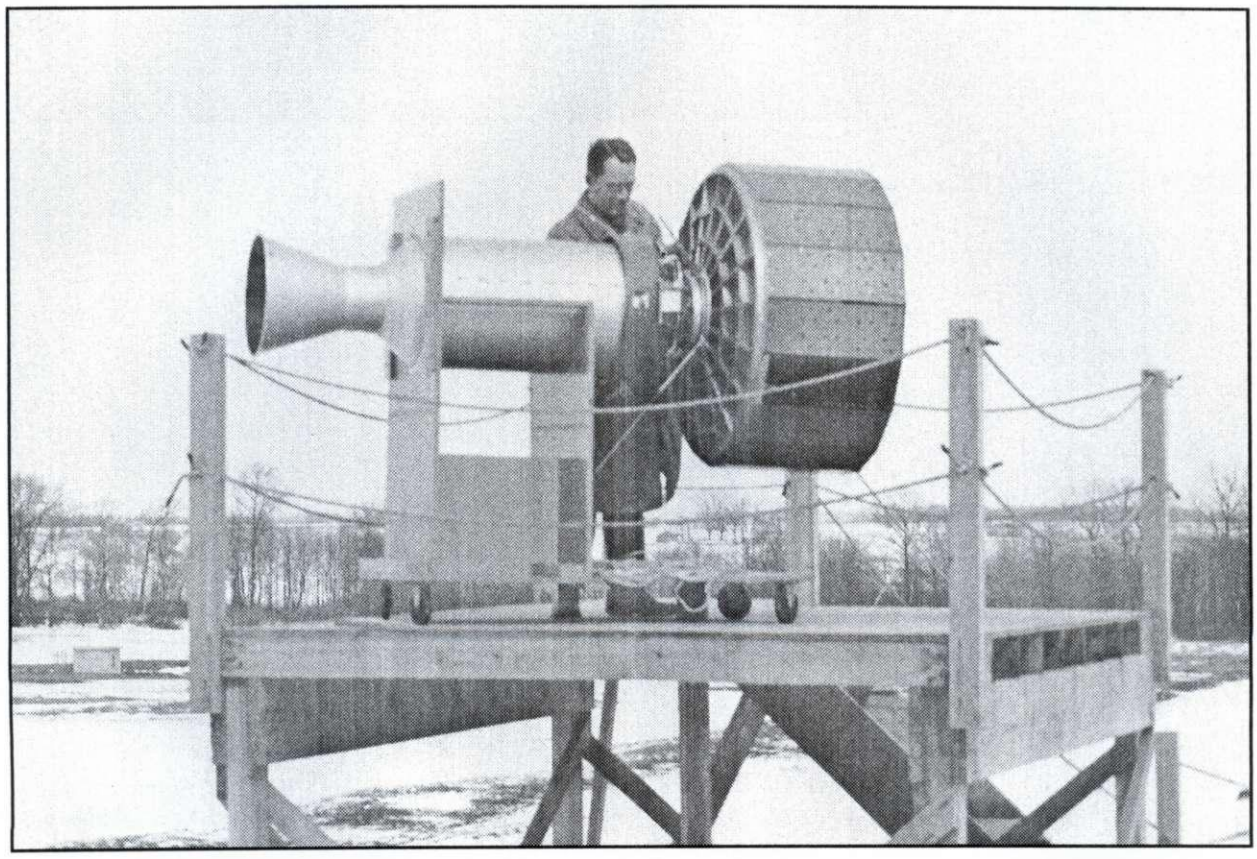

Photo 28-2.8. The author assembling an electrical test model of TIROS 1 to an empty third-stage booster rocket in 1959 in preparation for taking antenna radiation patterns to determine the effect of the rocket on the radiation patterns of the spacecraft antenna system.

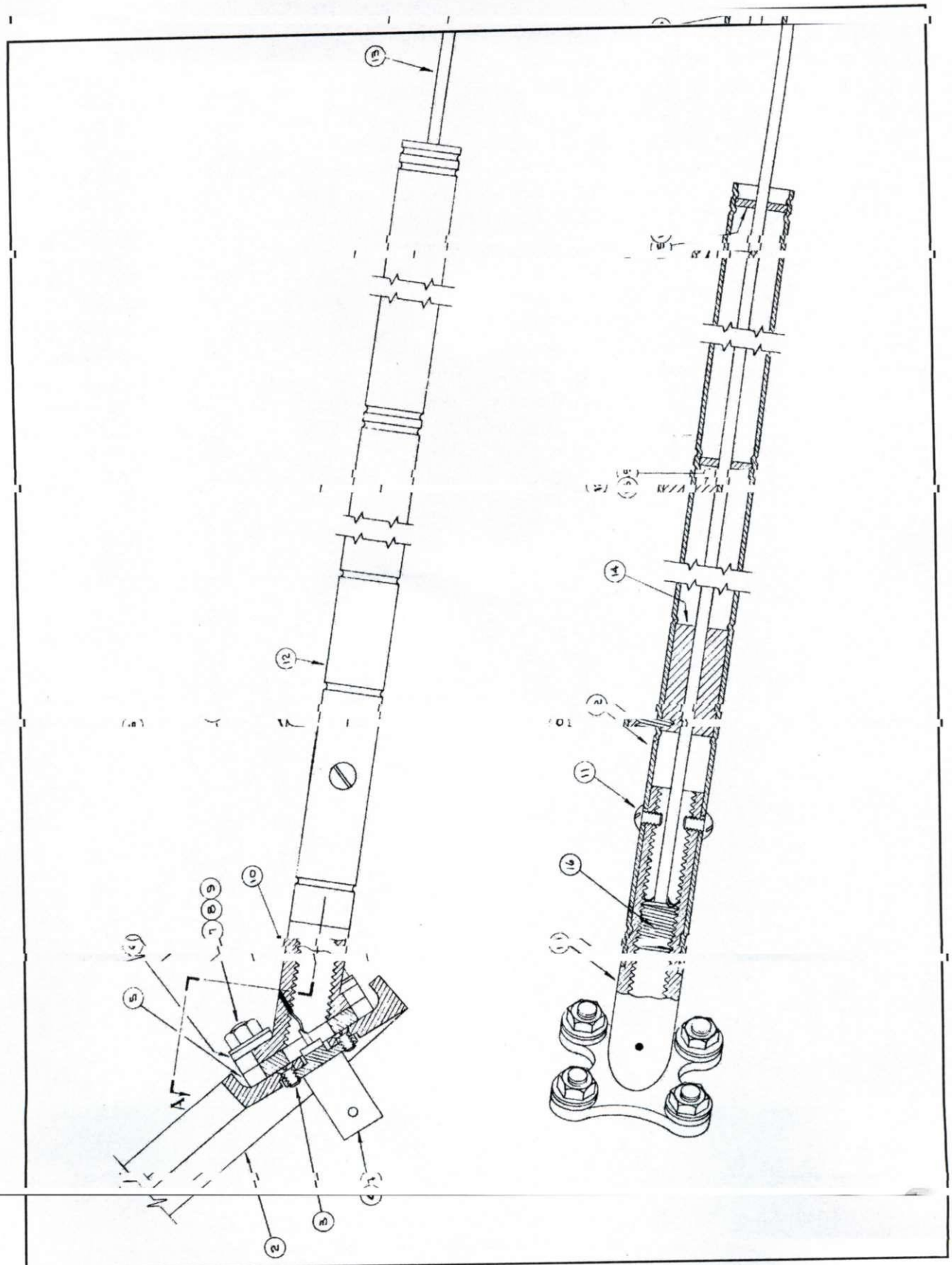

Fig 28-2.9. The layout diagram for the physical diagram of the sleeve and rod radaiator.

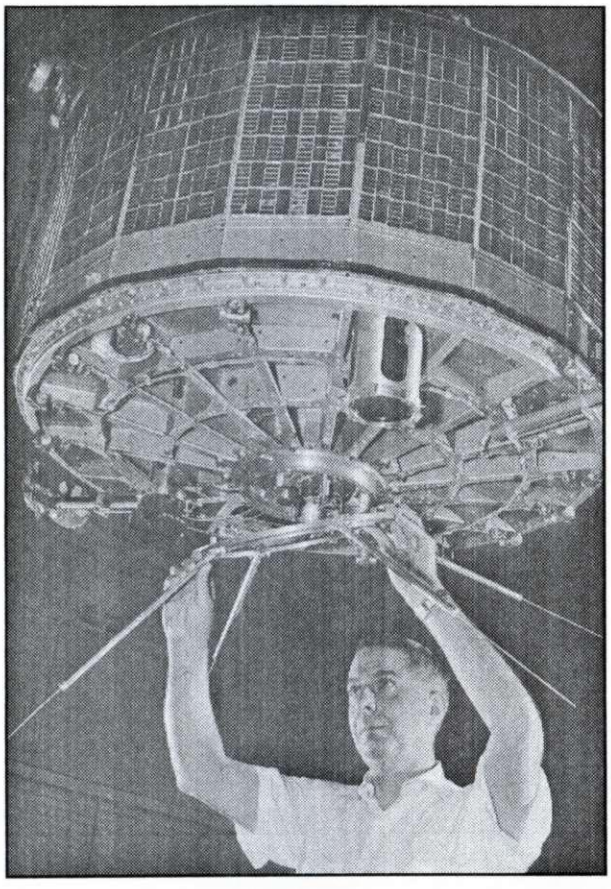

Photo 28-2.9. RCA mechanical technician Herb DeCerbo attaching the author's antennas to the TIROS 1 spacecraft.

pole, thus satisfying both the electrical and physical requirements for measuring the impedance of the single monopole.

We took the simplification of the design effort even further by using scale modeling during the development, thus reducing both the size of the design model and the space required to make valid impedance and radiation-pattern measurements. Accordingly, the size of the model was reduced by a ratio of 4-to-1, with a corresponding increase in frequencies by a ratio of 1-to-4. The simplified design and development model used for impedance measurements appears in Photo 28-2.4, just barely showing the half dipole (monopole) positioned on the 4-to-1 size half portion of the spacecraft mounted on a four-by-four foot square aluminum ground plane. Also shown in the photo is the Hewlett-Packard HP-805A Slotted Line, with which all impedance measurements (hundreds) were made and plotted on a Smith Chart. At that time, in 1958, the slotted line was the most advanced instrument available for measuring impedances at the frequencies involved. In addition, all calculations were performed on a slide rule, because desk-top computers and hand-held calculators had not yet been developed. The half-portion of the model is also shown in Photo 28-2.6. (Five-to-one scale models were used in the development of the antenna system for the earlier spy satellite, shown in Photo 28-2.5. The model at the top was used for measuring the radiation patterns and the half-portion shown at the bottom was used along with the aluminum ground plane for measuring impedances of the antenna, as seen in Photo 28-2.4.)

Signal generators used during the early antenna development were Hewlett-Packard HP-608C and HP-612. The HP-415B SWR indicator was used with the HP-805A slotted line for measuring the impedances of the scale model versions. The impedance measurements on the full-scale electrical test model of the spacecraft, shown in Photo 28-2.7, and all final testing of the flight model antennas, were made using the HP-608C signal generator, Polytechnic Research and Development's Standing Wave Detector (reflectometer) PRD-219 and the HP-415B SWR indicator. The PRD-219 indicates the magnitude of the reflection coefficient as a measure of the SWR, and the angle of the reflection coefficient is indicated at the null in the SWR curve, required to obtain the complex impedance appearing at the terminals of the antenna.

Delving more deeply into the description of the radiator assembly, we begin with the base mounting, which was machined to permit a tight fit for the aluminum tubing that serves as the sleeve radiator for the 236-MHz frequencies, as shown in Photo 28-2.10. The inner portion of the base was threaded to accommodate length adjustment of the rod extension for the 108-MHz frequencies. Because the sleeve radiator is approximately $\lambda/4$ in length, both inside and out, in conjunction with the coaxial rod extension as the center conductor, the inner portion of the sleeve becomes a shorted $\lambda/4$ section of coaxial transmission line at 236 MHz. The shorted $\lambda/4$ inner section thus performs as a trap at 236 MHz and isolates the portion of the rod extending beyond the sleeve at 236 MHz. Therefore, the input impedance at 236 MHz is

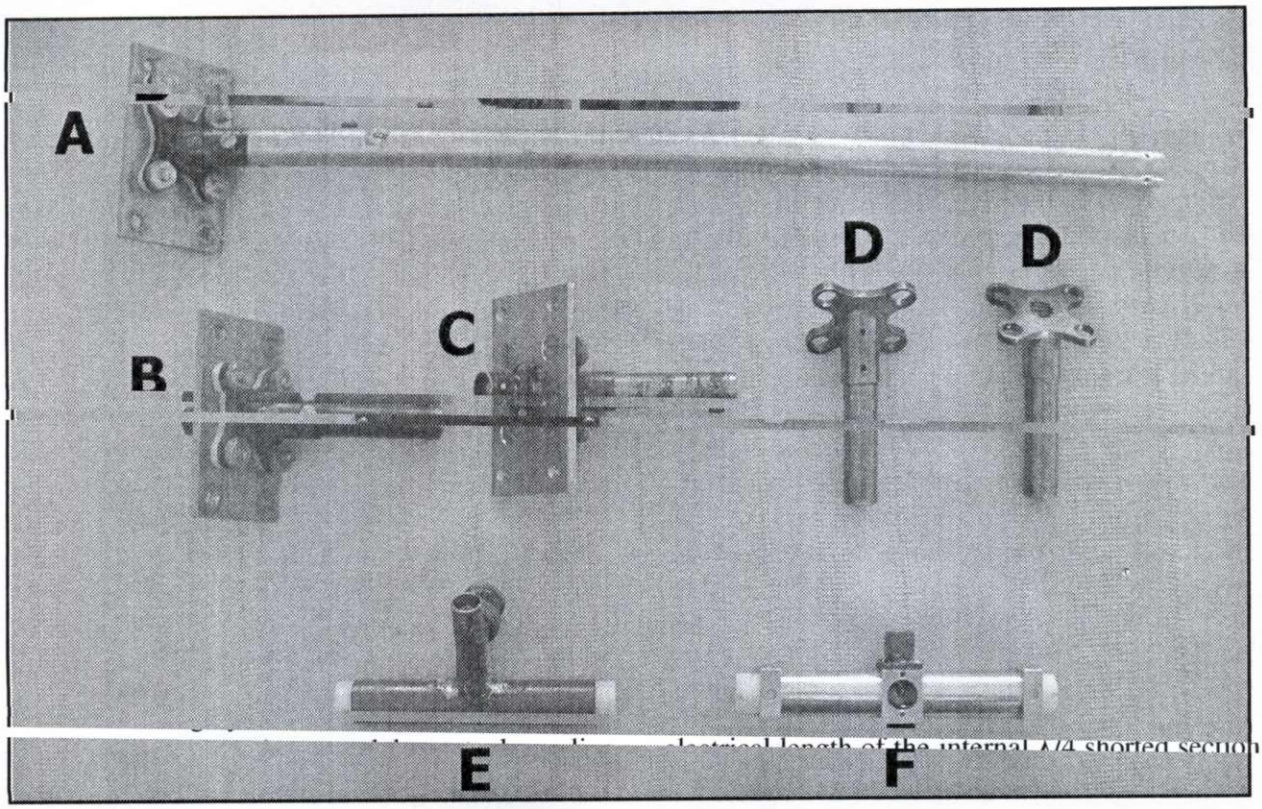

Photo 28-2.10. (A) TIROS 235-MHz sleeve radiator fitted to mounting base. (B, C, and D) Various views of the radiator mounting base. (E) Development model of 136-MHz notch filter. (F) Flight model of 136-MHz nnotch filter.

determined largely, but not entirely, by the length and diameter of the sleeve, and the mutual coupling of the collinear relationship between the sleeve and the extended portion of the rod.

For ease in developing the coupling and matching unit it was desirable to focus the mechanical design to achieve the terminal impedance of 50 + *j*0 ohms for the 236-MHz radiators. Then, by designing the matching unit to exhibit characteristic impedance Z_0 of 50 ohms throughout, no impedance matching was required to match the radiator to the 236-MHz transmitters. This feature simplified the design in that the only impedance matching circuitry required is for operation at 108 MHz. However, forcing the terminal impedance of the 236-MHz radiators to a resistive 50 ohms required a little fancy manipulation. First off, the bare λ/4-length sleeve yielded a resonant impedance of approximately 35 ohms. How can we increase it to 50 ohms? Black magic? Not really—just a little creative engineering.

It was discovered that by alternately varying the electrical length of the internal λ/4 shorted section of the sleeve and the length of the rod extension, we could control the mutual coupling between the rod extension and the sleeve, and thus force the input impedance of the half dipole to be 50 + *j*0 ohms at 236 MHz. A moveable Teflon® slug was inserted into the sleeve to vary the electrical length of the internal section. A narrow slot in the sleeve allowed adjustment of the slug position to obtain the required electrical length of the shorted section. A threaded screw brazed to the end of the rod extension and screwed into the mounting base allowed varying the length of the rod extension to control the mutual impedance between the sleeve and the rod extension.

The final length of the rod extension (adjusted by turning the rod) determined by obtaining the 50 + *j*0 impedance at 236 MHz, simultaneously determined the input impedance at 108 MHz to be 150 − *j*100 ohms. This is the impedance that requires

matching to 50 ohms by the circuitry in the coupling and matching network fabricated in stripline, described in the next section.

The Stripline Coupling and Matching Network

In Chapter 1 we briefly mentioned the spacecraft antenna system developed by the author that transmitted signals on four different frequencies from a single antenna array. In this section we'll describe and illustrate the multi-frequency antenna coupler used to couple four transmitters operating simultaneously on four different frequencies into one

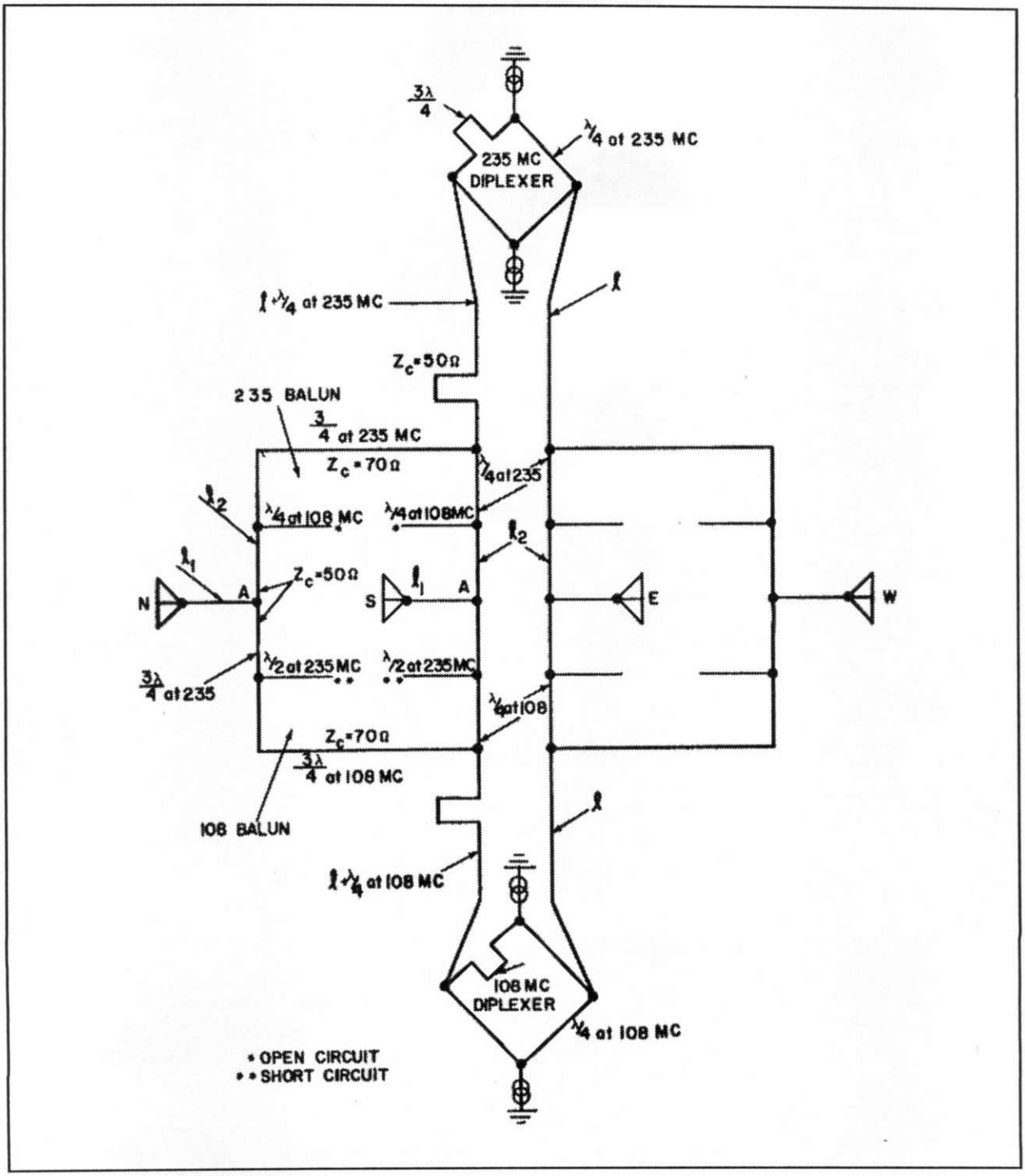

Fig 28-2.1. Circuit diagram of coupling and impedance-matching network for TIROS 1.

antenna array. Two frequency bands were used on the TIROS 1, 2, and 3 spacecraft, at 108 and 236 MHz, with two beacon frequencies at 108.0 and 108.03 MHz; the TV, or video, signal frequency at 235.0 MHz; and infra red (IR) signal frequency at 237.5 MHz, one transmitter on each of the four frequencies. However, beginning with TIROS 4, these two original beacon frequencies were changed to 136.23 and 136.92 MHz on all subsequent spacecraft through TIROS 8 to avoid interference with

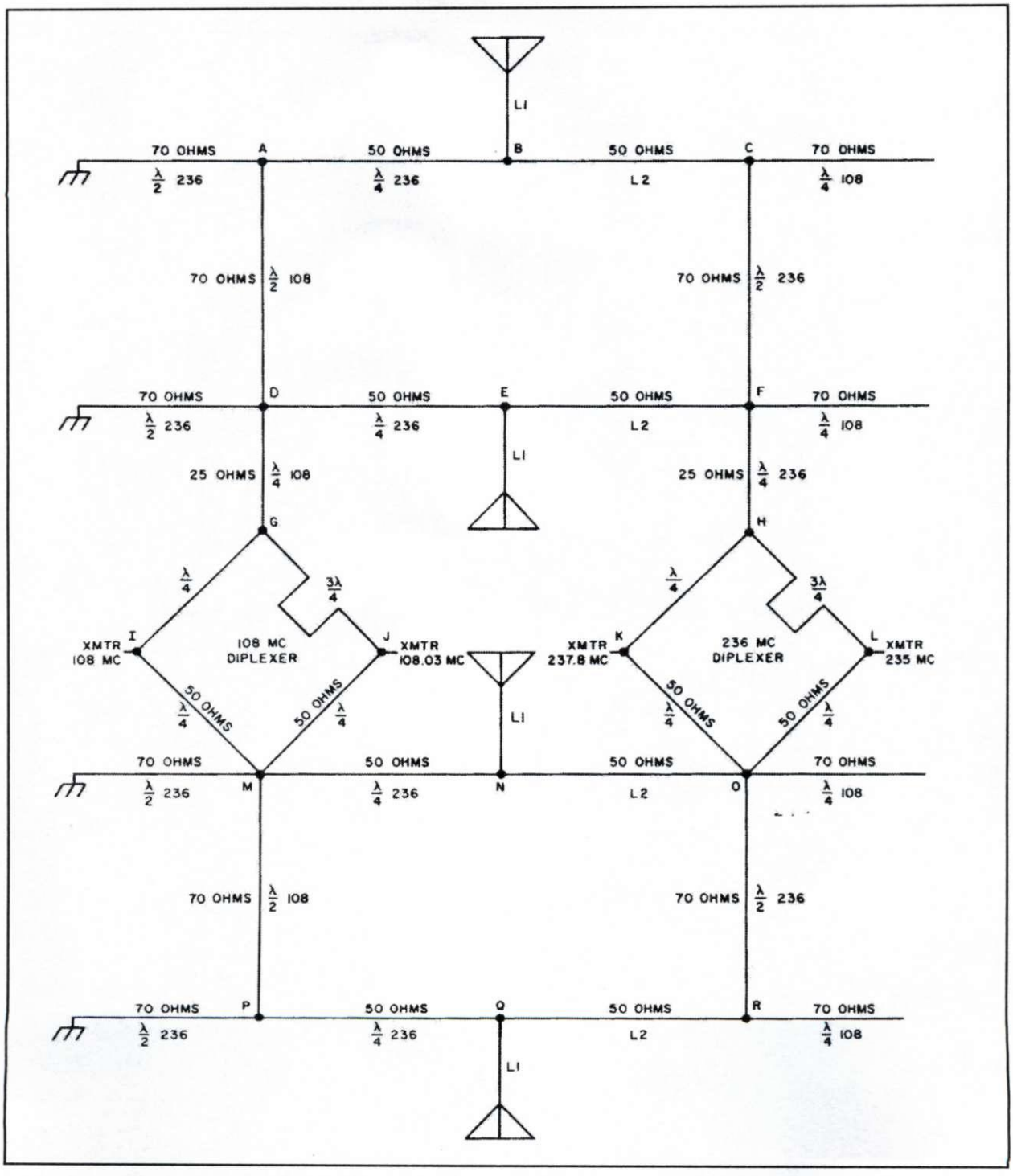

Fig 28-2.2. Circuit diagram for coupling and impedance-matching network for TIROS 2 and 3.

aircraft frequencies. The corresponding sections of the later antenna couplers were redesigned to 136.57 MHz, the mean frequency between the two operating frequencies. The TV and IR frequencies remained the same as before.

The problem when feeding multiple transmitters simultaneously into one antenna array is that of isolating the transmitters from each other to prevent mutual interference. Using frequency-selective isolation filters between transmitters of the two fre-

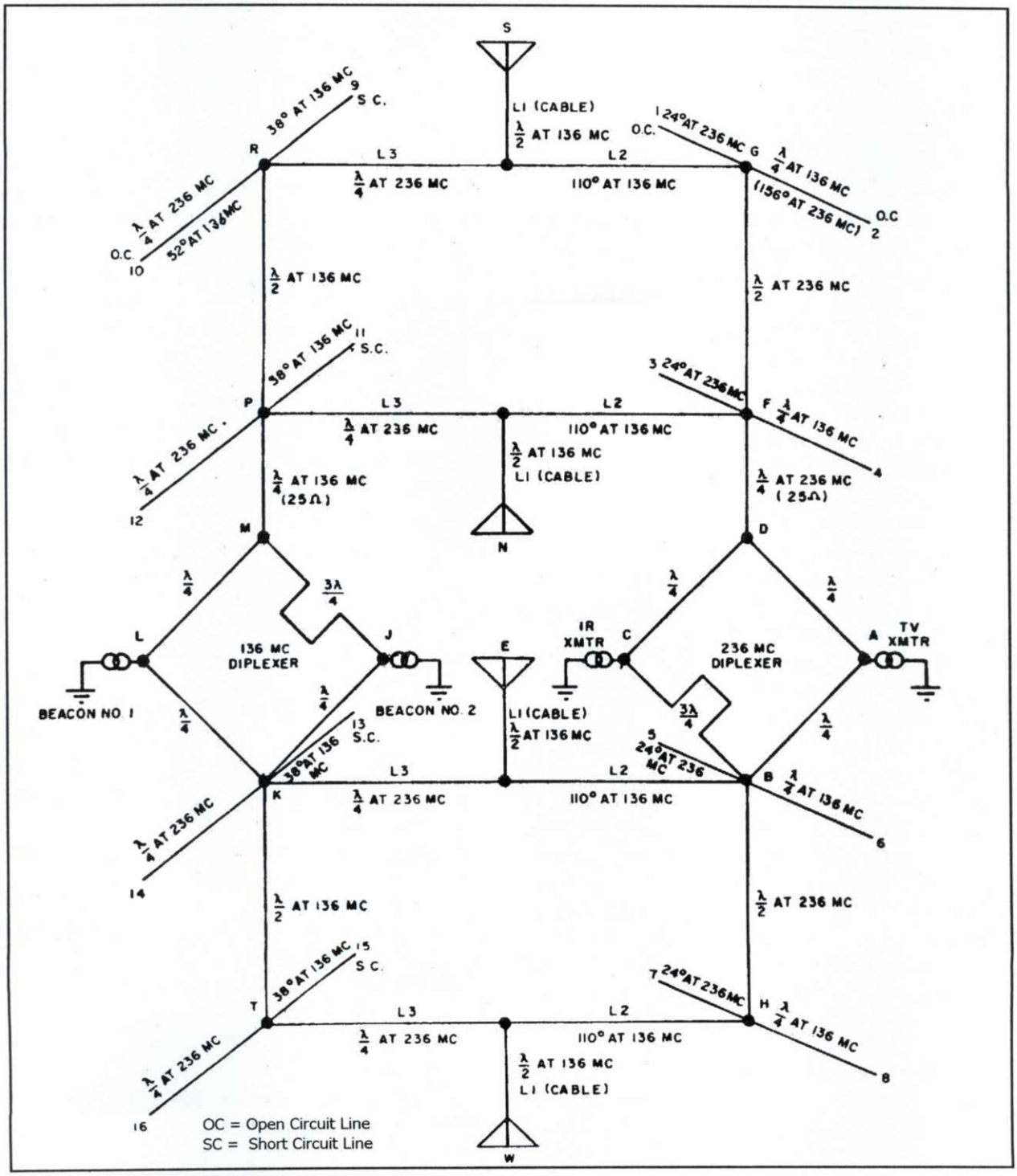

Fig 28-2.3. Circuit diagram for coupling and impedance-matching network for TIROS 4 through 8.

quency bands, and using ring hybrids to couple transmitters in the same band, solved the problem. The principles used in the solution are not new, having been used for decades—for example, two AM broadcast stations operating simultaneously on different frequencies, but using a common tower antenna. It is usual in these cases to construct the filter networks with lumped capacitors and inductors.

However, our solution was radically different—no lumped components. To save on precious weight and space the isolation and impedance matching unit was constructed entirely with stripline transmission-line circuitry (not microstrip) fabricated on printed circuit board. In stripline the center conductor is a flat ribbon conductor sandwiched between two flat layers of dielectric insulating material separating it from two outer layers of thin copper foil, with the outer foil becoming the outer conductor. (Think of coaxial line compressed until it's completely flat.) The width of the ribbon center conductor and the dielectric constant and thickness of the insulating material determine the impedance of the transmission line. In our case the thickness of each insulating layer is $^1/_{16}$ inch, and the dielectric material is Teflon®-fiberglass, with a dielectric constant of 2.42. Consequently, the completed transmission line is $^1/_8$ inch thick.

Diagrams of the transmission-line coupling and matching circuitry for TIROS spacecrafts 1, 2, and 3, along with the operating frequencies, appear in Figs 28-2.1, 28-2.2, and 28-2.3, respectively. The inside view of the printed circuits for the 136- and 235-MHz coupling and matching transmission line layout are shown in Figs 28-2.4 and 28-2.5, respectively. (Also see Photo 28-2.11.)

Because this project was our first experience in working with stripline, several test strips were fabricated to determine whether the characteristic impedance Z_0 and electrical length could be controlled to sufficiently-close tolerances to construct a workable system using stripline printed circuitry. It would have been nice to have fabricated the entire coupler in one unit, but with our lack of experience with stripline, coupled with a tight time schedule that could not tolerate the required learning curve, the initial coupler was constructed using six separate printed circuit boards interconnected with an unbelievable number of RG-141 cables and BNC elbow connectors. The six boards consisted of two frequency filters, two hybrid rings, and four baluns. However, the coupling network was redesigned for TIROS 2 and 3. Along with the experience gained while working with the new transmission medium with the first spacecraft, we bit the bullet and designed the new coupler into a single unit. The advantage in weight saving with the new design was tremendous, because the interconnecting cables and heavy elbow BNC connectors were eliminated, plus the complex mounting hardware for the six circuit boards, and the reduction in number of boards from six to two. The two final boards were sandwiched together into one board, thus eliminating the interconnecting cables and connectors.

We now show the steps taken during the matching procedure for the 108-MHz stripline coupler of TIROS 2 and 3 that resulted in the circuit diagram appearing in Fig 28-2.2, along with the corresponding Smith Chart presentation of Fig 28-2.6.

Degrees R (°R) = reflection degrees = electrical length in degrees × 2, and represents angular distance around the periphery of the Smith Chart.

Lower case y and z represent normalized values of Y and Z.

G = 1 defines the unity conductance circle on the Smith Chart

Z_M = Input impedance of single monopole

Z_M = 4.4:1 VSWR at –18° = 150 – j100 ohms (z_M = 3 – j2)

$Y_M = 1/Z_M$ = 4.4:1 VSWR at +161.5° (y_M = 0.24 + j0.16)

G = 1 matching point at 4.4:1 VSWR occurs at –51°

L_1 = distance from Y_M to G = 1 circle = 212.5°R

y_M at G = 1 circle = (1 – $j\beta$) = (1 – j1.62), residual susceptance $j\beta$ = –j1.62

Residual susceptance $j\beta$ cancelled at B, E, N, and Q by short-circuited lines L_2 providing susceptance $j\beta$ = + j1.62

Short circuits on L_2 at 108 MHz established by open-circuit stubs at C, F, O, and R

Normalized reactance j_x of L_2 = reciprocal of L_2 susceptance, $1/j\beta = 1/j1.62 = -j0.617$

Length of L_2 = j_x = $1/j\beta$ = –j0.617 = 148.33° (296.65°R)

L_2 = 148.33° electrical length of line fabricated in stripline matching unit.

Due to the change in the beacon frequency band from 108 to 136 MHz, the antenna impedance

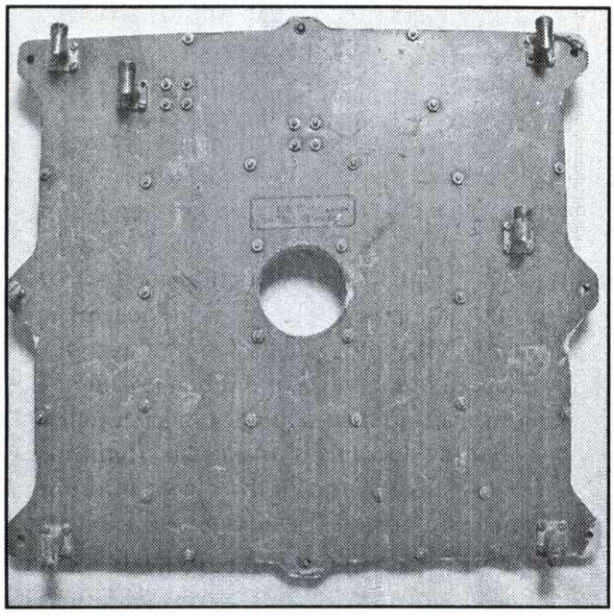

Photo 28-2.11. Stripline antenna coupling and Iimpedance matching unit, described in text and shown mounted in center of spacecraft in Photo 28-2.13. The hole in the center allowed the balancing shaft to go through the spacecraft during the spin balancing procedure.

changed from the original 150 – *j*100 ohms on the first three spacecraft to 26 – *j*85 ohms at 136 MHz, increasing the SWR from 4.4:1 at 108 MHz to 7.9:1 at 136 MHz, necessitating a redesign of the coupling circuit. However, although the increase in SWR presented no problem in designing the new matching circuitry, after the paper design was completed it was determined that with the narrower system bandwidth resulting from the increased mismatch, it would be more difficult to maintain adequate control of the mechanical tolerances in the fabrication of the stripline circuitry, and thus more difficult to assure an acceptable impedance match. Therefore, it was decided to redesign the antenna to bring its input impedance closer to 50 ohms in the 136-MHz band, and thus reduce the SWR to a more practical level. It is quite remarkable that while the input impedance of the antenna at 108 MHz was 150 – *j*100 ohms, for an SWR of 4.44:1, the input impedance of each monopole in the redesigned antenna was 43 + *j*15 ohms at 136 MHz, for an SWR of 1.43:1. In systems where there is an abundance of transmitter power available one wouldn't consider matching this impedance to 50 ohms for the purpose of saving power, because the mismatch loss for this small degree of mismatch would amount to only 0.13 dB. But the power available from the beacon transmitters was only 30 mw (milliwatts), which we didn't consider particularly abundant. Therefore, the decision was made to include a matching network in the coupling system for the 136-MHz band.

Because of the requirement to change the circuitry to accommodate the changes in impedances, the redesigned coupling and matching circuitry for TIROS spacecrafts 4 through 8 appears in Fig 28-2.3. The actual layout of the stripline circuits for 136 and 236 MHz as they appear in the printed-circuit boards appears in Figs 28-2.4 and 28-2.5.

We now show the steps taken during the matching procedure for the 136-MHz coupler of TIROS 4 through 8 which resulted in the circuit diagram appearing in Photo 28-2.3, along with the corresponding Smith Chart presentation of Fig 28-2.7.

Degrees R (°R) = reflection degrees = electrical length in degrees × 2, and represents angular distance around the periphery of the Smith Chart

Lower case y and z represent normalized values of Y and Z

G = 1 defines the unity conductance circle on the Smith Chart

Z_T = Total impedance of one dipole pair (two opposing monopoles) fed by cable balun of 180° differential length, referenced to center of BNC T junction.

$Z_M = 2Z_T$ = Impedance of single monopole of pair, fed as described in definition of Z_T.

Z_T = 2.4:1 VSWR at 160° = 21.5 + *j*7.5 ohms (z_T = 0.43 + *j*0.15)

Z_M = 1.426 VSWR at 106° = 43 + *j*15 ohms (z_M = 0.86 + *j*0.30)

$Y_M = 1/Z_M$ = 1.426 VSWR at (106° – 180°) = –74° = 0.0207 – *j*0.00742 mhos (y_M = 1.037 – *j*0.362)

G = 1 (matching point at 1.426 VSWR) occurs at –80°, 6°R from Y_M = length of L_1

L_1 of length 6°R is physically too short for a cable to reach from the matching device to the antenna terminal; add length λ/2, 360°R, L_1 = 366°R, 183° electrical.

y_M at G = 1 circle = (1 – *j*β) = (1 – *j*0.362), residual susceptance *j*β = – *j*0.362

Residual susceptance *j*β cancelled by short-circuited lines L_2 susceptance *j*β = + *j*0.362

Short circuits on L_2 at 136 MHz established at G, F, B, and H by open-circuit stubs 2, 4, 6, and 8, $\lambda/4$ at 136 MHz

Normalized reactance at G = 1 = reciprocal of susceptance, $1/j\beta\ 0.362 = -j2.762$

L_2 = length of 50-ohm line corresponding to $-j2.762$ = 19.9° of open-circuit line, or 109.9° of short-circuit line (short-circuit line required to satisfy operation of matching network at 236 MHz)

L_2 = 109.9° electrical length of short-circuit line fabricated in stripline matching unit.

As stated earlier, the antenna was designed physically to present a terminal impedance of $50 + j0$ ohms in the 236-MHz frequency band to make the circuitry of the coupler as simple as possible. This arrangement allows the TV and IR signal frequencies to pass through the 236-MHz side of the cou-

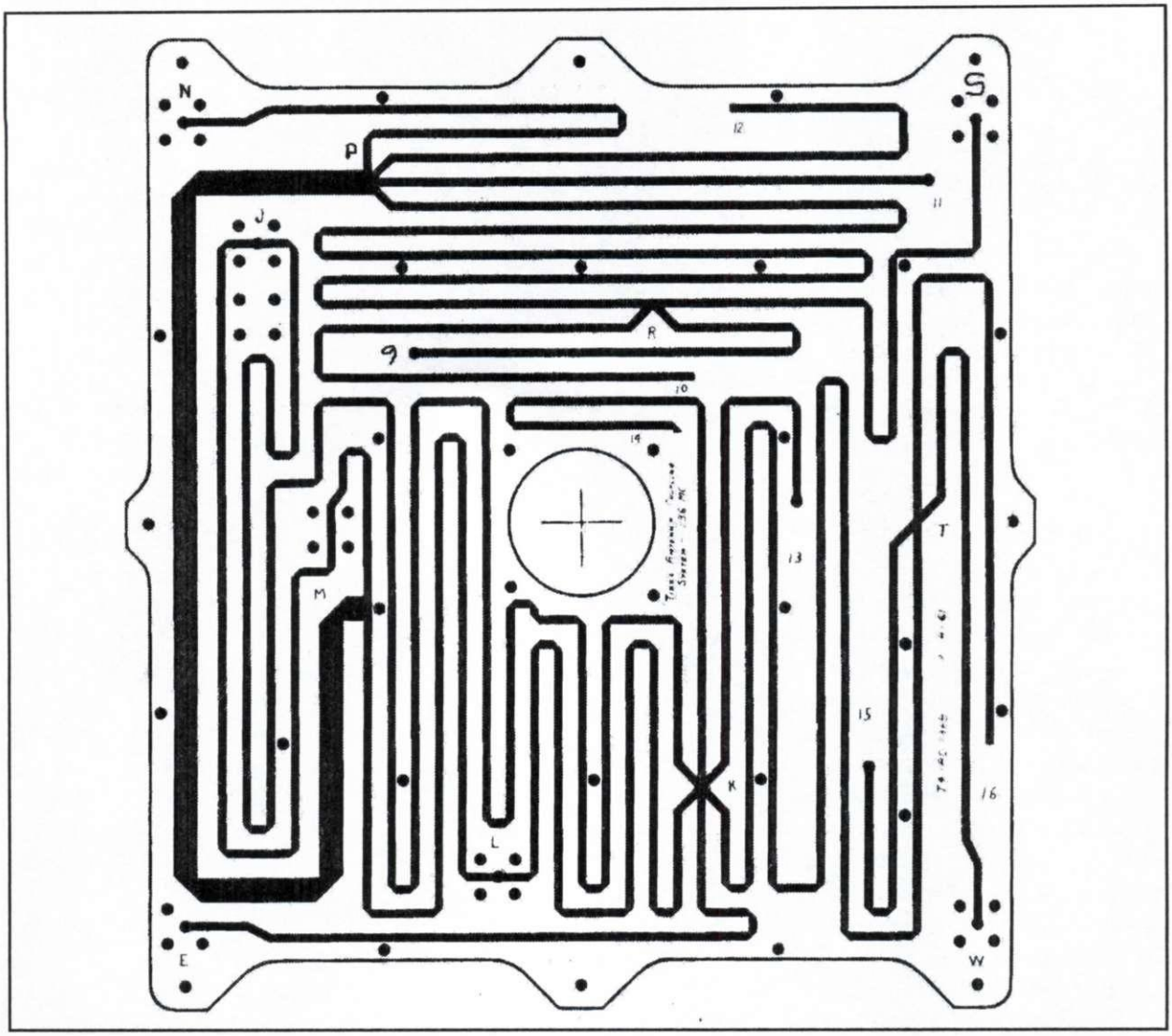

Fig 28-2.4. Inside view of the printed-circuit stripline transmission-line layout of the 136-MHz antenna-coupling and impedance-matching unit used on TIROS 4 through 8. Wide stripline Z_0 = 25 ohms, which is the extra $\lambda/4$ section required to insert the additional 90° phase difference between the orthogonally-related dipole elements to achieve circular polarization. All remaining stripline Z_0 = 50 ohms. Short-circuited lines have slightly circular endings to show short; open-circuited lines have abrupt endings to show open. A picture showing the coupler mounted in the center of the TIROS spacecraft appears in Photo 28-2.8. The hole in the center of the coupler is in the exact center of the spacecraft to allow a shaft to penetrate the entire spacecraft to support the spacecraft during the spin-balancing process.

pler with no need for impedance transformation from transmitter to antenna, requiring only isolation from the 136-MHz side. Consequently, only the 136-MHz side of the coupler required impedance transformation circuitry, but still required isolation from the 236 side. The impedance transformation and isolation were achieved through the numerous open- and short-circuit transmission-line stubs appearing in the circuitry, which will now be explained.

We'll first discuss the isolation of the 136-MHz section from the 236-MHz section. Referring to Fig 28-2.3, observe stubs 9-10 at the top left and stubs 1-2 at the top right. (Oc means open-circuited and Sc means short-circuited.) Stubs 9-10 and 1-2 are typical for all the stubs on their respective sides of the circuit. Now note L_3 and L_2, which are repeated in four places in the circuit. Continuing with the isolation from 236 to 136, note that length L_3 is $\lambda/4$ at 236 MHz, and that stub 10 is Oc $\lambda/4$ (90°) at 236 MHz. Oc stub 10 thus places a short circuit at 236 MHz at point R, making L_3 a shorted $\lambda/4$ section, causing an open circuit at 236 MHz to appear looking leftward at the L_1-L_2-L_3 junction.

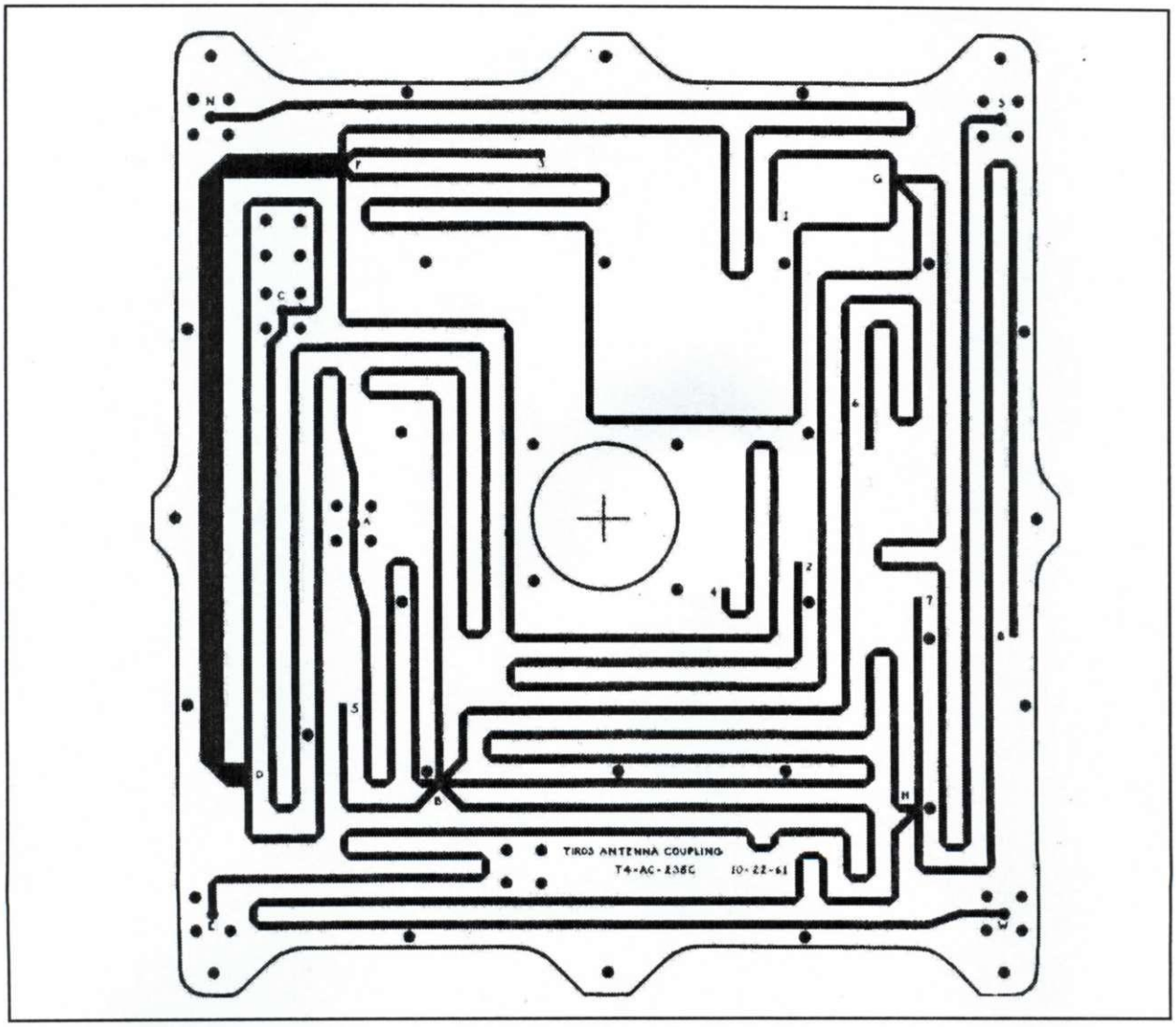

Fig 28-2.5. Inside view of the printed-circuit stripline transmission-line layout of the 235-MHz antenna-coupling and impedance-matching unit used on TIROS 4 through 8. Wide stripline Z_0 = 25 ohms, which is the extra $\lambda/4$ section required to insert the additional 90° phase difference between the orthogonally-related dipole elements to achieve circular polarization. All remaining stripline Z_0 = 50 ohms. Short-circuited lines have slightly circular endings to show short; open-circuited lines have abrupt endings to show open.

Consequently, no signal in the 236-MHz band travels leftward on L3 into the 136-MHz section. The same conditions hold at points P, K, and T.

However, Oc stubs 10, 12, 14, and 16 are 52° in electrical length at 136 MHz, creating shunt capacitive-reactance discontinuities of $-j39$ ohms at 136 MHz which disturb propagation through the coupler at that frequency. Consequently, to smooth the propagation we add 38° Sc stubs 9, 11, 13, and 15, making the total Sc stub length 90° at 136 MHz, thus canceling the reactances of stubs 10, 12, 14, and 16, removing the discontinuities and disturbances to the 136-MHz propagation through the coupler.

Next we'll proceed through steps in the matching of impedances between the antenna and the matching unit at 136 MHz. From here on we will be using the term "°R" meaning "reflection degrees," the angular degree scale found on the periphery of the Smith Chart. The value °R is twice the value of electrical degrees.

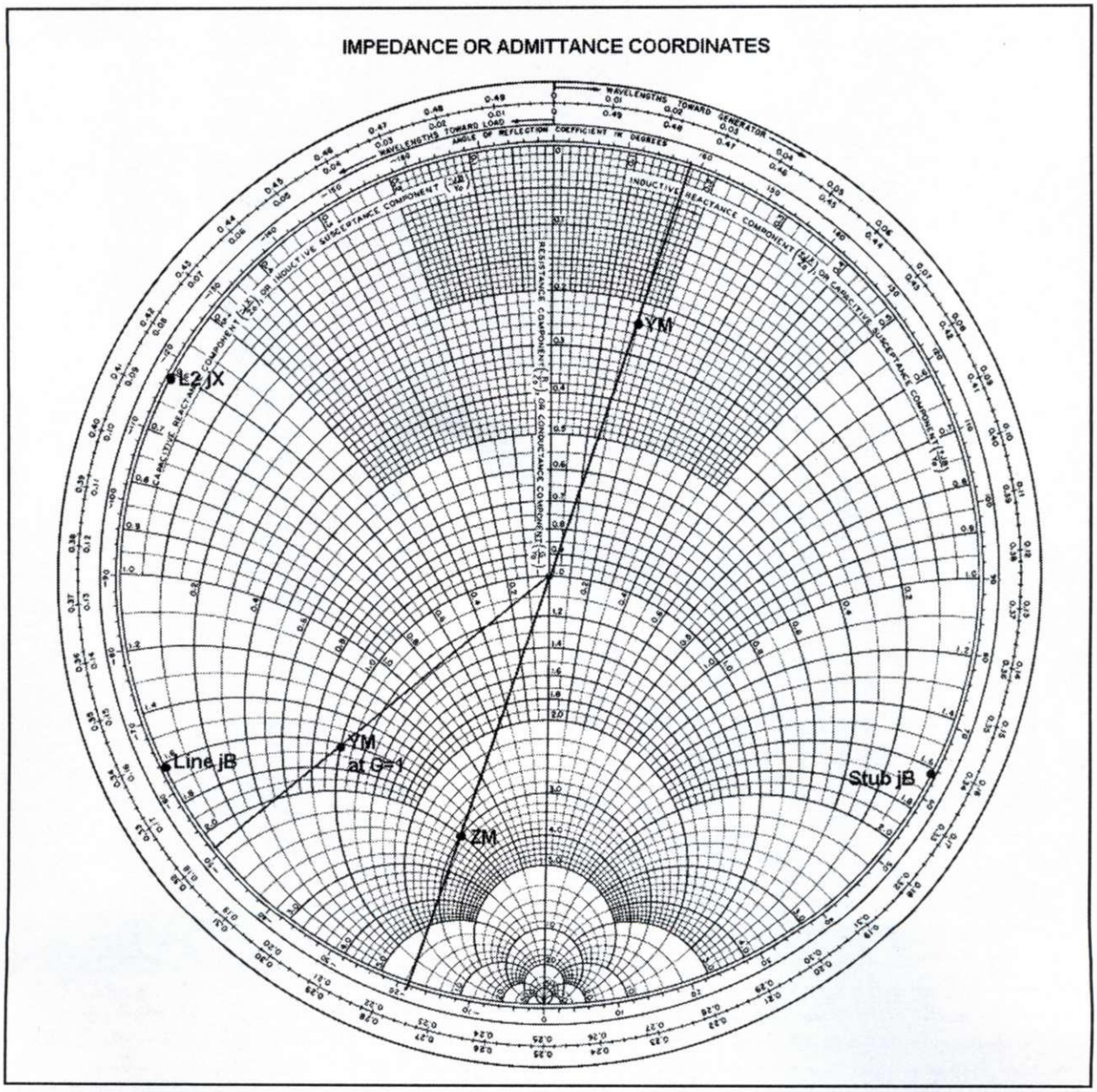

Fig 28-2.6. Impedance-matching data for 108-MHz network.

The terminal impedance of each single monopole M in the antenna array $Z_M = 43 + j15$ ohms at 136 MHz yields an SWR of 1.426 at 106°. The length of cable L_1 is approximately $\lambda/2$ (183°) at 136 MHz, thus closely repeating the terminal impedance at junction $L_1 - L_2$. To match $Z_M = 43 + j15$ ohms to $50 + j0$ ohms with a shunt stub requires transformer line L_1 to reach from the normalized value of the monopole impedance, $z_M = 0.86 + j0.43$ (VSWR 1.426 at 106°) to the unity conductance circle, G = 1, the location of the stub matching point. Because we are using a shunt stub, it is first necessary to convert impedance z_M to its reciprocal $y_M = 1/(0.86 + j0.43) = 1.037 - j0.362$ which appears at (106° – 180°) = –74°. The 1.426 VSWR circle intersects the G = 1 circle at $y_G = -80°$, where the normalized admittance $y_G = 1 - j0.362$.

To reach the –80° point on the G = 1 circle from y_M at –74° requires the length of L_1 to be either 6°R or 366°R, which is either 3° or 183° electrical

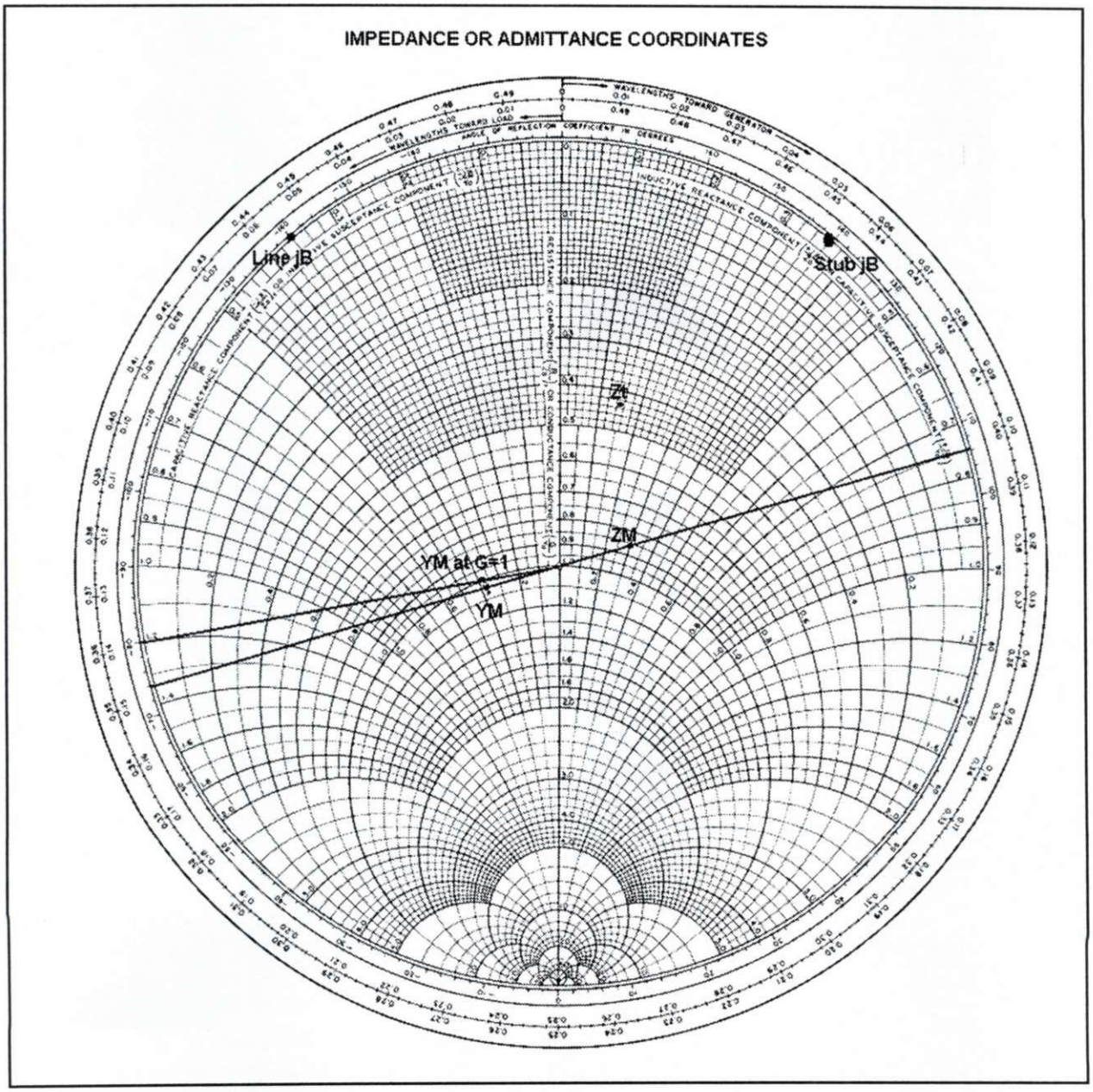

Fig 28-2.7. Impedance-matching data for 136-MHz network.

degrees. Because it is impossible for a cable length of 3° to reach the coupling circuit, a λ/2 (180°) length must be added, making the actual length of L_1 = 183°. The residual negative susceptance, $j0.362$ at the G = 1 point requires canceling with stub line L_2, having a positive susceptance $+j0.362$. However, to determine the length of L_2 in electrical degrees we use equation $\tan \theta = j\beta$, where θ = length L°, $j\beta$ = normalized residual susceptance. Thus, $\theta° = \arctan j\beta = \arctan 0.362 = 19.9°$ electrical degrees, or 39.8°R. Therefore, an Oc line of length 39.8°R is a correct length to cancel the residual susceptance, but is incorrect for 236-MHz operation. However, an Sc line 180° longer will

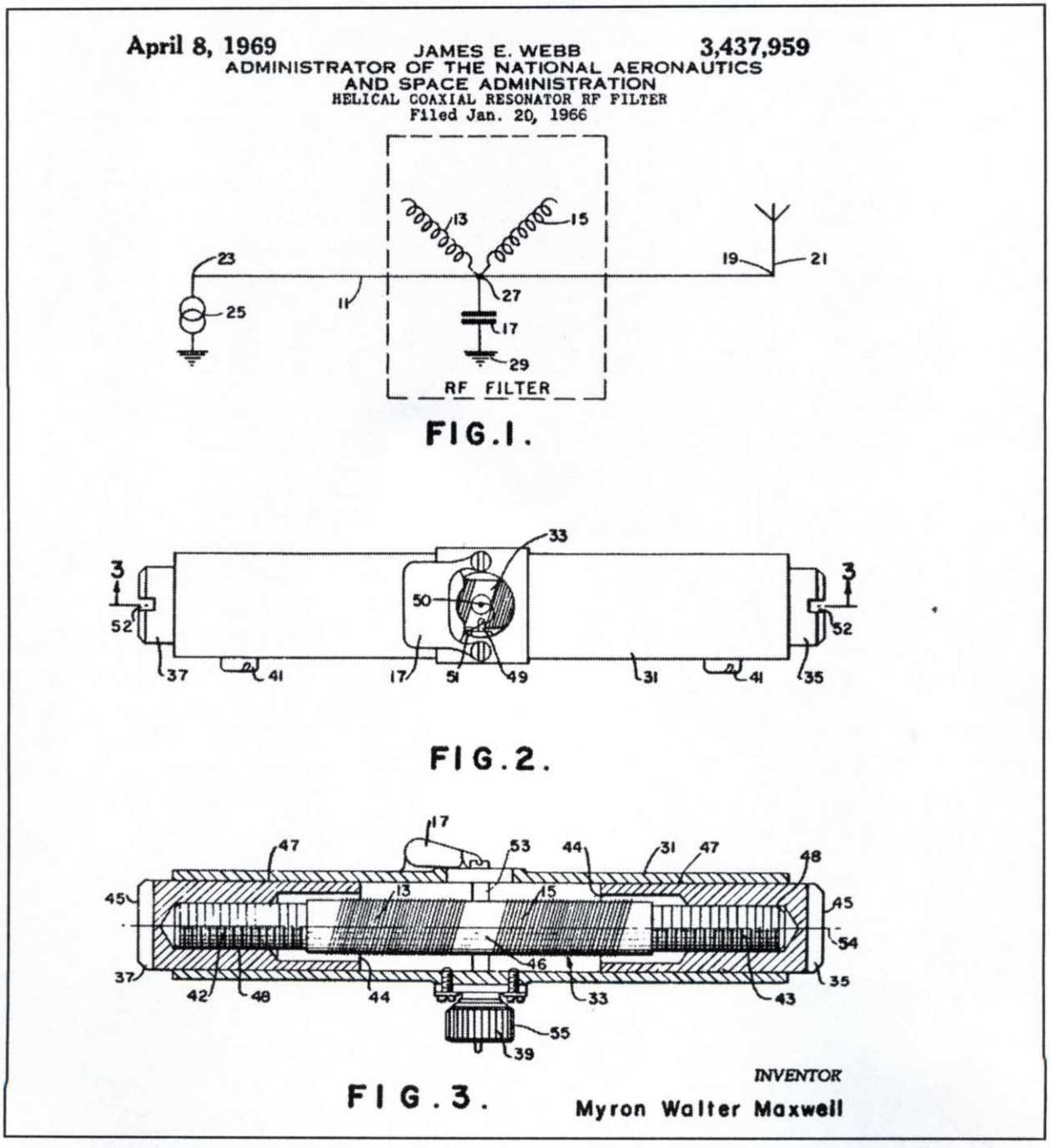

Fig 28-2.8. Patent for 136-MHz Helical Resonator Notch Filter.

work for both frequencies. Therefore, an Sc line of length 219.8°R is correct, but this length divided by 2 yields the electrical length $L_2 = 109.9°$.

We'll now discuss the isolation of the 236-MHz section from the 136-MHz section. Note that Oc stub 2 is $\lambda/4$ at 136 MHz (likewise Oc stubs 4, 6, and 8). These stubs place a short circuit at points G, F, B, and H at 136 MHz that prevent 236-MHz signals from passing past those points, thus isolating the 236-MHz transmitters from those operating at 136 MHz.

Next we'll discuss how the isolation between the two individual transmitters within each band is obtained. The method is the same for each band, so we'll use the circuitry of the 136 MHz in the discussion. The circuitry used to couple the two transmitters to the antenna which allows simultaneous operation with no significant mutual interference is well known as a ring diplexer. It is also well known as a "rat race" or "hybrid ring." The diplexer consists of a closed ring of transmission line having a circumferential length of six quarter wavelengths, $6\lambda/4$. Note in the circuit diagram of the 136-MHz diplexer, Fig 28-2.3, that the two transmission-line paths between the two transmitter input terminals L and J differ in length by 180°; the bottom path having two $\lambda/4$ sections for a total length of 180°, while the top path has one $\lambda/4$ section and one $3\lambda/4$ sec-

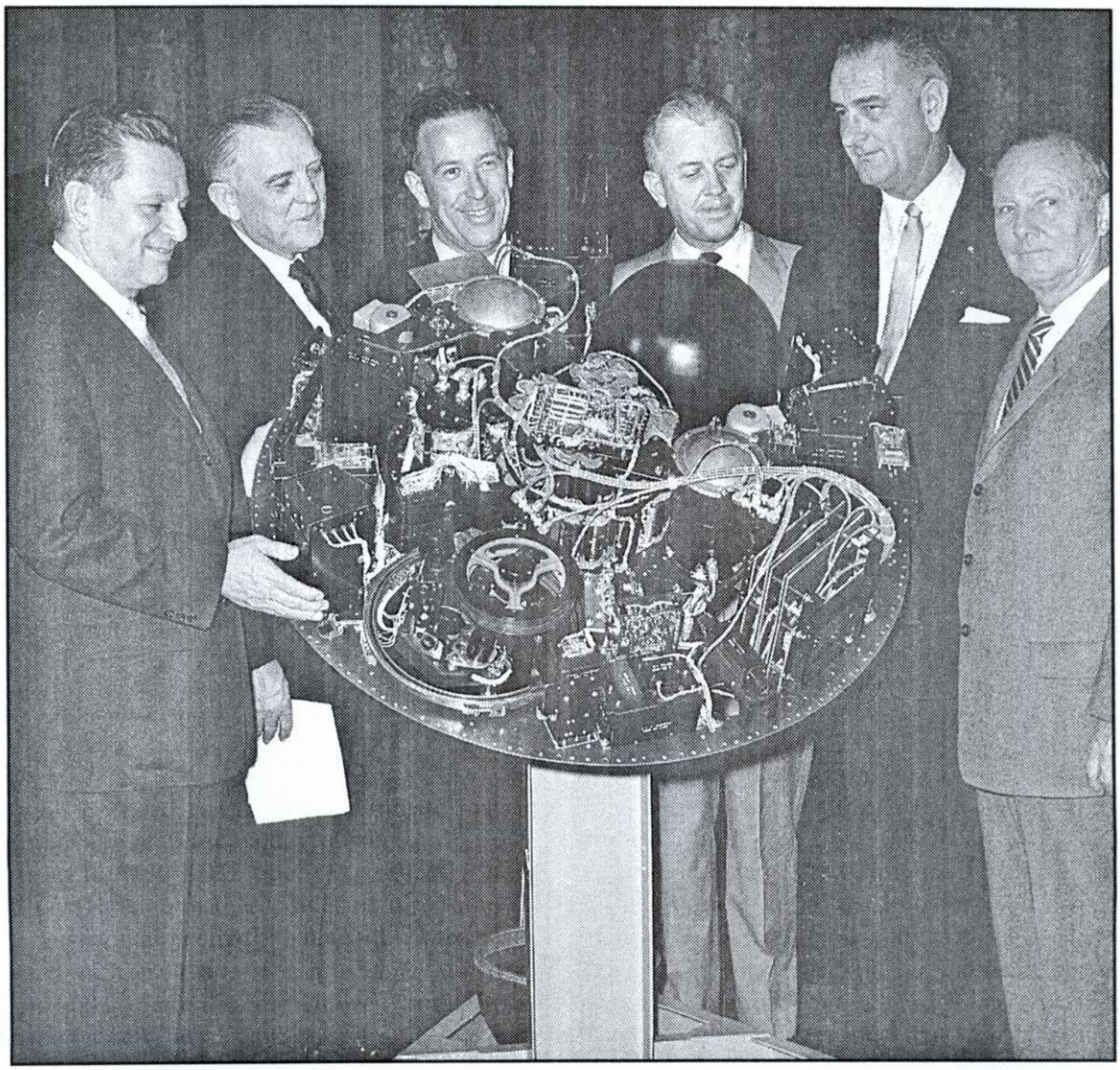

Photo 28-2.12. TIROS 1 with photo-cell cover removed showing initial multi-circuit-board antenna coupling system at bottom right. Also pictured, from left to right, Senator Stennis, Mississippi; Senator Jackson, Washington; P. B. Reed, RCA; Senator Lyndon Johnson, Texas; and Senator Young, Ohio.

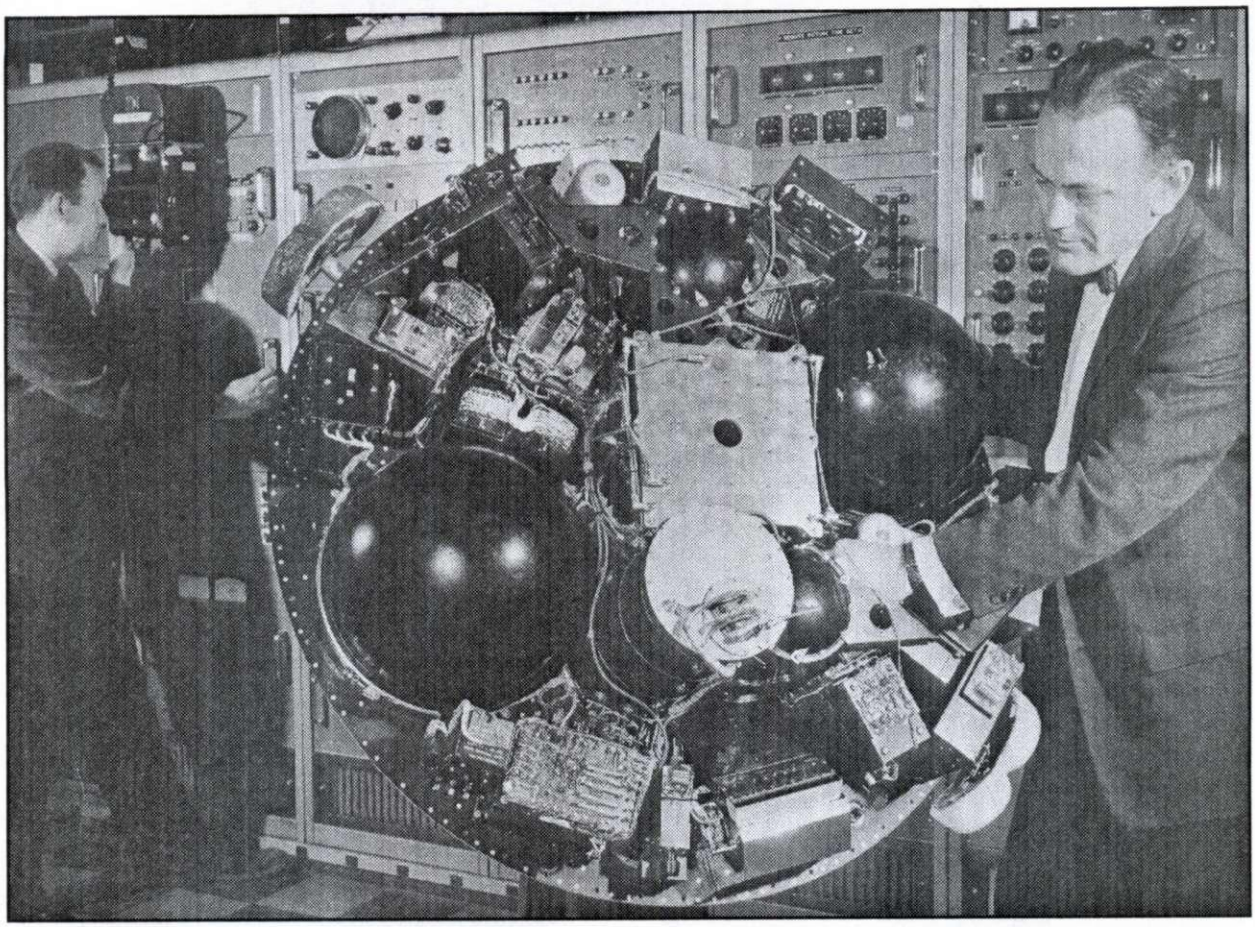

Photo 28-2.13. The internal assembly of the TIROS spacecraft. The bright rectangular unit with the hole in the center is the stripline antenna coupling and impedance-matching network (antenna tuners) that couples four VHF transmitters to the crossed-dipole antennas for simultaneous operation on four different frequencies. The matching network is described in the text. RCA engineers Marvin Harper and Glenn Corrington are testing various components of the spacecraft.

tion for a total length of 360°. This differential length of 180° is the heart of the isolation feature of the diplexer. As we progress we'll discover that the ring diplexer possesses some remarkable properties.

First, for this discussion we'll call beacon number 1 "B1" and beacon number 2 "B2." Consider now the signal waves delivered from B1 as they split at point L and travel the two differential-length paths toward B2. Because of the 180° difference in path lengths, the waves traveling the two different paths are 180° out of phase on arrival at B2. Consequently, due to the out-of-phase wave interference, a virtual short circuit (Sc) is established at the input of B2 to any further travel of waves delivered by B1. Thus, no signal from B1 enters B2. The same conditions apply reciprocally to signals delivered by B2 as they travel the reverse path toward B1. However, the virtual short circuit established by the out-of-phase wave interference is effective only in the direction from which it was established. It has no effect whatever on the waves delivered into the diplexer by either transmitter; each transmitter sees a $50 + j0$ impedance looking into the diplexer.

We'll now examine the activity occurring at the output terminals K and M of the diplexer, beginning with the signals delivered by B1. These signals travel out of the diplexer at terminals K and M, but after the steady state is reached no further signal travels into lines MJ and KJ, except the amount required to maintain the virtual Sc at the input of B2. The reason is that line lengths MJ and KJ are both odd multiples of $\lambda/4$, and thus the Sc appearing at point J establishes a virtual open circuit (Oc) at both points

M and K in the direction of point J. The two-section filtering action of the open-circuited odd-length λ/4 sections operating in tandem with the Sc established by the 180° out-of-phase wave interference at the inputs of the transmitters results in a significant increase in the mutual isolation between the same-band transmitters. Measurements indicated isolation values of 38 dB ± 2 dB.

As stated earlier, the 236-MHz diplexer performs in precisely the same manner as the 136-MHz diplexer just described. As one of its remarkable properties mentioned earlier, it should be strongly appreciated here that the ring diplexer has *no physical discontinuities,* yet its entire operation is based on the virtual open and short circuits developed only by wave reflections established by 180° out-of-phase wave interference.

The 148-MHz Receiving Antenna

The receiving antenna was a simple λ/4 monopole centrally mounted on the top of the spacecraft, with the body of the spacecraft as a reflecting ground plane. Its location in the center of the spacecraft placed it in the neutral plane of the transmitting antenna array at the bottom of the spacecraft, thus achieving a satisfactory isolation from the fields

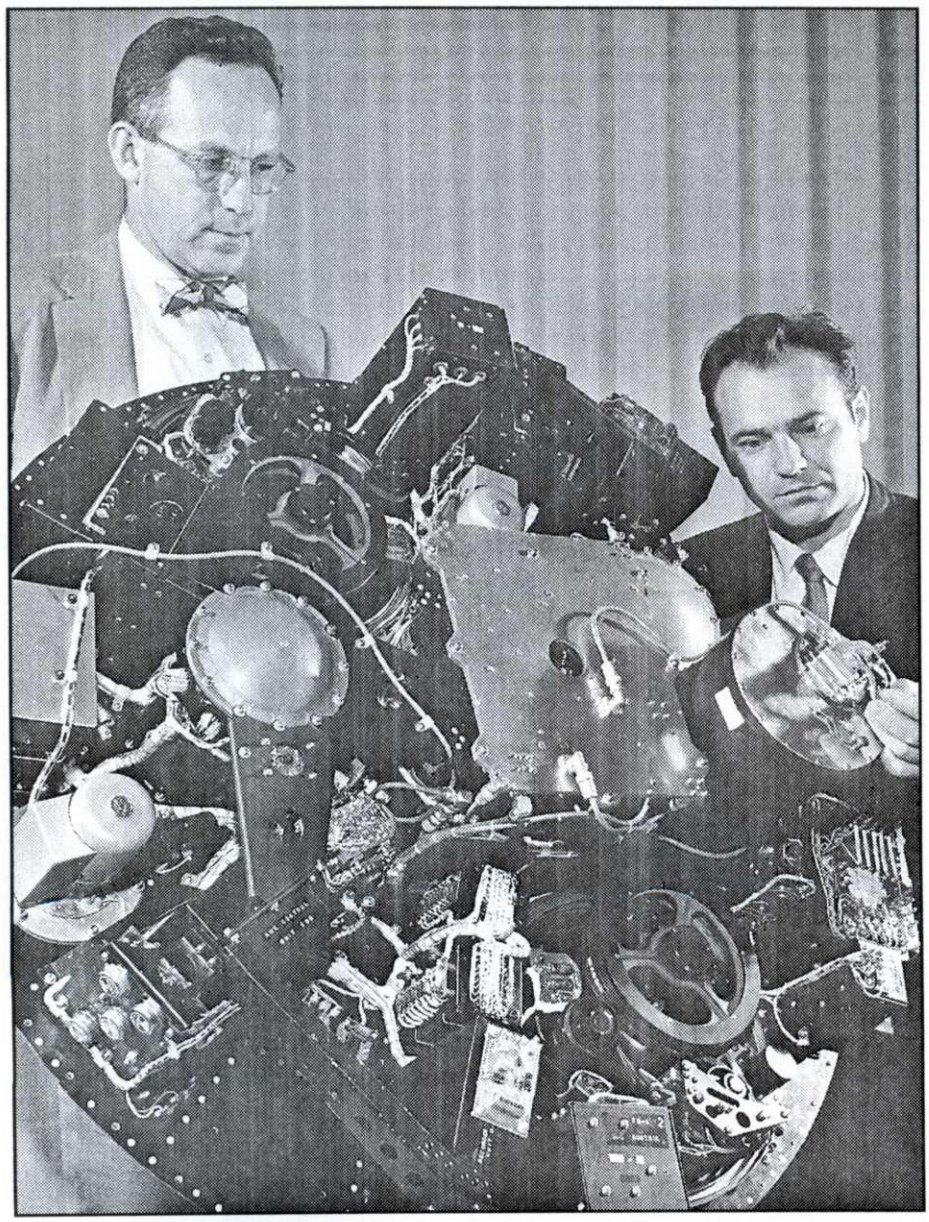

Photo 28-2.14. The internal assembly of the TIROS spacecraft, with TIROS Program Manager Abraham Schnapf on the left and Army Signal Corps Engineer on the right.

radiated from the array. Consequently, no desensing of the receivers' input-signal sensitivity occurred due to the transmitted signals.

However, an experimental system flew aboard TIROS 8 to determine the feasibility of the Automatic Picture Taking (APT) project that would allow real-time pictures to be transmitted continuously during each orbit to appropriate ground receiving stations throughout the world. The 137.5-MHz transmitter for this project was to share the receiving antenna, thus requiring a frequency filter to prevent the signal from the APT transmitter from entering the receivers, which leads us to the subject of the notch filter developed by the author.

The 136-MHz Helical Resonator Notch Filter

It is well known that an open-circuited $\lambda/4$ transmission-line stub provides a virtual short circuit at

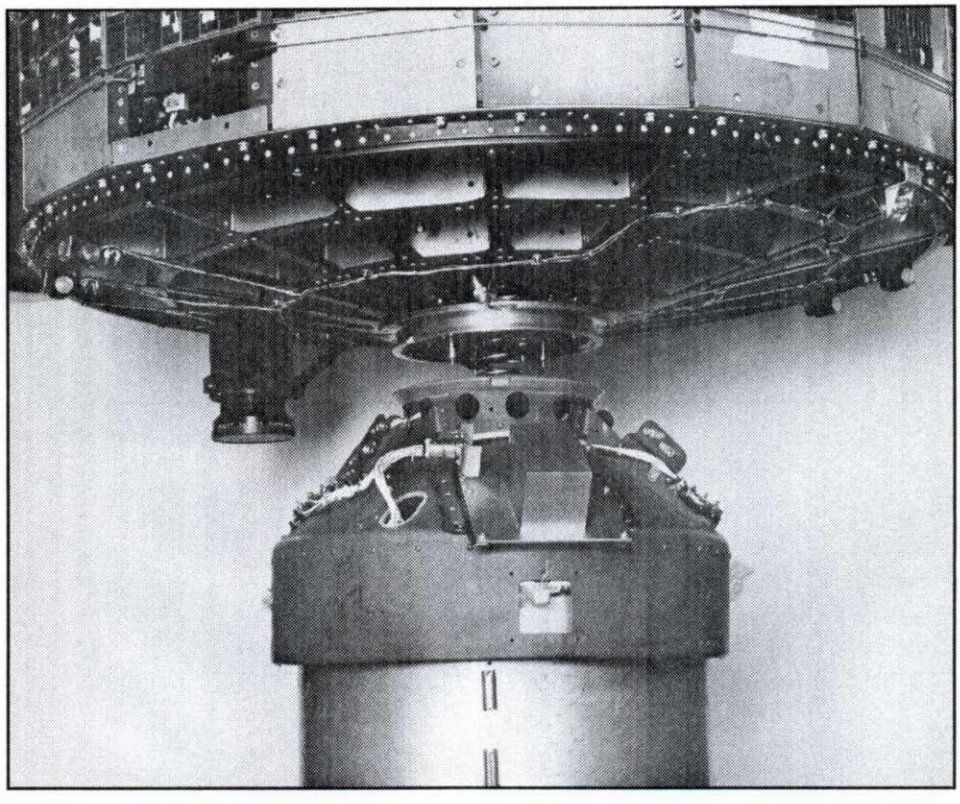

Photo 28-2.15. The TIROS spacecraft being attached to the third-stage rocket, showing the ejection spring between the spacecraft and the rocket. In launch configuration the spring is compressed and the spacecraft is firmly attached to the rocket with a ring clamp. On command from the ground at the appropriate time for separation, explosive bolts holding the clamp in place are fired, releasing the clamp. The thrust of the now-exposed ejection spring pushes the spacecraft and the rocket apart, allowing the spacecraft to orbit freely. The rocket remains in orbit, but drifts continually farther away from the spacecraft.
Directly above the bottom of the spacecraft two cables may be seen encircling the spacecraft. On one end of a cable is a weight (black) and on the other end is an eye caught around a hook. The other cable is similarly arranged. These two cables are used to de-spin the spacecraft from around 70 RPM down to around 5 RPM. The entire rocket system and spacecraft are spun up to 70 RPM immediately after launch to provide axial stability. However, to take pictures the spacecraft must rotate no more than 4 or 5 RPM. The spindown is accomplished by releasing the weighted cables on command from the ground station. When the cables are released, the centrifugal force on the weights at the end of each cable causes them to extend outward like a skater extending his arms. This action slows down the rotation, the same as with the skater, and after one revolution the cable and weights free themselves from the hooks seen in the picture and continue on their way into space away from the spacecraft.

its input terminals. I first measured the effectiveness of λ/4 stubs fabricated with RG-58 coax. These stubs provided satisfactory isolation at the desired frequency resulting from the very high conduction at 137.5 MHz (close to a virtual short circuit), but the conduction was still too high at the 148-MHz receiving frequency (where zero conductivity would be nice), resulting in unacceptable attenuation at that frequency.

My attention then turned to a helical resonator comprising a λ/4 transmission line having a high-Q coil of small-diameter wire for the center conductor inside a 3/8-inch diameter aluminum tube to obtain a much higher value of characteristic impedance than the 50 ohms of the RG-58. The reason for the higher characteristic impedance is to increase the steepness of the slope of attenuation when moving from the transmit frequency (the stop frequency) to the pass frequency (the receive frequency). One end terminal of the coil was left open-circuited to achieve a virtual short circuit at the opposite end terminal, which would then be shunted across the coaxial transmission line connecting the receiving antenna to the receivers and thus approximate a short-circuit shunt across the line at the 137.5-MHz frequency.

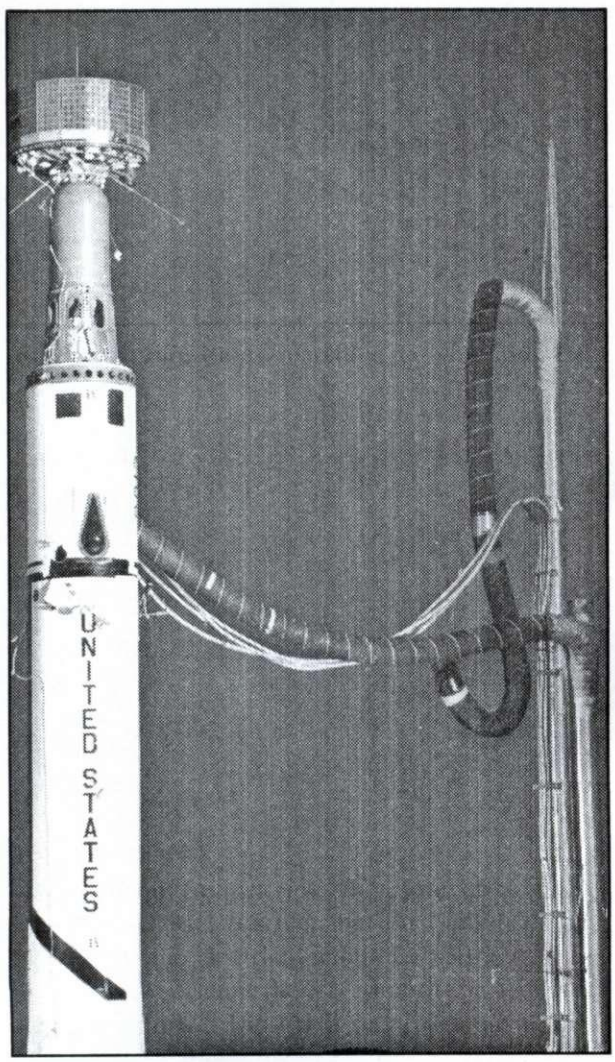

Photo 28-2.16. This photo shows the TIROS spacecraft atop a Delta 2 rocket on launch pad 17A at Cape Canaveral before the nose fairing is attached around the third-stage rocket and the spacecraft. The 12-story multi-level support gantry has been rolled away.

The model used during the development phase is shown at "E" in Photo 28-2.10, while the final flight model weighing 3.9 ounces is shown at "F." (A copy of the US Patent for the helical resonator showing the author as the inventor appears in Fig 28-2.8.)

The characteristic impedance Z_0 of the flight model resonator was 800 ohms; the attenuation at the 137.5-MHz transmit frequency was 28 dB and less than 0.2 dB at the 148 receive frequency. In actual operation in the TIROS 8 spacecraft two of the notch filters were shunted across the receiver coax spaced λ/4 apart, resulting in 56 dB of attenuation at the transmit frequency, which proved sufficient to reduce the amount of the transmit signal entering the receivers to prevent desensing, or decreasing the receiver sensitivity.

(See photos of the completed TIROS: 28-2.12, 28-2.13, 28-2.14, 28-2.15, 28-2.16, and 28-2.17.)

In Conclusion

TIROS 1was launched successfully from Cape Canaveral on April 1, 1960. Both beacons were first heard at the RCA Princeton ground station approximately three minutes after lift off at the beginning of the first orbit from a distance of approximately 1800 miles to the horizon. The signal level from the two 30-milliwatt beacons at this distance was 30 dB over S9, using four R-390 receivers with a Tapetone VHF-to-HF converter and a circularly-polarized multi-dipole array having a 16-dB gain at 108 MHz. The array was mounted on an az-el signal-tracking pedestal. The VHF receivers for the video and IR signals were Nems-Clark. A photo of typical Tapetone converters and R-390 receivers appears in Photo 28-2.20.

It is interesting to note that because each transmitter in each frequency band was fed into oppo-

site sides of their respective hybrids in the antenna coupler, the circular polarization radiated from the antenna array was of the opposite rotation with respect to the transmitters in each frequency band—i.e., right-hand circular from one transmitter and left-hand circular from the other. During reception of the signals from the orbiting spacecraft, it was immediately discovered that when the received signal level on one polarization went through a minimum during rotation of the spacecraft, the level of the opposite polarization was maximum. This fortuitous condition permitted using a separate receiver for each polarization, thus achieving polarization diversity, resulting in a practically constant signal level when combining the two signals into one output.

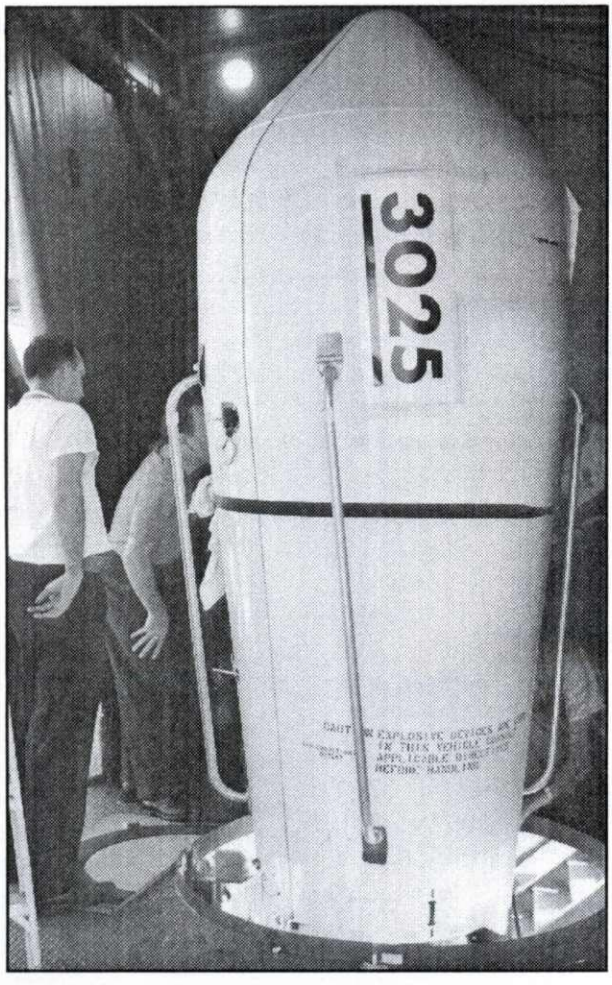

Photo 28-2.17. In this photo the gantry at launch pad 17A is in place around the entire height of the rocket structure and spacecraft. The photo was taken at the top level of the gantry, at the level of the spacecraft as shown in Photo 28-2.10 with the gantry rolled away. The photo shows author Maxwell peering into the fairing, or nose cone, that houses the third-stage booster rocket and the spacecraft. He is inspecting his antennas on the spacecraft atop the rocketry to determine whether the ends of the antennas fit properly into the fairing.

I was the engineer in charge of the Princeton ground station during the reception of the first signals received from TIROS 1 in orbit, the world's first weather spacecraft. I also engineered and installed the antennas at Cape Canaveral used for pre-launch check-out communications with the spacecraft while on launch pad 17A.

The TIROS ground-station tracking antenna array at RCA's Princeton Astro-Electronics Division (AED) Space Center (actually at Hightstown, N.J.) is shown in Photo 28-2.18. The array was constructed by the General Bronze Corporation, Valley Stream, N.Y. NASA's TIROS ground station tracking antenna at Wallops Island, V.A., is shown in Photo 28-2.19.

The 108- and 136-MHz telemetry data receiving equipment used at the RCA ground station comprised two Tapetone VHF-to-HF converters and two Collins R-390 HF receivers in combination, as shown in Photo 28-2.20. The Tapetone picture was obtained from the October 1958 issue of *QST*. The R-390 picture is shown via the courtesy of Charles Bautsch, III, W5AM's website: <www.radioing.com>.

Sec 28.3 The Echo 1 Spacecraft

Launched into space on August 8, 1960, Echo 1 was the world's first attempt to use an Earth-orbiting spacecraft as a means for achieving global TV broadcasting. When inflated after reaching orbit, Echo became a 100-ft spherical balloon made of aluminized mylar film of 1/2-mil thickness. The aluminized coating on the mylar was used to reflect TV RF signals globally from high-powered transmitters for direct reception to TV receivers on the ground. Although the spacecraft performed correctly while in orbit, its intended use was unsuccessful, because the power required of the TV transmitters was too great to obtain a satisfactory picture on reception after the signal was reflected from the spacecraft.

However, it is interesting to note that the spacecraft carried two beacon transmitters to verify a successful entry into space after launching from

Cape Canaveral. There was concern that it could become lost in clouds, with no way to determine its location thereafter. Hence, the two beacons operating at 108.0 and 108.03 MHz permitted continual radio tracking of the balloon if lost from visual contact.

The beacon units—mounted at opposite poles of the balloon, included the transmitter, batteries, antenna, and solar cells—were embedded in a plastic disc shaped like a dinner plate, as shown in Photo 28-3.1. The transmitter, shown with and without encasement in Photo 28-3.2, delivered a continuous-wave one-hundredth of a watt (10 milliwatts) into the antenna, which produced S9+ signals at the ground stations when the spacecraft was just above the horizon at 1800 miles distance. Photo 28-3.3 is a view of the bottom side of the unit, showing the transmitter, batteries, and printed circuit connecting

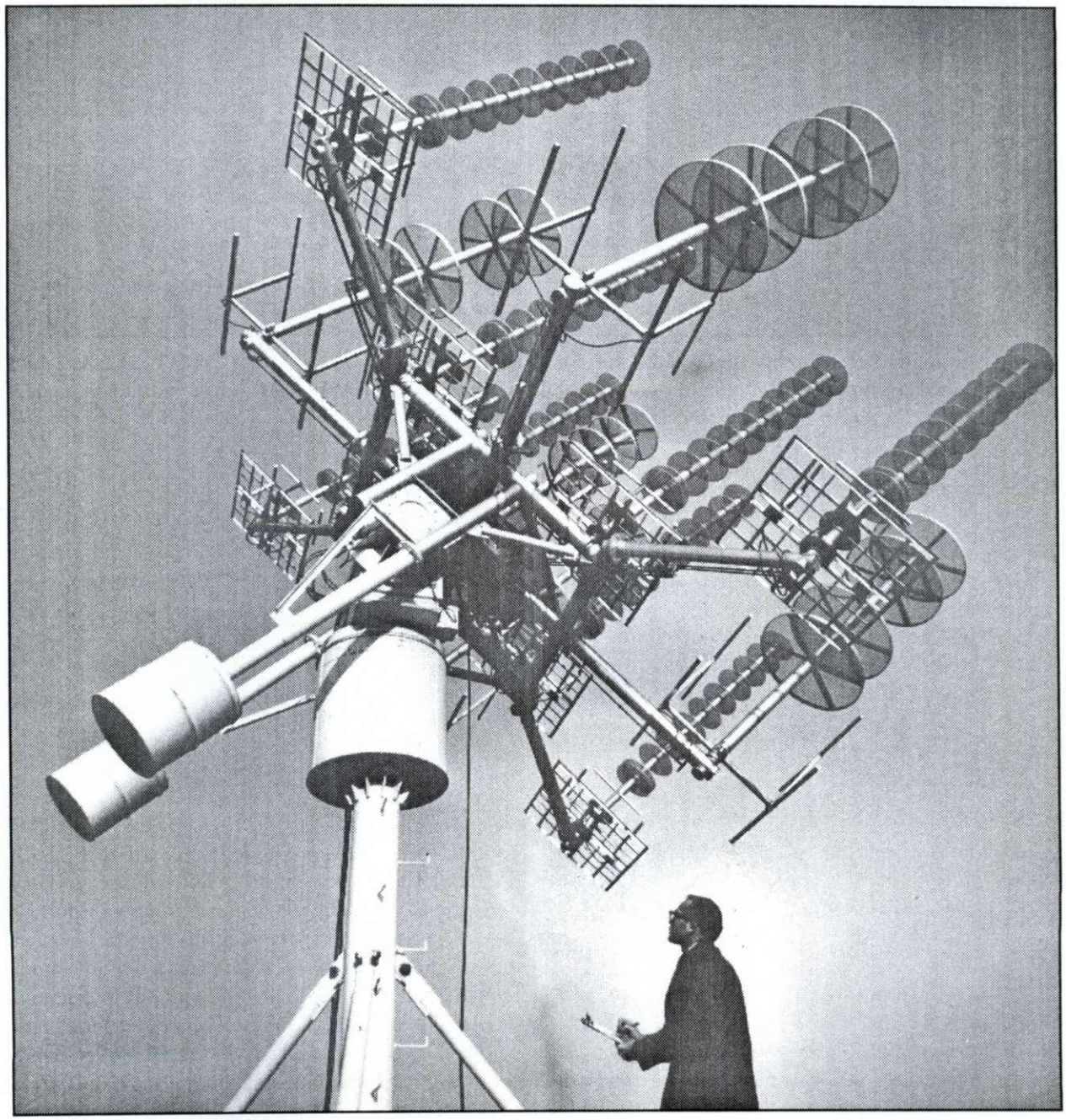

Photo 28-2.18. Az-El high-gain TIROS tracking Antenna at RCA's ground station at Princeton, New Jersey.

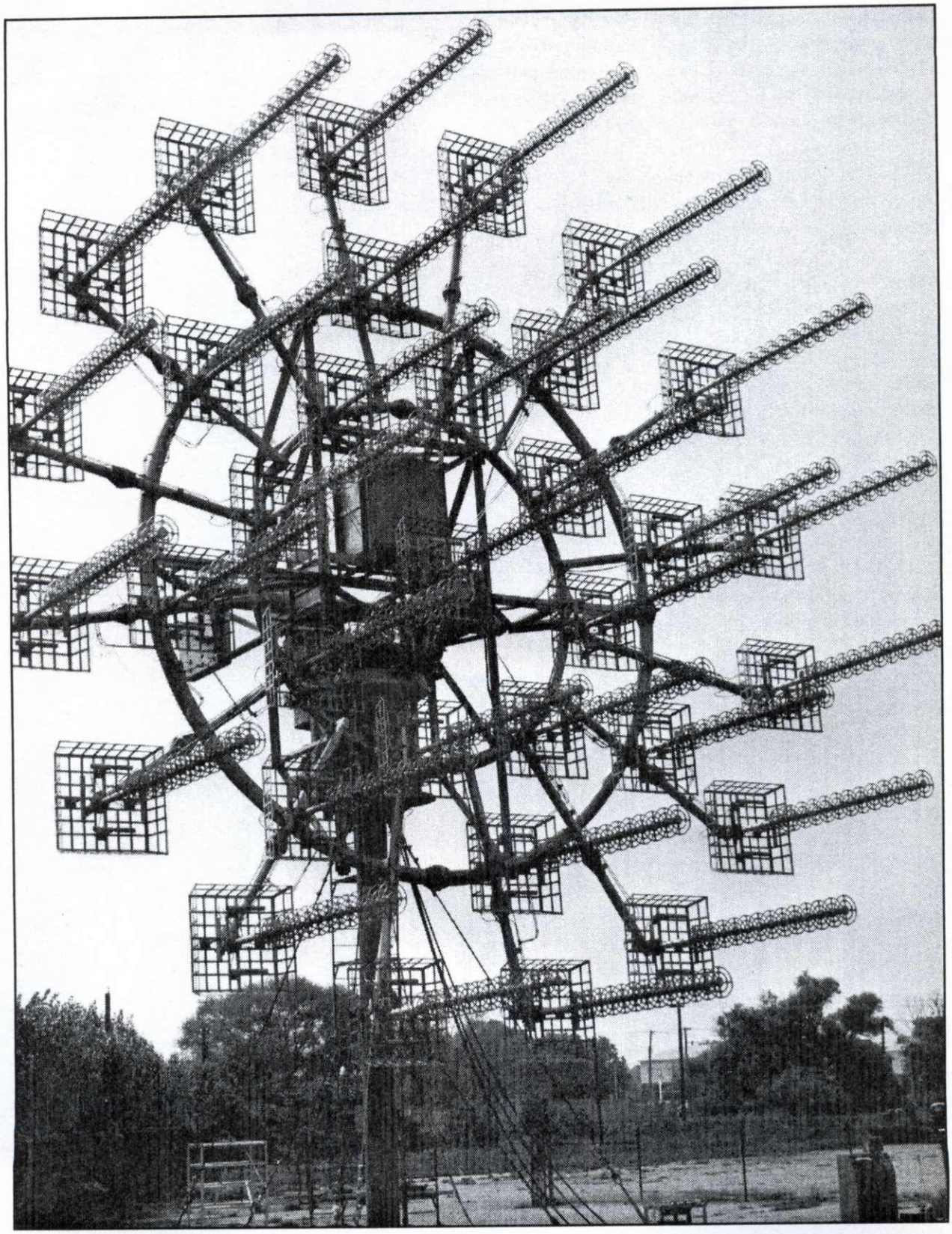

Photo 28-2.19. Az-El High-Gain TIROS Tracking Antenna at NASA's Ground Station at Wallops Island, Virginia.

Photo 28-2.20. TIROS 1 108-MHz Telemetry Data Receiver at RCA's Ground Station at Princeton, New Jersey.

the batteries to the solar cells. Photo 28-3.4 shows technicians attaching the beacon to the mylar balloon material with adhesive tape.

The antenna for Echo 1 was designed by the author, which in itself brings up an interesting story. The spacecraft was a child of NACA, the forerunner of NASA. RCA's involvement was to design and build the beacons. However, the engineers at NACA specified emphatically that no wire antenna could be involved due to the possibility of its inadvertently protruding into the skin of the balloon, allowing it to deflate. They strongly suggested that we design the beacon to use a slot antenna simply by making the slot opening in the surface of the balloon. We rejected the slot approach, indicating that while half of the RF energy delivered to the antenna would be radiated outward, the other half would be radiated inward, thus entering the space within the balloon. Inward radiation of RF energy would be disastrous, because the space inside the balloon would form a resonant cavity with extremely high Q. The result would be a highly unstable input impedance for the slot antenna.

Consequently, we at RCA suggested placing a cavity resonant at the beacon frequency directly behind the slot to prevent inward radiation, and

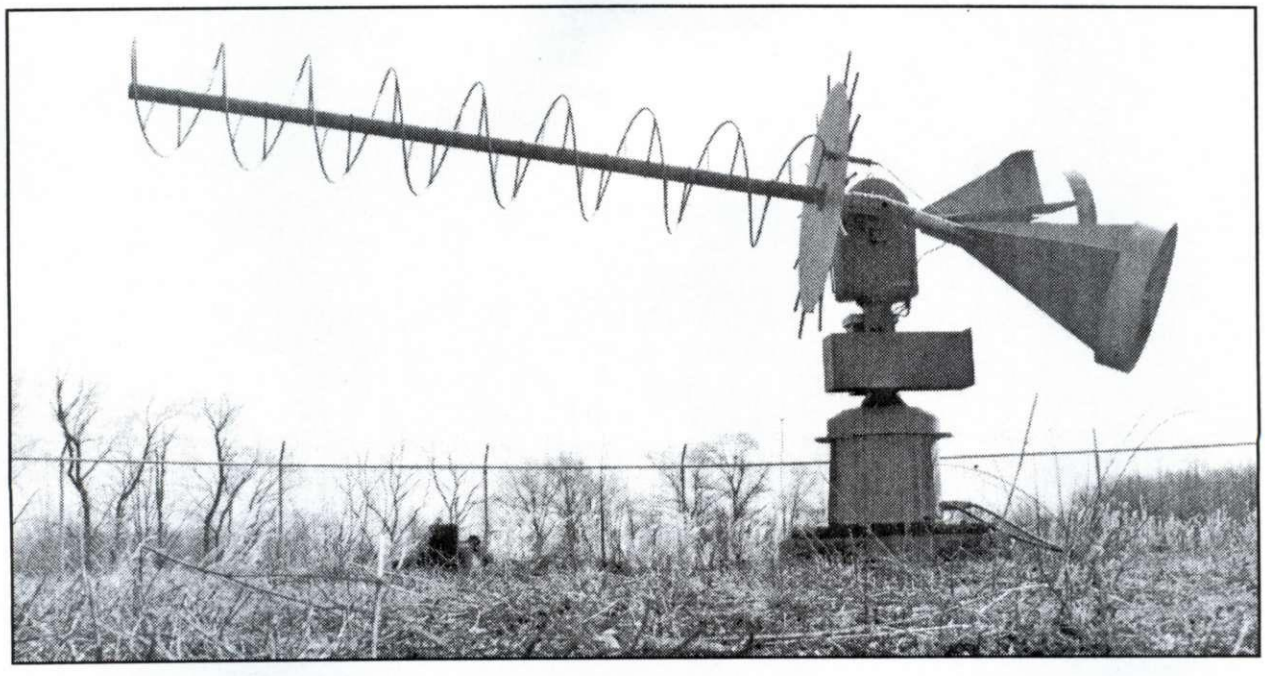

Photo 28-2.21. Original APT (Automatic Picture Taking) AZ-EL-mounted antenna, built by Fairchild, used at various locations worldwide for receiving real-time weather information on 137.5 MHz from the TIROS weather spacecraft.

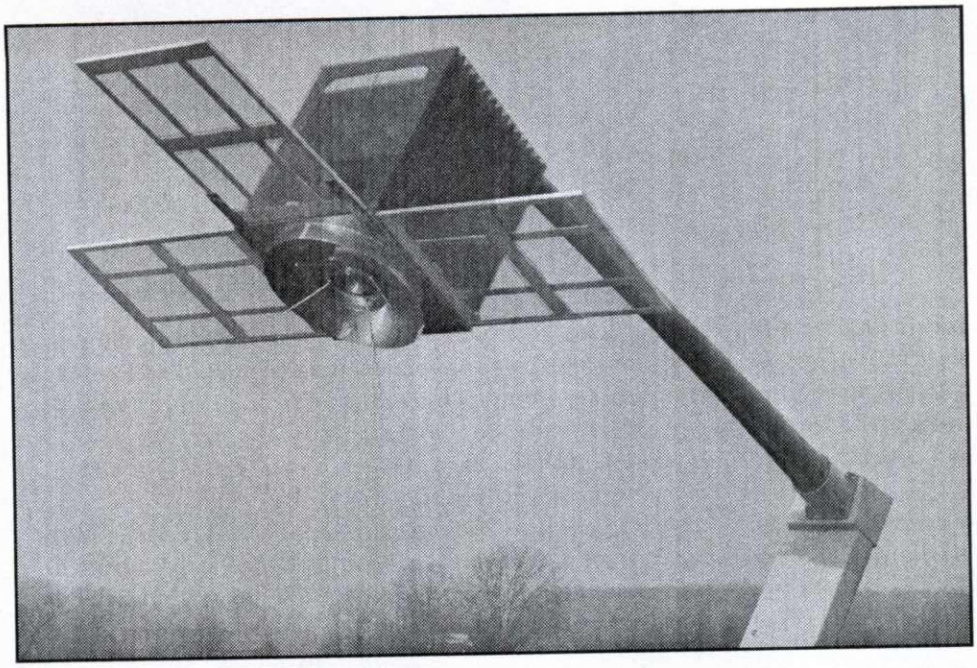

Photo 28-2.22. The electrical test model of TIROS 9, spacecraft ITOS, mounted on a Scientific-Atlanta pattern positioner during measurement of antenna patterns.

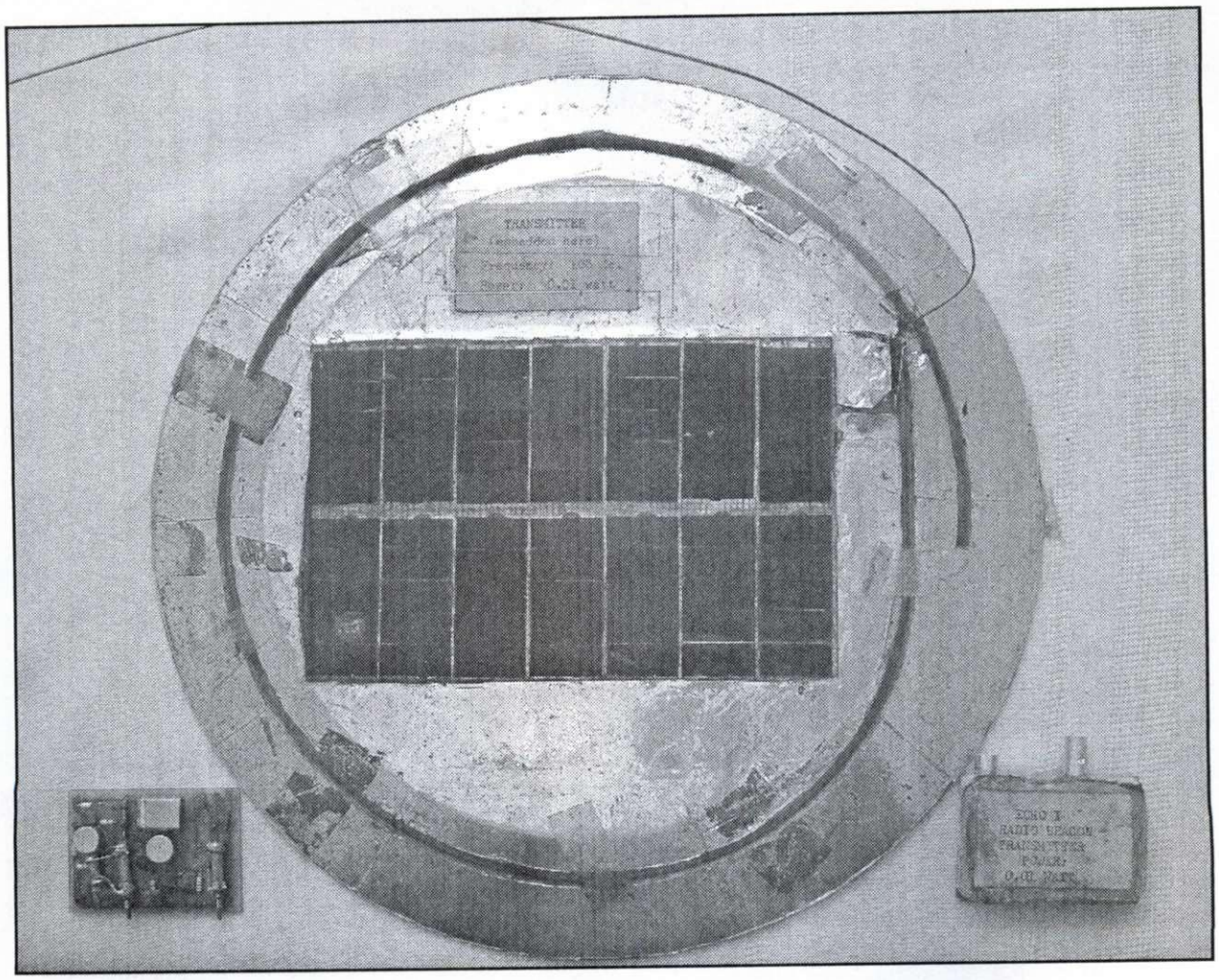

Photo 28-3.1. Echo 1 beacon unit, plus 108-MHz, 0.01-watt transmitters.

thus all the energy would be radiated outward. However, the NACA engineers were not only skeptical that the high Q of the cavity would cause an unstable impedance for the antenna, but also said building such a cavity behind the slot was impractical. Thus, it became incumbent on RCA to prove the instability of the antenna impedance in the absence of the resonant cavity behind the slot.

Because it was obviously impractical to take measurements on a balloon 100 feet in diameter, the proof had to be found using a scale model for the measurements. As the RF engineer assigned to the antenna development, I chose a 100-to-1 scale factor for a measurement model, making the diameter of the model sphere one foot and the measurement frequency 10,800 MHz, or 10.8 GHz. The RCA Laboratories model shop pressed a piece of 1/32-inch copper sheeting into a sphere of one-foot diameter.

A slot with the appropriate dimensions for the 10.8-MHz frequency was cut into the sphere and fed with RG-55 coaxial cable. As I predicted at the outset, the input impedance of the slot radiator proved to be immeasurable, because the values of SWR exceeded 100:1, varying wildly with small temperature changes in the model. The NACA engineers demanded a demonstration of the measurements performed at their location at Langley Air Force Base, Virginia, which I duly performed. The performance convinced the people at Langley that we were correct concerning the instability of the slot impedance without a resonant cavity backing the slot. They finally agreed to allow a stainless-steel spring wire antenna after we (RCA) promised to secure the wire embedded in the beacon plate until after the balloon had inflated to ensure that the wire would not damage the mylar skin of the balloon. Referring to Photo 28-3.1, observe the circular slot near the periphery of the beacon disc, with the wire antenna emerging on the right-hand side. The antenna wire was secured in this slot while the balloon was folded up prior to launch. However, when the balloon was inflated, the wire was released from the slot, becoming vertical in relation to the surface of the balloon. In addition, a switch at the point where the wire emerged was automatically turned to the ON position when the wire was released, connecting the batteries to the transmitter and thus turning on the beacon.

Had the NACA engineers believed us concerning the high-Q nature of the space within the balloon, the engineering of the simple quarter-wave vertical antenna mounted over the spherical ground plane supplied by the aluminized coating on the mylar balloon material would have been routine, requiring only designing the mechanical means for preventing the antenna from tearing a hole in the balloon..

Sec 28.4 The RELAY Communications Spacecraft

How the Author's Knowledge of Polarization Saved NASA from Scrubbing a Pre-Launch Test of Spacecraft RELAY at Cape Canaveral

This writing describes the events involving the author that occurred during a pre-launch test of the RELAY 1 satellite at Cape Canaveral, Florida in December 1962. Although AT&T's TELSTAR, launched from Cape Canaveral July 10, 1962, was the first active communication satellite capable of relaying transatlantic TV signals, NASA's RELAY,

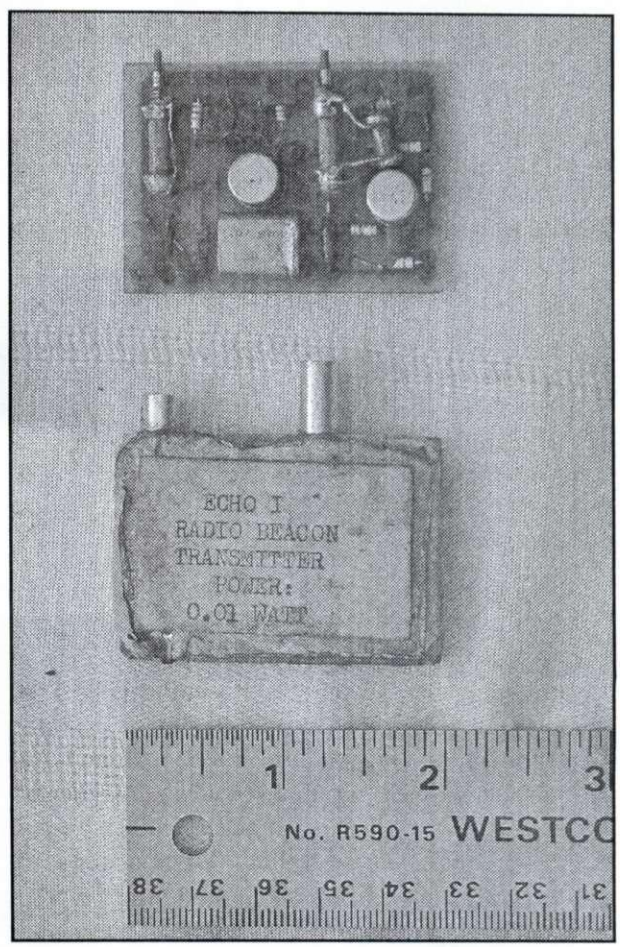

Photo 28-3.2. Echo 1 108-MHz, 0.01-watt transmitters used in beacon unit.

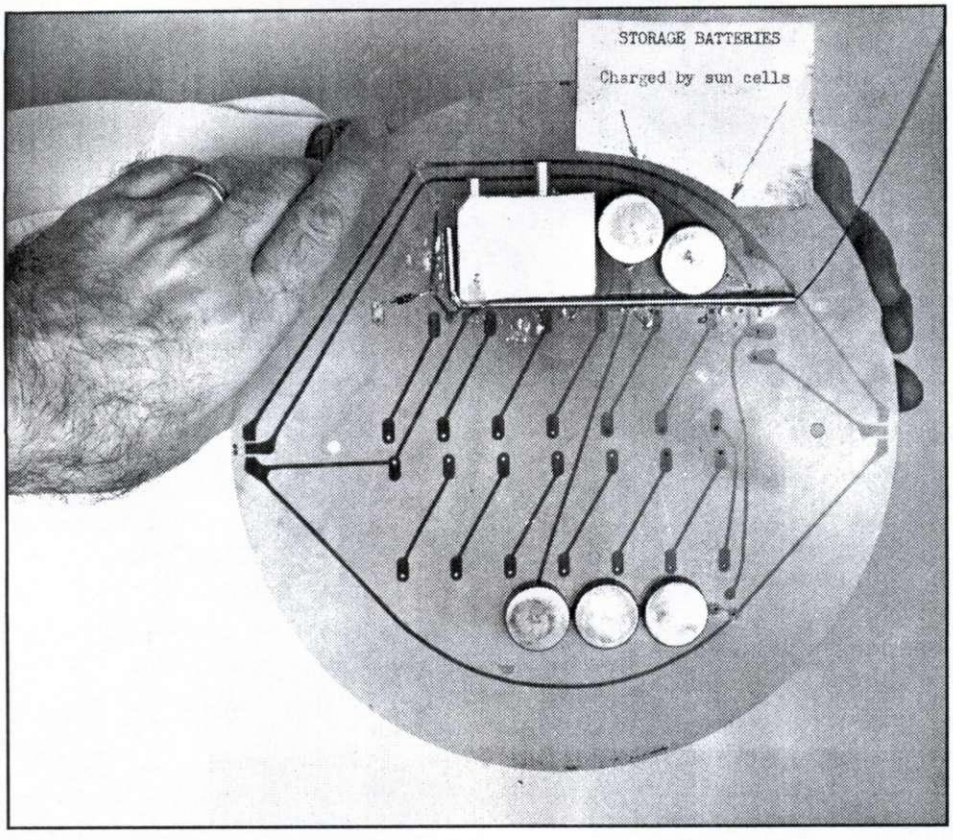

Photo 28-3.3. Bottom view of Echo beacon unit showing transmitter, batteries, and printed-circuit connections to solar cells.

Photo 28-3.4. Beacon unit being attached to Echo 1 balloon satellite (aluminum-coated mylar) prior to balloon being folded in preparation for launch configuration.

launched December 13, 1962, became the second such satellite. TELSTAR was built and owned by AT&T, and launched by NASA, but RELAY was owned by NASA and built by the Astro-Electronics Division of RCA (my employer) after being chosen over AT&T and Hughes (see Photo 28-4.1).

The NASA platform at Cape Canaveral that supported antennas communicating with various spacecraft on launch pads during pre-launch operations is shown in Photo 28-4.2.

Background

It should be remembered that in the early 1960s there was no booster rocket capable of lifting a spacecraft into the geosynchronous orbit altitude of 22,300 miles above the Earth, the altitude required for an orbiting spacecraft to appear stationary with respect to any point on Earth. Consequently, RELAY orbited with a perigee of 820 miles and an apogee of only 4623 miles above the Earth, at an inclination of 47.5°, which made it visible at any one Earth location for a maximum of around 110 minutes a day. (TELSTAR's perigee was 320 miles and apogee only 1895 miles.) Therefore, these communications spacecraft were not yet ready for continuous, prime-time television. Also, due to the generic aspect of the name RELAY, the public was never really aware of its existence, or its accomplishments in supporting the early transatlantic TV transmissions. Both TELSTAR and RELAY performed nearly identical missions. However, the name TELSTAR was so exotic at the time that the media referred to the missions of both spacecrafts as TELSTAR and seldom used the name RELAY. One example of the many times when RELAY performed the task, but for which TELSTAR received the credit, was the transmission of television signals among the US, Europe, and Japan during the 1964 Olympic Games held in Tokyo.

Let's Get Technical

During the time an active spacecraft is atop the launching rocket on the launch pad it is necessary to be in constant communication with it to perform housekeeping chores such as monitoring various voltages and component temperatures, plus activating the cameras and tape recorders to verify their state of readiness. In other words, communications that will continue during the launch phase and on

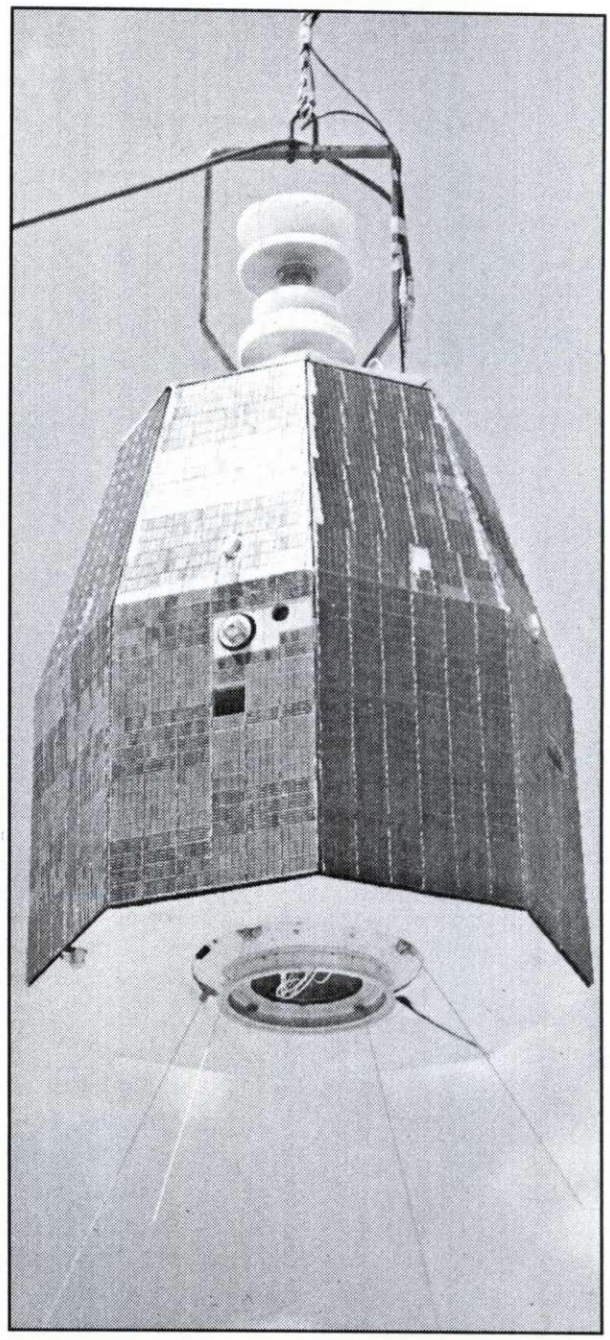

Photo 28-4.1. The RELAY Communications Spacecraft. The white disks at the top of the spacecraft are data-transmission (TV) antennas. The top disk is the 1.726-GHz receiving antenna, right-hand circular polarization (RHCP). The lower disk is the 4.71-GHz transmitting antenna, left-hand circular polarization (LHCP). The four monopoles at the bottom of the spacecraft are the antennas for receiving commands from the ground stations on 148 MHz, and transmitting telemetry data to the ground stations on 136 MHz.

into the operational phase after orbit is achieved. To accommodate the communications for these satellites during the pre-launch testing and launch-phase operations, a ground station containing the complementary instrumentation was established approximately three miles from the launch pad complex, which in this case was the launch pads using the Delta rockets, Complex 17. A 20-ft × 60-ft platform supported by wooden poles at approximately 40 feet above ground was built at the ground station to mount the antenna arrays aimed toward the spacecraft on the launch pad, shown in Photo 28-4.2. Yagis, and various other antenna arrays mounted on the right-hand end of the platform, were used to communicate at the VHF frequencies that involved reception of telemetry signals and transmission of command signals. The dish antennas on the left-hand end of the platform provided the UHF video links to the spacecraft, the large dish providing the uplink frequency of 1725 MHz and the small dish providing the downlink frequency of 4169.7 MHz.

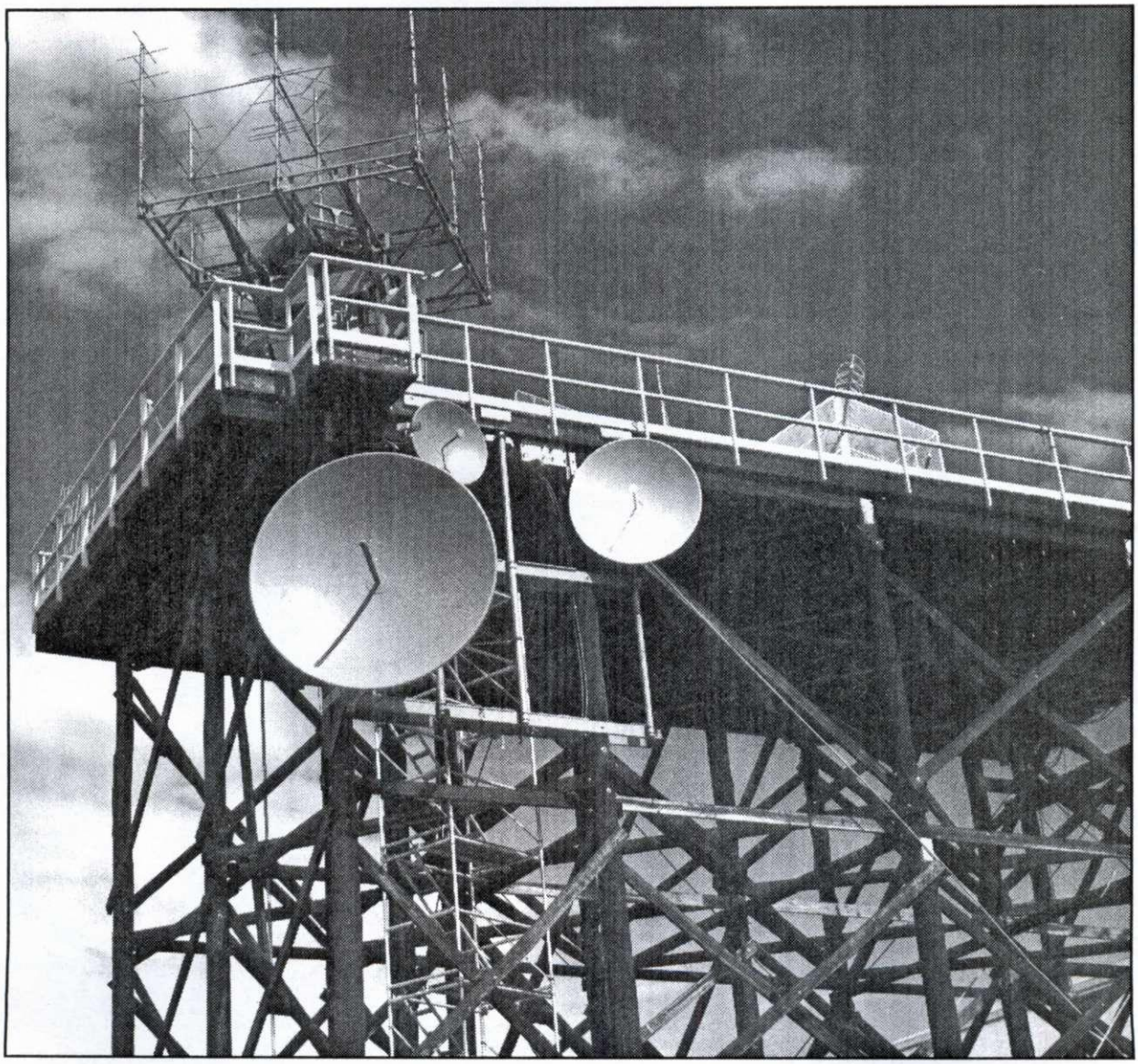

Photo 28-4.2. NASA platform at Cape Canaveral supporting antennas communicating with various spacecraft on launch pads during pre-launch operations. The two dish antennas were used for communicating with the RELAY spacecraft. The small dish is the 4.17-GHz downlink antenna, while the large dish is the uplink antenna. The dish antennas were engineered by the author.

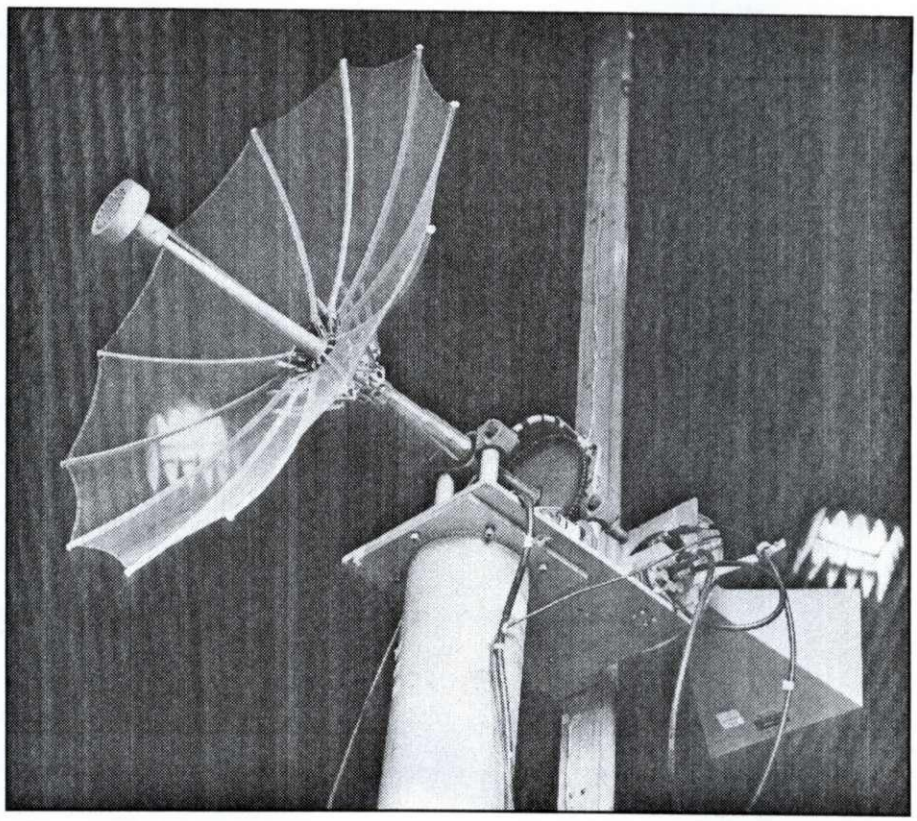

Photo 28-5.1. The strange device shown here that looks like a gossamer umbrella is actually the 3.6-GHz lunar rover parabolic dish antenna mounted on a test fixture designed and used by the author to measure the radiation pattern and gain during the development and the final measurements prior to delivering the antenna to NASA. It is presently mounted on one of the three lunar rover vehicles parked in one of NASA's used-car parking lots on the Moon.

On the appointed day, the initial pre-launch testing of RELAY 1 was in progress. The first portion of the test was performed with the gantry in place around the spacecraft and all tests went well. However, as the gantry was being moved away, the command signal from the ground station began fading at the input of the receiver in the spacecraft. When the gantry was completely away from the spacecraft the signal at the receiver was zero. With no way to further command the spacecraft with the gantry moved away, the launch director thought he had no alternative but to scrub the test for the day to allow the problem to be analyzed and repaired. Enter your author, Walt Maxwell, who had just finished installing the video-link dishes. Immediately sensing the cause of the signal failure he persuaded the launch director to take a short break in the test procedure to allow him to analyze and fix the problem. The director agreed. (I was knowledgeable concerning the RELAY antenna systems, because I had measured their antenna radiation patterns during the development phase of the spacecraft, in addition to measuring the final patterns proving that their performance conformed to the NASA specifications.)

I reasoned that the problem was due to cross polarization between the command transmitting antenna at the ground station and the receiving antenna on the spacecraft. The receiving antenna was vertically polarized, so I reasoned correctly that the wrong polarization was being used at the ground station. The NASA engineers at the ground station and I checked the patch panel that contained the connections to the RF coaxial cables leading to the antennas mounted on the platform. The indications inside the ground station were that the command transmitter was indeed correctly connected to the port labeled VERTICAL POLARIZATION TRANSMIT. I still insisted that the active antenna was horizontally polarized, and further insisted on checking the cable routings on the platform. It took some very diplomatic persuasion to get the NASA RF engineers to agree that the cables on the platform could be connected to the wrong antenna. However, the NASA engineers and I climbed onto the platform to investigate the problem and found the coaxial cable labeled VERTICAL POLARIZATION TRANSMIT was indeed connected to a *horizontally*-polarized antenna array, as I had predicted.

That cable was quickly disconnected from the

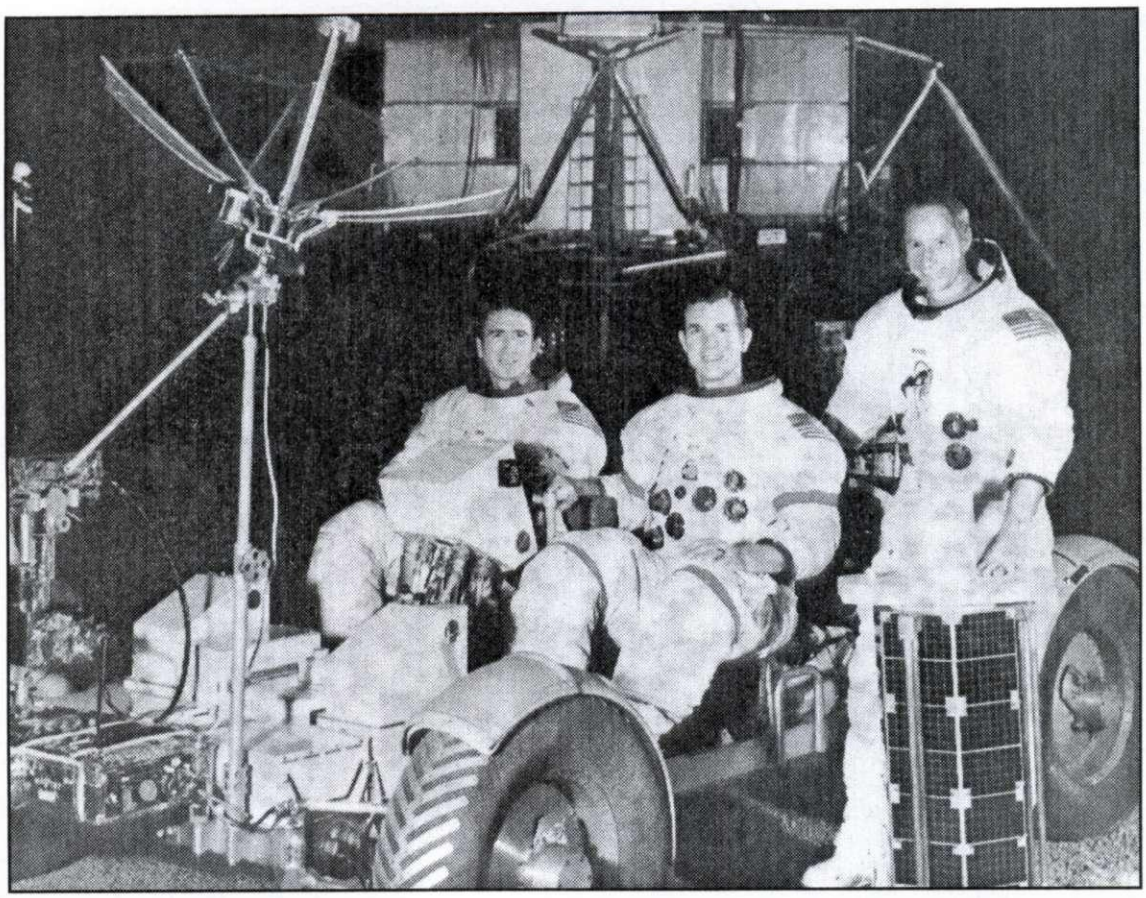

Photo 28-5.2. One of the three lunar rovers (Moon buggies) driven on the Moon's surface during the Apollo Program, shown with the 28-inch TV dish antenna described in the text. It is now parked in one of NASA's used-car parking lots on the Moon. Prime crew of the Ninth Manned Apollo mission, the astronauts shown left to right are James B. Irwin, David R. Scott, and Alfred M. Worden, Jr.

horizontal array and reconnected to a vertical array, when *voilá, the signal level at the command receiver in the spacecraft returned to normal.* The launch director was delighted, giving me a hearty congratulation for saving my test from being scrubbed until another day.

It's now quite reasonable to ask, "How could I be so certain that the problem was one of cross polarization?" To answer this question we must go back in time to December 1959 at Cape Canaveral. After completing the development of the antenna system for the spacecraft TIROS 1, I was assigned the task of designing, constructing, and installing the antennas at the ground station to be used for the prelaunch operations of the TIROS spacecraft at Cape Canaveral, which was launched April 1, 1960. After installing those antennas I proceeded to the 12th-story level of the gantry at launch pad 17A to take field strength measurements at the point where the spacecraft would be positioned. These measurements were necessary to determine the power needed at the ground station to communicate successfully with the spacecraft on the launch pad. The data obtained from these measurements revealed a surprising phenomenon. Because the girders used in the construction of the gantry were so tightly connected at each joint, the RF currents induced in them from the signals radiated from the antennas at the ground station flowed uniformly in both the vertical and horizontal girders regardless of the polarization radiated from the antennas at the ground station. Consequently, no matter which polarization was radiating from the antennas at the ground station, the field strength received by the test antenna at the spacecraft location within the confines of the gantry was identical, no matter

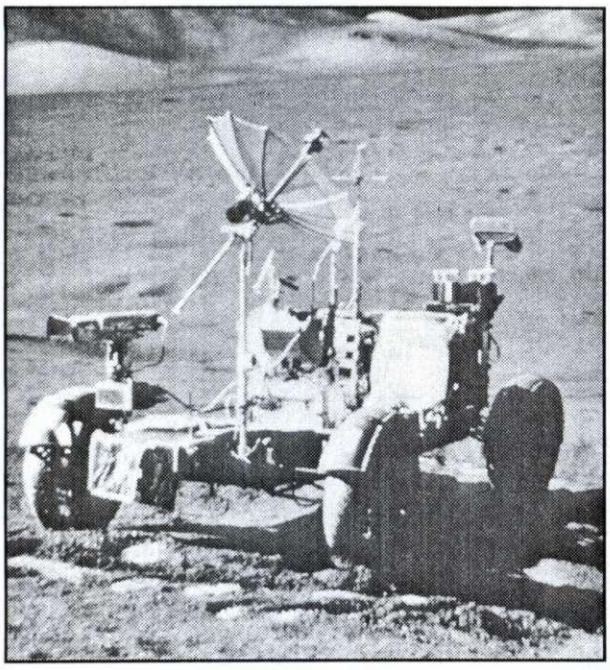

Photo 28-5.3. One of the three lunar rovers now parked in one of NASA's used-car parking lots on the Moon.

which polarization of the test antenna—horizontal, vertical, or any angle in between. In other words, within the gantry the incoming linearly-polarized waves were being converted to circular polarization due to the girder construction of the gantry. This, then, is the reason the vertically-polarized RELAY receiving antenna within the gantry received a normal-level signal with the transmitting antenna radiating horizontally-polarized waves, but which dropped to zero signal when the gantry was removed. A perfect example of loss of signal due to cross polarization—problem solved!

Sec. 28.5 The Lunar Rover (the Moon Buggy)

The TV dish antenna in Photo 28-5.1 was used by the Apollo astronauts during their Moon ride in one of the Moon Buggies. It transmitted TV signals directly from the Moon Buggy to Earth and into the TV networks from a camera and a 5-watt S-band transmitter mounted on the buggy. When the buggy was stopped for a TV broadcast, the astronauts aimed the dish toward Earth, using an optical telescope attached to the dish mounting. To facilitate aiming with the high accuracy required, the optics in the telescope were designed so that Earth just filled the viewing area. The 28-inch diameter dish, constructed of gold-plated fine-mesh wire, has a gain of 26 dBic at 3600 MHz and folds up like an umbrella.

The dish is shown in Photo 28-5.1 at RCA on a test fixture designed by the author, mounted atop the vertical stanchion of an antenna-positioner turntable (not shown). Here the dish received its final RF measurements of radiation pattern and gain. It is situated in an anechoic chamber, or RF darkroom. The room eliminates reflections that would affect the accuracy of the measurements. For the pattern and gain measurements, the dish is illuminated with RF from a transmitting antenna positioned 900 feet downrange. The pattern measurement is made by rotating the dish in azimuth (through the rotation of the turntable supporting the stanchion), recording the signal level received by the dish during the rotation. A standard-gain reference horn is visible in the lower right in Photo 28-5.1. The horn is mounted on the same shaft as the dish, so as the dish rotates in azimuth, so does the horn. As the dish-horn combination rotates through the 180° position in azimuth, the open end of the horn becomes illuminated by the downrange transmitting antenna. As this occurs, a coaxial switch just to the left of the horn is turned to switch the receiver from the dish to the horn recording the pattern of the horn as it rotates through the RF illumination. The gain of the dish antenna is then determined by comparing the recorded level of the signal received by the dish with that received by the reference horn. The uniformity of the radiation pattern around the axis of the dish is also measured. These measurements are performed by setting the dish at selected angles in azimuth relative to the downrange illumination while rotating the dish on its own axis, again recording the signal level. Measurements on all the antennas that went to the Moon on Lunar Rovers were performed by the author. In the event that you saw TV pictures sent from the Lunar Rover by the Apollo astronauts, the antenna in Photo 28-5.1 is one of the three that transmitted the TV signals from the Moon. Photo 28-5.2 shows three astronauts aboard one of the three Moon buggies. Photo 28-5.3 shows one of the three Moon buggies parked in one of NASA's used-car parking lots on the Moon.

Chapter 29

Broadcast Engineering

Sec 29.1 A Messy Ground Radial System can cause Radiation of Spurious Signals

In 1948 I was the consulting engineer for the proposed first AM broadcast station in Mt. Pleasant, Michigan, which resulted in a construction permit and license for WCEN, 500 watts on 1150 kHz. Using a National HRO receiver, I was performing a hands-on search for an available frequency for the new station, when I encountered an interesting and unusual signal that was entirely out of place in the AM broadcast band—a CW Morse-code station illegally transmitting five-letter-word code groups at 30 words per minute. The illegal signal was S9 +40 dB on 1297.8 kHz, producing a 2200-Hz beat-note with the 1300 kHz frequency of WOOD, Grand Rapids, thus producing an audible CW signal with the receiver BFO disabled.

The format of the coded messages appeared to be military, IDing as NSS. NSS is the flagship station of the U.S. Navy in Annapolis, Maryland, but in the AM broadcast band? It appeared that either an NSS transmitter was producing a spurious emission, or a station using NSS as a fraudulent call sign was operating clandestinely in the AM broadcast band. I deemed it important to find out which.

As a former FCC monitoring officer at the Allegan, Michigan monitoring station, the next step was to report the situation to the Allegan station. Although Allegan was 90 airline miles away, the monitoring personnel there could not hear the spurious signal, even though it was S9 +40 dB at Mt. Pleasant. I let the FCC monitors hear the signal through the telephone, but they still heard nothing on their receivers tuned to 1297.8 kHz. Thus, the signal must have been of local origin near Mt. Pleasant and not from NSS. However, to be on the safe side, the FCC notified the Navy of the spurious signals, and the NSS operators began combing all their transmitters for spurious signals; they found none. The situation now became even stranger.

I then copied five minutes of the coded text and sent a copy to the FCC, who relayed it to NSS for comparison to their transmissions. The situation was now both perplexing and frustrating, because the text I copied on 1297.8 kHz agreed exactly with a transmission that had been made by NSS. How could that signal have been transmitted on 1298.7 kHz if no spurious signals were emanating from NSS? It obviously was not a fraudulent station. What then?

A partial answer came shortly thereafter. As I resumed the search for a usable frequency for the new station, I proceeded downward from 1298.7 kHz, going through 1280 kHz and hearing WFYC, Alma, 1000 watts, 15 miles away, also S9 +40 dB. However, on continuing further downward I immediately came across another S9 +40 dB thumping CW signal. I switched on the BFO and discovered the CW was also a five-letter-word coded transmission at about 30 wpm, the same as NSS. I retuned to 1298.7 kHz and the NSS signal was also there, as before. Thus, I cranked up a second receiver to monitor both frequencies simultaneously. Surprise! Both frequencies were showing identical, simultaneous transmissions. I then measured the frequency of the lower-frequency signal—1262.2 kHz. *Voilá!* The higher CW frequency was 17.8 kHz above WFYC's 1280 frequency, and the lower CW frequency was 17.8 kHz below WFYC's frequency. A quick reference to the Berne frequency listing showed NSS assigned to 17.8 kHz. This situation now appeared to indicate something very wrong going on at WFYC. The low-frequency, worldwide ground-wave signal from NSS apparently somehow was mixing with the signal from WFYC and producing the 1297.8 and 1262.2 kHz sum and difference frequencies. However, what non-linear device in WFYC's system could perform that mixing? I didn't, but I reported this new information to the FCC and that was the last I heard of the situation … until:

Fast forward to 1955. I was now employed as an electrical engineer at the RCA Laboratories, the

David Sarnoff Research Center in Princeton, N.J. An assignment took me to Washington, D.C. to attend the annual conference of the NAB, the National Association of Broadcasters. President Dwight D. Eisenhower gave the keynote address. However, one of the technical forums was presented by Jack Young, Chief Engineer of the RCA Broadcast Division. His topic was the solution of mutual interference between two broadcast stations in Los Angeles, KFI and KNX.

It seems that in a section of the Los Angeles area it was impossible to hear one of these stations without hearing both simultaneously; when tuned to 640 kHz for KFI, both KFI and KNX were heard, and when tuned to 1070 kHz for KNX, both KNX and KFI were heard. Young was assigned the task of determining the cause of the interference and eliminating it. To make a long story short, he discovered that there were ancient and rusty oil-well derricks in the affected area. Currents from both KFI and KNX transmissions were being induced in the oil-well towers, and the rusty joints were acting as mixers for the two frequencies, producing both the sum and difference frequencies, as well as re-radiating both signals on their original frequencies. When the derricks were removed the interference stopped.

How is this incident relevant to the NSS problem? Well, at the conclusion of Young's presentation I had the opportunity to talk with him, and because of the similarity of the problems, I told him of my discovery of the NSS signals appearing in the AM broadcast band. Talk about coincidences! He was surprised and excited to learn that I had discovered the NSS problem at WFYC, because he was the one assigned to determine the cause of that problem. He had never been told how that problem originated, or how the problem had been discovered.

Young then explained that he had found the ground radial system under the WFYC antenna a horrible mess: cold solder joints throughout, and far ends of the radials hanging loose in the water of the nearby Pine River, establishing the non-linear mixer condition that resulted in the sum and difference frequencies being generated between the NSS and WFYC signals. Cleaning up the radial mess ended the appearance of the NSS signals in the AM broadcast band, thus concluding an interesting journey.

Chapter 30

How the FCC Played a Huge Part in Helping End WW II

(Adapted and revised from QST, *January 2007; won second cover award)*

Sec 30.1 Background

Have you ever heard of the RID, the Radio Intelligence Division of the FCC? Not likely, unless you were born before 1930. Due to the secrecy of its operations during WW II there was practically no publicity surrounding its existence. However, there was one article in *QST*, October 1944, "Hams in the RID," by Oliver Read, W9ETI, that described its operations at the primary FCC monitoring station at Allegan, Michigan. Thus, I believe you'll find it interesting to examine some of the contributions hams and commercial radio ops made to the WW II effort, as they were the operating personnel of the FCC's Radio Intelligence Division. What was the Radio Intelligence Division of the FCC? To answer that question I'm about to tell you some of the wartime history of the FCC. I say "some" of the history, because the secrecy act prohibits most of the intelligence cases from being divulged for 75 years following the end of WW II, leaving 10 years before those cases can be made public. However, this is the beginning of what can be told now, because some of the activities of the RID have been cleared for publication.

With the war already raging in Europe in 1939, people at the State Department knew they were missing vital war intelligence being exchanged by radio, especially that going between Germany and South America. They queried the FCC Field Division in early 1940 about monitoring to intercept the intelligence. The Field Division operated the original primary monitoring stations, performing regulatory and enforcement duties. However, at that time the Field Division personnel had their hands full just monitoring domestic operations and had no time for intelligence monitoring.

The President (FDR) and Congress were alerted to the need for additional personnel and equipment for the FCC to monitor intelligence, and they approved funds for establishing a new section, the National Defense Operations section, NDO. The NDO began operations September 3, 1940, and was later upgraded to a division, becoming the Radio Intelligence Division, RID. To head the NDO, the late George E. Sterling (W1AE/W3DF) was elevated from Assistant Chief Engineer, FCC,

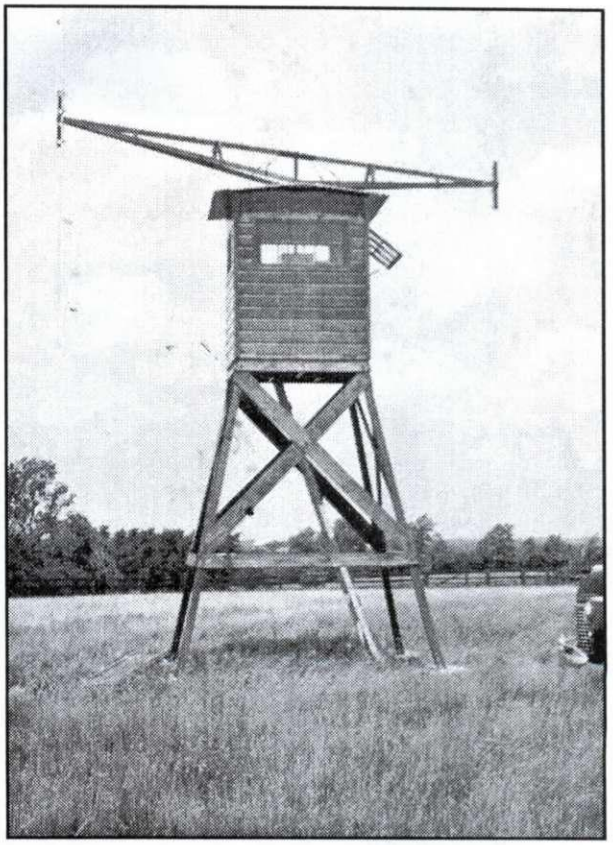

Photo 30-1. The FCC Adcock direction-finding station at Lexington, Kentucky, in 1941. This station is typical of FCC direction-finding Adcocks used at all FCC monitoring stations in the US mainland, Hawaii, Alaska, and Puerto Rico.

to Chief, NDO Section, and later to Chief, RID. To obtain personnel for the new Section he instructed one of his assistants, the late Harriette Koster, to search through the file cards containing the basic information on licensed amateur and commercial operators. She selected more than 500 operators from the file cards, and over T. J. Slowie's signature, she sent telegrams to those selected, offering them positions of Radio Operator ($1800 per annum), Assistant Monitoring Officer ($2400), and Monitoring Officer ($3200). The entire personnel for the new NDO Section, including myself, were obtained from responses to those telegrams. (Harriette later became my wife, and mother of our four children: Bill, W2WM; Rick, W8KHK; John, K4JRM; and Sue, KC4UBZ [Sue's license now has expired].) The Congressional funding also supported building many new secondary monitoring stations throughout the country, each equipped with Hallicrafters SX-28 and S-27 receivers, and Adcock (sky-wave) direction finders to determine the location of radio stations suspected of clandestine operation. In addition, Hudson automobiles equipped with the Hallicrafters receivers and a loop direction finder, used for mobile close-in surveillance, were a part of each secondary station.

Immediately following Pearl Harbor, December 7, 1941, the FCC RID mobilized a group from both primary and secondary monitoring stations to go to the Hawaiian Islands to set up and operate eight new secondary stations, one each on Oahu, Molokai, Kauai, Maui, and Lanai, and three on the Big Island, Hawaii. NDO Chief Sterling accompanied the group, of which the late Prose Walker, W4BW (then W2BMX and later WØCXA), and I (then W8KHK/W8VJR) were from the primary station at Allegan, Michigan. The late Charles Ellert, W3LO, Chief of the FCC Labs at Laurel, Maryland, who designed the eight Adcock antennas we carried with us for use at each secondary station, was also in the group. (Much later, after WW II, Walker became Chief of FCC's Amateur Radio and Special Services Division.)

After arriving on the islands and setting up the new stations, extensive 24/7 mobile monitoring around the shoreline of all the islands was pursued, with the intention of finding clandestine radio operation between local Japanese loyal to Japan and Japanese submarines cruising off shore. No such operations were found to occur, and no Hawaiians of Japanese descent were found to be disloyal to the U.S. During my stay on the islands I worked at stations on Oahu, Kauai, Molokai, and Hawaii. (I also worked at the Allegan station from September 1940 until leaving for Hawaii, returned to the Allegan station in October 1943, staying until April 1944, when I enlisted in the Navy, becoming an instructor in electronics.)

With Adcock direction finders at all eight secondary stations, plus the one at the primary station at the Punchbowl in Honolulu, the FCC saved the lives of thousands of military personnel and more than 600 military aircraft flying the Pacific between the mainland and the islands during WW II, after becoming lost due to errors in navigation with limited fuel supply. I'll now describe how this task was performed, and how a Beverage antenna was used to receive local Japanese AM broadcasts from JOAK, Tokyo.

Sec 30.2 Using the Beverage Antenna in WW II

As a monitoring officer with the Radio Intelligence Division (RID) of the FCC in Hawaii during WW II, I was privy to some interesting situations. Our State Department was, of course, aware of the operations occurring in the Pacific theater. The people there also were aware of the propaganda being spewed by the Japanese short-wave broadcasters. However, the State Department was curious concerning what the Japanese living on the homeland were being told—were they being told the truth, or the same propaganda as told on the short-wave broadcasts, or a totally different story. The State Department asked the RID to determine whether we could obtain such information.

We cruised the AM broadcast band and found several nighttime signals from Japanese mainland stations, but most were too weak to copy. However, JOAK, Tokyo, on 640 kHz was S9, but there was a problem in copying it. KFI, Los Angeles, was also on 640 kHz with an S9 signal—copying intelligence from JOAK was impossible. How could we eliminate, or reduce, KFI's signal level? A Beverage wave antenna perhaps?

We then proceeded to the northern portion of Oahu and constructed a Beverage one-half mile

long, 5 feet above ground, aimed at Tokyo, and terminated with a 1000-ohm pot resistor to ground at the Tokyo end. We discovered that by varying the pot resistance we could null the KFI signal to almost zero. The resistance terminating the Beverage that produced the null was around 600 ohms. Because the matching resistive termination rendered the Beverage a traveling-wave antenna with no standing wave, the signal arriving from JOAK was terminated by the input of our receiver, while the signal arriving from KFI was dissipated in the matched resistance at the Tokyo end of the Beverage—no KFI signal was reflected toward the receiver. *Voilá!* JOAK was now perfectly readable for recording!

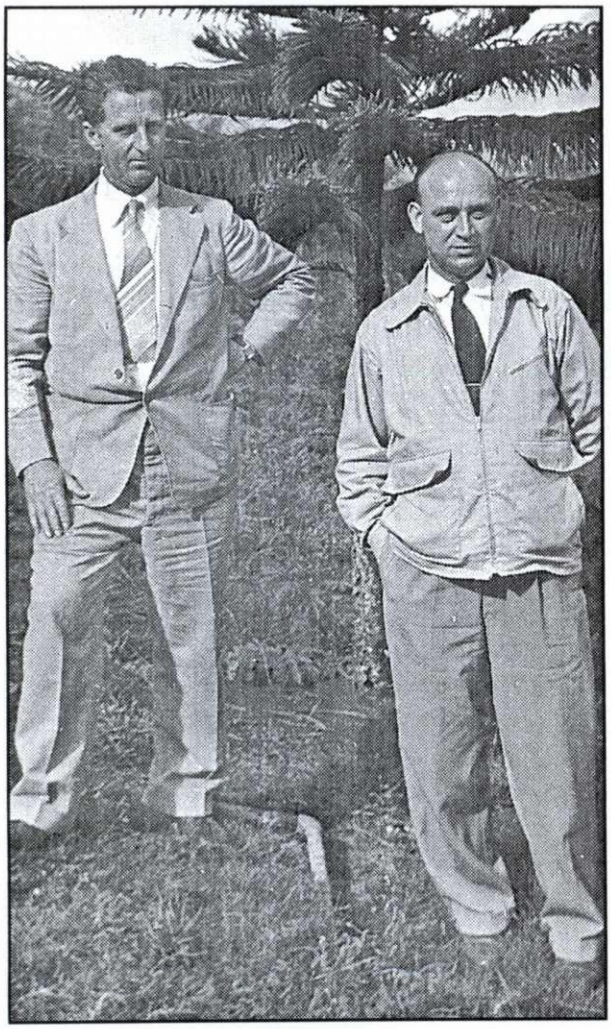

Photo 30-2. Shown on the left is the late George E. Sterling, Chief RID, W3DF/W1AE. Sterling was later elevated to Chief Engineer of the FCC, and still later was appointed FCC Commissioner by President Truman. Sterling was the only radio amateur to become an FCC Commissioner. The late Charles Ellert, W3LO, Chief of the FCC Laboratory, is on the right.

We sent the first recording to Washington, and the State Department was delighted—requesting that we continue recording JOAK nightly. Consequently, our recordings were flown daily to Washington from Hickam Field in Honolulu. We were left in the dark concerning the information on the recordings, and how it affected the war effort, because the State Department didn't share it with us. But it must have been pretty good, because the State Department was on our case every day to make sure we sent them the recordings.

Sec 30.3 The Correct Polarization Saves Lives During WW II

After arriving in Hawaii in 1942, Prose Walker was appointed chief of the newly established Radio Security Center (RSC) of FCC's RID, located in the Dillingham Building, Honolulu. (As stated above, long after WW II, Walker was Chief of the Amateur and Special Services Division of the FCC, succeeded by John Johnston, W3BE, President of QCWA.) In his position as Chief RSC, Walker learned that many military aircraft and its personnel were being lost due to ditching at sea while flying from the U.S. Mainland to Hawaii. There were two reasons for their being lost: (1) "navigationally impaired" pilots (government jargon for "lost"), and (2) totally drained fuel tanks. There was naturally a limit to the size of the fuel tanks, but what caused the pilots to become navigationally impaired? That point preyed on Walker's mind, and on investigating he discovered a deplorable situation that needed fixing. Here's what he found:

At the Boeing aircraft plant in Seattle they were building bombers as fast as possible. Dozens of green flight teams just out of flight school were awaiting their new aircraft and anxious to get aboard and proceed to the South Pacific area as soon as possible. The navigators and radio operators were taught how to use the loop direction finders (DFs) that were standard equipment on the aircraft. However, they were never told that loop DFs were incapable of obtaining reliable directional information from signals propagated by sky waves

reflected by the ionosphere. The DFs aboard the aircraft were capable of delivering reliable data only when the electromagnetic energy in the received signals was vertically polarized, but the navigators and radio ops didn't know that.

Unfortunately for them, on reflection and refraction through the ionosphere, a linearly-polarized wave, either vertical or horizontal, was converted into an elliptically-polarized wave, causing a continual shift in the null obtained by the loop DF as the polarization angle of the incoming signal rotates elliptically during propagation. Consequently, once the aircraft had left the mainland and could no longer receive the vertically polarized waves from AM broadcast stations, the only reception remaining was from sky waves propagated far beyond the range of the ground waves of the AM stations. Therefore, bearings taken using the loop DFs aboard the aircraft when at sea beyond the ground wave signal were useless. The only remaining means for the navigator to determine the position of the aircraft was through celestial navigation, using readings from the sun or stars. The situation was pretty bad on cloudy days, and that's when the pilots became navigationally impaired.

Photo 30-3. On the left is the late Prose Walker, W0CXA, licensing engineer with the FCC Broadcast division, consulting engineer with the Collins Radio Corp., engineering head of the NAB (National Association of Broadcasters), Chief of the FCC Amateur Radio Division. On the right is the late Charles Ellert, W3LO, Chief of the FCC Laboratory.

At this point Walker came up with a solution that ended the era of lost aircraft flying between the Mainland and Hawaii. Fortunately, every FCC monitoring station in the U.S., Hawaii, Alaska, and Puerto Rico had Adcock direction finders as standard equipment. Adcocks, as you may already know, are susceptible only to the vertical component of the arriving wave, regardless of its angle of polarization. Therefore, instead of constantly wandering, as with the loop DF, the null obtained with the Adcock remains stable at constant angle, even though the angle of polarization of the arriving wave is continually rotating elliptically. In other words, Adcocks give accurate directional information obtained from sky waves. Walker's reasoning was that triangulation from bearing measurements obtained by the FCC Adcocks taken on signals transmitted from the lost aircraft could determine its precise location, and thus determine a course for the aircraft to fly directly toward Hickam Field in Honolulu. The problem then was how to organize the communications to achieve the necessary procedure. Walker organized it in this manner:

The CAA (then the Civil Aeronautics Administration) operated a terminal in Honolulu with extensive operating facilities for communicating with all aircraft. A direct teletype connection was set up between the CAA and the RSC, which had a kilowatt transmitter used to communicate with the monitoring stations on all the islands, each of which had Hallicrafters HT-9 transmitters. When the pilot of the

aircraft determined he was lost, the radio operator signaled the CAA, who instantly put the aircraft's frequency on the teletype and rang its bell, alerting the RSC operator of the situation. The RSC operator then sent the following message in CW to all monitoring stations that were continuously monitoring the RSC frequency: "LOS LOS LOS 4250 4250 4250," where LOS meant lost aircraft and 4250 was the frequency being transmitted by the aircraft. The operator of the Adcock DF station immediately tuned to the 4250-kHz frequency, heard the aircraft, and began taking continuous bearings. The aircraft radio operator sent long dashes, MO MO MO, to enable the DF operator to be certain he was hearing the right signal and to obtain a satisfactory bearing angle on a moderately constant signal.

As each bearing was taken by all stations, the bearing angle was transmitted to RSC, where a great-circle map of the entire Hawaiian Pacific area was hanging on the wall. A compass rose was printed on the map at the location of every monitoring station on the islands, with a hole in the center of the rose through which a weighted string was hung. A pin was attached to the opposite end of the string, and the string was stretched across the compass and rose at the angle of the bearing obtained by the station represented by the rose. The pin was then pressed into the map, securing the string at that bearing angle. As the strings representing each station reporting were secured, they intersected at the point indicating the location of the lost aircraft, the intersection point called a "cocked hat." It was routine for the aircraft's position to be determined within ten minutes after the pilot alerted the CAA of its being lost.

After the aircraft's position was located, it was then given a course to fly toward Hickam Field, and the bearing measurements were reported continually until the pilot could see the field. During this time the aircraft's location was followed all the way in to the field, thus verifying the accuracy of the bearing measurements and the pilot's success in following the directions.

Once Walker's plan was in operation, no more aircraft were lost due to navigational impairment

Photo 30-4 . George E. Sterling making notes in front of the Little Grass Shack in Kealakekua, Hawaii. The 1930's tune with the above title became popular before the shack appeared. When visitors came to Kealakekua in Kona, on the west side of the Big Island, they were disappointed in not seeing the shack, so the people of Kealakekua built the one seen in the photo.

while flying between the Mainland and the Hawaiian Islands. In 1943 alone, 273 aircraft were saved by the FCC Adcocks, and more than 600 were saved during the duration of the war.

Unfortunately, planes continued to be lost on the run between Hawaii and the South Pacific, so the U.S. Military invited Walker to investigate. What he found there was almost unbelievable. The Army Air Corps was using Mercator projection maps for those runs, unaware that using maps of that projection produced directional errors of humongous and fatal proportions. On Walker's advice, once they acquired new maps with great-circle projection, the number of planes lost on the South Pacific run also dropped to zero.

These are just two of the stories of how the FCC assisted in the ending of WW II, of which I was privileged to be a part.

Sec 30.4 Addendum

George Sterling originated the science, art, and technique of radio intelligence while an officer in the US Army during World War I, reporting directly to General John J. Pershing. At the front line he organized and operated the first radio intelligence section of the Signal Corps in France which located enemy radio transmitters and intercepted their message traffic. For this work he received a citation from the Chief Signal Officer of the AEF for "especially excellent and meritorious service."

It is appropriate now to describe the Adcock antenna. The Adcock is a simple array of two parallel, center-fed vertical dipoles, fed 180° out of phase and spaced from 15 to 20 feet apart. The dipoles are connected with open-wire transmission line, transposed at the exact center, which we will call the *main line*. In other words, the transposition means that the conductor in the main line that connects to the top section of one dipole is connected to the bottom section of the other dipole, and vice versa. Thus, the out-of-phase relationship between the two dipoles results from the transposition of the main line that connects them together. A second open-wire line connects the receiver to the main line at its exact center. Consequently, when the two dipoles are positioned such that they both are equidistant from the source of the received signal, the phase of the signal received by one dipole is 180° out of phase with the signal received by the other dipole. Because the amplitudes of the signal received by each dipole are equal, the sum of the two signals resulting from their out-of-phase superposition is zero, producing a null in the received signal. Thus, when the dipoles are in the position producing a null, an imaginary line containing the dipoles is perpendicular to the direction toward the source of the received signal.

Appendix 1

Minimum-SWR Resistance Equation

I have never seen a reference to the minimum-SWR resistance in relation to terminating loads in any of the engineering or academic literature. Therefore, I believe I am the originator of the relationships represented by Eqs 5-1 and 5-2, discussed in Sec 11.3, and the derivation given here.

Theorem:

When a transmission line of characteristic impedance Zc is terminated with an impedance Z = R + *j*X, for every value of X there is corresponding value of R which yields the minimum value of SWR. For minimum SWR when R = Zc, X must be zero.

Prove that $r = \sqrt{x^2 + 1}$ (see Appendix 1 Fig 1)

where:
r = normalized resistance component of Z yielding minimum SWR
x = normalized reactance component of Z

r' = radius of resistance circle = $\frac{1}{r + 1}$

Uc = center of resistance circle = $\frac{r}{r + 1}$

$\frac{1}{x}$ = center of reactance circle

ρ = magnitude of reflection coefficient

$\tan \theta = \frac{1}{1/x} = x = \frac{\rho}{r'}$

$$\rho + \frac{1}{x} = \sqrt{(1/x)^2 + 1^2} = \frac{\sqrt{x^2 + 1}}{x}$$

$$\rho = \frac{\sqrt{x^2 + 1} - 1}{x}$$

$$r' = \frac{\rho}{x} = \frac{\sqrt{x^2 + 1} - 1}{x^2} = \frac{1}{r + 1}$$

Inverting:

$$\frac{1}{r'} = \frac{x^2}{\sqrt{x^2 + 1} - 1} = r + 1$$

Clearing the radical in denominator:

$$\frac{x^2}{\sqrt{x^2 + 1} - 1} \times \frac{\sqrt{x^2 + 1} + 1}{\sqrt{x^2 + 1} + 1} = r + 1$$

Multiplying and canceling:

$$\frac{x^2 \sqrt{x^2 + 1} + x^2}{x^2 + 1 - 1} = r + 1$$

$$\sqrt{x^2 + 1} + 1 = r + 1$$

$$\sqrt{x^2 + 1} = r$$

Therefore the theorem is proved.

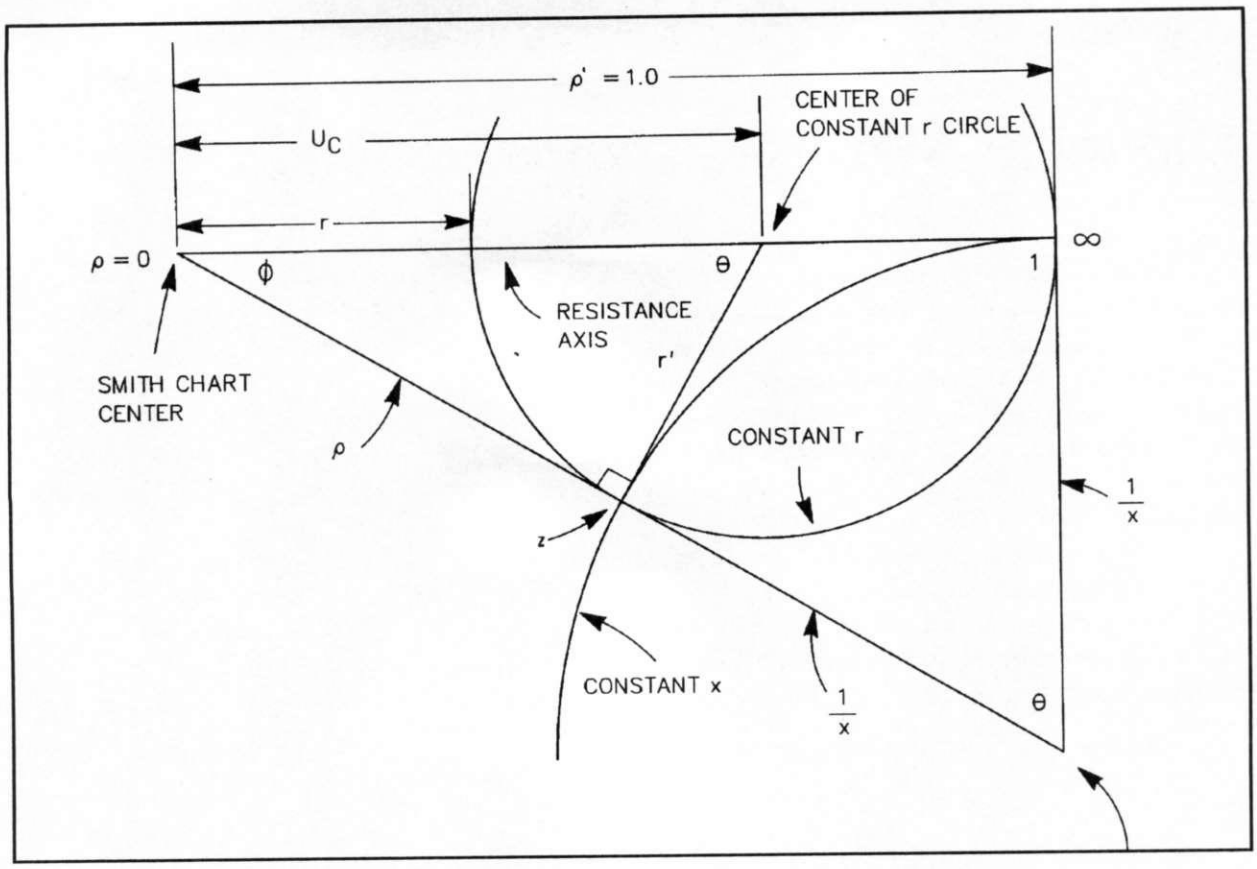

Appendix 1 Fig 1. Smith Chart geometry for Appendix 1 proof of minimum-SWR equation.

Appendix 2

Determining SWR from R + *j*X Method 1

The SWR resulting from an impedance mismatch may be obtained from the expressions SWR = R/Zc or SWR = Zc/R, *but only when the load is a pure resistance.* When the load is a complex impedance Z = R + *j*X, the exact SWR can be determined after finding the magnitude of the reflection coefficient ρ from Eq 3-1, repeated here in modified form.

$$\bar{\rho} = \rho\angle\theta = \frac{Z_L - Z_C}{Z_L + Z_C} = \frac{R - Z_C + jX}{R + Z_C + jX} \qquad \text{(Eq 3-1)}$$

where:

Z_L = the complex load impedance, R + *j*X

Zc = the characteristic impedance of the transmission line

The SWR may now be found from Eq 3-3, also repeated here.

$$SWR = \frac{1 + \rho}{1 - \rho} \qquad \text{(Eq 3-3)}$$

The SWR *cannot* be determined from any relationship between line impedance Zc and the magnitude |Z| of the complex load impedance, as shown in Appendix 2 Table 1. From the table, you can see that different values of load impedance Z_L can have the same magnitude |Z|, but produce different values of SWR on a feed line with a given Zc, which in this case is 50 ohms.

Polar Form		**Rectangular Form**		
|Z| at ± Angle		*R*	*± jX*	*SWR*
50	0.0°	50	0.0	1.0
50	25.84°	45	21.79	1.59
50	36.9°	40	30.0	2.00
50	45.0°	50	50.0	2.61803†
50	53.1°	30	40.0	3.00
50	66.42°	20	45.83	4.79
50	72.54°	15	47.7	6.51
50	78.46°	10	48.99	9.90
50	84.26°	5	49.79	19.95
50	87.13°	2.5	49.94	39.98
50	88.85°	1	49.99	99.99
50	90.0°	0	50.00	∞

†*See last paragraph of Appendix 3 for significance of this unusual value of SWR*

Appendix 2 Table 1. Complex load impedances versus SWR.

Appendix 3

Determining SWR from R + *j*X Method 2

I derived this method for calculating the exact value of SWR from R + *j*X from Eq 3-1 after a suggestion from the late Ken Miller, W2KF.

1. Normalize the load impedance by dividing by the characteristic impedance Zc of the transmission line.

$$\frac{R + jX}{Zc} = r + jx$$

2. Find the b term of the quadratic formula

$$\frac{b \pm \sqrt{b^2 - 4ac}}{2a}$$

using values of r and x in the equation

$$b = \left(\frac{x^2 + 1}{r}\right) + r$$

3. Calculate the SWR from the simplified quadratic equation

$$SWR = \frac{b + \sqrt{b^2 - 4}}{2}$$

The a and c terms of the complete quadratic equation reduce to 1 from normalizing the R and X terms of the load impedance. The negative root of the discriminant is ignored.

Let's now try an example by calculating the SWR on a 50-ohm line produced by a load impedance of 40 + *j*30 ohms.

Normalizing: $r + jx = \frac{40 + j30}{50} = 0.8 + j0.6$

Find the b term: $b = \left(\frac{0.6^2 + 1}{0.8} + 0.8 = 2.5\right)$

Calculate the SWR: $SWR = \frac{2.5 + \sqrt{2.5^2 - 4}}{2} = 2$

This is an excellent example because the answer is exactly 2:1 with no fractional remainder. To test your arithmetic, other examples to try which also give exact answers when Zc = 50 ohms are 30 + *j*40, SWR = 3:1; and 80 + *j*90, SWR = 4:1. It is also remarkable to note that the following different load impedances all produce an SWR of 2.618031 on 50-ohm lines: 25 + *j*25, 50 + *j*50, 100 + *j*50, and 130 + *j*10. See Appendix 4 for a hand-calculator program to compute SWR from the above equation.

Appendix 4

Program for Exact SWR from R + *j*X Method 2

Listed below is a calculator program for determining the SWR from R + *j*X, using Method 2 of Appendix 3. This listing is for a programmable Hewlett-Packard calculator or other brand using reverse Polish notation.

Line	Key Entry
1	H Label A
2	RCL 0
3	÷
4	g → x^2
5	1
6	+
7	x ↔ y
8	RCL 0
9	÷
10	STO 1
11	÷
12	RCL 1
13	+
14	ENTER
15	g → x^2
16	4
17	–
18	f → $\sqrt{\ }$
19	+
20	2
21	÷
22	H Return

Instructions:

1. Store line impedance Z_C in Register R_0
2. Key in R value of impedance R + *j*X
3. Press ENTER
4. Key in X value of impedance R + *j*X
5. RUN

Appendix 5

Derivation of Equations 6-1 and 6-2 in Chapter 6

I derived these equations to determine the power transmitted through a transmission line with attenuation and terminated in a mismatch (see Appendix 5 Fig 1).

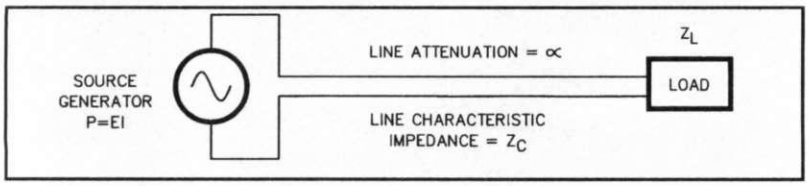

Appendix 5 Fig 1. Illustrating the transmission line for the Appendix 5 derivation of Eqs 6-1 and 6-2.

ρ_L = voltage reflection coefficient at load

$$= \frac{Z_L - Z_C}{Z_L + Z_C} = \frac{SWR - 1}{SWR + 1} \qquad \text{(Eqs 3-1 and 3-2)}$$

ρ_I at line input = $\rho\varepsilon^{-2\alpha}$

ρ_I^2 at line input = $\rho^2\varepsilon^{-4\alpha}$

ρ_L^2 = power reflection coefficient at load (equals reflected power)

where:

α = line attenuation in nepers = $\dfrac{dB}{20 \log \varepsilon} = \dfrac{dB}{8.6859}$

(one neper = 0.115129 decibel)

ε = 2.718282 (the base of natural logarithms)

The forward *voltage* wave encounters a reduction in level by the loss factor of $1/\varepsilon^{\alpha}$, or $\varepsilon^{-\alpha}$ in traveling from the source to the load. The reflected voltage wave encounters the same reduction factor $\varepsilon^{-\alpha}$ in its return to the source. Hence, the voltage reflection coefficient at the line input is $\rho_I = \rho\varepsilon^{-2\alpha}$.

The forward *power* encounters a *one-way* attenuation-loss factor $\varepsilon^{-2\alpha}$. Power returning to the source from a load reflection encounters a *two-way* loss—once during the trip to the load, and again during its return to the source. The power reflection coefficient at the line input is therefore $\rho_I^2 = \rho^2\varepsilon^{-4\alpha}$.

Let power supplied by the source = 1, and let reflected power reaching the input (which adds to the source power) = r. Then:

1 + r = total forward power at line input

$(1 + r)\varepsilon^{-2\alpha}$ = forward power arriving at the load, and

$\dfrac{r}{1 + r}$ = input power reflection coefficient = $\rho_I^2 = \rho^2\varepsilon^{-4\alpha}$

Now let $\dfrac{r}{1 + r}$ (and $\rho^2\varepsilon^{-4\alpha}$) = a

Then, total forward power (1 + r) at the line input = $1 + \frac{a}{1-a} = \frac{1-a+a}{1-a} = \frac{1}{1-a}$

Hence, it follows that

Forward power at line input		*Forward power at load after line atten.*		*Power reflected at load*		*Power absorbed in load*
$1 + r$	$\rightarrow$	$(1+r)\,\varepsilon^{-2\alpha}$	$-$	$\rho^2\,(1+r)\,\varepsilon^{-2\alpha}$	$=$	$(1+\rho^2)(1+r)\,\varepsilon^{-2\alpha}$

and

$$\frac{1}{1-a} \rightarrow \frac{\varepsilon^{-2\alpha}}{1-a} - \frac{\rho^2\varepsilon^{-2\alpha}}{1-a} = \frac{(1-\rho^2)\,\varepsilon^{-2\alpha}}{1-a}$$

But $a = \rho^2\varepsilon^{-4\alpha}$, so by substitution we have Eq 6-1:

$$\frac{1}{1-\rho^2\varepsilon^{-4\alpha}} \rightarrow \frac{\varepsilon^{-2\alpha}}{1-\rho^2\varepsilon^{-4\alpha}} - \frac{\rho^2\varepsilon^{-2\alpha}}{1-\rho^2\varepsilon^{-4\alpha}} = \frac{(1-\rho^2)\,\varepsilon^{-2\alpha}}{1-\rho^2\varepsilon^{-4\alpha}}$$

Translating the last expression on the right, it means that power absorbed in the load equals the source power times the quantity:

$$\frac{(1-\rho^2) \text{ times one - way line - attenuation factor}}{1-(\rho^2 \text{ times two - way line - attenuation factor})}$$

where $\rho = \rho_L$ from Eqs 3-1 and 3-2 above.

$$\frac{1}{1-\rho^2} \rightarrow \frac{1}{1-\rho^2} - \frac{\rho^2}{1-\rho^2} = 1$$

$$1 + r \rightarrow 1 + r - r = 1$$

When the SWR on a transmission line is $\approx$ 4.6:1 the total attenuation α_T is approximately two-times the attenuation of the line when matched.

Power Relationships on Mismatched Transmission Lines

The power relationships on a mismatched transmission line may be determined from the following equations.

ρ = magnitude of voltage reflection coefficient = $\frac{SWR - 1}{SWR + 1}$

ρ^2 = magnitude of power reflection coefficient (power reflected by mismatched load)

$(1 - \rho^2)$ = power absorbed by mismatched load

Example 1

Lossless line (attenuation $\alpha = 0$); line with matched load, SWR = 1:1, $\rho = 0$, $\rho^2 = 0$, and $(1 - \rho^2) = 1$. Transmitter matched to line-input impedance, Zc = 50 ohms. See Appendix 6 Fig 1. All the transmitter power, 100 W, is absorbed in the load.

Example 2

As in example 1, a lossless line (attenuation $\alpha = 0$); line with mismatched load, SWR = 3:1, $\rho = (3 - 1)/(3 + 1) = 0.5$. Transmitter initially matched to 50-ohm dummy load, then switched to the mismatched line without retuning and matching. The 3:1 load mismatch referred back to the line input results in a 3:1 mismatch to the transmitter; *transmitter not rematched* to the new line-input impedance. See Appendix 6 Fig 2. Here the transmitter reduces its delivered power by the amount of the reflected power, $\rho^2 = 25$ W, due to its mismatch to the line. Note that all the transmitter power delivered, 75 W, is absorbed in the load.

Example 3

As in example 2, a lossless line (attenuation $\alpha = 0$); line still mismatched with 3:1 SWR, but *transmitter rematched* (conjugate) to new line-input impedance. See Appendix 6 Fig 1C. The transmitter again delivers 100 W to the line, and 100 W are now absorbed in the Zc-mismatched, but conjugate-matched load. How is the 133.33 W of forward power obtained? From Chapter 6 Eq 6-2 (also in Appendix 5), forward power = $1/(1 - \rho^2) = 1/0.75 = 1.3333$ when the mismatch is 3:1. 100 W × 1.3333 = 133.33 W. (See Appendix 7 for explanation of the increase in forward power on line with mismatched load, but conjugately matched at line input by rematching pi-network in the transmitter, or with the use of an antenna tuner.)

Example 4

Line with attenuation $\alpha = 0.5$ dB, such as 87 feet of RG-59 or 175 feet of RG-8 at 4.0 MHz; matched load, as in example 1; SWR = 1:1. See Appendix 6 Fig 2A. The transmitter is matched to the line-input impedance Zc = 50 ohms. However, 100 W of forward power leaving the transmitter suffers 0.5 dB line attenuation loss; hence, only 89.125 W reaches the load, where it all is absorbed.

Example 5

Line with attenuation, $\alpha = 0.5$ dB, such as 87 feet of RG-59 or 175 feet of RG-8 at 4.0 MHz, as in Example 4, but line mismatched with 3:1 SWR at load. See Appendix 6 Fig 2B. The 3:1 load mismatch referred back to the line input through 0.5 dB of line attenuation results in a 2.61:1 mismatch to the trans-

mitter until matched by retuning, or with a transmatch. The rematched transmitter delivers 100 W to the line. With 0.5 dB of matched-line loss, plus 0.288 dB additional line loss from the 3:1 SWR, the total line-attenuation loss is 0.788 dB. The power lost to line attenuation with the 3:1 mismatch is 16.59 watts, in contrast to 10.87 watts lost when the line is matched (Example 4, Appendix 6 Fig 2A). The forward power, 124.78 W, suffers 0.5 dB loss to 111.21 W during the trip to the load; the reflected power, 27.8 W, suffers 0.5 dB loss to 24.78 W during the return trip to the transmitter, leaving 24.78 W to add to the source power, 100 W. The power absorbed in the load and the power lost in line attenuation account for all the power delivered by the transmitter!

With the conditions shown in Fig 6-2B, 100 watts of source power, line attenuation of 0.5 dB, and a 3:1 load mismatch, it should be understood that the forward and reflected powers, 111.21 watts and 27.80 watts, respectively, that appear at the load are the values that occur when the steady-state period has been

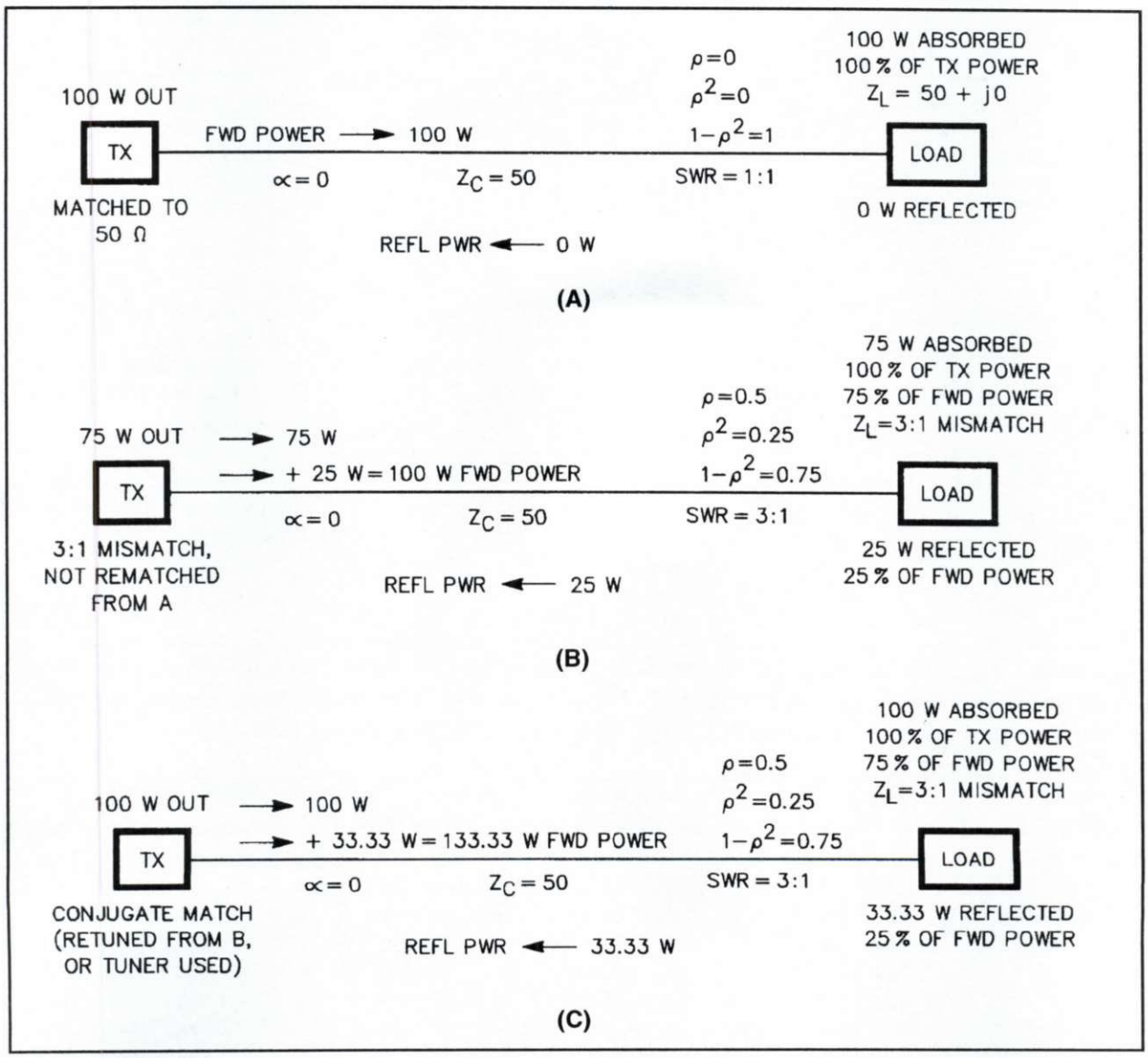

Appendix 6 Fig 1. Illustrating the transmission-line conditions for a lossless line with different loads and input matching conditions. Drawings A, B, and C, respectively, represent Appendix 6 examples 1, 2, and 3.

reached. Consequently, 111.21 watts of forward (or incident) power and 27.8 watts reflected leaves 83.41 watts absorbed in the load. Keep in mind that the decimal equivalent of 0.5 dB is 0.891251, and the power reflected at the load for a 3:1 mismatch is the forward power incident at the load times 0.25.

It is instructive to learn from Appendix 6 Table 1 how the magnitudes of the successive travels of the forward and reflected waves increase, but with smaller increments with each cycle as they progress from the first forward wave of 100 watts to the final steady-state condition, where the maximum available value of 124.78 watts is reached. From this time on, the change in magnitudes of both forward and reflected waves is vanishingly small, approaching zero with each successive cycle. Note that the steady-state condition is nearly reached after the fifth cycle is completed.

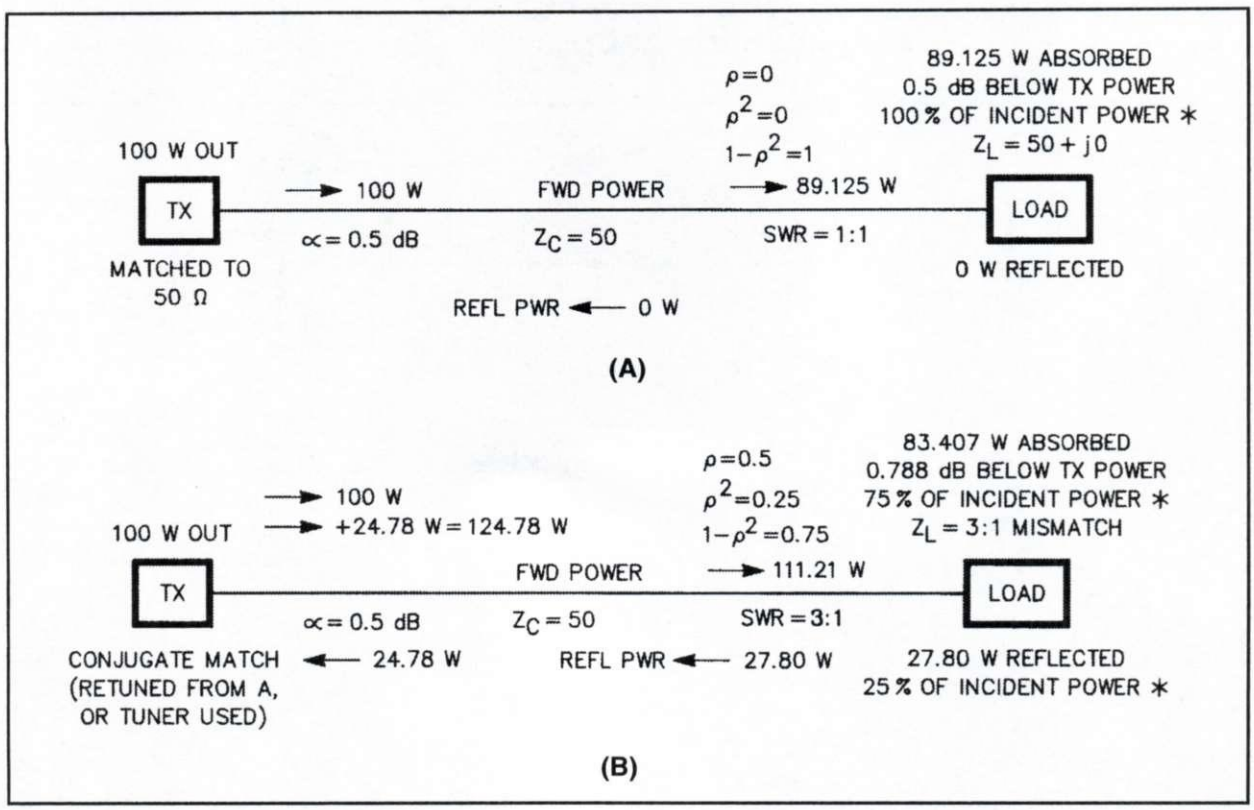

Appendix 6 Fig 2. Illustrating the transmission-line conditions for a line with 0.5-dB loss having different loads and input matching conditions. Drawings A and B, respectively, represent Appendix 6 examples 4 and 5. ****Incident* **power is the forward power that reaches the load.**

Wave Number	Forward Power at Input (w)	Forward Power at Load(w)	Reflected Power at Load (w)	Reflected Power on Return to Input (w)
1	100w	89.1251	22.2813	19.8582
2	119.8582	106.8237	26.7059	23.8017
3	123.8017	110.3384	27.5846	24.5848
4	124.5848	111.0363	27.7591	24.7403
5	124.7403	111.1749	27.7937	24.7712
6	124.7712	111.2024	27.8006	24.7773
7	124.7773	111.2079	27.8020	24.7785
8	124.7785	111.2090	27.8022	24.7788
9	124.7788	111.2092	27.8023	24.7788
Final Steady State	124.78w	111.21w	27.80w	24.78w

Appendix 6 Table 1. Integration of reflected waves to arrive at steady-state condition.

Appendix 7

On the Increase in Forward Power Resulting from the Conjugate Matching at the Input of a Mismatched Transmission Line

(Note: A calculator program for solutions using this procedure appears in Appendix 7A.)

When using coaxial transmission lines with a mismatched termination that gives rise to standing waves on the line, we must be concerned with the limitation that must be imposed on the magnitude of the standing waves by the voltage and power handling capability of the line. Thus, we must find a way to determine the amount of power traveling on the line with respect to the magnitude of the standing waves.

It is well known that when a transmission line has a mismatched termination, but which is conjugately matched at the input of the line, the forward power propagating along the line is greater than the source power by the amount of the reflected power. Consequently, on lossless lines, the power absorbed by the mismatched termination equals the total forward power minus the reflected power. However, for this phenomenon to occur the power traveling forward in the line must exceed that supplied by the generator. How can this be, you ask. The following discussion will explain this phenomenon (*Ref 18, p 99*).

When a wave of energy is first applied to the line, it sees only the characteristic impedance Z_0 in its travel along the line until it arrives at a mismatched termination. On arriving at the mismatch the wave is reflected with the reflection coefficient magnitude:

$$\rho = \frac{Z_L - Z_0}{Z_L + Z_0}$$

where

ρ = reflection coefficient of either voltage or current

Z_0 = characteristic impedance of the line

Z_L = impedance of the line termination.

The reflection at the mismatch gives rise to a second wave that travels back to the input of the line with the magnitude determined by multiplying the magnitude of the initial wave by the magnitude ρ. On arriving at the line input it sees total reflection $\rho = 1$ at the matching point in the network that achieved the conjugate match. Thus reflection of the second wave gives rise to a third wave of the same magnitude as that of the second wave, which also is reflected by the mismatched termination. This reflection thus gives rise to a fourth wave with the magnitude determined by multiplying the magnitude of the third wave by the magnitude ρ.

This process continues indefinitely, with each reflection smaller than the last. We thus have an infinite series of reflections, whose sum is convergent and represents the steady state condition, which is finally established. The infinite series can be written in the simplified form as $1 + a + a^2 + a^3 \ldots$, which converges to the value:

$$\frac{1}{1 - a} \quad \text{where } |a| < 1 \qquad \text{(Eq 1)}$$

We use this equation of convergence in solving for the total forward power in the line by letting "a" equal the *power reflection coefficient* ρ^2. Because the power absorbed in the load equals the forward power minus the power reflected, the *power transmission coefficient* becomes $1 - \rho^2$. We now replace "a" with ρ^2 in the convergence equation to get:

$$\frac{1}{1 - \rho^2} \qquad \text{Eq (2)}$$

which represents the sum of the infinite number of reflections appearing on a mismatched line when conjugately matched at the line input. Inserting the value of ρ^2 in the equation gives us the number to multiply by the source power to determine the total

power propagating in the forward direction toward the mismatched load, when the line is conjugately matched at the input with a matching network, such as an antenna tuner. The numerical result from calculating Eq 2 is called the *forward power increase factor.*

Let us illustrate this principle with an example. We will use the same values in the example that appear in the examples cited in Chapters 3 and 9, where the characteristic impedance of the transmission line is $Z_0 = 50$ ohms, and the mismatched load is a 150-ohm resistance, yielding a 3:1 SWR. The reflection coefficient $\rho = 0.5$, and therefore the power reflection coefficient $\rho^2 = 0.25$. Substituting 0.25 in the convergence equation, we get:

$$\frac{1}{1 - 0.25} = \frac{1}{0.75} = 1.3333$$

Thus, the forward power increase factor in this example is 1.3333. Consequently, if we supply 100 watts to the line with a 3:1mismatch, but conjugately matched to the RF generator at the input of the line, we find the total forward power to be 100 watts × 1.3333 = 133.33 watts

Continuing, let us determine the actual power incident on the mismatched load, the power absorbed by the load and the power reflected by the load. Recall that the power *transmission* coefficient $(1 - \rho^2) = 0.75$, which means that 75% of the power incident on the mismatched load will be *absorbed.* Also recall that the power *reflection* coefficient $\rho^2 = 0.25$, which means that 25% of the power incident on the load will be *reflected.* Multiplying out these percentages shows that 133.33 watts × 0.75 = 100 watts absorbed, and that 133.33 watts × 0.25 = 33.33 watts reflected. If we now add the 33.33 watts of reflected power to the 100 watts absorbed in the mismatched load we get 133.33 watts, thus proving that we have conformed to the Law of Conservation of Energy. We have also shown that, with lossless line, where there is no loss due to line attenuation, all the power delivered by the RF generator is absorbed in the load, even though mismatched 3:1 to the transmission line delivering the power.

Let us now apply the procedure to real transmission lines having loss due to attenuation. We perform this procedure by reducing the value of ρ by the amount of line attenuation α in decibels. We first convert the attenuation in decibels to its decimal value, and then multiply ρ by the decimal value to obtain the modified value of ρ that includes the effect of the line attenuation. The decimal number α_{DEC} of α is obtained from the expression:

$$\alpha_{DEC} = \text{anti } \log_{10}{}^{-\alpha/10} \qquad \text{(Eq 3)}$$

We will now illustrate the procedure with an example. We will use the example above where the mismatch yields reflection coefficient $\rho = 0.5$, but where the line attenuation $\alpha = 0.5$ dB. Dividing 0.5 by 10 yields 0.05. The expression "anti $\log^{-1}$" means taking the reciprocal of the number obtained by evaluating the number $10^{0.05}$, by raising 10 (the base of the logarithm) to the power 0.05. The number α_{DEC} can also be found by evaluating 10 with exponent –0.05 ($10^{-0.05}$) without taking the reciprocal.

Continuing the example, α_{DEC} = the reciprocal of $10^{0.05} = 0.89125$, the decimal value of 0.5 dB. ($10^{-0.05}$ also equals 0.89125.) Now we multiply ρ by α_{DEC} to obtain the new value of ρ' that includes the effect of the line attenuation.

$$\rho' = 0.5 \times 0.89125 = 0.44563$$

Squaring ρ' to obtain the new power reflection coefficient, $\rho'^2 = 0.44563^2 = 0.19858$. Replacing ρ^2 with $\rho'^2 = 0.19858$ in Eq 2 yields:

$$\frac{1}{1 - 0.19858} = \frac{1}{0.80142} = 1.2478$$

Thus, the forward power increase factor in this example is 1.2478. And as in the first example, if we supply 100 watts to the line having a 3:1mismatch, conjugately matched to the RF generator at the input of the line, but with the line now having a 0.5 dB attenuation, we find the forward power *at the input of the line* to be 100 watts × 1.2478 = 124.78 watts. However, due to the 0.5-dB line attenuation, the forward power encounters a 0.5-dB loss during its travel to the load, leaving 111.21 watts incident on the load. To confirm the incident power of 111.21 watts after 0.5 dB attenuation from the 124.78 watts at the line input, we see that:

$$\frac{111.21 \text{ watts}}{124.78 \text{ watts}} = 0.89125$$

which is the decimal number α_{DEC} that equals 0.5 dB obtained from the calculations above.

A diagram of this example, and further explanation from a different viewpoint, appears in Appendix 6, Fig 6-2B and *Example 5.*

Appendix 7A

Calculator Program for Determining the Increase in Forward Power Resulting from Conjugate Matching at the Input of a Mismatched Transmission Line

Listed below is a calculator program for determining the increase in forward power resulting from conjugate matching at the input of a mismatched transmission line, using the procedure described in Appendix 7. This listing is for a programmable Hewlett-Packard calculator, or other brand using reverse Polish notation.

Line	Key Entry	Comments
1	H Label A	
2	1	
3	–	
4	RCL 2	SWR
5	1	
6	+	
7	÷	
8	STO 8	
9	R/S ρ	
10	G → x^2	ρ^2
11	1	
12	↔	
13	–	
14	STO 5	
15	R/S	$(1 - \rho^2)$
16	RCL 1	α in dB
17	CHS	
18	ENTER	
19	1	
20	0	
21	÷	
22	g → 10^X	
23	STO 9	
24	R/S	α_{DEC}
25	RCL 8	ρ
26	×	ρ'
27	g → x^2	ρ'^2
28	1	
29	↔	
30	–	
31	STO4	
32	R/S	$(1 - \rho'^2)$
33	1	
34	↔	
35	÷	
36	H Return	

Instructions:

1. Store line attenuation α in Register R_1
2. Store SWR in Register R_2
3. RUN

Appendix 8

Determining the Increase in Power Lost due to Reflections and SWR

(A calculator program for solutions using this procedure appears in Appendix 8A.)

When using an antenna tuner with coaxial transmission lines to match the input impedance of the line to the transceiver, we often want to know how much additional power we will lose to line attenuation for a given value of SWR, over and above the power lost when the line is matched. Calculations to determine the additional power lost due to SWR are easy to perform using the reflection coefficient ρ, obtained by substituting the value of SWR in the following expression:

$$\rho = \frac{SWR - 1}{SWR + 1} \qquad \text{(Eq 3-2)}$$

It should be kept in mind that since standing waves result from reflections, the value of SWR is determined by the reflection coefficient. The scale of the SWR meter is designed to indicate SWR, but its needle deflection is determined by the reflection coefficient, which for an SWR of 3:1, reflection coefficient $\rho = 0.5$. Thus, the meter needle will be at half scale (0.5) for an SWR of 3:1. It is important to become familiar with using the reflection coefficient, because the entire procedure for calculating the additional power lost due to SWR will be with the reflection coefficient.

This procedure requires determination of the power transmission coefficients $(1 - \rho^2)$ at both the load and input ends of the transmission line. The difference between the two transmission coefficients gives the information we need to determine the amount of additional lost power. The power transmission coefficient at the load is determined from the reflection coefficient ρ at the load, and that at the input is determined by reducing the load ρ by the amount of the line attenuation α in decibels. Thus ρ represents the reflection coefficient at the load, and we will let ρ' represent the reduced reflection coefficient at the input. Consequently, the power transmission coefficient at the load is $(1 - \rho^2)$ and that at the input is $(1 - \rho'^2)$.

We first convert attenuation α in decibels to its decimal value α_{DEC}, using the expression:

$$\alpha_{DEC} = \text{anti log}_{10}{}^{-\alpha/10}$$

(Details for using this expression appear in Appendix 7.)

Next, we multiply ρ by α_{DEC} to obtain ρ' at the line input to include the effect of the line attenuation, and then substitute ρ and ρ' in the power transmission coefficients $(1 - \rho^2)$ and $(1 - \rho'^2)$, respectively. Due to the line attenuation, the power coefficient $(1 - \rho^2)$ at the load is less than coefficient $(1 - \rho'^2)$ at the input. The difference between the two power coefficients in dB gives us the amount of power lost because of the SWR.

We will now illustrate the procedure with an example, using the same values as in Chapters 3 and 9 (also Appendices 6 and 7). In those examples we used a transmission line having attenuation $\alpha = 0.5$ dB, terminated with a mismatched load that gives rise to reflections with the reflection coefficient $\rho = 0.5$, for an SWR of 3:1. Therefore, the power *reflection* coefficient at the load is $\rho^2 = 0.25$, and the power *transmission* coefficient at the load is $(1 - \rho^2) = 0.75$. Before we can determine the value of ρ' at the input, we must first calculate the decimal value of line attenuation α, using the expression repeated from above:

$$\alpha_{DEC} = \text{anti log}_{10}{}^{-\alpha/10}$$

Using the values obtained in the example appearing in Appendix 7, we find $\alpha_{DEC} = 0.89125$. Multiplying $\rho \times \alpha_{DEC}$ we get $\rho' = 0.44563$, which, after squaring, the power *reflection* coefficient at

the input is $\rho'^2 = 0.19858$. Therefore, the power *transmission* coefficient at the input is $(1 - \rho'^2) = 0.80142$. To find the difference between the two power transmission coefficients in dB, we perform the following division to find the decimal value of the loss:

$$\frac{(1 - \rho^2)}{(1 - \rho'^2)} = \frac{0.75}{0.80142} = 0.93548$$

which equals –0.288 dB, the additional power lost due to an SWR of 3:1 on a transmission line having an attenuation of 0.5 dB. The total loss includes the matched loss of 0.5 dB plus 0.288 dB due to SWR, which equals 0.788 dB. You may now find it interesting to review Example 5 in Appendix 6.

By using the procedure just described, the additional power lost to SWR can be found for any transmission line, once its matched-line attenuation and SWR are known.

Appendix 8A

Calculator Program for Determining the Amount of Additional Power Lost due to SWR on a Transmission Line

Listed below is a calculator program for determining the amount of additional power lost due to SWR on a transmission line, using the procedure described in Appendix 8. This listing is for a programmable Hewlett-Packard calculator, or other brand using reverse Polish notation.

Line	Key Entry	Comments
1	H Label A	
2	1	
3	–	
4	RCL 2	SWR
5	1	
6	+	
7	÷	
8	STO 8	
9	R/S	
10	G → x^2	ρ^2
11	1	
12	↔	
13	–	
14	STO 5	
15	R/S	$(1 - \rho^2)$
16	RCL 1	α in dB
17	CHS	
18	ENTER	
19	1	
20	0	
21	÷	
22	g → 10^X	
23	STO 9	
24	R/S	α_{DEC}
25	RCL 8	ρ
26	×	ρ'
27	g → x^2	ρ'^2
28	1	
29	↔	
30	–	
31	STO4	
32	R/S	$(1 - \rho'^2)$
33	RCL 5	$(1 - \rho^2)$
34	↔	
35	÷	
36	R/S	decimal value of additional loss
37	f → LOG	
38	1	
39	0	
40	x	additional loss in dB due to SWR
41	H Return	

Instructions:

1. Store line attenuation α in Register R_1
2. Store SWR in Register R_2
3. RUN

Appendix 9

Basic Axioms of the Conjugate Matching Theorem

It is well known that when a load impedance differs from the source impedance, a matching device is required to permit delivery of all the available power from the source to the load. In this condition we say the load is "matched" to the source. The term "matched" has been used universally for many decades to describe this condition. In earlier days, the term was used alone. However, when all the power available from the source is delivered to the load, the matching occurs because the source and load impedances are conjugates of each other. During the last fifty years, the term "*conjugate* match" gradually came into use synonymously with "match" to describe the term more accurately. In other words, "match," as used in this context, and "conjugate match" are often used interchangeably with no difference in meaning. Unfortunately, misinterpretation and misunderstanding of *conjugate* in the newer term has created confusion for many people when a routine impedance match is referred to as a "conjugate" match. However, do not confuse "impedance match" with "conjugate match," because there can be an impedance match at one or more points in a system without necessarily having a conjugate match in the entire system. For example, an impedance match (but a nonconjugate match) can exist at the junction of a transmission line and its load, while a mismatch may exist between the source and the input of the transmission line.

Now for the basic axioms of the Conjugate Matching Theorem:

Axiom 1. There is a conjugate match in an RF power transmission system when the source is delivering all of its available power to the load. (*Refs 120, 137, 35, 17, 69*)

Axiom 2. There is a conjugate match if the delivery of power decreases whenever the impedance of the load is changed in either direction. This follows from the Maximum Power-transfer Theorem. (*Refs 17, 69*)

Axiom 3. If there is a conjugate match at any junction in the system, and if there are no active or "pseudo active" sources within the network, there is a conjugate match *everywhere* in the system. (The phasors at any point along a transmission line are conjugates.) (*Refs 35, 17, 69*)

Axiom 4. The term "conjugate match" means that if in one direction from a junction the impedance is R + jX, then in the opposite direction the impedance will be R – jX. *(Refs 17, 69)*

Quoting Dr. W.L. Everitt's statement on the conjugate match (*Refs 17, 69*):

"**Theorem**—If a group of four-terminal networks containing only pure reactances [*includes lossless transmission lines*] are arranged in tandem to connect a generator to a load, then if at any junction there is a conjugate match of impedances, there will be a conjugate match of impedances at every other junction in the system."... *(Bracketed text is mine.)*

"If the dimensions [*values*] of the network elements are such that there is a conjugate match at any one of the junctions, there must be a conjugate match at all the junctions. Since the networks contain only pure reactances, there can be no dissipation, and all the power absorbed at the input of the first network must be transferred to the output. If at any junction there should not be a conjugate match, then by adjusting the impedance beyond the junction an increased absorption of power could be obtained. This would require an increase in power delivered by the generator, which is an impossibility. Therefore there must be a conjugate match at all junctions."...

"*The Conjugate Theorem also shows that in a sequence of matching networks it is necessary to match at only one junction if the networks are nondissipative. In actual practice, since there is usually some dissipation, it is frequently desirable to adjust at more than one point. An example is a*

radio transmitter feeding a line, which in turn is coupled to an antenna. If the line were non-dissipative it would be only necessary to adjust the matching conditions at one point."

Quoting from Robert W. Beatty, NIST, *Microwave Mismatch Analysis (Ref 120)*:

1. Conjugate match—The condition for maximum power absorption by a load, in which the impedance seen looking toward the load at a point in a transmission line is the complex conjugate of that seen looking toward the source.

2. Conjugate mismatch—The condition in the situation above in which the load impedance is not the conjugate of the source impedance.

3. Conjugate mismatch loss—The loss resulting from a conjugate mismatch.

[Conjugate mismatch loss is not a dissipative loss, but is identical to reflection loss, which represents only the inability of the source to deliver all of its available power to a mismatched load.]

4. Z_0 match—The condition in which the impedance seen looking into a transmission line is equal to the characteristic impedance of the line.

5. Z_0 mismatch—The condition in which the impedance seen looking into a transmission line is not equal to the transmission-line characteristic impedance Z_0. In general, a conjugate match is a case of Z_0 mismatch.

6. Z_0 mismatch loss—The loss resulting from a Z_0 mismatch, which is canceled by the reflection *gain* obtained with a conjugate match. (*Ref 19, Sec 4.1.3*).

7. Conjugate available power—*Maximum* available power.

8. Z_0 available power—The power a source will deliver to a Z_0 load.

More from Robert W. Beatty on the conjugate match in terms of "conjugate *mismatch*" *(Ref 137)*:

"*Conjugate mismatch is useful when one is given the available power P_A from a given generator, and wishes to determine the power P_1 that it will deliver to some specified load. If the powers are given in decibels relative to some convenient level, one subtracts the conjugate mismatch loss from the available power to obtain the power delivered to the load.*"

Definition: Conjugate mismatch loss is the ratio, expressed in decibels, of the available power from the generator to the power absorbed by the load connected to the generator."

Appendix 9A

Revealing Inherent Errors in Measurements of Network Output Impedance when Looking Rearward into the Network

Sec A9A.1 Background

As in the chapters that clarified misconceptions concerning SWR, reflections, and conjugate matching, the goal of this appendix is to clarify misconceptions concerning the procedure for calculating and measuring the output impedance of networks and transmission lines when the input impedance is known. Misuse of procedure in these calculations and measurements has given rise to a prevalent misconception that a conjugate match cannot exist in a system comprising networks and transmission lines having attenuation. If this were true, a conjugate match could never exist in practical systems, because all real networks and transmission lines have attenuation.

The misconception arises from improper application of Axiom 4 while attempting to determine the output impedance of networks and transmission lines when connected to real sources in contrast to that of the classical generator. The reason is that there is a potential for conflict between Axioms 1 and 2 with Axiom 4 that arises when comparing a system with a non-dissipative source with one having the dissipative source of the classical generator. The potential for conflict is especially true when attempting to determine the output impedance of a network by measuring rearward from the output terminals. A clue to the conflict is that the output impedance of a lossy network or transmission line obtained by measuring rearward from the output with the input terminated in a dissipative resistor is not the same as the actual output impedance of the network when the network is in normal operation. Thus, the impedance obtained by rearward measurement is incorrect. In addition, the same incorrect value of output impedance is obtained by using the attenuation factor incorrectly in *calculating* the output impedance when the input impedance is known. The difference between the correct output impedance and that obtained by rearward measurement (looking backward), and thus the error, is proportional to the amount of attenuation; the error is zero when attenuation is zero.

Sec A9A.2 Explanation

We'll now explain why the incorrect application of Axiom 4 and incorrect use of the attenuation factor leads to the misconception that a conjugate match cannot exist when network components and transmission lines have attenuation. It must be first understood that according to Axioms 1 and 2 there is a conjugate match when all available power from the source is being delivered to the load. During this condition the output impedance of the network or line is the conjugate of the load impedance by definition. However, while keeping in mind that the source resistance in the classical generator is inherently dissipative, the incorrect application of Axiom 4 arises when attempting to determine the output impedance of a network or line by measuring rearward from the output. During this measurement the input of the network or line is terminated in a real dissipative resistor that replaced the non-dissipative source resistance of the same value.

The reason this procedure is incorrect is that the output impedance of a lossy network or transmission line with attenuation while delivering power to the load is not the same as the impedance obtained by measuring rearward from the output terminals with the input terminated in a dissipative resistor. Consequently, the impedance obtained by rearward measurement is not the conjugate of the load impedance. Unfortunately, because the impedance obtained by rearward measurement of a lossy network is not the conjugate of the load impedance it is often assumed incorrectly that there is no conju-

gate match at the junction of the network output and its load. It is indeed disastrous that this incorrect measurement procedure to determine the output impedance has resulted in the misconception that no conjugate match exists, when in fact it does exist. Thus, let us examine the reason why this incorrect procedure produces the incorrect value of output impedance.

The principal concerns in obtaining the correct network output impedance when attenuation is present are the direction of travel through the network (or along a transmission line) and the correct use of the attenuation factor during the measurement. If the network or line is lossless, the direction of travel is irrelevant, because the resulting impedances are identical in traveling in either direction. However, when there is attenuation in the network or line, the direction of travel and correct use of the attenuation factor (which depends on the direction of travel) are of paramount importance in obtaining the correct output impedance. The basic reason direction of travel and correct attenuation factor are important is that in returning from a mismatched load terminating the network or line, the voltage and current reflected at the load mismatch decrease while traveling toward the source due to the attenuation. Thus the magnitude of the voltage and current reflection coefficients, and thus the SWR, is less at the input than at the output where the mismatched load terminates the network or line. Consequently, the impedance appearing at the input of the line is different than if the line were lossless. These differences of SWR and impedance due to attenuation are the basis for the problem concerning the direction of travel along the line, and the correct application of the attenuation factor during measurements or calculations to obtain the correct values of input and/or output impedance. As we will see, measuring rearward from the network output (source power now applied at the output) the attenuation factor applies in the opposite direction to that when the source power is applied at the input.

Sec A9A.3 Definition and Use of Attenuation Factor

We'll now define "attenuation factor," and explain how it is used correctly in measurements and calculations. The attenuation factor applied here is the decimal equivalent of the two-way voltage (and current) attenuation in dB. Its inherent effect is to change the magnitude of the voltage (and current) reflection coefficients at either end of a line or network in proportion to the amount of its attenuation. Whether the magnitude is increased or decreased at a given end depends on whether the calculation begins at the output or input.

If the magnitude of the reflection coefficient at the output is known, we start the calculation at the output to determine the reflection magnitude at the input using the expression $\rho_{IN} = \rho_{OUT}\, e^{-2\alpha}$, yielding a decrease in magnitude at the input. Conversely, when the reflection magnitude at the input is known, we start the calculation at the input to determine the magnitude at the output, using the expression $\rho_{OUT} = \rho_{IN}\, e^{2\alpha}$, yielding an increase in magnitude at the output. Note that the change in sign of the exponent in the expressions accounts for the difference in direction of travel along the network or line, with the negative exponent applying to the direction from output to input, and the positive exponent applies while going from input to load. The legends for the terms in the expressions are:

ρ_{IN} = magnitude of the reflection coefficients at the input

ρ_{OUT} = magnitude of the reflection coefficients at the output

e = 2.71828, the base of natural logarithms

α = attenuation in nepers = dB/20 $\log_e$ = dB/8.6859

(1 neper = 1/8.6859 dB = 0.115129 dB, and 1 dB = 8.6859 nepers)

However, the more simple and routine method for determining the attenuation factor is to convert the attenuation in dB to its decimal equivalent for two-way voltage attenuation (or one-way power attenuation) using the exponential expression $10^{dB/10}$ = the decimal attenuation factor. For example, the two-way attenuation factor for voltage and current for 1.0 dB is 0.79433,and for 2.0 dB it is 0.63096. To put these values in perspective, if 100 watts were applied to a line or network having 1.0 dB of attenuation, the power available at the output would be 79.433 watts, and for 2.0 dB, 63.093 watts.

Sec A9A.4 Importance of Direction of Wave Travel

To determine SWR and terminal impedance at

either line input or output, we will first be either multiplying or dividing the magnitude of the voltage reflection coefficient by the attenuation factor, depending on the starting point and direction of travel along the line. Both SWR and terminal impedance are then calculated from the modified magnitude of the reflection coefficient. (See Program HP2, "Transmission-Line Impedance Transformation," Chapter 15.) Because the magnitude of both reflection coefficient and SWR at the input are *less* than at the output due to attenuation, the known reflection coefficient at the output is **multiplied** by the decimal attenuation factor to determine the reflection coefficient at the input. Conversely, because both reflection coefficient and SWR at the output are *greater* than at the input, the known reflection coefficient at the input is **divided** by the decimal attenuation factor to determine the reflection coefficient at the output. (Alternatively, the coefficient may be multiplied by the *reciprocal* of the decimal attenuation factor.)

Consequently, if we begin with the output impedance to determine the input impedance, and then return along the line to transform from the input impedance back to the output, the output impedance determined by calculation must be identical to the output impedance appearing at the beginning. Thus, the net attenuation for the round trip is 0.0 dB, and the net attenuation *factor* is 1.0. Make careful note of this compensatory relationship as the attenuation factor functions as a loss going from load to input, but the loss is compensated on returning from the load to the input. Knowledge of this relationship is crucial to understanding why measuring the impedance rearward from the network output yields the incorrect value of output impedance.

Because the direction of travel during impedance-transfer calculations and measurements determine whether the attenuation factor will be used as a multiplier or divider, we'll use logical terms to indicate which argument will be used. When the direction of travel is from load to input (calling for multiplication) we'll consider the attenuation factor **positive**, because the attenuation is **additive** going in this direction to account for the loss that causes reduction in reflection coefficient and SWR at the input. Conversely, when the direction of travel is from input to load (calling for division) we'll consider the factor **negative**, because the attenuation is **subtractive** while going in this direction to account for the increase in the reflection coefficient and SWR at the load. However, calling the attenuation factor "negative" during this procedure does *not* imply gain. As stated earlier, correct use of *this positive/negative relationship of the attenuation factor is the crux of the problem in explaining why measurement of output impedance of the network or line by looking rearward from the output terminals yields incorrect results.*

Sec A9A.5 Example Demonstrating Importance of Direction of Travel

Let's now use an example to demonstrate how the difference in direction of travel affects the results. Although the procedure applies equally well to both networks and transmission lines, we will use a transmission line in the demonstration, because the explanation will be simpler. We'll begin using a $\lambda/2$ 50-ohm transmission line having zero attenuation terminated with a pure resistance, $100 + j0$ ohms. As we know, with zero attenuation, the input impedance of the $\lambda/2$ line is a repeat of the load impedance, $100 + j0$ ohms. Thus, everywhere along the line the magnitude of the reflection coefficient is 0.33333 and thus the SWR is 2:1 (see Eq 3-2). Consequently, when the line is lossless the direction of travel is irrelevant in determining the impedance at either end.

Now let's introduce a line attenuation of 1.0 dB, for which the decimal attenuation factor is 0.79433 While the impedance and SWR at the load remain at $100 + j0$ ohms and 2:1, respectively, to determine the reflection coefficient at the input the reflection coefficient at the load is multiplied by the attenuation factor 0.79433. Thus, the reflection coefficient at the line input is reduced to 0.26478 by **multiplying** 0.33333×0.79433. This lower reflection coefficient causes a reduction of the input SWR from 2:1 to 1.720:1, and a reduction of the input impedance from $100 + j0$ to $86.0 + j0$ ohms. Thus, in traveling from the load to the input we see the effect of the **positive** line attenuation factor has reduced both the input impedance and input SWR relative to those at the mismatched load. Conversely, to determine the output impedance when the input impedance is known, it is necessary to **reverse** this procedure by **dividing** the reflection coefficient at the input by the attenuation

factor (thus **negative**), also 0.79433. Thus, 0.26478 ÷ 0.79433 = 0.33333, the reflection coefficient at the output, the SWR of 2:1, and the original 100 + *j*0-ohm load impedance. Consequently, we have shown the net attenuation during the round trip—load-to-input and returning input-to-load is zero.

Continuing with the example above, let's assume the λ/2 transmission line is matching the load impedance of 100 + *j*0 ohms to a non-dissipative source whose output impedance is 86.0 + *j*0 ohms. Recall that when the λ/2 line is terminated with a 100-ohm load resistor the input impedance is reduced to 86.0 ohms due to the 1.0 dB line attenuation. Consequently, the source impedance is matched to the *input* impedance of the line, and the output impedance of the line is matched to its 100-ohm load. The result is that all of the available power from the source is delivered to the load, minus the amount dissipated in the line attenuation. Thus, the *output* of the line is now the true source delivering power to the load, and it is delivering to the load all of the power that is available at the line output. Ergo, there is a conjugate match by definition between the source and the line input and between the output impedance of the line and the load impedance (Axioms 1 and 2) *despite the 1.0-dB attenuation* in the line.

Sec A9A.6 Disastrous Results of Using Wrong Polarity of Attenuation Factor

Keep in mind from statements in the paragraph above that the network-output impedance is that which allows all of the power available at the network output to be delivered to the load. Therefore, let's now see what happens when we **fail to reverse the polarity** of the attenuation factor from positive to negative when transforming the input impedance to the output. The error resulting from this common failure is that which leads to the erroneous result when attempting to measure the output impedance looking rearward from output terminals. To measure the impedance looking rearward from the output terminals the active, non-dissipative source resistance of 86.0 ohms must be replaced with a *dissipative* physical resistor of 86.0 ohms at the line input, and the source for the measurement is applied to the line output. *The result is that both input and output of the line have been interchanged.*

From the previous discussion we know there is a conjugate match between the output and the load of 100 + *j*0 ohms, but will the impedance measured rearward at the output be 100 ohms? Because we have now interchanged the input and output terminals of the line to accommodate the measurement, the *direction of travel is reversed.* The 86.0-ohm resistor placed at what was the input is now the *load*, because in making the rearward impedance measurement we are now supplying source power at what was the output, but what is now the *input* during the measurement. Keep in mind that when going from load to input the attenuation factor is *always positive,* thus reducing the SWR and impedance. However, during rearward measurement we are again measuring at an **input**, because the original input and output are interchanged. Thus, we are again using *positive* attenuation in going from what is now the load to what is now the input, when we have already used positive attenuation in determining the 86.0-ohm resistance at the original line input with 100 ohms at the load. Consequently, we have *added another* 1.0 dB to the initial attenuation instead of subtracting 1.0 dB in returning to the output as required when returning to the output for a net attenuation of zero. (This is known as "double dipping: the attenuation.)

Thus, let's see what the output measurement will show using the *additional* 1.0 dB attenuation instead of correctly **subtracting** the 1.0 dB. With the 86.0-ohm resistor now terminating the original input as the load, both the resistance and SWR are lower yet at the new input terminals. The resistance now measured is 76.6 ohms and the SWR is 1.533:1, instead of 100 ohms and 2:1 SWR. This is not quite what we expected, is it, because we expected the output resistance to be 100 ohms to verify the conjugate match at the load. However, there really is a conjugate match, and this resistance of 76.6 ohms must be correctly interpreted to avoid believing incorrectly that the 76.6 + *j*0 ohms proves there is no conjugate match to the 100-ohm load. What has occurred is that the initial 1.0-dB attenuation reduced the 100-ohm load at the output to 86.0 ohms at the input, and the additional 1.0 dB (positive) has reduced the output resistance still further, from 86.0 ohms to 76.6 ohms. If the 1.0 dB had been used correctly as *negative* on the return to the load instead of positive, the output resistance would have returned to 100 ohms and the SWR

would have returned to 2:1. Unfortunately, the 1.0-dB attenuation factor cannot be negative using this procedure for *rearward measurement*, because, as described earlier, the input and output ports have been interchanged *inherently* during the rearward measurement. Thus, the direction of wave travel is reversed with respect to normal direction of operation, *forcing* the attenuation factor to be *positive* during the rearward measurement, resulting in the erroneous result.

Sec A9A.7 Emphasis on Difference between Rearward Measurement and Calculation

However, when *calculating* the output impedance from the input impedance we are not constrained to interchange the input and output ports as we are during rearward *measurement*. In calculating the output impedance from the known input impedance we can, **and must** use *negative* attenuation in the direction returning to the load, which yields the correct 100 + *j*0 ohms as the output impedance. On the other hand, if we were to calculate the output impedance with the 86.0-ohm resistance at the input, and then fail to reverse the attenuation factor from positive to negative, we also would arrive at the same incorrect 76.6-ohm output resistance obtained with rearward physical measurement. This failure to use negative attenuation factor during the calculation is prevalent, resulting in widespread error in attempting to determine the output impedance of lines and networks. Thus, it must be understood that for the rearward *measurement* we *are* constrained to using *positive* attenuation *twice*, once in the initial travel from the load (100 ohms) to the input (86.0 ohms), and again in returning to the load, for a total attenuation of 2.0 dB. (Again, double dipping.) This is because placing the physical 86.0-ohm resistor at the input forced the input to become the terminating load, thus reversing the direction of travel from the desired direction toward the output. It is this doubling of the attenuation factor, instead of compensating it to zero during the return to the load that causes the resulting difference between the measured output impedance and the correct output impedance that misleads one to believe there is no conjugate match when attenuation is present.

Sec A9A.8 Verification of Concept by Application of the Smith Chart

Let's now perform the same calculation on a Smith chart shown in Appendix 9A Fig 1 to verify the procedure and calculations performed above. By standard convention, traveling from the load toward the source on the Smith chart uses *clockwise* rotation and *positive* attenuation factor. Positive attenuation causes the impedance curve to spiral inward logarithmically while going from load to source, indicating a shorter chart radius at the source, corresponding to the lower magnitude of the reflection coefficient. Conversely, traveling from the source toward the load uses *counterclockwise* rotation and *negative* attenuation factor, causing the plot to spiral outward on returning to the starting point, the load.

In calculating the input impedance of the $\lambda/2$ (180°) transmission line having 1.0 dB of attenuation, we begin at the point on the chart that represents the 100 + *j*0 ohm load, 2 + *j*0 chart ohms when normalized to 50 ohms. This point is shown in the figure at the 2.0:1 point on the resistance axis of the chart where the 100-ohm load resistance appears. The chart radius at this point is 0.33333, equal to the magnitude of the voltage reflection coefficient of the 2:1 mismatch resulting from the 100-ohm load. We now move 360° **clockwise** on the chart, representing 180° of transmission line, (positive attenuation) along the **solid** spiral curve on the chart, returning to the resistance axis at the point of 1.72 mismatch that represents the input impedance of 86.0 + *j*0 ohms. The 1.0-dB line attenuation has caused the radius of the spiral curve to be reduced logarithmically to 0.26478 on reaching the 86-ohm point, the amount equal to the 1.0-dB attenuation factor, 0.79433 times the 0.33333 distance to the point with zero attenuation. Remember that the radius at any point on the chart is equal to the voltage reflection coefficient at that point. With zero attenuation the point of arrival at the load would have indicated 100 + *j*0 ohms with the original radius, 0.33333.

However, to determine the output impedance we must first determine the load impedance from our newly found input impedance. The output impedance is the conjugate of the load impedance. We begin at the 86.0-ohm input point just found and retrace the original solid spiral path, reversing the

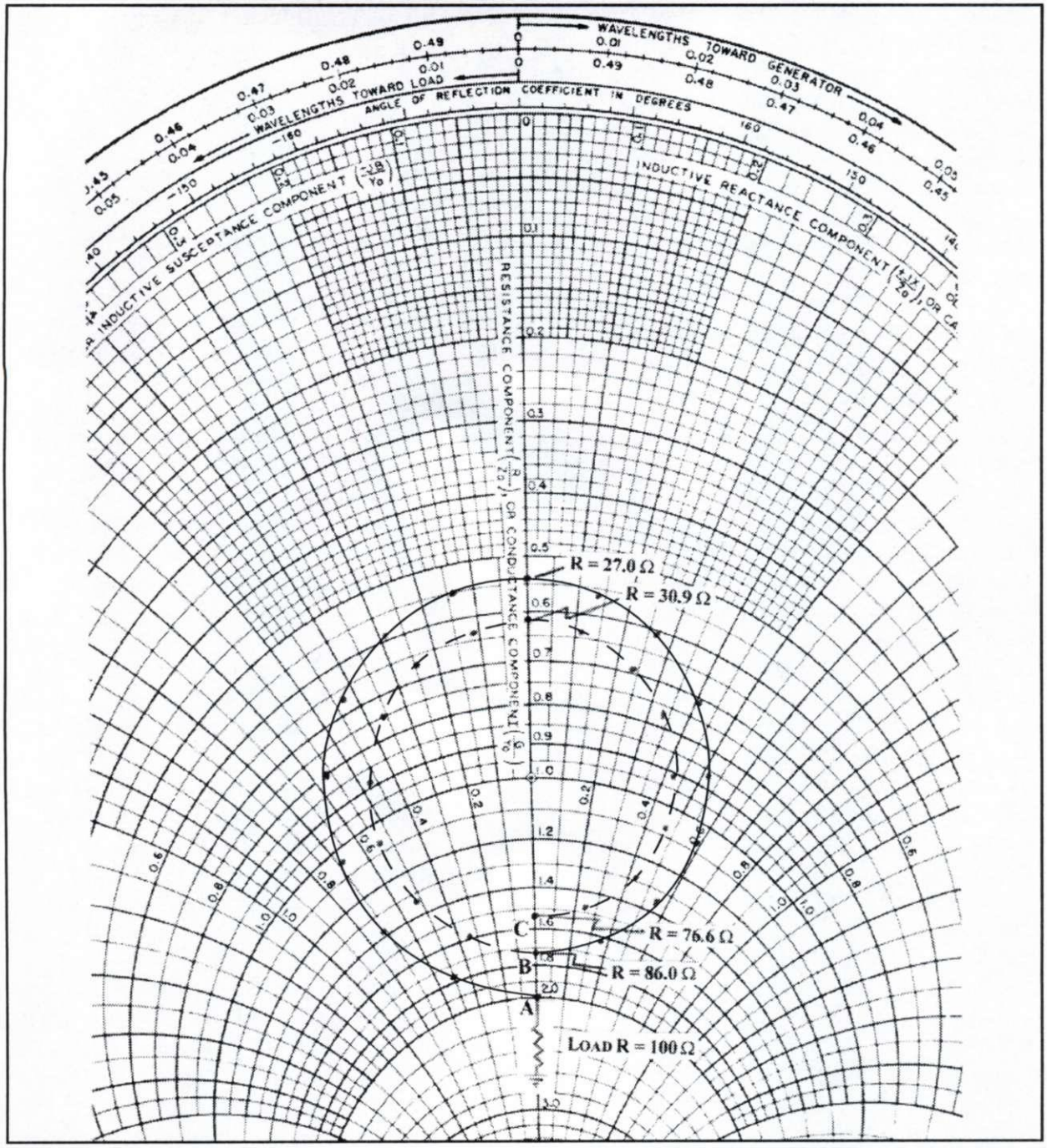

Appendix 9A Fig 1. Plot of impedances along a 50-ohm, half-wavelength (180°) transmission line, line attenuation 1.0 dB, terminated in pure resistance R = 100 + *j*0 ohms. Clockwise travel along spiral curve from A to B determines line-input resistance 86.0 ohms from load resistance 100 ohms; counterclockwise return travel from B to A determines load resistance from line-input resistance. Placing resistance 86.0 ohms at input of transmission line for rearward measurement to determine output impedance actually places the 86.0-ohm resistor as a new load resistance at B. Consequently, clockwise travel from B to C yields new line-input resistance 76.6 ohms, not line-output impedance as is prevalently considered. This incorrect procedure for determining output impedance of lines inherently requires clockwise travel along the spiral curve, resulting in an erroneous and meaningless value, prevalently considered to be the output impedance. It is imperative that counterclockwise travel be used from B to A to determine load impedance from input impedance; then output impedance is the conjugate of the load impedance, as explained in the text.

direction of rotation to travel 360° *counter*clockwise (*negative* attenuation) toward the load. The return travel thus spirals outwardly to return to the original starting point (the load) on the chart, 100 + *j*0 ohms, because the output impedance of the line has remained constant. Consequently, to return to the original starting point on the chart we must use *negative* attenuation to compensate for the positive attenuation used in the clockwise direction to determine the input impedance. Ergo, as previously stated, the net attenuation for the round trip—load-to-input and then input-to-load—is *zero.*

However, had we used positive attenuation for the return trip *the original travel would have continued for another 360° in clockwise rotation*, continuing from where the original spiral ended at the 86.0-ohm point. The continuation of the original clockwise spiral is the path shown by the *dashed* curve in the figure for a second 360° of travel, again returning to the resistance axis at the point of 1.533 mismatch. However, due to the continuation of the spiral inward, the radius has been reduced still further to 0.21023, where the impedance is 76.6 + j0 ohms. The radius at this point is 0.74933 (decimal equivalent of 1.0 dB) times shorter than the length at 86.0 ohms, and 0.63096 (decimal equivalent of 2.0 dB) times shorter than the original radius, instead of returning to the original radius of 0.33333 at the 100-ohm point. The point at this shortest radius of 0.21023, represents the impedance 76.6 + *j*0 ohms as determined in the earlier example where positive attenuation was used twice.

Sec A9A.9 Practical Effect of Difference between Correct Output Impedance and Incorrect Impedance obtained by Rearward Measurement

Before concluding this topic, here is an interesting exercise to determine the effect of the difference (error) between using the measured impedance and the correct output impedance in calculating the transfer of power to the load. We first determine the ratio of the correct output impedance and the measured impedance, and consider this ratio as a *virtual* mismatch. We then determine what the difference in power delivered to the 100-ohm load would be if the measured impedance were the correct output impedance. In other words, what would be the effect if the measured output impedance of 76.6 ohms were considered to be mismatched to the 100-ohm load? Using the data from the example above, the measured impedance resulting from using the 1.0 dB attenuation twice, or 2.0 dB, yields a virtual mismatch of 100 ÷ 76.6 = 1.305:1. This equates to a voltage reflection coefficient magnitude ρ of 0.13250, a power reflection coefficient ρ^2 of 0.01756, and a power transmission coefficient $(1 - \rho^2)$ of 0.9824. This indicates a 98.24 percent delivery of power to the load, representing a difference of 0.077 dB from that which is actually delivered to the load. Thus, this infinitesimal difference in power that would be delivered between using the measured impedance and the correct output impedance is insignificant. However, it must be remembered that this difference (error) *increases with attenuation*. Consequently, when one uses the measured impedance in attempting to disprove a conjugate match between output impedance and load, don't be misled to believe a conjugate match doesn't exist simply because the measured impedance isn't the exact mathematical conjugate of the load impedance.

Sec A9A.10 Conclusion

Finally, contrary to the prevalent misconceptions recited at the beginning, the preceding discussion and examples have shown that attenuation in a network or transmission line does not prohibit a conjugate match from existing in any RF system containing such a network or transmission line.

The following are axioms to remember concerning measurement of the output impedance of networks and lines:

1. Rearward measurement from the output of a line or a network with attenuation does not yield the correct output impedance.

2. Calculation of output impedance from input impedance using positive attenuation factor does not yield the correct output impedance.

(For further information on this subject please refer to Chapter 24, Sec 24.7 and Figs 24-1 through 24-9.)

To summarize the procedure described above it is appropriate to set forth some rules for guidance when transforming impedances from one end to the other on networks and transmission lines. It

will be helpful in understanding the basis for these rules to remember that in transforming impedances from load to input, both the magnitude of the reflected waves and the SWR decrease, due to network or line attenuation, and when transforming from input to load the magnitude and SWR increase. Now the rules:

1. When transforming impedance in the direction from load to input the attenuation is **always** positive.
2. When transforming impedance in the direction from input to load the attenuation is **always** negative.
3. When transforming load impedance to input impedance both phase and attenuation are positive.
4. When transforming input impedance to load impedance both phase and attenuation are negative.
5. When transforming input impedance to output impedance phase is positive and attenuation is negative.

Further discussion on this topic appears in Chapter 24, and computer and hand-held calculator programs for calculating impedance transformations in both directions on transmission lines appear in Chapter 15.

Appendix 10

The IEEE Definitions of Dissipative and Non-Dissipative Resistance

Are you aware that there is resistance that is non-dissipative? If not, you are not alone, because many otherwise knowledgeable electrical engineers are not only unaware of it, but due to a misunderstanding, some deny it exists. (We are not talking about a physical resis*tor*.) The concept of a non-dissipative resistance is one of the most misunderstood concepts in all electrical engineering. There are at least two reasons for this misunderstanding. First, we learned about dissipative resistance while studying DC circuits, but when moving on to AC theory, many may have failed to notice that *dissipative* resistance is not the *only* kind of resistance. In addition, the concept was seldom, if ever, discussed by the EE professors. Second, the IEEE chose to assign the same name, *resistance,* to both types, dissipative and non-dissipative, resulting in the present confusion.

Therefore, to assist in clarifying this unfortunate misunderstanding, I first quote the IEEE definitions, and then examine the real part of impedance, Definition 2 of Resistance.

From the *IEEE Standard Dictionary of Electrical and Electron Terms*, I quote the IEEE Std 100–1972 definitions of Impedance and Resistance:

Impedance:

(1) (linear constant-parameter system)

(B) The **ratio** of the phasor equivalent of a steady-state sine-wave voltage or voltage-like quantity (driving force) to the phasor equivalent of a steady-state sine-wave current or current-like quantity (response). The *real* part of impedance is the resistance. The *imaginary* part of impedance is the reactance. (C) A physical device or combination of devices whose impedance as defined in (B) can be determined. (*Note:* This sentence illustrates the double use of the word impedance, namely for a physical characteristic of a device or system [definition B] and for a *device* definition, C). In the latter case the word *impedor* may be used instead to reduce confusion. Definition (C) is a second use of **impedance** and is *independent* of definition (B). *Editors note:* The **ratio** Z is commonly expressed in terms of its orthogonal components, thus:

$$Z = R + jX$$

where Z, R, and X are respectively termed the impedance, resistance, and reactance, all being measured in ohms.

(2) **(electric machine)** Linear operator expressing the relation between voltage (increments) and current (increments). Its inverse is called the *admittance* of an electric machine.

(3) **(two-conductor transmission line)** The *ratio* of the complex **voltage** between the conductors to the complex **current** on one conductor in the same transverse plane.

Resistance:

(1) (network analysis)

(1) That physical property of an element, device, branch, network, or system that is the factor by which the mean-square conduction current must be multiplied to give the corresponding power lost by dissipation as **heat**, or as other permanent radiation or loss of electromagnetic energy from the circuit.

(2) The real part of impedance.

Note: Definitions (1) and (2) are not equivalent but are supplementary. In any case where confusion may arise, specify definition being used. (End of quote from the *IEEE Dictionary.*)

Summarizing the two resistances:

Definition 1 resistance is the heat-dissipative property of physical resistors.

Definition 2 resistance is the real part of impedance.

Definition 2 represents the general case, and Definition 1 is a special case of Definition 2, and is limited to resistors alone by the definition. In Definition 2 the real part of impedance may be the dissipative resistance of a physical resistor or it

may be a non-dissipative resistance representing only the transfer of energy.

We know that resistance is a ratio, the ratio of voltage divided by current. When taking measurements of voltage and current many people imagine they are measuring the dissipative characteristic of resistance when calculating the voltage–current ratio. However, unless it is known that they are dealing with a resistor, they cannot conclude anything about the presence of a Definition 1 resistance. Keep in mind that the impedance of a resistor is exactly equal to its Definition 1 resistance, so the *real* component of a resistor is always a Definition 2 resistance. In other words a resistor will have both a Definition 1 and a Definition 2 resistance that are exactly equal. However, in general, the only resistance we usually measure is the Definition 2 resistance.

When one measures voltage and current at a connection, the ratio is always resistance of the Definition 2 kind—i.e., you are measuring impedance. However, there is no way to postulate on the mechanisms that are causing the observed relationship strictly from the observed values. Similarly, without more information one cannot know the "source(s)" of the resistance. Thus, it doesn't matter at all whether one is dealing with dissipative or non-dissipative resistances; one cannot tell anything about that from measurements of voltage and current. We know only that the product of voltage and current tells us the power transferred at the connection, and that the ratio of voltage and current tells us the resistance between the terminals (impedance if reactance is involved). Also, we know that a ratio has no way of dissipating energy into heat, so unless we obtain additional information we can only conclude that the resistance (or impedance) is non-dissipative. A process for measuring Definition 1 resistance requires some form of thermal measurement, but we don't usually do this kind of measurement because we know where the resistors are located if there are resistors involved.

Now you may ask, "What resistance is there that is non-dissipative?" To answer this question let's first consider a lossless transmission line terminated in its characteristic impedance Z_0. In a lossless line Z_0 is a pure resistance, R. If we apply a voltage across the input terminals and measure the current flowing into the line, we will find that the current equals the voltage divided by Z_0. After manipulating this expression, we find that Z_0, or R, equals the ratio of the applied voltage to the resulting current flow into the line. Thus, by measuring the voltage and current we can determine the value of R. We also know that the product of the voltage and current equals the power delivered to the line. However, what is generally overlooked is that the power delivered to the line is not dissipated there, but is *transferred* along the line to the load where it is then dissipated. Thus, the resistance appearing at the input and all along the line up to the load termination is *non*-dissipative. *The dissipation to heat occurs only in the load resistor.*

Continuing, let's also examine the common ham installation consisting of a transceiver, an antenna tuning network, and an antenna. Also let's recall that dissipation in Definition 1 of resistance means dissipation as *heat*, and in Definition 2 resistance is the *real* part of impedance, which is often represented by the term "Re" to differentiate it from dissipative resistance "R." It will be instructive in this discussion to use impedance, with the emphasis on its real part Re, which represents only the *transfer* of energy across terminals connecting one component to another.

As we know, the transceiver delivers power to a transmission line, which *transfers* the power to the antenna-tuning network. The tuning network then *transfers* the power to the transmission line, and the transmission line *transfers* the power to the antenna, where the power is *then radiated* (or dissipated, if you prefer). At each point along the way from the transceiver to the antenna, the power is carried by voltage and current, the product of which is the power. However, at each of these points the *ratio* of the voltage to current is the *impedance* level at which the power is being *transferred.* For example, the usual impedance at which the transceiver delivers power to the transmission line is 50 ohms, where with a power of 100 watts, the voltage is 70.71 volts and the current is 1.414 amps. Verifying, the impedance is $70.71 \div 1.414 = 50$. (For the purpose of discussing the principles it is customary to consider the components in the system as lossless.)

Moving on to the output of the network we measure the voltage and current at the input of the line feeding the antenna, to find 122.47 volts and 0.8165 amps. Multiplying the volts times the amps yields the power transferred, 100 watts, but *divid-*

ing volts by amps yields the impedance level at which the power was transferred to the line, 150 ohms. Different impedance—same power. Observe that the power level remained constant, indicating that there was no dissipation to heat in the system. The impedance at the output of the transceiver is Z = 50 + *j*0 ohms, with 50 ohms the resistance Re. Re is the *real part* of the impedance, which simply means the power was *transferred* at the 50-ohm resistance level, but no power was *dissipated* to heat there. Likewise, the impedance at the input to the antenna line is Z = 150 + *j*0 ohms, where again, the 150 ohms is the real part of the impedance, but no power was dissipated to heat there either.

Thus, the real part Re of the two impedances just discussed are *non*-dissipative. If the line input impedance had been reactive, as it usually is, such as Z = 150 – *j*375 ohms, the real part of the impedance, Re = 150 ohms as before, and the –*j*375 ohms is simply the capacitive reactance, the reactive part of the impedance, which of course is also non-dissipative.

This concept of non-dissipative resistance also applies to the terminals of networks. The ratio of voltage to current at those terminals also yields the impedance, of which the real part is non-dissipative. The resistance Re simply represents the transfer of power *through* the terminals from one network to the next, with no dissipation *at* the terminals.

John Fakan, KB8MU, Ph.D. in Electrical Engineering, wrote the following illuminating discussion on non-dissipative resistance especially for this book, using a mechanical analogy. His mechanical analogy assists in developing a clear understanding of one of electrical engineering's most serious misunderstandings concerning non-dissipative impedance, and why a simple mathematical ratio such as voltage divided by current cannot dissipate energy into heat.

"Try this analogy to get your brain focused on the principle. Consider power transfer in a rotating mechanical system. The maximum power available at any connection (for example, at the end of the drive shaft) can be specified as some horsepower level at a given impedance. (I know it is not common practice to use the word impedance here, but it is appropriate and has precisely the same meaning as 'impedance' in electrical power transmission.) Usually the impedance is stated as the ratio of torque and rotational speed—the common variable pair for discussing rotational systems. In other words, the maximum power transfer can only occur at a specific speed and torque. The load connected to the shaft must be able to use all of the torque at that specific speed or it will not receive all of the available power. If the ultimate load has a different impedance (ratio of torque and speed) one must match the two impedances to transfer maximum power. That of course is easily done with gears—which simply change the torque/speed ratio. The product of torque and speed is the power, and the gears (impedance matching device) do not change this.

"Losses in the above system are due to friction and friction-like processes. Friction also has characteristics of torque (or drag) as a function of speed—i.e., at a given speed the frictional drag on the rotating shaft will produce a torque load. The losses will be proportional to the product of the speed and frictional torque. These losses will be due to the mechanical energy being changed to thermal energy—i.e., dissipated as heat. The frictional drag reduces the amount of torque available downstream of the point where the friction occurs. Giving the name 'resistance" to this phenomenon makes a lot of sense. Giving the same name to the other ratio (the speed/torque ratio at which power is transferred) would be a very dumb idea—although the units are the same. **This would certainly cause a great deal of confusion.**

"It is also exactly analogous to electrical power transfer. The available power is expressed as the product of some variable pair (we commonly use voltage and current) but this power level is available at a specific ratio of the variables—i.e., impedance. The common loss process in electrical power transfer is due to electrical 'friction' whereby when current flows through real materials the loss will depend on the amount of voltage 'dropped' while the current passes on through. The voltage loss reduces the amount of voltage available downstream of the point where the loss occurs. This process is named 'resistance,' which makes good sense. Unfortunately, the real part Re of the ratio of the voltage and current at which power is being transferred is also named 'resistance'—although it is an entirely different concept. **This *does* cause a great deal of confusion.**

"Electrical impedance is nothing more than the ratio of voltage and current with which electrical

energy is being transferred. It is just that simple. It is a mathematical ratio—like 12/5. In addition, because it is nothing more than a mathematical ratio (even if *it* sometimes happens to be a complex mathematical ratio) it cannot dissipate energy nor can it do anything else to the energy transfer process.

"The input impedance of a transmission line is simply the ratio between the applied voltage and the current that will be induced because of that voltage. (This is NOT the characteristic impedance of the line.) Again, just a ratio of numbers, and thus nothing to do with dissipation. It may very well be that the transmission line is connected to a dummy load, in which case all of the energy transferred to the transmission line may be dissipated in the dummy load, but nothing at the input of the line can tell us that. If you get focused on the need for impedance (in any kind of energy transfer process) it should all become obvious. It may help to consider 'lossless' systems at first. You still need to describe the ratio of the variables—that doesn't change. So you will still be dealing with electrical 'resistance,' **Definition 2**), but will not be dealing with resistance, **Definition 1**).

"Also, please note that impedance only deals with what is happening at the connections between components; it has nothing to do with how the values get to be what they are (i.e., the processes within the components)."

Another example of a non-dissipative resistance occurs between two terminals of a *lossless* network. Here the energy is transferred from one portion of the network to its adjacent component downstream with no energy dissipated as heat. The network components would get hot if there were dissipation. Therefore the voltage *across* the network terminals divided by the current *through* the terminals defines the impedance $Z = E/I$ appearing *at* the terminals, in accordance with IEEE definition (B) of impedance. In this case, where there is no dissipation, the "R" term in the IEEE equation $Z = R + jX$ may be replaced by the non-dissipative resistance term "Re," indicating that it is the "real part" of the impedance. In a real physical network, all the energy is transferred to the next component downstream, as in the lossless network, except for the loss due to dissipation in the *inherent* resistance in the components of the network.

If the discussion above didn't persuade you that the real part of impedance Re represents non-dissipative resistance in accordance with impedance definition (B), here's still another example, found in electric power transmission systems. Let's assume that at one point in a given distribution system the voltage across the line is 20,000 volts with 50 amperes flowing. With this voltage and current the transmission line is transferring one megawatt of power to its many loads, where the power is then dissipated. The impedance of the line at this point is 20,000 divided by 50, which is 400 ohms. At a point downstream in the system, after going through an impedance-matching device, a step-down transformer (like the gears in the rotating system), the voltage is 2,000 volts and the current is 500 amperes. The same amount of power is still being transferred, one megawatt, but the impedance has decreased to 4 ohms, 2,000 volts divided by 500 ohms. One megawatt of power was *transferred* at the new value of impedance, but *no dissipation* occurred (except for inherent, but insignificant wire-resistance loss), until reaching the loads down stream. There was *no dissipation* in either the 400- or 4-ohm impedances. If the voltage and current travel in phase, the impedance $Z = Re$ exactly; if the voltage and current travel out of phase, there is a reactance component in the impedance: $Z = Re \pm jX$, where jX is the reactive component. (Where there are reactive components [usually inductive] in the power being transferred, the power companies use compensating capacitors to maintain the power factor as close to 100% as possible.) However, in either case, no dissipation as heat occurred in the impedances. Thus, the resistance components R in the impedances are *non-dissipative*.

Of course, as stated above, there will always be some dissipation as heat in the wires of the transmission line, because they have inherent dissipative resistance according to Definition (1). However, this insignificant dissipation does not detract from the concept of the unrelated *non*-dissipative impedance determined by the ratio of the voltage *across* the line to the current *through* the line at any point along the line. If the impedance is complex, the energy storage in the reactances are unaffected when the resistance is non-dissipative. Thus, the voltage/current phase relationships are the same, whether the real part of the impedance is dissipative or non-dissipative.

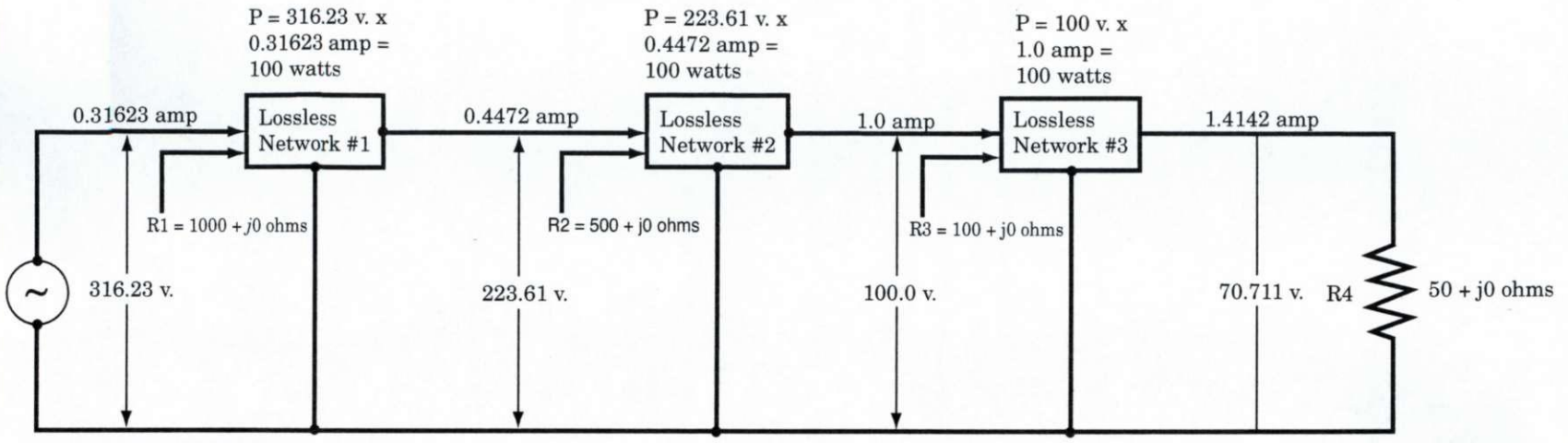

NON-DISSIPATIVE RESISTANCE
R1 =316.23 v./0.31623 amp = 1000 ohms

NON-DISSIPATIVE RESISTANCE
R2 = 223.61 v./0.4472 amp = 500 ohms

NON-DISSIPATIVE RESISTANCE
R3 = 100 v./1.0 amp = 100 ohms

DISSIPATIVE TERMINATIVE RESISTANCE
R4 = 70.111 v./1.4142 amp = 50 ohms

R1, R2, and R3 are non-dissipative energy-transfer resistances
R4 is a real resistor, dissipating 100 watts into heat.

Appendix 10 Fig 1. Example of non-dissipative resistances.

Appendix 11

Additional Measurements Proving the Existence of a Conjugate Match at the Output of RF Power Amplifiers

The purpose of this experiment is to provide proof, in addition to that presented in Sec 19.8, that a conjugate match exists at the output of an RF power amplifier when it is delivering all of its available power into its optimum load resistance R_L. It will be proved by showing that the power delivered by the amplifier into a mismatched load impedance decreases in accordance with the universally-known function of conjugate mismatch loss (return loss) versus load mismatch. The legend of the parameters measured during this experiment that are pertinent to the proof are as follows:

(1) Optimum load resistance R_L
(2) Impedance Z_{Lin} at input of pi-network tank
(3) Mismatch between R_L and Z_{Lin}
(4) Mismatch loss between R_L and Z_{Lin} at input of pi-network tank circuit
(5) Output impedance of amplifier R_{OUT}
(6) Load resistance R_{LOAD}
(7) Conjugate-mismatch loss at junction of R_{OUT} and R_{LOAD} at output of pi-network

Experiment 1

The measurement procedure used during this experiment is as follows:

1. The RF power amplifier, a Heathkit HW-100 transceiver, was tuned to resonance at 3.8 MHz and loaded with the drive level adjusted to deliver maximum available power of 114 watts into R_{LOAD}, a 52-ohm Bird 1500-watt dummy load terminating the pi-network.

2. Using a Hewlett-Packard HP-4815A RF Vector Impedance Meter, optimum load resistance R_L was then measured at the input of the pi-network tank circuit, and found to be 1350 + *j*0 ohms.

Mismatch				Mismatch Z_{Lin} vs R_L = 1350	Conjugate Mismatch Loss	
R_{LOAD} (ohms)	R_{LOAD} vs 52 ohms	Z_{Lin} (polar)	Z_{Lin} (R + jX)	At input of pi-network	At load	At input of pi-network†
240	4.6:1	950 @ 58°	503.4 + *j*805.6	3.74:1	–2.3 dB	–1.77 dB
160	3.17	980 @ 48°	655.7 + *j*728.3	2.78	–1.37	–1.09
100	1.92	1060 @ 32°	898.9 + *j*561.7	1.90	–0.45	–0.44
83	1.6	1050 @ 20°	986.7 + *j*359.1	1.55	–0.24	–0.21
52	1.0	1350 @ 0°	1350 + *j*0	1.0	0.0	0.0
41	1.22	1260 @ –14°	1222 – *j*304.8	1.29	–0.04	–0.07
34.2	1.52	1630 @ –18°	1550 – *j*503.7	1.45	–0.19	–0.15
26.0	2.0	1780 @ –32°	1509 – *j*943.3	1.93	–0.51	–0.46
20.6	2.52	1900 @ –41°	1433 – *j*1245	2.39	–0.90	–0.80
17.5	2.97	2000 @ –48°	1338 – *j*1486	2.88	–1.23	–1.16

† *The numbers in the column "At the input of pi-network" are not intended to imply a conjugate match exists at the input, but only to indicate the decrease of the RF pulsed energy delivered to the pi-network when the network input impedance is other than R_L = 1350 ohms.*

Appendix 11 Table 1

3. Nine resistors of different values of R_{LOAD} from 240 ohms down to 17.5 ohms were then used separately to terminate the output of the pi-network to obtain the corresponding transformed values of Z_{Lin} at the input of the pi-network with each separate value of R_{LOAD}.

4. After measuring each of the separate values of Z_{Lin} the data resulting from the measurements appear in Appendix 11 Table 1.

The output loading of the amplifier was initially adjusted for delivery of all the available power into a 52-ohm load to provide a reference from which to evaluate the mismatch loss encountered with various mismatched loads relative to *conjugate* mismatch loss. Accordingly, observe in Table 1 that the amplifier output is shown to be matched to R_{LOAD} = 52 ohms with zero loss showing in the Conjugate Mismatch Loss column. Note also that resistance R_{LOAD} = 52 ohms is transformed upstream through the network to R_L = 1350 ohms at the input of the network.

Now note particularly that magnitudes of the mismatches occurring between R_L = 1350 and the various values of complex impedances Z_{Lin} appearing at the input of the network are nearly the same as those at the output of the network between R_{LOAD} = 52 ohms and the corresponding mismatched values of R_{LOAD}. The differences between the corresponding mismatch values at the network input relative to those at the output are principally due to losses in the real-world network, and partially to limitations of measurement accuracy. However, because the mismatches appearing at the network input and output are correspondingly similar, the reduction in the amount of average integrated pulsed energy delivered to the pi-network tank with the various input impedances also corresponds to the mismatch losses appearing at the output of the network.

Experiment 2

For this experiment we set a maximum reference level of output power delivered to R_{LOAD} = 52 ohms at each of five different power levels. The values of R_{Lin} appearing at the input of the network were measured at each reference power level for each of the three loads shown in Appendix 11 Table 2. Leaving the tuning and loading controls of the

Nominal Output	R_{LOAD}	Measured Zin	Mismatch at Load	Mismatch at Pi Input	Power Out	Conjugate Mismatch Loss	Ideal Conjugate Mismatch Loss†
100 watts	52	1500 + *j*0	1:1	1:1	95.9 ref	0.0 dB	0.0 dB
	26	1509.6 – *j*980.4	2.0	1.79	80.0	–0.78	–0.51
	17.5	1271.3 – *j*1412	2.97	2.7	59.2	–2.09	—1.23
75	52	2100 + *j*0	1:1	1:1	71.7 ref	0.0	0.0
	26	1677 – *j*1089	2.0	1.85	60.1	–0.77	–0.51
	17.5	1312 – *j*1509	2.97	2.68	45.6	–1.96	–1.23
50	52	2850 – *j*0	1:1	1:1	48.8 ref	0.0	0.0
	26	1951 – *j*1219	2.0	1.88	38.8	–1.0	–0.51
	17.5	1472 – *j*1635	2.97	2.72	31.2	–1.94	–1.23
25	52	5100 + *j*0	1:1	1:1	20.2 ref	0.0	0.0
	26	3380 – *j*1505	2.0	1.72	16.8	–0.80	–0.51
	17.5	2409 – *j*1951	2.97	2.50	14.7	–1.38	–1.23
20	52	5600 + *j*0	1:1	1:1	17.7 ref	0.0	0.0
	26	3472 – *j*1546	2.0	1.8	14.9	–0.75	–0.51
	17.5	2451 – *j*2057	2.97	2.65	11.1	–2.01	–1.23

†*The ideal conjugate-mismatch loss assumes lossless components in the pi-network. The difference between "conjugate mismatch loss"and "ideal conjugate mismatch loss" is the result of the inherent loss in the network.*

Appendix 11 Table 2

SWR	ρ	ρ^2	$(1 - \rho^2)$	Mismatch Loss (dB)	Relative Power (watts)	Measured Power
1.0:1	0.0	0.0	1.0	0.0	100	100
1.5:1	0.200	0.040	0.960	0.177	96	96
2.0:1	0.333	0.111	0.889	0.512	88.9	89
2.5:1	0.429	0.184	0.816	0.881	81.6	80
3.0:1	0.500	0.25	0.75	1.249	75.0	74

Appendix 11 Table 3

amplifier undisturbed after setting the reference level at each power level, R_{LOAD} is changed to provide separate mismatches of 2:1 and 3:1 at the output. Then the network input impedance Z_{Lin}, and the output power delivered to each mismatched load, respectively, were measured.

Now comes the revealing part. Examination of the tabular data in Table 2 reveals that the decrease in power delivered to R_{LOAD} is directly proportional to the loss resulting from the conjugate mismatch between loads Z_{Lin} at the input of the pi-network and the corresponding amounts of average integrated power delivered by the source at each power level.

Experiment 3

The purpose of this experiment is to measure the decrease in power delivered by the amplifier to various *complex*-impedance loads with specific degrees of mismatch to show again that the decrease in power due to mismatch conforms to the function of *conjugate mismatch loss* (return loss) versus load mismatch. The impedances that presented specific mismatches to the output of the amplifier were obtained using a T-network antenna tuner terminated in a load of 50 + *j*0 ohms. The network was first adjusted to obtain a one-to-one input-output ratio to yield a 50 + *j*0 ohm resistance at the input to provide a matched impedance reference. The network was then re-adjusted to provide various complex impedances at the input that yield specific desired values of load mismatch at the output of the amplifier for the measurements of power delivered through the mismatches to the 50-ohm load terminating the tuner. The power delivered to the 50-ohm load terminating the tuner was determined by measuring the load voltage with a Hewlett-Packard HP-8405A RF Vector Voltmeter, and calculating the power using the measured resistance of the load. The resistance of the load was measured with a Hewlett-Packard HP-4815A RF Vector Impedance Meter.

In Appendix 11 Table 3 is the voltage reflection coefficient corresponding to the SWR measured at the input of the antenna tuner to obtain the desired reactive mismatched load impedances to terminate the output of the amplifier. Power reflection coefficient ρ^2 represents the power *reflected* from the mismatched load impedances, and $(1 - \rho^2)$ represents the power *transmitted through* the mismatched loads and absorbed in the 50-ohm load terminating the tuner. Table 3 also shows the relationship between the SWR mismatch and conjugate mismatch loss, in relation to the decrease in power absorbed in the 50-ohm load due to the load mismatch. The reference for the 0.0-dB conjugate mismatch loss was set with the impedance at the input of the tuner adjusted to 50 + *j*0 ohms, for a 1:1 SWR, and reflection coefficient $\rho = 0$. In this reference condition all power delivered is absorbed in the 50-ohm matched load at the output of the tuner. The measured power absorbed in the 50 + *j*0-ohm load terminating the tuner versus the various mismatched impedances at the tuner input terminating the output of the amplifier is based on 100 watts measured at zero conjugate mismatch loss—i.e., with the input impedance of the tuner adjusted to 50 + *j*0 ohms. The tuner was then readjusted to obtain the various desired values of mismatch appearing at the input of the tuner. Power loss in the tuner network is excluded, because all measurements, including the 50-ohm reference load at the input of the tuner, were taken through the network while continuously terminated with the 50 + *j*0-ohm load resistor in which the delivered power was measured.

The data in the relative power column indicates the theoretical *calculated* power that would be absorbed in the load versus the varying degrees of SWR and conjugate mismatch. The data in the

measured power column indicates the power actually absorbed by the 50 + *j*0-ohm load terminating the network. Comparison of these two columns shows that the values of measured power agree with the theoretical calculated values based on conjugate mismatch loss within the limitations of measurement accuracy. Hence, a condition of conjugate matching is proved when the measured conjugate mismatch loss is zero and the power absorbed by the mismatched loads terminating the amplifier decreases uniformly according to the standard return loss vs conjugate mismatch curve.

Thus, the data obtained from these measurements also provides additional conclusive proof that a conjugate match exists at the output of the RF power amplifier when the amplifier is delivering all of its available power.

Appendix 12

Measuring the Output Resistance of RF Power Amplifiers

Sec A12.1 Introduction

The purpose of the experiments described below is to determine the output resistance of RF power amplifiers using the load-variation method of measurement. The conventional procedure for determining the optimum load resistance R_L appearing at the input of the pi-network tank circuit for RF power amplifiers that will result in delivery of its maximum available power is by calculation from the design parameters—i.e., the plate voltage, plate current, and grid drive, etc. However, the procedure used in the experiments described below is the reverse of the conventional. In these experiments the output load resistance R_{OUT} is the starting point, and the parameters of the amplifier are then adjusted to obtain delivery of all the available power into that load at a given drive level. Therefore, these experiments show that when the amplifier is adjusted to deliver the maximum available power into a specified load, the output resistance can be measured by the load-variation method described below. Consequently, *within the limits of experimental error,* the results of these experiments reveal that **when the correct output resistance is obtained by tuning and loading the amplifier to deliver its maximum available power into the load at any appropriate drive level, the output resistance of the amplifier is equal to the load resistance.**

The measurements taken to obtain the data in the following experiments were performed using the load-variation method to determine the output resistance R_{OUT} of an RF power amplifier in which $R_{OUT} = \Delta E \div \Delta I$. ΔE and ΔI represent the corresponding change in load voltage and load current, respectively, with each change in load resistance R_{LOAD}. In these experiments all values of R_{LOAD}, R_1 and R_2, are pure resistances, $R + j0$.

The equipment used in these experiments consisted of a Heathkit HW-100 transceiver with two parallel 6146 tubes and pi-network tank circuit for the RF power amplifier; a Hewlett-Packard HP-4815A RF Vector Impedance Meter with digital readout, along with ESI 250-DA universal impedance bridge, for measuring RF and DC resistance of non-inductive load resistors, R_1 and $R_2 = R + j0$; an HP-8405A Vector Voltmeter with digital readout for measuring voltage appearing across load resistors R_1 and R_2; and an HP-410B RF Voltmeter with HP-455A Coaxial Adapter, also equipped with digital readout for voltage readings. The Vector Voltmeter was used to confirm that the load resistors contained zero reactance. The experiments were conducted at 4.0 MHz.

Sec A12.2 Procedure

The pi-network output of the amplifier is initially terminated with R_1, then tuned and loaded to deliver a specific maximum available output power with a given level of grid drive. The load voltage E_1 is then measured with load R_1, then the load is changed to R_2 and E_2 measured. Load currents I_1 and I_2 are then determined by calculation of $I = E/R$, using the measured values of R and E. Finally, as stated above, $R_{OUT} = \Delta E \div \Delta I$, as shown in the data of Experiment 1.

It should be noted that values of R_{OUT} obtained from the measurements are the average of several scattered values obtained from several measurements for each value of R_{OUT} recorded. The reason for the necessity of several measurements for each recorded value is because of sag in the output power of the amplifier. Obtaining valid output resistance data using the load-variation method requires that the change in the delta-R load be a small percentage of the load at which all the available power is delivered. However, the sag in the output power during the measurement is uncomfortably large for this type of measurement, making accurate measurements difficult without taking the average of several scattered data points.

Experiment 1

Amplifier tuned and loaded with drive level set to deliver maximum available power of ≈ 120 watts. All adjustments remain undisturbed thereafter.

$R_1 = 51.2\ \Omega$	$E_1 = 75.9$ volts	$I_1 = 1.482$ amps	
$R_2 = 44.6$	$E_2 = 70.6$	$I_2 = 1.583$	
	$\Delta E = 5.3$	$\Delta I = 0.101$	$R_{OUT} = 52.7\ \Omega$
$R_1 = 51.2$	$E_1 = 76.9$	$I_1 = 1.502$	
$R_2 = 44.6$	$E_2 = 71.6$	$I_2 = 1.605$	
	$\Delta E = 5.3$	$\Delta I = 0.1034$	$R_{OUT} = 51.2\ \Omega$
$R_1 = 51.2$	$E_1 = 69.75$	$I_1 = 1.36$	
$R_2 = 46.4$	$E_2 = 66.29$	$I_2 = 1.43$	
	$\Delta E = 3.46$	$\Delta I = 0.70$	$R_{OUT} = 49.4\ \Omega$
$R_1 = 51.2$	$E_1 = 62.5$	$I_1 = 1.22$	
$R_2 = 46.4$	$E_2 = 59.4$	$I_2 = 1.28$	
	$\Delta E = 3.1$	$\Delta I = 0.60$	$R_{OUT} = 51.7\ \Omega$
$R_1 = 51.2$	$E_1 = 77.8$	$I_1 = 1.519$	
$R_2 = 46.4$	$E_2 = 74.1$	$I_2 = 1.597$	
	$\Delta E = 3.7$	$\Delta I = 0.078$	$R_{OUT} = 47.8\ \Omega$
$R_1 = 51.2$	$E_1 = 75.22$	$I_1 = 1.469$	
$R_2 = 47.75$	$E_2 = 72.43$	$I_2 = 1.517$	
	$\Delta E = 2.79$	$\Delta I = 0.477$	$R_{OUT} = 58.5\ \Omega$
$R_1 = 51.2$	$E_1 = 77.5$	$I_1 = 1.5137$	
$R_2 = 47.75$	$E_2 = 74.9$	$I_2 = 1.5686$	
	$\Delta E = 2.6$	$\Delta I = 0.0549$	$R_{OUT} = 47.35\ \Omega$

Load resistance when adjusted for maximum power out $R_1 = 51.2\ \Omega$
Average measured source resistance $R_{OUT} = 51.9\ \Omega$

Note changes in reference load R_1 from here on:

Amplifier tuned and loaded with drive level set to deliver maximum available power of ≈ 120 watts with $R_1 = 25.7\ \Omega$.

$R_1 = 25.7\ \Omega$	$E_1 = 53.57$ volts	$I_1 = 2.084$ amps	
$R_2 = 24.5$	$E_2 = 52.12$	$I_2 = 2.127$	
	$\Delta E = 1.45$	$\Delta I = 0.043$	$R_{OUT} = 33.7\ \Omega$
$R_1 = 25.7$	$E_1 = 54.129$	$I_1 = 2.106$	
$R_2 = 24.5$	$E_2 = 52.679$	$I_2 = 2.150$	
	$\Delta E = 1.450$	$\Delta I = 0.044$	$R_{OUT} = 33.0\ \Omega$

Load resistance $R_1 = 25.7\ \Omega$ when adjusted for maximum power out
Average measured source resistance $R_{OUT} = 33.35\ \Omega$

Amplifier tuned and loaded with drive level set to deliver maximum available power of ≈ 120 watts with R_1 = 16.66 Ω.

R_1 = 16.66 Ω	E_1 = 40.2 volts	I_1 = 2.413 amps	
R_2 = 15.91	E_2 = 39.4	I_2 = 2.476	
	ΔE = 0.80	ΔI = 0.063	R_{OUT} = 12.7 Ω
R_1 = 16.66	E_1 = 40.2	I_1 = 2.413	
R_2 = 15.45	E_2 = 38.8	I_2 = 2.511	
	ΔE = 1.40	ΔI = 0.099	R_{OUT} = 14.1 Ω
R_1 = 16.66	E_1 = 39.4	I_1 = 2.365	
R_2 = 14.13	E_2 = 36.4	I_2 = 2.576	
	ΔE = 3.0	ΔI = 0.211	R_{OUT} = 14.2 Ω

Load resistance R1 = 16.66 Ω when adjusted for maximum power out
Average measured source resistance R_{OUT} = 13.66 Ω

Experiment 2

Amplifier tuned and loaded with drive level set to deliver maximum available power of ≈ 120 watts with R_1 = 51.2 Ω. Power then reduced as indicated by decreasing only the drive level, leaving the loading and plate tuning controls undisturbed from their original positions. (Note same change in R_{LOAD} at each power level.)

Power out ≈ 120 watts:

R_1 = 51.2 Ω	E_1 = 75.9 volts	I_1 = 1.482 amps	
R_2 = 44.6	E_2 = 70.6	I_2 = 1.583	
	ΔE = 5.3	ΔI = 0.10	R_{OUT} = 53.0 Ω

Power reduced to ≈ 50 watts by decreasing drive level only:

R_1 = 51.2	E_1 = 47.0	I_1 = 0.918	
R_2 = 44.6	E_2 = 44.4	I_2 = 0.996	
	ΔE = 2.6	ΔI = 0.078	R_{OUT} = 33.3 Ω

Power reduced to ≈ 25 watts by decreasing drive level only:

R_1 = 51.2	E_1 = 34.2	I_1 = 0.668	
R_2 = 44.6	E_2 = 32.2	I_2 = 0.722	
	ΔE = 2.0	ΔI = 0.054	R_{OUT} = 37.0 Ω

Experiment 3

Amplifier drive level and loading adjusted to deliver maximum available power of 50 watts:

R_1 = 51.2 Ω	E_1 = 47.3 volts	I_1 = 0.924 amps	
R_2 = 44.6	E_2 = 44.7	I_2 = 1.002	
	ΔE = 2.6	ΔI = 0.078	R_{OUT} = 33.3 Ω

Amplifier drive level and loading adjusted to deliver maximum available power of 25 watts:

R_1 = 51.2 Ω	E_1 = 34.6 volts	I_1 = 0.656 amps	
R_2 = 44.6	E_2 = 32.6	I_2 = 0.731	
	ΔE = 2.0	ΔI = 0.054	R_{OUT} = 37.0 Ω

Experiment 4

In this experiment the amplifier drive and loading were adjusted to deliver its maximum available power at each of the power levels indicated, with R_{LOAD} = 51.2 Ω.

Power Delivered (watts)	Z_{OUT} (ohms)
100	57.6
75	43.0
50	41.4
25	40.9
20	40.5
12.5	39.4

Experiment 5

In this experiment the amplifier loading was adjusted initially to deliver 100 watts into the load, R_{LOAD} = 51.2 ohms. The output power was then reduced in the steps indicated by reducing ***only the drive***. All other adjustments were left undisturbed. Two sets of five measurements at each power level were made to determine the output resistance of the amplifier. However, it should be noted that as the power output is reduced, plate voltage increases somewhat due to the unregulated power supply, ***which accounts for the increase in output resistance with decrease in output power.***

Power Out (watts)	Output Resistance (ohms, measured†)	Conjugate Mismatch to 51.2-ohm load	Conjugate Mismatch Loss in dB
Set #1 (4-3-99)			
96.6	45.7	1.12	0.014
75.0	56.4	1.10	0.010
50.0	56.7	1.11	0.012
25.0	65.1	1.27	0.062
12.5	63.5	1.24	0.050
Set #2 (3-19-99)			
100	53.5	1.04	0.002
75	56.9	1.11	0.012
50	55.1	1.08	0.012
25	63.9	1.25	0.054
12.5	71.5	1.40	0.122
Average at 12.5 watts	67.5	1.35	0.097

† *The measured values of output resistance at lower power levels shown above are somewhat higher than the true values, because the unregulated plate voltage increased as the plate current decreased with the decrease in output power. Consequently, the measured output resistance increased because of the increase in plate voltage, which would not have occurred if the plate voltage had remained constant. The measurements are intended to show that the output resistance remains relatively constant with changes in output power due to changes in drive level. This is so because the load line conditions have not changed since they were first adjusted to deliver maximum available power into the load.*

Sec A12.3 Conclusion

Within the limits of measurement error, the experiments above prove that if the output and load resistances are substantially equal when the RF power amplifier is delivering all of its available power into the load, the voltage/current relationship at the output of the pi-network tank is linear, and a conjugate match exists between the output impedance and load impedance.

References

(Note that some references may refer to material that is no longer available in print, some of which were available the time of the original printings of Reflections *and* Reflections II. *In addition, an asterisk [*] indicates material that contains misleading or erroneous information, as discussed in various chapters)*

1. *The ARRL Handbook,* any recent edition (Newington, CT: The American Radio Relay League).

2. *The ARRL Antenna Book,* 10th ed. (Newington, CT: The American Radio Relay League, 1964), pp 70–80 and 90–136.

3. G. Grammer (W1DF), "The Whys of Transmission Lines," *QST,* in three parts: Jan 1965, p 25; Feb 1965, p 24; Mar 1965, p 19.

4. G. Grammer (W1DF), "Simplified Design of Impedance-Matching Networks," *QST,* in three parts: Mar 1957, p 38; Apr 1957, p 32; May 1957, p 29.

5. G. Grammer (W1DF), "Antennas and Feeders," *QST,* in three parts: Oct 1963, p 30; Nov 1963, p 36; Dec 1963, p 53.

6. "Standing Waves—Good or Bad?" Technical Topics, *QST,* Dec 1946, p 56.

7. B. Goodman (W1DX), "My Feedline Tunes My Antenna," *QST,* Mar 1956. Reprint: "My Feed Line Tunes My Antenna," *QST,* Apr 1977, pp 40–42.

8. L. G. McCoy (W1ICP), "Choosing a Transmission Line," *QST* in two parts: Dec 1959, p 42; Feb 1960, p 40.

9. L. G. McCoy (W1ICP), "Antennas and Transmatches," *QST,* Oct 1964, p 18.

10. L. G. McCoy (W1ICP), "A Versatile Transmatch," *QST,* Jul 1965, p 58.

11. L. G. McCoy (W1ICP), "A Completely Flexible Transmatch for One Watt to 1000," *QST,* Jun 1964, p 39.

12. L. G. McCoy (W1ICP), "A Transmatch for Balanced and Unbalanced Lines," *QST,* Oct 1966, p 38.

13. L. G. McCoy (W1ICP), "When is A Feed Line Not A Feed Line?" *QST,* Aug 1965, p 37.

14. C. C. Drumeller (W5JJ), "The Mismatched RF Transmission Line," *73 Magazine,* Nov 1969, p 68.

15. P. H. Smith, "The "Mega-Rule," *QST,* Mar 1969, p 24.

16. Y. Beers (WØJF), "Match or Not to Match," *QST,* Sep 1958, p 13.

17. W. L. Everitt, *Communication Engineering,* 2nd ed. (New York: McGraw-Hill Book Co., 1937).

18. W. C. Johnson, *Transmission Lines and Networks,* 1st ed. (New York: McGraw-Hill Book Co., 1950).

19. P. H. Smith, *Electronic Applications of the Smith Chart in Waveguide, Circuit and Component Analysis* (New York: McGraw-Hill Book Co., 1969, and Malabar, FL: Robert E. Krieger Pub Co., 1983).

20. G. H. Brown, R. F. Lewis (W2EBS), and J. Epstein, "Ground Systems as a Factor in Antenna Efficiency," Proc IRE, Jun 1937, pp 753–787. (Discusses ground resistance versus number of radials, a classic work on which FCC standards for AM broadcast ground-radial systems are based.)

21. R. M. Smith (W1FTX), "Getting the Most Into Your Antenna," *QST,* Jul 1952, p 21.

22. "Impedance Matching With an Antenna Tuner," Technical Topics, *QST,* Oct 1946, p 38.

23. M. Ferber (W1GKX), "Coaxial Cable Attenuation," *QST,* Apr 1959, p 20.

24. R. Leo (W7LR, ex-K7KOK), "An Impedance-Matching Method," *QST,* Dec 1968, p 24.

25. G. L. Hall (K1TD, ex-K1PLP), "Smith-Chart Calculations for the Radio Amateur," *QST,* in two parts: Jan 1966, p 22; Feb 1966, p 30.

26. L. A. Cholewski (K6CRT), "Some Amateur Applications of the Smith Chart," *QST,* Jan 1960, p 28.

27. P. C. Amis (W7RGL), "Antenna Impedance Matching," *CQ,* in two parts: Nov 1963, p 63; Dec 1963, p 33.

28. J. R. Fisk (W1HR), "How to Use the Smith Chart," *Ham Radio,* Nov 1970, p 16. (Also see Ref 29 for corrections.)

29. W. Maxwell (W2DU), "Correspondence on How to use The Smith Chart," *Ham Radio,* Dec 1971, p 76 (corrections to information of Ref 28).

30. P. H. Smith, "L-Type Impedance Transforming Circuits," *Electronics,* Mar 1942, p 68.

31. R. E. Gordon (WØKFI), "L Networks for Reactive Loads," *QST,* Sep 1966, p 30.

32. J. J. Schultz (W4FA), "Broad-Band Balun," *CQ,* Aug 1968, p 66.

33. *Reference Data for Radio Engineers,* 4th ed. (New York: Federal Telephone and Radio Co, 1956), p 564.

34. R. C. Fenwick (K5RR, ex-W5KTR), "Antenna and Transmission Line Quiz," *QST,* Questions: Jul 1965, p 19; Answers: Aug 1965, p 55. Reprinted in *QST,* Technical Correspondence, Questions: Jan 1981, p 43; Answers: Feb 1981, p 46.

35. J. C. Slater, *Microwave Transmission* (New York: McGraw-Hill Book Co., 1942), pp 7–69.

36. W. I. Orr (W6SAI), "Broad Band Balun For A Buck," *CQ,* Feb 1966, pp 42–45.

37. R. W. P. King, *Transmission Line Theory* (New York, McGraw-Hill Book Co., 1955, and New York: Dover Publications, Inc, 1965), pp 77–83.

38. W. B. Bruene (W5OLY, ex-WØTTK), "An Inside Picture of Directional Wattmeters," *QST,* Apr 1959, p 24.

39. Radio Research Laboratory Staff, Harvard University, *Very High-Frequency Techniques,* Vol I, ed. I (New York: McGraw-Hill Book Co., 1947), pp 10–15.

40. J. Hall (K1TD, ex-K1PLP), "Accuracy of SWR Measurements," *QST,* Nov 1964, p 50.

41. L. G. McCoy (W1ICP), "The Ultimate Transmatch," *QST,* Jul 1970, p 24.

42. W. W. Mumford (W6CU), "Directional Couplers," *Proc IRE,* Feb 1947, p 160.

43. H. H. Skilling, *Fundamentals of Electric Waves,* 2nd ed. (New York: John Wiley and Sons, 1948), p 123.

44. S. C. Shallon (W6EL), "The Monimatch and SWR," *QST,* Aug 1964, p 54.

45. L. G. McCoy, "Is a Balun Required?" *QST,* Dec 1968, p 29.

46. J. Hall (K1TD, ex-K1PLP), and J. Kaufmann (WA1CQW), "The Macromatcher, An RF Impedance Bridge for Coax Lines," *QST,* Jan 1972, p 14.

47. G. H. Brown and O. M. Woodward, Jr, "Experimentally Determined Impedance Characteristics of Cylindrical Antennas," *Proc IRE,* Apr 1945, p 257.

48. R. W. P. King, *Theory of Linear Antennas* (Cambridge, MA: Harvard University Press, 1956), pp 169–176.

49. R. W. P. King and F. G. Blake, "The Self-Impedance of the Symmetrical Antenna," *Proc IRE,* Jul 1942, p 335.

50. J. Sevick (W2FMI), "The Ground-Image Vertical Antenna," *QST,* Jul 1971, p 16.

51. J. Sevick (W2FMI), "The W2FMI Ground-Mounted Short Vertical," *QST,* Mar 1973, p 13.

52. J. D. Kraus (W8JK), *Antennas,* 1st ed., New York: McGraw-Hill Book Co., 1950; 2nd ed. New York: McGraw-Hill Book Co, 1988.

53. E. C. Jordan, *Electromagnetic Waves and Radiating Systems* (New York: Prentice-Hall, Inc., 1950) p 415.

54. D. L. Fayman (WØGI), "A Simple Computing SWR Meter," *QST,* Jul 1973, p 23.

55. W. H. Anderson (VE3AAZ), "SWR's Significance," *CQ,* Oct 1970, p 8.

56. C. E. Smith and E. M. Johnson, "Performance of Short Antennas," *Proc IRE,* Oct 1947, p 1026.

57. E. A. Laport, *Radio Antenna Engineering* (New York: McGraw-Hill Book Co., 1952).

58. H. Jasik, *Antenna Engineering Handbook,* 1st ed. (New York: McGraw-Hill, 1961). Also R. C. Johnson and H. Jasik, *Antenna Engineering Handbook,* 2nd ed. (New York: McGraw-Hill, 1984).

59. W. Schreuer (K1YZW), "Notes on Directional SWR Indicators," *Ham Radio,* Dec 1969, p 65.

60. J. S. Belrose (VE2CV) "Short Antennas for Mobile Operation," *QST,* Sep 1953, p 30. Information also contained in any edition of *The Mobile Manual for Radio Amateurs* (Newington, CT: The American Radio Relay League), now out of print (the 4th ed. appeared in 1968).

61. R. Leo (W7LR, ex-K7KOK), "How To Design L-Networks," *Ham Radio,* Feb 1974, p 26.

62. W. Maxwell (W2DU), "A Revealing Analysis of the Coaxial Dipole Antenna," *Ham Radio,* Aug 1976, p 46.

63. L. Gray and R. Graham, *Radio Transmitters* (New York: McGraw-Hill Book Co., 1961), pp 115–133.

64. F. D. Schottland, "Pi Networks as Coupled Circuits," *Electronics*, August 1944.

65. *J. T. Kroenert (WA1YTC), "What Your

Wattmeter Really Reads," *QST,* Feb 1981, p 26.

66. S. Gibilisco (W1GV), "How Important is Low SWR?" *Ham Radio,* Aug 1981, p 33.

67. *H. Woods (W9IK), "Exploding the Power Myth," *73 Magazine,* Dec 1976, p 120.

68. *C. C. Drumeller (W5JJ), "Logic and Reflected Power," *73 Magazine,* Jun 1973, p 65.

69. W. L. Everitt and G. E. Anner, *Communication Engineering,* 3rd ed. (New York: McGraw-Hill Book Co., 1956), p 330.

70. R. A. Chipman, "Theory and Problems of Transmission Lines," *Schaum's Outline Series* (New York: McGraw-Hill Book Co., 1968).

71. G. L. Hall (K1TD), ed., *The ARRL Antenna Book,* 15th ed., (Newington, CT: The American Radio Relay League, 1988), Chapter 28.

72. D. DeMaw (W1FB), "Murch UT-2000-B Transmatch," Product Review, *QST,* Apr 1980, p 50.

73. L. G. McCoy (W1ICP), "To Use Or Not To Use A Transmatch," *CQ,* Feb 1986, p 13.

74. E. A. Wingfield (W5FD), "New And Improved Formulas for the Design of Pi and Pi-L Networks," *QST,* Aug 1983, and "Feedback," *QST,* Jan 1984, p 49.

75. L. G. McCoy (W1ICP), "Set the Record Straight," Correspondence, *QST,* Mar 1981, p 56.

76. L. G. McCoy (W1ICP), "The 50-Ohmer Transmatch," *QST,* Jul 1961, p 30.

77. D. DeMaw (W1FB), "Ultimate Transmatch Improved," Technical Correspondence, *QST,* Jul 1980, p 39.

78. J. Rusgrove and G. Woodward, Eds., "A Transmatch for Balanced or Unbalanced Lines," *The Radio Amateur's Handbook,* 58th ed. (Newington, CT: The American Radio Relay League, 1981), p 19-10.

79. See Fig 26B of Ref 78, p 19-12.

80. J. Nagle (K4KJ), "RF Impedance Bridge Measurement Errors and Corrections," *Ham Radio,* May 1979.

81. G. L. Hall (K1TD), ed., *The ARRL Antenna Book,* 14th ed. (Newington, CT: The American Radio Relay League, 1982), p 5-5.

82 J. Reisert (W1JR), "Simple and Efficient Broadband Balun," *Ham Radio,* Sep 1978, p 12.

83. W. Orr (W6SAI), "Multiple Dipole for Portable Use," *Ham Radio,* May 1970, p 14.

84. D. DeMaw (W1FB), *Ferromagnetic-Core Design and Application Handbook* (Englewood Cliffs, NJ: Prentice-Hall Inc, 1981), Chap 4.

85. *Reference applies to a previous edition* Reflections.

86. O. M. Woodward, Jr, "Balance Measurements on Balun Transformers," *Electronics,* Sep 1953, p 188.

87. *Transmission Line Catalog and Handbook,* Pub No. TL-6 (Wallingford, CT: Times Wire and Cable Co, 1972).

88. R. W. Bricker and H. H. Rickert, "S-Band Resonant Quadrifilar Antenna for Satellite Communications," *RCA Engineer,* Vol. 20, No. 5, Feb-Mar 1975. (Reprint from original published in 1974 International IEEE AP-S Symposium Digest, Atlanta.)

89. R. W. Bricker, "A Shaped-Beam Antenna for Satellite Data Communication," *1976 International IEEE AP-S Symposium Digest* (Amherst).

90. G. H. Brown and O. M. Woodward, Jr, "Circularly Polarized Omni-Directional Antenna," *RCA Review,* Vol. 8, Jun 1947, pp 259–260.

91. C. C. Kilgus, "Multi-element Fractional Turn Helices," *IEEE Trans,* Vol. AP-16, Jul 1968, pp 499–500.

92. C. C. Kilgus, "Resonant Quadrifilar Helix," *IEEE Trans,* Vol. AP-17, May 1969, pp 349–351.

93. C. C. Kilgus, "Resonant Quadrifilar Helix Design," *Microwave Journal,* Dec 1970, pp 49–54.

94. M. W. Maxwell (W2DU), Some Aspects of the Quadrifilar Helix Antenna (private distribution).

95. M. W. Maxwell (W2DU), "Cover Story: 2304 MHz Quadrifilar Antenna for AMSAT-OSCAR 7," *AMSAT Newsletter,* Vol. 7, No. 1, Mar 1975. See Fig 22-12.

96. M. W. Maxwell (W2DU), "Some Aspects of the Quadrifilar Helix Antenna," Trends in HF and VHF/UHF Antenna Design, IEEE Electro 77 Professional Program, New York, Apr 19–21, 1977.

97. *H. Woods (W9IK), "Power in Reflected Waves," *Ham Radio,* Oct 1971, p 49, and Dec 1972, p 76.

98. *G. T. DeLaMatyr (W5GO), "Reflections on 'Reflected Power,'" Technical Correspondence, *QST,* Nov 1972, p 46.

99. *P. M. Chamberlain (K5KEO), "SWR and Tank Coil Heating," *CQ,* Aug 1966, p 76.

100. *R. T. Hart (W5QJR), "The Case for the Half-Wave Feed Line," *73 Magazine,* Mar 1969, p 58.

101. *K. (Judge) Glanzer (K7GCO), "More Words on Antennas," *CQ,* Jul 1957, p 48.

102. *L. R. Houghton (K8ZVF), "Converts SWR Into Watts," *CQ,* Jun 1970, p 36. (See Ref 55 for Anderson's correct rebuttal.)

103. *W. M. Scherer (W2AEF), "*CQ* Reviews the Knight Kit P-2 SWR Power Meter," *CQ,* Mar 1963, p 31.

104. S. Gibilisco (W1GV), "What Does Your SWR Cost You?" *QST,* Jan 1979, p 19.

105. S. Gibilisco (W1GV), "The Imperfect Antenna and How it Works," *QST,* Jul 1979, p 24.

106. W. B. Bruene (W5OLY, ex-WØTTK), "Distortion in Single-Sideband Linear Amplifiers," *QST,* Nov 1954, p 24.

107. W. B. Bruene (W5OLY), "Introducing the Series-Parallel Network," *QST,* Jun 1986, pp 21–23.

108. E. W. Pappenfus, W. B. Bruene (W5OLY), and E. O. Schoenike, *Single-Sideband Principles and Circuits* (New York: McGraw-Hill Book Co., 1964).

109. D. K. Belcher (WA4JVE), "RF Matching Techniques, Design and Example," *QST,* Oct 1972, p. 24.

110. R. W. P. King, H. R. Mimno and A. H. Wing, *Transmission Lines, Antennas and Waveguides* (New York: Dover Publications, Inc, 1965).

111. G. H. Brown, "The Phase and Magnitude of Earth Currents Near Radio Transmitting Antennas," *Proc IRE,* Feb 1935.

112. L. Varney (G5RV), "The G5RV Multiband Antenna ... Up-to-Date," *The ARRL Antenna Compendium,* Volume 1, G. L. Hall (K1TD), ed. (Newington, CT: The American Radio Relay League, 1985), p 86.

113. W. B. Bruene (W5OLY), "How to Design RF Coupling Circuits," *Electronics,* May 1952, p 134.

114. S. Ballantine, "On the Radiation Resistance of a Simple Vertical Antenna at Wave Lengths Below the Fundamental," *Proc IRE,* Dec 1924, p 823.

11.5 S. Ballantine, "On the Optimum Transmitting Wave Length for a Vertical Antenna Over Perfect Earth," *Proc IRE,* Dec 1924, p 833. (Basis for 5λ/8, or 0.64λ antenna.)

116 *T. W. Swafford, Jr (W5HGU), "Improved Coax Feed for Low-Frequency Mobile Antennas," *QST,* Dec 1951, p 40.

117. *W. I. Orr (W6SAI), ed., *The Mobile Handbook,* 1st ed. (Port Washington, NY: Cowan Publishing Corp, 1953) p 100.

118. R. Lewallen (W7EL), "Baluns: What They Do And How They Do It," *The ARRL Antenna Compendium,* Volume 1, G. L. Hall (K1TD), ed. (Newington, CT: The American Radio Relay League, 1985), p 157.

119. D. Reynolds (K7DBA), "The 5/8-Wavelength Antenna Mistique," *The ARRL Antenna Compendium,* Volume 1, G. L. Hall (K1TD), ed. (Newington, CT: The American Radio Relay League, 1985), p 101.

120. "Microwave Mismatch Analysis," Hewlett-Packard Application Note 56, Oct 1967.

121. R. W. Beatty, "Intrinsic Attenuation," *IEEE Trans on Microwave Theory and Techniques,* Vol. MTT-11, No. 3, May 1963, p 179.

122. F. J. Witt (AI1H), "Broadband Dipoles—Some New Insights," *QST,* Oct 1986, pp 27–37. (Note that a printing error exists on p 31, column 3. The value 2.8 in line 16 should be 2.28.)

123. F. Witt (AI1H), "The Coaxial Resonator Match and the Broadband Dipole," *QST,* Apr 1989, pp 22–27.

124. F. Witt (AI1H), "The Coaxial Resonator Match," *The ARRL Antenna Compendium,* Volume 2, G. L. Hall (K1TD), ed. (Newington, CT: The American Radio Relay League, 1989), pp 110–118.

125. J. M. Haerle (WB5IIR), *The Easy Way, HF Antenna Systems* (Denton, TX: Overtones, Inc, 1984).

126. F. E. Terman, *Radio Engineers' Handbook,* 1st ed. (New York and London: McGraw-Hill Book Co., 1943).

127. A. Roehm (W2OBJ), "Some Additional Aspects of the Balun Problem," *The ARRL Antenna Compendium,* Volume 2, G. L. Hall (K1TD), ed. (Newington, CT: The American Radio Relay League, 1989), pp 172–174.

128. *C. R. Ward (WA5LVG), "Transmatches," Technical Correspondence, *QST,* Oct 1984, pp 41–42.

129. *C. C. Whysall (W8TV), "The 'Double-Bazooka' Antenna," *QST,* Jul 1968, pp 38–39.

130. R. D. Snyder, "The Snyder Antenna," *RF Design,* Sep/Oct 1984, pp 49–51. Also R. D. Snyder, "Broadband Antennae Employing Coaxial Transmission Line Sections," United States Patent no. 4,479,130, issued Oct 23, 1984.

131. M. W. Maxwell (W2DU), "Cover Story: 2304 MHz Quadrifilar Antenna for AMSAT-OSCAR 7," *AMSAT Newsletter,* Vol. 7, No. 1, Mar 1975.

132. J. S. Belrose (VE2CV), "Tuning and Constructing Balanced Transmission Lines," Technical Correspondence, *QST,* May 1981, p 43.

133. R. L. Measures (AG6K), "A Balanced Balanced Antenna Tuner," *QST,* Feb 1990, pp 28–32.

134. J. S. Belrose (VE2CV) and P. Bouliane (VE3KLO), "The Off-Center-Fed Dipole Revisited," was scheduled for appearance in *QST,* Aug 1990, or shortly thereafter.

135. M. W. Maxwell (W2DU), "Helical Coaxial Resonator RF Filter," United States Patent no. 3,437,959, issued Apr 8, 1969. (Invention is an isolation filter that prevents receiver desensitization from adjacent-channel transmitters flying on TIROS weather satellites and on RELAY television satellites.)

136. Donald G. Fink and H. Wayne Beaty, editors, *Standard Handbook for Electrical Engineers,* 13th Edition, McGraw-Hill, 1993 ISBN 0-07-020984-7.

137. Robert W. Beatty (Senior Member IEEE, also with NTIA), 'Insertion Loss Concepts," *Proc of the IEEE,* Vol. 52, No. 6, June 1964, p. 663. (Beatty's definitions also appear in Hewlett-Packard Application Note 56, Microwave Mismatch Error Analysis, October 1967 [Ref 120].)

138. M. Walter Maxwell, W2DU, "Another Look At Reflections," *QST,* a series of articles: 1973 April, June, August, October; 1974 April, December; 1976 August. (Specific attention to matching by wave interference.) Same example as in present the article, but illustrated through use of the Smith Chart.

139. M. Walter Maxwell, W2DU, *Reflections – Transmission Lines and Antennas,* 1st Edition, Newington, CT, ARRL, 1990, pp 4-3 to 4-10, p 9-3 (ditto Ref 138).

140. *Dr. Steven R Best, VE9SRB, "Impedance Matching," *Communications Quarterly,* CQ Communications, Fall 1999.

141. M.W. Maxwell, W2DU, "Letter to the Editor," *QEX,* Sept/Oct 2000, p 60. This letter rebuts the material appearing in the final issue of *Communications Quarterly,* Ref. 140.

142. *Warren Bruene, W5OLY, "RF Power Amplifiers and the Conjugate Match," *QST,* November 1991, p 31.

143. William E. Sabin, WØIYH, "Dynamic Resistance in RF Design," *QEX,* Sep 1995, pp 13–18.

144. *Warren Bruene, W5OLY, "Letter to the Editor," *QEX,* Jan/Feb 2001, pp 59–61.

145. William E. Sabin, WØIYH, "Letter to the Editor," *QEX,* May/June 2000, pp 57–58.

146. William E. Sabin, WØIYH, "Letter to the Editor," *QEX,* Sept/Oct, 2000, pp 62–63.

147. William E. Sabin, WØIYH, "Letter to the Editor," *QEX,* Jan/Feb 2001, p 60.

148. *S. R. Best, "Wave Mechanics of Transmission Lines, *QEX,* Part 1, Jan/Feb 2001; Part 2, July/Aug 2001; Part 3, Nov/Dec 2001.

149. W. Maxwell, *Reflections,* Chapter 3, Sec 3.1, 1990.

150. W. Maxwell, *Reflections II and III,* Chapter 3, Sec 3.1, and Chapter 23.

151. W. Maxwell, "Examining the Mechanics of Wave Interference in Impedance Matching," *QEX*, Mar/Apr 1998, and Chapter 23, *Reflections II* and *III.*

152. W. Maxwell, "Another Look at Reflections," Part 4, *QST,* October 1973, and Chapter 4, *Reflections II* and *III.*

153. W. Maxwell, "Examining the Mechanics of Wave Interference in Impedance Matching, *QEX,* Mar/Apr 1998.

154. W. Maxwell, "A Tutorial Dispelling Certain Misconceptions Concerning Wave Interference in Impedance Matching," *QEX,* Jul/Aug 2004, p 43.

155. J. Kelley, AC6XG, personal correspondence.

156. W. Klocko, N3WK, personal correspondence.

157. Kraus and Carver, *Electromagnetics,* McGraw-Hill, New York, 1973, pp 515–517.

158. Robert Lay, W9DMK, personal correspondence.

159. W. L. Everitt, *Communication Engineering,* 2nd Edition.

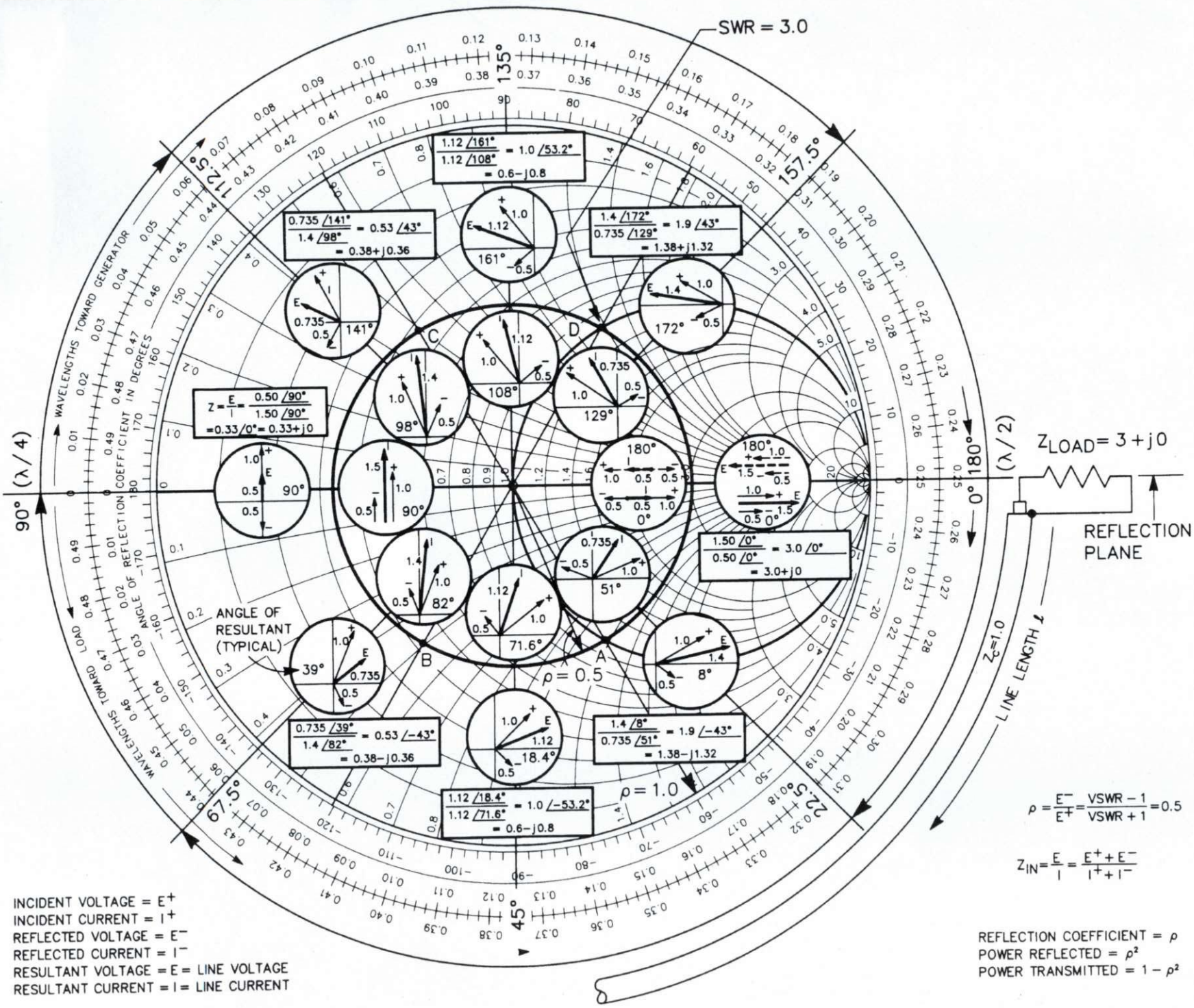

Fig 3-2 & 9-2. The W2DU Reflection Mechanics Vector Graph.

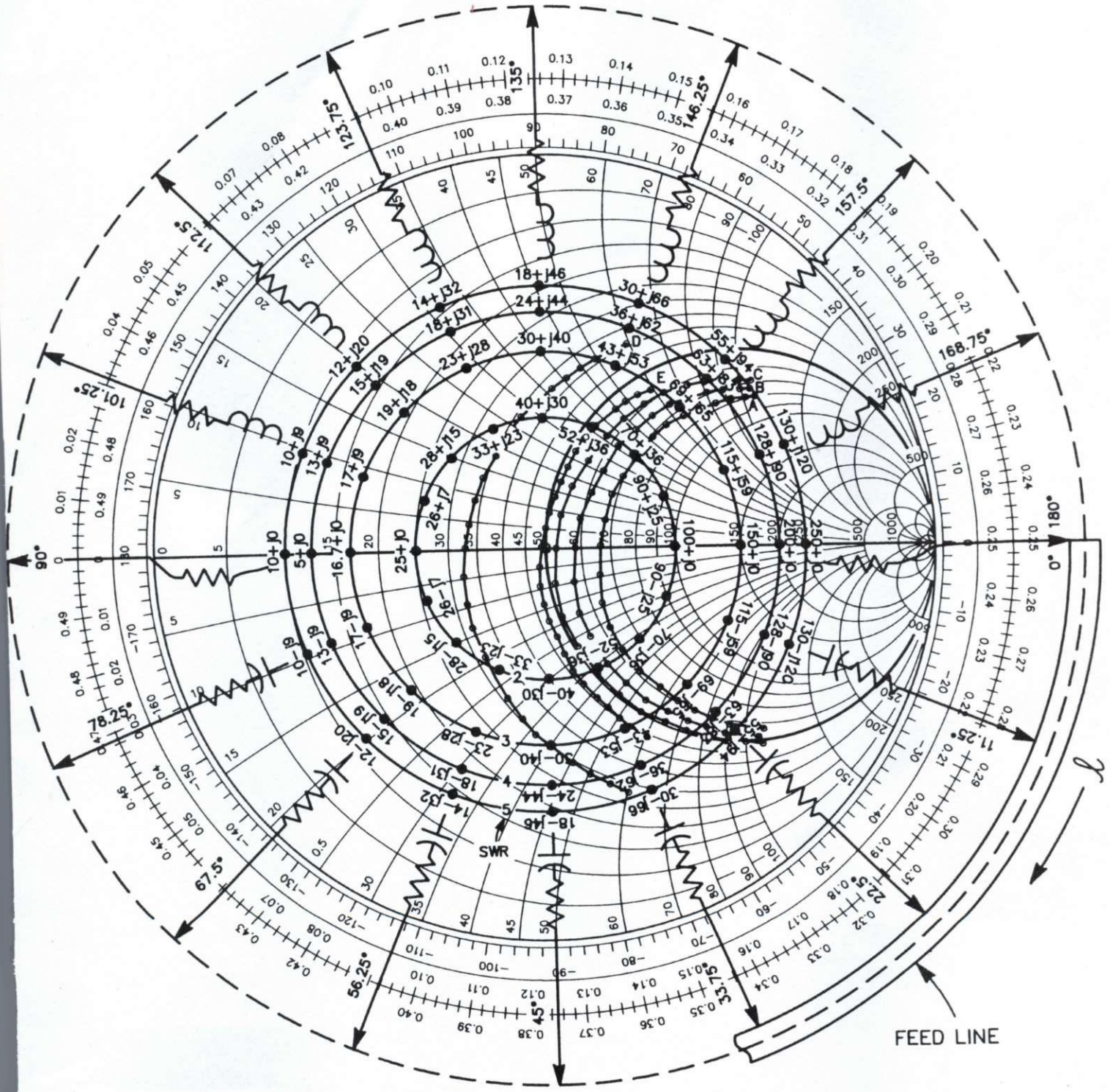

Fig 10-1. The W2DU Antenna-Impedance Feed-Line Transformation Graph.

Walt Maxwell, W2DU, at the Antenna Lab of the David Sarnoff Research Center in 1959.

About The Author

Few people have had as durable and successful a career in the field of antennas and transmission lines as has Walt Maxwell, W2DU. Fewer still have been able to create an unimpeachable legacy of understanding of the entire field of transmission-line theory, a complex and multi-faceted field rife with misconceptions and myths. Despite suffering some misguided challenges to his explanations in the 1990s, Walt's science has survived with renewed acclaim. This Third Edition brings it all together in a single, thoroughly documented and updated volume. Reflections III must be the cornerstone of any library of antenna literature, whether for the professional or the amateur.

ISBN-13: 978-0-943016-43-6
ISBN-10: 0-943016-43-6
53995 >
EAN
9 780943 016436